

AFFDL-TR-72-3

AD 745335

RINGSAIL PARACHUTE DESIGN

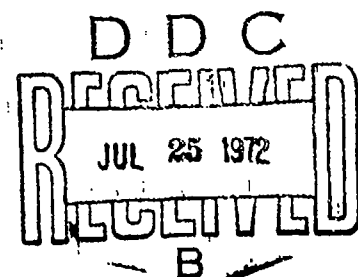
Edgar G. Ewing

NORTHROP CORPORATION
VENTURA DIVISION

TECHNICAL REPORT AFFDL-TR-72-3

JANUARY 1972

Details of illustrations in
this document may be better
studied on microfiche



Approved for Public Release; Distribution Unlimited

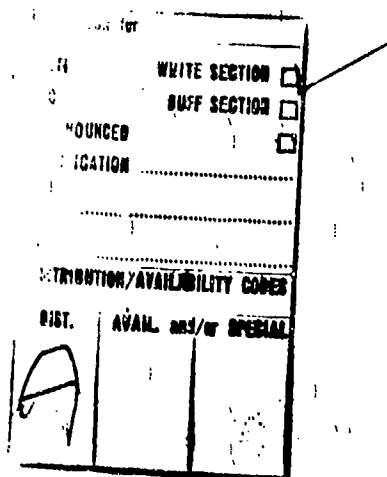
Reproduced by
NATIONAL TECHNICAL
INFORMATION SERVICE
U.S. Department of Commerce
Springfield VA 22151

AIR FORCE FLIGHT DYNAMICS LABORATORY
AIR FORCE SYSTEMS COMMAND
WRIGHT-PATTERSON AIR FORCE BASE, OHIO

386

NOTICES

When Government drawings, specifications, or other data are used for any purpose other than in connection with a definitely related Government procurement operation, the United States Government thereby incurs no responsibility nor any obligation whatsoever; and the fact that the Government may have formulated, furnished, or in any way supplied the said drawings, specifications, or other data, is not to be regarded by implication or otherwise as in any manner licensing the holder or any other person or corporation, or conveying any rights or permission to manufacture, use, or sell any patented invention that may in any way be related thereto.



Copies of this report should not be returned unless return is required by security considerations, contractual obligations, or notice on a specific document.

UNCLASSIFIED

Security Classification

DOCUMENT CONTROL DATA - R & D

(Security classification of title, body of abstract and indexing annotation must be entered when the overall report is classified)

1. ORIGINATING ACTIVITY (Corporate author) Northrop Corporation, Ventura Division 1515 Rancho Conejo Blvd. Newbury Park, California 91320		2a. REPORT SECURITY CLASSIFICATION Unclassified
		2b. GROUP N/A
3. REPORT TITLE Ringsail Parachute Design		
4. DESCRIPTIVE NOTES (Type of report and inclusive dates) Final Report		
5. AUTHOR(S) (First name, middle initial, last name) Edgar G. Ewing Jack R. Vickers		
6. REPORT DATE 31 January 1972	7a. TOTAL NO. OF PAGES 359	7b. NO. OF REFS 36
8. CONTRACT OR GRANT NO. F33615-71-C-1815	9a. ORIGINATOR'S REPORT NUMBER(S) None assigned.	
b. PROJECT NO. 412A	9b. OTHER REPORT NO(S) (Any other numbers that may be assigned this report) AFFDL-TR-72-3	
c.	10. DISTRIBUTION STATEMENT Approved for Public Release; Distribution Unlimited	
11. SUPPLEMENTARY NOTES	12. SPONSORING MILITARY ACTIVITY Air Force Flight Dynamics Laboratory AFFDL/FER Wright-Patterson AFB, Ohio 45433	
13. ABSTRACT This document is intended for use as a design handbook for the Ringsail parachute. It begins with an historical review of the aerodynamic and structural development of the parachute, including the development of the modified Ringsail Design used in the Apollo ELS main parachute cluster. Salient characteristics of all Ringsail parachutes fabricated and tested over the past 16 years are summarized. An exposition of the present status of Ringsail design and operational theory, with special emphasis on a general theory of the inflation characteristics of clustered canopies, is given. Accumulated performance and weight data are presented in tabular and graphical form. A detailed step-by-step procedure for the design of the Ringsail parachute is given and illustrated by numerical example. Pertinent design analysis methods are described including the recently improved computer methods of opening load prediction and stress analysis. Construction details and fabrication and assembly procedures in which the Ringsail parachute differs from other parachute types are delineated. Additional design data, specifications and pertinent information are presented in appendices.		

DD FORM 1 NOV 68 1473

UNCLASSIFIED

Security Classification

ia

UNCLASSIFIED
Security Classification

14. KEY WORDS	LINK A		LINK B		LINK C	
	ROLE	WT	ROLE	WT	ROLE	WT
Ringsail Parachute Parachute Design Parachute Fabrication Space Vehicle Recovery Parachute Structural Analysis						

AFFDL-TR-72-3

RINGSAIL PARACHUTE DESIGN

Edgar G. Ewing

**NORTHROP CORPORATION
VENTURA DIVISION**

Approved for public release; distribution unlimited.

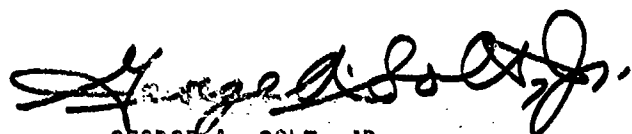
FOREWORD

This final technical report was prepared by Northrop Corporation, Ventura Division, Newbury Park, California, under Contract F33657-71-C-1815. The study was sponsored by the Life Support System Program Office, Wright-Patterson Air Force Base, Ohio. Mr. Anthony S. Mastriana of the sponsoring organization served as the Program Manager for this effort under Life Support SPO Endeavor A0211. Mr. W.R. Pinnell of the Air Force Flight Dynamics Laboratory, Air Force Systems Command was the Air Force Project Engineer.

This report was prepared by Northrop Corporation, Ventura Division at Newbury Park, California. The principal author was Mr. Edgar G. Ewing, the inventor of the Ringsail parachute and a noted parachute designer. Mr. Ewing is presently retired from Northrop and performed this effort under a consulting contract to Northrop. Mr. Ewing was assisted in this effort by Mr. Jack R. Vickers, Project Engineer, and received aid and encouragement from the noted parachute designer, Mr. Theodore W. Knacke.

Publication of this report does not constitute Air Force approval of the reports findings and conclusions. It is published only for the exchange and stimulation of ideas.

This technical report has been reviewed and is approved.



GEORGE A. SOLT, JR.
Chief, Recovery and Crew Station Branch
Vehicle Equipment Division
AF Flight Dynamics Laboratory

ABSTRACT

This document is intended for use as a design handbook for the Ringsail parachute. It begins with an historical review of the aerodynamic and structural development of the parachute, including the development of the modified Ringsail design used in the Apollo ELS main parachute cluster. Salient characteristics of all Ringsail parachutes fabricated and tested over the past 16 years are summarized. An exposition of the present status of Ringsail design and operational theory, with special emphasis on a general theory of the inflation characteristics of clustered canopies, is given.

Accumulated performance and weight data are presented in tabular and graphical form. A detailed step-by-step procedure for the design of the Ringsail parachute is given and illustrated by numerical example. Pertinent design analysis methods are described including the recently improved computer methods of opening load prediction and stress analysis. Construction details and fabrication and assembly procedures in which the Ringsail parachute differs from other parachute types are delineated. Additional design data, specifications and pertinent information are presented in appendices.

TABLE OF CONTENTS

Foreword	ii
Abstract	iii
Section 1 - Introduction	1
Section 2 - Historical Development	3
2.1 Descriptive Historical Review	3
2.1.1 Conception of the Ringsail Design Principle	3
2.1.2 Evolution of the First Working Models	4
2.1.3 Evolution of Canopy Shape and Construction	15
2.1.4 Ringsail Parachute Cluster Development	34
2.1.5 Summary of Ringsail Parachutes	55
2.2 Present Status of Ringsail Design and Operational Theory	55
Section 3 - Performance Characteristics	65
3.1 Drag Coefficient	65
3.1.1 Effect of Unit Canopy Loading (W/C_{DS_0})	65
3.1.2 Effect of Scale	65
3.1.3 Effect of Suspension Line Length	68
3.1.4 Effect of Canopy Porosity	68
3.1.5 Variation in Rate of Descent	70
3.1.6 Effect of Clustering	70
3.2 Opening Load Factors	74
3.2.1 Opening Force-Time Characteristics	83
3.3 Filling Intervals (Time, Distance, K_f)	91
3.3.1 Filling Time and K_f	91
3.3.2 Filling Distance	91
3.4 Stability	96
3.5 Reefed Drag Area	101

3.6	Opening Reliability and Repeatability	105
3.7	Tolerance for Damage	110
Section 4	-	
4.1	Weight and Volume	117
4.2	Individual Parachutes Without Risers	117
4.3	Line to Riser Links	117
4.4	Riser Assemblies	117
	Complete Parachute Systems	120
Section 5	-	
5.1	Design Procedures	121
5.2	Calculation of Basic Dimensions.....	123
5.2.1	Selection of Materials.....	130
5.2.2	Canopy Cloth	131
5.2.3	Suspension Lines and Vent Lines	133
5.2.4	Radial Tapes	133
5.2.5	Risers	134
5.2.6	Circumferential Bands	134
5.2.7	Vertical and Intercostal Tapes	135
5.2.8	Miscellaneous Textile Components	135
5.3	Hardware	136
	Ringsail Design by Computer	136
Section 6	-	
6.1	Design Analysis Methods	139
6.2	System Trajectory Computations	139
6.2.1	Ringsail Aerodynamics	140
6.2.2	Rate of Descent	140
6.2.3	Drag Coefficient	141
6.2.4	Reefed Drag Area	142
6.2.5	Calculation of Reefing Line Length	146
6.2.6	Filling Time	147
6.2.7	Derivation of the Dimensionless Filling Interval	149
6.3	Stability	151
	Prediction of Opening Loads	155

6.3.1	The Load Factor Method	155
6.3.2	The Mass-Time Method	157
6.3.3	The Area-Distance Method	160
6.4	Stress Analysis	165
6.4.1	Structural Design Factors	165
6.4.2	The Short Method	166
6.4.3	The Computer Method	178
6.5	Calculation of Ringsail Weight	178
6.5.1	Canopy and Lines	178
6.5.2	Risers	180
6.6	Calculation of Ringsail Porosity	180
Section 7	Construction Details	187
7.1	Sail Patterns	187
7.2	Sail Edge Tapes (Intercostals)	187
7.3	Radial Tapes	187
7.4	Vertical Tapes	187
7.5	The Gore Subassembly	188
7.6	Radial Seams	188
7.7	Circumferential Bands	188
7.8	Suspension Lines and Vent Lines	189
7.9	Pilot Chute Bridle Harness	189
7.10	Risers	190
Section 8	Fabrication and Assembly	191
8.1	Cloth Layout and Cutting	191
8.2	Sail Edge Tapes	191
8.3	Radial Tapes	192
8.4	Vertical Tapes	192
8.5	The Gore Subassembly	192
8.6	Circumferential Bands	193
8.7	Suspension Lines and Vent Lines	193

8.8	Risers	193
8.9	The Canopy Assembly	193
8.10	The Parachute Assembly	194
8.11	Dimensional Tolerances	195
8.12	Quality Control	195
References		199
Appendix A	- Prominent Ringsail Parachutes	203
Appendix B	- Special Ringsail Parachute Applications.....	293
Appendix C	- Sample Design Problem	303
Appendix D	- Specification, Trip Selvage Cloth	317
Appendix E	- Ringsail Parachute Design Computer Program	323

ILLUSTRATIONS

Figure		Page
1	Skysail Geometry	5
2	Sail Fullness Distribution of First Ringsails	7
3a	First Ringsail Drop Test 4 February 1955 (Note Infolded Gores on RH Side).	3
3b	Same Parachute with Two of Forty Eight Gores Removed	8
4	Skysail Model A Tethered in the Wind	10
5	Skysail Personnel Parachute Coordinates	11
6	Effect of Restrictor Tapes on Slot Openings of Skysail Model XB-1	13
7a	USN Parachute Test Jumper Landing with 29.6 ft D₀ Skysail Model D El Centro, California February 1969 . . .	14
7b	Jumper's View of Skysail Canopy.	14
8	Ringsail - Skysail Coordinates	16
9	Typical Ringsail Gore Layout Developed by the Original Standard Method (Schematic)	17
10	Lapped-Sail Gore Assembly Method of 64.7 ft D₀ Ringsail No. 1	18
11	Ringsail Construction	20
12	Ringsail Parachute Basic Dimensions	24
13	Gemini 84.3 ft D₀ Ringsail - Boiler Plate Capsule Splashdown in the Salton Sea, California	25
14	Termination of "Little Joe" Test Simulating Apollo Off-Pad Abort with 88.1 ft D₀ Ringsail Parachutes in First Experimental Earth Landing System	26
15	Comparison of Ringsail Canopy Constructed Profiles	27
16a	124.5 ft D₀ Ringsail Opening Configuration Associated with the "Soft" Opening Mode	29
16b	124.5 ft D₀ Ringsail Parachute in Steady Descent with 9650 pounds	29
17	Two Stages During Reefed Operation of 124.5 ft D₀ Ringsail Showing Typical Irregular Shape	31

Figure		Page
18	Fullness Distribution of 127 ft D_o Bi-Conical Ringsail Canopy Relative to Calculated Width of Conical Gore	33
19	128.8 ft D_o Lightweight Version of the Century Ringsail Descending at 27.9 fps (EAS) with 9762 pounds (Bottom of Damaged Gore Visible on RH Side)	35
20	Results of Full Scale Wind Tunnel Air Flow Studies with 88.1 ft D_o Ringsail Reefed	43
21	Ringsail Geometric Porosity of Crown Ventilation	60
22	Variation of Ringsail Drag Coefficient with Unit Canopy Loading and Effective Line Length	66
23	Variation of Ringsail Drag Coefficient with Scale	67
24	Effect of Suspension Line Length on Ringsail C_{D_o}	69
25	Effect of Canopy Porosity on Ringsail Drag Coefficient	71
26	Cluster Effects on Ringsail Drag Coefficient	73
27	Opening Load Factor (C_K) vs Unit Canopy Loading	75
28	Opening Load Factor (C_K) vs Mass Ratio	76
29	Apparent Trend of Ringsail Opening Load Factor with Altitude	78
30	Ringsail Opening Load Factors at Altitude (see Table XII for Code)	79
31	Effect of Flight Path Angle at Line Stretch on C_K (Results of Computer Study of 128.8 ft D_o Ringsail)	82
32	Enlargement of Coleman Tensiometer Record Obtained with Non-Reefed 56.2 ft D_o Ringsail Deployed at 130 KEAS, 15,000 ft Altitude	84
33	Opening Forces Correlated with Canopy Shape, Gemini 84.2 ft D_o Ringsail Reefed 10.5% D_o for 8 Seconds, Deployed at 272 fps (TAS) at 9630 Feet Altitude (Weight = 4450 pounds)	85
34	Opening Forces and Trajectory Data for ASSET 29.6 ft D_o Ringsail with two Reefed Stages	86

Figure		Page
35	Opening Force-Time History for Cluster of Two 128.8 ft D ₀ Ringsails Reefed 13% D ₀ for 8 Seconds, Deployed at 299 fps (TAS) at 10,246 feet Altitude (Weight = 17,720 pounds)	87
36	Opening Force - Time History for a Cluster of Two 85.6 ft D ₀ Modified Ringsails with Two Stages of Reefing Deployed at 167 KEAS at 10,000 feet Altitude Weight = 12,989 pounds)	88
37	Opening Force - Time History for a Cluster of Three 88.1 ft D ₀ Ringsails Each Reefed 13% D ₀ for 6 Seconds Deployed Under Simulated Abort Conditions (Weight = 9500 pounds) Apollo Test 50-11	89
38	Opening Force - Time History for a Cluster of Three 85.6 ft D ₀ Ringsails with Two Stages of Reefing (8.4% D ₀ /24.8% D ₀) Deployed under 90% Design Limit Conditions (Weight = 13,000 pounds) Apollo Test 83-6 ...	90
39	Pendular Oscillations of ASSET 29.6 ft D ₀ Ringsail During Terminal Descent at 45.5 fps (EAS) with 1115 Pounds	97
40	Pendular Oscillation of 29.6 ft D ₀ Skysail During Jump Test Program at El Centro in 1959	98
41	Typical Coning Oscillation Record of Gemini 84, 2 ft D ₀ Ringsail (Development Test No. 19)	99
42	Oscillation of 128.8 ft D ₀ Ringsail Descending at 26.4 fps (EAS Average) with 9786 Pounds	100
43	Statistical Comparison of Angular Deflections of Apollo Two-Canopy Clusters of Standard and Modified Ringsails	102
44	Oscillation Data, Three Canopy Cluster, Apollo Modified Ringsail, Test 73-3	103
45	Oscillation Data, Three Canopy Cluster, Apollo Modified Ringsail, Test 73-1	104
46	Typical Ringsail Parachute Reefing Ratios	106
47	Mercury, Gemini, and Apollo Development Test Data Averages	107

Figure		Page
48	Century Ringsail Reefed Data	108
49	85.6 ft D_o Ringsail (Modified. -75% of 5th Ring Removed) with Mid-Gore Reefing	109
50	Mercury 63.1 ft D_o Ringsail Damaged by Falling Compartment Cover During Qualification Test-Salton Sea, California	112
51	Century 128.8 ft D_o Ringsail (Lightweight Model) Opening Damage (Rate of Descent 27.9 fps with 9762 lb)	113
52	88.1 ft D_o Ringsail Descending Safely with One Gore. Split from Vent to Skirt.....	114
53	Ringsail Parachute Weight vs Diameter (Without Risers)	118
54	Ringsail Fullness Distribution	128
55	Full-Scale Wind Tunnel Data	145
56	Typical Reefing Line Splice	146
57	Idealized Ringsail Drag Area Growth with Time	148
58	Variation of Filling Distance with Mach No. (Reference 23).....	152
59	Typical Static and Dynamic Stability Characteristics of Parachutes	153
60	Drag Area Growth Exponent vs Filling Time (Disreef to Full Open).....	159
61	Mass-Time Method; Calculated vs Measured Opening Loads (Apollo Test 80-1R)	161
62	Area-Distance Method, Apollo Cluster Test 81-2	163
63	Mass-Time Method, Apollo Cluster Test 81-2	164
64	Differential Pressure Distributions Across 85.6 ft D_o Ringsail (Modified) Deduced from Shape Measurements and Strain Analysis by CANO Program	170
65	Method of Estimating the Design Load for a Mid-Canopy Circumferential Reinforcing Band	173
66	Method of Calculating Reefing Line Tension	175
67	"Stress" - Strain Characteristic of Nylon Textiles	177

Figure		Page
68	Variation of Relative Porosity with Δp for Typical Parachute Cloth	182
69	Assumed Shapes of Crescent Slots	184
70	Cross Section of Vertical Tape Cut on Gore Centerline	188
71	Bridle Harness for Permanently Attached Pilot Chute	190
72	Acceptable Tolerances for Finished Dimensions of the Ringsail Parachute	196
73	Mercury Capsule Landing System, 63.1 ft D_o Ringsail	205
74	Gemini Spacecraft Landing System, 84.2 ft D_o Ringsail	206
75	Apollo Spacecraft Earth Landing System, Cluster of Three 85.6 ft D_o Ringsail Parachutes	207
76	128.8 ft D_o Century Ringsail Parachute	208
77	Guide to Fullness Distribution Curves Presented in Figures 78 through 105	209
78	Gore Pattern and Fullness Distribution, 29.6 ft D_o Ringsail Parachute	210
79	Gore Pattern and Fullness Distribution, R5044-501 41.0 ft D_o Ringsail Parachute	212
80	Gore Pattern and Fullness Distribution, R5157-333 63.1 ft D_o Ringsail Parachute	214
81	Gore Pattern and Fullness Distribution, R6220-525 84.2 ft D_o Ringsail Parachute	216
82	Gore Pattern and Fullness Distribution PDS 808-1 88.1 ft D_o Ringsail Parachute	218
83	Gore Pattern and Fullness Distribution, PDS 926-1 88.1 ft D_o Ringsail Parachute	220
84	Gore Pattern and Fullness Distribution, PDS 927-1, 88.1 ft D_o Ringsail Parachute	222
85	Gore Pattern and Fullness Distribution, PDS 1226-1 through -505 88.1 ft D_o Ringsail Parachute	224
86	Gore Pattern and Fullness Distribution, PDS 1543-1, -535 and -553 88.1 and 85.6 ft D_o Ringsail Parachute	229

Figure		Page
87	Gore Pattern and Fullness Distribution, PDS 1543-521 and -523 88.1 ft D_o Ringsail Parachute	233
88	Gore Pattern and Fullness Distribution, PDS 1543-529 88.1 ft D_o Ringsail Parachute.....	236
89	Gore Pattern and Fullness Distribution, PDS 1543-531 and -543 88.1 ft D_o Ringsail Parachute	238
90	Gore Pattern and Fullness Distribution, PDS 1543-525, -533, -539 and -551 88.1 and 85.6 ft D_o Ringsail Parachute	241
91	Gore Pattern and Fullness Distribution, PDS 1543-547 88.1 ft D_o Ringsail Parachute	246
92	Gore Pattern and Fullness Distribution, PDS 1543-555 85.6 ft D_o Ringsail Parachute	248
93	Gore Pattern and Fullness Distribution, PDS 1544-1 and -501 88.1 ft D_o Ringsail Parachute	250
94	Gore Pattern and Fullness Distribution, PDS 1650-1 and -501 87.1 ft D_o Ringsail Parachute	253
95	Gore Pattern and Fullness Distribution, PDS 2021-1 88.1 ft D_o Ringsail Parachute	256
96	Gore Pattern and Fullness Distribution, PDS 2071-1 88.1 ft D_o Ringsail Parachute	258
97	Gore Pattern and Fullness Distribution, PDS 2072-1 87.9 ft D_o Conical Ring/Solid Parachute	260
98	Gore Pattern and Fullness Distribution, PDS 3120-1 88.3 ft D_o Ringsail Parachute	262
99	Gore Pattern and Fullness Distribution, R7118-1, -501, -503 and -513 88.1 ft D_o Ringsail Parachute	264
100	Gore Pattern and Fullness Distribution, R7118 -507 88.1 ft D_o Ringsail Parachute	269
101	Gore Pattern and Fullness Distribution, R7118-515 88.1 ft D_o Ringsail Parachute	271
102	Gore Pattern and Fullness Distribution, R7527-1 and -503 85.6 ft D_o Conical Ringsail Parachute	273
103	Gore Pattern and Fullness Distribution, DR 7661-1 and -527 83.5 ft D_o Conical Ringsail Parachute	276

Figure		Page
104	Gore Pattern and Fullness Distribution, R7661-1 thru -519 83.5 ft D_o Conical Ringsail Parachute	279
105	Gore Pattern and Fullness Distribution, R7811-1 128.8 ft D_o Ringsail Parachute	291
106	63 ft D_o Glidesail Parachute Gliding at L/D (max) ~0.7 with 2580 pounds	294
107	Aerial Engagement of 17.5 ft D_o Ringsail Target Canopy on 42 ft D_o Annual Parachute with 800 lb Dummy Payload	296
108	Schematic of the PEPP Ringsail (40 ft D_o)	299
109	Opening Load Fluctuations of PEPP Parachutes Following Line Stretch at Mach 1.4 - 1.6	301
110	Trail Gore Layouts of Crown Ventilation per Gore	306
111	Prototype Design Dimensions and Materials for 60.6 ft D_o Ringsail Parachute	315

TABLES

I	Measured Opening Forces-Clusters of Three 100 ft Parachutes (Reference 10).....	37
II	Ringsail Parachute Design Modifications for Cluster Development	40
III	Porosity Variation of the Wing Tunnel Models Tested	45
IV	Apollo Cluster Development - Measured Opening Forces for Cluster Tests Showing Maximum Divergence	47
V	Maximum Force Ratios from Table IV	49
VI	Measured Opening Forces of Two 128.8 ft D_o Ringsails in Cluster	52
VII	Cluster Opening Time Sequence of Two 128.8 ft D_o Ringsails in Cluster	52
VIII	Comparison of Unit Canopy Loadings of Three Apollo Parachute Systems	54
IX	Standard Ringsail Parachutes - Design and Performance Data	57
X	Effect of Crown Porosity on C_{D_o} of 88.1 ft D_o Ringsail	70
XI	Summary of Rate of Descent Data	72
XII	Ringsail Opening Load Factors at Altitude	80
XIII	Comparison of Filling Intervals of Standard Ringsail Parachutes and the 85.6 ft D_o Modified Ringsail of Apollo Block II	92
XIV	Filling Intervals of the 85.6 ft D_o Modified Ringsail with Two Reefed Stages (Apollo Block II H)	93
XV	Measured Filling Distances of Large Ringsail Parachutes	94
XVI	Relative Filling Distances of Large Ringsail Parachutes	95
XVII	Typical Suspension Line-to-Riser Link Weights	119
XVIII	Typical Riser Assembly Weights	119

TABLES (Continued)

XIX	Weight of Spacecraft Landing Systems	120
XX	Wind Tunnel Test Data for Two Configurations of the Apollo 88.1 ft D_o Ringsail	143
XXI	Wind Tunnel Test Data of Configuration A-2 Apollo 88.1 ft D_o Ringsail with Mid-Gore Reefing	144
XXII	Shock Factors for Synchronous and Non-synchronous Inflating Ringsails in Cluster	156
XXIII	Measured Reefing Line Loads on the 85.6 ft D_o Modified Ringsail	176
XXIV	Textiles Commonly used in Ringsail Parachutes	179
XXV	Typical Unit Weights of Ringsail Canopies	180
XXVI	Representative Ringsail Parachutes	203
XXVII	Measured Glidesail Performance	295
XXVIII	Ringsail Target Performance as a Drogue in the UAR System	298
XXIX	PEPP Measured Drag Coefficients	300
XXX	Summary of Crown Geometric Porosity	308
XXI	Canopy Dimensional Calculations	310
XXXII	Sail Pattern Dimensions	311
XXXIII	Material List for the 60.6 ft D_o Ringsail Parachute	314

SYMBOLS

Primary		Subscript
Width of sail pattern upper edge, allowable strength factor	A	Sail upper edge, allowable
Acceleration, length of short edge of sail	a	Added air mass
Width of sail pattern lower edge	B	Sail lower edge
Length of long edge of sail	b	Circumferential band
Coefficient, constant, factor, chord	C	Canopy
	c	Crown, Critical, steady state
Diameter, drag, a characteristic dimension	D	Drag
Diameter	d	
Abrasion loss factor	e	Effective, equilibrium
Force, load	F	Full
	f	Filling
Acceleration of gravitation	g	Geometric, slot
Height of gore pattern	H	
Height, altitude	h	
Shape factor, dimensionless interval, a constant	K	
Fatigue loss factor, spring constant	k	Opening load

Primary		Subscript
Lift	L	Lift, limit, leading canopy of cluster
Length	l	Lagging canopy of cluster
Total mass of system, Mach number	M	Aerodynamic moment
Mass	m	Mass, material (cloth), canopy mouth
Number of gores, an integer	N	
Exponent of drag area growth equation, any number	n	The n^{th} member of a series
	o	Initial, nominal, at sea level
Strength of material, pressure (absolute)	P	Projected, parachute, strength
Differential pressure	p	Pressure, pack
Dynamic pressure	q	
Radius, reefed, ratio	R	Radial, rated, reefed, risers, crescent-shaped slot
Radius, local radius of curvature	r	
Area	S	Suspended
Distance, load distribution ratio	s	Suspension line, sail, snatch
Unit tensile load	T	Proof test, total
Time	t	
Seam or joint efficiency	u	
Volume	v	Vehicle
Velocity	v	Vent

Primary		Subscript
Weight	W	
Unit weight	w	Woven
Opening shock factor ($= C_K$)	X	
Displacement along "x" axis	x	
Displacement along "y" axis	y	
Number of identical members or plies	z	
Angle of attack, filling distance coefficient	α	
Angle of yaw	β	
Flight path angle from horizontal	γ	
Difference, small increment	Δ	
Density	δ	
Angle between longitudinal axis and vertical	θ	
Vacuum loss factor	ι	
Relative porosity of cloth	Λ	
Porosity	λ	
Viscosity of air	μ	
Humidity loss factor	σ	
3.1416	π	
Density of air	ρ	

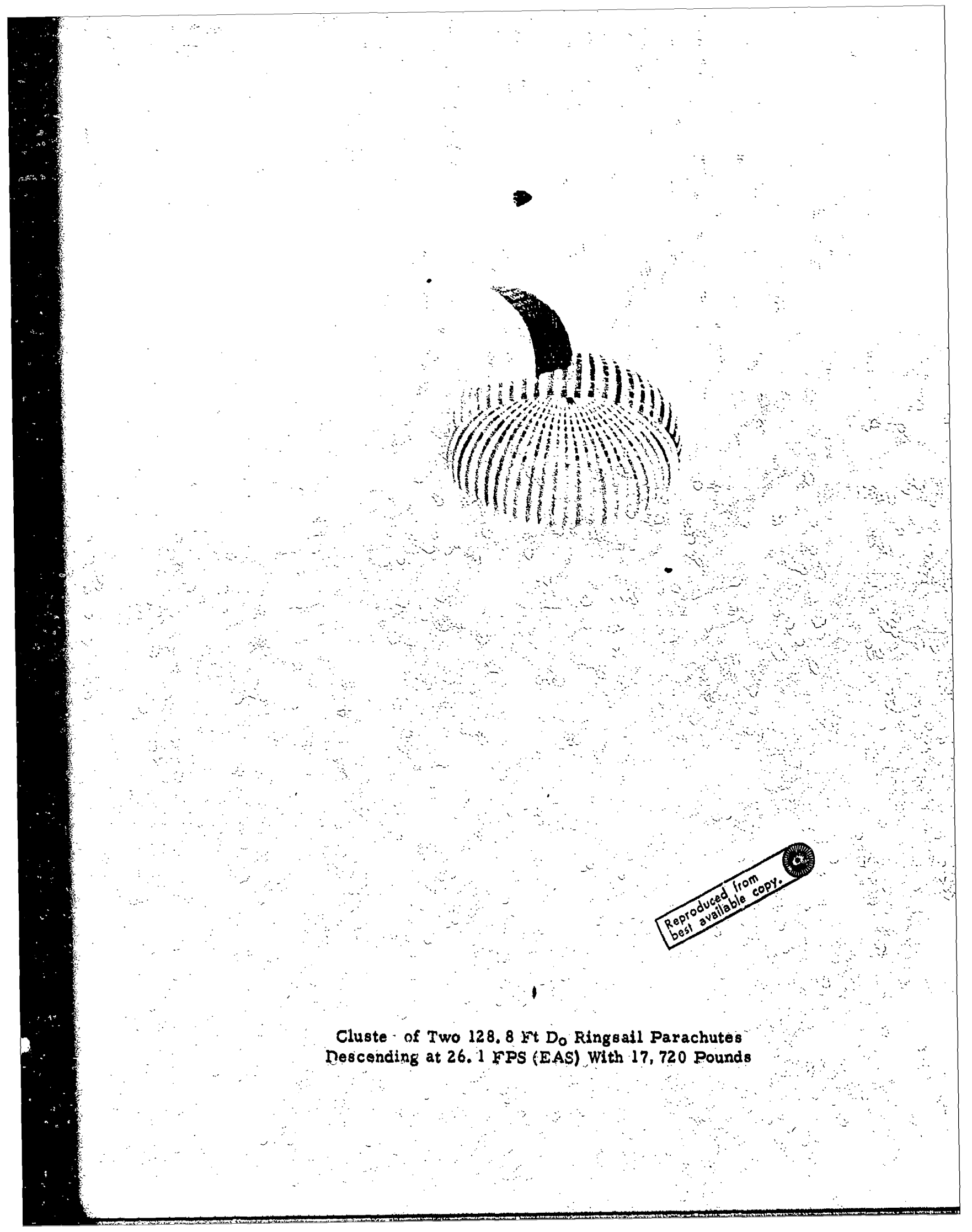
<u>Primary</u>	<u>Subscript</u>
Summation	Σ
Standard deviation	σ
Temperature loss factor	τ
Suspension line angle from longitudinal axis	ϕ
Skirt angle from longitudinal axis, drag area ($= C_D S$)	ψ
Approximately	\approx
Approximately equal to	\approx
<u>Superscript</u>	
Reference value	*
Average or mean value	—
Similar value, reference value	†
Rate of change of variable with time	•

Abbreviations and Definitions

$C_{D,R}^S$	Reefed drag area
$C_{D,o}^S$	Full open drag area
EAS	Equivalent air speed
FO	Full open
fps	Feet per second
D. F.	Design factor
DOF	Degrees of freedom
DR	Disreef
KEAS	Knots equivalent air speed
LIM	Limit
max	Maximum
chute	Parachute
LS	Line stretch
in	Inflow
out	Outflow
psf	Pounds per square foot
S. F.	Safety factor
Fn	Froude number ($gD \sin \gamma / v^2$)
Re	Reynolds number ($Dv\rho/\mu$)
S_o	Area of design drag surface including slots and vents
M. S.	Margin of safety

Definitions

Differential fullness	The difference in lengths of adjoining sail edges.
Fullness	The difference between the width of the sail and the chord of the gore at any radial ordinate (h).
Pendular	Pendulum-like
Squidding	Behavior of a parachute which stops filling at any stage prior to the normal full condition for that stage.



Reproduced from
best available copy.

Cluster of Two 128.8 Ft D₀ Ringsail Parachutes
Descending at 26.1 FPS (EAS) With 17,720 Pounds

SECTION 1

INTRODUCTION

The first Ringsail parachute started out as a rather unprepossessing modification of the Ringslet design, but after surviving two embarrassing proof tests, it was found to have some desirable performance advantages. Since that day in February 1955 the Ringsail parachute has been improved in both performance and method of design, and has seen extensive use in missile and drone recovery systems. It has also been used in a variety of space vehicle recovery or landing systems including those of Mercury, Gemini, and Apollo.

The purpose of this work is to provide designers with all of the detailed information required to produce a successful Ringsail parachute of near-optimum performance for a given application. The presentation begins with a historical review of Ringsail development aimed at exposing the pitfalls that lie in the path of the innovative designer, hopefully to spare him repetition of errors made by his predecessors.

One of the earliest designs of the Ringsail was the "Skysail" personnel parachute developed for the Navy. The first Skysail jump test was performed in 1958 over the Salton Sea by Chief H. W. Piccard of the Naval Parachute Unit, flying out of the Naval Air Station, El Centro, California on a routine jump test mission. Since that time hundreds of Navy airmen and a number of skydivers have jumped the Skysail without incident.

The historical review pays special attention to the development of the modified Ringsail for the Apollo ELS parachute cluster. Although this parachute has been widely publicized as having a nominal diameter of 83.5 feet, it is referred to throughout this document by its true-scale diameter of $D_o = 85.6$ feet. The smaller figure was calculated by subtracting the area of the wide slot from the canopy area, producing a value for S_o which cannot be used in performance comparisons.

The historical review includes a summary of the salient characteristics of all existing Ringsail parachutes, supplemented by a set of diagrams in Appendix A covering the construction details of the most familiar operational models. Significant data on several special-purpose Ringsail parachutes of modified design are given in Appendix B. The history concludes with an appraisal of the present status of Ringsail design and operational theory.

Presented in Section 3 is a digest of Ringsail parachute performance data accumulated from a number of different programs in which instrumented aerial drop tests were performed. An attempt has been made to discard wild points and reduce the data to a form most useful to the designer. The data scatter remains wide. The validity of the measurements reported for some Ringsail models is open to question, but to reject the results completely would leave unjustified gaps in the picture. The quality of the performance picture has been blurred in another way also; the documentation is incomplete. Some important test reports could not be found in the morgue and are presumed lost or destroyed. Other test reports were incomplete in basic essentials. Everything that is known about Ringsail parachute performance has been put together in Section 3 as accurately as possible for the guidance of the designer. Accumulated weight data for all Ringsail parachutes manufactured are summarized in Section 4.

A step-by-step design procedure for the Ringsail parachute is detailed in Section 5. This is a minimal procedure which will produce as an end item all the dimensional data and material requirements needed to manufacture a prototype model. The design procedure is illustrated by numerical example in Appendix C, concluding with a preliminary weight and volume estimate. Design analysis methods are given in Section 6 by means of which the prototype design can be refined, reefing requirements determined, performance characteristics and opening loads predicted, a rigorous stress analysis performed, and weight, volume and porosity calculated. The design analysis is usually a preliminary to the performance of a number of aerial drop tests aimed at completing the design development of the parachute through verification of both aerodynamic performance and structural integrity. After such tests have been successfully completed is the time to prepare detailed production drawings of the new parachute.

Construction features peculiar to the Ringsail parachute are described in Section 7 as a guide to the preparation of manufacturing drawings. The fabrication and assembly techniques used in Ringsail parachute manufacture are described in Section 8 along with a discussion of unusual quality control methods.

SECTION 2

HISTORICAL DEVELOPMENT

2.1 DESCRIPTIVE HISTORICAL REVIEW

The purpose of presenting this historical review in what is nominally a "design handbook" for Ringsail parachutes is to give parachute designers (and innovative designers in particular) a view of the many different configurations and methods of construction tested. Of particular interest will be those features that were tested, found wanting, and discarded.

2.1.1 Conception of the Ringsail Design Principle

In 1953, during an engineering research program aimed at advancing the development of the Ringslot parachute as an aircraft deceleration parachute, it was recognized that there was a large number of ways in which an annulate canopy with alternating rings of slots and sails could be formed. Indeed, the number of possible combinations of slots per gore, slot/sail width ratios, variable slot width distributions, and canopy profile shapes was so large as to preclude testing more than a fraction of them in the wind tunnel. Thus, it is not surprising that when the suggestion was offered that the belly or "fullness" of the sails could also be varied between leading and trailing edges, the idea was not received with enthusiasm. However, it was recorded in Reference 1 as follows:

"It is evident that the gore geometry of the Ringslot is open to considerable variation, not only in the number and width of slots and sections, but also in the angle of radial cut on each panel. In addition to the usual methods of affecting the overall canopy shape by varying the width of the gore pattern, the opportunity is presented of varying the fullness and angle of attack of each section (i.e., each ring) independently of the others. While the effects of different combinations of slot width and ring height have been investigated to some extent, the independent variation of section fullness and angle of attack has not, and is sufficiently promising of results to warrant careful evaluation. Two possibilities are immediately evident:

- (1) An increase in the average angle of attack of the individual rings in the skirt region beyond the mid-radius could have a beneficial effect on both C_{D_0} and opening characteristics.
- (2) An increase in the section width in the crown area will reduce transverse fabric stresses by reducing the local radius of curvature."

Subsequent events have proved the first surmise to be quite correct with little qualification. The second, it was found could be effected better by simply adding fullness to conventional Ringslot construction in the crown of the Ringsail canopy.

2.1.2 Evolution of the First Working Models

An opportunity to test the Ringsail design concept did not arrive until 1955 and then simultaneously on two different programs. The first of these programs had been initiated in April 1954 with a proposal to the Bureau of Aeronautics for development of the Ringsail personnel parachute (Reference 2). The purpose of this program was to produce an improved escape system for Naval airmen in which the parachute opening shock would not exceed 25g in a 400 knot bailout and the pack weight and bulk would be a minimum.

The Skysail configuration illustrated in Figure 1 was justified by the following statement of Ringsail design theory (Reference 2).

"Although the possibility exists of effecting the desired improvement by the stepwise development of a set of gore coordinates for a solid shaped canopy, experience with the Ringslot parachute suggests that the use of carefully distributed geometric porosity holds greater promise. However, the delicate balance between drag efficiency and opening reliability on the one hand and stability and opening shock on the other is easily upset if the size and shape of the geometric openings are poorly proportioned. The central problem is one of providing the geometric porosity needed to satisfy the stability requirement in a form which properly controls airflow through the canopy. The flow control must be twofold:

- (1) The openings shall provide good ventilation during inflation in order to limit opening shock.
- (2) The lips of the openings shall inhibit ventilation during steady descent in order to provide a maximum drag coefficient.

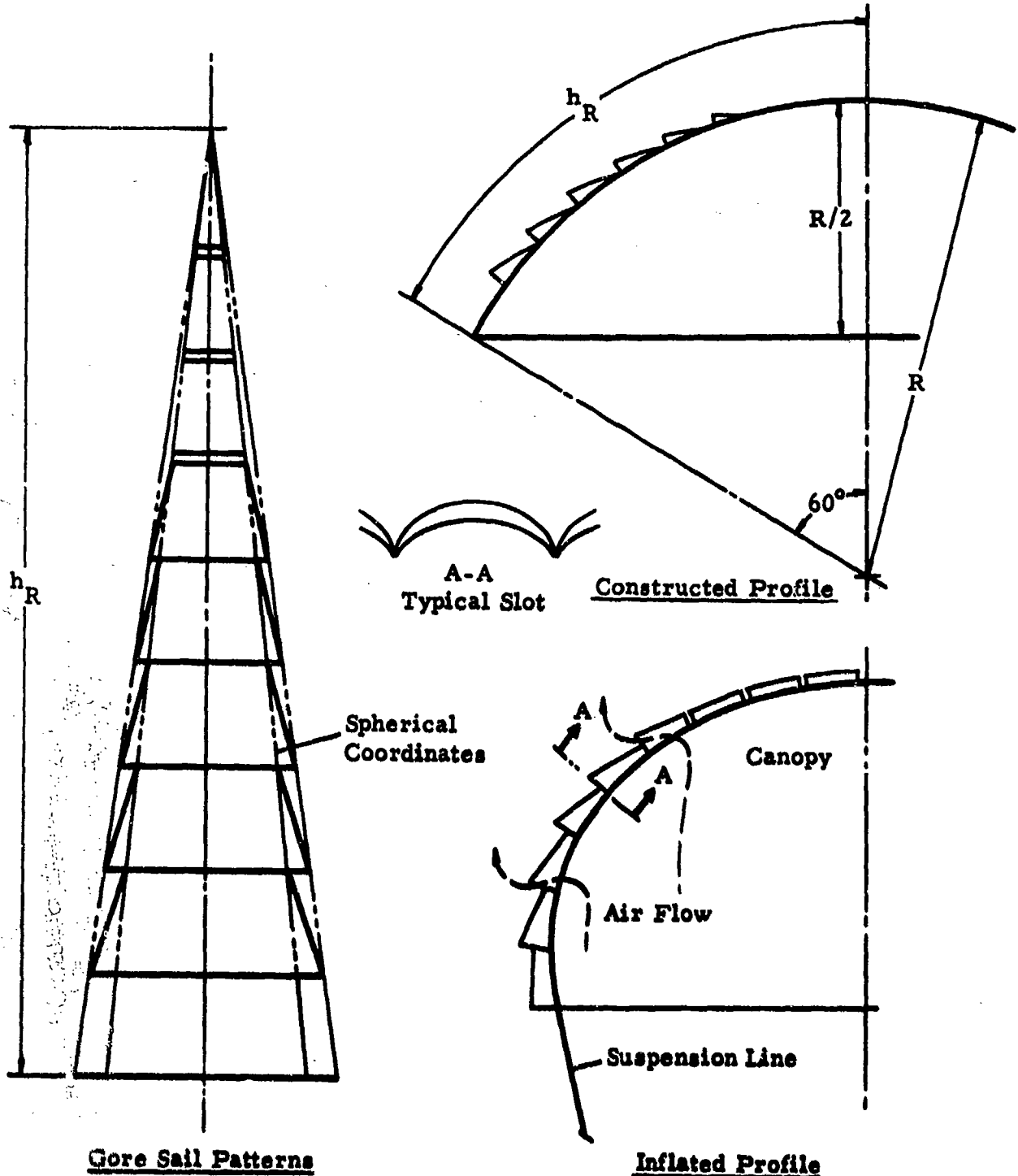


Figure 1. Skysail Geometry

Solution of this problem is possible only because both the shape of the canopy and the character of the flow field during each of these phases is different. The geometric porosity of the Skysail, like that of the Ringslot, is distributed among a number of narrow concentric annular rings (Figure 1). However, the similarity between the two parachutes ends here. Aside from important structural differences, the essential difference between the Ringslot parachute and the Skysail is...(that described in the quotation from Reference 1 above). Precise and virtually independent control of each annulus of the canopy is achieved by this means. Thus, during inflation the absolute magnitude of canopy porosity may be relatively large, but after inflation the projected geometric porosity is small and through-flow interference becomes a maximum. At the same time, the leading edge of each fabric annulus in succession meets the airstream at a high angle of attack, thereby promoting reliability of inflation.

It is estimated that a geometric porosity of between 5% and 10% will satisfy all requirements, but the uncertainty factor inherent in the aeroelastic properties of any new gore design can only be resolved by appropriate experiments. For the same reason, it cannot be assumed that the sail geometry shown in Figure 1 is necessarily the best, but on theoretical grounds its probability of success is high."

In December 1954, before the Skysail development contract award was made, the need for a high performance recovery parachute on the XQ-4A drone program motivated the design, fabrication and testing of the first Ringsail parachute. In the form first tested in February 1955 (Reference 3), the canopy had nominal diameter (D_0) of 64.7 ft, 48 gores, 10 rings of sails, and the sail dimensions were derived from the coordinates of a shaped-gore as shown in Figure 2. In searching for a rational method of computing sail widths that would be structurally conservative, the coordinates of a flat gore were adopted as a base reference and the coordinates of a surface of revolution approximating the inflated shape were used as a lower boundary reference. The result was a shaped-gore with considerably more allowance for bulging between radials than was actually needed for stress relief.

When the first 64.7 ft D_0 Ringsail prototype was drop tested (February 1955, El Centro, California), it exhibited the same general behavior as that seen much later in the 84.2 ft D_0 Gemini Ringsail---the fully inflated canopy was slack and puffy with several gores folded inward on one side (Figure 3a).

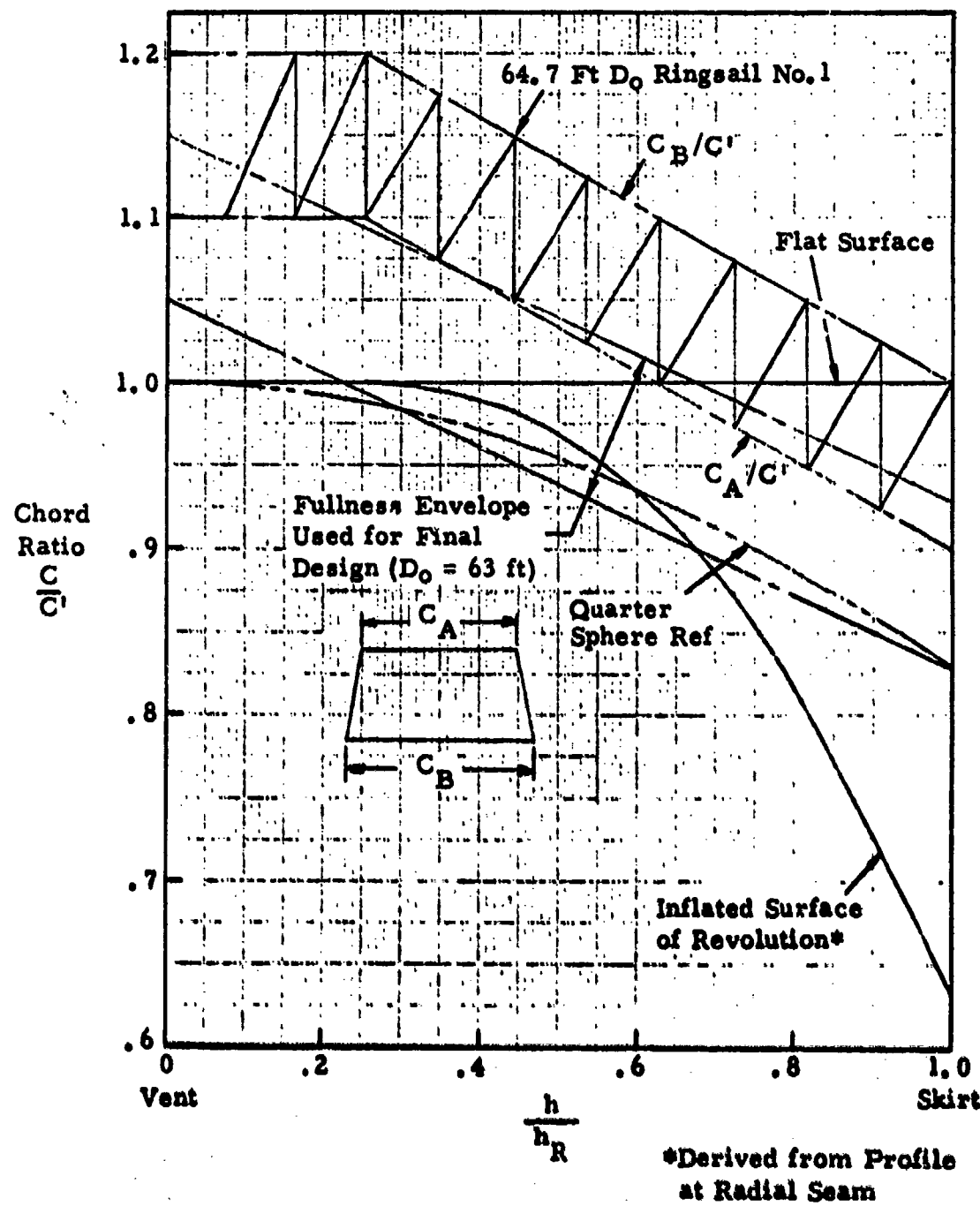
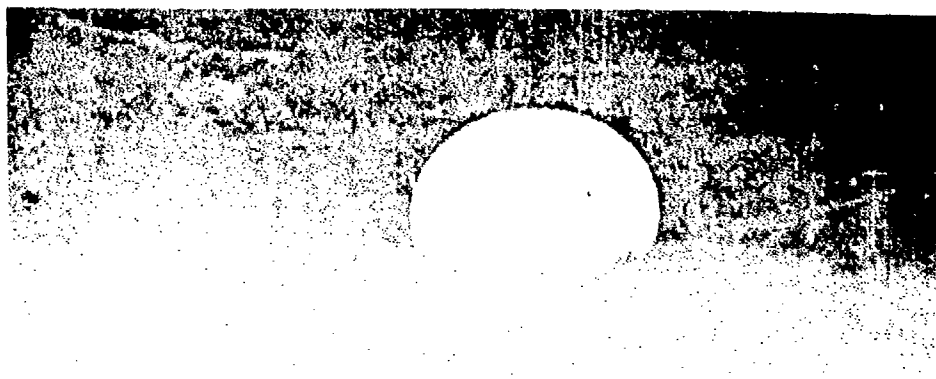


Figure 2. Sail Fullness Distribution of First Ringsails



Figure 3a. First Ringsail Drop Test 4 February 1955
(Note Infolded Gores On RH Side)



Reproduced from
best available copy.

Figure 3b. Same Parachute With Two of 48 Gores Removed

In order to continue the test program with minimum delay, the infolding was corrected by removing two gores from the canopies of the existing test specimens (Figure 3b). The modified parachutes (with 46 gores $D_o = 63$ ft) were used until new 48 gore models could be fabricated with sail dimensions corrected as shown in the Figure 2 with a reduction in width of approximately 10%.

During the subsequent development and qualification tests, the drag coefficient derived from rough rate of descent measurements averaged $C_{D_o} = 0.73$, an increase of 30% over that of the 56 ft D_o Ringslot canopy that the new parachute replaced. However, this was tempered by a 40% increase in the average amplitude of pendular oscillations, i.e., from $\pm 5^\circ$ to $\pm 7^\circ$. Since the stability was still acceptable for recovery purposes in a system utilizing an airbag impact attenuation system, the gain in drag efficiency was almost entirely on the plus side, and it could be said that the Ringsail design principle had proved to be reasonably successful.

In the Skysail program, progress was made more difficult by the small size of the canopy ($D_o = 27$ - 30 ft). Ringsails in the 18 to 41 ft D_o range could not be made to develop as much drag per unit area as those of $D_o = 56$ ft and larger. In this respect the Ringsail appeared to exhibit a C_{D_o} change with size, similar to a solid conical or extended skirt parachute. Average drag coefficients ranged from $C_{D_o} = .67$ to $C_{D_o} = .71$ approximately, with no improvement in stability relative to oscillations of $\pm 7^\circ$, while in some cases average amplitudes of ± 10 to 15° were recorded. Thus, in the Skysail size range the gain in drag coefficient for parachutes of equal stability was less than 20% relative to the Ringslot. Along with this gain, the opening shock was moderate and the increased sail angle of attack made the opening tendency strong.

Skysail Model A (26.9 ft D_o with 20 gores) designed in June 1955 (Figure 4), was the first Ringsail with gore coordinates developed for a canopy shape of a quarter sphere. The fact that the performance of this model was deficient in all categories is attributed to the use of only six cloth rings of which the three in the major area of the canopy were 36 inches wide and the skirt ring had no fullness, i.e., the constructed profile had a skirt angle of 60 degrees as shown in Figure 1. The sail fullness distribution used in this first Skysail model is shown in Figure 5. The angle of attack of the sails was not adequately developed in this model and the geometric porosity was low.

Skysail Model B (29.4 ft D_o with 20 gores) was made with nine cloth rings all approximately 18 inches in width, but again with no fullness in the skirt ring. This model went through three modifications aimed at gaining an acceptable drag coefficient:



Figure 4. Skysail Model A Tethered In the Wind

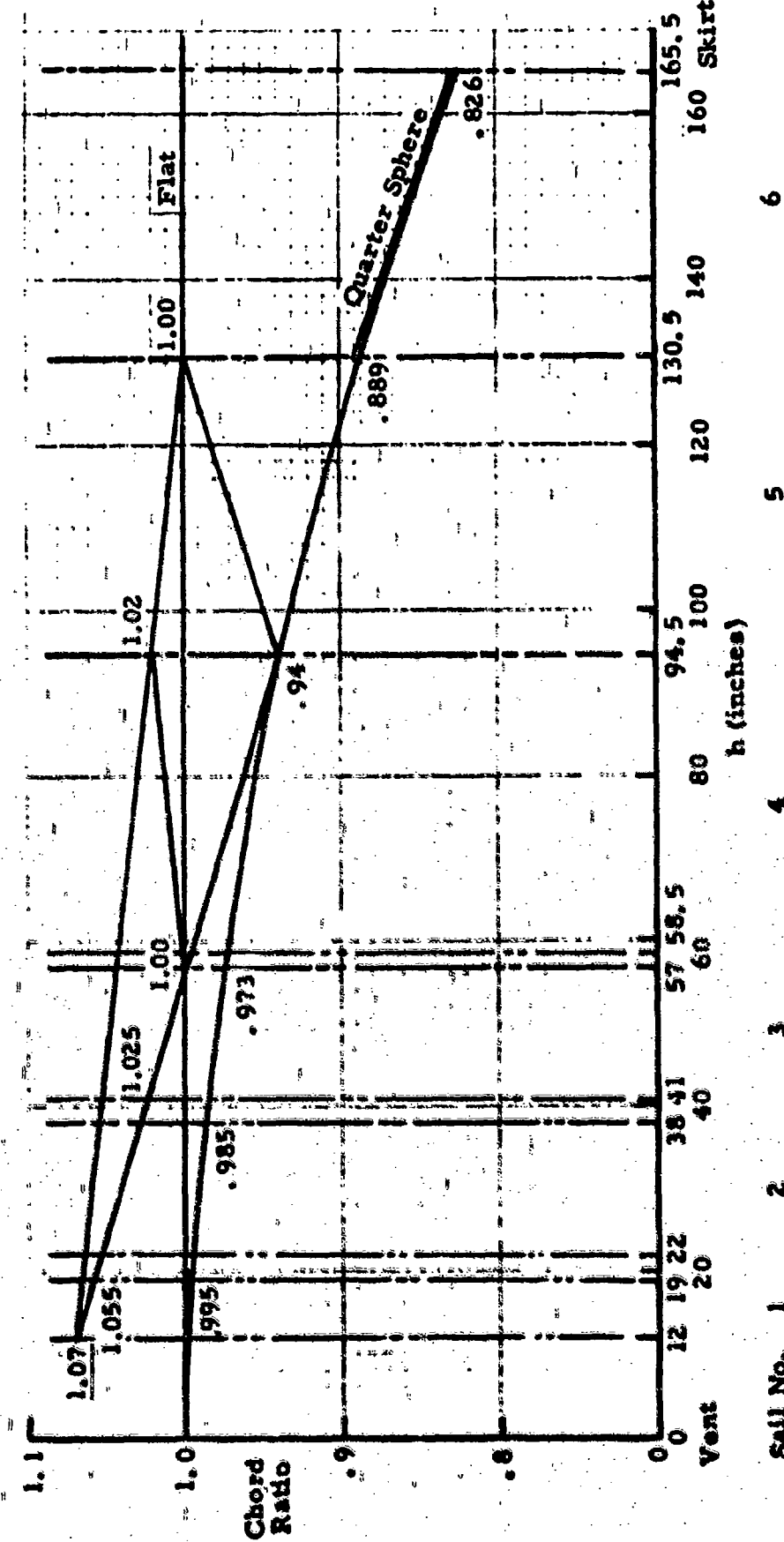


Figure 5. Skystail Personnel Parachute Coordinates

- (1) XB-1: Restrictor tapes were installed on the gore centerline across the four slots in the peripheral area of the canopy above the skirt. These changed the crescent shaped slots to double openings as shown in Figure 6. This modification was abandoned when tests showed the filling time to be excessive, giving the first indication that the Ringsail filled through the side slots as well as through the mouth.
- (2) XB-2: Pocket bands derived from FIST ribbon parachute design documentation were added to the canopy. These were discarded to simplify construction after a few tests showed no overt improvement in opening characteristics, but it is now believed the tests measurements were too rough to constitute conclusive evidence. Pocket bands on the Ringsail should be as effective as they are on other parachute types.
- (3) XB-3: The skirt ring (#9) was removed from the canopy, decreasing the basic skirt angle from 60° to 54° . This change also reduced the nominal diameter to $D_0 = 26.8$ ft, but more important, it produced a canopy having a flared skirt with a fullness of 17.5% in the bottom sail (#8). However, with an average leading edge fullness in the sails of approximately 13%, the crescent shaped slots were relatively large in the fully inflated canopy and the low drag coefficient obtained was attributed to excessive geometric porosity. ($\lambda_g = 13.5\%$, $\lambda_v = 16.6\%$).

Skysail Model C (28.3 ft D_0 with 24 gores) was designed to overcome the deficiencies of Model B: 24 gores (in place of 20) for narrower sails and average sail leading edge fullness reduced to 9% (in place of 13%). However, the canopy was again made to the quarter spherical shape with a 60 degree skirt angle. The justification for this was the full skirt of Model B did not inflate tautly and tended to flutter, but this retrogression was an over-reaction, and the drag coefficient of Model C was no better than that of Model B.

Skysail Model D (29.6 ft D_0 with 24 gores) was the final configuration developed under the original Bureau of Aeronautics contract and the one selected for the qualification program (Figure 7). It combined what were believed to be the best features of Models B & C:

- a) Basic shape a spherical segment with a skirt angle of 54 degrees.*
- b) Average sail leading edge fullness 8.8%.
- c) Nine rings each 18 inches wide with four open ring slots in the crown

* In Figure 1 this would change the height of the spherical segment from $R/2$ to $0.439R$.

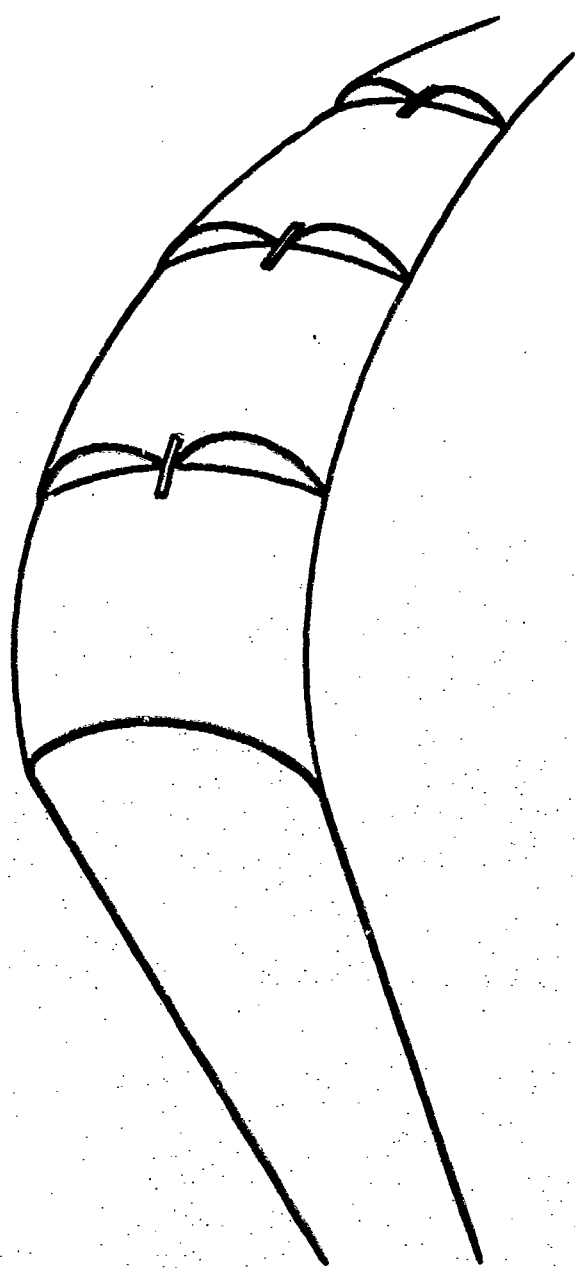


Figure 6. Effect of Restrictor Tapes on Slot Openings of Skysail Model XB-1

Reproduced from
best available copy.



Figure 7a. USN Parachute Test Jumper Landing With 29.6 ft
D₀ Skysail Model D - El Centro, California Feb. 1969

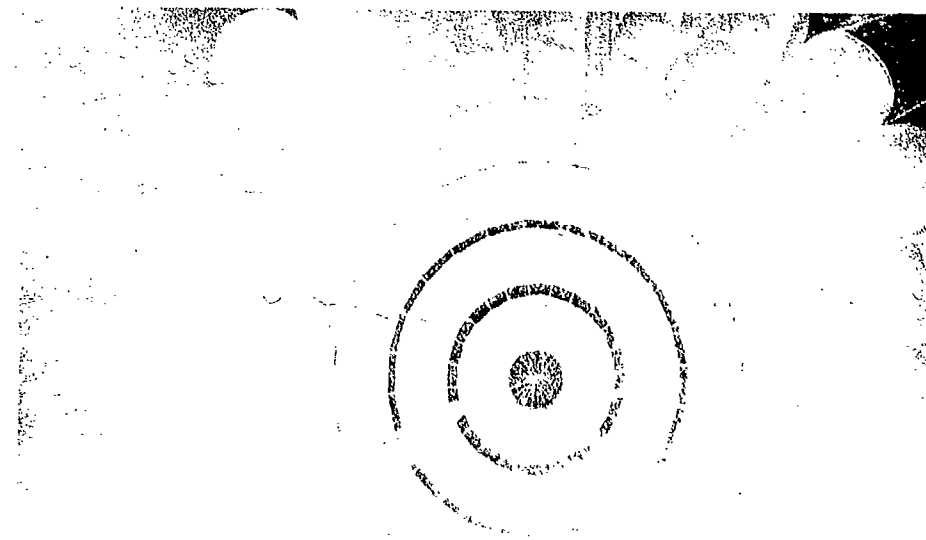


Figure 7b. Jumper's View of Skysail Canopy

d) Calculated porosity based on photo measurements

Geometric 10.9% Total 14.2%.

e) Effective suspension line length 0.91 Do.

A U.S. patent was applied for 15 May 1956 and Patent No. 2,929,588 was issued 22 March 1960. In June 1956, at the same time the Skysail design was frozen, the method of computing Ringsail gore coordinates and sail widths was standardized in the non-dimensional form illustrated in Figure 8. The difference in sail fullness between the standard Ringsail and Skysail Model D in the peripheral region is indicated. The chord ratio (C/C') was based on the width, C' , of a flat triangular gore because it could be calculated easily at any radial height, h , as

$$C' = 2h \tan (360^\circ / 2N)$$

for a canopy embodying N gores of height, h_R , from center line vent to skirt. In practice, the h dimensions used corresponded to the upper and lower edges of both slots and sails, and the values of h/h_R were calculated. Then, at each value of h/h_R the curves were read to obtain C_A/C' and C_B/C' from which the lengths of the upper and lower edges were calculated. It will be seen that the spherical profile is controlled accurately in the peripheral region of the canopy below $h/h_R = 0.65$ by the upper edges of the sails. Above this point the introduction of fullness in both upper and lower sail edges for stress relief modifies the shape slightly. The resulting sail layout for one gore is illustrated schematically in Figure 9.

This is the method of gore coordinate and sail-width calculation that was used for all Ringsail parachutes designed prior to September 1965, including the Apollo main parachutes. Although a few modifications were tested experimentally during the Apollo ELS development program, none proved acceptable. These are described in Section 2.1.4.

2.1.3 Evolution of Canopy Shape and Construction

During the early aerodynamic development of the Ringsail a number of innovations in the methods of parachute construction and assembly were tested. Traditionally, Ringslot parachutes were assembled sail by sail to form rings and then the cloth rings were joined with radial tapes. This appeared to be an inconvenient procedure for shops geared to the gore by gore assembly sequence of solid cloth and ribbon canopies. Since Ringsail No. 1 had no open slots other than the crescent shaped openings developed in the inflated surface between contiguous sails, it appeared feasible to sub-assemble the gores by shingle-lapping and basting as shown in Figure 10. First, the edges of the individual sails were hemmed or taped to augment tear resistance in the areas of greatest

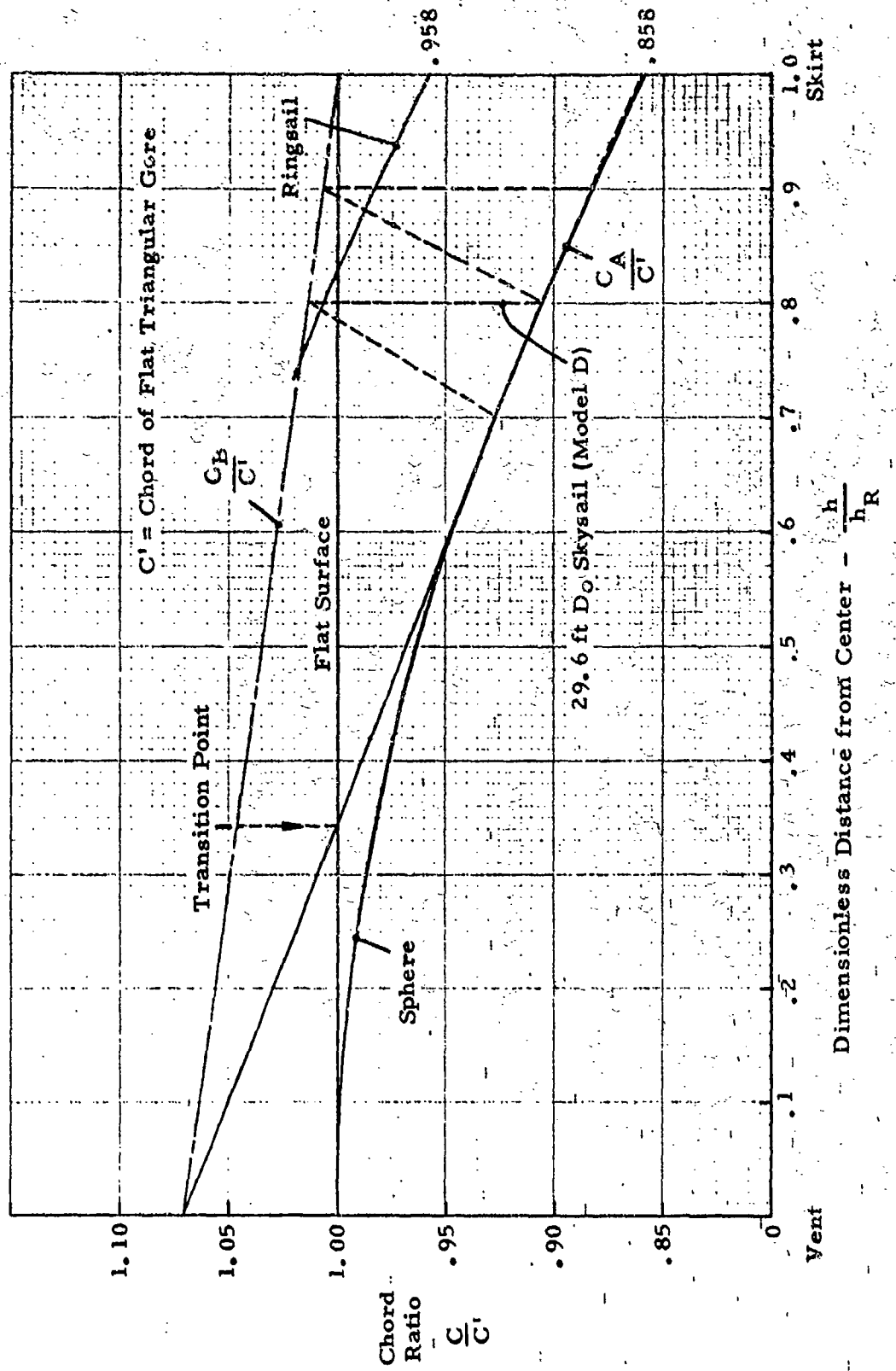


Figure 8. Ringsail - Skysail Coordinates

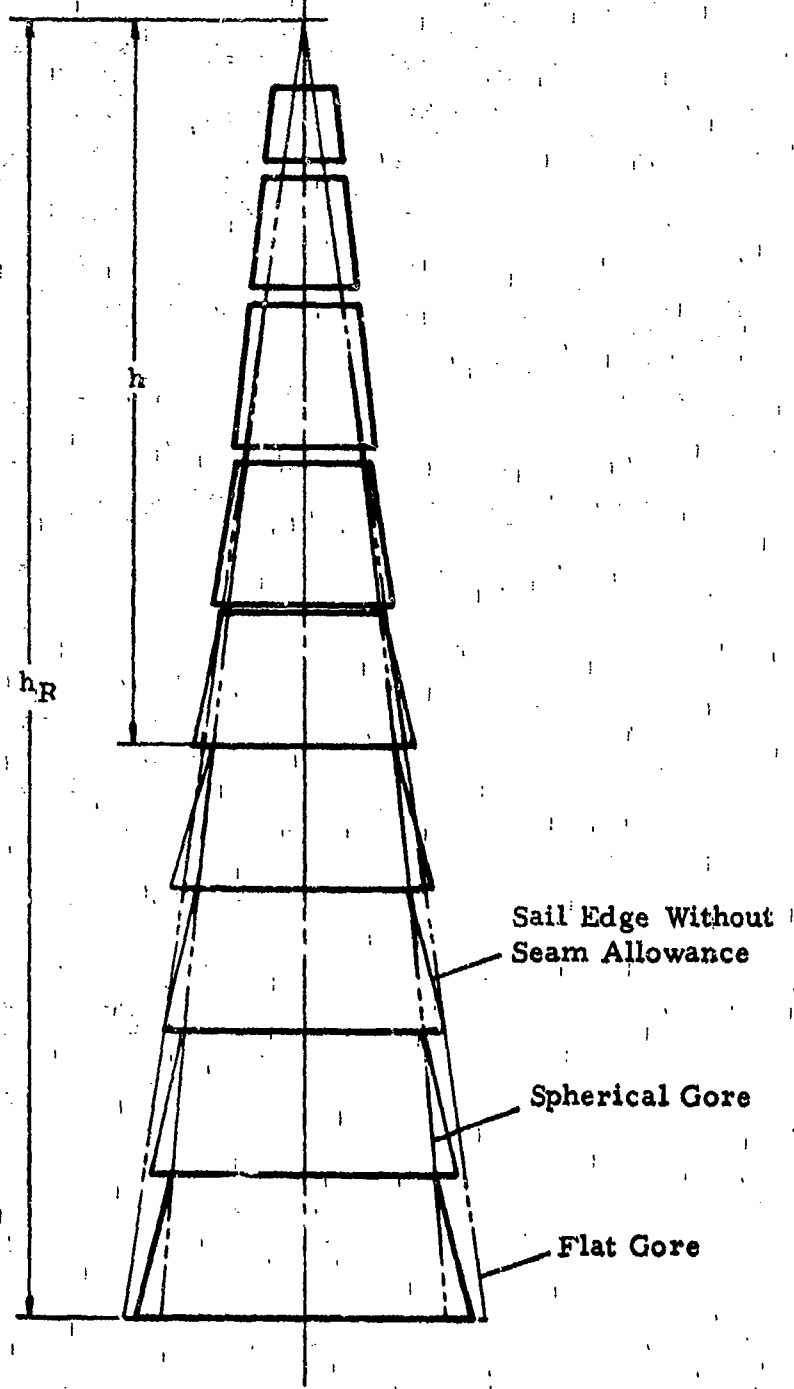
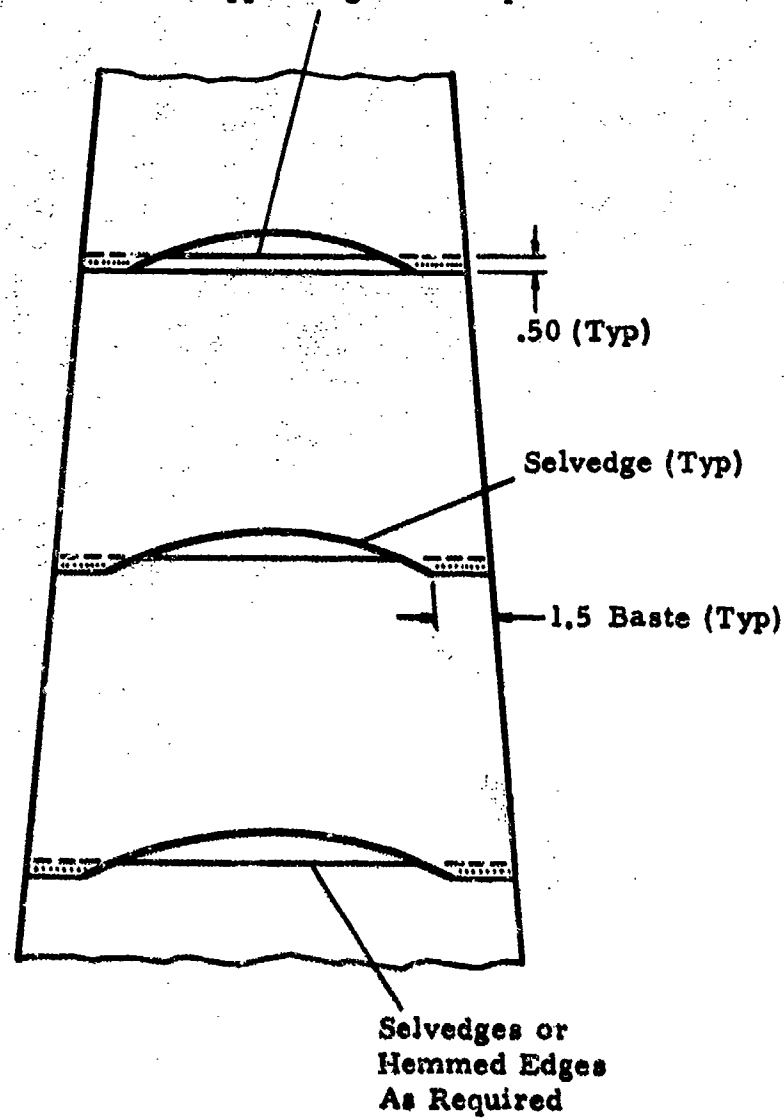


Figure 9. Typical Ringsail Gore Layout Developed by the Original Standard Method (Schematic)

**Intercostal Tape On Sail
Upper Edges As Required**



**Figure 10. Lapped-Sail Gore Assembly Method of
64.7 ft D₀ Ringsail No. 1**

stress. (Cloth selvedges were generally strong enough only in the peripheral region of the canopy where bulging of the sails between radials was pronounced.) Second, the sails were basted together into gore subassemblies. Third, the gores were joined in the conventional manner with one-inch fell seams stitched on a four-needle sewing machine. The final parachute assembly operations also were conventional, including the running of suspension lines over the entire canopy through the center channels of the radial seams.

This assembly method worked reasonably well as long as the intercostal tapes on the sails were light and thin. However, the tape joints in the radial seams were strong enough to develop substantial hoop strength which created the general misapprehension that the tapes could also function effectively as reinforcing bands. During the test program when the 63 ft D₀ Ringsail experienced opening shock damage in the crown, heavier intercostal tapes were placed on the sail edges in lieu of reinforcing bands. The multiplied thickness of these tape ends in the fell seam made it difficult to pass the material through the sewing machine, and the usual seam forming guides could not be used.

Since the lapped-sail gore construction was not amenable to the introduction of adequate geometric porosity in the crown of the canopy, as well as being structurally inefficient and difficult to assemble, a better assembly method was sought for the Skysail parachute. The drive for minimum weight and bulk motivated the design of a narrow (1/2 inch) radial seam to reduce seam allowances, while the need for tape reinforced radial seams to overcome the shortcomings of the line-in-channel construction produced the construction methods illustrated in Figure 11. These methods have been standard for all Ringsail parachutes produced to date with minor exceptions, e.g., the radial seams of a few early lightweight models were stitched with two-needle machines instead of three, vertical tapes were introduced in 1962, and tapered line joints a year later. The subassembly of sails and radial tapes came from traditional ribbon canopy assembly methods, but the rolling of the one-inch radial tapes to one half width in the fell seams was novel; it reduced the variations in gore width caused by under and overfolding to a negligible factor. This was important to the basic Ringsail principle inherent in the fullness distribution of the individual sails between radials.

The fell-folded radial tapes have other advantages. The lower ends extended below the skirt provide a convenient means of forming an efficient tapered splice for the suspension lines, thus eliminating the need for additional reinforcements such as the "butterfly" tab commonly used. Also, a recent experiment by NASA with a modified Ringsail assembled ring by ring with single lapped seams reinforced with radial tapes revealed indirectly another structural advantage. In this modified parachute the tear resistance of the

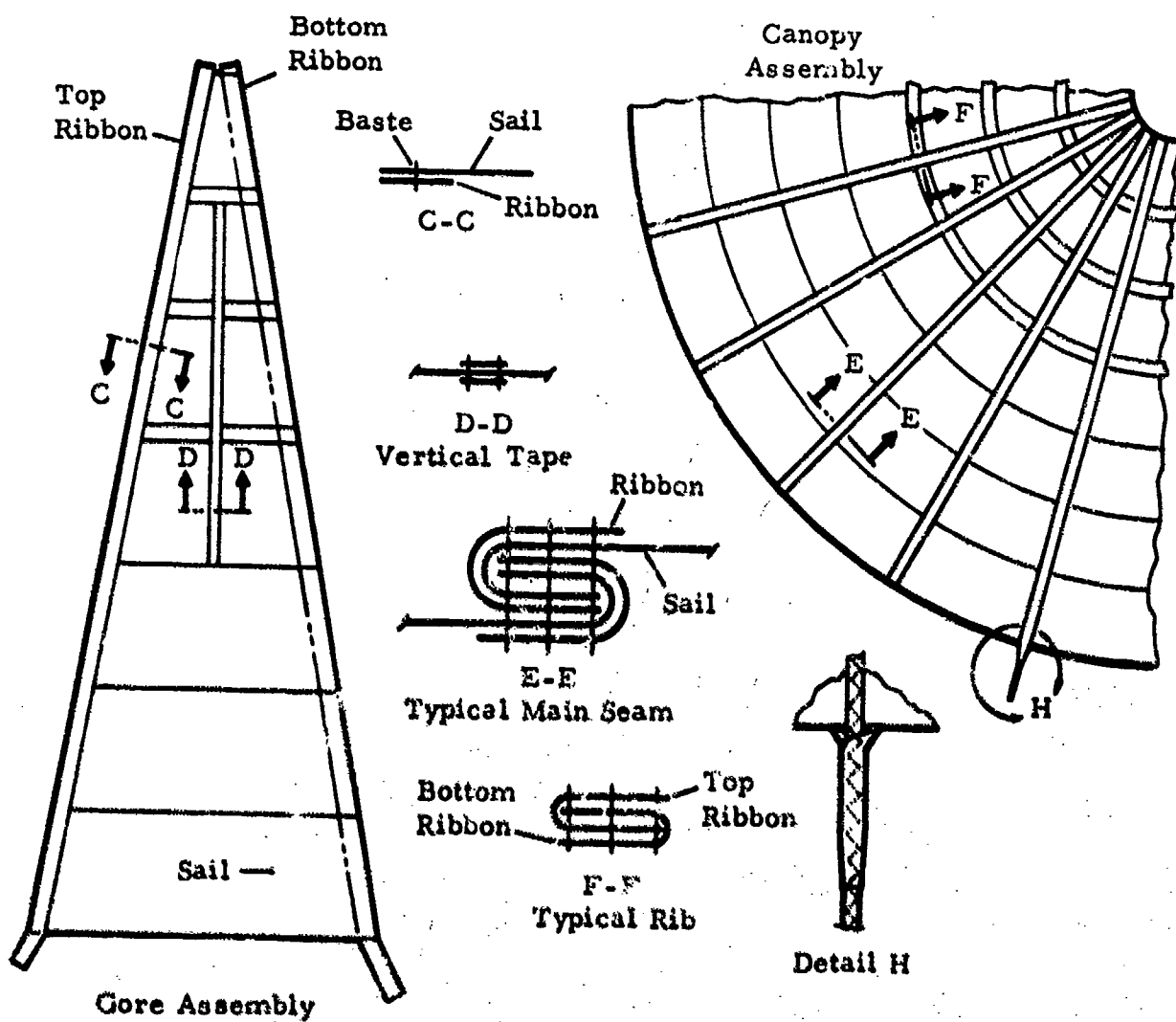
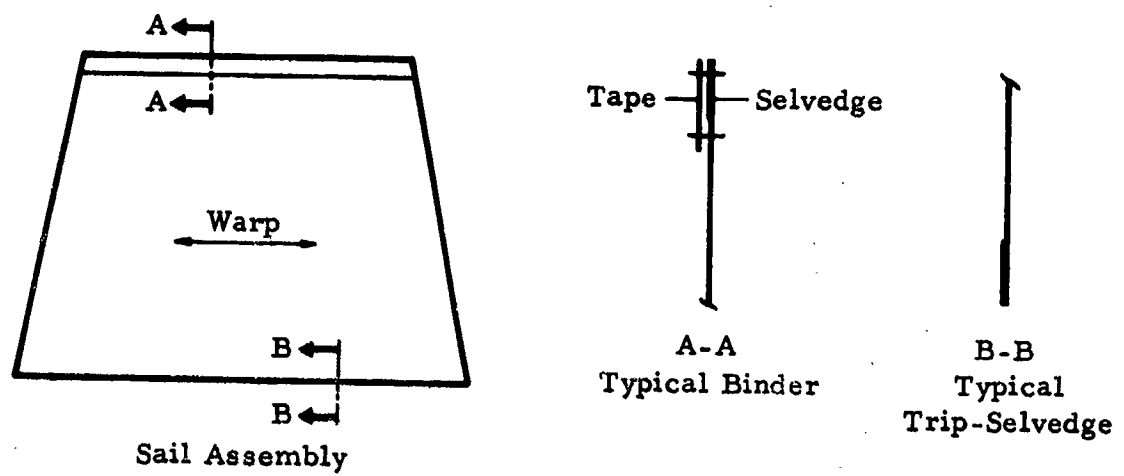


Figure 11. Ringsail Construction

sail edges was so poor it became necessary to add hundreds of short reinforcing tapes to the edges across each radial seam. A plausible explanation is that the narrow reinforcing tapes, being at least four times thicker and much stiffer than in the standard Ringsail construction, provided a stress concentrating mechanism that degraded the tear strength of the sails along the radial seams.

It is important to emphasize that the intercostal tapes on sail edges joined end to end in the fell seam provide an effective means of augmenting the tear resistance of cloth selvedges and as such need not be very heavy; 70 to 90 lb 5/8 inch tapes attached with two rows of "B" or "E" nylon thread have been adequate. However, the misapprehension that these tapes should also carry hoop stresses persisted well into the 1960's, so most of the Ringsail parachutes built prior to 1965 have excessively heavy intercostal tapes in the crown area, i.e., heavy relative to the strength of the end-to-end joints in the radial seams. In some cases, such tapes were replaced with continuous reinforcing bands where excessive hoop loads were encountered.

Ringsail parachute construction also borrowed from early Ringslot developments which produced cloth woven to a desired sail width with special reinforced selvedges. Some "doupe" selvedge cloth was available but Skysail requirements motivated the design of new weaves with triple-strength selvedges, whence the term "trip" selvedge cloth. With trip-selvedges, one half inch along each edge of the cloth is reinforced with additional warp yarns to a strength three times greater than that of the basic cloth. Woven widths of 18, 24, 36, and 42 inches in nylon cloths weighing 1.1, 1.6, and 2.25 oz/yd² were used. The trip-selvedges, of course, substantially reduce the need for additional reinforcements on the sail edges.

The Bureau of Aeronautics, in 1960, after supporting the development and qualification of Skysail Model D as a minimum bulk parachute for high speed bailout emergencies, decided to incorporate it in the Martin Baker ejection seat system then being adapted for use in all single place Naval aircraft. Although this parachute opened fast enough to pass the Navy's low altitude qualification requirements at normal flight speeds (200 ft at 100 Kts and 500 ft with pre-twisted lines), it could not pass the "off-the-deck" ejection seat test in the Martin Baker system with tandem pilot chutes and peak altitudes of only 70 to 120 ft. Therefore, Skysail Model E with $D_0 = 29.7$ ft was designed as a minimal modification of Model D.

At that time the effectiveness of vertical tapes across the crown ringslots in promoting positive and repeatable opening of the Ringsail was unknown and, as noted earlier, pocket bands were believed to be of small value, having had no measurable effect on Model B. Thus, relative to Model D,

Skysail Model E was made with seven rings of 24 inch sails in place of 9 rings at 18 inches, a flared-skirt ring with 5% leading edge fullness in place of the 54 degree spherical skirt ring, and a total porosity of approximately 11.5% in place of 14.2%.

Although Skysail Model E passed the off-the-deck ejection tests and was retrofitted in all of the Navy's Martin Baker seat system, it constituted a step backward in Ringsail development because its performance was not outstanding when compared to that of the standard flat service parachute it replaced. In qualitative terms, although its stability was significantly better, its opening shock was only marginally lower and its drag coefficient was less ($C_{D_0} = 0.7$ vs 0.76).

This bit of Ringsail history is noteworthy because a few years later (1962) Skysail Model D was adapted for recovery of the ASSET lifting body entry vehicle through the addition of two reefed stages. When it was observed that canopy filling during the first reefed stage was slow and erratic, the deficiency was corrected by placing a single vertical tape on the center line of each gore across the ring slots in the crown. The tapes prevented the slots from opening widely during the initial phase of filling when the crown of the canopy was slack, thereby eliminating random delays and greatly improving the repeatability of the filling time. Had this same innovation been introduced in 1960, the Skysail Model D may have passed the Martin Baker ejection seat off-the-deck tests and the regression to Model E avoided.

After Skysail Model XB-2, pocket bands were not again tested on the Ringsail parachute until the Apollo wind tunnel program of February 1963 (Reference 15). The wind tunnel models also had vertical tapes across the crown slots. Although the two devices have similar effects, they are not mutually exclusive and their use together can be justified on theoretical grounds in any Ringsail application for which total opening time is critical. Pocket bands, by limiting the extent to which the skirt sails can blow inward when they first meet the airstream, promote the early admission of air through the mouth. Taped crown slots, as noted, prevent excessive outflow from the first mass of ingested air to flow the length of the canopy. The net result is a considerable reduction in random delays in getting effective filling started, and the total filling time is made more repeatable about its minimum value for any given set of operational conditions.

In September, 1965, the method of calculating the basic dimensions, gore coordinates, and sail pattern dimensions of the Ringsail parachute was revised. The purposes of the revision were:

- a) To standardize the Ringsail design in an advanced form
- b) To simplify the computational procedure and improve the accuracy of determining gore coordinates and sail pattern dimensions

- c) To minimize the possibility of producing new Ringsail parachutes having subnormal characteristics such as a slack, infolded canopy when fully inflated (84 ft D_0 Gemini) or excessive stress concentrations during opening (127 ft D_0 bi-conical).

The new basic dimensions scheme summarized in Figure 12 is the product of a number of different developments generated by the Gemini, Apollo, and Century programs. The 84.2 ft D_0 Gemini Ringsail was designed in 1959 as a backup recovery parachute on the Q-4B drone program. A few years later exigencies of the Gemini Paraglider development program led to its adoption as a backup for and ultimate use as the Gemini primary landing system (Figure 13). As noted, the fully inflated canopy was slack and exhibited an infolding tendency that was never fully corrected, although a number of "tight" peripheral bands were added to the canopy for this purpose. The deficiency was traced to a slide-rule error in computation of the gore coordinates which increased the average sail fullness from 4.42 to 4.71% of the gore width, i.e., an actual increase of 6.1% in the cloth perimeter. Since the width of one gore in a 72 gore canopy is only 1.39% of the perimeter, it is not surprising that several gores tended to fold inward in the fully inflated canopy. In other respects the basic dimension scheme of this Ringsail was identical to that of the Mercury 63.1 ft D_0 canopy and also of the 88.1 ft D_0 canopy from which the Apollo main parachute was derived. Neither of these exhibited the infolding tendency, but the latter was slack enough to have some difficulty in maintaining a polysymmetric shape in a three-canopy cluster (Figure 14).

Early in the development program for the Apollo Earth Landing System, it was found that the drag of the 82.1 ft D_0 Ringsail in clusters of two and three canopies was considerably greater than the design requirement at that time. The chronic need to reduce parachute weight and bulk motivated removal of four gores from the canopy rather than design a completely new one. Of course, it was known from previous experience that this change would also correct the slackness of the fully inflated canopy. The result of the modification was an 85.6 ft D_0 canopy with 68 gores and a conical apex of 19 degrees (measured below the horizontal). The shape of the constructed profile of the canopy was described as a "truncated ogive" having a base angle of 57 degrees. (See Figure 15b).

In May 1963, the first of two "Century" Ringsail programs was initiated with the design of an experimental model having a nominal diameter of 124.5 feet. The design logic employed was necessarily conservative (for want of any previous experience with Ringsails larger than 88.1 ft D_0) and is described in Appendix A of Reference 5. Quoting from the design notes relating to the canopy shape:

$$\text{Canopy Area } S_0 = \frac{C_{DS} \text{ req'd}}{C_{D_0}}$$

$$\text{Nominal Dia. } D_0 = \left[\frac{4 S_0}{\pi} \right]^{\frac{1}{2}}$$

$$\text{Number of gores } N = .76 - .88(D_0 \text{ in feet})$$

$$\text{Effective line length } l_e = 1.15 D_0$$

$$\text{Riser length } l_R = 2 - 4 \text{ feet}$$

$$\text{Line length } l_s = l_e - l_R$$

$$\theta = 15^\circ$$

$$h_R = .519 D_0$$

H = Width of cloth

$$A = C_A + 1.6 \text{ in. } B = C_B + 1.6 \text{ in.}^*$$

$$C_A = K_A C \quad C_B = K_B C$$

$$C = 6.44 \left[\frac{h}{N} \right] \sin \left[\frac{h}{h_R} \times 54^\circ \right] \quad K_A = 1.06 - 0.1 \left[\frac{h}{h_R} \right]$$

$$\text{Vent diameter } D_V = 2 h_V \cos 15^\circ = 1.932 h_V$$

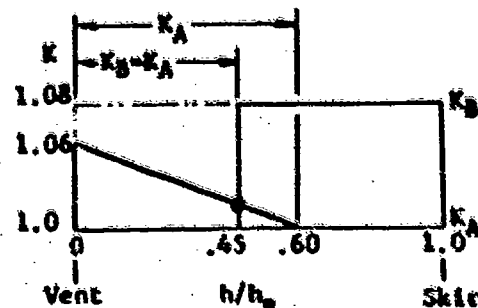
As shown below:

$$K_A = K_B \text{ from } \frac{h}{h_R} = 0 - .45$$

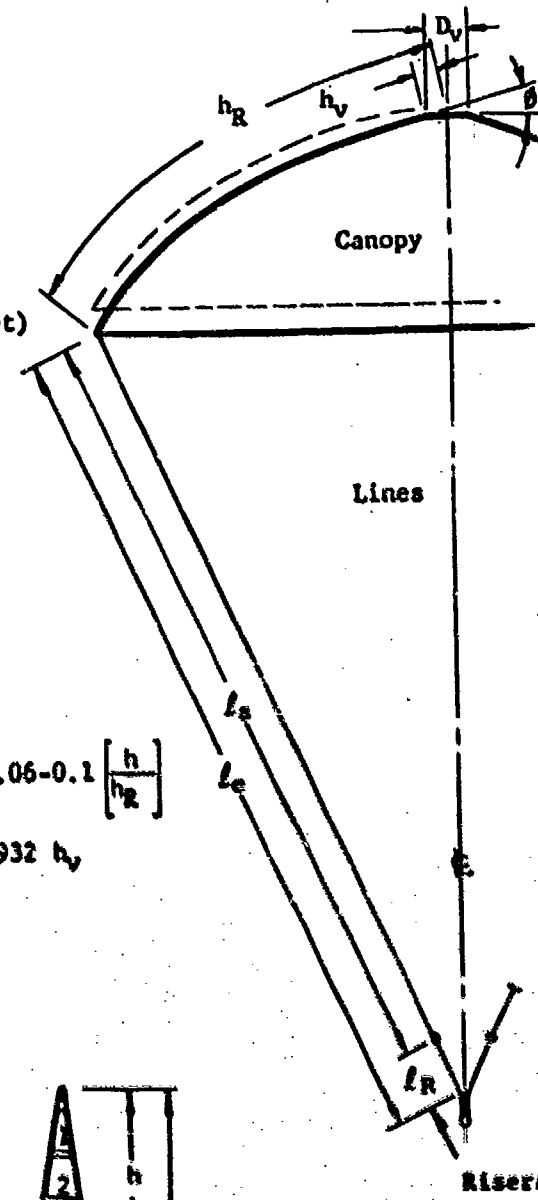
$$K_A \text{ varies from } 1.06 - 0$$

$$\text{from } \frac{h}{h_R} = 0 - .6$$

$$K_B = 1.08 \text{ from } \frac{h}{h_R} = .45 - 1.0$$

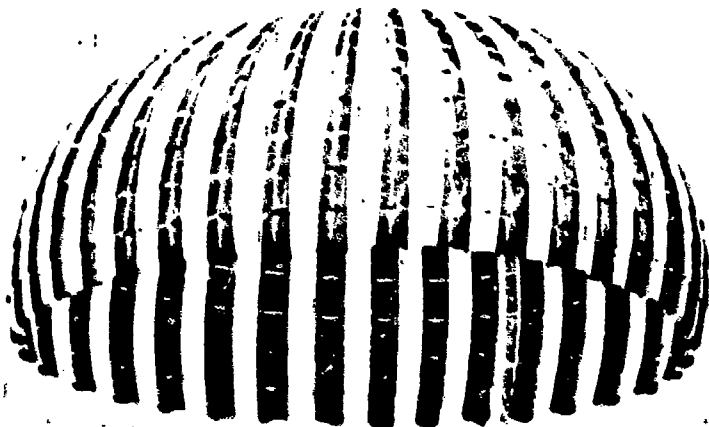


Fullness Distribution



*Includes seam allowance

Figure 12. Ringsail Parachute Basic Dimensions



Reproduced from
Bell available copy.

**Figure 13. Gemini 84, 2-ft D₀ Ringsat - Boiler Plate Capsule
Splashdown in the Salton Sea, California**

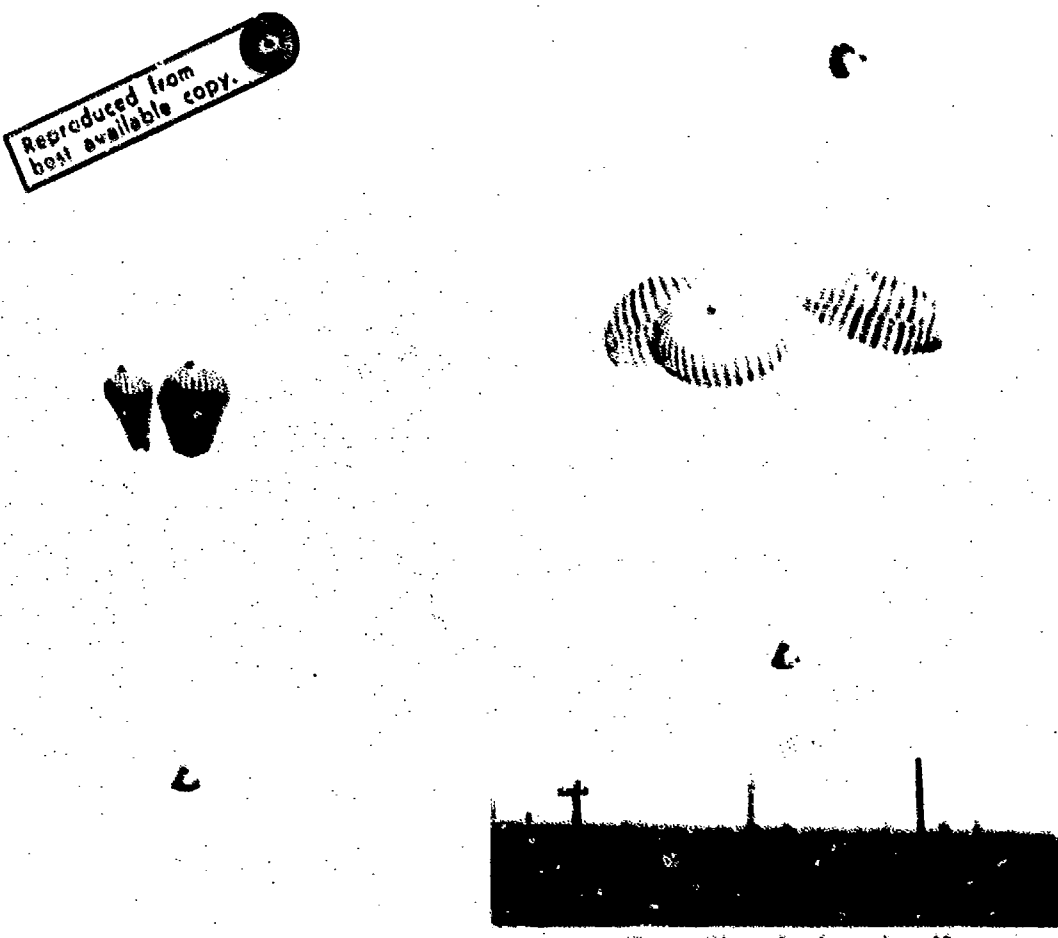


Figure 14. Termination of "Little Joe" Test Simulating Apollo Off-Pad Abort with 88, 1 ft D_o Ringsail Parachutes in First Experimental Earth Landing System

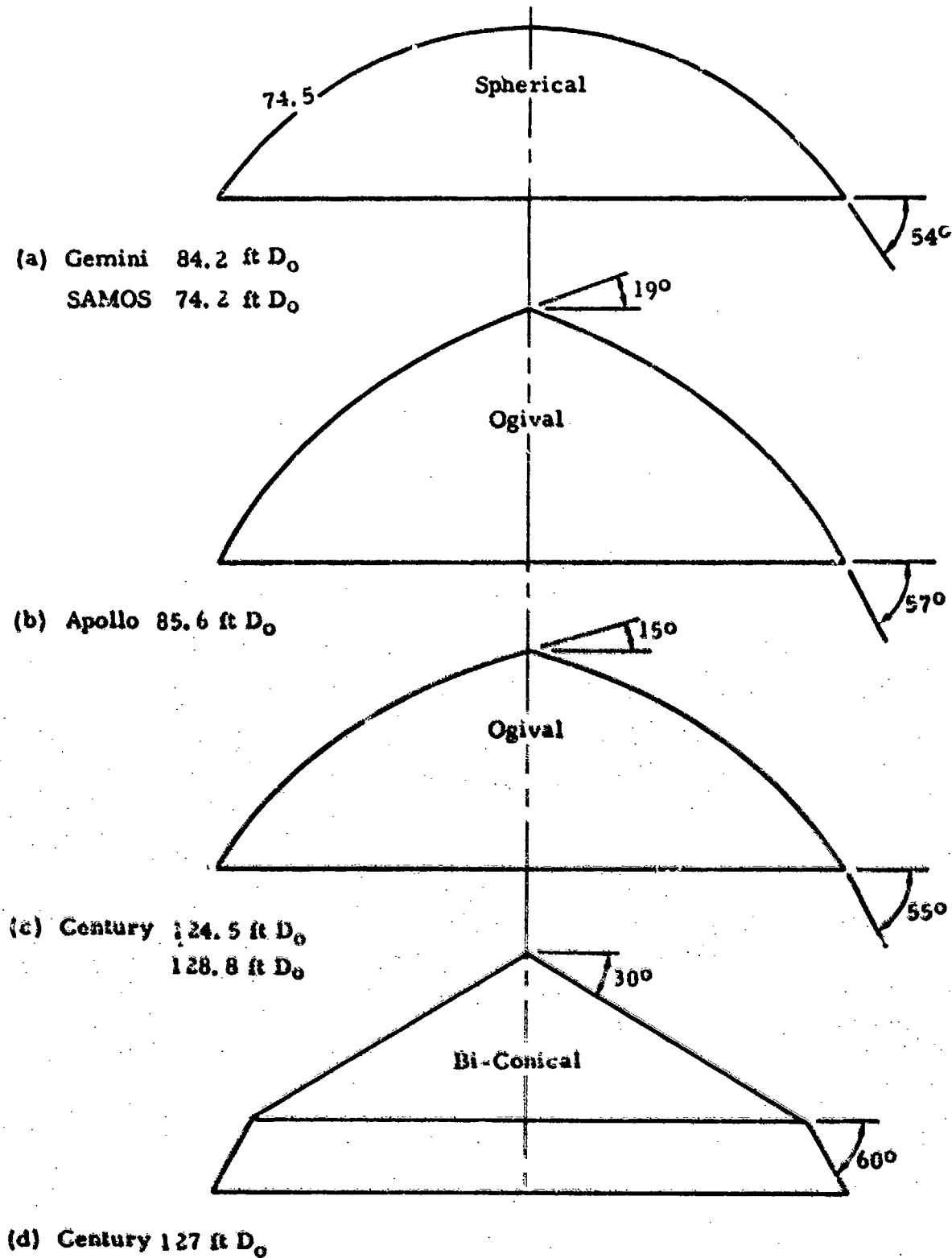


Figure 15. Comparison of Nimsail Canopy Constructed Profiles

"A taut canopy minimizes the infolding tendency and can be obtained readily by modifying the spherical profile to that of a truncated ogive. This is accomplished by removing gores from an otherwise full canopy. In this instance the desired result was obtained by designing an oversized canopy with 116 gores and utilizing 112 gores in the final assembly. This had the effect of reducing the circumferential fullness of the spherical canopy by 3.4 percent."

The expedient described produced an ogival profile with an apex angle of 15° and a base angle of 55° . (Figure 15c). Because the performance of the new Ringsail throughout a series of five aerial drop tests with a gross weight of 9650 lbs was unusually good in all categories, the decision was made to use the design as a basis for the design of all new Ringsail parachutes (see Figure 16).

To quote Reference 6: "Analysis of the canopy shape of the 124.5 ft Ringsail produced the gore coordinate formula given in Figure (12) for the revised basic dimension scheme. In the interest of further design simplification, the distribution of circumferential fullness was simplified by a conservative revision of that found in the 124.5 ft model. This introduced 0.5 to 3.0 percent (points) more fullness in the crown area for further stress relief and reduced the graduated differential fullness of the major (ringsail) area from an average of 9.83% to a flat 8.0 percent. The latter is expected to slightly reduce the strong expansion tendency of the skirt on disreefing by reducing the average angle of attack of the sails, but the performance of an 87 ft model with 5-6% differential fullness (see Table II and Figure 94 (Appendix A)) gives assurance that the effect will be virtually undetectable by present methods." It will be noted that this redistribution of differential fullness also slightly reduces the area of the crescent slots near the skirt and increases it in the mid-gore region, but this is another second-order effect. The most significant aspect of the change is the reduction in average overall sail fullness from 4.91 to 4.0 percent of the gore width or a net reduction of 18.6 percent in the cloth perimeter near the major inflated diameter. Although the relative magnitude of the change is large, its effect is slight, the increase in peripheral tautness merely reducing the amount the sails bulge outward between radials. This further augmentation of the aeroelastic forces maintaining the canopy's polysymmetric shape, reflects continued concern for avoidance of canopy slackness and infolding, particularly in very large Ringsails.

The effective suspension line length of $1.15 D_0$ given in Figure 12 is optimum for large lightweight Ringsails, yielding, as shown by analysis in

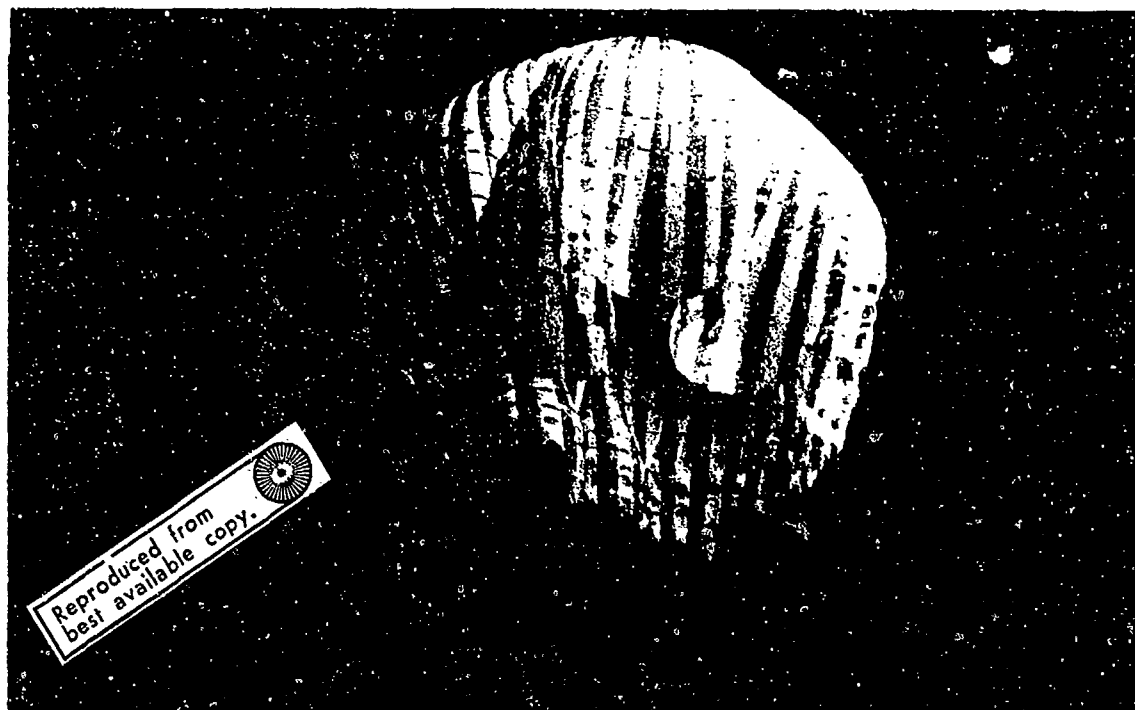


Figure 16a. 124.5 ft D_0 Ringsail Opening Configuration Associated with the "Soft" Opening Mode

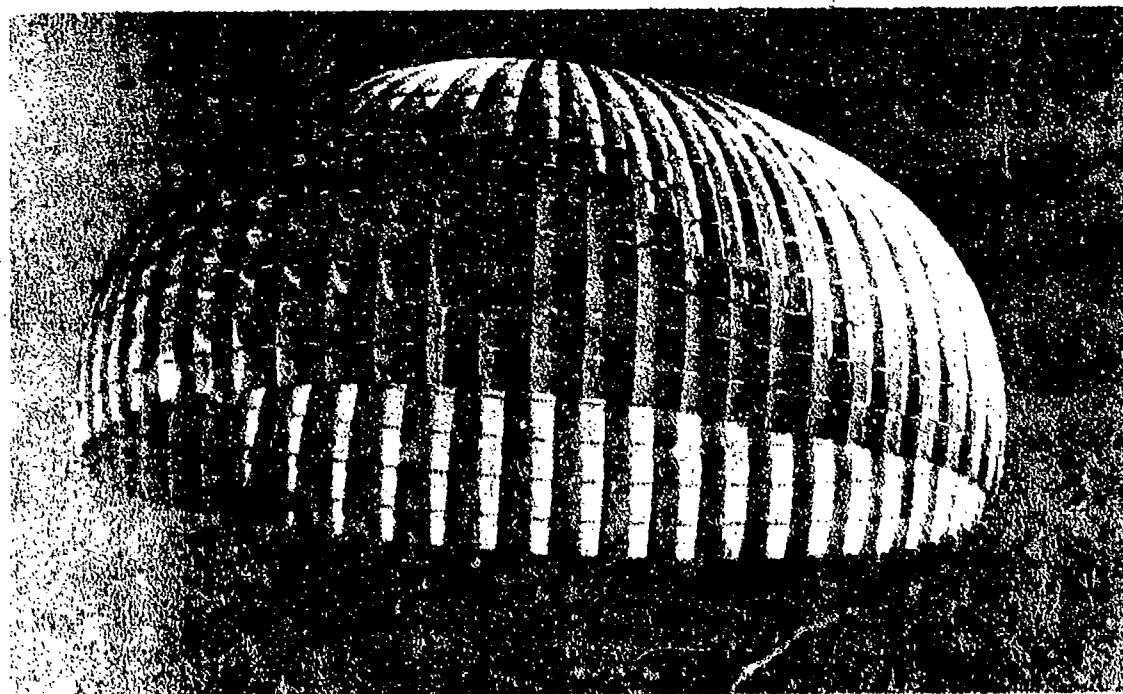


Figure 16b. 124.5 ft D_0 Ringsail Parachute In Steady Descent with 9650 Pounds

Reference 5, a parachute of minimum weight W_p , or maximum specific drag area ($C_D S_0 / W_p$)*. The seam allowance given for sail pattern layout is that required to form the typical 0.5 inch with fell seam shown in Figure 11 using two 1.0 to 1.06 inch wide radial tapes folded together,

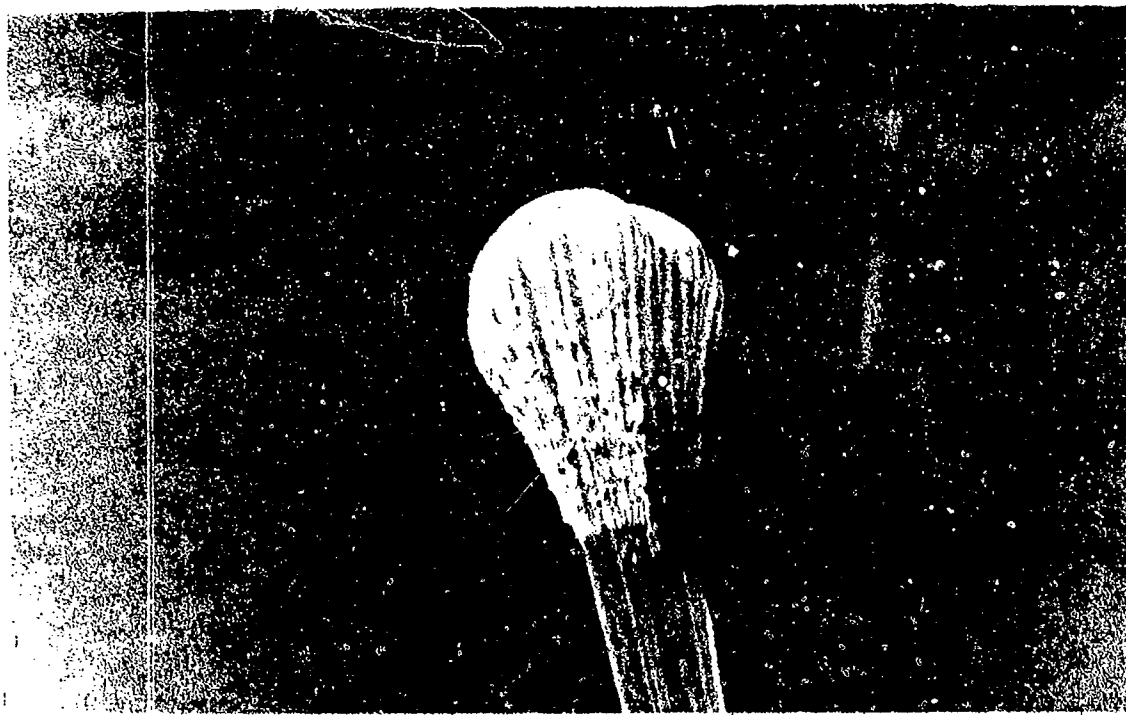
The second Century Ringsail program was initiated in September 1964 with the design of a 127 ft D_o canopy having the bi-conical profile illustrated in Figure 15d. This departure from the proven design of the 124.5 foot model was precipitated by two ideas:

- a) It had been demonstrated that a solid cloth conical parachute had a higher drag efficiency than the solid flat parachute, consequently a conical Ringsail would have a higher drag efficiency than the original Ringsail.
- b) The unsymmetrical infolded shape of the reefed 124.5 ft D_o Ringsail (Figure 17) was undesirable and could be corrected by changing the canopy shape.

The mechanical difference between a solid cloth canopy of 45 degrees bias construction and an annulate canopy with cloth warp horizontal is sufficiently marked to warrant little elaboration. In a conical canopy, the bias-cut cloth stretches freely at near-zero stress to assume an ellipsoidal/inflated shape, and, having less redundant material than the flat canopy the conical canopy can develop a higher drag coefficient. The conical annulate canopy on the other hand tends to hold the conical shape and the strain resulting from inflation to a rounded, or even ogival, shape is attended by hoop stresses which reach a maximum in the mid-radius region. In short, the ogival constructed profile of the Apollo 85.6 ft D_o canopy with 19 degree apex is about as close to a conical shape as appears structurally safe for any annulate canopy of lightweight construction. All conical ribbon and Ringslot canopies, for example, are either of uniformly heavy construction or carry added reinforcing bands in the crown and mid-radius regions. Therefore, neither the drag coefficient nor the specific drag area of a straight conical Ringsail could be expected to be higher than for the proven design.

As to the unsymmetrical reefed shape of the 124.5 ft model, it was argued that this could be a source of non-uniform loading of the parachute structure during opening and might lead to early failures thereby preventing attainment of the very lightweight parachute sought. In general, reefed canopies are not noted for their symmetry and all Ringsail parachutes have exhibited

* The design drag coefficient of $C_D o = 0.81$ proved to be a minimum value (see Section 3.1.1).



Canopy Configuration 0.2 Seconds After the Reefed Load Peak

Retroduced from
best available copy.

Canopy Configuration at Disreef

Figure 17. Two Stages During Reefed Operation of 124.5 Ft D₀
Ringsail Showing Typical Irregular Shape

this characteristic. However, there is no test evidence that under near-ultimate loading conditions the irregular shape of the reefed canopy was the source of a critical stress level. Indeed, critical loading conditions of the Ringsail causing extensive damage are generally encountered after disreefing as the canopy approaches full inflation. At this time, because infolding relaxes the load in the several gores and lines affected, the average load in the balance of the canopy would be increased possibly as much as 10 percent. However, use of the ogival shape had already been shown to correct this condition in the fully inflated canopy and the adoption of a straight conical profile did not appear to be warranted. Actually, no method of improving the symmetry of a reefed canopy was known at that time, the efficacy of the conical shape being pure conjecture.

The 30/60 biconical profile illustrated in Figure 15d represents the compromise made with conflicting requirements for the design of a highly efficient lightweight Ringsail of 127 ft D_o . The profile is a straight-line approximation of the desired ogival profile over the major canopy area based on the assumption that the sharply conical apex could be coped with by reinforcement of the normally heavy crown rings at small weight cost. Since, one design goal of the new program was to simplify the method of computing Ringsail gore coordinates, a tri-conical design canopy with a 15° crown, 30° midrif, and 60° skirt was never pursued.

The fullness distribution of the bi-conical Ringsail canopy illustrated in Figure 18 represents an attempt to reconcile two conflicting requirements in an optional fashion for a lightweight parachute. These two requirements are:

- a) Introducing sufficient fullness in the leading edge of the sails to provide necessary stress relief
- b) Maintaining canopy shape with the trailing edge

It is clear that the bias cut solid cloth conical canopy does not hold the conical shape as it inflates and it obtains stress relief from the great bi-axial elongation inherent in the cloth weave. To approximate this action in the annulate canopy it is necessary to make the gore wider in the critical stress region with the result that the conical profile becomes onion-shaped, which is even more complex than the tri-conical.

Aerial drop testing of the new 127 ft D_o bi-conical Ringsail was initiated in March 1965 (Reference 8). After four successive failures of three successively heavier modifications at low load levels, the parachute design was discarded as essentially unworkable. In each case the canopy split along a

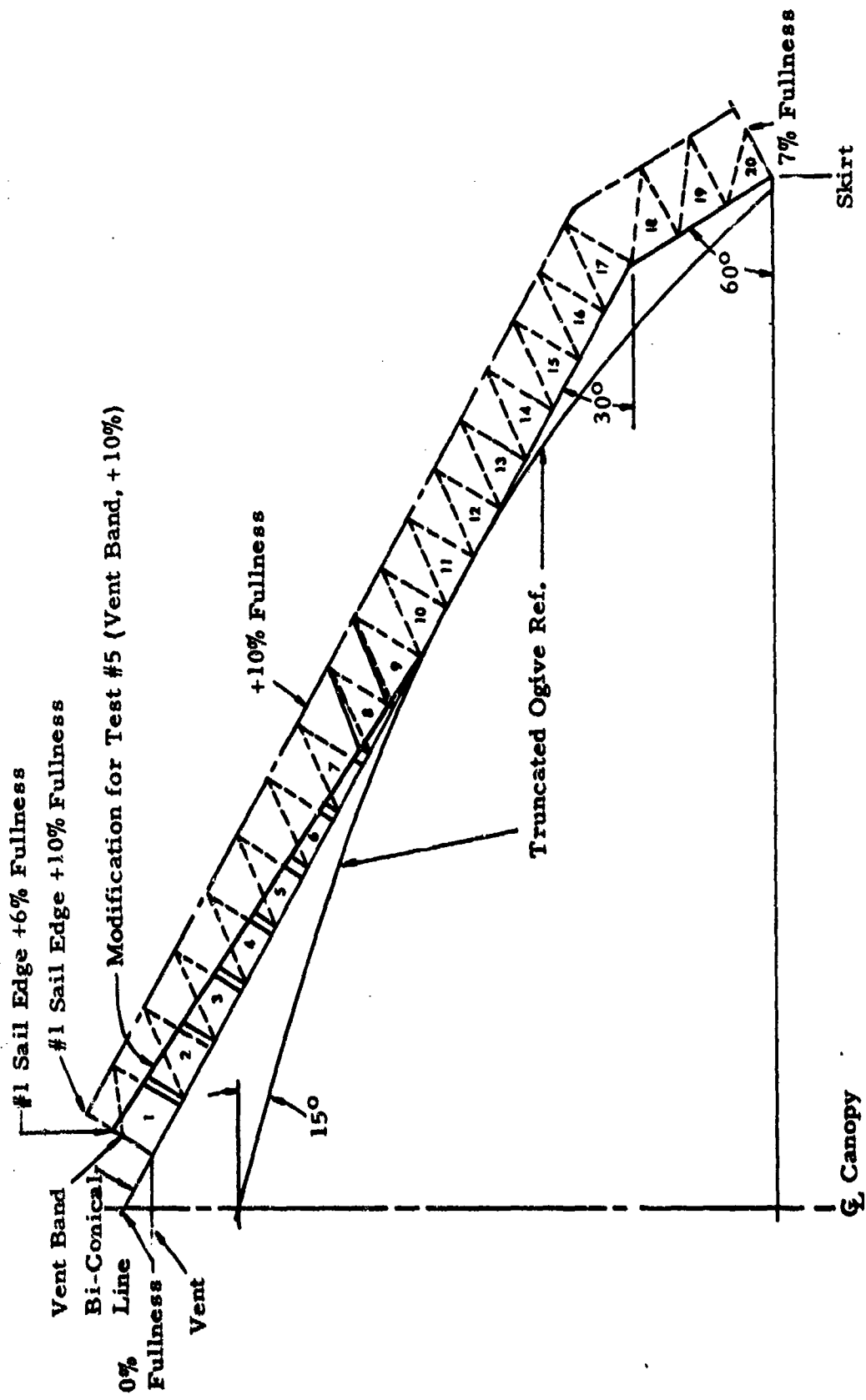


Figure 18. Fullness Distribution of 127 ft D_o Bi-Conical Ringsail Canopy
Relative to Calculated Width of Conical Gore

gore after disreefing, the rupture starting in ring #6 in test No. 1, in ring #5 in tests No. 2 & 3 and in ring #7 in test No. 5. (The catastrophic failure of test No. 4 triggered by a faulty pilot chute link is not pertinent.) A comparison of the 30 degree conical shape with the inflated profile of the canopy at the time of failure showed rings 5 through 7 to be in a region of maximum strain; hence, prohibitively heavy cloth and/or reinforcing bands would be required to prevent rupture.

The 128.8 ft D_o Century Ringsail (designed in March 1966) was the first Ringsail parachute to be designed in accordance with the new basic dimension scheme of Figure 12 utilizing at the same time the new IBM 7090 digital computer program designated WG 176 (see Section 5.4).

The results of three aerial drop tests of this "all new" Ringsail, one a cluster of two canopies with a weight of 17,720 pounds, were sufficiently impressive aerodynamically to justify unqualified acceptance of the revised design. For example, the single parachute performance included $C_{D_o} = .87 - .90$ at a rate of descent of 27 fps, average amplitude of pendular oscillations ± 7 degrees and a specific drag area of $C_{DS_o}/W_p = 51 \text{ ft}^2/\text{lb}$. Although the two canopies of the cluster exhibited the characteristic divergence of inflation observed in the 88.1 ft D_o Ringsail clusters during the Apollo program, the ratio of maximum to average forces for this one test was about half that of the maxima recorded previously. Figure 19 is the only good photograph obtained from the two single canopy tests.

2.1.4 Ringsail Parachute Cluster Development

Ringsail cluster development embraces the Apollo Earth Landing System (ELS). Perhaps if a new program were to begin wherein suitable time and money was available, a Ringsail cluster possessing characteristics other than those of Apollo would emerge. However, due to schedule pressures which accompany development programs of the magnitude of Apollo, and lack of any experience in clustering Ringsail parachutes, a sequential order of events led to the development of the modified Ringsail used on Apollo. The design, in its present form, is a composite of changes which were necessitated during the development to solve the clustering problem. Whatever improvements might be conceived in retrospect, the Apollo Ringsail cluster performs exceedingly well and has safely and reliably returned all of this nation's astronauts from space. The following paragraphs recapitulate the development of the Apollo modified Ringsail and, so far as practical, gives the reasons and rational behind the decisions that were made.

The proposed Apollo Earth Landing System (ELS) was to have as its principal components a cluster of three identical parachutes. Each of these was to be deployed independently of the others so that a system redundancy of

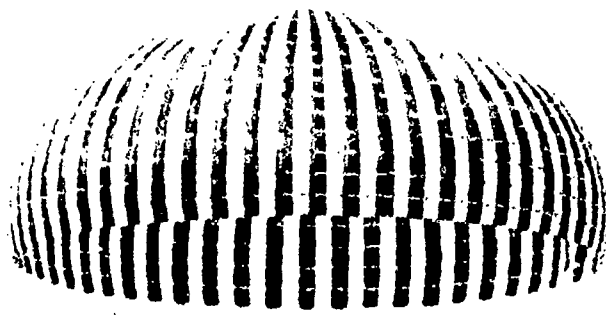


Figure 19. 128.8 ft D_0 Lightweight Version of the Century Ringsail
Descending at 27.9 fps (EAS) with 9762 Pounds (Bottom of
Damaged Gore Visible on RH Side)

50 percent could be provided by designing for safe recovery with any two of the three parachutes operable. At the outset of the development program the design descent weight of the command module (CM) including parachutes was 9500 lbs and the rate of descent with two main canopies was not to exceed 33 fps at 5000 ft msl. With allowance for an observed 6 percent scatter in measured rates of descent, a design value of 31 fps at 5000 ft was used. The corresponding EAS was 28.8 fps under standard sea level conditions with an equilibrium dynamic pressure close to 0.99 psf. The latter numbers are significant because they show the unit canopy loading of the cluster ($W/C_D S$) to be high relative to that of previous large parachute cluster experience. One of the consequences is that the peak opening load after disreefing occurs much later in the filling process as the canopy is approaching full inflation, even in the ideal case of perfectly synchronous inflation.

Prior to the Apollo ELS development program experience with the Ringsail parachute in clusters was too limited to be represented by either useful test data or definition of the problems. In April 1962 the design of the original 88.1 ft D_0 Apollo main parachute for use in clusters of two and three was carried out with no clear understanding of the magnitude of the operational problem faced. The need for a conservative approach to the structural design was indicated by Reference 10 in which the opening force data for clusters of three 100 ft D_0 solid cloth canopies* exhibited the load sharing characteristics given in Table I.

These clusters were deployed from a common rigid container, housing three deployment bags, by a single 12 ft extraction chute. As shown in Table I, the measured maximum opening forces compared to the estimated synchronous opening load varied from nearly equal to +16% reefed, and from +17% to +108% on disreefing. This dramatic demonstration of the magnitude of the cluster nonsynchronous inflation problem was not fully appreciated at the time, and the Apollo ELS parachute development program was initiated in July 1962 with aerial drop tests of very lightweight single canopies. These early tests were exploratory in character and had as their objectives: (1) evaluation of reefing parameters and opening load factors for the nominal design conditions, and (2) to produce the lightest possible parachute structure. Some of the experimental lightweight models were so extensively damaged by opening loads that they could not inflate; however, it was noted that if the skirt band was not broken, the canopy would inflate despite split gores and massive crown damage.

* Several different canopy shapes were used: flat, 27° conical, and tri-conical (18° - 30° - 67.5°).

TABLE I
MEASURED OPENING FORCES-CLUSTERS OF THREE
100 ft SOLD CLOTH PARACHUTES (Reference 10)

AF Test No.	Gross Weight (lb)	Unit Ld W/C S (psf)	Canopy No.	Measured Opening Forces			Canopy Damage
				Received Max. lb	Discreet Max. lb	Ratio	
58-828	10,616	0.60	1	13,200	1.16	19,450	2.08
			2	(9700) Δ	.84	(660) Δ	.07
			3	11,600	1.01	8,000	.85
			Cluster	33,000	2.87	28,000	2.99
			Average	11,500	1.00	9,370	1.00
58-921	11,620	0.66	1	12,200	1.02	10,800	.90
			2	11,900	.99	14,000	1.17
			3	11,800	.99	11,200	.93
			Cluster	30,300	2.53	30,000	2.50
			Average	11,970	1.00	12,000	1.00
				Δ			

NOTE: Δ Estimated from the total cluster load -- no recording was obtained due to instrument failure

- Δ The average load is taken to represent the probable opening load for each of three canopies inflating synchronously. This assumption was found to be a reasonable approximation by application of the load prediction method for the Apollo cluster given in Reference 12 to the synchronous opening case.

Thus, at the conclusion of the first series of single parachute tests with one stage of reefing, structural integrity of the lightweight 88.1 ft D_0 Ringsail had been demonstrated for maximum opening loads of 17,300 lbs reefed and 19,000 lbs on disreefing; these were about equal to the probable synchronous opening loads of a two-canopy cluster.

In anticipation of cluster rigging requirements, the 88.1 ft D_0 Ringsail had been designed with an effective suspension line length of 1.40 D_0 . This was done to increase the drag efficiency of the cluster relative to the conventional approach using 1.0 D_0 lines along with long risers to obtain effective canopy separation at a moderate angle of attack. It will be recognized that the general configuration of a two-canopy cluster can be made similar to an equivalent single parachute of area $2 S_0$, having an effective line length equal to its nominal diameter, by providing a combined length of lines and risers equal to $\sqrt{2} D_0$ on each of the two canopies.

The first three-canopy cluster test was performed in December 1962. The failure of one canopy to inflate caused by a fouled reefing line did not signal the existence of a serious problem. However, the second cluster test a month later with two canopies was characterized by "some blanketing" in which the leading canopy was subjected to a maximum load of 29,370 lbs on disreefing with a total cluster load of 31,500 lbs. Now, the worst aspects of the cluster operational problem had been demonstrated: nonsynchronous inflation tended to degrade system reliability and substantially augmented the peak loads to which each member of the cluster might be subjected.

One initial reaction to this, which overlooked the evidence of Reference 10, was to ascribe the source of the trouble to the unique inflation characteristics of the Ringsail itself: the large bulbous development at the end of the reefed interval caused by filling through the side slots (as well as the canopy mouth) and the rapid growth to full inflation following disreefing. Later, it was demonstrated that these characteristics aggravated non-synchronous opening but did not cause it. Thus, a concerted attack on the problem that was launched early in 1963 was mainly concerned with reducing the canopy growth during the reefed interval and increasing the filling time after disreefing. While these objectives are not mutually exclusive, some of the canopy modifications tested during the initial phase of the investigation attacked one at the expense of the other and only succeeded in worsening cluster operation.

The experimental approach reflected the general weakness of cluster operating theory prevailing at that time. Interference between canopies, sometimes called "blanketing", was considered to be the prime source of the trouble.

Two other tributary factors were recognized. (1) non-synchronous deployment causing the canopies to arrive at line stretch and start filling at different times and (2) non-synchronous disreefing due to variations in reefing line cutter initiation and timing.* The former was of relatively small effect and, being difficult to control with three independently deployed parachutes, was neglected. The latter, on the other hand, was not negligible so long as cutter timing variations remained a large fraction of the disreef filling time. Hence, considerable thought and effort was devoted to both reduction of pyrotechnic cutter timing tolerances and the creation of a synchronous disreefing system. However, no practical synchronous disreefing system was developed, and the best that could be done with pyrotechnic line cutters was a reduction in timing variations at any given temperature from $\pm 10\%$ to $\pm 7\%$ approximately. Therefore, the most promising course was to effect a substantial increase in the filling time of the parachutes after disreefing.

The experimental test program was carried forward in the wind tunnel as well as with full scale aerial drops of two- and three-canopy clusters. Two different series of tests were performed in the Ames 40 by 60 wind tunnel at Moffet Field. The wind tunnel models consisted of both full scale single parachutes reefed and one-half and one-third scale models. The one-third scale models were allowed to disreef and inflate fully in the tunnel. A one-third scale cluster was also tested.

Presented in Table II is a summary of the different modifications of the basic Ringeail design that were tested during the experimental attack on the cluster non-synchronous opening problem. Additional variations of these modifications and a few novel configurations were tested in the wind tunnel as noted in the following discussion.

The first group of wind tunnel models tested in February 1963 consisted of five full scale ($D_0 = 28$, 1 ft), two half scale ($D_0 = 44$ ft), and two one-third scale ($D_0 = 48$ ft) test specimens, plus an assortment of four different shaped canopies of 24 to 32 ft D_0 (Reference 19). Thirteen different Ringeail configurations were evaluated including one cluster of two 28 ft D_0 canopies. However, due to a rigging error the cluster test was inconclusive.

* A fairly well defined correlation was found between the differences in disreef loads of the leading and lagging canopies and their respective disreefing times, as first reported in Reference 11, and as developed more fully later in Reference 12.

TABLE II
RINGSAIL PARACHUTE DESIGN MODIFICATIONS FOR CLUSTER DEVELOPMENT

Model Designation	D_o ft.	Design Modification	Justification
PDS 1543	88.1	(none) 72 gores; 12 rings; open ringslot crown to $h/h_R = .45$; sail leading edge fullness 7.5 - 11.7%; $\lambda_T = 7.21\%$; $t_s/D_o = 1.40$ effective	Basic Reference
PDS 1544	88.1	Sail leading edge fullness reduced by the addition of tight tapes	To reduce inflow through side slots causing bulbous canopy development reiced
PDS 1650	87.1	Sail leading edge fullness reduced by reducing width (5.6% was 7.5-11.7%) $\lambda_T = 6.6\%$	To reduce inflow through side slots
PDS 2021	88.1	Suspension lines shortened to $t_s/D_o = .93$ effective	To increase filling time
PDS 2071	88.1	Open ringslot crown expanded to $h/h_R + .53$; $\lambda_T = 7.4\%$	To increase filling time
PDS 2072	88.1	Ventilated crown replaced with solid cloth crown extending to $h/h_R = .53$; Lower slots widened to maintain $\lambda_T = 7.2\%$	(No record)
PDS 3420	88.1	(All new) 72 gores; 14 rings; conical apex 15.4°, distributed increase in geometric porosity $\lambda_T = 10.7\%$	To substantially increase filling time (and to reduce slackness of fully inflated canopy)

TABLE II (Continued)
RINGSAIL PARACHUTE DESIGN MODIFICATIONS FOR CLUSTER DEVELOPMENT

Model Designation	D_0 ft.	Design Modification	Justification
PDS 1543 -523	88.1	Upper 35% of ring 5 removed; $\lambda_T = 9.38\%$	To reduce reefed canopy bulb diameter
PDS 1543 -533	88.1	Upper 50% of ring 5 removed; $\lambda_T = 10.35\%$	To reduce reefed canopy bulb diameter
PDS 1543 -535	88.1	Vertical tapes on gore centerlines extended from crown across all slots to skirt	To reduce inflow through side slots
PDS 1543 -547	88.1	All of ring 5 removed; $\lambda_T = 13.8\%$	To reduce reefed canopy bulb diameter
PDS 1543 -557 -561	85.6	68 gores; conical apex 190° ; $r_s/D_0 = 1.44$ effective; upper 75% of ring 5 removed; $\lambda_T = 12.5\%$	To reduce weight and to reduce reefed canopy bulb diameter
R 7661 -501 -507	85.6	(Block I final design) 68 gores; conical apex 190° , $1 \times 1/4$ rings; upper 75% of ring 5 removed; $r_s/D_0 = 1.44$ effective; $\lambda_T = 12.5\%$	Acceptable cluster performance for Apollo Block I with one reefed stage of 9.5% D_0 (mid-gore)

NOTE: For detailed configuration of these models, see the figures and data sheets presented in Appendix A.

Configurations in Table II represented by wind tunnel models included PDS-1543 and PDS 1543-535. All full-scale models had a 10 ft D_o Ringslot pilot chute attached. The canopy modifications evaluated were relatively minor. Pocket bands and skirt stiffeners were added to promote more uniform reefed inflation by reducing random variations in the initiation of effective filling. As noted, vertical tapes on the gore centerlines extending across all slots to the skirt were aimed at reducing aerodynamic interference between canopies by reducing inflow through side slots.

Steady state airflow studies of the unmodified parachute reefed in the range of 8 to 13% D_o (with rings on radials) produced the results illustrated in Figure 20 as an aid to understanding how clustered canopies might interfere with each other while reefed. The effect of the modifications on the inflated shape of the reefed canopy was evaluated in terms of maximum inflated to skirt mouth diameter ratios and the distance from the skirt to the maximum diameter. The extended vertical tapes had no significant effect on the inflated shape but increased from one to four the number of skirt rings stabilized with all sails blown inward between radials (Figure 20b). A measured reduction in reefed drag of approximately 18 percent was attributed to this change in airflow over the canopy.

The variation of reefed drag with reefing ratio and with canopy scale was evaluated for the unmodified Ringsail design. The results had no bearing on the cluster operational problem but appeared to confirm the general increase of drag coefficient with scale observed with fully inflated Ringsails of different sizes in free descent.

Reefed inflation time of the full scale models was evaluated, the results indicating no significant effect of the stiffened skirt, early development of a steady inflation rate with pocket bands, and slower inflation with vertical tapes extended over the lower slots. Evaluation of the reefed filling time in terms of the dimensionless ratio vtf/D_o for the three canopy sizes yielded values within 10% of a constant 8.5. The disreef inflation time was evaluated for the one third scale Ringsail model and the other small parachute models. Of possible significance is the observation that the Ringsail value of $vtf/D_o = 1.09$ was 20% greater than for the solid cloth circular canopy and 40% less than for the solid cloth conical canopy.

Steady state reefing line loads were also measured, adding to the useful general information produced by the wind tunnel program. On the whole,

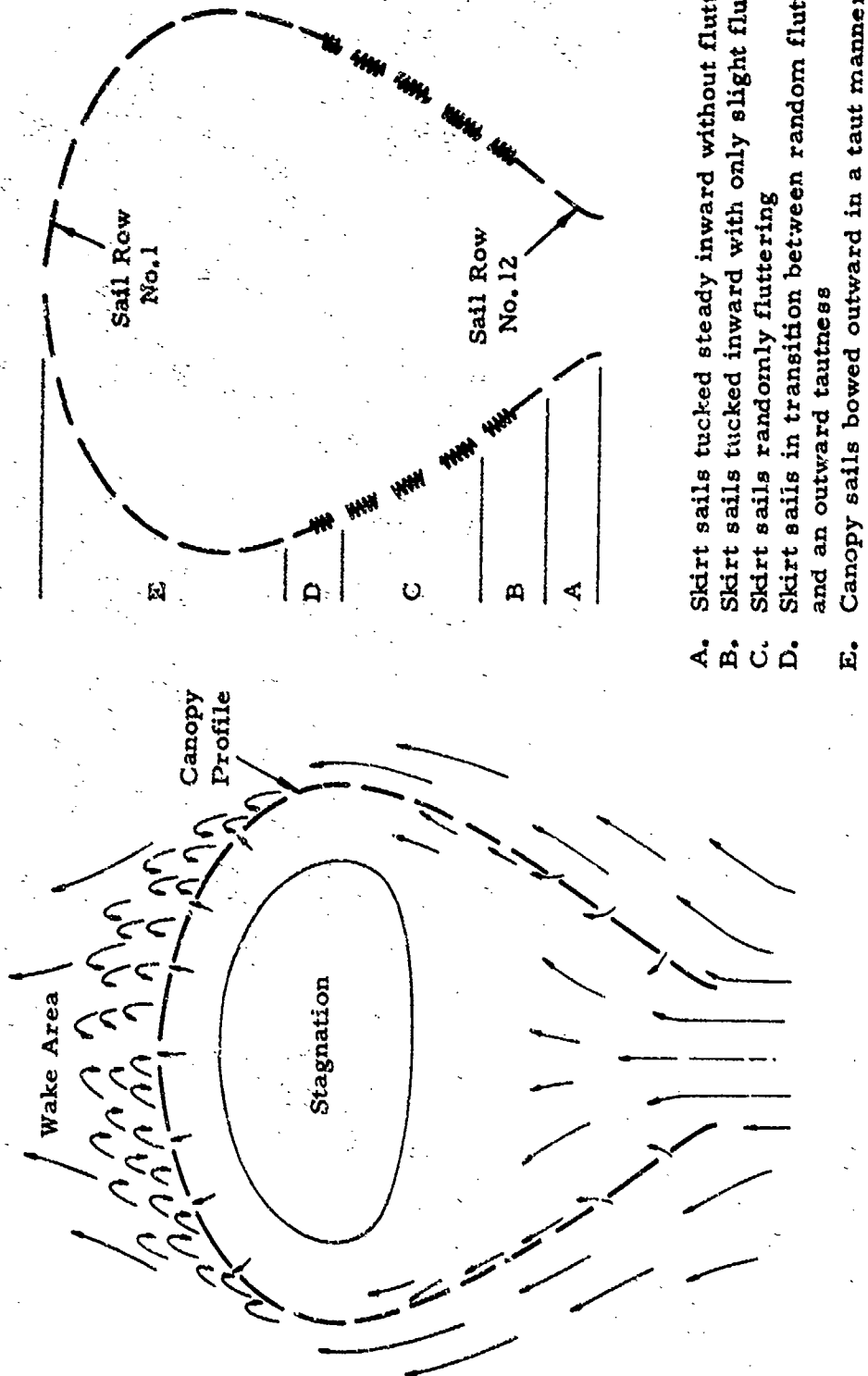


Figure 20. Results of Full Scale Wind Tunnel Air Flow Studies
with 88.1 ft D_o Ringsail Reefed

the results of this first series of wind tunnel tests of modified Ringsail parachutes produced no conclusive evidence bearing on the cluster operational problem. It was observed that pocket bands "promoted rapid initial reefed inflation" which could be construed to also promote more uniform reefed inflation of clustered canopies. The vertical tapes extended to the skirt appeared to have the desired effect of reducing inflow through the side slots, but whether or not this would benefit cluster operation remained to be demonstrated. Additional wind tunnel testing of two-canopy clusters of one-third scale models was recommended as an economical method of evaluating the effects of further modification of the Apollo main parachutes.

The second group of wind tunnel models tested in October 1963 consisted of six full scale and one, one-third scale test specimens by means of which it was possible to evaluate 35 different configurations, of which three full scale configurations were duplicated in one-third scale (Reference 16). Configurations in Table II represented by wind tunnel models included PDS 1543-535 (vertical tapes extended to skirt); PDS 1543-547 (all of ring 5 removed); PDS 3120 (increased geometric porosity); PDS 1543-533 (upper 50% of ring 5 removed). Other configurations had all of the crown slots covered in combination with 25%, 50% and all of rings 4, 5, & 6 removed plus provisions for both radial and mid-gore reefing. Intermediate canopy reefing for the purpose of forcibly reducing the diameter of the inflated bulb was tested in both full and one third scale models with a second reefing line installed inside ring 7. This proved to have a very unfavorable effect on the shape of the reefed canopy.

Most of the one third scale models were tested with different reefing ratios both with and without an attached pilot chute of 3.4 ft D_o . Two full scale "high" porosity configurations were tested in which 1.9 inches and 3.8 inches of material were removed from the trailing edges of all ringsails below the ringslot crown to increase the total porosity by 25% and 50% respectively. The effect of these changes in canopy ventilation on the calculated porosity of the different wind tunnel models is summarized in Table III. For the most part, these modifications were aimed at reducing the reefed canopy bulb diameter, but one full scale test was made with a 10 ft diameter guide surface canopy riding inside the mouth of the 88.1 ft D_o Ringsail restrained only by a long riser. The reason for this is not now clear because the technique was designed to accelerate the opening of the canopy mouth where a very short total filling time was needed in a non-reefed parachute. Altogether, 159 wind tunnel runs were made at low dynamic pressures ranging from 2.5 to 20 psf. Data were accumulated on reefed drag areas, projected diameters, and, for several one third scale models, reefed filling times and the filling time from the disreef to full open. The results indicated that a wide slot bordering the ringslot crown

TABLE III
POROSITY VARIATION OF THE WIND TUNNEL MODELS TESTED

Model Description Basic Model With:	Geometric Porosity				Material Porosity	Total Porosity		
	Skirt Area		Crown Area					
	$\lambda_s(\%)$	$\lambda_s/2.12$	$\lambda_c(\%)$	$\lambda_c/1.50$				
Open Crown	2.12	1.00	1.50	1.00	3.59	7.21	1.00	
Closed crown	2.12	1.00	0.17	0.11	3.60	5.89	0.82	
*50% Row No. 4 removed open crown	2.12	1.00	4.36	2.91	3.55	10.03	1.39	
*100% Row No. 4 removed open crown	2.12	1.00	6.80	4.53	3.48	12.40	1.72	
25% Row No. 5 closed crown	2.12	1.00	1.88	1.25	3.58	7.56	1.05	
50% Row No. 5 removed closed crown	2.12	1.00	3.40	2.27	3.54	9.06	1.26	
100% Row No. 5 removed closed crown	2.12	1.00	6.43	4.28	3.50	12.05	1.67	
100% Row No. 5 open crown	2.12	1.00	7.10	4.73	3.49	13.38	1.85	
25% Row No. 6 closed crown	2.12	1.00	2.17	1.45	3.57	7.86	1.09	
50% Row No. 6 removed closed crown	2.12	1.00	4.11	2.74	3.50	9.73	1.35	
100% Row No. 6 closed crown	2.12	1.00	8.32	5.55	3.34	13.78	1.91	
100% Row No. 6 open crown	2.12	1.00	9.48	6.32	3.33	15.11	2.10	

* Material removed from leading edge of sail row rather than trailing edge as on Row Nos. 5 and 6. Porosity values calculated per Reference 5.

produced the greatest reduction in reefed bulb diameter and that ring 5 was the best location for it. The bulb diameter decreased with increasing width of the slot and the reefed filling time decreased at the same time because the volume to be filled was reduced. On the other hand, the filling time after disreefing increased significantly with increased slot width.

Quantitative evaluation of the effects the Ringsail modifications had on cluster operation was possible only for those that were subjected to full scale aerial drop tests with suitable instrumentation. The following analysis is based on the opening loads reported in Appendix A of Reference 13. The criterion of cluster performance is the same as that applied to the 100 ft D_0 solid cloth parachutes in Table I. However, in Table IV only the data for tests showing a maximum ratio of opening force to the average are given for each modification.

It is clear that maximum measured values of F/F_{av} for most of the configurations tested might be increased by performance of a statistically adequate number of tests, but in some cases the results of one or two tests were sufficiently extreme to justify rejection of the modification. Outstanding examples are PDS 1544, PDS 1650, PDS 2071, PDS 1543-535, and PDS 1543-549. A reduction in sail leading edge fullness to minimize inflow through the side slots also reduced total porosity and simply accelerated the rate of inflation after disreef. Increasing the crown porosity by enlarging the ringslot area of the canopy did not increase the total porosity enough to lengthen the filling time after disreef. Extending the vertical tapes the full length of the gore to restrict filling through the side slots did not have the desired effect and canopy filling after disreef was accelerated. The use of short suspension lines to slow down canopy filling was largely ineffectual because only the reefed filling time was increased.

PDS 2072, a hybrid Ringsail with a solid cloth crown, was not rejected because of its cluster performance (Table IV) but because of the exaggerated balloon-like development it exhibited at the end of the reefed interval. This modification sharply accelerated filling after disreef. A total of six full scale drop tests, two of them with clusters, was conducted and the decision was made to abandon this idea.

Considerable effort also was devoted to optimization of the width of the slot in ring 5 by means of full scale aerial drop tests. The object was to obtain the smallest possible reefed bulb diameter without jeopardizing opening reliability; one of the one-third scale models had been marginal in this respect on disreefing in the wind tunnel. The reduction in reefed bulb diameter by the addition of the wide slot was given considerably more weight than the increase in filling time after disreefing that attended it. Consequently, a new high porosity Ringsail model (PD 3120) that showed no

TABLE IV
APOLLO CLUSTER DEVELOPMENT - MEASURED OPENING FORCES
FOR CLUSTER TESTS SHOWING MAXIMUM DIVERGENCE

Test No.	Date	Model Designation	Modification Characteristic	Measured Opening Forces			
				Canopy No.	Ib	Ratio	Ib
13-1	3/21/63	PDS 1543	none $D_o = 88.1 \text{ ft}$	1 2 3 (Avg.)	6436 10110 9710 8752	.73 1.16 1.11 1.00	4208 7270 10290 7256
26-5	2/8/63	PDS 1543	none $D_o = 88.1 \text{ ft}$	1 2 (Avg.)	15810 14450 15130	1.05 .95 1.00	5840 21970 13905
26-1	1/11/63	PDS 1544	Sail leading edge fullness reduced with tight tapes to reduce λ_T $D_o = 88.1 \text{ ft}$	1 2 (Avg.)	13200 13390 13295	.99 1.01 1.00	6910 29370 19140
26-3	1/28/63	PDS 1650	Sail fullness reduced 41% av. $D_o = 87.1 \text{ ft}$	1 2 (Avg.)	23230 10700 16965	1.37 .63 1.00	28200 7700 17950
26-8	5/13/63	PDS 2071	Ringslot crown area enlarged $D_o = 88.1 \text{ ft}$	1 2 (Avg.)	13140 12450 12795	1.03 .97 1.00	5550 28410 16980
26-9	5/15/63	PDS 2072	Solid Cloth Crown replaced ringslots $D_o = 88.1 \text{ ft}$	1 2 (Avg.)	13150 9470 11310	1.16 .84 1.00	26420 24160 25290

TABLE IV (Continued)

APOLLO CLUSTER DEVELOPMENT - MEASURED OPENING FORCES
FOR CLUSTER TESTS SHOWING MAXIMUM DIVERGENCE

Test No.	Date	Model Designation	Modification Characteristic	Canopy No.	Measured Opening Forces		
					Reeled	Ib.	Disagree Ratio
40-2	3/30/64	PDS 1543 -535	Vertical tapes extended to skirt $D_o = 88.1$ ft	1 2 (Avg.)	.9840 10540 10190	.97 1.03 1.00	.5710 26610 16160
41-1	4/7/64	PDS 1543 -527	4 gores removed (to reduce weight) $D_o = 85.6$ ft	1 2 (Avg.)	21330 16090 18210	1.12 .38 1.00	22580 7310 14945
44-8	4/27/64	PDS 1543 -547	Large slot formed by removing all of ring 5 $D_o = 88.1$ ft	1 2 (Avg.)	22400 19000 20700	1.08 .92 1.00	8800 13400 11100
44-6	4/30/64	PDS 1543 -549	Lines shortened to $l_s/L_o = 1.2$ effective $D_o = 88.1$ ft	1 2 (Avg.)	14200 17900 16050	.88 1.12 1.00	5400 21100 13250
29-2 (one pilot chute separated)	8/4/64	PUS 1543 -557	75% of ring 5 removed 4 gores removed $D_o = 85.6$ ft	1 2 3 (Avg.)	12640 9110 4860 8870	1.42 1.03 .55 1.06	12900 6250 4620 7923
29-4	11/6/64	PDS 1543 -561	75% of ring 5 removed, 68 gores $D_o = 85.6$ ft	1 2 3 (Avg.)	13260 10160 10074 11145	1.19 .91 .90 1.00	13540 5680 7617 8946
48-4	12/21/64	R 7661 -507	Final design 75% ring 5 removed 68 gores $D_o = 85.6$ ft	1 2 (Avg.)	14091 16630 15360	.92 1.08 1.00	27320* 9321 18320

* with split gore

significant reduction of the reefed bulb in the wind tunnel yet which promised a substantial increase in both reefed and disreef filling times was dropped from the program without further test evaluation.

Due to schedule pressures, experimental model performance in the wind tunnel dominated technical decisions. The adoption of mid-gore reefing is an example. The full-scale models tested in the wind tunnel with mid-gore reefing exhibited a high degree of poly-symmetry, each sail being held tauntly inward between radials. Drop tests made prior to this on an experimental basis had exhibited no overt difference in reefed opening characteristics of the Apollo parachutes with mid-gore reefing. At least two reasons for this can be cited: (1) the reefed filling time was not long enough for the poly-symmetric shape produced by a taut reefing line to develop; (2) only the skirt ring of sails was controlled by the reefing line, the others remaining free to flutter in and out at random, (except on those models with vertical tapes on the gore centerlines extended across all slots to the skirt). While mid-gore reefing has worked very effectively, we cannot show conclusive data that it was superior.

While it cannot be said that a statistically adequate number of instrumented cluster tests has been performed with either the original 88.1 ft D_o Ringsail, the 85.6 ft D_o model with four gores removed, or the modified 85.6 ft D_o design adopted for the Apollo Earth Landing System, comparison of the maximum force ratios in Table IV indicates that some improvement in cluster operation may have been realized. Recognizing the possibility that the number of canopies in the cluster also may have an effect on synchronism of inflation, the comparison is made in Table V.

TABLE V

MAXIMUM FORCE RATIOS FROM TABLE IV

Number of Canopies in Cluster	Original Ringsail		Modified Ringsail	
	Test No.	Disreef F_{max}/F_{av}	Test No.	Disreef F_{max}/F_{av}
2	26-5**	1.58	48-4	1.49
	41-1	1.51		
3	13-1	1.42	29-2*	1.63
			29-4	1.51

* Test 29-2 may be considered invalid because a pilot chute separated from one of the main canopies.

** Test 26-5 may be considered invalid because a planned difference in reefing line cutter operation of 1.0 second was used and the actual difference was 1.33 seconds.

The fact that the results of the three-canopy cluster data are negative was apparently overlooked at the time, because the individual parachute loads are greater in the two-canopy cluster than in the three canopy cluster. The ratios shown in Table V indicate that the maximum probable opening load after one stage of reefing may have been reduced from 151 percent to 149 percent of the maximum synchronous opening load of one parachute in a two-canopy cluster. This difference is small and the comparison is inconclusive because of significant differences between the two parachute systems and the way in which they were tested. The secondary goal of the development program was attained in that the bulbous development of the reefed canopy was substantially reduced. The design modification responsible for this change in Ringsail behavior was the wide slot in the crown of the canopy formed by removal of the upper 75 percent of the width of ring 5. This increased the total porosity of the canopy by 73 percent (from 7.5% to 12.5%) and reduced the drag coefficient by 12% (from $C_{D_0} = .85$ to $C_{D_0} = .75$). The effect on canopy growth during the reefed interval in terms of drag area (C_{DS}) was marked (down from 90% to 20% approximately), the wide slot falling at the periphery of the reefed canopy at disreef. The reefed filling time was reduced because the volume to be filled was smaller. The filling time from disreef to full open was increased by two factors: (1) the greater differential volume to be filled starting with a smaller reefed volume, and (2) the increased ratio of outflow to inflow produced by the higher canopy porosity. The increase in filling time from disreef to full open was estimated to be approximately 50 percent. The stability of two-canopy clusters was improved, the average amplitude of pendular oscillations being reduced from ± 8 to ± 3 degrees.

The design limit loads applicable to each of the three parachutes in the cluster as reported in Reference 12 are:

Reefed opening	21,400 lbs
Disreef to full open	25,000 lbs

The maximum cluster load calculated was 49,700 lbs for three canopies opening reefed. Probable synchronous opening loads calculated by the same method are:

Reefed opening	16,300 lbs (ea of 3)
Disreef to full open	17,000 lbs (ea of 2)

The maximum load ratio corresponding to the limit design case on disreefing is:

$$F_{max}/F_{av} = \frac{25,000}{17,000} = 1.47$$

While this may appear to be slightly unconservative in view of the test results in Table V, the difference is small relative to the errors inherent in the method of load prediction (e.g., see Reference 14).

Several reasons for the improvement in cluster operation of the modified Ringsail have been given:

- a) Reefed drag area growth stopped at the 5th ring.
- b) The smaller reefed canopy volume to be filled made it easier for a lagging canopy to catch up with its mates by the end of the reefed interval.
- c) Reduction of the bulbous reefed development reduced aerodynamic interference between canopies.
- d) The increased filling time after disreefing reduced the retarding effect of the disreef time differential on subsequent inflation of the lagging canopy.

The changeover to two stages of reefing for the Apollo Block II Heavyweight after the gross landing weight increased from 11,000 to 13,000 lbs (approximately) did not degrade cluster performance. The maximum recorded force ratio for the final qualification tests with three-canopy clusters was $F_{max}/F_{av} = 1.49$, the same as that for two-canopy clusters in the Block I system. Since the synchronous opening load for normal entry with 2 drogues and 3 mains is in the order of 10,000 lbs on each parachute in the cluster the probability of any one parachute being subjected to a peak load greater than 15,000 lbs appears small. Structural integrity of the parachutes has been demonstrated for each opening stage with measured individual loads of 30,000 to 33,000 lbs (approximately). Therefore, the structural reliability of the Apollo Block II Heavyweight main parachute cluster is very high.

As noted, the history of Ringsail cluster development includes one aerial drop test of two 128.8 ft D_0 "Century" parachutes with a gross load of 17,720 lbs. (See Frontispiece.) The test was performed on 27 October 1966.

The system was launched from an aircraft in level flight at approximately 150 KEAS and 10,000 ft altitude. The canopies were reefed 13 percent D_o for 8 seconds. Deployment and opening took place in a normal manner and the peak loads are presented in Table VI.

TABLE VI
MEASURED OPENING FORCES OF TWO
128.8 ft D_o RINGSAILS IN CLUSTER

Canopy No.	Max Reefed F_R		Force	Max Disreef F_o	
	lbs.	Ratio	at Disreef lbs	lbs.	Ratio
M-1	19,400	.94	7,050	13,800	.67
M-2	21,800	1.06	13,900	27,600	1.33
(Avg.)	20,600	1.00	--	20,700	1.00

The time sequence of events is given in Table VII.

TABLE VII
CLUSTER OPENING TIME SEQUENCE OF TWO
128.8 ft D_o RINGSAILS IN CLUSTER

Canopy No.	Event time after line stretch-seconds			
	F_R max	Disreef	F_o max.	Canopy full open
M-1	1.88	8.41	9.59	18.25
M-2	2.69	8.59	9.67	11.26

With a unit canopy loading of 0.81 psf, the system descended at an average velocity of 26.1 fps EAS ($C_{D_o} = .84$), and the average amplitude of pendular oscillations was ± 2 degrees. The cluster specific drag area for this test was $\Sigma C_D S_o / \Sigma W_p = 48$ ft²/lb.

It will be noted that although the lagging canopy disreefed first, the small lead of 0.18 seconds did not prevent it from continuing to lag on a divergent course as the lead canopy contributed an increasing major fraction of the total force causing deceleration of the system. With a maximum force ratio of 1.33, the cluster nonsynchronous inflation characteristic is roughly

comparable to the average performance recorded for all parachutes tested during the Apollo Block I main parachute development program. Had the lead parachute disreefed first, then the maximum force ratio would have been much higher.

In order to understand the basic cause of the cluster inflation problem it is necessary to employ more precise language. Terms like "aerodynamic interference" and "blanketing" do not describe what is actually happening in a cluster system, and it has not been possible to quantize a flow field through and around clustered canopies that fits such a description. For example, when all of the canopies begin to fill, their mouths lie in the same plane normal to the airstream, and their initial inlet areas are nearly equal. The only change in inlet geometry visible during subsequent inflation is the flattening of common boundaries as the canopies come together and their areas begin to diverge, i.e., there is no blanketing in the sense that one canopy obstructs airflow into another.

During the course of the detailed study of the Apollo parachute system reported in References 13 and 14, an analysis of parachute load prediction methods brought to light a possible mechanism behind the cluster inflation problem. It has been described loosely as "inflation instability induced by system deceleration." The physical process is clarified by consideration of the equation for the tangential force produced by an inflating parachute,

$$F_p = C_D S q + m_a v + (m_a + m_p) \dot{v} + W_p \sin\gamma$$

(1) (2) (3) (4)

The first term represents simple aerodynamic drag. The second term is the momentum of the incoming airmass, a large positive quantity. The third term represents the inertial force of the parachute and the air mass moving with it caused by system deceleration, a negative quantity which is sometimes greater than the first two terms combined. This latter event becomes visible as a momentary dimpling or flattening of the canopy at the end of a period of rapid inflation (e.g., see Figure 33 at 15.1 seconds). The fourth term is the tangential weight component of the parachute, small enough to be neglected in most systems.

It is the third term that identifies the source of inflation instability in clustered canopies. \dot{v} , the system deceleration which unlike that of the single parachute system, is uncoupled from or independent of the drag growth of the individual canopies. The system is indifferent to the source of the deceleration, whether produced by all, part or only one of the canopies in the cluster. The effect of this common deceleration on the airmass in each canopy is felt as a reduction in differential pressure across the canopy.

the air mass tending to continue moving at its initial velocity, and, of course, this diminishes the motive power forcing air to flow into the canopy at a time when the free stream dynamic pressure is decaying. The slightest hesitation on the part of one canopy to ingest air at the same rate as its mates will cause it to fall behind or lag in a divergent manner until the system deceleration drops to a low level. Lacking any stabilizing mechanism, inequitable inflation and load sharing is the most probable mode of operation, as all test evidence indicates.

In the comparison of different cluster systems, maximum and average deceleration levels during canopy inflation would be the governing criteria. These are functions of unit canopy loading reefed and disreefed and of the average flight path angle. These factors were neglected in the foregoing comparison of the Apollo cluster systems. The actual difference in unit canopy loading was not negligible because the modified Ringsail was both smaller and had a lower drag coefficient than the original design. The effect of this on the unit canopy loading of fully inflated two and three-canopy clusters with $W = 9500$ lbs is shown in Table VIII for both the 72 and 68 gore models.

TABLE VIII
COMPARISON OF UNIT CANOPY LOADINGS OF
THREE APOLLO PARACHUTE SYSTEMS

Ringsail Design	Original		Revised		Modified (Apollo)	
Model Designation	PDS 1543		PDS 1543 - 527		R 7661-507	
Nominal diameter D_o (ft)	68.1 (72 gore)		55.6 (68 gore)		#5.6 (68 gore)	
Number of canopies in cluster	2	3	2	2	2	3
Drag coef. C_{D_0} (Table VI Ref.)	.345	.325	.845	.742	.725	
$\Sigma C_D S_o$ (ft^2)	10,300	15,075	9,730	8,540	12,515	
$W/\Sigma C_D S_o$ (psf)	.922	.635	.976	1.112	.758	
Ratio: 2 canopies	1.0	--	1.06	1.206	--	
3 canopies	--	1.0	--	--	1.214	
Approximate deceleration ratio	1.0	1.0	.94	.83	.82	

In general, the average system deceleration is inversely proportional to the unit canopy loading for parachutes of similar inflation rates. Thus, in the absence of an inflation stabilizing mechanism, the effects of nonsynchronous inflation could be expected to be more severe on the average for the original Apollo cluster than for the modified system on this ground alone.

2.1.5 Summary of Ringsail Parachutes

Design and performance data for the different Ringsail parachutes of standard design built and tested in single canopy systems are summarized in Table IX. For purposes of clarification, a "standard" Ringsail is one which has a spherical or ogival constructed profile without any wide slots or modifications of that nature. A "modified" Ringsail is one which has a constructed profile other than spherical or ogival in nature (such as conical or bi-conical) or incorporating wide slots such as the Apollo or PEPP Ringsails. A symbol code is provided for identification of the different Ringsail models in the graphs. Additional symbols for models not listed in Table IX will be found in Table XII. The characteristics of the modified Ringsail used in the Apollo ELS main parachute cluster are outlined in Section 2.1.4 and Appendix A and performance data are given in Section 3. Similar data for modified Ringsails designed for other more specialized uses are given in Appendix B. The special purpose Ringsails included a steerable version known as the "Glidesail" (Reference 17); a target canopy of an aerial recovery system in which the primary was an annular parachute (Reference 4); and a candidate design in the NASA program for development of a planetary entry parachute for the Viking Mars Lander (Reference 18).

2.2 PRESENT STATUS OF RINGSAIL DESIGN AND OPERATIONAL THEORY

The present concept of an optimized Ringsail parachute design for general use is represented by the 128.8 ft D_p Century Ringsail of "mid-weight" construction. This parachute conforms with the basic dimension scheme given in Figure 12 and has exhibited superior performance in all categories, both individually and in a cluster of two (Reference 8). When comparison is made with other parachute types under conditions of equal scale, canopy loading ($W/C_D S = 0.83$ psf), and stability of descent ($\theta = \pm 7^\circ$) a drag coefficient of $C_{D_0} = 0.9$ appears to be exceptional. Even the lightweight model descending with two split gores had $C_{D_0} = 0.61$, which equaled the design drag coefficient. Although the canopy filling time remains relatively short, the opening load factor is moderate, enabling a specific drag area greater than $C_{D_0} S_0 / W_p = 51$ psf to be attained in a well balanced structure designed for deployment at 15,000 feet altitude and $q = 100$ psf. The design limit opening load for these conditions would be $F_g + F_a = 26,000$ lbs.

The statements in paragraph 2.2 are qualified by the following considerations pertinent to the performance evaluation.

- a. The number of tests performed was insufficient to establish firm averages.
- b. The pilot to main parachute drag area ratio was 0.005 and the pilot chute was permanently attached to a special bridle harness on the apex of the main canopy.

The drag of the attached pilot chute was believed to be large enough to influence the reefed opening characteristics of the main canopy by retarding its rate of growth. This appears to be borne out by the quasi-flattened shape of the reefed peak load for approximately 1.5 seconds as shown in Figure B8 of Reference 9. An examination of Figure B15 of Reference 9 (see Figure 35) also indicates similar peak load flattening in the force tracings of the individual parachutes of the cluster. The characteristic "spike" which accompanies reefed inflation of Ringsail parachutes without attached pilot chutes (see Figure 34) is not there. The force tracing of the Gemini parachute however (see Figure 33) shows what could be interpreted as a quasi-flattened shape at the reefed peak load similar to that of the Century parachutes referenced above. The Gemini parachute however did not have an attached pilot chute. Therefore, the total effect of an attached pilot chute on Ringsail performance is still not clear and should be subject to system analysis. The following deployment options are open to the designer:

- a. Use of the drogue as a pilot chute when compatible with the system configuration and reliability goal.
- b. A free pilot chute which carries the deployment bag away with it.
- c. A permanently attached pilot chute stowed outside the deployment bag, both being retained on the apex of the main canopy with a strong bridle.

T

STANDARD RINGSAIL PARACHUTE

Symbol	Ringsail Basics					Reeling		Design Conditions				(Design)	Perf.		
	D _o (ft)	No. Gores	No. Rings	L _R D _o	λ _c /λ _T (%)	% D _o	Δt (Sec.)	Weight (lb)	Altitude (ft)	V max (EAS) (KTS)	q Lim (psf)	F _o Lim (lb)	V _e (fps)	C _D	
⚠															
◇	15.0	16	5	.89	7.2 / 17.0		(none)	200 4730 (R) 230 (DR)	7,000	200 190 134	135 120 (R) 61 (DR)	2,100	(34)	(.56)	
○	18.3	16	6	.93	3.7 / 11.2	8	6		10,000			3,000	42	.59	
□	24.1	24	7		3.7 / 10.8		(none)	200	7,000	200	135	2,500	(24)	.65	
▢	24.1	24	7		3.7 / 10.8	10	4	325	1,000	377	482	4,000	(31)	(.64)	
—	29.5	28	9	.93	2.7 / 13.0	10	4	1,650	15,000	272	250	6,200	(55)	(.68)	
▽	29.6	24	9	.93	2.7 / 14.2		(none)	270	1,000	400	542	6,700	22	.67	
△	29.6	24	9	.93	2.74 / 14.2	10/20	6/6	1,085	25,000	232	182	4,400	44.5	.67	
▽	29.7	24	7	.93	1.97 / 11.5		(none)	270	1,000	350	410	6,000	(21.6)	(.70)	
▽	37.0	32	6	1.03	12.8 / 12.2	12	3	545	1,000	351	422	7,500	25	.68	
△	40.5	40	7	.91	3.15 /	10	4	550	1,000	350	410	6,000	23.3	.66	
□	41.0	32	9	.93	2.42 / 7.8	10	2	635	1,000	351	422	7,500	24.1	.70	
—	41.0	32	9	.93	2.42 / 7.8	9	2	694	21,000	285	274	7,600	25	.70	
▢	41.0	32	9	.78	2.42 / 7.8	14	8	1,300	20,000	150	76	6,000	35	.62	
□	56.2	48	9	.97	1.94 / 7.1	10	6	950	15,000	130	57	4,500	20.5	.68	
—	56.2	48	9	.97	1.94 / 7.1	10	4	900	1,000	172	100	5,000	(20)	(.78)	
○	63.0	48	10	.92	-	11	4	1,900	15,000	217	159	8,000	26.5	.73	
○	63.1	48	10	.97	1.4 / 7.1	12	4	2,340	10,000	150	76	10,000	14.0	.91	
◇	74.2	60	12	.94	1.56 / 7.6	12	6	1,700	50,000	139	66	11,250	27.9	.75	
□	84.2	72	13	.94	1.28 / 7.7	8.3	4	2,980	12,000	205	142	10,000	20.5	.79	
▢	84.2	72	13	.94	1.28 / 7.7	10.5	8	4,400	10,000	190	120	16,000	29.6	.76	
▽	88.1	72	12	1.40	1.5 / 7.2	13	6	4,750	10,000	151	77	22,000	27.8	.85	
—	88.3	72	14	1.40	1.79 / 10.7	13	6	4,750	10,000	190	122	23,000	(27.5)	(.85)	
○	124.5	112	17	1.40	1.96 / 8.7	11.5	6	9,500	15,000	137	64	28,000	(27.8)	(.85)	
▢	128.8	112	21	1.15	2.08 / 9.8	12.5	8	M 9786	15,000	137	64	28,000	26.4	.90	
○	189.5	156	27	1.18	2.24 /	NR	8/5	L 9762	20,560	18,000	153	80	40,000	26.0	.90
														26.9	.85

(1) Average pack density

(2) With cylindrical bomb

(3) At altitudes below approx. 20,000 ft;
θ = 15-40 degrees between 20,000 - 50,000 ft

(4) Lightweight design had parts of 2 gores split

() Denotes design values not verified by test

M, L Des

Sym

N.R. = No

TABLE IX
PARACHUTES - DESIGN AND PERFORMANCE DATA

Performance				Weight		Status	References		Date		Total Number of Tests
V_e (fps)	C_{D0}	θ Avg. (\pm Deg)	$\frac{C_{DS_0}}{W_p}$ (ft 2 /lb)	W_p (lb)	δ (lb/ft 3)	(1)	Drawing No.	Program &/or Application	Design	First Test	
(34) (.56)	5	-	4.6	22	Retired - λ_T too high	62746	RP-76 Recovery I	8/57			N. R.
42 .59	5-10	29.1	5.6	-	Active	R-6204	Gemini R&R Pilot/Drogue	6/62	8/62	4	
(24) .65	-	-	7.1	22	Active	80165	RP-76 Recovery II				
(31) (.64)	-	-	8.3	22	Inactive	R-3656	Redstone FITR				
(55) (.68)	5-10	-	14.0	22	Inactive	66850	Test Vehicle Recovery				
22 .67	7	38.6	11.9	22	Inactive	R-3220	Skysail Mod D	6/56			
44.5 .67	5	22.8	14.0	-	Active	R-5616	Asset Recovery	10/62	11/62	9	
(21.6) (.70)	10-15	-	12.2	28	In navy mart in Baker System	R-3230	Skysail Mod E	9/60			
25 .68	15-25	-	19.0	25	Retired - θ too large	R-5001	B-58 CES Recovery I	1/60	3/60		
33.3 .66	10-15	31.2	27.4	22	Retired - W_p too high	SK-7036	RP-77A Recovery	7/55	10/55	5	
15.1 .70	5-10 11 (2)	42.3	21.9	45	Operational	R-5044	B-58 CES Recovery II	5/60	6/60	33	
10.25 .70	-	47.2	19.6	-	Inactive	PDS-1859	Sud Nose Cone	7/63			
11.35 .62	6	37.0	24.0	-	Inactive	R-3877	GE E-6 Recovery	7/62			
(.68) 9	6	50.2	38.6	33	Active	R-3303	GAM-72 Recovery	5/56	7/56	14	
10.5 .78	-	-	38.6	24	Active	62341	RP-77D Recovery				
16.5 .73	6	-	53.0	31	Retired - Obsolete	33023	Q-4A Recovery	3/55	4/55		N. R.
14.0 .91	-	57.4	55.4	28	Active	R-5157	Mercury Cap. L. S.	4/59	4/59	77	
17.9 .75	5	43.0	-								
10.6 .78	5-15 (3)	46.2	73.0	38	Operational	R-4444	Lockheed E-5 Recovery	8/60	9/60		
10.5 .79	-	42.2	104.3	-	Inactive	R-4177	Q-4B Recovery Backup	10/59			
9.6 .76	7	41.9	101	22	Active but obsolete	R-6220	Gemini Cap. L. S.	10/59			
17.8 .85	8	49.1	105.4	33	Retired - Obsolete	PDS-1543	Apollo Exp. I	4/62			
17.5 (.85)	-	-	-	-	Active	PDS-3120	Apollo Ext. II	12/63			
17.8 (.85)	-	-	218	22	Active	R-6853	Century I	6/63			5
14 .90	7	51.3	230	25	M	R-7811	Century II M	3/66	6/66		
19 .81	4	51.4	206	22	L	R-7812	L (4)	3/66	7/66	1	
10 .90	-	45.6	-	-	Inactive						
19 .85	2	-	557	-	Inactive		20K System				5/66

Designates medium and light construction
Symbol used in data plots (see Table XII also)

= No record

- d. Forcible ejection by thruster, mortar, ejector bag, etc., with pilot chute stowed on the deployment bag, the bag being free to separate after canopy-stretch.
- e. Any other means compatible with system operational requirements.

The geometric porosity of crown ventilation is a small but important part of Ringsail parachute total porosity. By governing the inflation rate and growth of the reefed canopy it determines the magnitude of the reefed opening load factor. The crown geometric porosity has varied somewhat erratically throughout the development period between excessively high (in small Ringsails) and unnecessarily low (e. g., Mercury 63 ft D_o), depending somewhat on how much conservatism appeared to be called for. The general downward trend of crown geometric porosity with increasing canopy diameter is shown in Figure 21. After the value of vertical tapes had been firmly established, the earlier design trend was superseded by the recommended design curve given. The use of a lower porosity crown without vertical tapes is not recommended.

Calculation of the crown geometric porosity is simplified by neglecting the area covered by the radial and vertical tapes and by the vent lines. The sum of the areas of the central vent and all of the open ringslots above $h/h_R = 0.5$ is used to define the crown geometric porosity number $\lambda_{gc} = \sum S_{gc}/S_0$. This simplified approach is useful for comparison of one Ringsail design with another but should not be applied as a general criterion.

It will be recognized that there is a sound theoretical basis for the difference in performance between small and large scale parachutes (Reference 14). The size effect (increase in C_{D_0} with D_o) can be accounted for. Reference 24, indicates an increase in C_{D_0} with D_o for extended skirt and conical canopies, and Ringsails apparently follow the same pattern. Also, some of the differences in performance between the Ringsail and other parachute types can be explained on theoretical grounds. The following considerations derived from both theory and experiments are pertinent.

Differences that can be accounted for (plausibly explained):

- a. The relative elasticity of the parachute structure increases with scale (Reference 14).
- b. The unit loading of parachute suspension lines and canopy radials (W_S/N) increases with scale (when N/D_o is approximately constant).

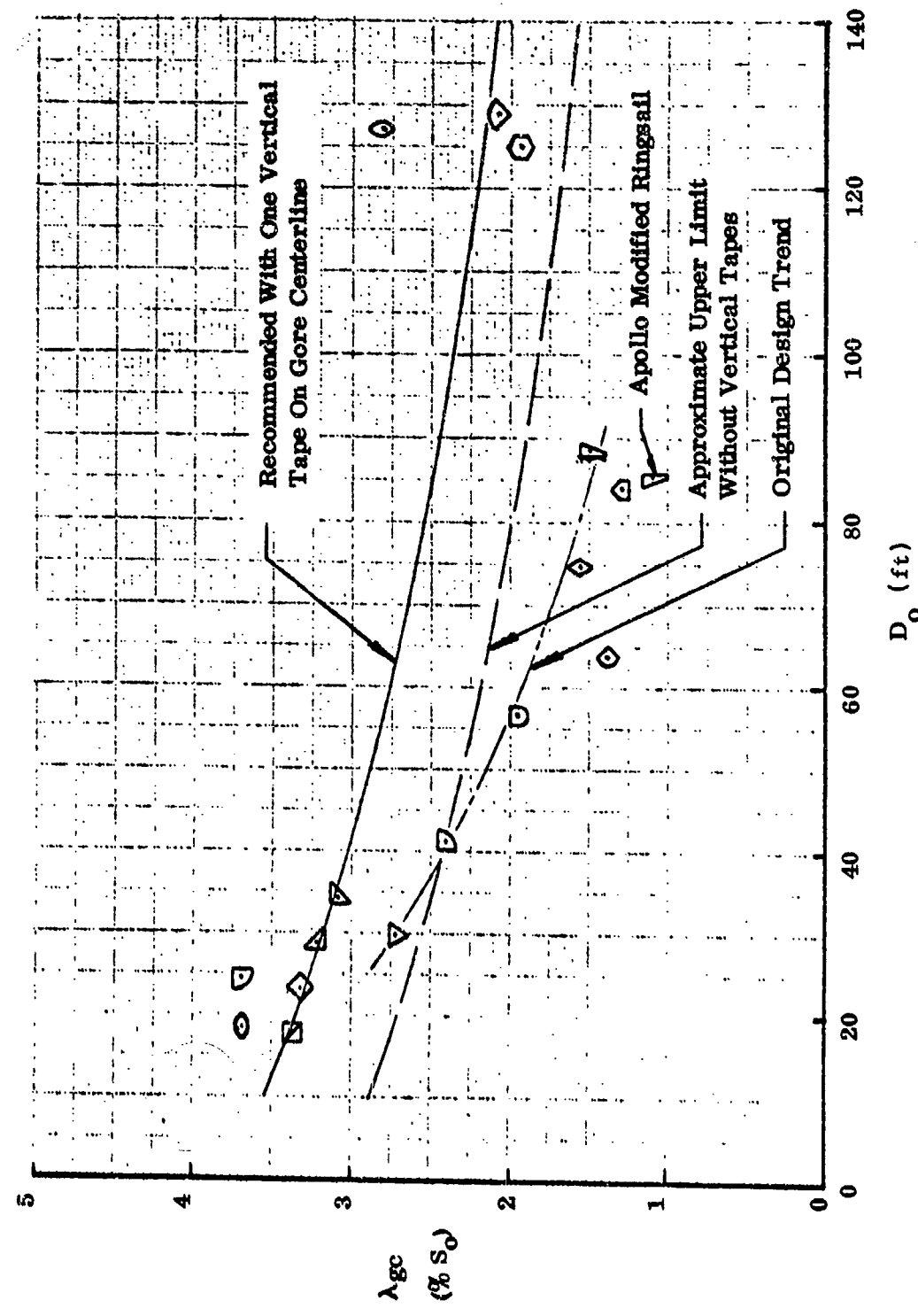


Figure 21. Ringsail Geometric Porosity of Crown Ventilation

- c. The relative porosity of the canopy may increase with scale due to (a) above.

Differences which are theoretical:

- d. The bulbous development of the canopy at disreef accelerates canopy growth and shortens the final filling interval.
- e. The contribution of skin friction to total canopy drag is augmented by the surface roughness produced by the differential fullness in sail leading edges.
- f. Resistance to air through-flow is greater in crescent-shaped slots than in rectangular slots due to increased interference flow in the sharp corners.
- g. The positive angle of attack of the sails promotes continued filling through the side slots during the reefed interval.
- h. The flared skirt augments the radial component of the opening forces acting on the canopy.

The scale effects may combine to produce a larger increase in canopy drag area than is lost to reduced through-flow resistance, the result being a net gain in total drag coefficient with increasing scale. Augmented canopy roughness undoubtedly accounts for an increment of Ringsail drag coefficient over that of other canopy types such as a Ringslot parachute of equal total porosity and/or stability of descent. Another increment would be accounted for by the effect of augmented radial forces on the projected area of the fully inflated canopy. The accelerated filling rate after disreefing would account for an increment of Ringsail opening load factor over that of other canopy types of equal total porosity.

Some thought has been given to the measures that might be taken to further improve the Ringsail design, i. e. :

- a. To make its performance more repeatable and hence more predictable.
- b. To make it adaptable to requirements for different inflation rates, slow as well as fast.

For example, the wind tunnel tests of Reference 15 showed that pocket bands regulated initial opening of the canopy mouth so that filling started earlier. This, through elimination of random delays, would make the reefed filling time more repeatable about its minimum value. Pocket bands were installed for this purpose on the small Ringsail target canopies of the UAR systems described in Reference 4. There is some indication that the repeatability of reefed filling was improved, but numerous changes in system parameters diluted the data. The addition of pocket bands to new Ringsail parachutes is recommended for serious consideration when improved repeatability of canopy inflation is desired.

Another direction for Ringsail design improvement was suggested by the two opening modes exhibited by the Century Ringsails in the seven single canopy tests performed. These modes were called "hard" and "soft" rather than "fast" and "slow" because there was no consistent relationship between the magnitude of the opening loads and the filling time after disreefing. Rather, the correlation appeared to be with the shape assumed by the canopy mouth as it expanded after disreefing. The soft opening mode resulted when the mouth assumed a roughly symmetrical shape of large lobes alternating with infolded flutes extending up the canopy to the crown (e.g., Figure 16). The hard opening mode resulted when the lobulation and infolding was grossly unsymmetrical. Because the soft opening mode occurred spontaneously in two of the seven tests, indications are that a relatively minor modification of the skirt shape might convert it to a wholly repeatable process. The specific modification contemplated was to invert N/8 skirt sails in four equal groups spaced N/8 sails apart, the purpose being to induce the formation of a symmetrical pattern of four flutes and four lobes in the expanding canopy by varying the radial force components on alternate zones of the skirt. This concept still appears to merit experimental investigation.

Finally, the question of what can be done with the Ringsail to improve its cluster performance must be answered. As noted, theory suggests that non-synchronous inflation effects could be mitigated (but not eliminated) by a reduction in the peak and average deceleration levels of the system. This is synonymous with increasing both reefed and disreef filling times substantially, something the modified Ringsail of the Apollo ELS cluster does only in part; i.e., the disreef filling time was increased roughly 50%, the reefed filling time was shortened due to the reduction in bulbous development and the test evidence shows that the net overall benefit was small. The main problem with any increase in filling time is that the methods used seriously degrade drag efficiency. Another problem arises from the current military requirement for a fast opening cluster in which the time from deployment

to full open steady descent must be a minimum. Theory also suggests the strong probability that a fast opening cluster of any type of parachute will exhibit the effects of nonsynchronous inflation in exaggerated form, with no predictable opening time from one operation to the next.

SECTION 3

PERFORMANCE CHARACTERISTICS

The performance of standard Ringsail parachutes in single canopy systems is well established by test data from many programs. The performance of Ringsail parachutes in clusters was derived primarily from the Apollo program since only one other adequately instrumented test was performed, that of the Century Ringsail program. Some data applicable to single canopy systems at high rates of descent was obtained from Reference 4 for Ringsail target canopies functioning as Stage I drogue chutes in the UAR system (see Appendix B).

Since all Ringsail performance data is derived from full scale aerial drop tests, the common types of data plots obtained from wind tunnel tests such as static stability coefficients as a function of canopy angle of attach are missing. (The results of very small scale model tests reported in Reference 21 cannot be accepted as valid for comparative evaluations because the test specimen was not a faithful scale model in respect to number of gores, canopy shape, or sail fullness).

3.1 DRAG COEFFICIENT

3.1.1 Effect of Unit Canopy Loading ($W / C_D S_o$)

The variation of Ringsail drag coefficient with unit canopy loading is presented in Figure 22 in the familiar form expressed as a function of rate of descent under standard sea level conditions. The actual variation with air-speed is slight, if any, and cannot be detected by present methods. The effects of varying both effective suspension line length and canopy scale are indication but the data scatter yields only a rough correlation at best. Most of the small parachutes performed below the desired norm, while the century series and 20K parachutes exhibited remarkably high drag coefficients. Even the 128.8 ft D_o' model that descended with a split gore fell on the norm expected for $l_e/D_o = 1.15$, while the two-canopy cluster (indicated for reference by the double symbol) gave $C_{D_o} = .84$. These were the averages for single tests, however; only the solid curves are faired through data points which are mainly the averages for many tests.

3.1.2 Effect of Scale

The variation of Ringsail drag coefficient with nominal diameter presented in Figure 23 exhibits characteristics which are closely related to those of the conical and extended skirt parachutes. The conical parachute C_{D_o} ranges

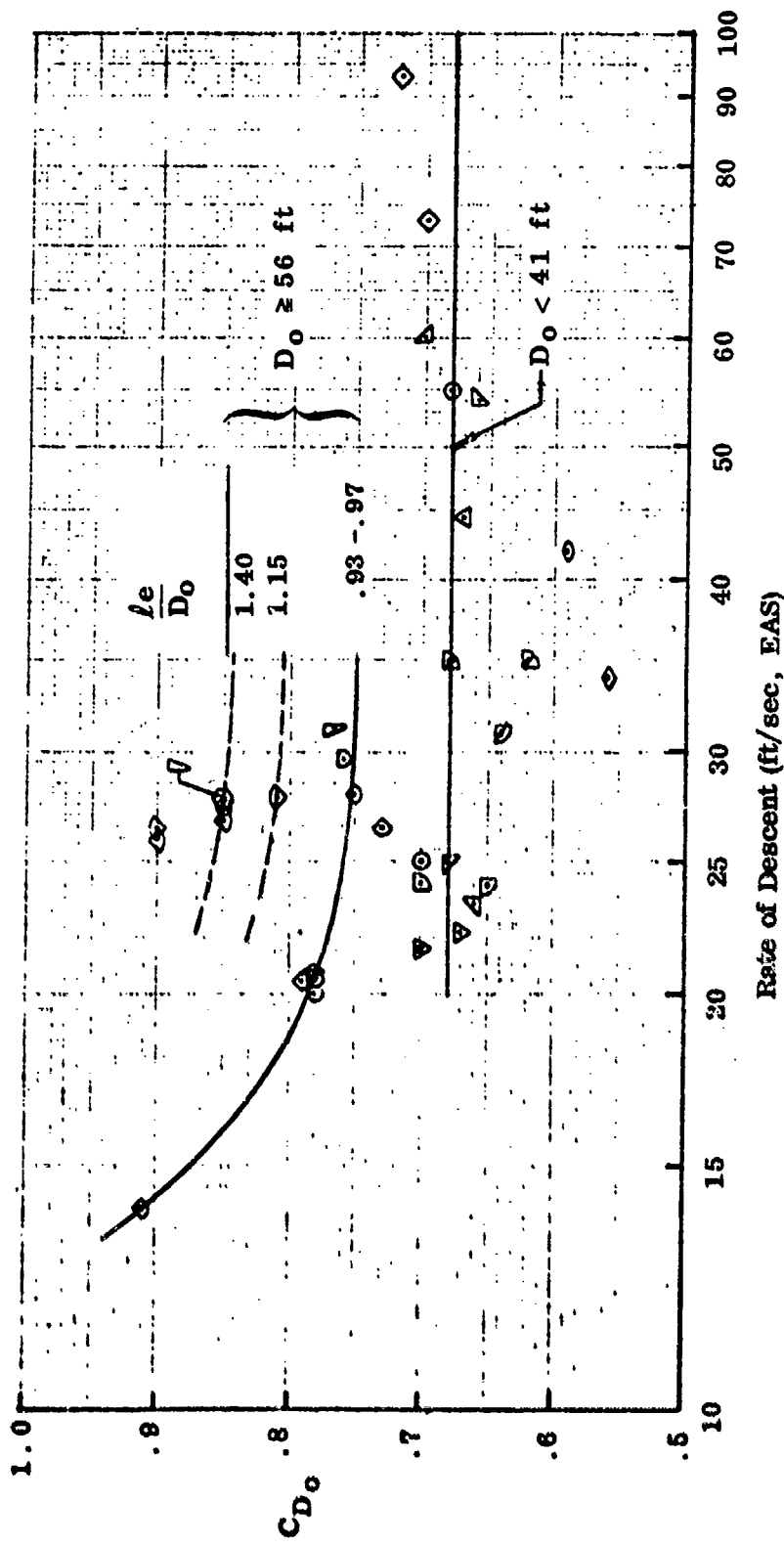


Figure 22. Variation of Ringsail Drag Coefficient With Unit Canopy Loading and Effective Line Length

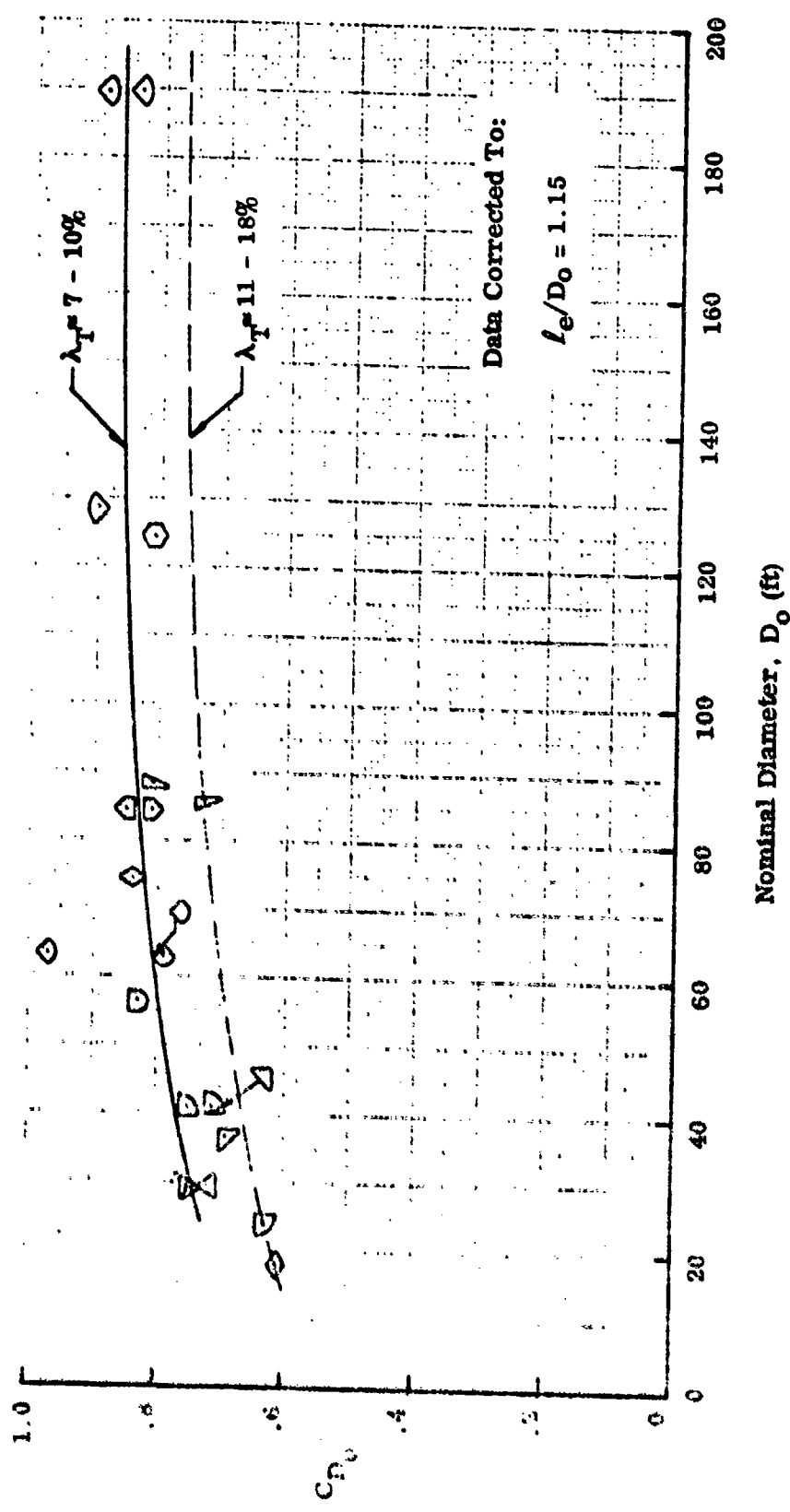


Figure 23. Variation of Ringsail Drag Coefficient with Scale

from 0.62 to 0.95 depending on size, cone, angle, suspension line length and rate of descent. The extended skirt parachute C_{D_0} also varies with size, rate of descent and suspension line length. The data presented in Figures 22 and 23 show this same effect for the Ringsail parachute.

3.1.3 Effect of Suspension Line Length

The variation of Ringsail C_{D_0} with the effective length of the suspension lines ($l_e = l_s + l_R$) is shown in Figure 24a corrected to $v_e = 28$ fps and to $D_0 > 50$ ft using Figures 22 and 23 respectively. The faired curve may be considered representative of Ringsails having nominal diameters in the range of 50 to 100 feet approximately. The two curves for l_e/D_0 of 1.15 and 1.40, is consistent with the data derived from the century series Ringsail program wherein increase is C_{D_0} with size and increased line length was obtained.

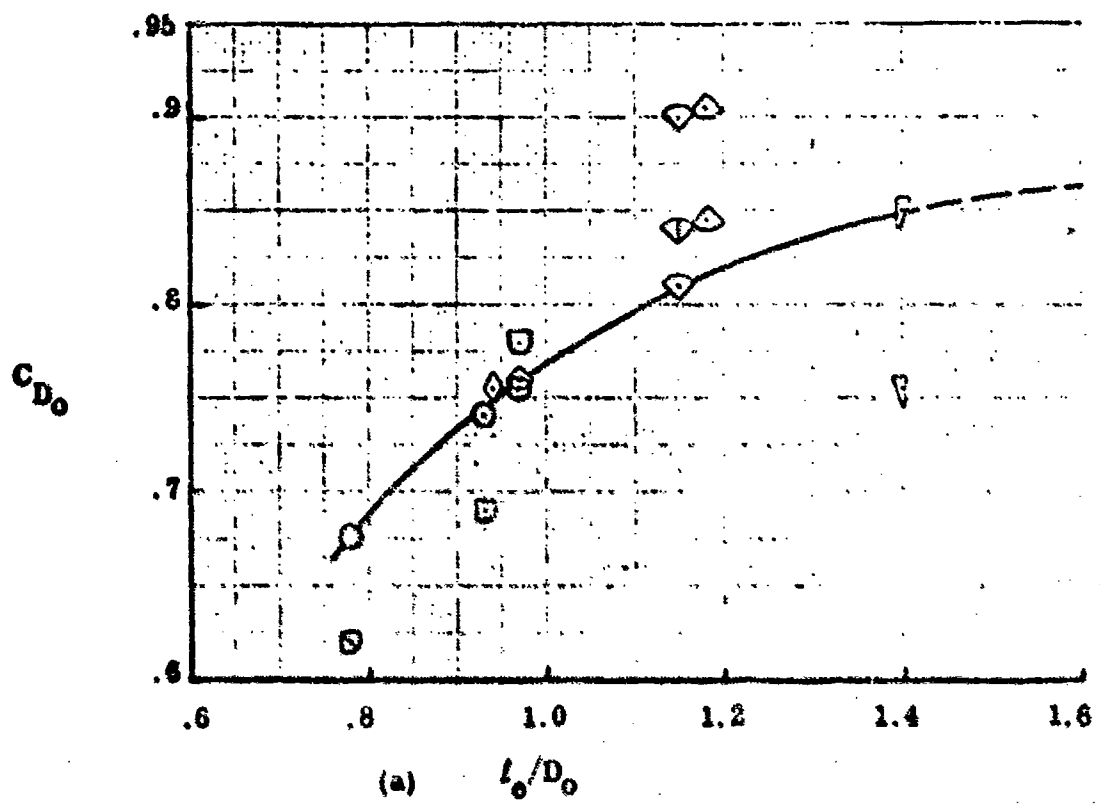
The faired data have been normalized in Figure 24b relative to $l_e/D_0 = 1.15$ with $C_{D_0}^* = 0.81$ as representative of the optimized lightweight Ringsail design. As developed, $C_{D_0}/C_{D_0}^*$ vs l_e/D_0 should be essentially invariant with scale over the entire range of parachute sizes. From this relationship it was shown in Reference 5 that the length ratio for a minimum weight parachute was $l_e/D_0 \approx 1.15$ for $D_0 = 128$ ft. A similar analysis in Reference 35 showed the optimum length ratio to be $l_e/D_0 = 1.72$ for $D_0 = 183$ ft.

3.1.4 Effect of Canopy Porosity

The 88.1 ft D_0 canopy of the Apollo ELS development program was the only Ringsail model in which a wide range of porosities was evaluated in adequately instrumented tests. However, the porosity variation was simply the effect on the geometric porosity of the crown area of removing different fractions of the width of ring number 5. The only raw data reported were average rates of descent from drop tests made with constant weight. The effect on C_{D_0} of the changes in crown porosity were deduced from the relationship

$$C_{D_0}/C_{D_0}^* = (v_{eo}/v_e)^2$$

The data and results are summarized in Table X and plotted in Figures 25(a) and (b).



(a) l_0/D_0

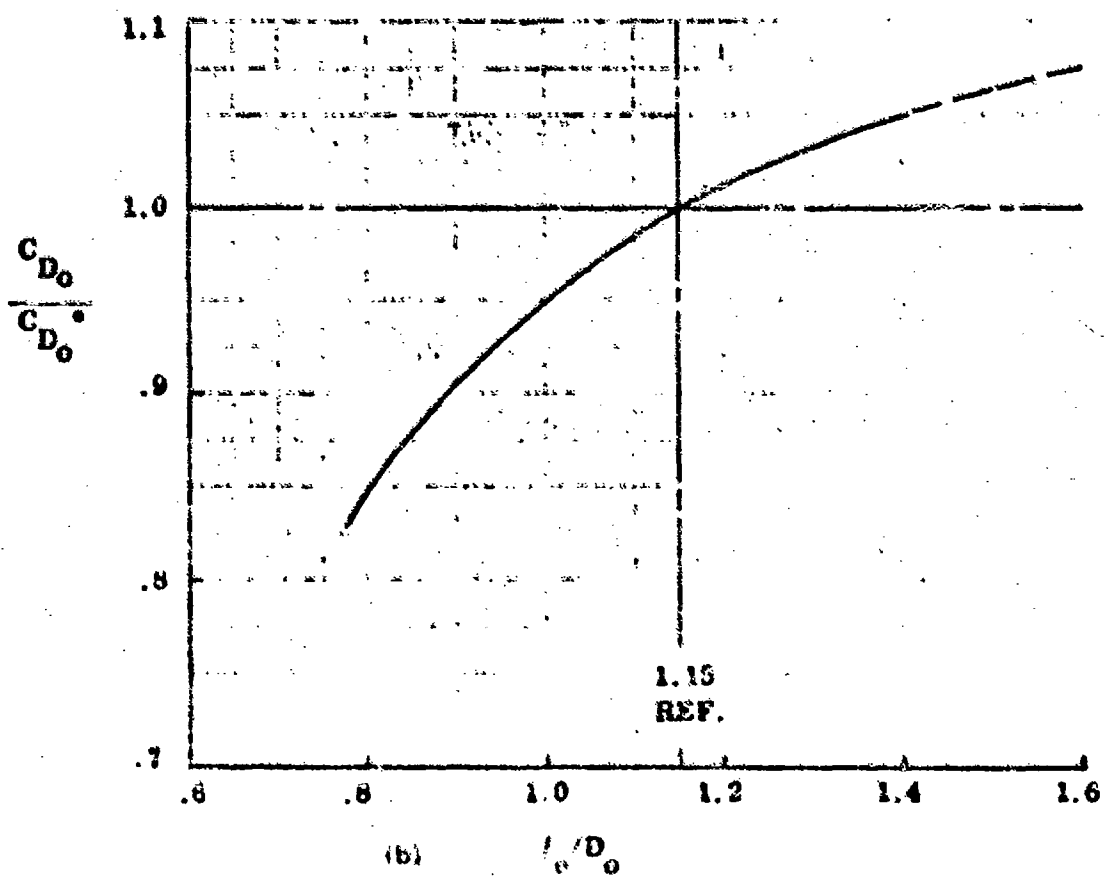


Fig. 24. Effect of Suspension Line Length on Ringall C_{D_0}

TABLE X
EFFECT OF CROWN POROSITY ON C_{D_0} OF 88.1 ft D_0 RINGSAIL

Fraction of Ring 5 removed, (% h_w)	0	50	75	100
Area of Slot 4-5 (S_s) (% S_0)	0.281	3.421	5.111	7.050
Crown $\lambda_{ge} = S_s + 1.22$, (% S_0)	1.59	4.64	6.33	8.72
Avg measured v_e , (fps)	30.0	31.1	32.1	33.2
Ratio v_{eo}/v_e	1.00	.964	.935	.904
Calculated $C_{D_0}/C_{D_0}^*$	1.00	.930	.876	.812
Average C_{D_0}	.85	.79	.745	.69

Because the accuracy of these data is uncertain and the porosity variation strictly localized in the crown of the canopy, Figure 26b should be viewed more as an example than as a basis for design.

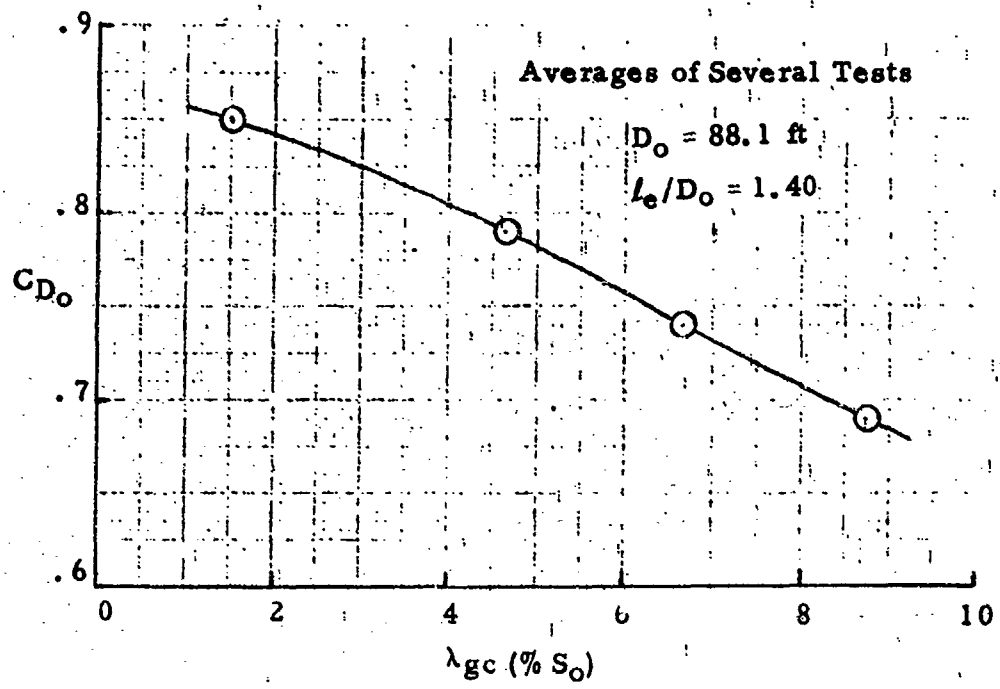
3.1.5 Variation in Rate of Descent

Parachute drag coefficients are derived from rate-of-descent measurements. The rule-of-thumb variation in parachute rate of descent used for Ringsail design to meet a specified maximum rate of descent was ± 6 percent. A study of rate-of-descent data from the Mercury, Gemini, and Apollo parachute development programs reported in Reference 19 produced the evaluation of standard deviations presented in Table XI. It will be seen that the rule-of-thumb variation used is approximately ± 6 for one and two canopies and ± 9 for three-canopy clusters.

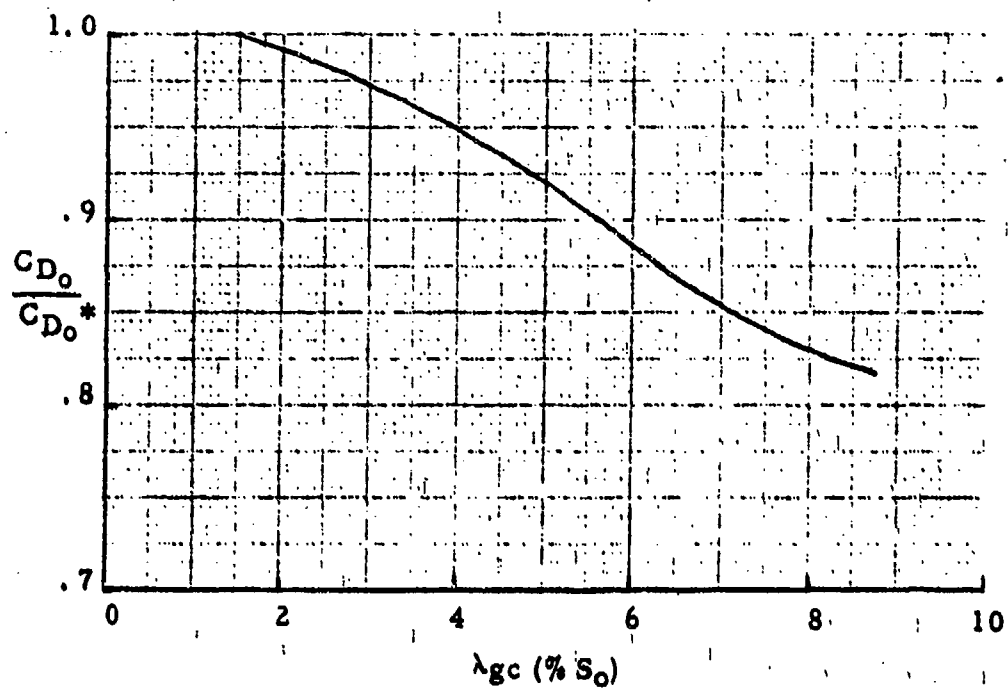
3.1.6 Effect of Clustering

The effect of clustering on drag coefficients is shown in Figure 36 as a function of the number of canopies in the cluster. The data point for the three-canopy cluster was corrected from .825 to .810, using the steps of the curves in Figure 22, to account for the difference in rates of descent.* The calculated three-canopy cluster system weight that would have the same unit loading (i.e., rate of descent) as the one and two-parachute systems is 13,850 lbs. The effective line + riser lengths were the same for all clusters ($l_e/D_0 = 1.4$) but as noted, the effective line length of the individual Century parachutes was $l_e/D_0 = 1.15$.

* For $C_{D_0} = .825$ W = 9500 lbs and $v_e = 23.0$ fps compared with $v_e = 27.8$ fps for the single and two-canopy cluster cases.



(a)



(b)

Figure 25. Effect of Crown Geometric Porosity
On Ringsail Drag Coefficient

TABLE XI

SUMMARY OF RATE OF DESCENT DATA

Project Parachute	Vehicle Weight (lb)	No. of Canopies	No. of Tests	Rate of Descent			Standard Deviation	Average C_{D_0}
				Computation Method For Average Values	\bar{v}_{sl} (ft/sec)	ft/sec		
Apollo $(D_0 = 88.1 \text{ ft})$	4750	1	7	Average of Askania v_e each 1000 ft ± 300 ft	29.9	27.8	0.85*	2.8*
	9500	2	6	Same as above	30.0	27.9	0.81*	2.7*
	9500	3	8	Askania Data each second 5000 ft to 200 ft	24.8	23.0	0.59	2.4*
Apollo (Block II) $(D_0 = 85.6 \text{ ft})$ (1)	10,950	3	4	Askania Data each second 2000 ft to 500 ft	28.5	26.5	1.22**	4.6**
	12,920	3	5	Askania Data Each Second 2000 ft to 500 ft	33.2	30.8	1.87**	6.1**
Apollo (Block II) Heavyweight $(D_0 = 85.6 \text{ ft})$ (1)	-	-	-	-	-	-	-	-
	-	-	-	-	-	-	-	-
Gemini $(D_0 = 84.2 \text{ ft})$	4400	1	16	Average Askania v_e from 5000 ft to 2000 ft	31.9	29.6	0.92**	3.1**
	-	-	-	-	-	-	-	-
Mercury $(D_0 = 63 \text{ ft})$	2160	1	34	Average of Askania v_e at 5000 ± 300 ft and 500 ± 200 ft	29.7	27.6	0.90**	3.3**
	-	-	-	-	-	-	-	-

(1) Note that S_0 is based on 83.5 ft D_0

* 5000 ft values

** Sea level values

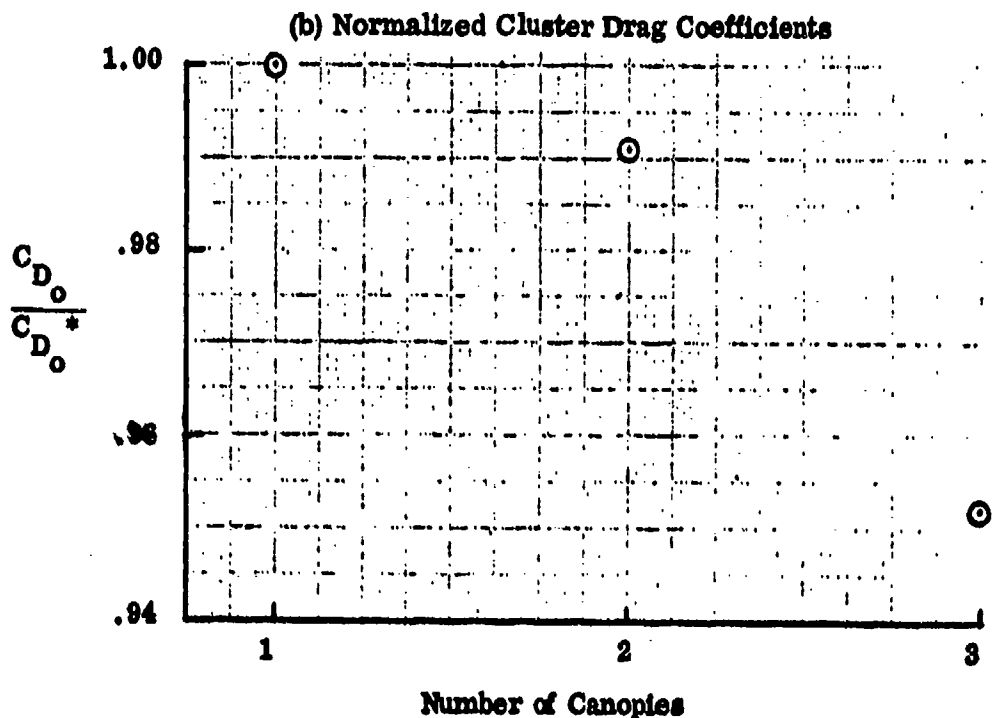
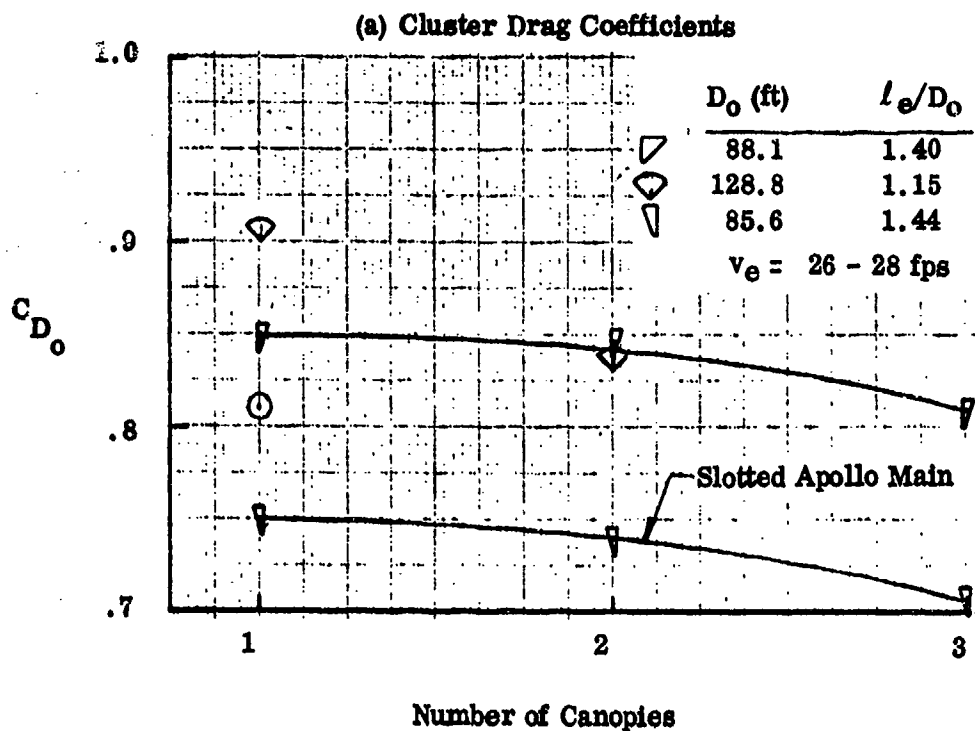


Figure 26. Cluster Effects on Ringsail Drag Coefficient

3.2 OPENING LOAD FACTORS

The opening load factor (C_k) determined experimentally by the ratio $F_{max}/C_{DS} q$ provides a convenient means of making quick estimates of the probable opening loads of a given parachute system. At best, the method yields predicted loads having an accuracy of about ± 10 percent when applied within a narrow range of speeds and altitudes. The principal sources of error are:

- a. Mensuration of parachute forces and flight conditions
- b. The element of randomness in the parachute opening process
- c. Variations in reefing line cutter timing
- d. Limitations of the analytical methods employed in the prediction of dynamic pressures at line stretch and at the end of each reefed stage.
- e. Limitations of the methods of predicting parachute reefed drag areas.

A substantial quantity of data has been accumulated over the years presenting C_k as a function of unit canopy loading (W/C_{DS}) as shown in Figure 27. In this form C_k varies widely with both altitude and dynamic pressure or equivalent air speed (EAS). The Ringsail data plotted in Figure 27 are for tests performed in the altitude range of 10 to 16 thousand feet. The faired curves indicate the general trend of C_k as a function of W/C_{DS} and EAS, but data scatter makes the quantitative effect of EAS highly uncertain. In general, higher opening load factors are associated with lower velocities (EAS) or dynamic pressures at the beginning of the filling process. The disreef data also reflect the accelerated filling rate of the Ringsail caused by the large canopy growth during the reefed interval.

The presentation in Figure 28 of measured opening load factors as a function of mass ratio (R_m) is derived from the model law developed in Reference 20. (See Section 6.3.1). This includes the effect of altitude. The general trend of the scattered data is indicated by the faired curves. The effect of the other related variables, velocity and flight path angle (Froude Number) is lost in the "noise." The sharp separation of the disreef data reflects the difference in inflation process noted above. Stage 1 reefed data should logically fair into the non-reefed data as a limit. The width of the trend-bands shown emphasizes the difficulty of applying this methods of load prediction to new system designs.

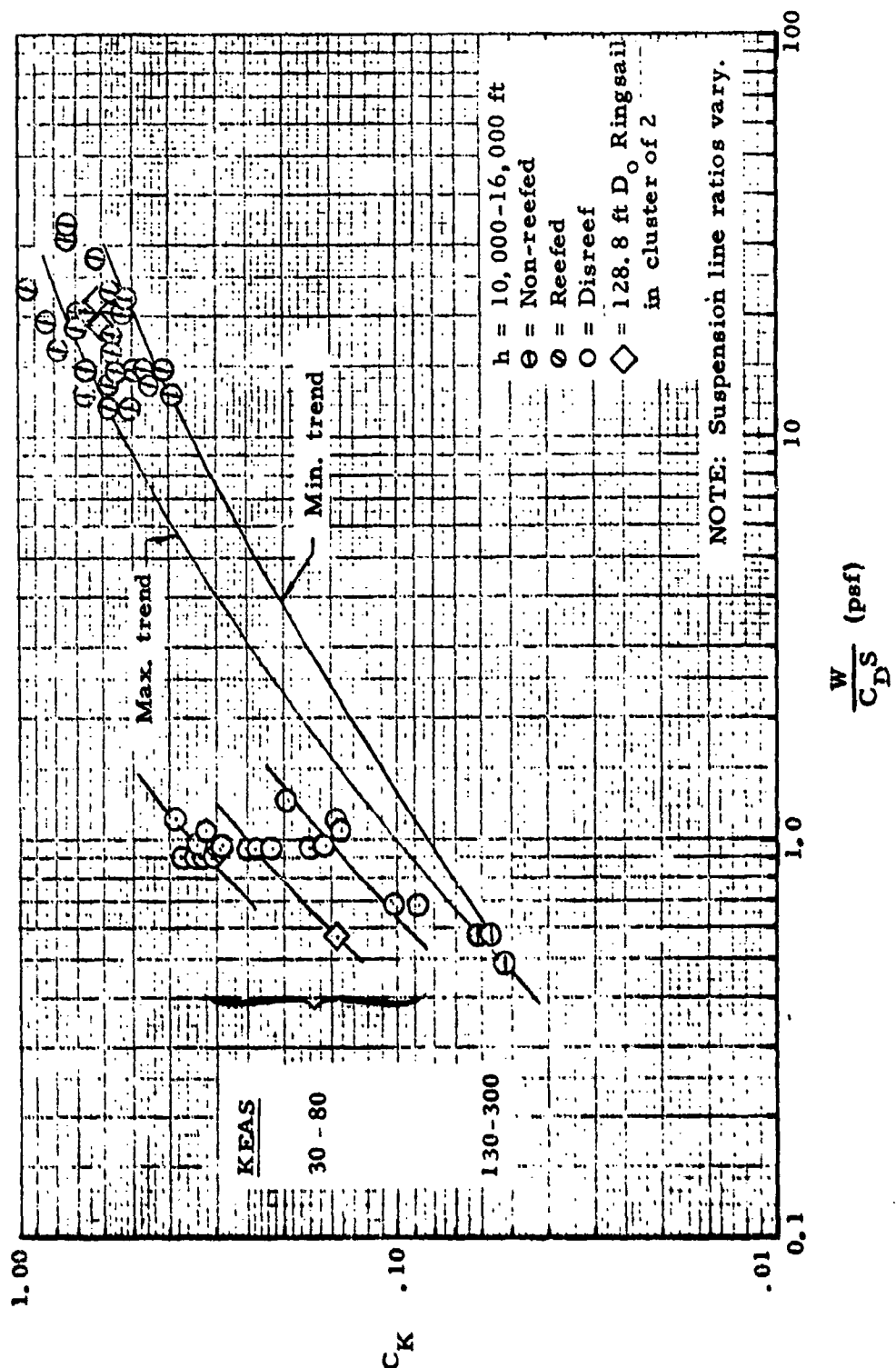


Figure 27 : Opening Load Factor (C_K) vs Unit Canopy Loading

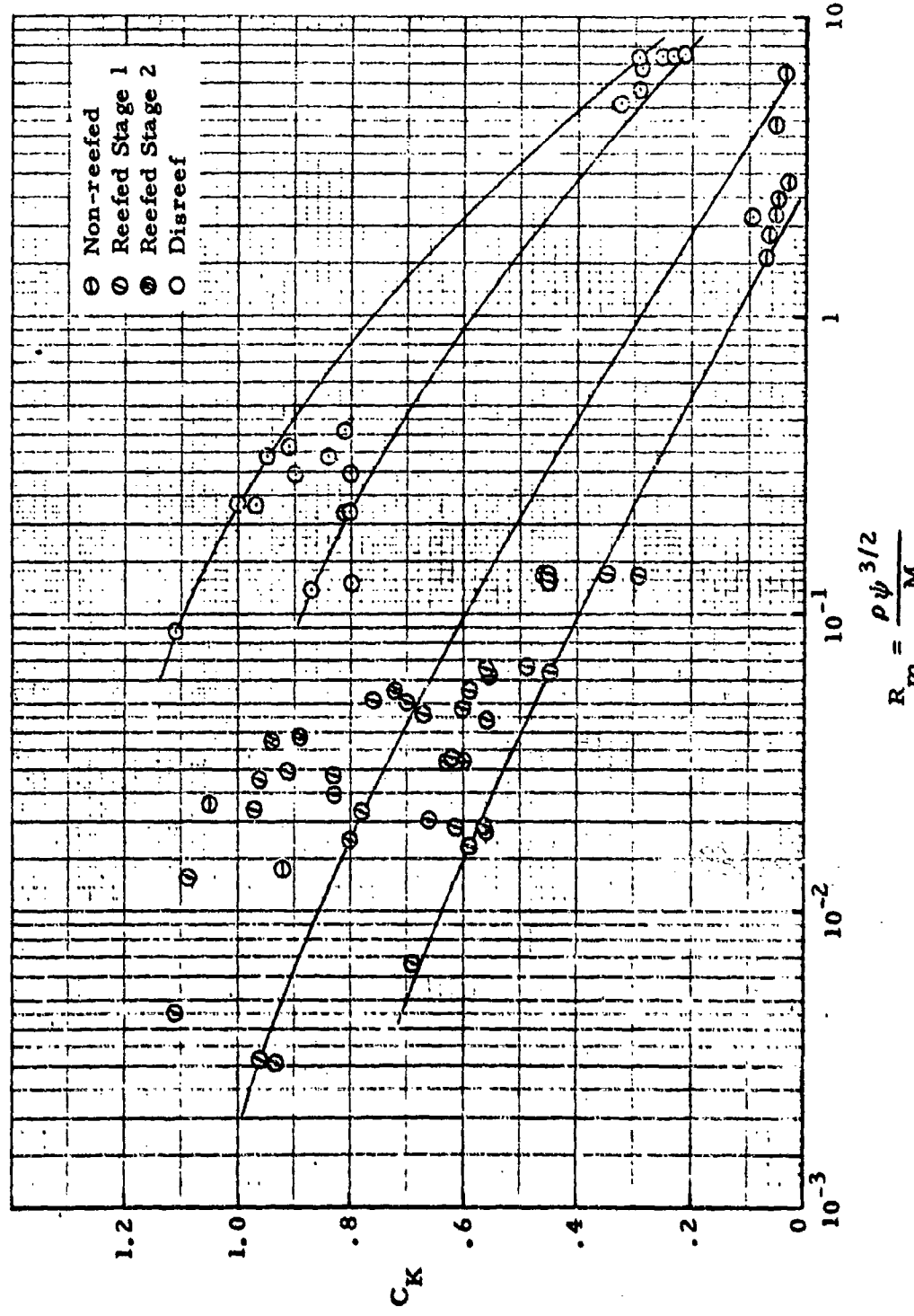


Figure 28 . Opening Load Factor (C_K) vs Mass Ratio

The apparent effect of altitude on Ringsail opening load factor, with unit canopy loading constant, is shown in Figure 29. This was derived, as illustrated, by interpolation of the data in Figure 30 to W/C_{DS} = 10 psf. The interpolation is based on the postulate previously noted that the reefed and non-reefed data points are related. Figure 30 is similar to Figure 27 with data points keyed for identification of the different Ringsail models listed in Table XII. The disreef data are irrelevant to this study and so are not shown. The symbol code does not apply to Figure 29, the points merely locating the data interpolated at W/C_{DS} = 10 psf. The ladder at 15-16 thousand feet represents the great majority of the data, and the horizontal bars indicate the altitude uncertainty of some load factor interpolations. The extrapolation of the data per the non-reefed modified Ringsails at altitudes over 100,000 feet is somewhat speculative but the broad trends shown in Figure 28 provided some guidance. The tendency for opening load factors to level off somewhere between 1 and 2 at high unit canopy loads is supported by general wind tunnel experience, i.e., "infinite mass" inflation tests. The effect of deployment velocity on Froude number has not been identifiable and no doubt contributes to data scatter along with the several sources of error cited.

Since $(g \sin \gamma)$ is also important component of Froude number, the effect of flight path angle on opening load factors is not always negligible. A computer study of this effect on the opening forces of the 128.8 ft Century Ring-sail produced the variation of C_k with flight path angle at line stretch plotted in Figure 31. With the velocity and altitude at line stretch constant, the load increases 21 percent between $\gamma_0 = 10^*$ and $\gamma_0 = 90$ degrees, while the increase in dynamic pressure is only 14 percent, the net result being an increase in C_k of 8.5 percent. Since this is within probable error tolerance, the effect on predicted opening loads would be detectable only under unusual circumstances, but obviously contributes to the variation in test measurements.

* 8-10 degrees is generally representative of parachute systems deployed from aircraft in level flight.

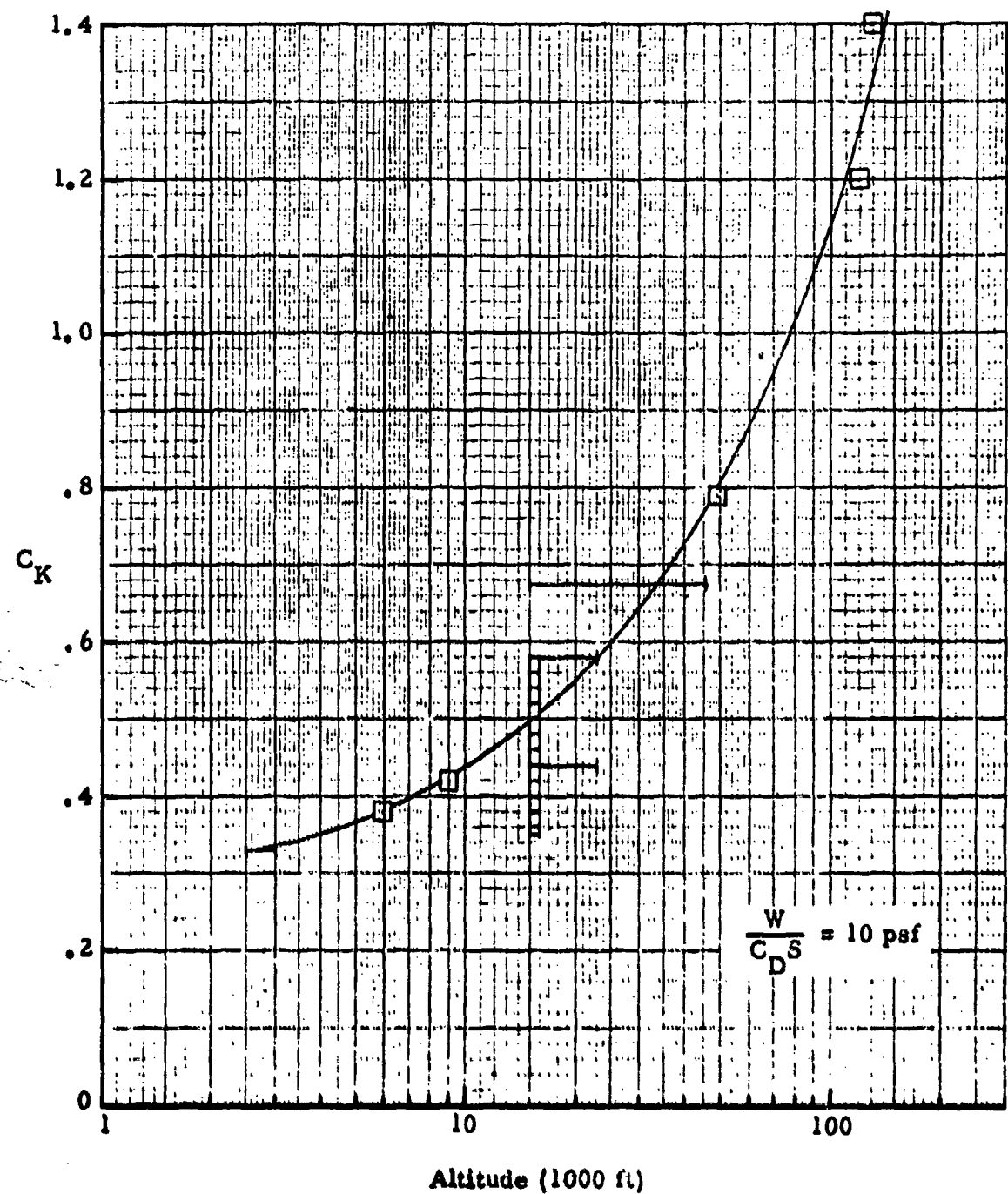


Figure 29 . Apparent Trend of Ringsail Opening Load Factor with Altitude

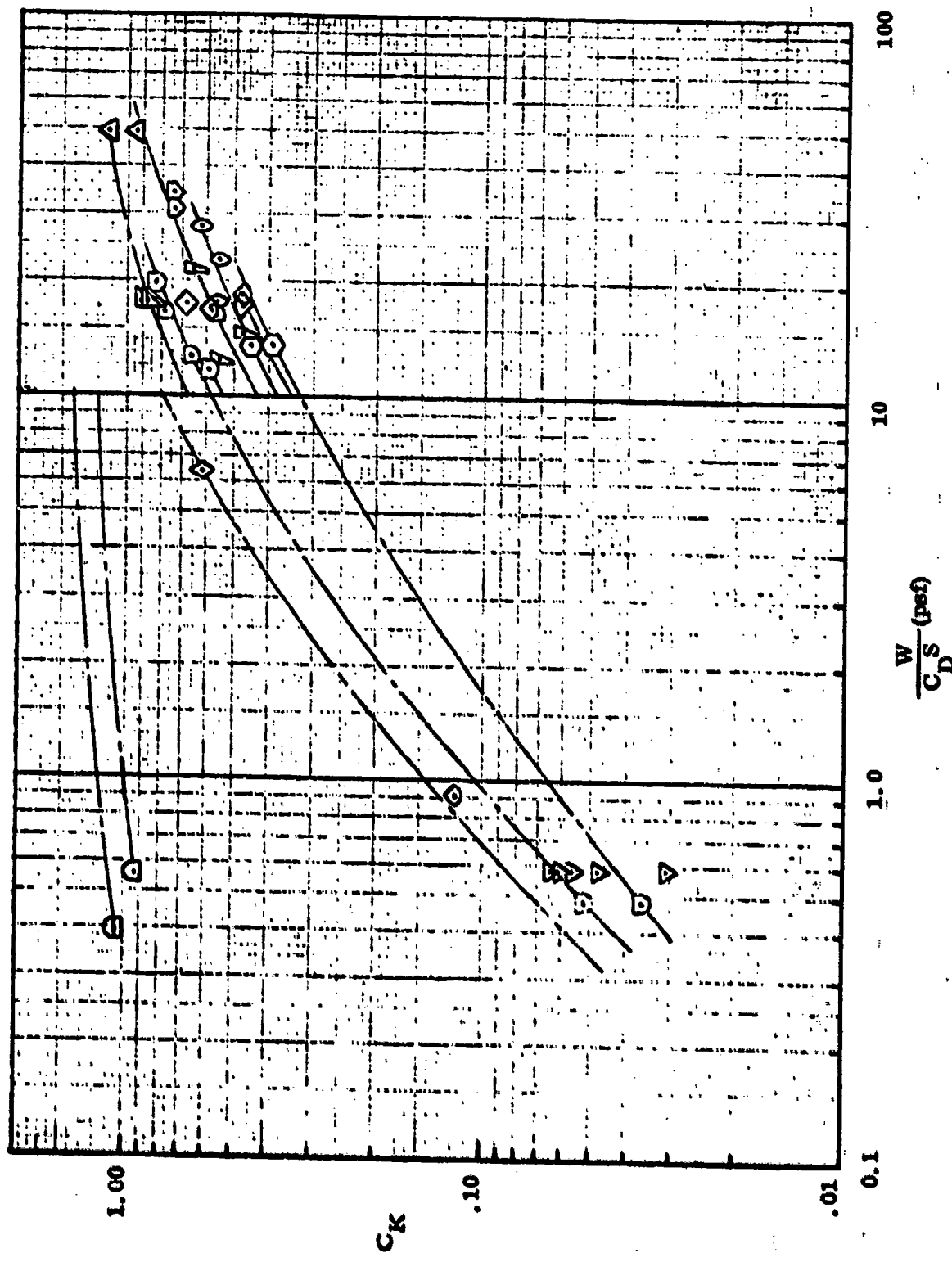


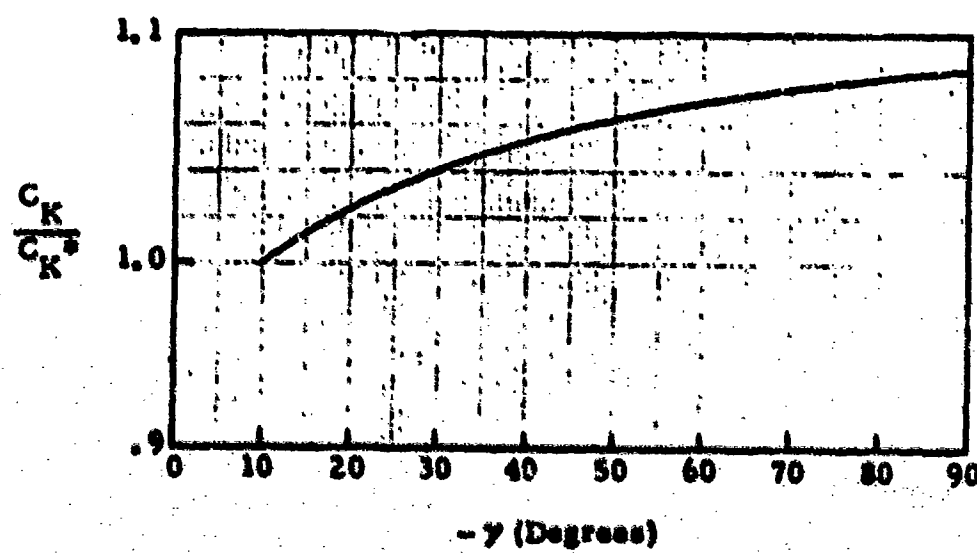
Figure 30. Ringsail Opening Load Factors at Altitude (see Table XII for Code)

TABLE XII
RINGSAIL OPENING LOAD FACTORS AT ALTITUDE

D ₀ ft	W/C _{DS} psf	C _K		Altitude Feet	Symbol
		Nonreefed	Reefed		
23.0	17.2	--	.68	46,200	◇
34.0	17.6	-- -- --	.91 .84 .87	12,560 19,660 46,630	▷
29.6	.58	.0306 .0477 .0562 .0610 .0642	-- -- -- -- --	1,100 5,000 10,000 15,000 20,000	▽
41.0	16.1 12.6 16.4	-- -- --	.56 .66 .78	15,000 22,300 22,900	▷
56.2	.48	.036	--	2,000	□
		.052	--	15,000	
	11.7 19.6	-- --	.59 .83	2,500 15,000	
63.1	.91	.12	--	10,000	◇
	18.2	--	.47	2,700	
	16.4	--	.58	10,400	
74.2	6.43	--	.61	48,800	◇

TABLE XII (Continued)
RINGSAIL OPENING LOAD FACTORS AT ALTITUDE

D _o ft	W/C _{Ds} psf	C _K		Altitude Feet	Symbol
		Nonreefed	Reefed		
84.2	33.9	--	.74	9,000	◆
	30.6	--	.74	9,100	
88.1	12.3	--	.55	15,900	□
	14.4	--	.47	15,700	
	21.1	--	.65	15,500	
124.5	13.4	--	.39	3,600	○
		--	.45	6,000	
127.0	27.7	--	.62	15,000	○
	22.6	--	.55	15,500	
	17.5	--	.56	15,550	
128.8	17.1	--	.47	15,750	◆
29.6	49.1	--	1.11 .95	15,000 26,200	△
31.2	.56	.92	--	119,500	○
54.4	.39	1.05	--	129,300	■



NOTE: Use for C_{K^*} a value pertinent to the system under consideration, when deployment is initiated in level flight.

Figure 31. Effect of Flight Path Angle at Line Stretch on C_K (Results of Computer Study of 128.8 ft D_0 Ringsail)

3.2.1 Opening Force-Time Characteristics

Opening load factors are derived from parachute force-time recordings in conjunction with system trajectory measurements that yield dynamic pressure data and canopy effective drag areas at several points of critical interest as follows:

- a. Main canopy line stretch
- b. Reefed opening and/or Fmax
- c. Disreef
- d. Fmax after disreef
- e. Full open

The way in which the opening force-time history of the Ringsail parachute varies from system to system is illustrated in Figures 32 through 38 depicting traces obtained from tensiometer recordings and telemetered force transducer records.* Figure 33 is particularly instructive because it illustrates the development of the inflated shape of the canopy at numerous points in the opening history enabling important deductions to be made about the physical events. Note that the force of the reefed canopy increases significantly while the deployment bag is still being withdrawn from the canopy. The canopy is still an elongated sock when the initial air mass reaches the apex to generate a preliminary force peak. At the peak reefed opening load the canopy development angle ($\psi - \phi$) is almost zero indicating very little tension in the reefing line (see Section 6.4.2.6). The bulbous growth of the canopy is continuous through most of the reefed interval. After disreefing, the canopy is only partially inflated when the force passes its second peak. The rebound following full inflation, attended by a dip in the force trace, clearly demonstrates the tendency of the added air mass to decelerate at a lower rate than the parachute system. (See Section 2.1.4.)

* All tests were performed at the DOD Joint Parachute Test Facility,
El Centro, California

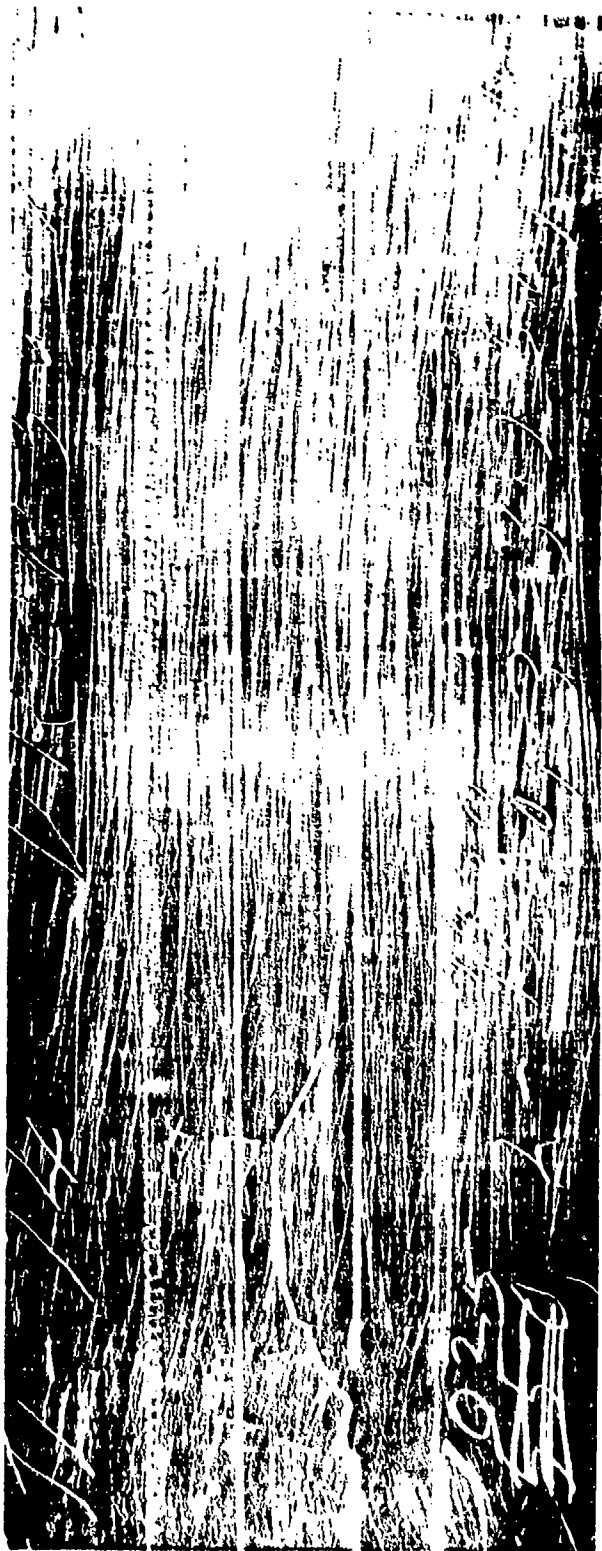


Figure 32. Enlargement of Coleman Tensionmeter Record Obtained with Non-Reefed 56.2 Ft D_o Ringsail Deployed at 130 KEAS, 15,000-Foot Altitude (Weight = 950 Pounds)

Reproduced from
best available copy.

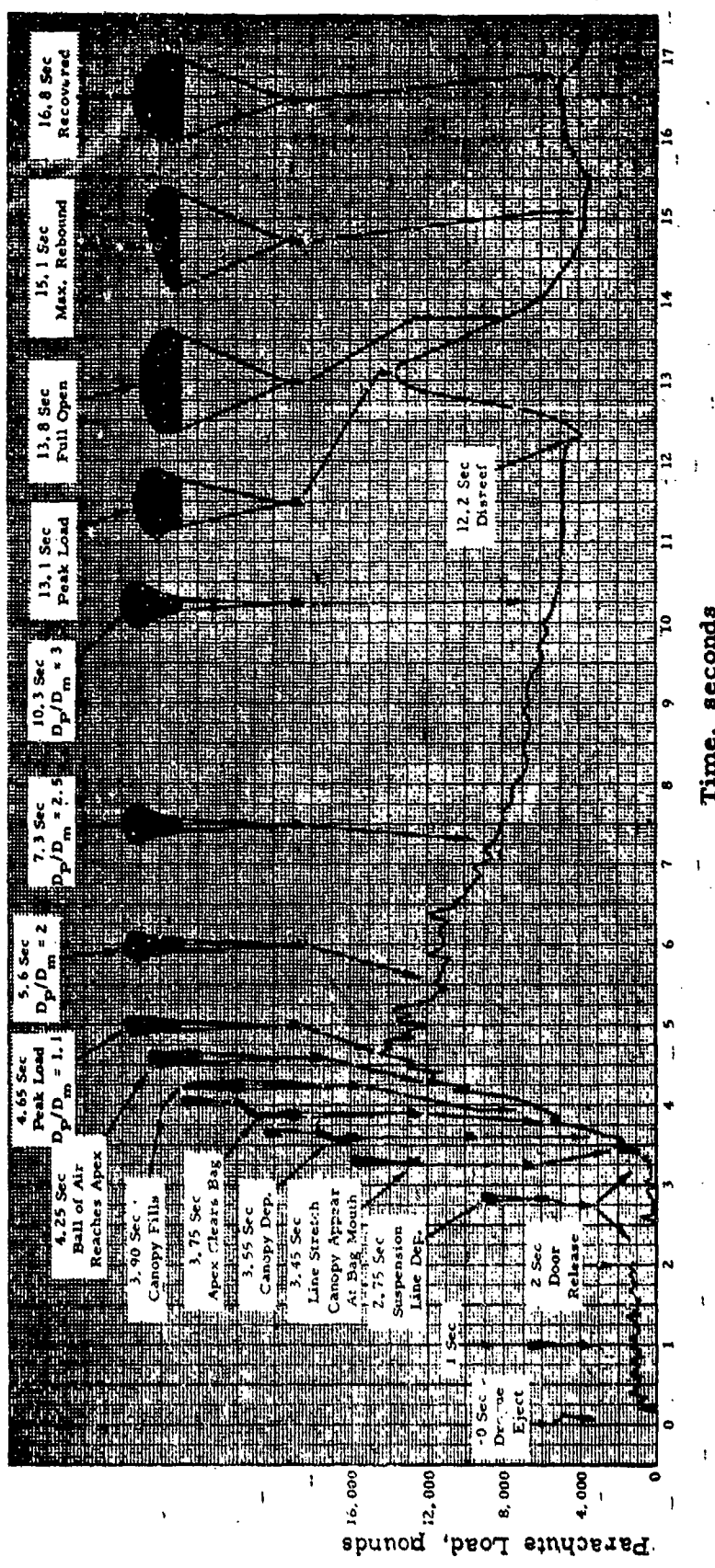


Figure 33. Opening Forces Correlated with Canopy Shape, Gemini 84.2 ft Do Ringsail Reefed 10.5% D_0 for 8 Seconds, Deployed at 272 fps (TAS) at 9630 Feet Altitude (Weight = 4450 lb)

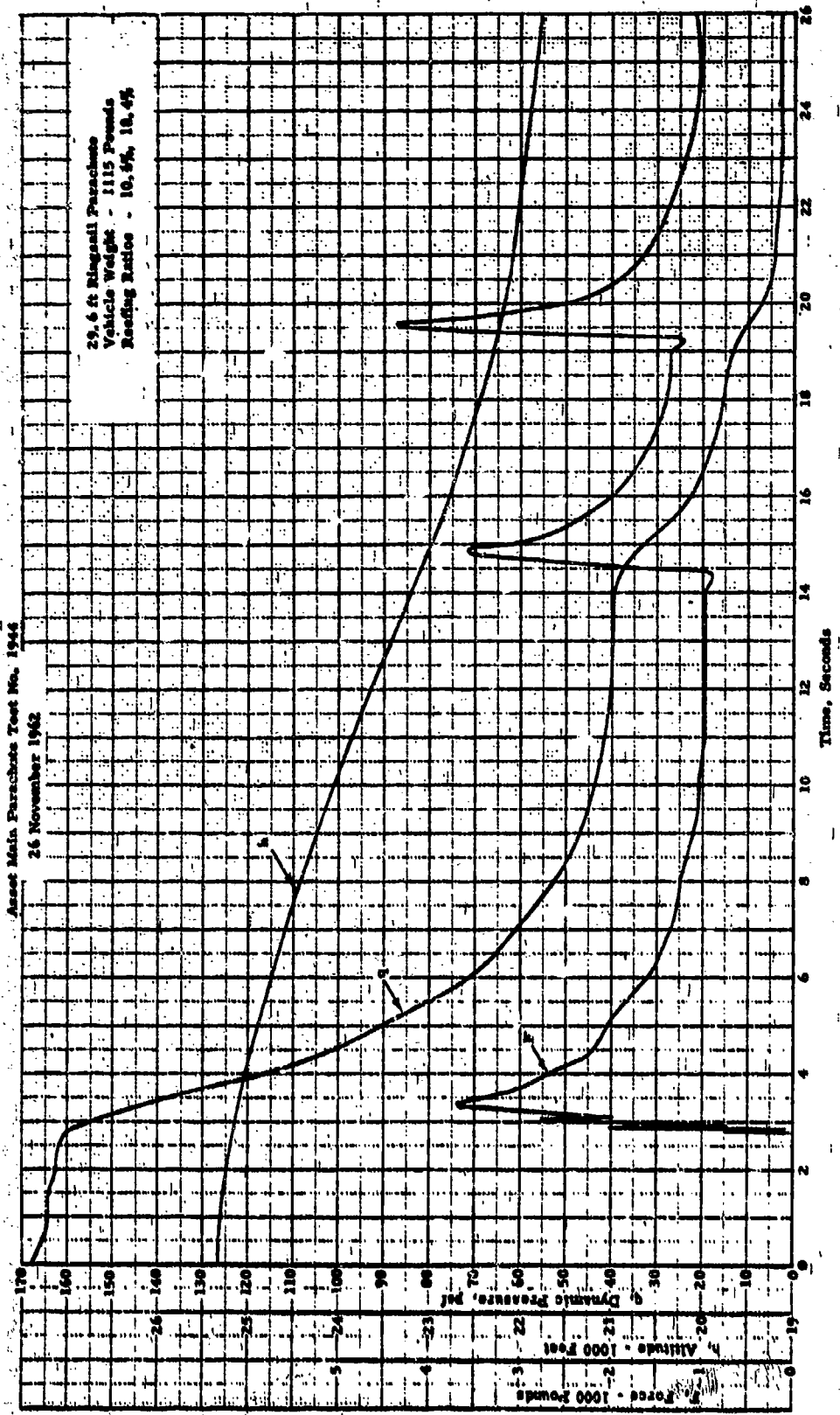


Figure 34. Opening Forces and Trajectory Data for ASSET 29.6 ft D₀ Ringtail with Two Reefed Stages

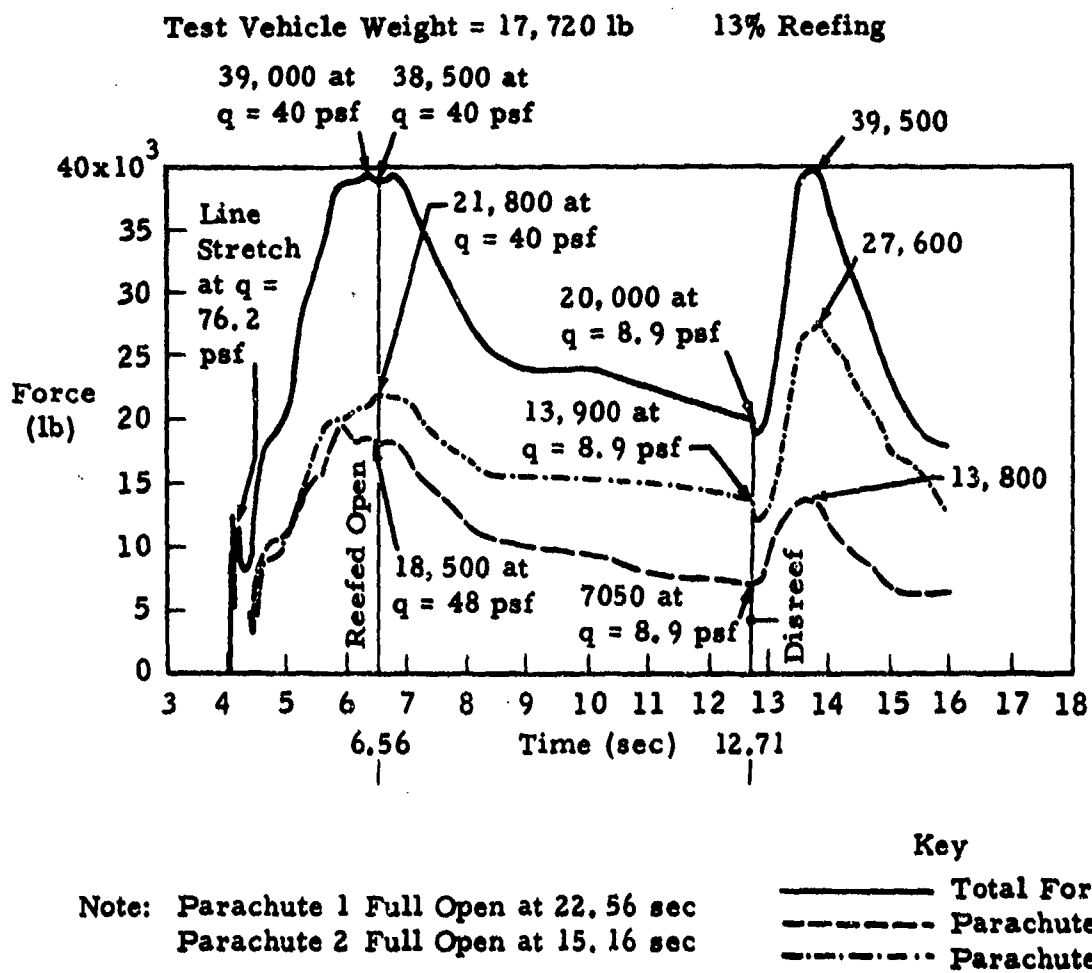


Figure 35. Opening Force-Time History for Cluster of Two 128.8 ft D_o Ringsails Reefed 13% D_o for 8 Seconds, Deployed at 299 fpm (TAS) at 10,246 Feet Altitude (Weight = 17,720 pounds)

Apollo Test 81-2

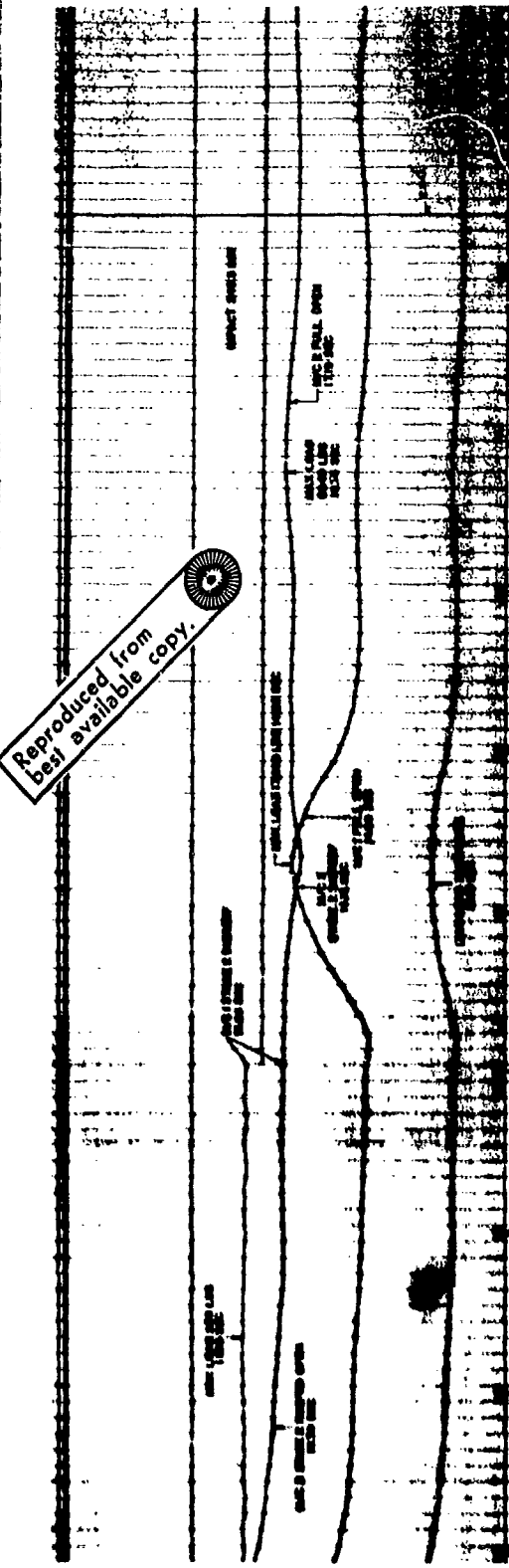
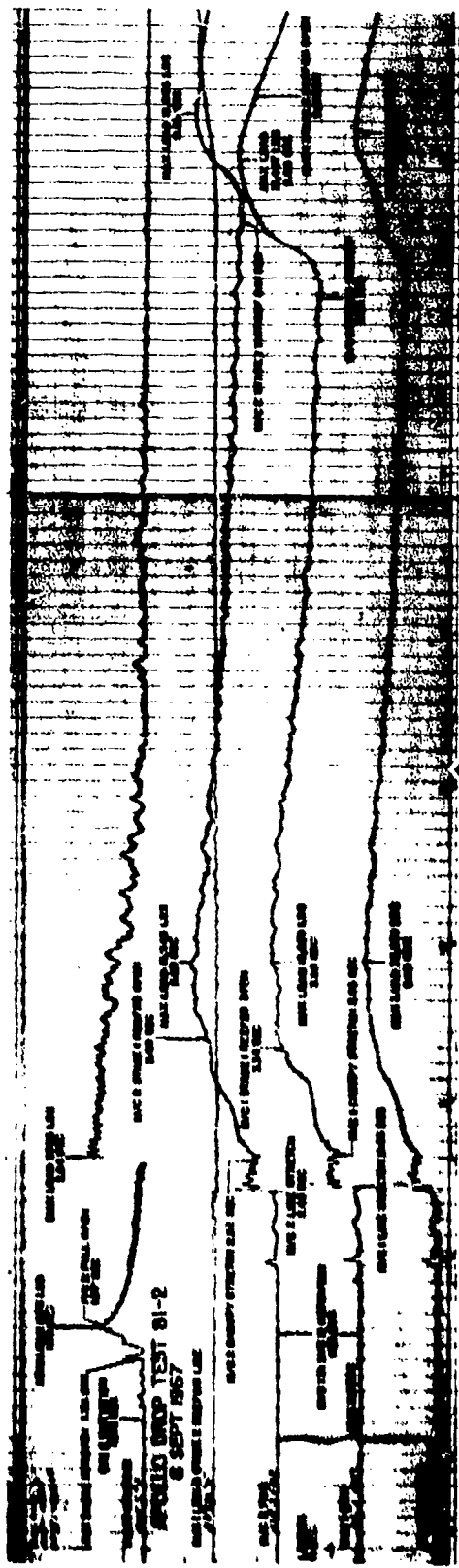


Figure 36. Opening Force - Time History for a Cluster of Two 85.6 ft D_0 Modified Ringsails with Two Stages of Reefing Deployed at 167 KEAS at 10,000 feet Altitude (Weight = 12,989 pounds)

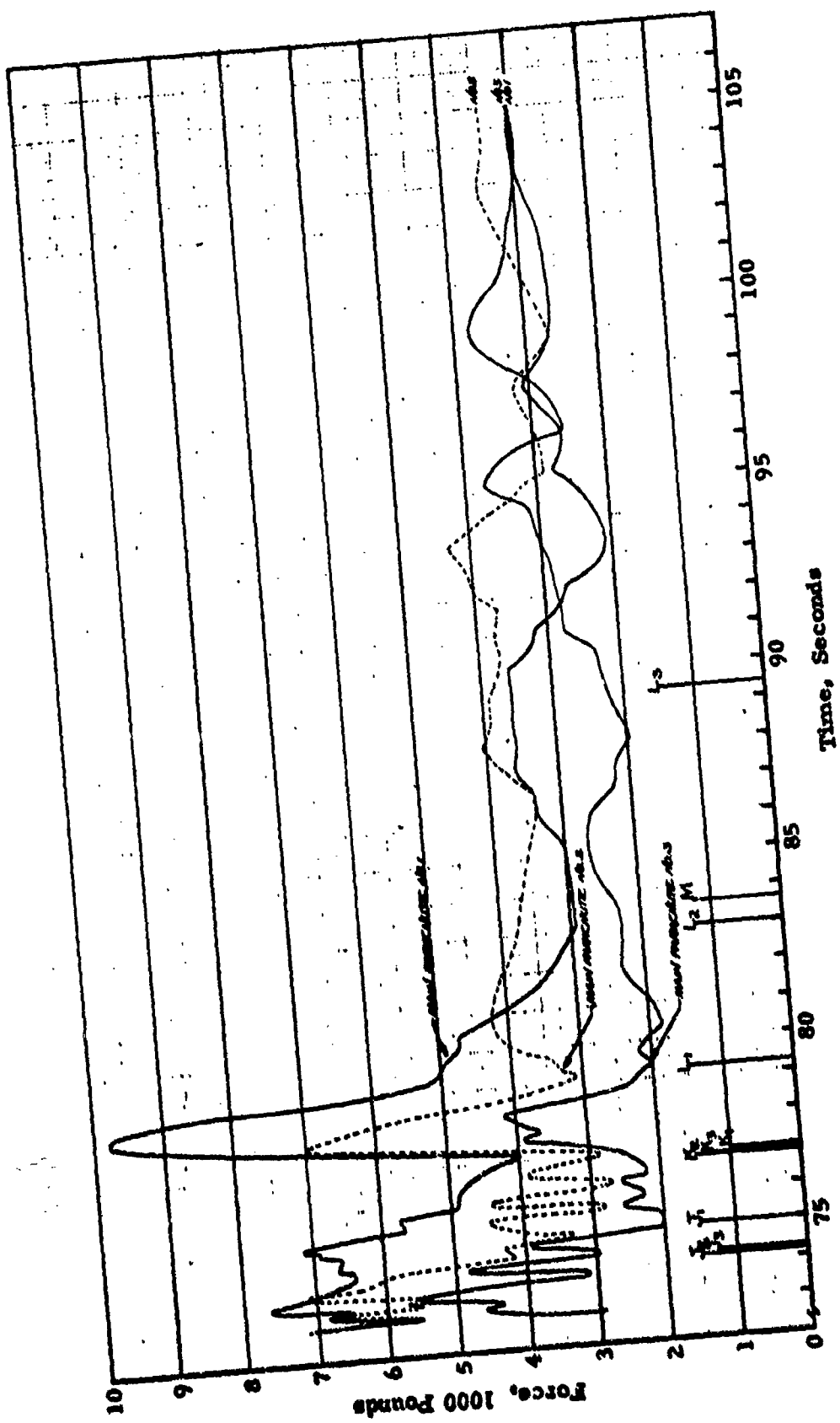
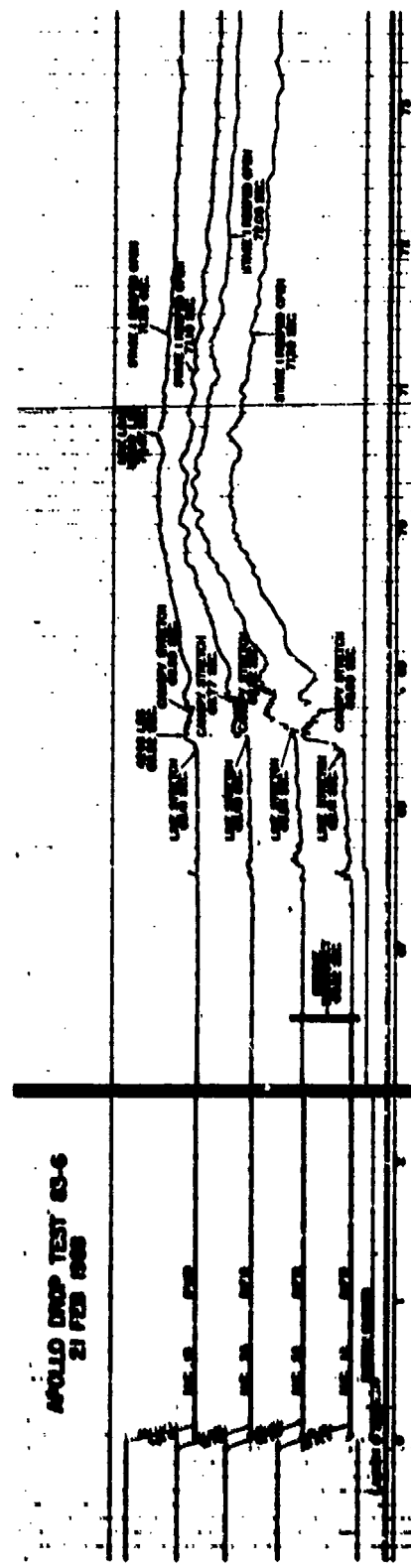


Figure 37. Opening Force-Time History for a Cluster of Three 88.1 ft D. Ringsails Each Reefed 13% Do
 for 6 Seconds, Deployed Under Simulated Abort Conditions (Weight = 9500 pounds)
 Apollo Test 50-11



90

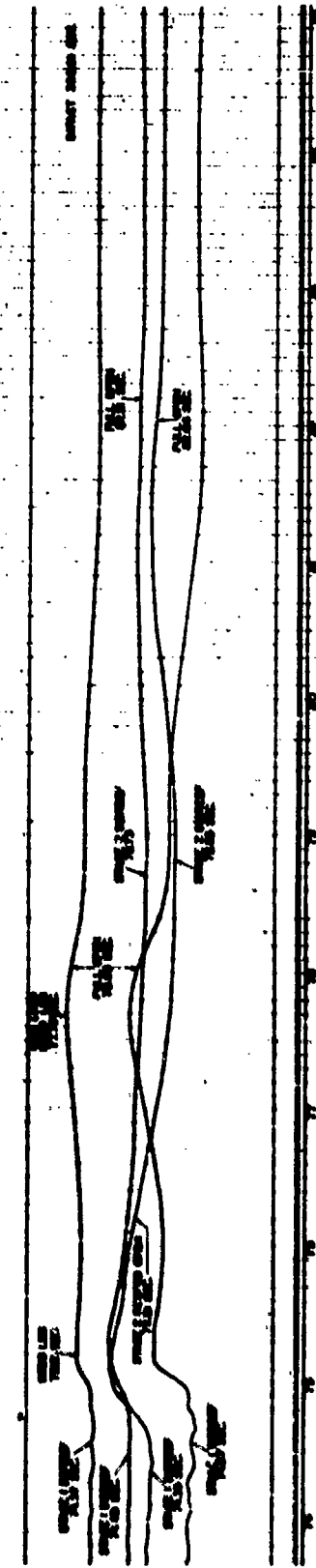


Figure 38. Opening Force-Time History for a Cluster of Three 85.6 ft D_0 Ringsails with Two Stages of Reefing (8.4% D_0 /24.8% D_0) Deployed Under 90% Design Limit Conditions (Weight = 13,000 pounds) Apollo Test 83-6

3.3 FILLING INTERVALS (TIME, DISTANCE, K_f)

3.3.1 Filling Time and K_f

Derivation of the filling time equation used in Ringsail parachute analysis is given in Section 6.2.

Test data for the filling intervals of the Ringsail parachute with one stage of reefing are given in Table XIII in terms of time and the dimensionless constant, $K_f = \Delta t_f v_1 / (\psi_2^{1/2} - \psi_1^{1/2})$, along with those of the 85.6 ft D_o modified Ringsail used in the Apollo Block II system. Evaluation of a good average for the latter parachute was handicapped by the lack of adequate data. However, a comparison of the average values of K_f obtained shows a 30 percent shorter reefed filling interval and a 54 percent longer filling interval after disreefing, which confirms the estimate made (page 50), that the reefed filling time was shortened and the disreefing filling time increased by 50%. The data given in Table XIV show that when the same parachute is reefed in two stages, K_f for the first and final stages is altered significantly. The stage 1 filling characteristic approaches that of the unmodified models and the filling interval after disreefing becomes shorter; both are close to 91 percent of the averages for the standard Ringsail. Of course, the magnitude of the stage 2 reefing ratio is the governing factor and its effect needs to be determined over a broader range.

Data for the leading canopy of the Century Ringsail cluster are included in Table XIII because it appears to have filled at the normal rate. This was not the case for selected Apollo cluster tests examined and so may be an atypical event.

3.3.2 Filling Distance

The actual distance traveled by the parachute while it is filling may be a matter of critical importance in low altitude operations. Measured filling distances of two Century Ringsails and the 85.6 ft D_o modified Ringsail are given in Table XV. Data for the unsuccessful 127 ft D_o bi-conical model are presented as pertinent to the effects of different porosities and reefing ratios on the distance traveled during the reefed interval (where the constructed shape of the canopy has little influence). Crown geometric and canopy total porosities are given in Table XVI.

* See Section 6.2.6 for derivation.

TABLE XIII
COMPARISON OF FILLING INTERVALS OF STANDARD RINGSAIL PARACHUTES AND THE 85.6 ft D_o MODIFIED RINGSAIL OF APOLLO BLOCK II

D_o (ft.)	λ_{gc} (% S_o)	Reefing		Δt_f - (sec.)		v_1 - (fps)		K_f		Test No.
		(% D_o)	Δt (sec.)	Reef	Disreef	Reef	Disreef	Reef	Disreef	
128.8	2.08	12.5	8	2.33	2.40	380	104	37.3	3.41	6
				2.44	3.00	368	98.3	37.4	4.36	7 
				2.69	2.67	299	101	37.2	4.14	8 
88.1	1.50	11	6	2.1	3.3	315	-	37.0	-	
				1.8	3.4	375	-	37.7	-	
				1.7	3.4	380	-	36.1	-	
				2.4	2.3	283	-	38.0	-	
				2.2	3.3	305	-	37.5	-	
84.2	1.28	10.5	8	(.95 - 1.48)	(1.41 - 2.43)	(265 - 453)	(96.4 - 109)	37.4	4.76	
				-	(1.37 - 3.10)	-	(94.2 - 116)	-	5.44	
63.1	1.40	10 - 14	4 - 6	(.5 - 4.25)	(.3 - 5)	(150 - 375)	(90 - 154)	-	-	
85.6	7.04	9.5 (mid-gore)	8	.82	2.62	432	140	21.5	7.45	70 - 1 
				1.90	2.20	240	137	27.8	6.15	70 - 2
				1.67	-	281	-	28.6	-	30 - 2
								26.0	6.80	Averages
Standard Ringsail Averages								37.3	4.42	

- NOTES:
-  Two gores partially split after disreef.
 -  Leading canopy of two in cluster.
 -  Typical tests of PDS 1226 version (See Figure 85) performed in 1962.
 - The velocity at disreef was not recorded.
 -  Averages for 10 development tests performed in 1963.
 -  Average for 10 qualification tests performed in 1964. The reefed filling time was not recorded.
 -  Reported Mercury filling time data are not useable because they fail the constant filling distance test in a way that reflects use of inadequate mensuration techniques.
 -  These may be considered representative tests. All are single parachutes

TABLE XIV

FILLING INTERVALS OF THE 85.6 ft D_o MODIFIED RINGSAIL
WITH TWO REEFED STAGES (APOLLO BLOCK II H)

Reefing (Mid-Core) (% D _o)	Filling Time - (seconds)				Velocity - (fps)				K _f		Test No.
	Reef 1	Reef 2	Disreef	LS	DR1	DR2	R1	R2	FO		
8.0/21.3	1.44	.57	1.79	335	154	89.8	32.0	7.33	4.52		80-1R
8.0/23.4	1.33	.69	1.48	374	179	107	32.9	9.20	4.67		82-2
8.2/26.0	1.58	.54	1.26	374	180	93.8	36.3	7.56	3.79		80-3R1
8.2/24.2	1.60	.70	1.34	339	165	165	33.3	9.13	3.98		80-3R2
8.2/24.2	1.81	.55	1.18	306	226	102	34.0	9.25	3.69		82-2
9.3/24.2	2.36	.63	1.10	295	182	109	36.2	9.34	3.68		82-4
NOTE: K _f = Δt _f v _f / (ψ ₂ ^{1/2} - ψ ₁ ^{1/2})						34.1	8.64	4.06	Averages		

TABLE XV

MEASURED FILLING DISTANCES OF LARGE RINGSAIL PARACHUTES

D_o (ft)	Reeling (% D_o)	Stage 1			Stage 2			Disreef to Full Open		
		Δt_f (sec.)	\bar{v} (fps)	Δs_f (ft)	Δt_f (sec.)	\bar{v} (fps)	Δs_f (ft)	Δt_f (sec.)	\bar{v} (fps)	Δs_f (ft)
128.8	12.5	1.40	352	493	-	-	-	2.40	70	168
		2.90	303	879 (676)	-	-	-	3.00	63	189 (180)
		2.43	270	656	-	-	-	2.67	68	182
127	11	1.64	293	481	-	-	-	-	-	-
	13	1.36	298	406	-	-	-	-	-	-
	16	2.80	278	778 (663)	-	-	-	-	-	-
	16	2.03	270	548	-	-	-	1.96	65	127
85.6	8.0/21.3	1.44	305	578 (593)	.57	145	86	1.79	62	111 (112)
	8.0/23.4	1.33	347	608	.69	166	123	1.48	76	113
	8.2/26.0	1.58	340	648 (632)	.54	169	114	1.26	69	87
	8.2/24.2	1.60	304	588	.70	156	138	1.34	73	98 (92)
	8.2/24.2	1.81	302	659	.55	211	128 (129)	1.18	77	91
9.3/24.2	2.36	284	669	.63	174	121	1.10	82	91	-

NOTE: Δ The occurrence of split gores after disreefing produced atypically long filling times.

TABLE XVI
RELATIVE FILLING DISTANCES OF LARGE RINGSAIL PARACHUTES

D_0 (ft)	Reefing (% D_0)		Porosity (% S_0)		$\Delta S_f/D_0$		
	R1	R2	λ_{gc}	λ_T	R1	R2	DR
128.8	12.5	-	2.08	9.77	5.25	-	1.40
127	11	-	2.81	10.51	3.78	-	-
	13	-			3.20	-	-
	16	-			5.22	-	1.00
85.6	8.0	21.3	7.04	12.54	6.92	1.0	1.31
	8.2	23.4			7.38	1.44	-
	9.3	24.2			7.82	1.51	1.08
		26.0			-	1.33	1.02

Because the average velocity during initial inflation of the canopy is high, most of the distance traveled is covered during reefed stage I; also the effects of small differences in filling time are amplified, which emphasizes the importance of taking every measure possible to regularize the opening process and eliminate random delays in the initiation of canopy inflation. At the other end, the distance traveled after disreefing is very short, scarcely more than the nominal diameter of the canopy as shown in Table XVI. Here, the relative filling distance in canopy diameters is another dimensionless form of the Ringsail filling interval that has been particularly useful in the analysis of minimum altitude recovery trajectories. Additional test measurements are needed at very low deployment velocities to determine whether the total filling distance of non-reefed parachutes is under such conditions.

Of course, with a reefed canopy the distance traveled during the reefed interval is a substantial increment added to the total. At high speeds this can only be minimized by reducing the reefed interval to the shortest time allowed by the design limit case. At low speeds, if the reefed interval is no longer than two or three seconds, the normally slower filling rate of the canopy may embrace the reefed interval to the extent that the canopy inflates as though non-reefed.

3.4 STABILITY

The principal mode of instability exhibited by the Ringsail parachute, like that of any other circular parachute, is described as a "pendular"^{*} oscillation in which the axis of the descending system describes a series of alternating angular deflections in random directions from the vertical. Because the center of gravity of the system with added air mass is generally closer to the canopy than to the suspended load, the similarity to a pendulum is marked (when the out-of-plane components of the motion are not clearly evident). The actual deflections of the system axis in three-dimensional space may be characterized as an irregular "coning" oscillation (Figures 39 and 41). When the coning motion becomes roughly circular it tends to be sharply periodic and this mode has been observed occasionally. (Figure 42).

Synchronous phototheodolite measurements from several stations have enabled both amplitude and direction of axial deflections of some recent Ringsail parachute systems to be determined, as indicated in the Figures. Most early measurements obtained from motion picture records indicated angular deflections in the plane of the picture only (Figure 40) but in some cases out-of-plane data was obtained by scaling the changing ellipticity of the canopy skirt and correcting the result for the angle of elevation at which it was viewed.

The average amplitude of pendular oscillation ($\bar{\theta}$) characteristic of different Ringsail parachute systems during steady descent is given in Table IX. It will be seen that $\bar{\theta} \approx 7$ degrees is a fairly typical average. In normal descent the amplitude of oscillations varies widely in a random manner as influenced by atmospheric disturbances (wind gradients, thermal currents, turbulence and gusts) so that occasional excursions of up to three times the average may be encountered (Reference 30). However, the Ringsail damping characteristic is strong enough to reduce greater than average oscillations to small amplitudes in approximately one full cycle. Also it is not unusual for well-balanced systems to descend steadily without perceptible oscillation for protracted periods (e. g. see the note in Figure 40).

Undamped oscillations of large amplitude have occurred in some Ringsail parachute systems under the special circumstances described in Section 6.3.7. These are not typical and resultant problems have been minimized by design revisions.

* A word coined by parachute people to signify a pendulum-like motion, not necessarily periodic like a pendulum, however.

ASSET Main Parachute Test No. 1944 26 November 1962

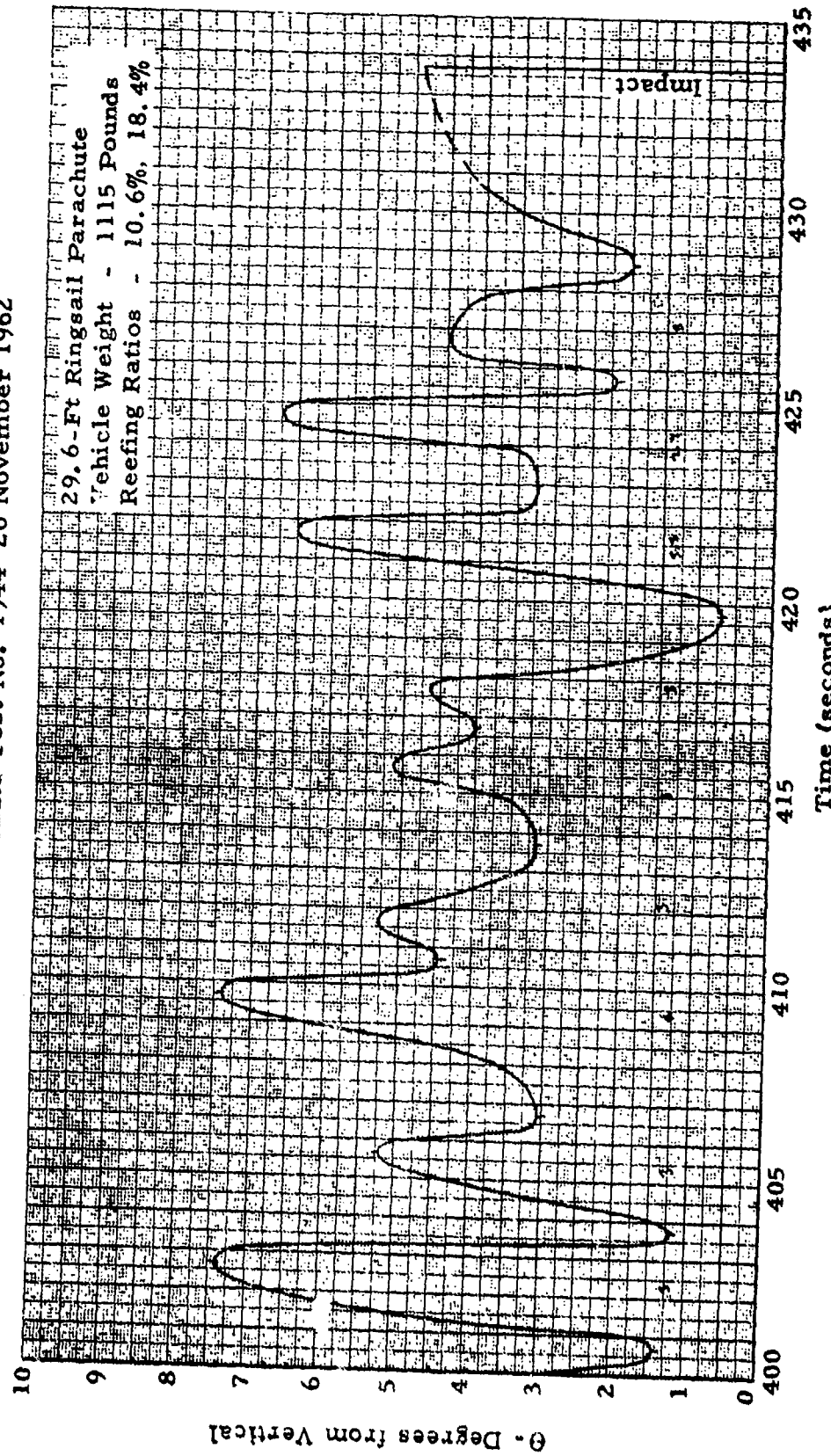
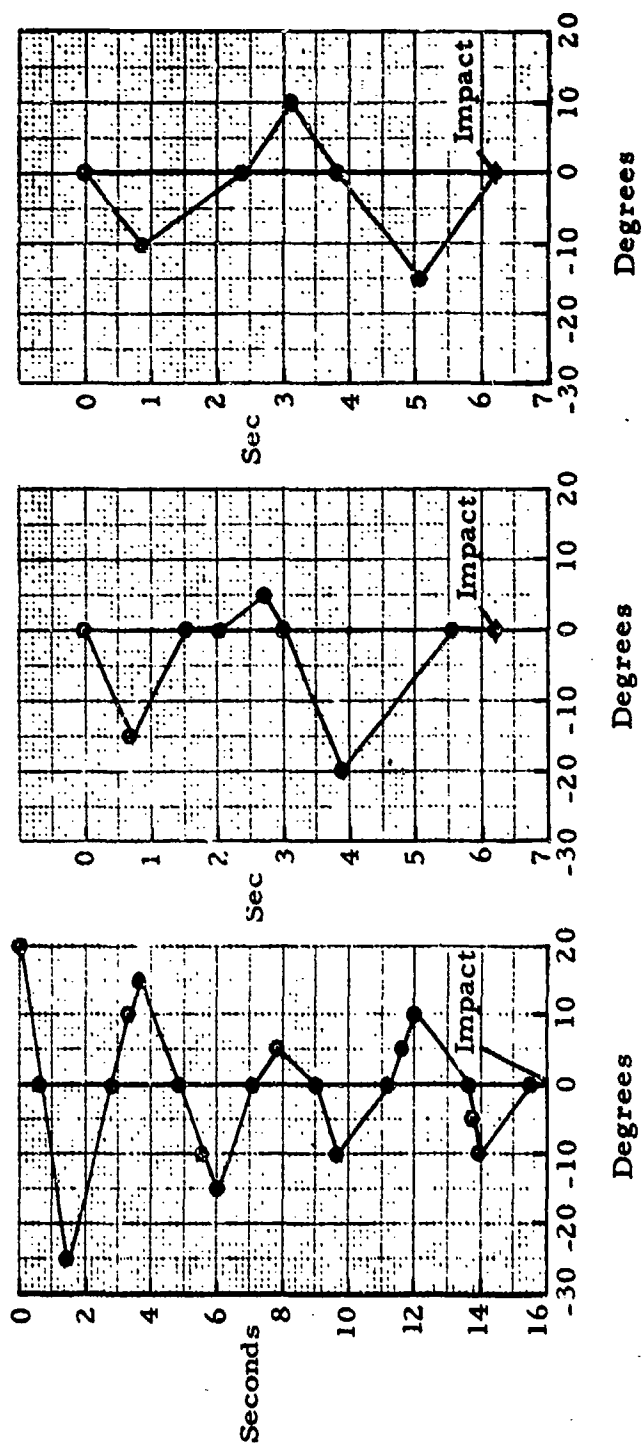


Figure 39. Pendular Oscillations of ASSET
29.6 ft D₀ Ringsail During Terminal Des-
cent at 45.5 fps (EAS) with 1115 Pounds

Note: These records represent 3 of 8 live jump tests.
 Oscillations during the 5 remaining tests were
 imperceptible in film records.



$$v_e = 17 - 21 \text{ fps}$$

Weight = 200 - 270 pounds

Figure 40. Pendular Oscillation of 29.6 ft D_0 Skysail Model D During Jump Test Program at El Centro in 1959

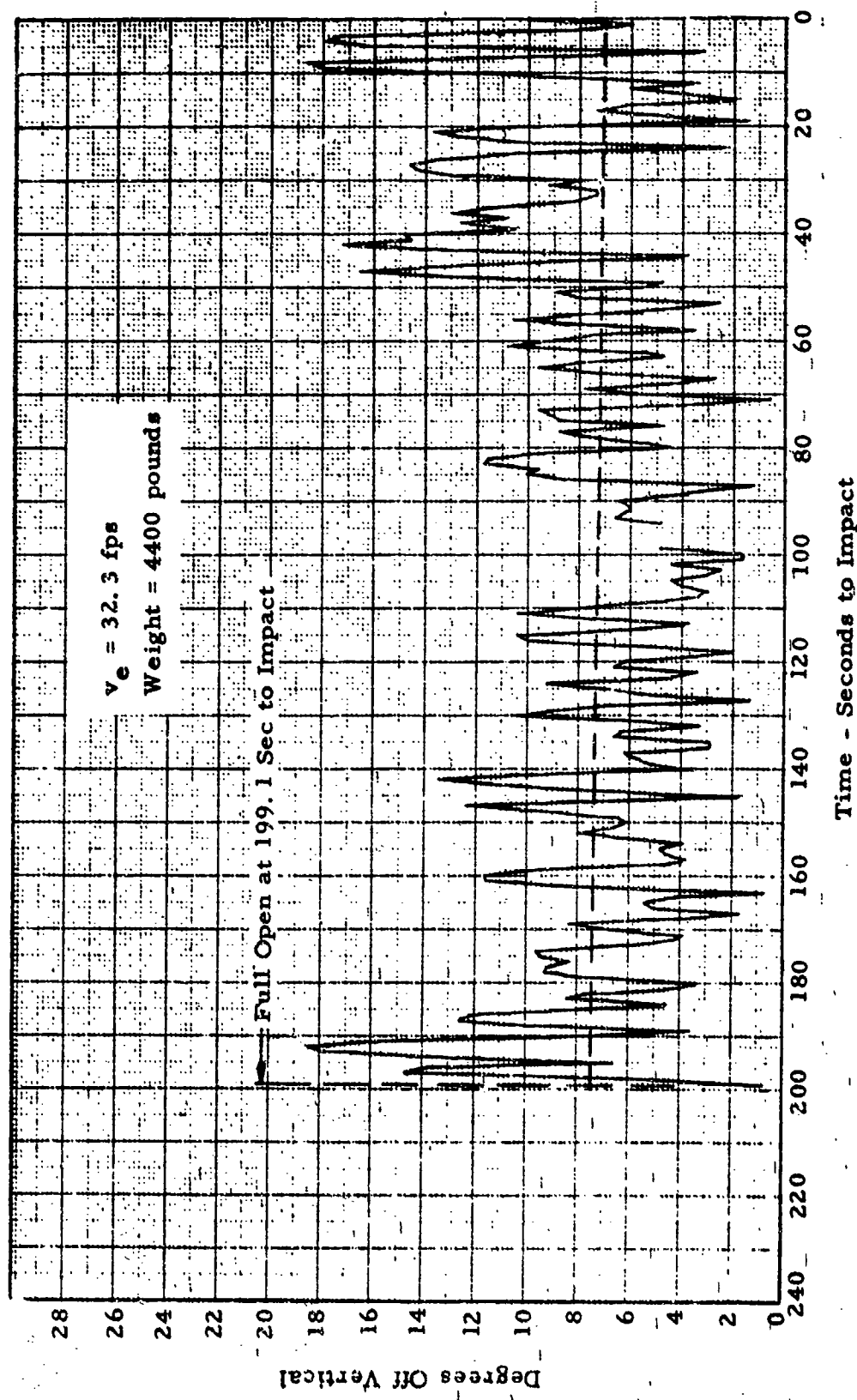


Figure 41. Typical Coning Oscillation Record of Gemini 84.2 ft Do Ringsail (Development Test No. 19)

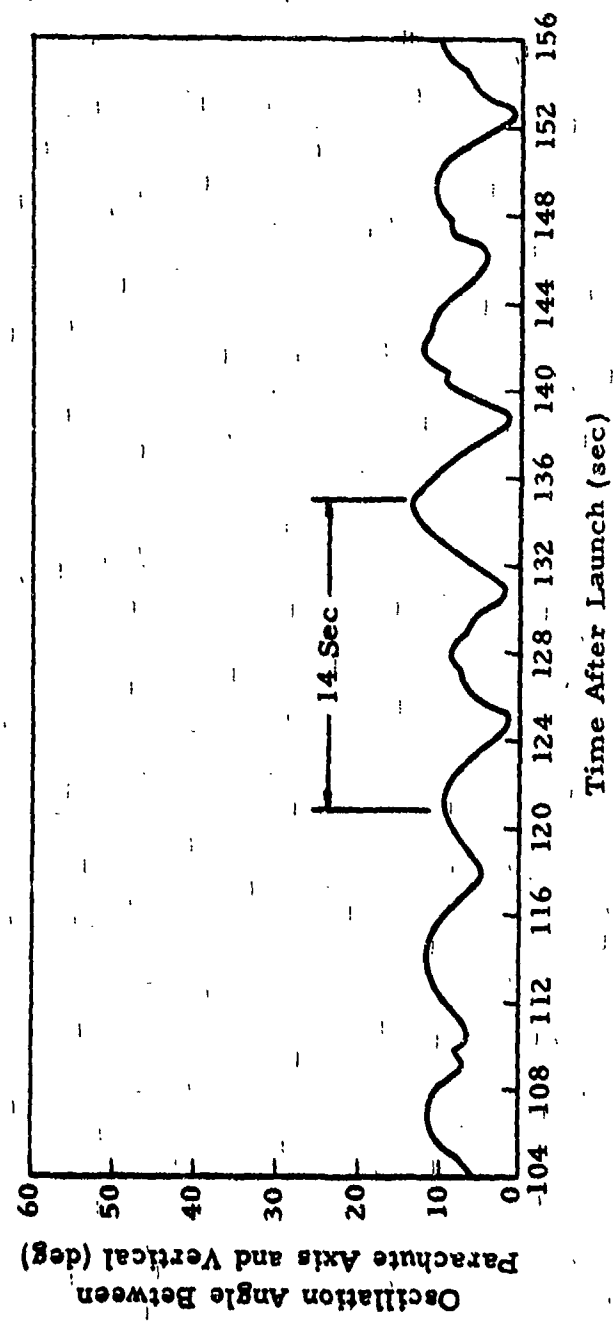


Figure 42. Oscillation of 12.8.8 ft D₀ Ringsail Descending at 26.4 fps (EAS) with 9786 Pounds

Distribution curves for angular deflection of the Apollo cluster system are shown in Figures 44 and 45. These are not typical for either the 88.1 ft D_o standard Ringsail or the 85.6 ft D_o modified Ringsail but they are indicative of the improved stability resulting from the higher total porosity of the latter. It will be recognized that the two systems in Figure 43 are not quite equivalent because the average rate of descent of the modified Ringsail system was 13 percent higher.

The stability of the 41 ft D_o Ringsail varied from system to system and posed some unusual problems. The B-58 escape capsule recovery system parameters fell in the critical Reynolds number range (described in Section 6.2.4) where oscillation amplitudes have been greatly amplified. With a cylindrical bomb test vehicle the averaged measurements of seven drop tests showed oscillation amplitudes greater than 10° 41% of the time, greater than 15° 19% of the time and greater than 20° 6% of the time. The maximum was 24° and the average 11.4° (Reference 28). However, with the "boiler-plate" * capsule, system stability was observed to be greatly improved, and an average amplitude of 5 to 10 degrees was estimated on the basis of limited test data, no measurements being available. Stability of descent was particularly important to the B-58 capsule operation because of the highly directional type of impact attenuation mechanism employed.

In the much heavier E-6 Satellite capsule system, average oscillations of $\bar{\theta} = 9$ degrees with maximum up to 18 degrees were found objectionable, so the suspension lines on the 41 ft D_o canopy were shortened from 32 feet to 26 feet and limited test measurements indicated that the average amplitude of oscillations had been reduced to approximately 6 degrees with maxima up to 10 degrees. However, additional tests of the short line configuration performed later put the average back to $\bar{\theta} = 9$ degrees with maxima up to 23 degrees. It should be noted that while the suspension line length was only $0.64 D_o$ and no risers were used, the effective line length was made close to $0.78 D_o$ by spacing the line attachment points some distance apart on the base of the capsule.

3.5 REEFED DRAG AREA

The reefed drag area of Ringsail parachute expressed in the nondimensional form C_{DSR}/C_{DS_0} appears to vary widely from system to system for a given reefing ratio. How much of this variation is real is uncertain because of the technical difficulties associated with getting drag area measurements during

* Designating a rugged dummy vehicle usually made of welded steel plate

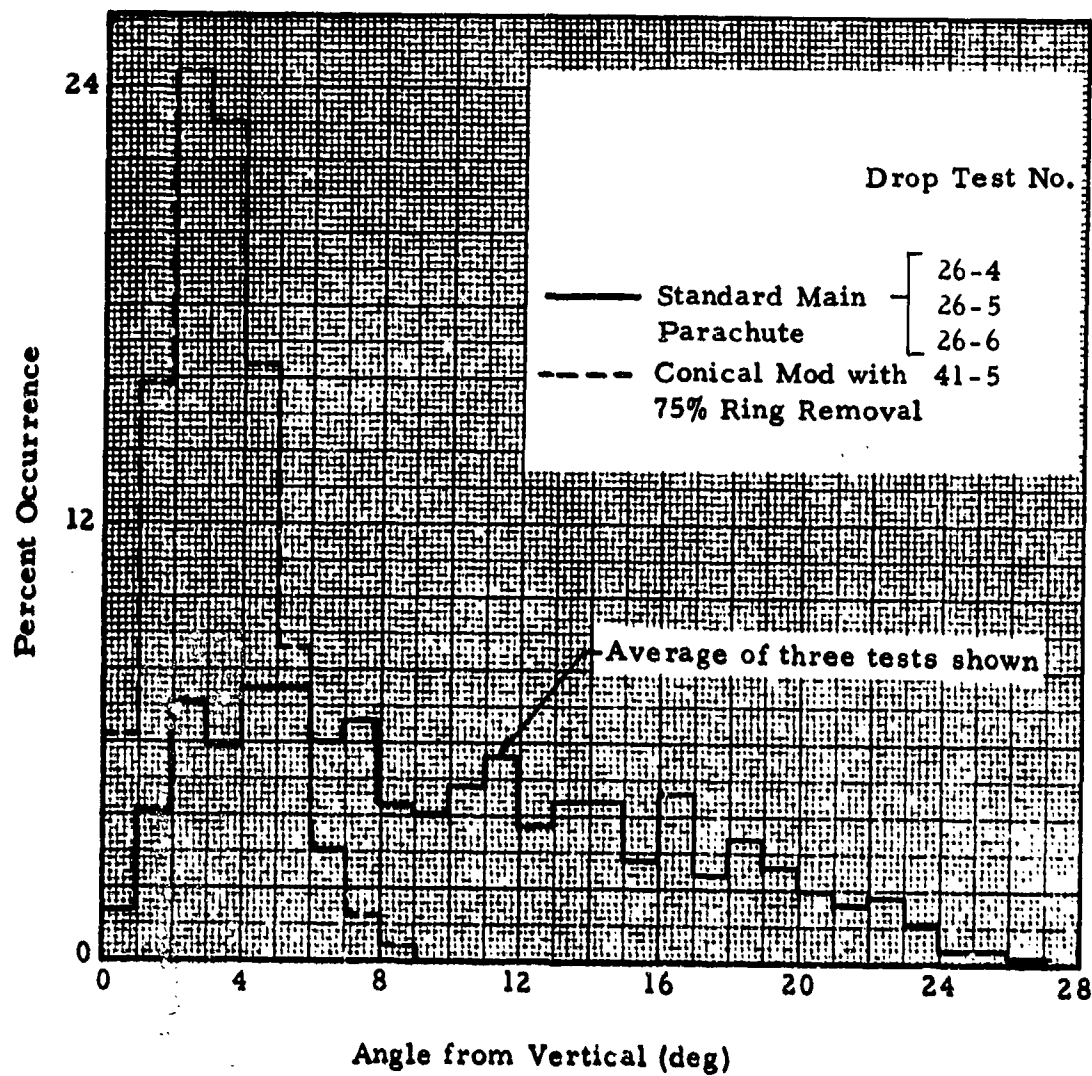


Figure 43. Statistical Comparison of Angular Deflections of Apollo Two-Canopy Clusters of Standard and Modified Ringsails

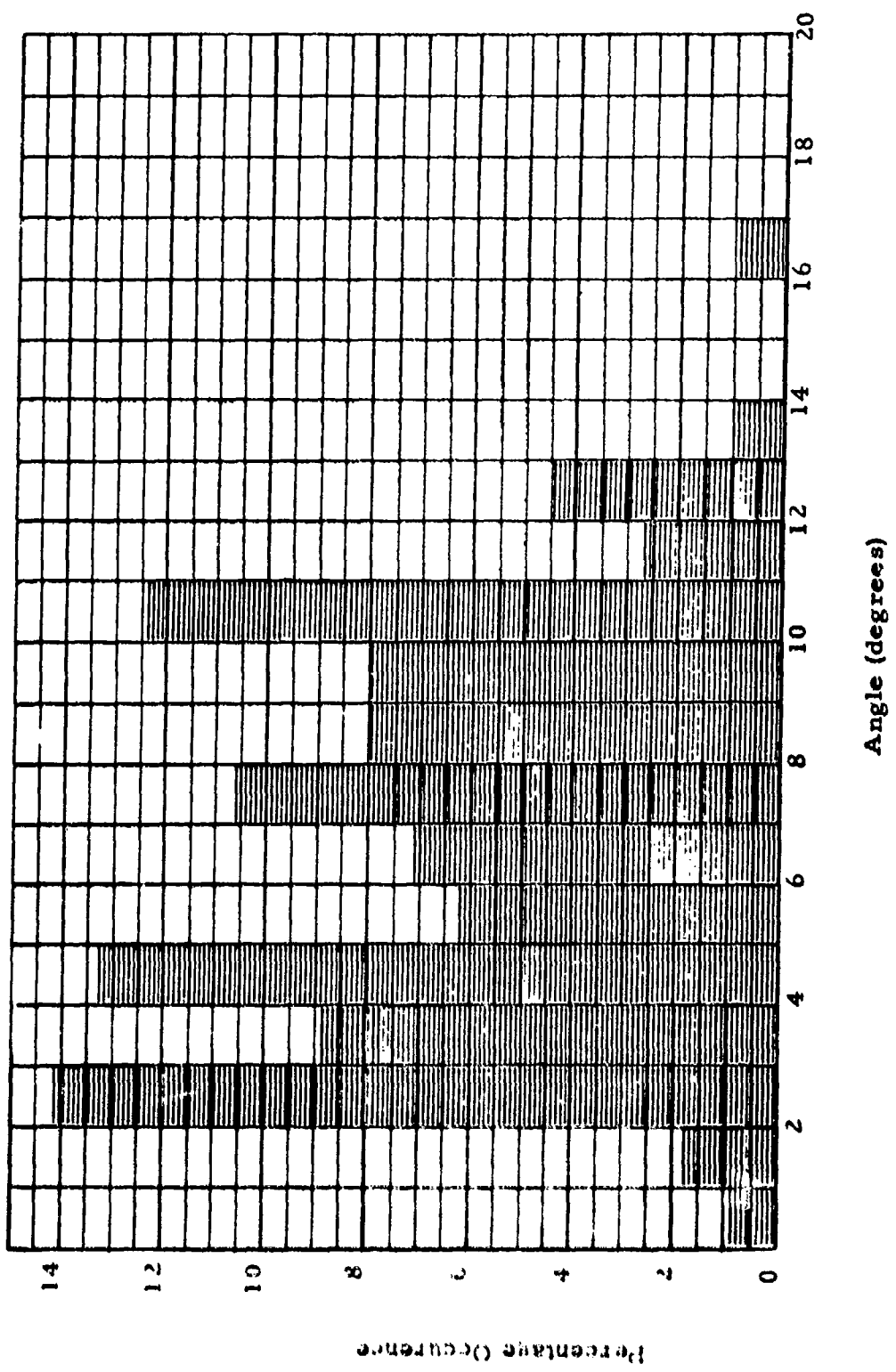


Figure 44. Oscillation Data, Three Canopy Cluster, Apollo
Modified Ringsail, Test 73-3

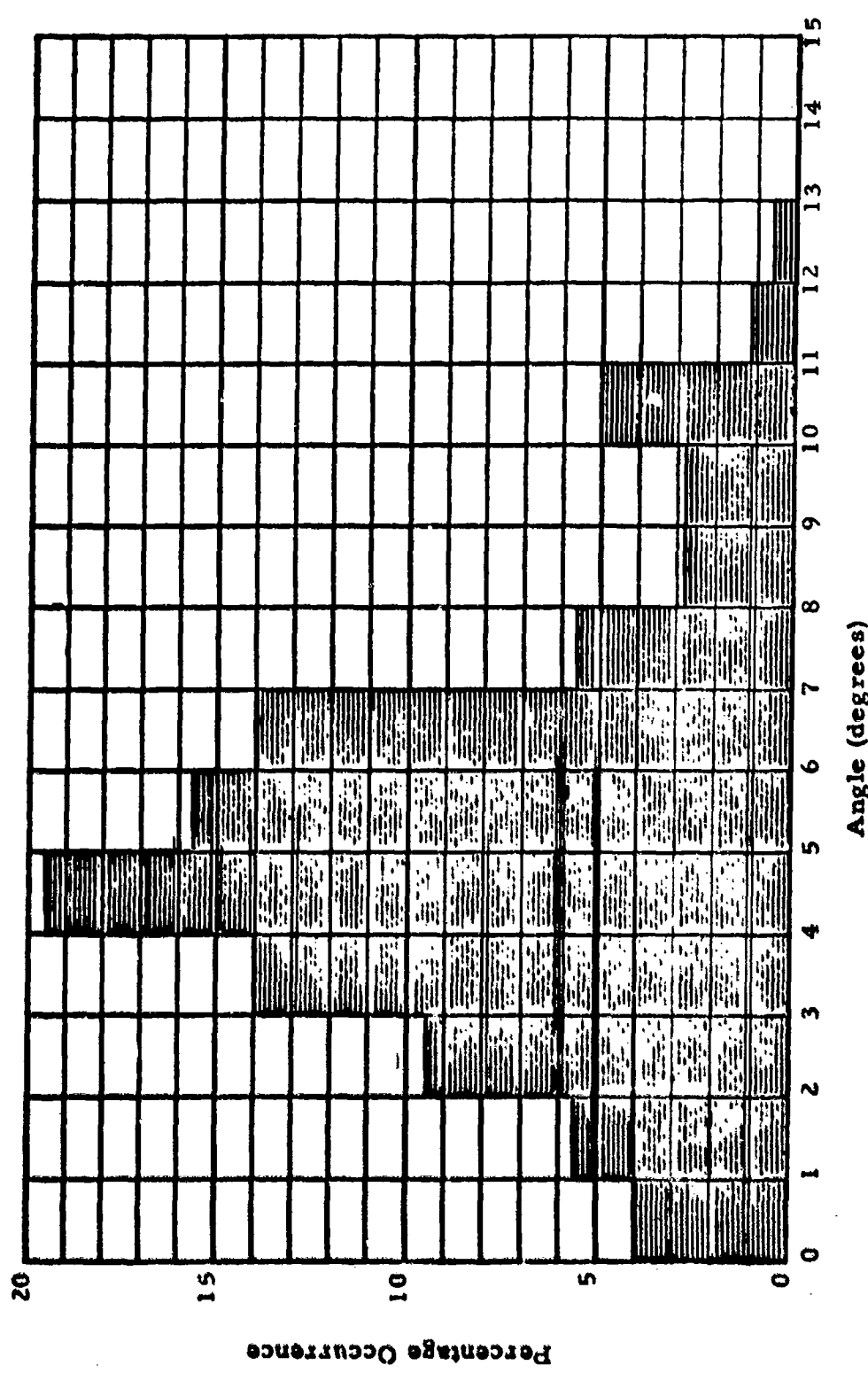


Figure 45. Oscillation Data, Three Canopy Cluster, Apollo
Modified Ringsail, Test 73-1

unsteady flight conditions. Theoretically the initial reefed drag area (at F_R max) should show some correlation with the geometric porosity of the crown area of the canopy that is pressurized at that time. Along with this effect, the reefed drag area at disreef is dependent to some extent on the duration of the reefed interval. But while the canopy appears to fill steadily at a low rate during the reefed interval, there are some indications that equilibrium between inflow and outflow may be reached after a short time (3 to 4 seconds).

In view of these sources of uncertainty, the typical curves relating reefed drag area ratios to reefed diameter ratios given in Figure 46 can be treated only as indicative of general trends. The reefing data compiled during various Ringsail development programs presented in Figures 47 through 49 give a more realistic picture of the performance to expect under similar conditions. For example, the data obtained from the Century program (Figure 48) shows a separation that correlates with the crown geometric porosities of the two canopy designs. However, the difference between the Mercury and Gemini data cannot be accounted for on this basis; the validity of the Gemini data is suspect.

At $D_R/D_o = 0.16$ the 127 ft D_o Century parachute is seen to revert to the augmented growth characteristic of the lower porosity 128.8 ft D_o model at disreef. Apollo cluster data show no significant difference in reefing ratios relative to the single parachute system.

3.6 OPENING RELIABILITY AND REPEATABILITY

The opening reliability of the Ringsail like that of any other proven parachute design is a function of factors unrelated to its aerodynamic properties. A parachute can be prevented from opening by faulty rigging, a fouled reefing line, failure of reefing line cutters to fire, and extensive damage in the crown. One of the sources of crown damage other than opening shock is the whiplash impact of a broken pilot chute bridle or attachment link.

A faulty pilot chute bridle link precipitated the catastrophic failure of one of the 127 ft D_o bi-conical Ringsails reported in Reference 8. A broken radial member in the critical pressure area of the crown was clearly the result of a whiplash impact following failure of the link and this provided the focus for a ruptured gore that subsequently split full length and through the skirt band.

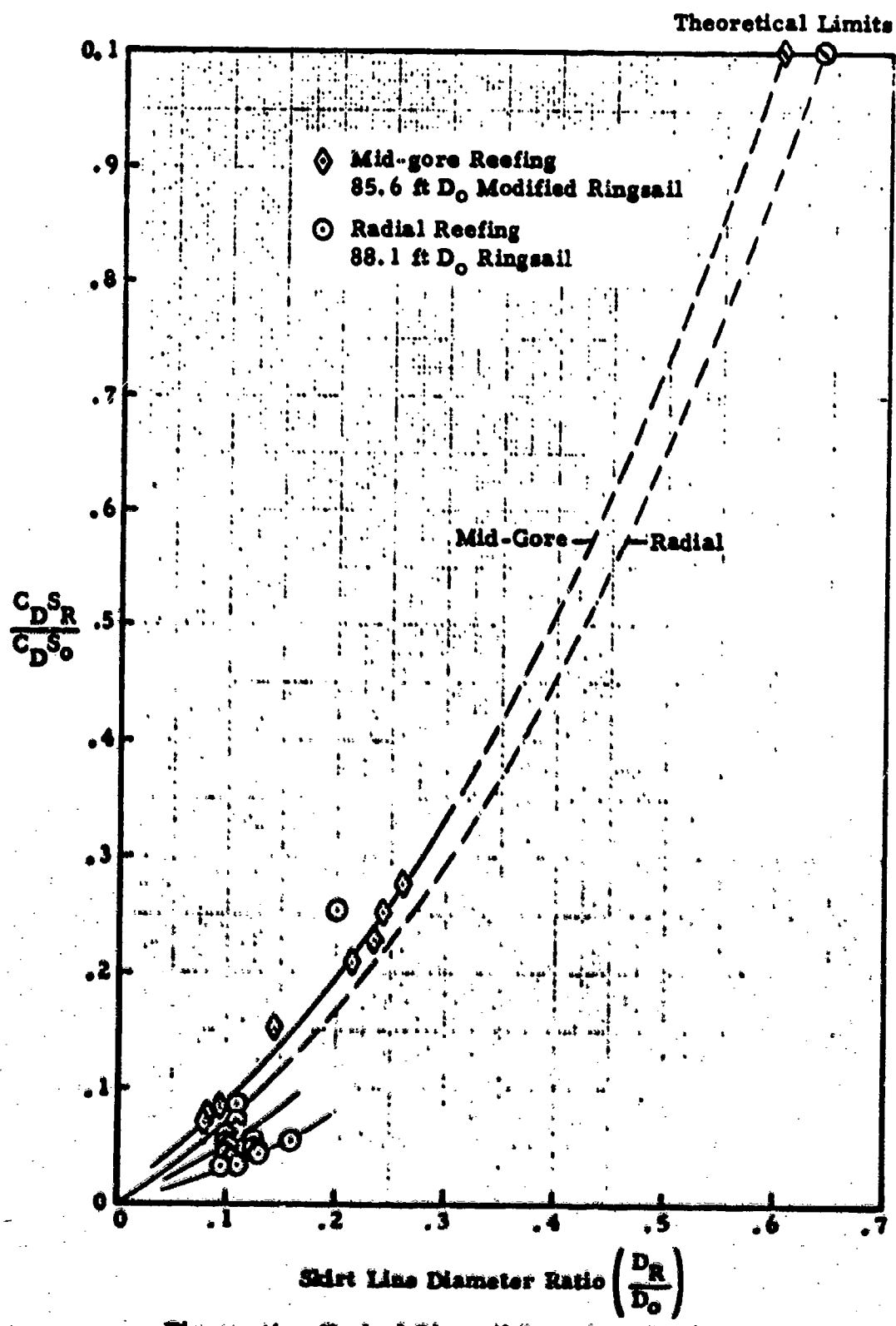
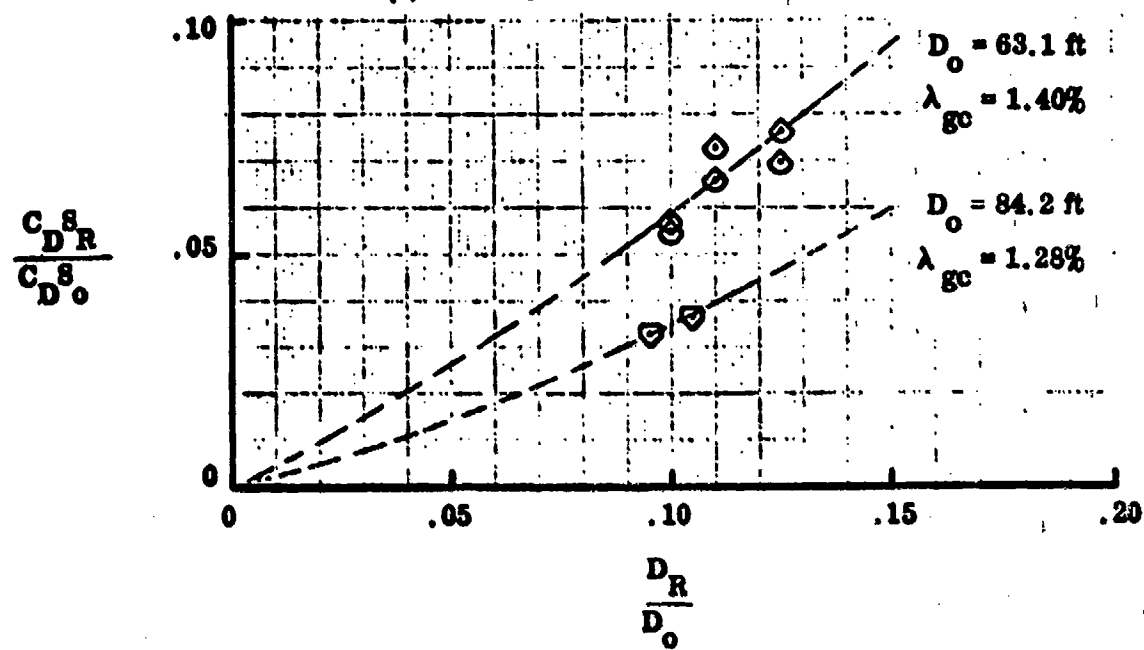


Figure 46. Typical Ringsail Parachute Reefing Ratios

$$\frac{C_{DSR}}{C_{DSO}} \text{ vs } \frac{D_R}{D_o} \text{ (General Trends)}$$

(a) Mercury and Gemini Data Averages



(b) Apollo Development Test Data Averages

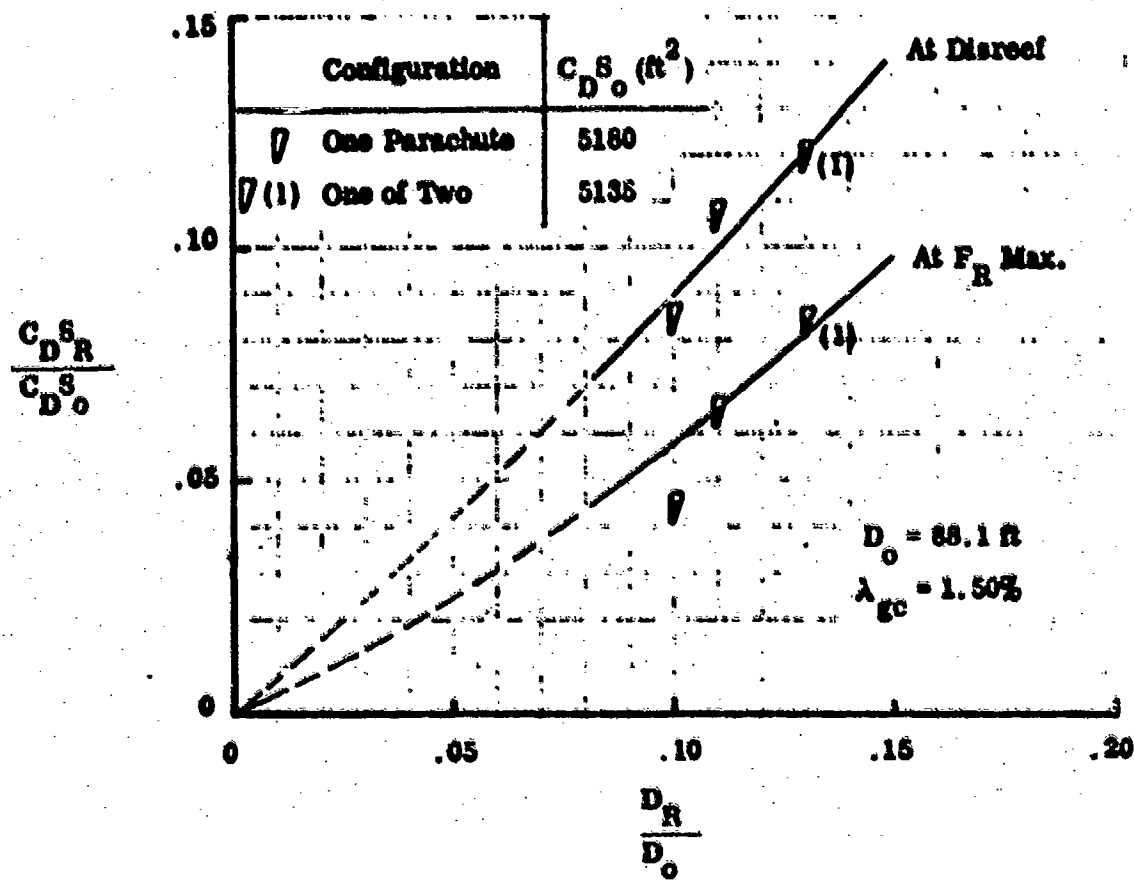


Figure 47. Mercury, Gemini, and Apollo Development Test Data Averages

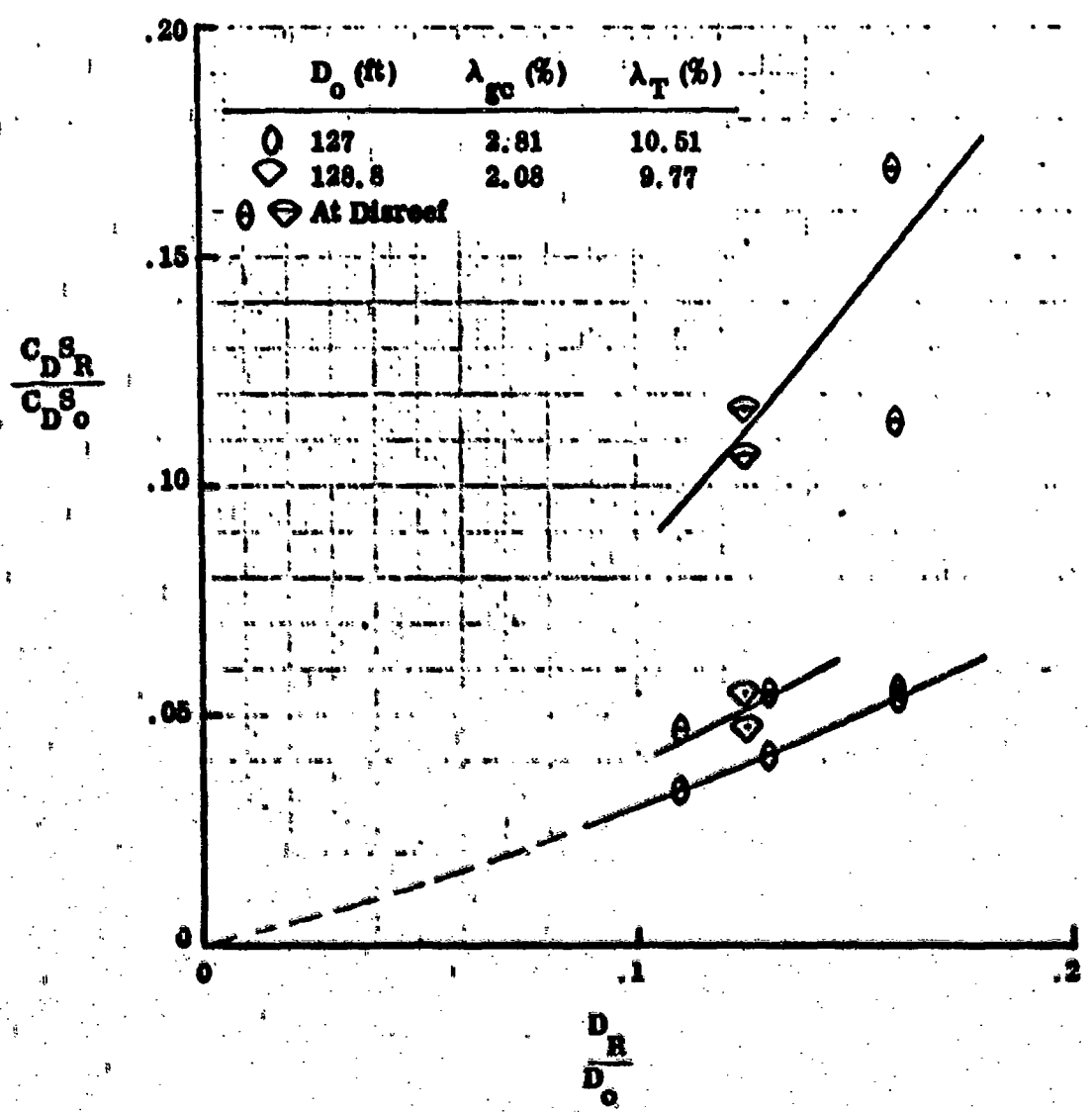


Figure 48. Century Ringsall Roofed Data

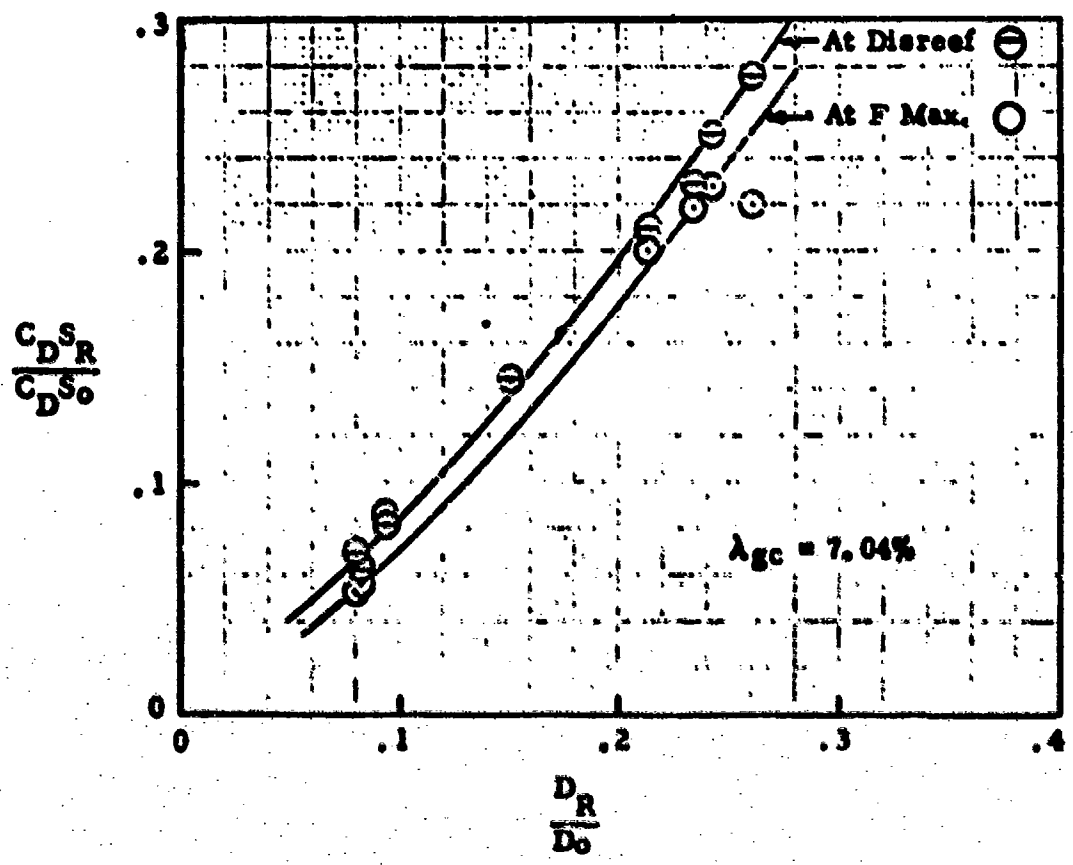


Figure 49 . 85.6 ft D_O Ringsail (Modified -75% of 5th Ring Removed)
with Mid-Gore Roofing

The strong opening tendency of the Ringsail parachute provides added insurance that once deployed it will inflate. This is born out by its high tolerance for opening damage as described in Section 3.7.

The repeatability of the Ringsail opening process is subject to the same random variables found in any parachute system that does not have a positive mechanical means of opening the canopy mouth as soon as it is exposed to the air stream. The slack fabric in the skirt area flutters in and out between the lines according to no fixed pattern such that the initial influx of air is obstructed in varying degrees. It is known that the flared skirt configuration augments the radial opening force component when the sails flutter outward, more than it is inhibited when the sails flutter inward, because such canopies open reliably with a higher than normal total porosity. Also, pocket bands, by limiting the inward deflection of the skirt panels, significantly reduce random delays in getting effective filling started. Stiffening the skirt band is believed to have a similar effect but the amount of stiffening required for useful results may be impractical for packing. Initial inflation of the reefed canopy is also promoted by vertical restrictor tapes across the crown slots.

Insofar as the Ringsail parachute has a flared skirt, stiffened skirt band, and tapes across the crown slots, and may have pocket bands to meet critical opening requirements, its opening process can be said to be more repeatable than that of other types of parachutes lacking any or all of these features. A measure of such repeatability would be provided by statistical evaluation of the time lapse between line stretch and first opening of the canopy mouth to form a positive flow inlet in a series of tests all performed under identical conditions. The practical obstacles in the way of so doing are considerable, and such a survey has never been made, at least not with the Ringsail parachute.

Another less rigorous, yet meaningful, measure of Ringsail opening repeatability is the dimensionless filling interval, K_f , given in Table VIII, Section 3.3. Some data showing the variation of K_f from test to test are given in both Tables VIII and IX.

3.7 TOLERANCE FOR DAMAGE

Tolerance for damage may be considered an unusual criterion of parachute performance. However, the ultimate reliability of any parachute system hinges on the ability of the canopy to remain inflated and limit the descent velocity when severely damaged. The critical area for opening damage is the crown where an excessive outflow of air can prevent inflation from

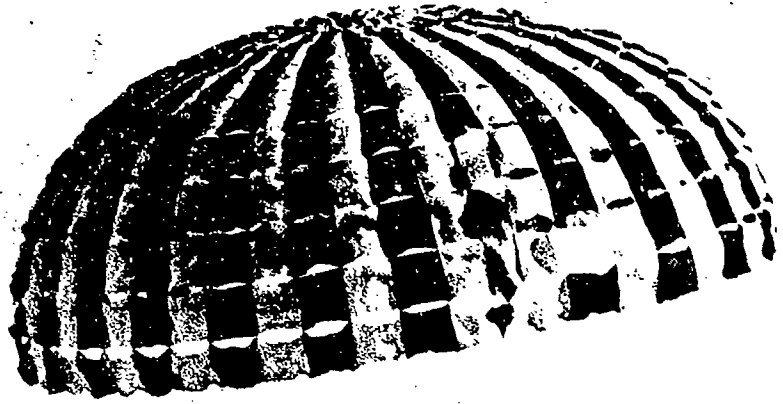
progressing beyond a low-drag "squidding"* configuration. The normal geometric porosity of the Ringsail crown is between 1 and 2 percent (Figure 21). Tests performed during the Apollo ELS parachute development program demonstrated that the 88.1 ft D_0 Ringsail would inflate reliably with a crown geometric porosity of $\lambda_{gc} = 8.1$ percent of which 6.9 percent was concentrated in ring 5 between $h/h_R = .37$ and .45. This is equivalent to a very heavily damaged canopy because strong cloth is used in the crown rings. Normally, the area of critical stress is lower in the gore between $h/h_R = .53$ and .76.

The split gore is a more typical form of Ringsail parachute damage, and two gores split from vent to skirt will not cause the canopy to collapse, nor is the rate of descent increased to a dangerous level. The Ringsail has also remained inflated and descend safely with one split gore and both vent and skirt bands broken. This occurred in one of the early Apollo development tests of very lightweight Ringsail. The canopy split (one gore) from skirt to vent, including skirt and vent band. During descent the canopy slowly unwrapped itself and turned inside out, forming a canopy shape, then proceeded to reverse itself and formed a canopy (right-side-out) and descended in a gliding mode. However, in the most cases the dynamic rebound from this type of failure is so violent that the torn edges are driven too far apart to recover and the event is followed by canopy collapse and streaming.

A partial measure of the Ringsail parachute's tolerance for damage is indicated by Figures 50, 51 and 52.

A split gore or other large rent in the canopy may have as its point of origin a minor defect or rupture in a region that is subjected to critical stress levels during inflation. This is most certainly the case when major damage is sustained by a parachute of sound design at a low load level. Such failures have occurred with opening loads below the design limit. The presence of minor damage prior to inflation is also highly probable when the major damage originates in those gores of the canopy identified as the "packing axis" (Gores 1, $N/2 \pm 1$, and N), because the gores on the packing axis are on the outside of the pleated canopy as it is folded into the deployment bag. Therefore, these same gores are the ones exposed to the dynamic effects that cause pre-opening damage. (Only rarely can the damage be traced to faulty packing technique.) The damage charts of parachutes (large ones in particular) which performed successfully frequently show a scattering of minor damage and friction burns across the canopy with a greater than average concentration in the gores on the packing axis. The number of such defects tends to be a direct function of the test dynamic pressure at deployment.

* A term coined by parachute people acknowledging the similarity of the streaming canopy configuration to that of the familiar marine creature; however, the direction of motion is reversed.



Reproduced from
best available copy.

Figure 50. Mercury 63.1 ft D₀ Ringsail Damaged By Falling Compartment Cover During Qualification Test - Salton Sea, California

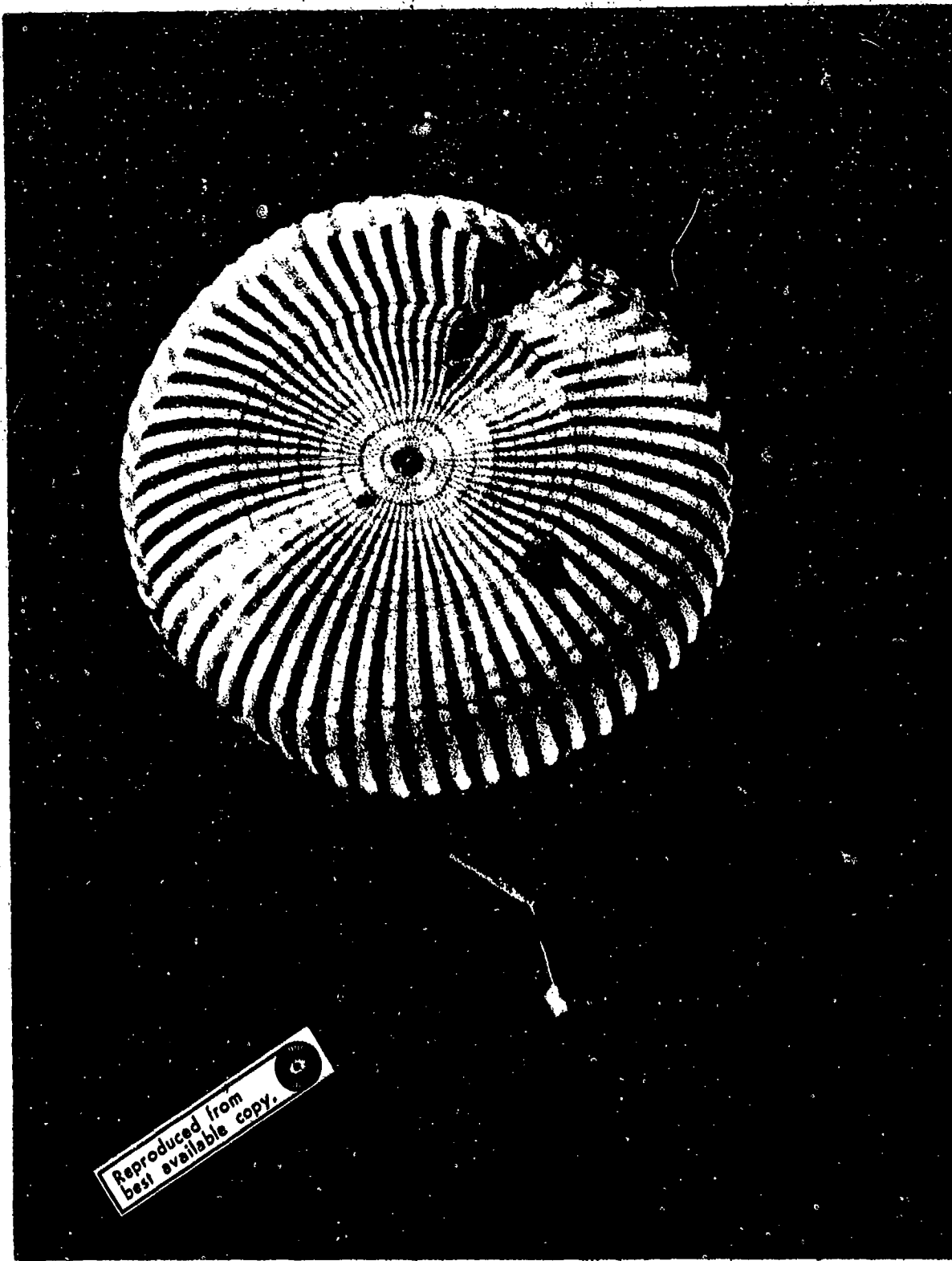


Figure 51. Century 128.8 ft D₀ Ringsail (Lightweight Model) Opening Damage (Rate of Descent 27.9 fps with 9762 lb)

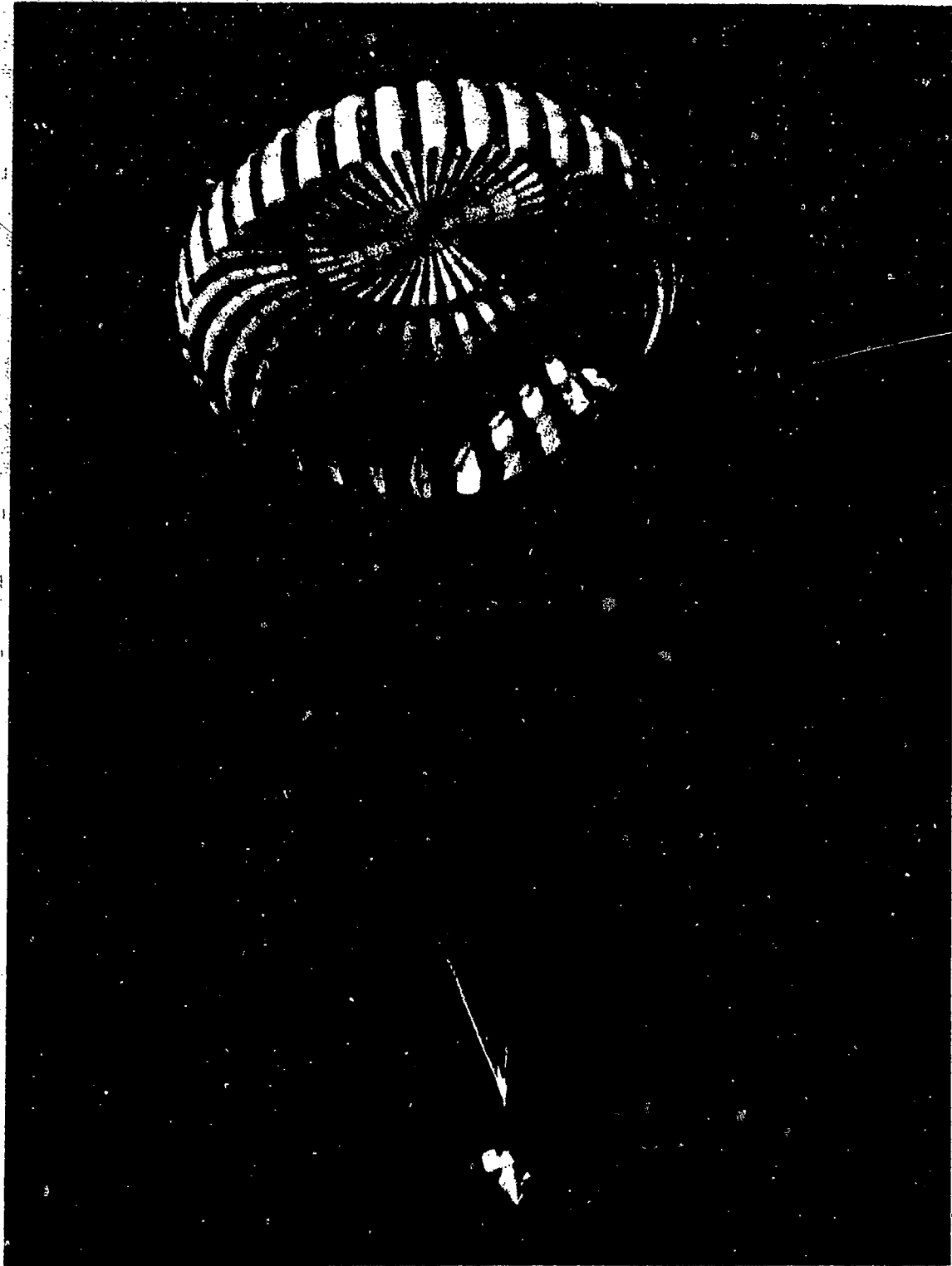


Figure 52. 88.1 ft D₀ Ringsail Descending Safely with One Gore Split from Vent to Skirt

Evidence of this sort compiled during the Century Ringsail test program supports the theory that pre-opening damage is caused by dynamic pressure blowouts at small spots in the canopy that have been temporarily weakened by frictional heating. Friction burns in nylon can be identified after the event only when the material was heated to the melting point. In such spots embrittlement occurs after cooling and the material has no strength. But any spot that was heated to less than the melting point cannot be identified afterwards because there is no embrittlement and the material recovers most of its original strength. Therefore, it is logical to assume that the majority of small pressure bursts found in the canopy without brittle edges were earlier hot spots and that were exposed to dynamic pressure before they had time to cool. Since the heat capacity of nylon cloth is very small, it is clear that the time between heating and exposure must be very short, i. e., of the same order of magnitude as the time required for the affected area to move out of the mouth of the deployment bag. This is also the time during which the outer surface of the canopy is rubbing rapidly across the deployment bag lining.

The presence of pre-opening damage generally across the canopy, suggests that inter-laminar friction is the primary source, while the concentration along the packing axis would reflect only the added contribution of the deployment bag. Therefore, it is not something that could be controlled effectively by employing a reversible lining in the deployment bag, unless measures were also taken to reduce inter-laminar friction. The other approach would be to prevent penetration of high pressure air into the canopy until the deployment bag has been stripped off, a difficult mechanical problem requiring both zero leakage and unfailing release at canopy stretch.

SECTION 4

WEIGHT AND VOLUME

4.1 INDIVIDUAL PARACHUTES WITHOUT RISERS

Ringsail parachute weights without risers are listed in Table IX and are plotted in Figure 53. These are average measured values. In addition to the weights shown, 12% must be added to obtain the pack weight which include risers, links, reefing line, reefing cutters and deployment bag. The weights presented in Figure 53 fall into three categories which are representative of the following basic structures.

Light Construction:	90% S_o of 1.1 oz/yd ² cloth 10% S_o of 1.1 to 1.6 oz/yd ² cloth Suspension lines of 400-450 lb cord
Medium Construction:	85% S_o of 1.1 oz/yd ² cloth 15% S_o of 1.6 to 2.25 oz/yd ² cloth Suspension lines of 550-650 lb cord
Heavy Construction:	75% S_o of 1.1 oz/yd ² cloth 25% S_o of 2.25 to 3.25 oz/yd ² cloth Suspension lines of 750-1000 lb cord

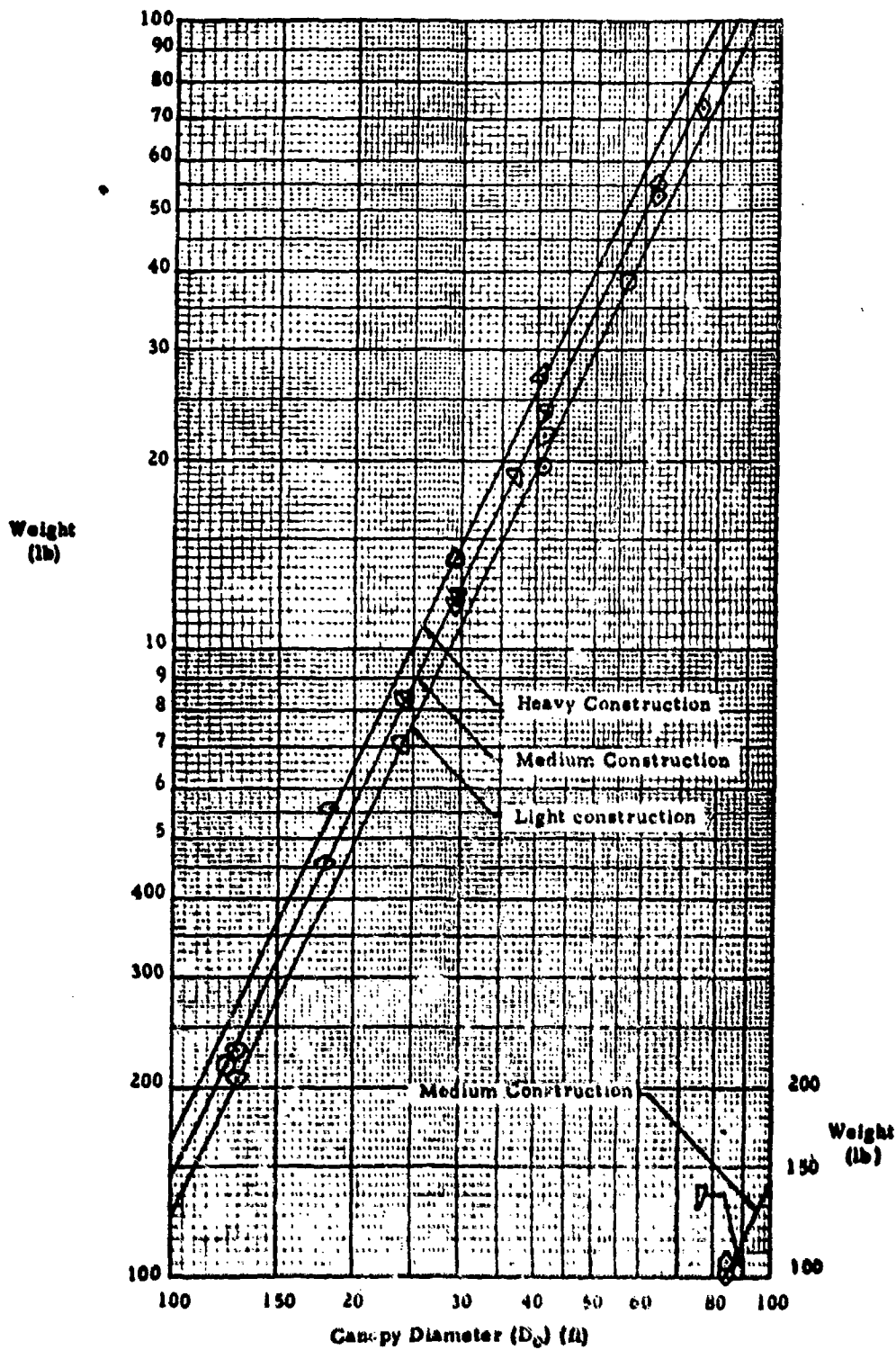
Parachute volumes vary with the pack density δ_p which is a function of the packing method employed. Average pack densities also are given in Table IX. The installed volume depends on the weight and density of other components stowed in the deployment bag along with the parachute and even on the skin thickness of the bag itself.

4.2 LINE TO RISER LINKS

Table XVII presents weights of some of the line to riser links used in Ringsail parachute assemblies.

4.3 RISER ASSEMBLIES

The weight of riser assemblies varies widely from system to system. Table XVIII presents some typical examples.



NOTE: Weights from Table IX (average measured); add 12% to obtain pack weight including riser links, reefing lines, cutters and deployment bag.

Figure 53. Ringsail Parachute Weight vs Diameter (without risers)

TABLE XVII
TYPICAL SUSPENSION LINE TO RISER LINK WEIGHTS

Part No. or Drawing No.	Rated Strength (lb)	Weight (lb)
Capewell 101740 (for 1 inch webbing)	6000	.144
MS 22021-1	6000	.184
USAF 52B6660	9500	.190
R7666-1 (Northrop)	6650 (ULT)	.267
MS 24553-1	23,000	.540

TABLE XVIII
TYPICAL RISER ASSEMBLY WEIGHTS

System	D _o (ft)	Part No. or Drawing No.	Lengths		Weight (lb)
			Branch (ft)	Trunk (ft)	
Mercury	63.1	R5107-301	3.5	0.5	1.50
Gemini	84.2	R6222	1.1	4.1	1.82
Apollo	85.6	R8061-1	3.5	1.3	2.50
	88.1	PDS 1356-501	3.5	3.0	5.80
Century	128.8	R7805-1	3.0	32	18.43 

 This riser was designed for cluster operation

4.4 COMPLETE PARACHUTE SYSTEM

Significant statistics on the weight breakdown of Ringsail parachute system components are summarized in Table XIX for the Mercury, Gemini and Apollo spacecraft landing systems.

TABLE XIX
WEIGHT OF SPACECRAFT LANDING SYSTEMS

SYS- TEM	SUBSYSTEM	QTY. PER S/C	FABRIC LB	OTHER LB	TOTAL LB	PER S/C LB
MERCURY - 2500 LB	Drogue	1	7.1	4.0	11.1	11.1
	Pilot	1	2.8	1.5	4.3	4.3
	Main	1	69.3	0.7	70.0	70.0
	Reserve	1	67.0	0.3	67.3	67.3
	Location Aids	1	0	6.5	6.5	6.5
	Sequencer	1	0	9.8	9.8	9.8
	Totals	-	146.2	22.8	169.0	169.0
	% Recovered Weight:					
GEMINI - 4400 LB	4.8 Total					
	4.1 Without Sequencer & Location Aids					
	3.4 Without Backup					
	Drogue	1	8.5	4.7	13.2	13.2
	Pilot	1	8.9	4.7	13.6	13.6
	Main	1	115.3	1.6	116.9	116.9
	Disconnects	3	0	2.0	2.0	6.0
	Bareswitch	2	0	1.3	1.3	2.6
APOLLO - 11000 LB	Personnel	2	17.0	2.8	19.8	39.6
	Totals	-	-	-	-	191.9
	% Recovered Weight:					
	4.4 Total					
	4.2 Without Bareswitches & Disconnects					
	3.3 Without Backup					
	Drogue	2	26.8	23.2	50.0	100.0
	Pilot	3	3.7	6.3	10.0	30.0
APOLLO - 11000 LB	Main	3	136.0	9.2	145.2	435.6
	Retention	3	1.1	0	1.1	3.3
	Sea Sling	1	2.6	0	2.6	2.6
	Sequencer	2	0	6.6	6.6	13.2
	Totals	-	-	-	-	584.7
	% Recovered Weight:					
	4.5 Total					
	4.4 Without Sea Sling & Sequencers					
	2.8 Without Redundant Drogue, Pilot & Main					

SECTION 5

DESIGN PROCEDURES

The design procedures outlined in this section are applicable to Ringsail parachutes of all sizes. The solution of a sample design problem is given in Appendix C. The design of a Ringsail parachute, like that of any other type, is carried out along two parallel courses -- geometric and structural -- with some interplay between them aimed at one or more of the following potential objectives:

- a. Minimum weight
- b. Maximum specific drag area ($C_D S/W_p$)
- c. Maximum structural reliability
- d. Facility of manufacture

System operational requirements for the parachute yield basic design criteria which may include the following:

- a. The maximum allowable rate of descent at a given altitude.
- b. Maximum allowable opening load or load factor.
- c. Maximum or average amplitude of pendular oscillations.
- d. Installed weight and/or volume.
- e. Maximum allowable elapsed time from deployment to full open under a given set of conditions.
- f. Geometrical factors affecting the lengths of suspension lines and risers.
- g. Type of deployment system.
- h. Type of reefing system.

Usually some of these criteria are given greater weight than others, some may be set up only as design goals, and in areas of possible conflict an order of precedence may be established.

The decision to use a cluster of parachutes rather than one parachute is made on the basis of preliminary design calculations and tradeoff studies. With the exception of specific details to be identified, the design procedure for the cluster Ringsail is the same as that for the single parachute.

Design of the parachute proper is preceded by a number of preliminary computations. System true airspeed and free stream dynamic pressure at parachute line stretch and at disreef for each reefed stage are determined for given design conditions by trajectory computations using a digital computer program of the type described in Section 6.1. The size of the parachute or cluster is determined by calculating the total effective drag area ($\Sigma C_D S$) required using the method given in Section 6.2.1 along with the applicable drag coefficient (C_{D_0}) determined from Figures 22 through 26, as follows:

- a. Enter Figure 22 with the design rate of descent, and estimated suspension line length and estimated D_0 range and read C_{D_0} , interpolating l_e/D_0 as required.
- b. Calculate S_0 and D_0 to verify size of single canopy.
- c. Enter Figure 23 with D_0 to verify C_{D_0} for $l_e/D_0 = 1.15$.
- d. For effective line lengths other than $l_e/D_0 = 1.15$, enter Figure 24b with design value and read $C_{D_0}/C_{D_0}^*$, where $C_{D_0}^*$ is the value for $l_e/D_0 = 1.15$.
- e. If the crown geometric porosity is significantly higher than standard for the design as given in Figure 21, consider the need for a C_{D_0} correction derived from Figure 25, with due allowance for the specialized nature of the source data given.
- f. For clusters, use Figure 26 to determine $C_{D_0}/C_{D_0}^*$, where $C_{D_0}^*$ is the single canopy value derived from steps (a) through (e) above.

Design limit loads of single and clustered canopies are calculated by the method given in Section 6.3.1. When design safety factors are not given in the system specification, those given in Section 5.2 should be used for preliminary estimates. The overall design factor is calculated as $D.F. = S.F. / A_p$. The components of the allowable load factor (A_p) are given in Section 6.4.1.

It should be noted that most of the empirical methods given for Ringsail parachute design are derived from tests in which unit canopy loadings were in the order of $W/C_D S = 0.5$ to 1.5 psf; uncertainty as to their accuracy will be greater for systems having lower or higher unit loads.

5.1 CALCULATION OF BASIC DIMENSIONS

The aerodynamic analysis through determination of the required effective drag area and applicable drag coefficient defines the drag surface area (S_o). This provides the basis for the bulk of the basic dimension calculations. Salient aspects of the design procedure, summarized in Figure 12, are repeated here in greater detail, each discrete step being numbered for clarity.

1. Calculate the nominal diameter of the canopy

$$D_o = (4 S_o / \pi)^{1/2}$$

2

2. Determine the number of gores as a convenient even number divisible by the number of risers for good structural design between $N = .76 D_o$ and $N = .88 D_o$, with D_o expressed in feet. Since the number of suspension lines is equal to the number of gores, structural efficiency will be benefitted if the product $N P_g$ is about five percent greater than the product (D. F.) F_{Lim} obtained from the structural analysis (see Section 6.4). The margin allowed for future growth depends on the firmness of the design criteria and somewhat on the availability of textile cords of the proper rated strength (P_g). However, the possibility exists (and has been taken advantage of) of uprating the strength of some mil-runs of "MIL Spec" materials by performing acceptance tests to ensure compliance.

3. Calculate the length of the suspension lines.

$$l_s = l_e - l_R$$

3

where

$$l_e = 1.15 D_o$$

4a

and the riser length (l_R) is any convenient number, usually between 2 and 4 feet. For two-canopy clusters the recommended effective line length is

$$l_e = \sqrt{2} D_o$$

4b

and for three canopy clusters of high efficiency

$$l_e = \sqrt{3} D_o$$

4c

might be justified by a tradeoff study of length vs C_D to obtain a cluster of minimum weight for a given $\Sigma C_D S$, as was done for single parachutes in References 5 and 35.

Make certain that the drag coefficient used in the aerodynamic analysis was based on the effective line length selected.

4. Calculate the gore height equal to the canopy radial dimension.

$$h_R = 0.519 D_o \text{ (see Figure 12)}$$

5

For convenience this dimension is rounded off to the nearest inch.

5. Calculate the combined area of the central vent and the ring slots in the crown of the canopy.

$$\Sigma S_{gc} = \lambda_{gc} S_o$$

6

Where λ_{gc} is read from the top curve of Figure 21 at the pertinent D_o .

6. Select the woven width (h_w) of cloth to be used in the sails. Integral widths of 18, 24, 36 and 42 inches have been used depending in part on the size of the parachute. However, the use of 42 inch cloth may not be desirable since models with 36 inch sails ranging from $D_o = 56.2$ to 128.8 feet have exhibited very satisfactory performance. Select a width such that the number of sails in the final gore layout is not less than nine. Note that at sail number 1 allowance must be made for folding under the vent band as shown in Figure 70 in Section 7.

7. Determine the vertical spacing of sails in the gore. This is necessarily an iterative procedure, initiated by making a rough estimate and then refined by subsequent steps of adjustment and computation. In general the number of sails (n) is the nearest whole number less than h_R/h_w , but when $D_o > 100$ feet the number of sails is one less than this. Since the top sail is usually narrower than h_w the number of full sails (n_f) is approximately $(h_R/h_w - 1)$.

Note in Figure 12 that the ring slots in the crown of the canopy extend to approximately 0.4 h_R . Assume that the number of slots (n_g) is the nearest integer less than $(0.4 h_R/h_w) + 1$.

- a. Determine the number of sails and number of ring slots with the above relationships. Let the vent dimension be any convenient number between $h_v = 0.02 D_o$ and $0.03 D_o$ rounded off to the nearest inch. Estimate the slot width dimension (Δh_g) by defining a mean slot as follows:

- Let the position of the mean slot be

$$\frac{h_g}{g} = (.4 h_R - h_v) / 2 + h_v$$

7

- Then the length of the mean slot is

$$\bar{C}_g = 6.44 (h_R / N) \sin(h_g / h_R) 54^\circ \text{ (Figure 12)}$$

8

- The open area per gore is $\Sigma S_{gc} / N$ (See step 5)

- Estimate the area of the vent sector and calculate the area of the mean slot in one gore $\bar{S}_g = [(\Sigma S_{gc} / N) \cdot S_v] / n_g$

- Then $\Delta h_g = \frac{\text{area of mean slot}}{\text{length of mean slot}} = \bar{S}_g / \bar{C}_g$

Present best practice is to make all slots the same width because experience gained from the Apollo Ringsail development program demonstrated that having slot widths inversely proportional to the ring diameter was a needless complication.

The final step in completing the first approximation of the sail spacing is to calculate the height (h_t) of the top sail as the difference:

$$h_t = h_R - (n_F h_W + n_g \Delta h_g + h_v)$$

9

This dimension will usually be less than the woven width of the cloth and is rounded off to the nearest inch. Allow 2.0 inches for the vent hem as shown in Figure 70.

- b. The second approximation begins by making any dimensional adjustments that appear necessary upon appraisal of the following:

- Is the height of the top sail too wide or too narrow?
If too wide, consider adding one sail to the layout.
If too narrow, consider reducing the vent diameter.

Compare the radial position of the mean slot obtained from the calculated dimensions with the first estimate. This will indicate whether the slot width should be increased or decreased. This step is clarified by the numerical example given in Appendix C.

After making the dimensional adjustments indicated, check the size of the central vent. Because the average Ringsail vent is relatively small, there is considerable latitude in the area acceptable. The following criteria may be applied; only one need be satisfied.

$$S_v / S_o = .0015 \text{ to } .0035 \quad (\text{Let } S_v = \pi D_v^2 / 4)$$

$$h_v / D_o = .02 \text{ to } .03$$

$$C_v = 2.0 \text{ to } 2.5 \text{ inches} \quad (\text{Let } C_v = \pi D_v / N)$$

An approximate vent diameter is obtained from

$$D_v' \approx 1.932 h_v \quad 10a$$

The finished vent diameter is

$$D_v = N C_v / \pi \quad 10b$$

and

$$S_v = \pi D_v^2 / 4 \quad 11$$

Note that the vent diameter is not increased by the fullness factor because the vent lines are marked to hold this dimension, causing the vent band to arch upward between radials. In order to prevent the vent band from shrinking the vent, it is marked under nominal tension to a dimension C_v based on its outside diameter which is close to $D_v + 2$ inches for a 1 inch band. An additional allowance for takeup due to thread tension in the seams may be made.

With the preliminary crown geometry thus defined, the geometric porosity is calculated and compared with the value obtained in step 5. Note that this computation entails determination of the gore width at each slot in place of a mean slot length.

c. The result will indicate the adjustment to be made in the slot width. If the adjustment is large, the number of slots may be increased or reduced by one. Since these changes also change the radial spacing of the slots in the gore, the third approximation consists of repetition of all the operations required to verify the crown geometric porosity. If good agreement with the desired design value is obtained, say within ± 5 percent, no further dimensional adjustments need be made the vertical spacing of the sails in the gore is determined.

8. Calculate the gore coordinates at the upper and lower edges of the sails.

$$C = 6.44 \left(\frac{h}{R} \right)^N \sin \left(\frac{h}{h_R} \right) 54^\circ \text{ (from Figure 12)} \quad 12$$

These are the coordinates of a truncated ogival surface having the constructed profile illustrated in Figure 15c. Mathematically and geometrically, it is the equivalent of a spherical surface with small sector, i.e., several "gores", removed and the cut edges joined together.

9. Determine the fullness factors K_A and K_B using the diagram showing how K varies with h/h_R for the upper and lower edges of the sails in Figure 54.

10. Calculate the widths of the sails at the upper and lower edges.

$$C_A = K_A C \quad 13a$$

$$C_B = K_B C \quad 13b$$

These are the distances between the centerlines of the radial seams.

11. Calculate the sum of the areas of vent, slots and sails to verify S_o .

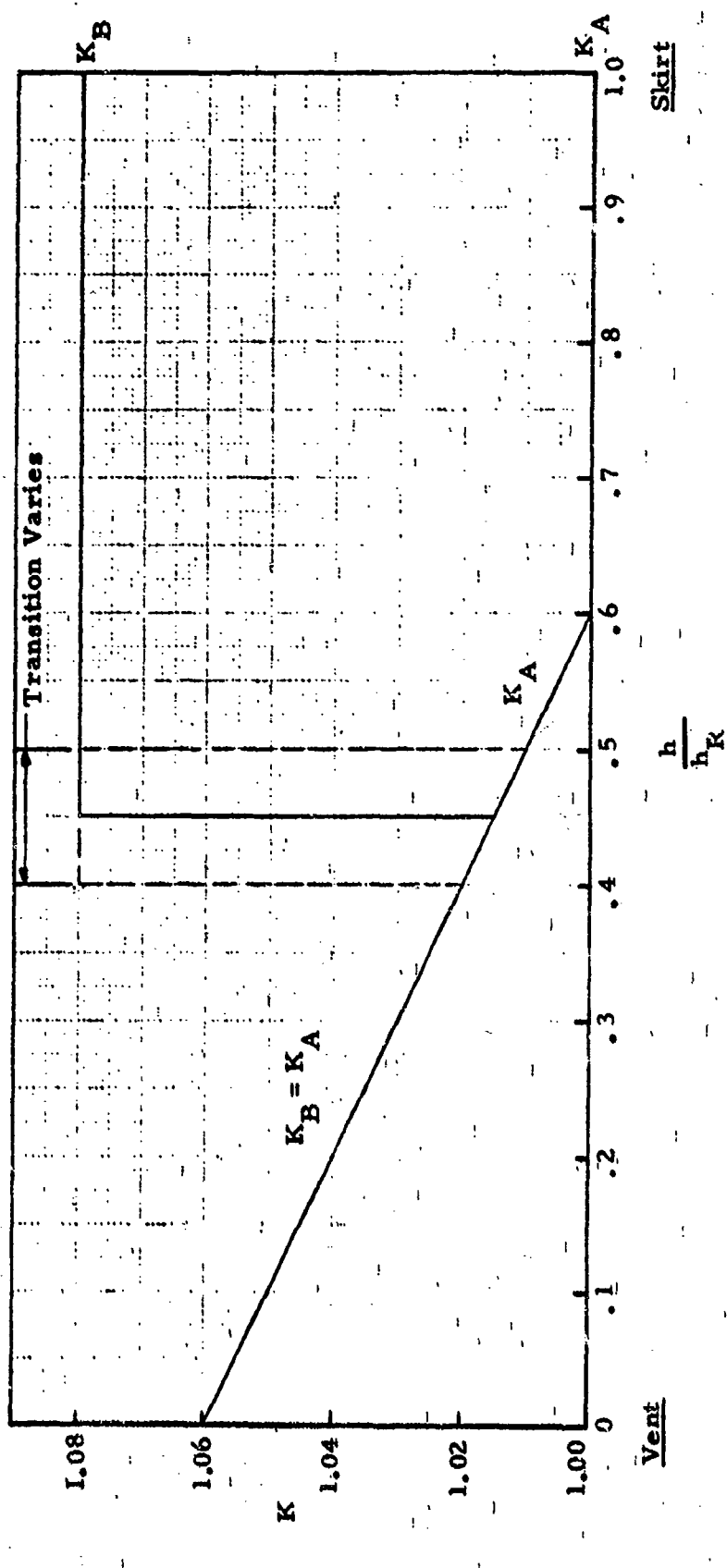
$$S_o = S_v + \sum S_g + \sum S_s \quad 14$$

The area of each slot or sail is calculated as the product of its height and its mean length

$$\Delta S = \Delta h (C_A + C_B)/2 \quad 15$$

And the area of each ring is simply $N(\Delta S)$.

Figure 54 . Ringsail Fullness Distribution



The value of S_0 thus obtained usually is slightly different from the design value and the nominal diameter is corrected to reflect the difference. However, there is no pressing need to correct the design drag area ($C_D S_0$) because the change is small relative to the probable accuracy of the drag coefficient.

12. Calculate the sail pattern dimensions. Seam allowances are added for the radial fell seams and the rolled hem on the upper edge of Sail No. 1. The allowance made for the 1/2 inch fell seam shown in Figure 11 is 0.8 inches or 1.6 inches for two overall. The allowance made for a 1.0 inch rolled vent hem is +2.0 inches on the height of Sail No. 1. With reference to the pattern diagram:

$$H_1 = h_1 + 2.0 \text{ (inches)}$$

$$H_2 \text{ to } H_n = h_w \text{ (woven width)*}$$

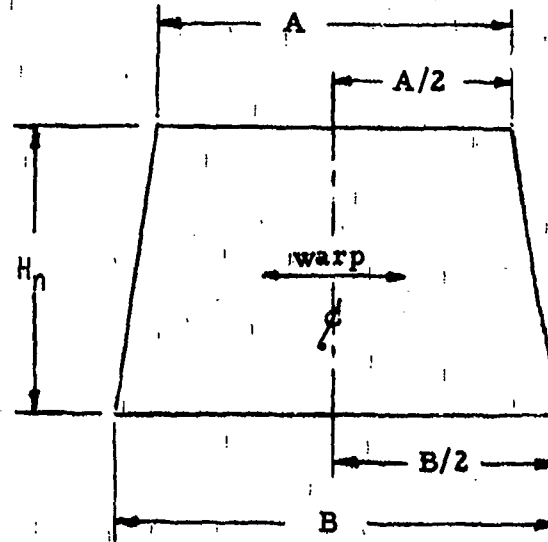
$$A = C_A + 1.6 \text{ (inches)}$$

$$B = C_B + 1.6 \text{ (inches)}$$

The upper edge of Sail No. 1

$$A_1 = C_A + 1.6 - \Delta C$$

Where ΔC is the change in width over the 2 inch seam allowance.



13. Calculate the gore assembly height: $h_a = h_R - h_v$

16

This completes the basic dimension scheme and the lengths of all components are determined.

* Note that h_w is subject to a manufacturing tolerance which is shown on the pattern drawing only. All calculations are based on the nominal width which is the minimum value; e.g., $h_w = 36 \frac{1}{2} \pm \frac{1}{2}$ inches for a nominal width of 36 inches.

5.2 SELECTION OF MATERIALS

Selection of materials is based partly on experience and partly on a preliminary stress analysis employing empirical formulae to estimate the strength of materials required. The structure so defined provides a basis for weight calculations and for a detailed stress analysis by more rigorous methods supplemented by laboratory strength tests. The results may dictate changes in the weight of cloth and in the rated strengths of other members with a consequent revision of the weight estimate.

The stress analysis, more properly called an internal loads analysis, is based on limit opening loads applied by the parachute to the attached vehicle through the main riser. These design limit loads are supplied by the loads analysis and may be different for each opening stage. Since the shape of the reefed canopy differs greatly from the shape of the disreefed canopy at the instants of peak loading, a separate internal loads analysis must be made for each opening stage.

A preliminary selection of materials may be made without going into the various factors affecting the allowable strengths because a suitable design factor can be estimated for any safety factor required. For example, commonly specified safety factors are 1.5 for canopy and lines and 2.0 for risers. Corresponding design factors for a sound lightweight parachute structure are: (Reference Section 6.4.1).

$$D.F. = 1.9 \text{ (canopy and lines)}$$

$$D.F. = 2.5 \text{ (risers)}$$

Very conservative structures of mid- to heavy-weight are obtained with design factors of 2.1 to 2.3 for canopy and lines. The actual weight class of the structure also depends on the magnitude of the opening load factor.

The required minimum rated unit strength (P'_R) of the textile member is determined as the product of the design factor and the maximum or critical internal load

$$P'_F = (D.F.) T_c$$

17

and it is good practice to select the lightest available material for which the rated strength

$$P_R \geq P'_R$$

18

The following empirical formulae provide a convenient basis for the preliminary calculation of internal loads and the required strength of materials. (See Section 6 for derivations.)

$$\text{Canopy cloth: } T_c = F_L / \pi D_p \quad 19$$

$$\text{Suspension line cord: } T_c = F_L / N \quad 20$$

5.2.1 Canopy Cloth

The projected diameter of the canopy at the instant of $F_L = F$ (max) during inflation is

$$D_p = (4 S_p / \pi)^{1/2} \quad 21$$

where

$$S_p = C_D S / C_{D_p} \quad 22$$

and $C_D S$ is derived from trajectory calculations for reefed stages and C_{D_p} comes in Figure 55. (See Section 6.2.3)

It can be assumed that the reefed opening load reaches its peak at the end of reefed inflation, but on disreefing the load peak occurs prior to full inflation.

Fortunately, only the reefed condition is critical in the great majority of cases, because for many years the lightest available parachute cloth has been more than strong enough for the major area of the canopy outside the crown. Therefore, the problem is reduced to a simple determination of how much of the crown area should be made from cloth stronger than 1.1 oz Ripstop (normally rated at 42 lb/in). (See Table XXIV in Section 6.5.)

The maximum reefed opening load obtained from the loads analysis is based on a particular reefed drag area ($C_D S_R$). For rough calculations it may be assumed that the drag coefficient $C_{D_p} = 1.0$ but this is very conservative for small reefing ratios. A somewhat less conservative approach is justifiable using a C_{D_p} value corresponding to the given reefing ratio (D_R / D_o) as given in Figure 55 (Section 6.2.3).

Calculate $P'_R = (D.F.) T_c$ and compare the result with the unit strengths of available parachute fabrics.

$$T_c = F_L / \pi D_{pl} \quad (\text{Equation 19})$$

The crown area to be covered with the heavy cloth should be a minimum because the weight increases rapidly with increasing radius. This area can be estimated in terms of a radial dimension (h_c) on the pressurized portion of the canopy defined as a hemisphere of diameter D_{p1} (see Figure 66 in Section 6).

$$h_c = \pi D_{p1} / 4$$

23

Comparison of this dimension with the table of gore coordinates will indicate the number of rings of heavy cloth required.

The crown of the reefed canopy is not a hemisphere but photogrammetric analysis shows the radius near the vent to agree well with this assumption, e.g., see Reference 13. The profile radius decreases toward the periphery, as does the differential pressure across the canopy also, which may account for the concentration of damage close around the vent when the crown cloth is not strong enough. With two stages of reefing the above is true of both stages and the method of calculation is the same as for stage 1.

If a transition annulus of intermediate weight cloth between the crown and the major area of the canopy is needed, the strength required may be determined by estimating the unit loading after disreefing when the pressurized portion of the canopy has expanded to a larger radius such that

$$h/h_R \approx 0.5^*$$

when $h_{c2} < h/h_R = .5$ the transition annulus is not required. Since the parachute force will not have reached its peak at this time a calculation based on the limit load will be quite conservative.

Let

$$D_{p2} = (4/\pi) \cdot 5 h_R$$

24

and

$$T_c = F_L / \pi D_{p2} \quad (\text{Equation 19})$$

*Observation indicates the inflated periphery to be roughly in this region shortly after disreefing.

The conservative nature of both of the above calculations allows the designer some freedom in the selection of materials for the rings in the upper half of the canopy. For example, in the interest of minimizing structural weight a fabric could be selected for which P_R was somewhat less than the calculated P'_R on the ground that the prototype model will be subject to more rigorous evaluation later both analytically and in aerial drop tests for demonstration of structural integrity. This approach has been used successfully in some programs where weight was a critical factor.

Having determined the number of crown rings to be made of heavy cloth, the remainder will be made of 1.1 oz ripstop nylon or its equivalent. In many cases, if lighter weight fabrics of the proper porosity were available, such material could be used. A listing of the unit strengths and unit weights of currently available parachute textiles is given in Table XXIV, Section 6.5.

5.2.2 Suspension Lines and Vent Lines

Although the vent line load is less than the suspension line load, it is good practice to use the same cord for both members, because the weight increment is negligible. As noted in step 2 of the basic dimension calculations the strength of cord selected for the suspension lines is coordinated with determination of the number of gores in the canopy such that P_R is roughly 5 percent greater than

$$P'_R = (D.F.) F_{LIM} / N$$

25

Of course $P_R = P'_F$ is also acceptable but allows no margin for growth.

5.2.3 Radial Tapes

The canopy load transferred to the suspension lines is shared by two tapes and the cloth in each radial seam. As a minimum the strength of each of the two tapes in the radial seam must have

$$P_F = (0.9 P'_R \text{ of suspension lines}) / 2$$

(See 6.4.2.3)

26

but the limited choice of suitable textiles usually results in radials considerably stronger than the lines. New textile forms are needed here to support the design of Ringsail structures of maximum efficiency.

5. 2. 4 Risers

Of the many nylon webbings available a few have unusually high strength/weight ratios in combination with good flexibility, e. g., 6000 lb 1.0 inch and 10,000 lb 1.75 inch. These are used in preference to the stiffer and less efficient webbings even when choice of the latter is indicated by the required strength

$$\frac{P}{F} = \frac{(D.F.) F_{LIM}}{N_R}$$

27

Because the riser assembly is usually quite short, the weight increment of using stronger webbing than required is very small.

5. 2. 5 Circumferential Bands

These are the bands that form continuous hoop members around the canopy, as opposed to the intercostal tapes placed on sail edges to increase tear strength.

Vent Band: Because the vent band is so short, it is made much stronger than can be justified by any internal load analysis. Good practice is to make the vent band from 4000 lb 1 inch tubular nylon webbing or an equivalent textile form or plied assembly.

Skirt Band: Under normal operating conditions the skirt band is lightly loaded. Substantial strength may be required only to resist whipping loads and to hold the canopy together when a gore is split. Because this band also serves to stiffen the skirt as an opening aid, good practice is to make the skirt band of a one-half inch wide tape or web having a strength at least equal to that of the suspension lines. However, the practice in large Ringsails has been to employ a 1,000 lb 1/2 inch tubular web for this member.

Intermediate (ripstop) Bands: Parachutes subject to high stress levels in the mid gore region after disreefing are reinforced with one or two continuous bands on the upper edges of selected rings. These are redundant members and in order to be effective in preventing the radial spreading of rips in the canopy they must be quite strong. Consequently they are heavy and the number used must be sharply limited to obtain a parachute structure of good efficiency. One such band made of 1000 lb 1/2 inch tubular webbing at $h/h_R = .416$ in the lightweight 128.3 ft D_0 Century Ringsail proved to be an adequate ripstop member.

5.2.6 Vertical and Intercostal Tapes

Good practice is to make these members of 5/8 inch tape with $P_R = 70$ lbs in low stress areas and $P_R = 90$ lbs elsewhere. The vertical tapes on gore centerlines across the crown slots are generally double members of 90 lb tape. The weight increment of the 90 lb tape over the 70 lb tape is negligible except on sail edges below $h/h_R = 0.45$, where the tear-stress level is low and 70 lb tape can be used to good advantage.

Distribution of the tapes on sail edges along the gore is made as follows:

90 lb tapes:

- on both edges of all ring slots in the crown
- on upper sail edges only to $h/h_R \approx .40 - .45$

70 lb tapes:

- on upper sail edges only between $h/h_R = .45$ and 0.60 approximately

Beyond $h/h_R = 0.60$ no tapes are required on "Trip" selvage cloth. (See Appendix E.)

Where a ripstop band is installed, the intercostal tape is omitted from the sail subassembly.

5.2.7 Miscellaneous Textile Components

Thread: In general, Ringsail structures of all weights are stitched with the same weight nylon threads as follows:

B (5.5 lb) -- Basting gore subassemblies

E (8.5 lb) -- All seams except radials and vent band

F (11.0 lb) -- Radial seams and vent band

Use of B thread may be considered optional for stitching intercostal tapes to sail edges. Riser assemblies are generally stitched with #6 nylon cord.

Reefing Line: Use 1000 lb braided nylon cord except where the structural analysis or test data show the need for an allowable strength greater than 500 lbs approximately. Although 550 lb and 750 lb reefing lines have been used successfully in some systems, there is nothing to be gained by using a cord lighter than the proven capacity of available miniature reefing line cutters.

5.2.8 Hardware

Reefing Rings: Of the many reefing ring designs available, the best for a given application will be the smallest that allows the reefing line complete running freedom. The ring selected must also be rigid, very smooth with fully rounded edges, and wide enough so that it can be rigidly attached to the canopy skirt. The ring should also be of corrosion resistant materials or design.

Line to Riser Links: The preferred design is a separable link of maximum specific strength that is rigid and smooth with fully rounded edges all over. The proof test load for the link should be not less than

$$P_T = F_{LIM} / N_R \quad 28$$

and the minimum ultimate strength or certified rated strength should be equal to or greater than

$$P'_R = 1.5 F_{LIM} / N_R \quad 29$$

Suitable links of different strengths are given in Section 4.2, Table XVII.

A rough weight estimate of canopy and lines is made with the aid of Figure 53 based on the weight class into which the new parachute design falls. This weight increased by 12 percent will provide a representative pack weight including reefing components, risers, links, and deployment bag. The pack volume is then calculated for an average pack density based on the packing method to be employed.

When the parachute design has been completed to this point, it is ready for a more detailed and rigorous analysis by the methods outlined in Section 6 and for the preparation of detail drawings or sketches suitable for the fabrication of the first test specimens.

5.3 RINGSAIL DESIGN BY COMPUTER

A digital computer program designated WGI76 was developed in 1966 to facilitate solution of Ringsail parachute design problems. The program was designed around the basic dimension scheme of Figure 12 to carry out the design procedure described in preceding Section 5.1, including an iterative determination of the sail spacing on the gore. In addition, it performs a porosity computation similar to that illustrated in Section 6.6 and a weight computation by the exact method given in Section 6.1. The program was

originally written for the IBM 7090 digital computer in FORTRAN IV. It has since been modified for use in the IBM 360/65 digital computer and exists in two forms: WG176A-10 punched IBM input cards and requires all sails below the ringslot crown to be of equal width; the -11 version employs 11 input cards and variable sail widths may be used throughout.

As a minimum the input must specify either the desired effective drag area ($C_D S_0$) or the nominal diameter (D_0) of the Ringsail parachute to be designed. Given one of these, the computer will develop the basic dimensions and gore coordinates of a standard Ringsail design having an even number of gores divisible by the proper number of risers, the correct crown porosity, the correct number of rings in the canopy for a cloth width of 36 inches, and an effective suspension line length of $\ell_e/D_0 = 1.15$ (with risers 3.0 feet long). The printout includes a summary of the porosity computation (λ_{gv} , λ_{gc} , λ_g , λ_m and λ_T); the drag coefficient $C_D \delta$ (corrected for scale) used to calculate $C_D S_0$, plus corrected values of S_0 and D_0 derived from a summation of the sail and slot areas. The printout also includes the sail pattern dimensions.

When the program input is augmented to include a listing of the unit weights of selected materials, the print-out will also include the total weight of parachute and risers down to the confluence point and a breakdown summary of the component weights: sail fabric, suspension lines, risers, radials, skirt and vent bands, and all reinforcing tapes and bands.

The input provisions of the program are comprehensive and flexible, enabling the designer to specify as many of the design parameters as he wishes, including the vertical spacing of sails of varying widths along the gore. After a preliminary design run on the computer, the designer is free to adjust any of the basic dimensions specified and learn their precise effects on the area, porosity, and weight of the modified configuration by performing a second computer run. WG176 is a valuable adjunct to the CANO stress analysis program described in Section 6 and Reference 25.

SECTION 6

DESIGN ANALYSIS METHODS

The design of parachute systems requires a variety of computations employing a combination of analytical procedures based on empirical data describing the performance and other characteristics of the type of parachute to be utilized. Presented in this section are the major design analysis methods used in the development of Ringsail parachute systems. The material is presented under the following subheadings:

- a. System Trajectory Computations
- b. Ringsail Aerodynamics
- c. Prediction of Opening Loads
- d. Stress Analysis
- e. Calculation of Ringsail Weight
- f. Calculation of Ringsail Porosity

6.1 SYSTEM TRAJECTORY COMPUTATIONS

Parachute system trajectory computations are made to produce a graphic presentation of vehicle motion and dynamic response data following deployment of the component parachutes in operational sequence. Preliminary trajectory calculations also are a necessary part of the parachute design process and are usually based on a given set of initial conditions at deployment (vehicle weight, velocity, and flight altitude and path angle).

Such computations are best done with a digital computer using a simple two-degree-of-freedom program in which the equations of motion are:

$$\dot{x} = v \cos \gamma \quad 30$$

$$\dot{y} = v \sin \gamma \quad 31$$

$$\dot{v} = -(F_p + D_v + W_v \sin \gamma) / m_v \quad 32$$

(See equation 52 in Section 6.3.2)

$$\dot{\gamma} = -(g \cos \gamma) / v^2 \quad 33$$

For rough preliminary work the parachute force and the drag of the vehicle are approximated by

$$F_p + D_v = (C_D S_p + C_D S_v) q \quad 34$$

and $C_D S_p$ is represented by a simple step function of time corresponding to the reefed program desired. Significant variations of $C_D S_v$ with time or Mach number also are represented by step functions. For any given set of initial conditions (W_0 , h_0 , v_0 , and Y_0) this method will yield dynamic pressures at the beginning and end of reefed intervals suitable for prediction of opening loads by the load factor method. The loads indicated by the computer itself are excessive because the drag area step-function is not realistic. However, with the introduction of filling times in the drag area step-function, e.g., Figure 56, the reefed opening forces predicted by the computer can be made quite accurate as shown in Section 6.2.6. Unfortunately the same is not true of the final opening load after disreefing because this process is dominated by the influence of the added air mass on system dynamics.

The determination of parachute reefing parameters (D_R/D_0 and Δt_R) for a given system prior to flight test is done through a series of trajectory calculations made primarily for the purpose of determining the dynamic pressure at the beginning and end of each reefed interval. This is done in conjunction with opening load calculations aimed at attainment of a favorable balance of peak loads from stage to stage for the critical design conditions on the performance envelope of the vehicle. In the general case the maximum opening load of one stage is not necessarily associated with the same set of initial conditions for which the opening loads of other stages are maxima.

6.2 RINGSAIL AERODYNAMICS

Due to aeroelasticity and porosity the aerodynamics of parachutes is so complex that only rudimentary calculations can be made with any confidence. Even so, the results are subject to statistical variations of a random character, as the data of Section 3 clearly demonstrate.

6.2.1 Rate of Descent

In equilibrium descent the total drag of the system (F_c) is very nearly equal to its weight (W) such that

$$W = F_c = \sum C_D S q_e \quad 35$$

Whence the equilibrium dynamic pressure

$$q_e = W / \Sigma C_D S \quad 36$$

and the rate of descent

$$v_e = (2 q_e / \rho)^{1/2} \quad 37$$

Generally at low rates of descent the drag of the suspended vehicle is negligible, permitting the effective drag area of the parachute to be calculated for a desired rate of descent as simply

$$C_D S_o = W / q_e \quad 38$$

Since system oscillation and gliding are limited by design to magnitudes that pose no hazard to the payload at touchdown, there is seldom any need in the operational analysis to consider horizontal velocity components other than that of wind drift. The latter is a totally random factor to which all non-steerable parachute systems are subject.

6.2.2 Drag Coefficient

The drag coefficient is calculated from test data relating the tangential force (F_c) of the parachute to the free stream dynamic pressure (q)

$$C_{D_o} = F_c / S_o q \quad 39$$

With large parachutes this becomes a matter of measuring the descent velocity and atmospheric properties over a substantial altitude interval. An attempt is made to obtain aerological data as a function of altitude at the time of the test ± 30 minutes so that the air density can be evaluated with reasonable accuracy. The descent velocity is subject to errors of observation and mensuration of phototeleodolite data and includes an unknown increment due to vertical air motion. The system weight can be measured very accurately to yield F_c , and while the canopy area (S_o) is known within narrow limits, the inflated (projected) area (S_p) is not. S_p is known to vary somewhat due to the breathing phenomenon which tends to be periodic. However, it is suspected that S_p also may vary from test to test due to the effects of hysteresis after the canopy has been stretched by opening loads of different magnitudes. Thus far, attempts to correlate these factors have been unsuccessful. While some photogrammetric data show the Ringsail adhering closely to the two-thirds rule ($D_p/D_o = 2/3$) other measurements yield

$D_p/D_o = .74$ to $.80$ following heavy overloads. In any event, when the corrected rate of descent during a given test is found to vary widely in a non-periodic fashion, the resultant average value cannot be relied upon for evaluation of the drag coefficient. When this behavior was found in the results of Ringsail drop tests, such data points were rejected from the performance evaluation.

For design purposes the drag coefficient is estimated with the help of Figures 22 through 26 by taking into account all of the governing factors:

- a. Unit canopy loading as measured by the equivalent rate of descent
- b. Scale effects
- c. Effective length of suspension lines
- d. Crown geometric porosity
- e. Number of canopies in a cluster when pertinent

6.2.3 Reefed Drag Area

Reefed drag area calculations are made for both single and clustered parachutes on the basis of empirically derived curves of the two reefing ratios $C_{D,S,R}/C_{D,S,o}$ vs D_R/D_o such as those of Figures 46 through 48. Accurate determination of Ringsail reefed drag area is handicapped by the fact of its growth during the reefed interval. Thus, the easily measured value, under near-equilibrium conditions at disreefing, is a function of the duration of the reefed interval, while the smaller initial drag area associated with the peak opening force is obscured by system deceleration. It has been a common practice to report measured values of F/q as equal to $C_{D,S}$, ignoring the dynamics of the added air mass. Consequently, the data obtained by this uncritical treatment tends to be unique for each different system and cannot be relied upon for general use.

Note that by defining the diametral reefing ratio in terms of D_o , the canopy is fully inflated at $D_R/D_o \approx 2/\pi = .636$ for any parachute in which $D_p = 2/3 D_o$. This is necessarily only an idealized theoretical limit.

As noted in Section 5, the short method of estimating internal loads would be improved by more accurate knowledge of the reefed drag coefficient $C_{D,p}$.

Steady state measurements made in the wind tunnel give results corresponding to conditions at the end of a long reefed interval. For example, the full scale tests of single Apollo 88.1 ft D_o experimental parachutes described in Section 2.1.4 yielded the drag coefficient data presented in Table XX for reefed canopies having the same crown porosity as the unmodified design.

TABLE XX

WIND TUNNEL TEST DATA FOR TWO CONFIGURATIONS OF
THE APOLLO 88.1 ft D_o RINGSAIL

Wind Tunnel Test Configuration	$\frac{D_R}{D_o}$	D_p (ft)	C_{DSR} (ft ²)	$\frac{C_{DSR}}{C_{DSo}}$	$\frac{D_p}{D_o}$	C_{Dp}
A-2 (1) (Full length vertical tapes) $C_{DSo} \approx 5180 \text{ ft}^2$.10 .13	27.8 30.5	397 641	.0766 .1235	.316 .346	.652 .876
A-11(2) (Overall λ_g increased to 9%) $C_{DSo} \approx 5020 \text{ ft}^2$.10 .13	26.3 29.7	399 563	.0795 .1121	.298 .337	.733 .813

NOTE:

- (1) W. T. Mod A-2; PDS 1543-553 Figure 86 Appendix A
- (2) W. T. Mod A-11; PDS 1543-543 Figure 89 Appendix A

Comparison of the area ratios with those in Figure 40b at the corresponding diameter ratios shows reasonably good agreement at $D_R/D_o = 0.10$ and only fair agreement at $D_R/D_o = 0.13$ for conditions at the end of the reefed interval.

Table XXI presents results obtained with Wind Tunnel Test Configuration A-2 (see Table XX for definition) using mid-gore reefing in place of radial reefing.

TABLE XXI

WIND TUNNEL TEST DATA OF CONFIGURATION A-2
APOLLO 88.1 ft D_o RINGSAIL WITH MID-GORE REEFING

$\frac{D_R}{D_o}$	D_p (ft)	C_{DSR} (ft ²)	$\frac{C_{DSR}}{C_{DSo}}$	$\frac{D_p}{D_o}$	C_{Dp}
.08	28.0	402	.0775	.318	.652
.10	30.5	553	.1067	.346	.757
.13	32.6	743	.1435	.370	.890

These data are plotted in Figure 55a to show the difference between mid-gore and radial reefing. For equal drag areas the difference in reefing ratio is close to $\Delta(D_R/D_o) = .02$. The drag coefficients plotted in Figure 55b show good agreement when this difference is applied to correct D_R/D_o for mid-gore reefing. The drag coefficient of the fully-inflated canopy was calculated with the assumption that $D_p = (2/3) D_o$.

$$C_{Dp} S_p = C_{Do} S_o$$

$$C_{Dp} = C_{Do} (S_o/S_p) = C_{Do} / (2/3)^2$$

and with

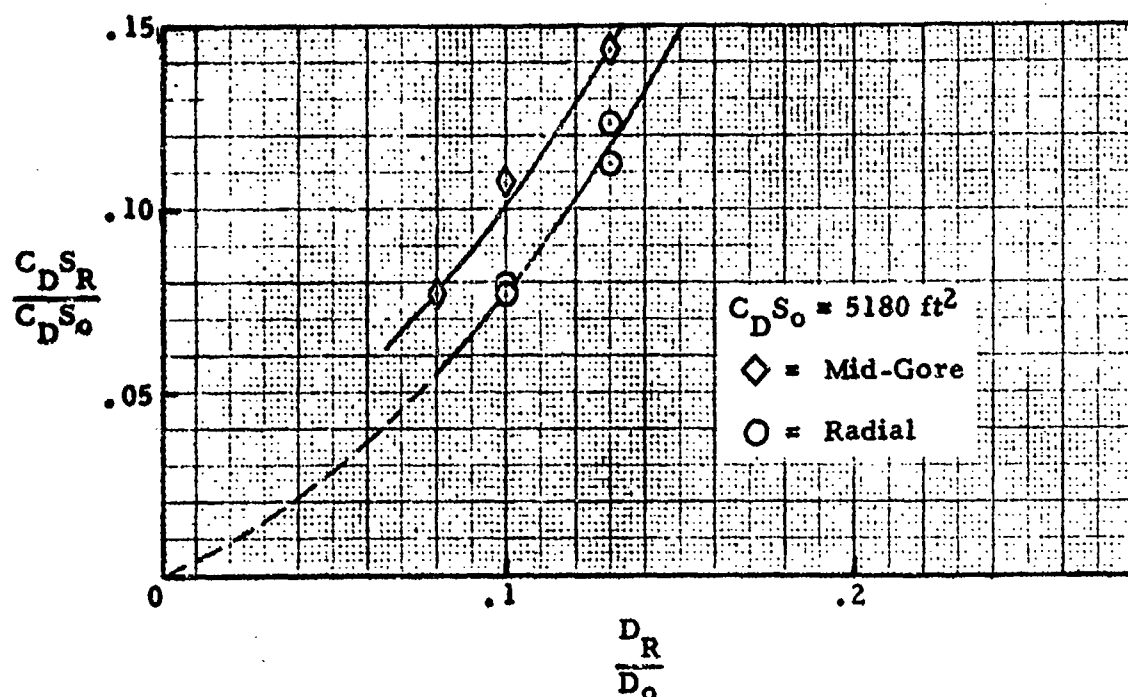
40

$$C_{Do} = .85$$

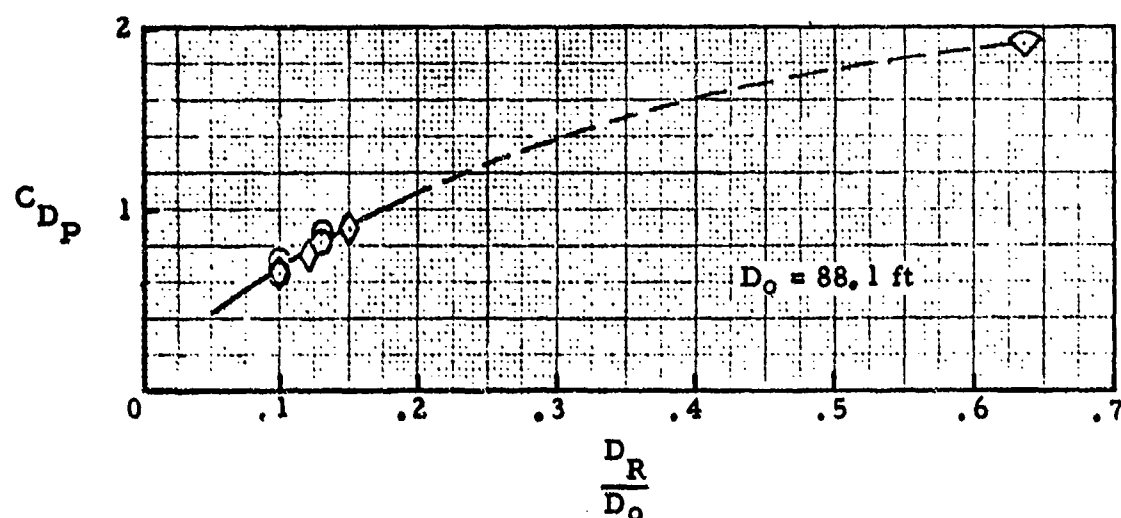
$$C_{Dp} = 1.91$$

The indication is that C_{Dp} increases continuously with canopy inflation as the shape changes from that of a tubular sock to that of an ellipsoidal cup. Since the canopy inflated diameter is considerably smaller initially (at the instant of peak loading) than it is at the end of the reefed interval, Figure 55b provides a conservative means of evaluating the projected area of the canopy for stress calculations.

(See Figure 46 for larger reefing ratios)



(a) Comparison of Mid-Gore and Radial Reefing



(b) Reefed Ringsail Drag Coefficients

Figure 55 . Full-Scale Wind Tunnel Data

The wind tunnel data is presented here rather than in Section 3, because it cannot be translated into a form representative of the performance of the reefed parachute under the dynamic conditions of free flight.

6. 2. 4 Calculation of Reefing Line Length

The length of the reefing line is simply $L_{RL} = \pi D_R + \text{length of splice overlap}$ (Figure 56) where D_R is the desired reefed diameter of the canopy mouth at the skirt. Determination of the reefed diameter ratio (D_R/D_o) for a given drag area ratio (C_{DSR}/C_{DSo}) prior to test depends on the quality of the empirical data available. The method given in Reference 24 is satisfactory for Ribbon and Ringslot canopies but not for the Ringsail. Two values of C_{DSR}/C_{DSo} must be taken into account.

a. At completion of rapid reefed inflation (marked by $F_{R\max}$)

b. At disreef

The first value is associated with reefed opening force calculations, and the second with velocity and dynamic pressure calculations at disreef. Where both values are plotted, as a function of D_R/D_o as in Figures 40, 41 and 42, such curves can be used to make a preliminary estimate of the reefed diameter required. Since C_{DSR} at disreef is the easiest to determine from test data with reasonable accuracy, this is the value commonly represented by single curve data plots as in Figure 39. Such curves can also be used to make a preliminary estimate of D_R and the reefing line length. However, when opening force calculations are carried out, it is necessary to make an

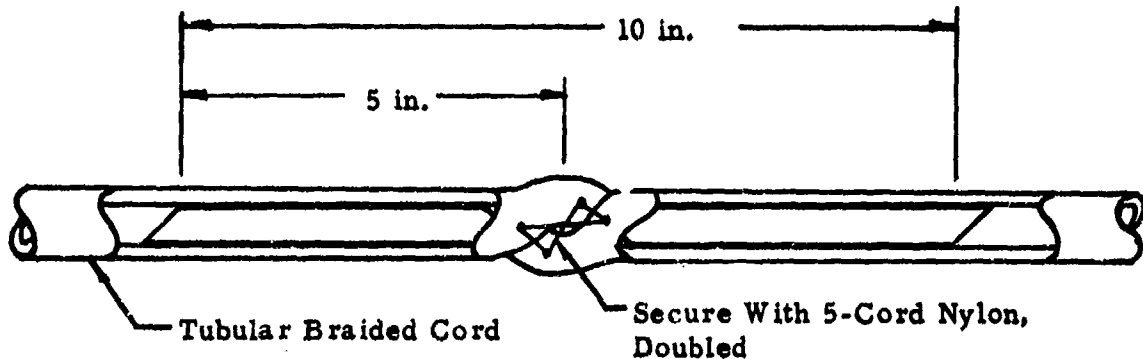


Figure 56. Typical Reefing Line Splice

assumption about the drag area growth during the reefed interval. As indicated in Figures 40 and 41 this may be in order of 100% for the standard Ringsail design. Also it should be noted that the determination of reefing line length should not be based on the wind tunnel data of Figure 55a, because it represents an equilibrium condition of canopy growth reached after a much longer period than the typical reefed interval.

6.2.5 Filling Time

Parachute filling time is defined as the interval, or intervals, between the following events in the deployment and opening sequence:

- a. Line-stretch to full open (non-reefed)
- b. Line-Stretch to reefed open
- c. Disreef to reefed open (two reefed stages)
- d. Disreef to full open

Actual canopy filling usually begins somewhere between line-stretch and canopy stretch after the mouth has opened far enough to admit an effective flow of air. This short randomly variable delay can be minimized by good design and is neglected. It has been found (e.g., Ref. 14) that the best indicator of reefed opening is the maximum load peak. This has also been true of the second reefed stage when the reefing ratio is in the range of 15 to 30 percent D_0 approximately. After disreefing of the final stage the peak load occurs before the canopy is fully inflated. The instant at which full inflation of the canopy is completed is difficult to determine accurately due to the rapid change in canopy shape and the over-expansion attending the peak pressure load. Thus, the definition of the "full open" configuration has varied from program to program and this contributes to the considerable variation in filling times reported.

It is also necessary to allow for the filling that occurs during the reefed interval as shown in the diagram of Figure 57 illustrating how the canopy drag area increases with time. Two stages of reefing are shown in the interest of generality.

The determination of canopy filling times reefed and after disreefing with sufficient accuracy to be useful in the prediction of opening loads is difficult because of the wide scatter of empirical data. However, there

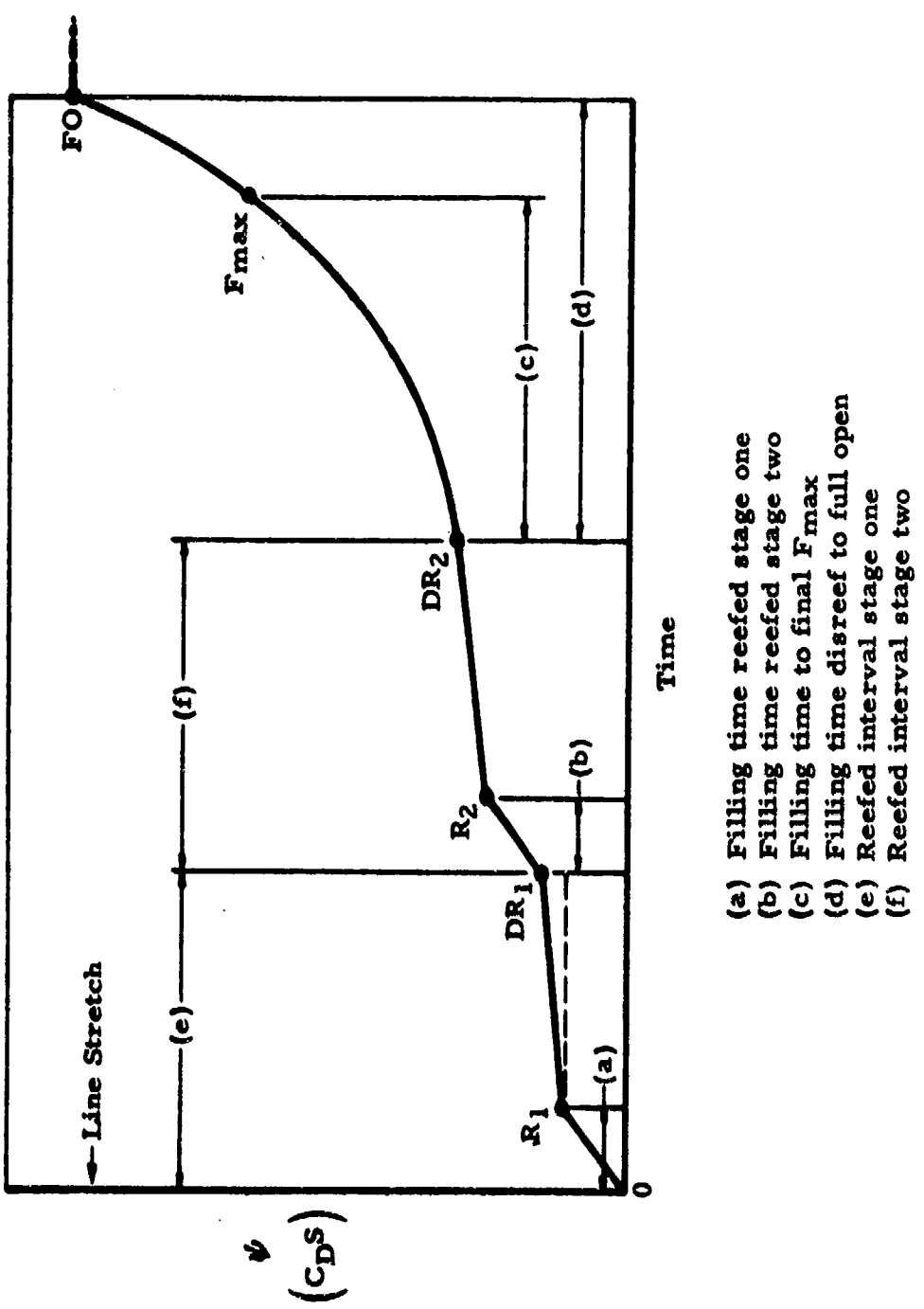


Figure 57. Idealized Ringsail Drag Area Growth With Time

is no practical alternative to the use of such empirical data in the form of the dimensionless filling interval (K_f) as given in Table XIII. By this definition the filling time is calculated from

$$\Delta t_f = K_f (\psi_2^{1/2} - \psi_1^{1/2}) / v_1 \quad 41$$

and in order to do so it is necessary to know the true air speed (v_1) at the beginning of the interval in addition to the initial and final drag areas. This unavoidably leads to an iterative trajectory computation, except for the first reefed stage when the conditions at line-stretch are defined.

Evaluation of average values of K_f from Ringsail test data justifies use of the following formulae for the calculation of filling times.

$$\text{Reefed (stage 1): } \Delta t_f = 37.3 (C_D S_R)^{1/2} / v_1 \quad 42$$

$$\text{After disreef: } \Delta t_f = 4.42 (\psi_2^{1/2} - \psi_1^{1/2}) v_1 \quad 43$$

Presumably the addition of a second reefed stage would alter the filling characteristics in the way indicated in Table XIII and XIV for the 85.6 ft D_o modified Ringsail, but the prediction of quantitative effects on this basis would be highly speculative.

6.2.6 Derivation of the Dimensionless Filling Interval

It will be recognized that the dimensionless filling interval corresponds to the parachute filling process described by the concept of a "constant filling distance"; ie, the distance traveled by a parachute while filling is a constant, irrespective of speed and altitude, and is unique for each different parachute. Understanding of the origin and limitations of this concept is helpful in guiding its utilization in Ringsail parachute design.

In the general case for filling any plenum:

$$\text{Filling time} = \frac{\text{Volume to be filled}}{\text{Inflow rate-outflow rate}} \quad 44$$

In the case of an inflating parachute the volume to be filled can be expressed as a function of the cube of a characteristic canopy dimension such as D_o , i.e.,

$$V = f(D_o^3) \quad 45$$

The inflow rate, being a function of the canopy mouth area and the air flow velocity, with the assumption of incompressible flow, can be expressed as a function of the square of a characteristic canopy dimension multiplied by an average air inflow velocity, i. e.,

$$\dot{V}_{in} = f(D_o^2 \bar{v}_{in}) \quad 46$$

With the further assumption that the relative porosity of the canopy is a constant fraction of the canopy area (S_o), the outflow rate can be similarly represented, i. e.,

$$\dot{V}_{out} = f(D_o^2 \bar{v}_{out}) \quad 47$$

The average flow velocities in and out are both proportional to the average flight speed (\bar{v}) of the system so that the functional relationships (46) and (47) remain true with \bar{v} substituted for these velocities. Thus, with the introduction of constants of proportionality, substitution of the expressions for V_{in} , V_{in} , and V_{out} in equation 44 yields:

$$\begin{aligned} \Delta t_f &= K_1 D_o^3 / (K_2 D_o^2 \bar{v} - K_3 D_o^2 \bar{v}) \\ &= K_1 D_o / \bar{v} (K_2 - K_3) \end{aligned}$$

combining constants

$$\Delta t_f = K D_o / \bar{v} \quad 48$$

or

$$K = \Delta t_f \bar{v} / D_o \quad 49$$

which expresses the filling distance in canopy diameters. But so defined the filling distance is not useful in a practical sense because the average airspeed can only be determined by a series of iterative trajectory computations. Also the volume of a reefed canopy is not a simple function of the nominal diameter. Therefore, the dimensionless filling interval used in this work is defined as follows. (See also References 14 and 22.)

$$K_f = \Delta t_f v_1 / (\psi_2^{1/2} - \psi_1^{1/2}) \quad 50$$

Where Δt_f is the filling time while the canopy is growing from an initial drag area Ψ_1 to a final drag area Ψ_2 and v_1 is the true air speed at the start of the filling process. Use of $\Psi^{1/2}$ as the characteristic canopy dimension in place of D_o permits reefed filling to be expressed in the same form as filling after disreef.

This formulation should be used circumspectly, because the constant filling distance concept breaks down at high speeds due to compressibility. Reference 23 indicates the possibility of a large discrepancy at Mach 0.5 increasing drastically at supersonic speeds as shown in Figure 58 for the modified Ringsails of the NASA Planetary Entry Parachute Program (Reference 18).

Also, at very low speeds ($v_1 < 60$ KEAS) there is justification for the expectation that the filling distance will be reduced by a sharp decline in the effective porosity of the canopy due to the low differential pressure (e.g., Figure 68). This hypothesis requires experimental verification.

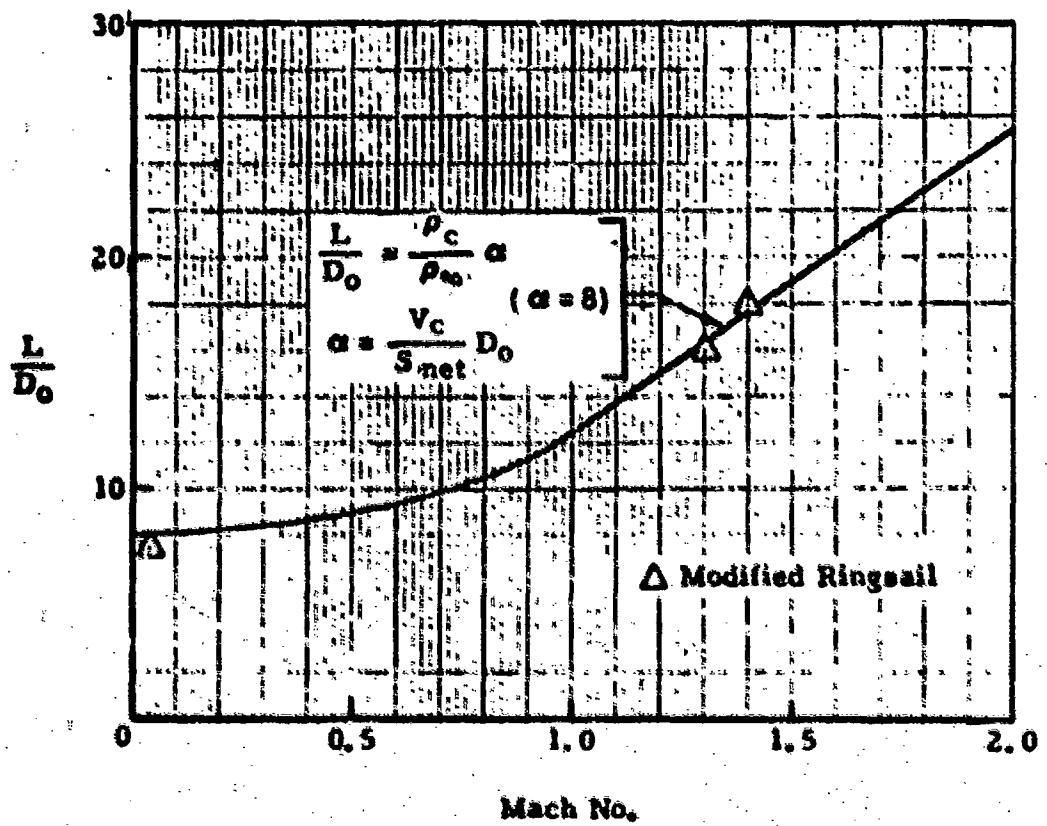
6.2.7 Stability

From a practical standpoint the stability of a parachute system must be considered in relation to the stability of the atmosphere through which it descends, this being the source of the disturbances affecting normal system motion. Also, the condition of crucial interest is the probable nature of system motion at the moment of touch-down.

Parachute instability takes several forms of which pendular oscillations and coning oscillations are of prime concern. Breathing and longitudinal pulsations are of secondary interest because they seldom become critical at normal rates of descent. Since the air is always in motion, the average amplitude of pendular oscillations observed in aerial drop tests might be considered misleading. However, the damping function of parachutes is generally strong for any excursion beyond the normal characteristic angle of attack for static stability, (θ_o) as illustrated schematically in Figure 59a.

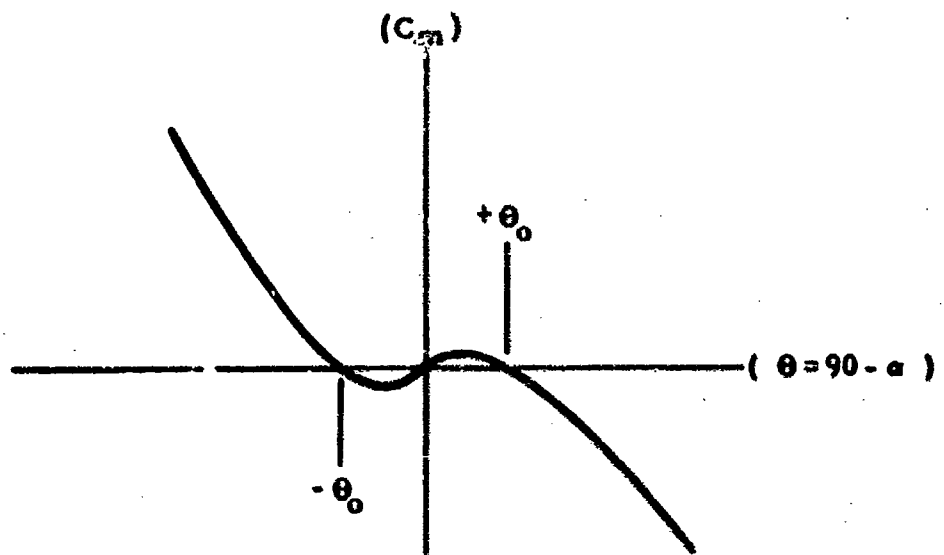
For example, a non-reefed parachute deployed in level flight follows the first downswing of the suspended mass with one excursion of large amplitude which is virtually damped down to the average amplitude (θ) in the next half cycle (Figure 59b).

Ringsail parachute systems that have exhibited unacceptable instability in the form of undamped periodic oscillations of large amplitude relative to those of Figures 42 (etc.) fall in what appears to be a special category along with a variety of other parachute types. There is some evidence pointing to the existence of a critical Reynolds number near which any type of parachute

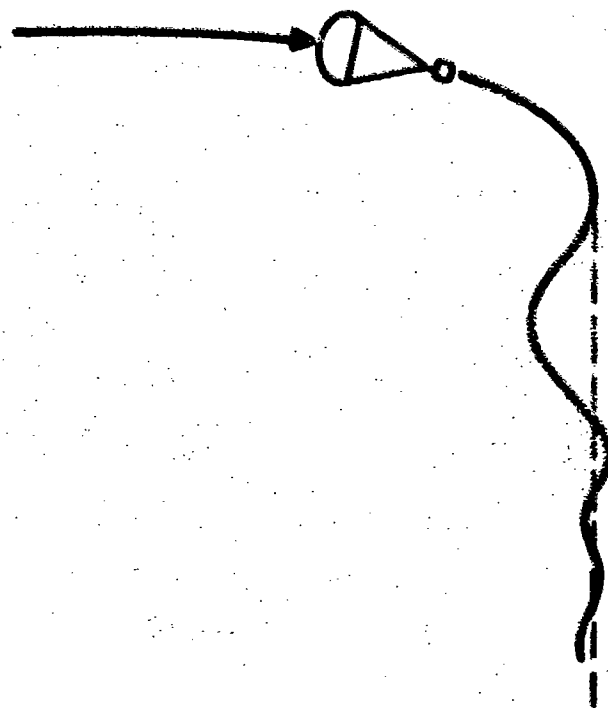


NOTE: The modified Ringsail referred to here is the PEPP parachute incorporating a wide slot near the skirt (see Appendix B).

Figure 58. Variation of Filling Distance with Mach No. (Ref. 23)



(a) Variation of Parachute Moment Coefficient with Canopy Angle of Attack



(b) Damped Oscillation Transient Following Horizontal Deployment

Figure 59. Typical Static and Dynamic Stability Characteristics of Parachutes

system begins to oscillate widely with the sharp periodicity of a pendulum. The first instance of this behavior reported was an oversized model of the personnel guide-chute design (approximately 40 feet in diameter) tested at El Centro in the mid-1950's. While the average amplitude of oscillations of the AF type C-11 personnel version of this design is in the order of ± 10 degrees, the 40 ft model was said to have oscillated steadily at ± 30 to 35 degrees. Early in 1960 a 37 ft D_0 Ringsail with a suspended load of 520 lbs exhibited sharply periodic oscillations of as much as ± 25 degrees throughout its descent from 10,000 ft altitude. Because the motion looked like a forced oscillation, resonance of pulses caused by vortex shedding with the natural frequency of the parachute system was postulated. The same type of behavior was encountered at high altitudes with three different large parachute systems:

- a. A cluster of four 35 ft T-10 Extended skirt canopies
- b. A 67.3 ft D_0 Full Extended skirt parachute
- c. A 74.2 ft D_0 Ringsail parachute

The suspended load in each case was 1640 lbs, and these systems exhibited strong periodic oscillations (up to ± 45 degrees) throughout the first half of the descent followed by more normal behavior below approximately 20,000 feet altitude.

In the case of the 74.2 ft D_0 Ringsail it was found that the Reynolds number* at 45,000 feet altitude was the same as that for the 37 ft D_0 model at sea level ($R_e = 3.64 \times 10^6$). It will be seen that during any parachute descent Reynolds number increases continuously because the ratio ρ/μ for air increases faster than v_g decreases. Consideration of the possible relationship between Reynolds number and the natural frequency of the parachute system suggests the existence of a critical combination of scale or effective line length and altitude at which large undamped oscillations are most likely to occur. Shortening the suspension lines of the above Ringsail by about 14 percent to increase its natural frequency appeared to mitigate the problem by raising the critical altitude somewhat.

Therefore, in view of the complexity of the problem and the varied behavior exhibited by parachute systems descending through a real atmosphere, no method of predicting the probable stability of a given Ringsail parachute system can be presented. Once the average amplitude has been established by

*Defined as $R_e = (C_p) v_g \rho/\mu$

a number of drop tests, the data given in Section 3.4 suggest that a probable maximum amplitude that would not be exceeded 90 percent of the time is approximately $3\bar{\theta}$. As shown in Table V, $\bar{\theta}$ ranges from 5 to 8 degrees for the majority of the single Ringsail parachute systems developed.

6.3 PREDICTION OF OPENING LOADS

Three different methods of predicting Ringsail opening loads are available to the parachute designer.

- a. The Load Factor Method
- b. The Mass-Time Method
- c. The Area-Distance Method

Although the Load Factor method has been highly refined in its application to Ringsail parachute systems (References 11, 12 and 14), its accuracy at best is no better than ± 10 percent. The Mass-Time and Area-Distance methods were developed in order to get better results, and accuracies of ± 5 percent have been obtained in the limited context of the Apollo main parachute development program.

6.3.1 The Load Factor Method

The simplicity of the load factor method makes it quite useful despite its heavy dependence on full scale drop test data and the uncertainty of its accuracy in any new design situation. The peak opening load is

$$F_{\max} = C_D S q_s C_k$$

51

Where q_s at the start of the filling process (reefed or disreefed) is determined from trajectory computations and the load factor (C_k) is estimated with the aid of Figure 27 or Figure 28. When entering Figure 27 with an appropriate value of the unit canopy loading ($W/C_D S$) considerable judgment is required to make a realistic allowance for the effect of initial velocity, as reflected by the data spread. The effect of altitude on C_k can be estimated with the aid of Figure 29, using the assumption that the trend indicated by the faired curve is invariant with $W/C_D S$.

Figure 28 is useful for making preliminary estimates of the opening loads of both single and clustered canopies. Conservative results are obtained by reading the upper faired curves for the reefed and disreefed cases. R_m is evaluated in terms of $\psi^{3/2}$ instead of D_o^3 to make reefed C_k data directly comparable with that for non-reefed and disreefed canopies. The synchronous inflation of a cluster can be treated the same as for a single parachute using $\psi = \sum C_D S$ and $M = W/g$. Non-synchronous cluster opening loads can be estimated by making an assumption about the fraction of the total mass applicable to one parachute of the cluster. Worst cases for two and three-canopy clusters, for example, will be obtained by using $R_{ms}/2$ and $R_{ms}/3$ respectively, where R_{ms} is the mass ratio for the synchronous case, i.e., the leading canopy is assumed to open before the other members of the cluster develop any drag. The ratio of the load factors obtained for the non-synchronous and synchronous cases will be comparable to the ratio of the maximum to the average opening forces given in Tables I, IV, V and VI.

Taking a typical disreef case as an example, enter Figure 28 with $R_{ms} = 7.4$, $R_{ms}/2 = 3.7$, and $R_{ms}/3 = 2.47$ and read from both upper and lower curves corresponding values of C_k as presented in Table XXII:

TABLE XXII

SHOCK FACTORS FOR SYNCHRONOUS AND NON-SYNCHRONOUS
INFLATING RINGSAILS IN CLUSTERS

Cluster Opening Configuration	Synchronous	Non-Synchronous	
Number of canopies	2 or 3	2	3
R_m	7.4	3.7	2.47
C_k	maximum .3 minimum .21	.47 .35	.57 .43
Ratio: C_k (nons)/ C_k (sync)	-	1.57 1.67	1.90 2.05

Apollo test data representative of the two-canopy case is given in Table V with $F_{max}/F_{av.} = 1.58$ for test 26-5 in which the disreef time differential was artificially increased by one second (nominal). Test data representative of the three-canopy case is given in Table I with $F_{max}/F_{av} = 2.08$ for

test 58-828 in which two of the three solid cloth canopies were heavily damaged*. However, it appears from Apollo statistics that the Ringsail three-canopy case may never reach the extreme inequity of load sharing assumed; i. e., each of the canopies will always develop a significant fraction of the total force. Therefore, for preliminary design purposes in systems having a unit canopy loading in the order of $W/\Sigma C_D S_0 = 1.0$ psf a conservative assumption for both two- and three-canopy clusters based on the data in Table V would be a load ratio $F_{\max}/F_{\text{sync}} = 1.5$ applied to the calculation of the design limit load for each parachute. For systems having a design unit canopy loading significantly different from 1.0 psf, this ratio will tend to be smaller or larger than 1.5 in proportion to the synchronous mass ratio (R_m), due to the slopes of the curves in Figure 28.

After a few suitably instrumented aerial drop tests have been performed, the accuracy of the load factor method improves and it is useful in predicting the probable opening loads of subsequent tests as well as the design limit loads for conditions that it may not be economical to duplicate in the test program. The opening load factor of each stage is derived from the test data by using Equation 51 in the form $C_k = F_{\max}/C_D S_{q_s}$.

6.3.2 The Mass-Time Method

The Mass-Time method of predicting parachute opening loads, developed in detail in Reference 14, is summarized here. The parachute force (F) used in Equation 32 is calculated from

$$F_p = \psi q + v \dot{m}_a + (m_a + m_p) \ddot{v} + W_p \sin \gamma \quad 52$$

Both the effective drag area of the canopy (ψ) and the added air mass (m_a) are expressed as functions of time in equations having empirically based coefficients and exponents as follows:

$$C_D S(t) = \psi = \psi_1 + (\psi_2 - \psi_1) (t - t_1)^n / (t_2 - t_1)^n \quad 53$$

$$\dot{m}_a = \rho K_a \psi^{3/2} \quad 54$$

$$\ddot{m}_a = (3/2) \rho K_a \psi^{1/2} \dot{\psi} \quad 55$$

$$\dot{\psi} = n [(\psi_2 - \psi_1) / (t_2 - t_1)] [(t - t_1) / (t_2 - t_1)]^{n-1} \quad 56$$

*When the damage occurred is not stated in Reference 10, but the results indicate that extensive reefed opening damage of the lagging canopies may have been responsible for the high leading canopy load after disreef.

The computation is carried out in steps using equations 30 through 33 to describe system motion and a program of drag area changes similar to that in Figure 57 for determination of the values of ψ_1 and ψ_2 pertinent to each step. The growth that occurs during the reefed interval can be estimated with the aid of Figure 47. Figure 47b is for the 88.1 ft D_o Ringsail only. If another size parachute is used we cannot be certain. The reefed intervals are assigned first on a tentative basis and the filling times are calculated with empirical formulae such as 42 and 43. As the computation progresses through several iterations, optimum reefed intervals will be developed.

The added-mass shape factor (K_a) is equal to 0.66 for modified Ringsails of the Apollo type but has not been evaluated for the standard design. Because this is pertinent only to the final stage of inflation after disreefing when the effect of the crown geometric porosity is diminished, K_a for the standard Ringsail design may not be greatly different. The results of two or three well-instrumented drop tests would be sufficient to provide substantiating data.

The instrumental measurements required as a minimum are:

- a. Weights of parachutes and vehicle during deployment and steady descent
- b. Photo theodolite flight trajectory elements coordinated with parachute force-time and atmosphere density-altitude measurements,
- c. Onboard and ground-based motion picture records

It was found that reefed opening loads could be predicted accurately neglecting the added air mass, i.e., $K_a = 0$ for reefed stages. Further, with the end of reefed filling marked by the instant at which the parachute force reached its peak, the assumption of linear area growth with time gave good results. Thus, in the area growth equations (53 and 56), the exponent $n = 1.0$ for the reefed stages. On the other hand, in the final stage of inflation after disreefing, n proved to be a function of the filling time, varying with Δt_{fo} as shown in Figure 60. The applicability of this data derived from tests of the Apollo main parachute (slotted design) to the standard design also is uncertain; additional test evidence is needed.

The Mass-Time method of opening load prediction gives good results when the computation is carried out with a two DOF digital computer program designed around the equations of motion given (30 through 33) and incorporating the variation of atmospheric density with altitude. When the empirical

3.5

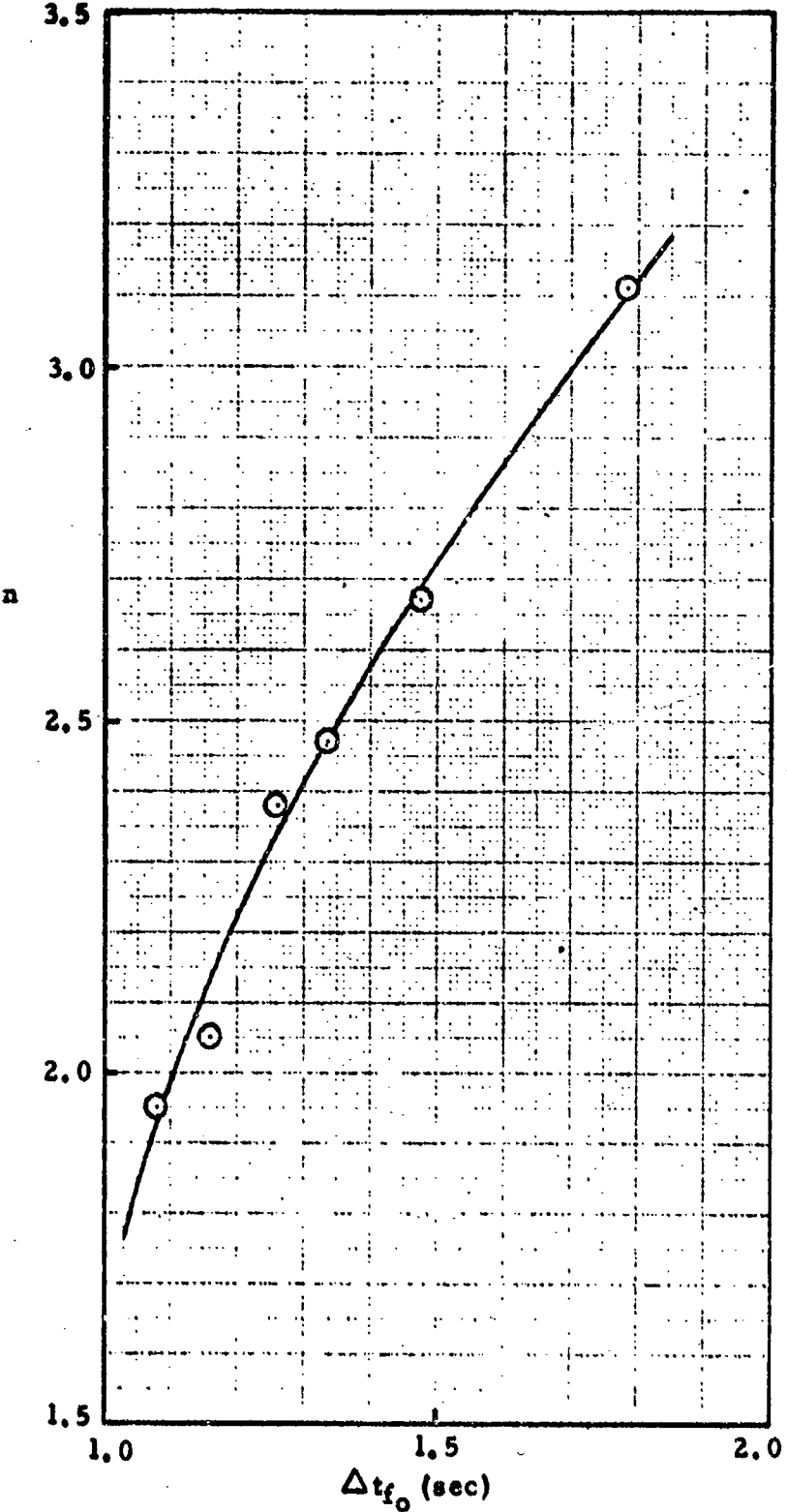


Figure 60. Drag Area Growth Exponent vs Filling Time
(Disreef to Full Open)

coefficients and exponents have been correctly evaluated, the peak loads will be within $\pm 5\%$ of actual and the final peak after disreefing will occur at the correct time prior to full inflation. An example of the results obtained during the Apollo program is illustrated in Figure 61.

The example in the form presented was computed to provide partial verification of the data reduction process; i.e. average values of C_{DSR}/C_{DS0} and K_a obtained from all tests were used as inputs along with measured filling time and reefed intervals for this test. Exponent n was read from Figure 59. The pre-test computation is carried out step by step for each area stage to determine the velocity at the start of each filling interval. Then, average values of K_f for each stage (e.g., Table IX) enable appropriate filling time to be calculated. Nominal reefed intervals also are used as inputs. A pre-test computation superimposed on Figure 60 would show the peak loads shifted in time where actual reefed intervals departed from the nominal and actual filling times varied from the averages calculated with K_f values derived from all prior tests.

In order to evaluate the parameters of the Mass-Time method from the results of aerial drop tests it is necessary to obtain coordinated velocity, dynamic pressure and parachute force histories. The filling time from disreef to full open must be measured independently from photo records, because this does not appear in the force-time record. Other measurements required to define inputs to the computer program include: initial altitude, velocity, path angle, system weights; system descent weight when this differs from the initial value; parachute weight (A detailed breakdown by components should be recorded at the time the parachutes are rigged and packed.) and the reefing parameters used (reefing line length or D_R/D_0 and reefing line cutter nominal timed intervals). The computer program was made double-ended and can be run backward to facilitate data reduction, i.e., inputting trajectory data to obtain C_{DS} vs time and K_a , for example.

6.3.3 The Area-Distance Method

The Area-Distance method of predicting parachute opening loads is identified in Reference 14 as the "Modified Mass-Time" methods. This method is similar to the Mass-Time method in all particulars except that the distance traveled by the parachute while it inflates through each stage is expressed as a function of the drag area growth. The reduced test data showed the filling distance of each reefed stage to be a linear function of the change in effective drag area during the stage. The computer program was modified to accept these filling distances and to calculate how far the vehicle traveled after the beginning of inflation, by integrating the velocity and "remembering" where it started.

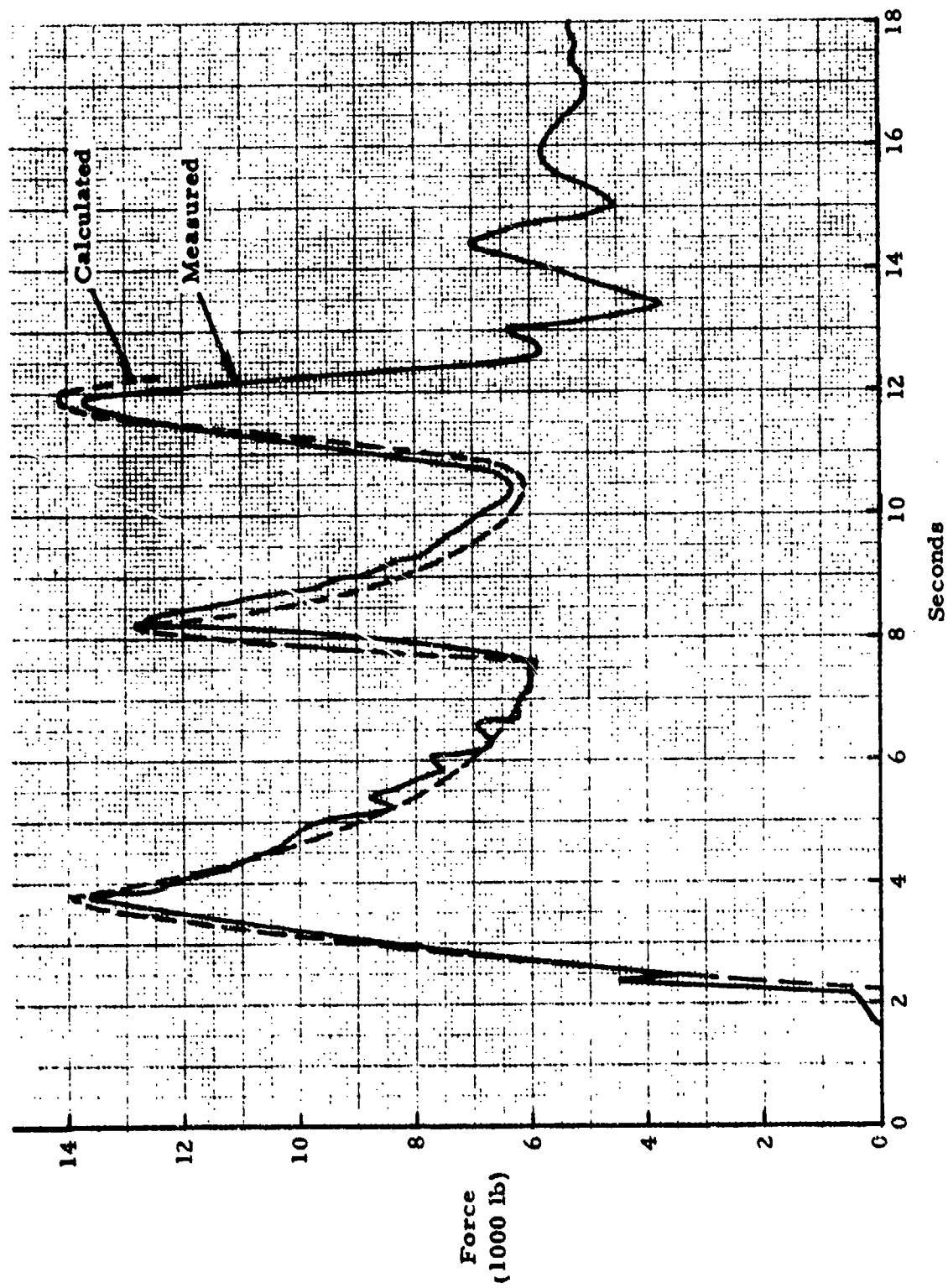


Figure 61. Mass-Time Method; Calculated vs Measured Opening Loads (Apollo Test 80-1R)

The non-linear function of the final stage of inflation expressed C_{DS} in terms of lineal constants and a function of s^* derived from averaged test data where s^* is the distance traveled since passing a reference point a fixed distance before the completion of filling. There are other complications that introduce discontinuities and make the final stage calculation somewhat specialized. The drag area values between inflation intervals were determined as time functions in the manner specified for the Mass-Time method.

One of the important advantages of the Area-Distance method is that the filling times fall out of the calculation. They do not have to be calculated in advance. This greatly simplifies the approach to prediction of clustered parachute opening loads, which was a prime objective. Applied to single parachute cases the method predicted reefed opening loads with an accuracy slightly better than that of the Mass-Time method. Both methods had large errors in the loads predicted for final opening stages of clustered canopies. Also, both methods were not fully developed for the cluster calculations, because only empirical coefficients for single parachutes were available eg ... K_g and $ds/d\psi$. The observed discrepancies suggested that the added mass terms caused each parachute to have a strong effect on the loads of the others through the mechanism of system deceleration.

The promising potential of both methods for further development is shown in Figures 62 and 63, comparing measured and calculated forces for two-canopy cluster cases.

One of the significant aspects of the computed force-time histories is that they were generated by the equations of motion and parachute forces with the input of single canopy inflation characteristics. Only the disreef time differentials derived from the cluster test data were included to trigger the nonsynchronous inflation process. The fact that the force-time history of the lag canopy is reproduced with good fidelity is ample evidence that the momentum of the added air mass coupled with system deceleration is the prime factor. As noted, the equation for parachute force (Equation 52) accounts for the effect of system deceleration on dynamic pressure in the drag term during the reefed intervals and on both drag and added air mass after disreefing, each parachute in the cluster being computed individually such that $F = F_1 + F_2 + \dots + F_n$. There is nothing in the equations corresponding to the mechanical and aerodynamic interference seen to take place between the inflating canopies in the film records. While this interference distorts the canopies by flattening or caving in adjacent surfaces, the evidence shows that this does not inhibit air ingestion or the inflation rate. The theory of deceleration induced inflation instability of clustered canopies was first presented in Reference 34.

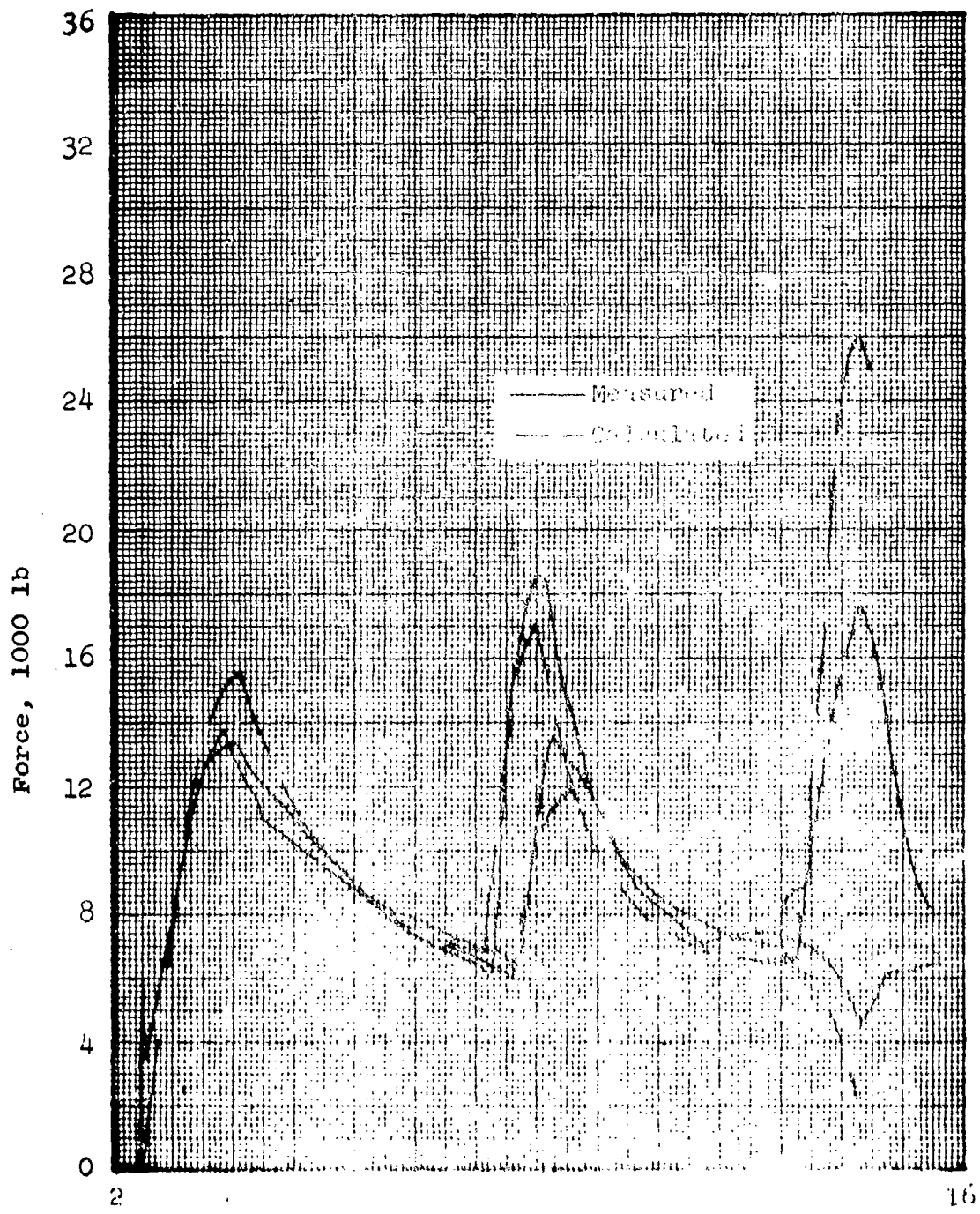


Figure 6.

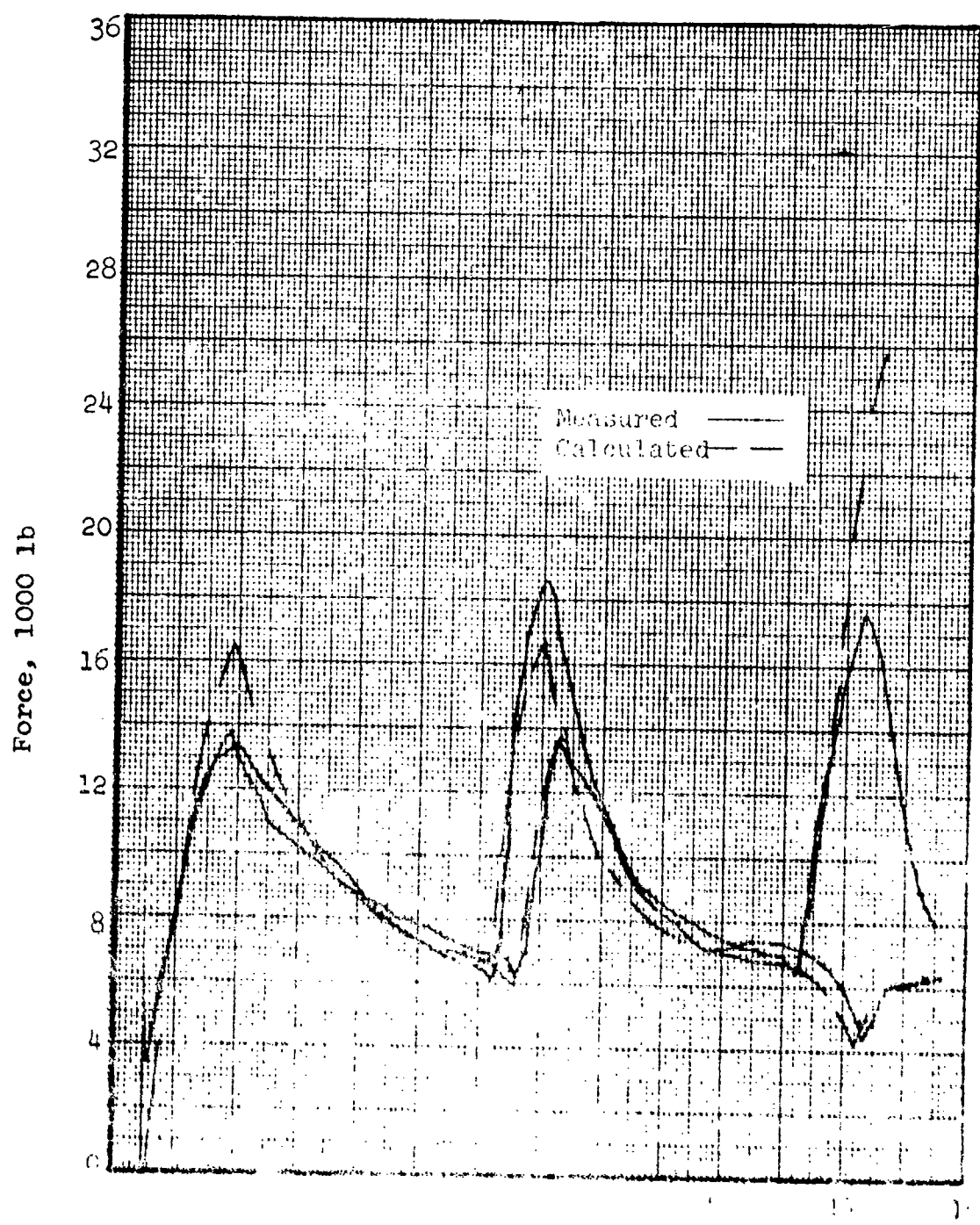


Fig.

1.1.2.1.2

6.4 STRESS ANALYSIS

Today, there are essentially only two practical methods of calculating the internal loads of a parachute structure.

- a. The Short Method (Illustrated in Section 5 and Appendix C)
- b. The Computer Method (Described in References 13 and 25).

There is no intermediate analytical approach of a general nature that will yield results any more dependable than the short empirically-based method. All of the intermediate quasi-analytical methods developed are complex, laborious, and time consuming and their usefulness is limited to a particular type of parachute structure or a particular set of operational conditions (Reference 24).

6.4.1 Structural Design Factors

The structural design factors (D. F.) are derived from required safety factors (S. F.) and allowable strength factors (A_p) as the ratio

$$D. F. = S. F. / A_p \quad 57$$

The allowable strength factor is the product

$$A_p = u \cdot e \cdot o \cdot k \cdot \tau \cdot s \cdot \cos\phi \quad 58$$

where the subfactors used in Ringsail design are defined as follows. (The typical values given in parenthesis are seldom all used at the same time, some being equal to unity for each design case.)

u = joint or seam efficiency (.85 applied only to MIL-Spec rated minimum strengths)

e = abrasion loss (.95)

o = humidity loss (.95)

k = fatigue loss (.95)

τ = temperature loss (.97 @85°F to account for the loss in the strength of nylon due to dynamic heating, for example)

ϵ = vacuum loss (*)

s = load distribution ratio (.95)

ϕ = line convergence angle or similar deflection of the applied load (0 to 20° or $\cos \phi = .94$ max. applied to the opening load after disreefing)

For other values typically assigned to these allowable strength factors see References 6 and 24. The allowable strength of the textile form is

$$P_A = A_P P_R$$

59

For design purposes, the required minimum strength of material (P'_R) for a given member is

$$P'_R = (D.F.) (\text{Limit Load})/z$$

60

where z is the number of identical cords, webs, or tape plies in the member (for fabric $z = 1.0$).

In the stress analysis the margin of safety (M. S.) of each member subject to an applied load (T_c) is

$$M.S. = (P_A / T_c) - 1$$

61

6.4.2 The Short Method

6.4.2.1 Canopy

The short method of estimating canopy internal loads is based on membrane theory and depends heavily on empirically derived coefficients and to some extent on the judgment of the designer. A general expression for the circumferential unit load or hoopstress in an ellipsoidal surface of revolution having no bending strength is

$$T_c = p r_e + T_2 (r_e / r_2)$$

62

*The vacuum factor was ≈ 0.8 for the first Apollo parachutes to allow for the estimated effects of outgassing and dehydration in a hard vacuum, but later it was concluded that the materials recovered sufficiently during atmospheric entry that this factor could be neglected.

where p is a uniformly distributed pressure, r_c is the local radius of curvature in the circumferential direction, T_2 is the unit load in the meridional direction, and r_2 is the local radius of curvature of the meridian.

As noted in Reference 22, "The difficulty inherent in attempting to apply equation (62) to a decelerator surface that is not a surface of revolution is evident, although it is well suited for computing unit loads of bi-axial structures like woven fabric."

The short method employs the simplest form of equation (62) to develop empirical formulas for the unit loads in the canopy fabric, i.e.,

$$T_c = K p r \quad 63$$

where $K = 1.0$ for simple curvature (cylindrical, conical) and $K = 0.5$ for a spherical surface. For other shapes, K falls between 0.5 and 1.0.

From these relationships for unit pressure,

$$p = F/S_p \quad 64$$

and for radius of curvature,

$$r = D_p / 2 \quad 65$$

The formula given in Section 5 is obtained by substitution in equation (63) with $K = 0.5$.

$$T_c = F/\pi D_p \quad 66$$

To estimate D_p for the reefed canopy, the effective drag area must be known in order to calculate

$$S_p = C_D S_R / C_{D_p} \quad 67$$

using C_{D_p} from Figure 55b for a given reefing ratio (D_R/D_o).

The problem is more difficult when the canopy is not reefed because the projected diameter of the canopy at the instant of peak loading is not predictable. The same is true after disreefing, where various strategies are used to define a local radius of curvature.

When the unit canopy loading is low (say when $W/C_D S_0 < 1.0$) the peak opening load occurs early in the inflation interval, and the non-reefed canopy can be treated like a reefed canopy by simply estimating from empirical data what the equivalent reefing ratio would be. Sometimes a more accurate estimate of radius of curvature can be obtained from damage statistics, with the assumption that the cloth developed its rated strength at the time of failure when the parachute force was a known value. Then from Equation 66

$$D_p = F/\pi T_c \quad 68$$

where $T_c = s u P_R$, using $u = 1$ when the cloth failure did not occur along a seam and $s = 0.6$ for full sails in which the trailing edge stress is critical.*

When the unit canopy loading is relatively high the peak load of the non-reefed canopy, like that following disreefing of the reefed canopy, occurs later in the filling interval and in the limiting case may be coincident with full inflation. This occurred in disreef overload tests of the 85.6 ft D_n Apollo main parachute with $W/C_D S_0 \approx 2$. The results of one of these tests provide an instructive example of the empirical approach described above. In the test in question (30-3) the parachute canopy was destroyed by a load which reached a peak at the onset of failure of 14,350 lbs. The rated strength of the cloth was $F_g = 42$ lb/in., and the average seam efficiency measured $u = .72$. With the assumption that failure occurred at a unit load of

$$T_c = (.6) (.72) (42) = 18.12 \text{ lb/in.}$$

Equation 68 yields $D_p = 60.4$ ft or .76 D_n . This falls between $D_p/D_n = 2/3$ (nominal) and $D_p/D_n = .74$, the latter value being the result of canopy measurement's made at the peak load instant for a similar test in which ultimate damage was not sustained.

*The stress analysis presented in Reference 11 shows the average unit load across the sail section to be about + 5% of the maximum at trailing edges.

Other significant aspects of the design problem brought out by this example are:

- a. In the design limit case the unit canopy loading would be much less (because the test was performed with an overweight vehicle) and the peak load, occurring earlier in the filling interval, would likely cause the critical hoopstress to occur higher in the canopy.
- b. The elasticity of the structure results in substantial over-expansion of the canopy under heavy loads, i.e., well beyond the nominal projected diameter.

Consider the parachute of the above example from the designer's viewpoint with a given limit load of $F = 25,000$ lbs and required S. F. = 1.35. Applying Equation 66, he would let $D_p = 2/3 D_o = 57$ ft and obtain $T_c = 14$ lb/in. For S. F. = 1.35 a design factor of D. F. = 2.7 should be used when $s = 0.6$, whence $P'_R = 38$ lb/in. and 1.1 oz ripstop cloth rated at 42 lb/in. would be selected. The fact that laboratory test data on hand showed a minimum breaking strength of 45 lb/in. would boost the design factor to a realized value of D. F. = 2.9 for added confidence.

The conservative nature of Equation 66 is brought out by examination of its underlying assumptions. The Ringsail canopy is not a surface of revolution but an ellipsoid made up of radial ribs and a large number of small semi-conical surfaces supported only along the edges attached to the ribs. The profile radius at any stage of inflation is everywhere less than $D_p/2$ except in the region close around the central vent. Here the assumption of a spherical surface in which $r = D_p/2$ is a good approximation.

The unit differential pressure is not uniformly distributed across the inflated area of the canopy but varies along the radials approximately as shown in Figure 64. However, across the central spherical region of the canopy the differential pressure is essentially constant. These pressure distributions are those of several different ones tested in the CANO computer analysis of the 85.6 ft modified Ringsail that gave best results in terms of canopy shape and total load vs measured data as reported in Reference 13. Since the shape and structure of the standard Ringsail is similar, it is probable that such pressure distributions are representative and could be used in the analysis of new Ringsail designs. Thus, the pressure calculated as $p = F/S_p$ would be less than actual if all of the parachute force was the product of pressure loading. However, an unknown but possibly significant fraction of F is due to skin friction, which tends to mitigate the unconservative assumption about the pressure distribution.

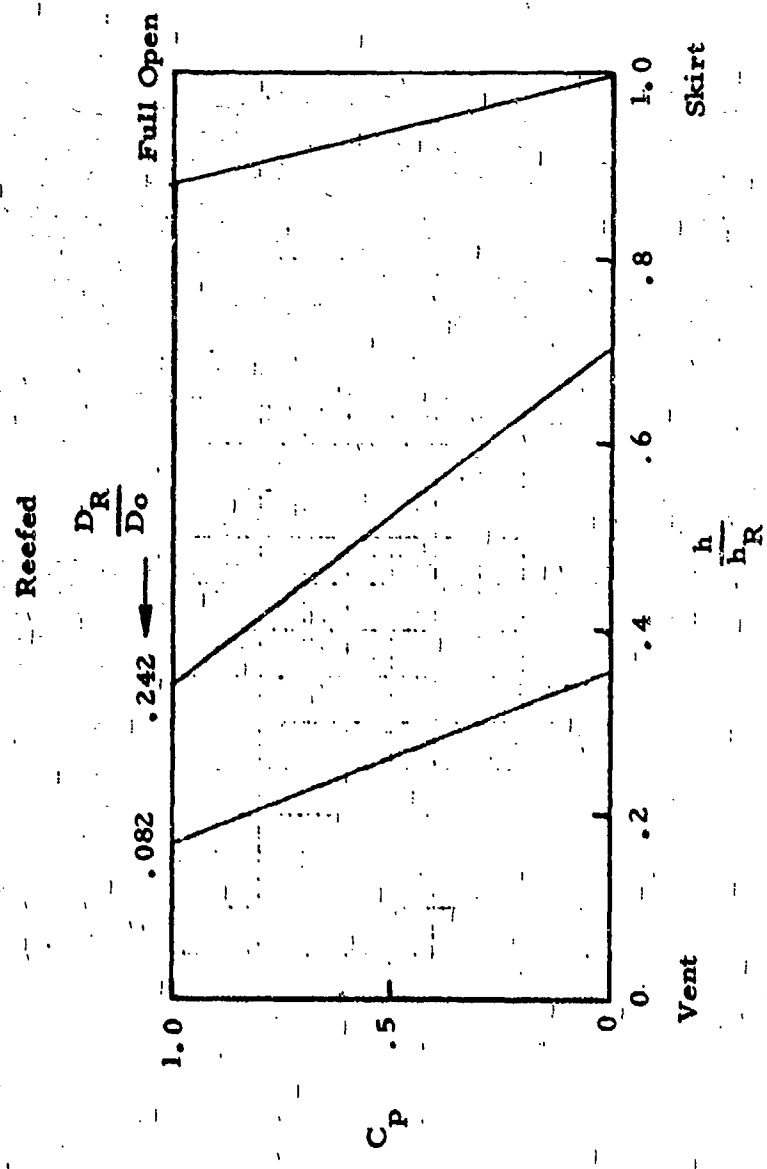


Figure 64.

Differential Pressure Distributions Across 85.6 ft D_o Ringsail (Modified)
Deduced from Shape Measurements and Strain Analysis by CANO Program

6.4.2.2 Suspension Lines

The load in one suspension line can be calculated with precision using

$$T_c = F_{LIM}/N \cos\phi \quad 69$$

However, the required strength of material based on its allowable strength is determined as given in Section 5 from

$$P'_R = (D.F.) F_{LIM}/N \quad (\text{Equation 25})$$

in which the design factor includes $\cos\phi$ along with the other allowable strength factors. With $P_R = P'_R$ for suspension line cord (using Equation 69) the margin of safety, in expanded form for clarity, is

$$M.S. = \frac{A_p P_R}{F_{LIM}/N \cos\phi} - 1 \quad 70$$

6.4.2.3 Radial Tapes

The load in each pair of radial tapes is equal to the load in the suspension lines up to the point of tangency with the pressurized bulb of the canopy, both reefed and after disreefing. But after the reefed load peak, when the canopy continues to grow and build up tension in the reefing line, the tension in the radial will become greater than in the suspension line in proportion to the canopy development angle between them. This is not a critical loading condition for the radial but is for the reefing line as shown in Section 6.4.2.6.

The fact that a radial tape strength (in pairs) of 90% P'_R for the lines is acceptable merely recognizes the fact that the efficiency of the suspension line joint is generally about 90% and the tape joint is reinforced by the canopy cloth.

6.4.2.4 Risers

The load in one riser is calculated by the same method used for the suspension lines simply by substituting N_R for N in Equation 69.

6.4.2.5 Circumferential Bands

Because circumferential reinforcing bands are largely redundant members, the only way to obtain a realistic load estimate is to assume that the cloth in one gore is cut for part or all of its length as shown in Figure 65. This approach is illustrated in Reference 6. The validity of the result was substantiated by a test reported in Reference 8 in which the lightweight Century Ringsail sustained gore failures above and below the reinforcing band but the band held and prevented the vent from opening widely. The design analysis was aided by existing data for another Century parachute test in which the canopy split from vent to skirt. From the failure analysis it was possible to deduce approximate values for the unit running load and radius of curvature at the point where the band appeared to be needed.

A similar method is based on the observation that the peak load after disreefing occurs at a time when the projected area of the canopy is between $S_p = 0.7$ and $0.8 S_{p_0}$ for $W/C_D S_0 = 1.0$ to 1.3 psf (Reference 14). Use $S_p = 1.0 S_{p_0}$ for higher canopy loading. At this same time the linear dimensions of the canopy are elongated about 10 percent by the design limit load so that

$$D_p = 1.1 (4 S_p / \pi)^{1/2}$$

71

With reference to Figure 65, the unit running load T_c is calculated with Equation 66 using $F = F_{LIM}$ disreef and the assumptions are made that the hoop tensions in the bands are equal and that

$$T_b + T_v = (h_b - h_v) T_c$$

72

Whence

$$T_b = (h_b - h_v) T_c / 2$$

73

Experience teaches that a good location for the band is on the upper edge of a ring about midway between the vent and the "equator" * of the inflated canopy. The equator of the fully inflated canopy is close to $h/h_R = 0.85$. When the canopy is partially inflated the location of the equator is assumed to be at $h = \pi D_p / 4$.

* Term used to designate the point at which the periphery of the inflated canopy is a maximum

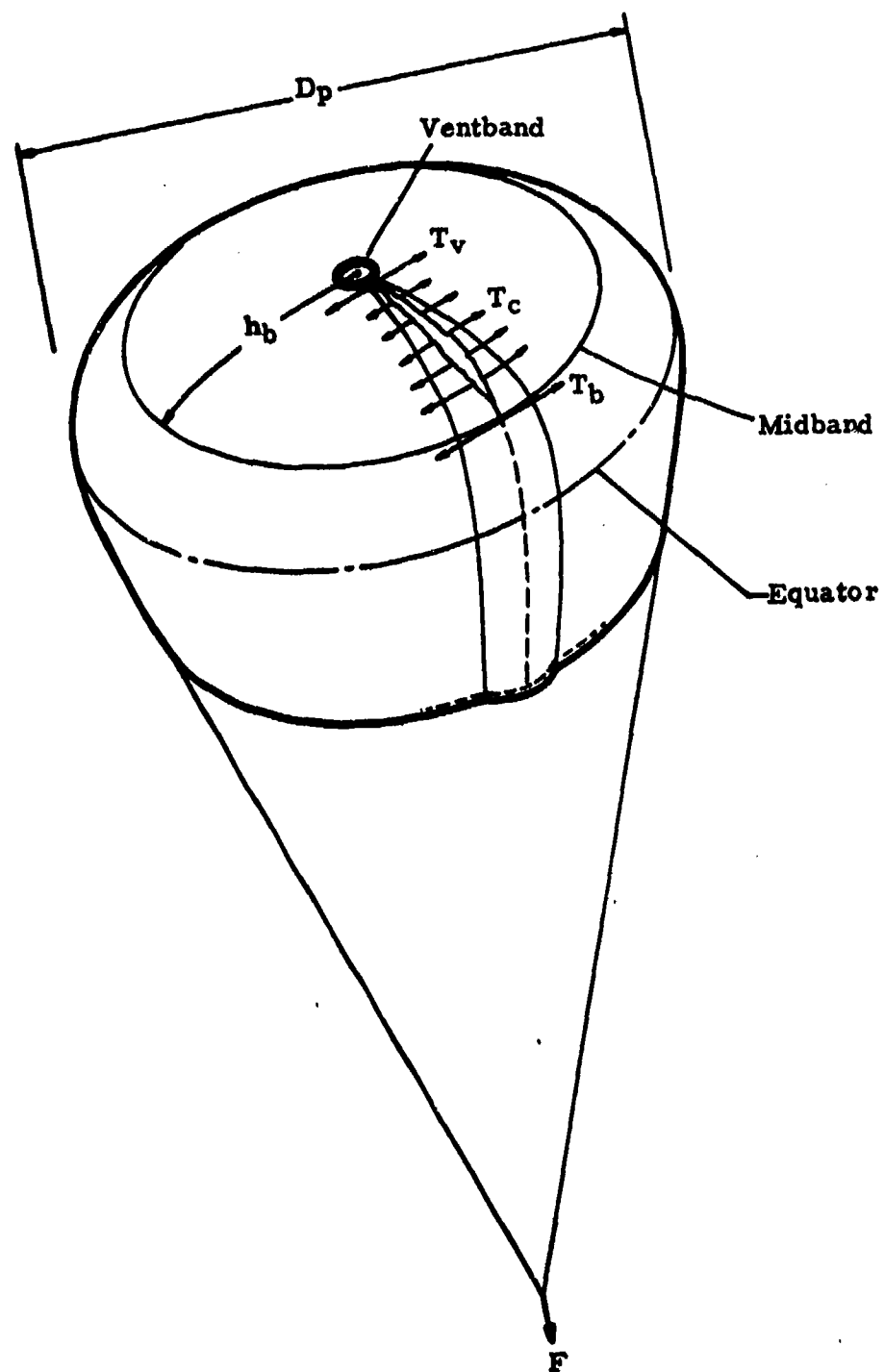


Figure 65. Method of Estimating the Design Load for a Mid-Canopy Circumferential Reinforcing Band

6.4.2.6 Reefing Line

Calculation of the tension in the reefing line is straightforward when the riser load and the canopy development angle are known. From the vector relations given in Figure 66, it can be shown that

$$T_R = F (\tan \psi - \tan \phi) / 2\pi$$

74

Unfortunately neither of the governing factors can be determined accurately. Initially the canopy development angle ($\psi - \phi$) is zero and is still quite small when F reaches its peak. Then as the force decays with $\psi - \phi$ continuing to increase the tension in the reefing line reaches its peak. In other words, the peak reefing line load is not directly related to the peak parachute force, and steady state wind-tunnel measurements are not applicable.

A few measurements of reefing line loads were made during the Apollo parachute development program. These are presented in Table XXIII. The maximum values turned out to be much less than expected on the basis of data given in Reference 24, as the following table of measurements shows. Inasmuch as somewhat higher load ratios can be expected in standard Ringsails due to the more rapid rate of increase in ($\psi - \phi$) associated with their characteristic growth while reefed, the designer should base his reefing line material selection on a more conservative load evaluation. It appears that an amply conservative load could be calculated as

$$T_R = 2.5\% F_R \text{ max.}$$

75

or select a reefing line material of

$$P_R = 5\% F_R \text{ max.}$$

76

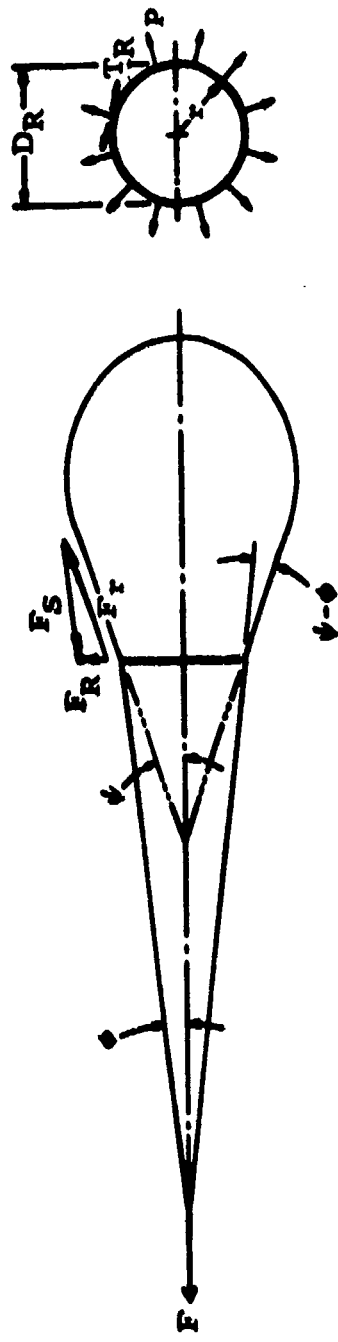
but not less than 1000 lb coreless braided cord in any event, this being the allowable maximum for standard miniature reefing line cutters.

6.4.2.7 Pilot Chute Bridle and Harness

The bridle and attaching harness of a pilot chute is subject to an initial impact load that has been of critical magnitude in some Ringsail systems, notably those of the Apollo and Century parachute development programs. When it is feasible to neglect drag, the bridle and lines can be treated as a linear spring and the probable magnitude of the snatch force estimated from the expression:

$$F_s = \Delta v (\text{km})^{1/2}$$

77



$$T_R = P r \quad r = \frac{D_R}{2} \quad P = \frac{F_R}{\pi D_R}$$

$$T_R = \frac{F_R}{2\pi}$$

$$F_R = F_S + F_T = F (\tan \psi - \tan \phi)$$

Figure 66. Method of Calculating Reefing Line Tension

where Δv is the velocity differential between vehicle and pilot chute at line stretch, k is the effective spring constant and m is the mass of the pilot chute canopy plus one-third of the mass of bridle and lines. The stress-strain characteristic of nylon cord shown in Figure 67 is typically non-linear, but two average spring constants are identified: k_1 is applicable to limit load calculations and k_2 to ultimate load calculations. Δv is determined from two-body trajectory computations.

Of course, the drag of the permanently attached pilot chute is not negligible when the main canopy comes taut and the fully inflated pilot chute is impulsively accelerated to the vehicle velocity. Computation of the impact load in this case is best accomplished with a digital computer program written for a two-body spring-mass system. However, the results should be used circumspectly because the computed load will not be conservative when the shock onset is sufficiently high to generate traveling stress waves in the bridle. (See Reference 13.)

TABLE XXIII

MEASURED REEFING LINE LOADS ON THE 85.6 ft D₀
MODIFIED RINGSAIL

Test No.	Reefing Data		Maximum Loads		Ratio T _R /F _R
	Stage	D _R (% D ₀)	F _R -(lb)	T _R -(lb)	
81-1	2	24	(1) 19052	229	.0120
			(2) 13692	132	.0096
80-3	2	28.5	14760	121	.0082
80-3R	2	26.7	21184	307	.0145
80-3R1	2	26.7	19491	121	.0062
81-3	2	26.7	(1) 14710	225	.0153
			(2) 19925	257	.0129
81-4	1	8.4	(1) 16318	--	--
			(2) 15834	143	.0111
81-2	2	26.7	(1) 18597	259	.0139
			(2) 13391	--	--

NOTE: This reefing line loads were measured with strain gage force transducers in the lines having electrical leads running down the suspension lines to the telemetry transmitter in the vehicle.

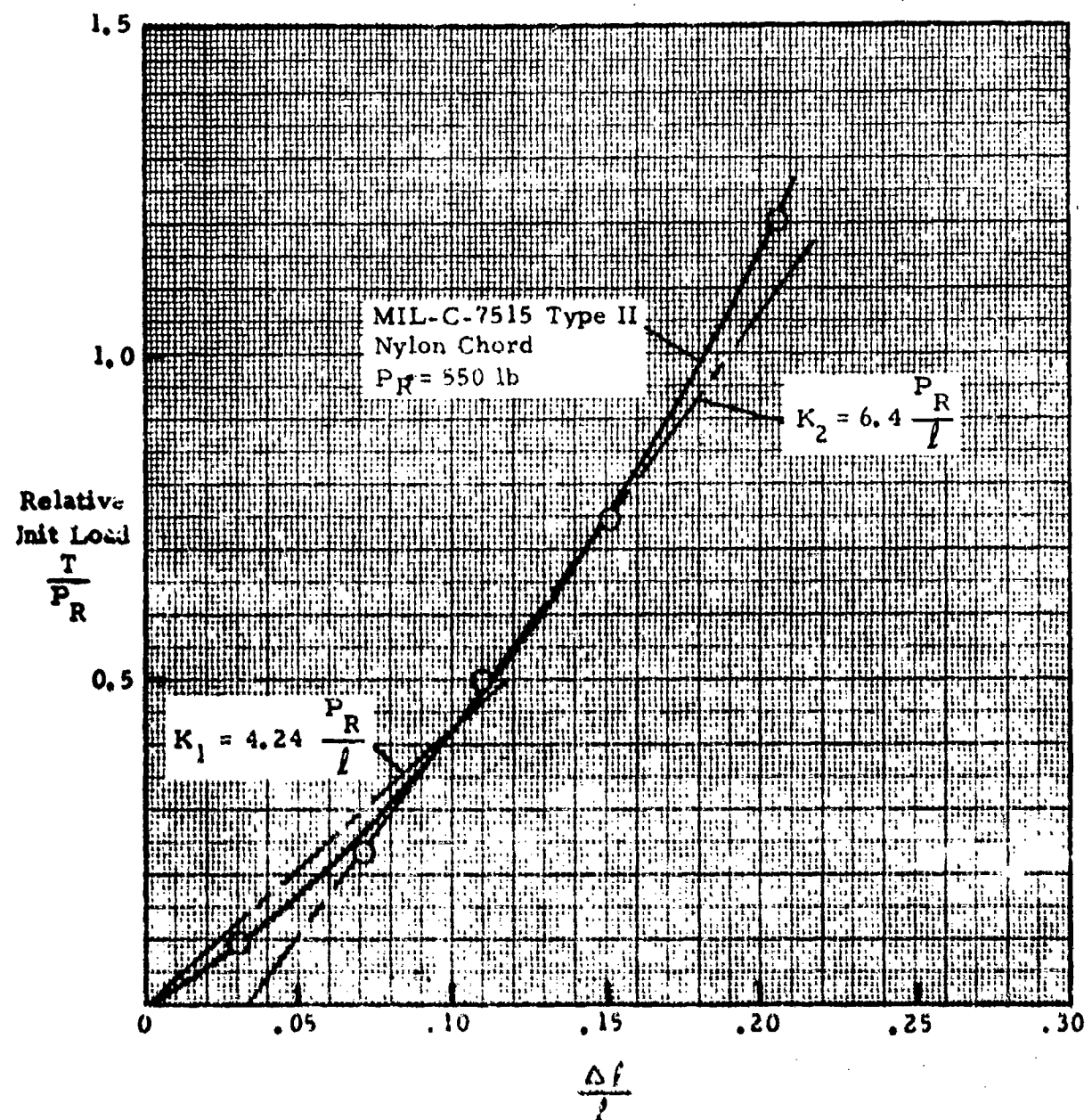


Figure 67. "Stress" - Strain Characteristic of Nylon Textiles

6.4.3 The Computer Method

A digital computer program identified as CANO was developed for poly-symmetric annulate parachute structures (Ribbon, Ringslot, and Ringsail) through which a complete internal loads analysis can be performed using an IBM 60-90 computer. The mathematical model includes the dimensions of every structural member in the parachute, together with the stress-strain characteristics of each different material (e.g., Figure 67), the pressure distribution across the canopy (e.g., Figure 64), the shape of the canopy, and the applied riser load. Stress-strain computations are iterated in small steps throughout the structural model until the calculated shape of the canopy agrees with the observed shape and the calculated net pressure load agrees with the applied load. The print-out includes a tabulation of internal loads for each structural member with sufficient accuracy to identify critical areas and probable points of failure. This enables optimization of the structure for consistent small margins of safety throughout the parachute.

A CANO user's manual which includes a listing of the program is given in Reference 25. Its application to the stress analysis of the Apollo parachute system is demonstrated in Reference 13.

6.5 CALCULATION OF RINGSAIL WEIGHT

In making weight calculations it is convenient to prepare a table listing all the members in the structure, their lengths (or areas) and their unit weights. Total lengths (or areas) are summed and multiplied by the corresponding unit weights to obtain the weight of each set of components. Table XXIV presents a list of the unit weights of textiles frequently used in Ringsail parachutes.

6.5.1 Canopy and Lines

A less accurate yet useful estimate of the weight of canopy and lines can be made fairly quickly with this relationship.

$$W_p = S_0 w_c + N L_s w_f \quad 78a$$

Where w_c is the unit weight of an existing canopy of similar design and w_f is the unit weight of the cord. Table XXV presents some typical unit weights of Ringsail canopies calculated with the same formula, i.e.,

$$w_c = (W_p - N L_s w_f) / S_0 \quad 78b$$

TABLE XXIV
TEXTILES COMMONLY USED IN RINGSAIL PARACHUTES

Textile Form	Unit Strength		Unit Weight (1)	
	lb	lb/inch	lb/ft	lb/ft ²
Cloth: 1. 1 oz ripstop (2) 1. 6 oz ripstop 2. 25 oz cloth		42-45		.0076
		50-58		.0110
		90		.0155
Cord: (coreless braid)	400		.00303	
	550		.00392	
	650		.00354	
	750		.00527	
	1000		.00710	
Tape: 5/8 inch 5/8 inch 1.06 inch one inch one inch	70		.000926	
	90		.000996	
	200		.00215	
	300		.00302	
	525		.00624	
Webbing: 9/16 inch 1/2 inch one inch one inch 1-3/4 inch	500		.0050	
	1000		.0081	
	4000		.0271	
	6000		.0344	
	10000		.0563	

NOTE: (1) Representative measured values are given where known
 (2) Trip salvage cloth per Appendix D

TABLE XXV
TYPICAL UNIT WEIGHTS OF RINGSAIL CANOPIES

D_o (ft)	S_{o_2} (ft)	l_e/D_o	W_p (lb)	$N/l_s w_f$	w_c (lb/ft ²)
29.6	688	.93	11.9	2.35	.01388
41	1322	.93	21.9	5.90	.01210
56.2	2483	.97	38.6	7.56	.01248
63.1	3130	.97	53.0	10.91	.01343
88.1	6091	1.42	105.4	23.50	.01345
128.8	13,035	1.15	230	63.6	.01276

6.5.2 Risers

A good weight estimate for a conventional short riser assembly may be made with

$$W_R = 1.1 N_R (l_g + 1.0) w_w \quad 79$$

where l_g is the length of one leg in feet and w_w is the unit weight of the webbing in lbs/ft.

When the main riser trunk is longer than 6 inches add the difference in feet to $l_g + 1$.

6.6 CALCULATION OF RINGSAIL POROSITY

At best, the methods of calculating parachute porosity yield only approximate results due to the elasticity of the structure and the flexibility of ventilation boundaries. This causes the relative porosity of the canopy to vary with differential pressure over a wide range, such that during opening the relative porosity of the pressurized crown area may be an order of magnitude greater than that of the fully inflated area during steady descent. Since it is customary to characterize the porosity of a parachute with only one number, it is important to understand to which phase of the parachute operation it is related.

The rated air permeability of parachute cloth (λ_R) is measured in this country at a differential pressure head of 0.5 inches of water, i.e., $\Delta p = 2.60 \text{ psf}$. From the relationship

$$F = \Delta p S = C_D S q$$

80

the equivalent dynamic pressure is

$$q = \Delta p / C_D$$

81

and for flat panels of parachute cloth at $\alpha = 90^\circ$, $C_D = 1.74^*$

whence

$$q = 2.6 / 1.74 = 1.49 \text{ psf}$$

which corresponds to a velocity of

$$v_e = 35.4 \text{ fps E.A.S.}$$

The cloth permeability is expressed in $\text{ft}^3/\text{ft}^2/\text{min.}$, and defines the average through-flow velocity in $\text{ft}/\text{min.}$ at a given Δp . In these terms, any change in Δp causes a marked change in λ . The relative porosity defined as the ratio $\Lambda = \lambda/v$, where v is the free stream velocity, does not change as rapidly, but below $\Delta p = 3$ inches of water the rate of change is still significant as shown in Figure 68 for a typical parachute cloth of $\lambda_R = 125 \text{ ft}/\text{min.}$. Note that the relative porosity corresponding to this number is $\Lambda_R = 4.45\%$ and the ratio $\lambda_R/\Lambda_R = 28.1 \text{ ft}/\text{min.}/1\%$. But in the calculation of parachute porosity the number $27.4 \text{ ft}/\text{min.}$ was established to represent 1% of relative porosity and has been used as standard for many years. This corresponds to the introduction of a drag coefficient $C_D = 1.05$ into the calculation, an expedient for which no justification can be found. It would seem more logical to apply the cloth drag coefficient given above and use a value of $21.3 \text{ ft}/\text{min.}/\text{percent of relative porosity}$ to obtain a total parachute porosity compatible with steady descent conditions. Then in calculating the canopy porosity pertinent to deployment and opening conditions a value of say $12.0 \text{ ft}/\text{min.}/1\%$ applied to λ_R would be more realistic, i.e., $q = 60 \text{ psf}$.

*Unreported data from wind tunnel tests of rectangular cloth panels supported on two sides with leading and trailing edges free.

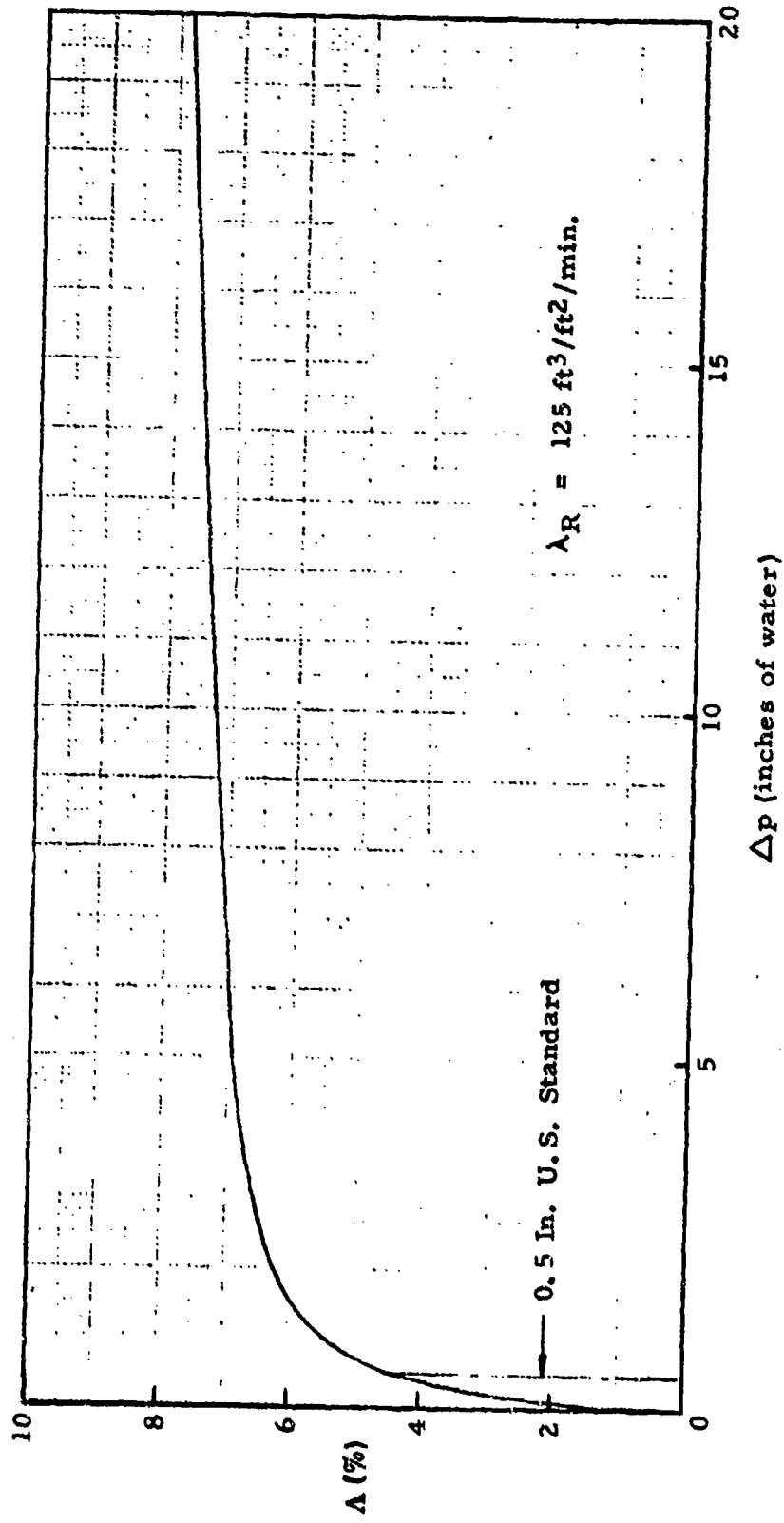


Figure 68. Variation of Relative Porosity with Δ_p for Typical Parachute Cloth (Reference 1)

Also for such conditions, the calculated geometric porosity should be based on the area of ventilation in the pressurized area of the canopy rather than in the entire area (S_o). However, these are refinements that lack of time has made impractical to incorporate into the calculation of Ringsail porosity.

The total porosity of the canopy is defined as

$$\lambda_T = \lambda_g + \lambda_m \text{ (in percent)} \quad 82$$

where

$$\lambda_g = \lambda_{gc} + \lambda_{gs} \quad 83$$

$$\lambda_m = \frac{\lambda_R}{27.4} \left[1 - .01 (\lambda_g + \lambda_{\sigma}) \right] \quad 84$$

$$\lambda_{gc} = (\text{Area of crown ventilation}) (100)/S_o$$

$$\lambda_{gs} = (\text{Total area of crescent slots}) (100)/S_o$$

$$\lambda_R = \text{Cloth rated porosity in ft}^3/\text{ft}^2/\text{min. at } \Delta p = 0.5 \text{ in. water}$$

$$\lambda_{\sigma} = (\text{Imporous area of canopy}) (100)/S_o$$

Because of the difficulty of making an accurate appraisal of some of these components, several assumptions were made to simplify the computation.

- a. Ventilation area covered by tapes is negligible.
- b. The area of the crescent-shaped slots can be characterized in terms of an average slot.
- c. The imporous area is a constant 2.5%.
- d. The cloth porosity is a constant $\lambda_R = 105$ ft/min.

On this basis, the open area of the crown ventilation is

$$S_c = s_v + h_g \sum (\text{slot lengths}) \quad 85$$

$$\sum S_s = .00353 S_o n_R \quad 86$$

where n_g is the number of rings of crescent slots in the canopy. The average value of the crescent slot area was derived from photogrammetric data applied to the basic dimensions of the 88.1 ft D_o Ringsail which indicated that the area of the slot nearest the skirt was 0.408 percent of the gore area (S_G) and that of the uppermost crescent slot was 0.298% S_G . These relative areas were calculated for slots of the shapes shown in Figure 69.

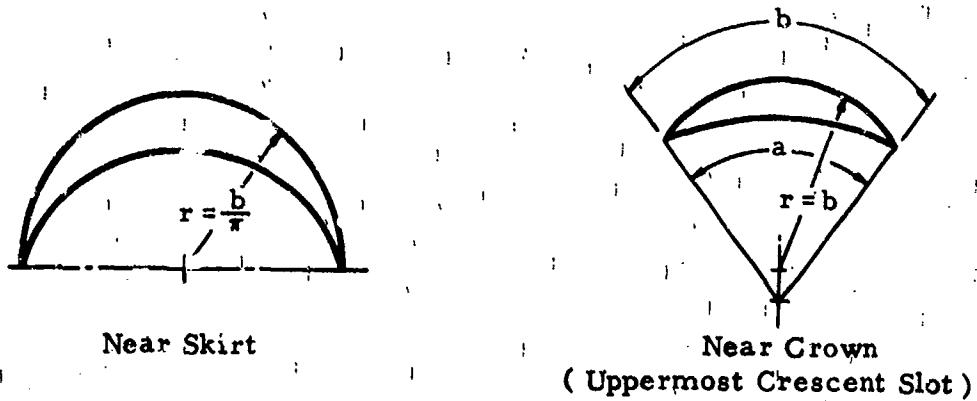


Figure 69. Assumed Shapes of Crescent Slots

The expression for the relative porosity of the cloth reduces to

$$\lambda_m = 3.83 \left[1 - .01 (\lambda_g + 2.5) \right]$$

87

The porosities given in Table IX for Ringsails of $D_o = 41$ ft and larger were calculated by the above method. The porosities of the smaller models were estimated from photogrammetric data, because the simplified method produced answers that were clearly too low.

A more accurate method of calculating the relative area of each ring of crescent slots is expressed as follows.

$$\frac{S_R}{S_G} = .67 \left(\frac{D_o}{N} \right)^2 \left(\frac{b}{a} \right) \left[.007175 \left(\frac{h}{h_R} \right) - .003384 \left(\frac{h}{r_R} \right)^2 \right] \quad 88$$

This allows for the varying shape of the slot with its position in the gore and for variations in the relative widths of gores in different canopy designs. In one test case utilizing dimensional data for the 63.1 ft D_o model the calculated value of λ_{gs} came out 15 percent greater than that obtained with the simplified method. This refined method has not seen much use because it is laborious and time consuming.

Inasmuch as the method of calculating porosity incorporated in the Ringsail computer design program (WG 176), yields totals that are about 20 percent less than those produced by the above methods, it is clear that considerably more work could be done in this area to put Ringsail design analysis on a firmer footing.

Ideally, the relative porosity of a parachute canopy should be presented as a function of dynamic pressure for three different operational conditions: reefed opening, opening after disreefing, and steady descent. The total porosity for each condition might be defined as

$$\lambda_T = S_g / S_{\Delta p} + \Lambda_{\Delta p} \quad 89$$

where S_g is the open area of the ventilation in the pressurized area ($S_{\Delta p}$) and $\Lambda_{\Delta p}$ is the relative porosity of the cloth in the same area. Although the practical difficulties in the way of obtaining such data are formidable, the end result finally attained would be a marked improvement in the predictability of parachute performance.

Since, most design needs can be satisfied with the crown geometric porosity

$$\lambda_{gc} / 100 = (S_v + \sum S_g) / S_o \quad 90$$

it is the only porosity calculation presently required for Ringsail design. The precise determination of total porosity can be left for future development.

SECTION 7

CONSTRUCTION DETAILS

The preparation of detail drawings of a Ringsail parachute assembly for use in the shop entails consideration of a number of features peculiar to the Ringsail design along with many others common to the art.

7.1 SAIL PATTERNS

A table of sail pattern dimensions including seam allowances is provided. These are calculated from the gore coordinates as described in Section 5. Note that the warp of the cloth is always horizontal.

7.2 SAIL EDGE TAPES (INTERCOSTALS)

The lengths of these tapes are determined automatically by the sail sub-assembly procedure described in Section 8. Hence, no dimensions other than the sail pattern dimensions are needed. The use of Trip Selvedge cloth minimizes the number of tapes required.

7.3 RADIAL TAPES

A radial tape marking diagram is provided in which the dimensions between marks are identical to those on the gore assembly layout, i.e., neglecting the angularity of the radial seams. This introduces a small increment of radial fullness in the sails in addition to that resulting from the fact that the woven width of the cloth is always greater than its nominal width. Another increment of fullness results from take-up due to thread tension along the seams.

Two sets of radial tapes are identified, one extending one inch below the skirt, the other two inches. When assembled in pairs the bottom extensions provide a wrap-around tab of tapered thickness for the suspension line joint.

7.4 VERTICAL TAPES

Each vertical tape is made of one length of tape doubled with the fold at the bottom end. The tape passes around the lower edge of the sail below the last ring slot in the crown so that half the tape is on top and the other half on the underside of the canopy. Since the 1-2 slot is small it need not be crossed by the tape and the ends can be finished off by folding them over the upper edge of sail 2 as shown in Figure 70. It should be noted that, with a few recent exceptions, Ringsails up to this point have utilized vertical tapes across the 1-2 slot as shown in Appendix A.

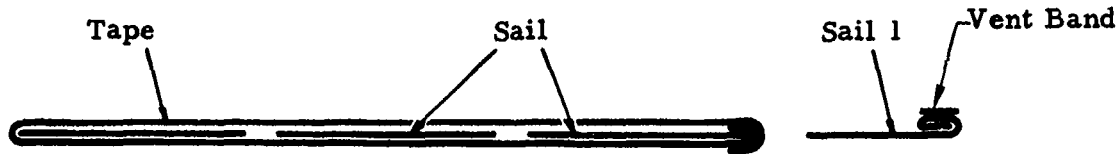


Figure 70. Cross Section of Vertical Tape Cut on Gore Centerline

A marking diagram is provided in which the sail spaces are made approximately two percent longer than the nominal woven width of the cloth to minimize the distortion caused by take-up along the seams when the tape is stitched to the sails.

7.5 THE GORE SUBASSEMBLY

The gore subassembly consists of one set of sails and one pair of radial tapes basted together. The radial tape on one side of the gore is placed on top of the sails and the other underneath so that when the gores are joined along the radial seams the two layers of cloth will be sandwiched between the tapes.

One vertical tape is also made part of the gore subassembly. It is stitched in place with a continuous two-needle seam of "E" nylon thread running full length.

7.6 RADIAL SEAMS

The one-inch radial tapes are folded together with the cloth in the one-half inch fell seams to minimize the variation in gore widths produced by over and under-folding. A three-needle seam of "F" nylon thread is used because comparative strength tests have shown this yields a maximum seam efficiency. (With 300 lb radial tapes and 8 to 10 stitches per inch the seam efficiency in 1.1 oz. cloth is 81 percent and in 2.25 oz. cloth, 86 percent.)

7.7 CIRCUMFERENTIAL BANDS

In conformance with common good practice marking diagrams are provided for vent, skirt, and intermediate bands to provide N equal spaces equal to the gore width at the latitude of each. The calculated band dimensions are increased by shrink allowances as follows:

Vent: $C_b = C_v^1 + (0 \text{ to } 3\%)$

Intermediate: $C_b = C_A + 2\%$

Skirt: $C_b = C_s + 2\%$

In practice these allowances are negotiated between the shop and engineering when cloth stretch or gathering along the seam poses an assembly problem.

Band lap splices are usually made 4 to 6 inches long and are located far apart around the canopy, each centered on a different radial seam.

7.8 SUSPENSION LINES AND VENT LINES

Line marking diagrams are provided in conformance with common good practice.

The vent line attachment is a simple 4 to 6 inch lap over the main seam secured with one row of double-throw zig-zag stitches. The vent line length is made equal to the vent diameter (Figure 71).

The skirt line attachment is a 4 to 6 inch lap over the main seam with the lower ends of the radial tapes wrapped snugly around the cord below the skirt for a distance of 2 inches all secured with one row of double-throw zig-zag stitches.

7.9 PILOT CHUTE BRIDLE HARNESS

When a permanently attached pilot chute is part of the system and predicted impact loads are high, a special bridle harness is employed to relieve the vent lines of the strain and abrasion produced by such loads, and to minimize the vent closing tendency of bridle tension. The number of lines in the harness is made equal to N divided by an even integer, and the ends are lap-spliced to the under side of the radial seams parallel to the vent line splices but offset enough to prevent superposition of the zig-zag stitching. The harness includes a confluence keeper and centering loop, and the length of the lines is made equal to the length of the vent lines, i. e., vent diameter, as shown in Figure 71.

7.10 RISERS

The riser design conforms with common good practice, employing a keeper at the confluence constrained to prevent slippage and having all plies stitched together between the keeper and the attachment loop to prevent interlaminar slippage. Buffers are installed in each attachment loop.

Standard line to riser links of the separable types are used except when weight limitations dictate the design of special links that more closely match the strength required. The links may be covered with envelopes of dacron felt to protect the textile members from abrasion, particularly when the packing pressure under the ram foot is high.

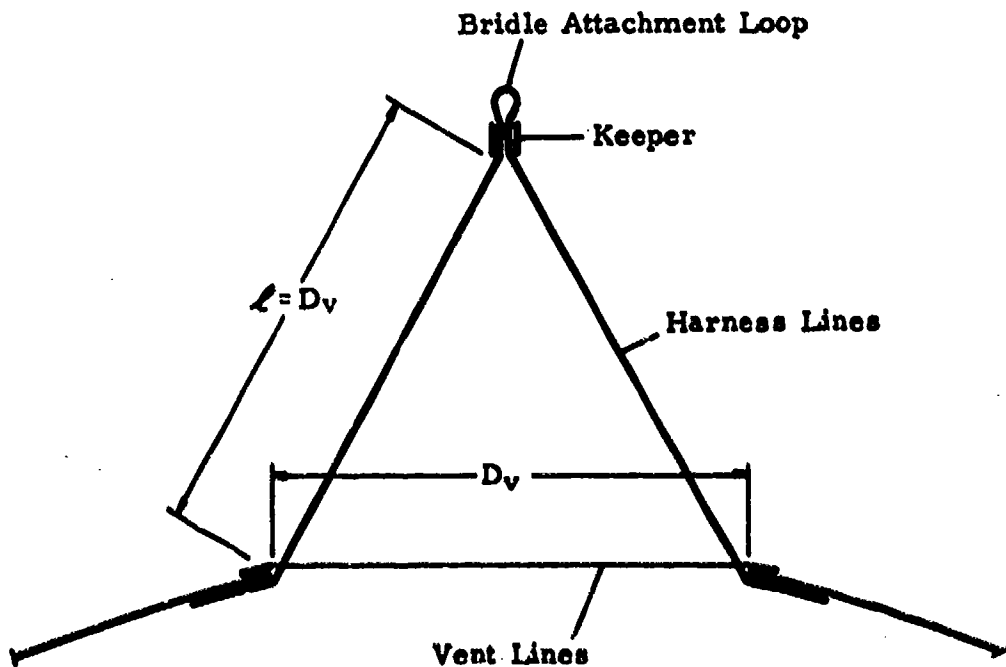


Figure 71. Bridle Harness for Permanently Attached Pilot Chute

SECTION 8

FABRICATION AND ASSEMBLY

Fabrication and assembly of the Ringsail parachute follows conventional shop practices with the exception of the specific construction details described in Section 7 wherein the Ringsail differs from other types of parachutes.

8.1 Cloth Layout and Cutting

The sail dimensions, as described on the engineering drawing, are transferred to heavy pattern material in the shop and trimmed to size. These serve as master marking patterns. For each cutting operation, the master pattern is used to layout a cutting pattern on a single long sheet of pattern paper, alternating the upper and lower sail edges to minimize material waste. Some wastage is unavoidable because the angle of cut is different for each sail. The difference may be negligible in the small sails near the vent but not for the majority. Care should be taken to insure that the pattern is followed because neglecting, to any degree, the angle of cut could seriously degrade the performance of the finished parachute. A large cutting table is used and sail material is distributed over the length of the table (under no tension, back and forth) so as to create a stack of sail material. Care must be taken to insure that each layer of the material is smooth and the edges straight and even. The thickness of the stack of cloth will vary depending upon the size of the parachute and the number of parachutes to be cut at any one time. This generally is worked out by the manufacturer. After insuring that the stack is uniform in smoothness and straightness, the cutting pattern is placed upon the material stack and secured into position with weights. The cloth stack is cut with a power shear along the lines marked on the cutting pattern. Note that the cutting pattern is cut simultaneously with the sail stack. Each cut set of sails should be stamped with the sail number near the center lower edge of each sail to aid in future identification and assembly.

8.2 SAIL EDGE TAPES

Sail edge tapes are stitched directly to the sails chainwise off the roll and cut off even with the edge of each sail to separate the sail subassemblies. The cloth and tape are fed through the two-needle sewing machine in a manner that will minimize gathering or take-up in either member. A minimum thread tension is used, and "B" nylon thread may be substituted for "E" thread on sails of 1.1 oz/yd² ripstop cloth.

8.3 RADIAL TAPES

Radial tapes are marked under nominal tension* in accordance with the marking diagram. An allowance of about 1/2 inch is made at each end for turning under to cover cut ends. One of each pair of tapes is made one inch longer than its mate at the lower end to provide for the tapered suspension line joint (see Figure 11).

8.4 VERTICAL TAPES

The double vertical tapes are marked under nominal tension* in accordance with the marking diagram. An allowance of about one inch is made at one end for turning that end over the other cut end when finishing the gore sub-assembly.

8.5 THE GORE SUBASSEMBLY

The gore subassembly consists of one set of sails, one pair of radial tapes and one vertical tape. About one-half of the sails will be subassemblies carrying tapes on one or both selvages, the remainder will have trip selvage. The upper edge of sail 1 will have a 1-inch rolled hem basted with "B" nylon thread. One of the radial tapes will be about an inch longer than the other.

The radial tapes are placed even with the cut edges of the sails and basted with one or two rows of "B" nylon thread through each sail in proper order holding upper and lower edges even with the marks on the tapes. The tape on one side of the gore is placed on the undersurface and the other on the upper surface, always in the same order from gore to gore. Cloth fullness is distributed uniformly between marks. The basting seam is placed where it will not interfere with subsequent folding and stitching of the main radial seam.

The double vertical tape is stitched in place along the gore centerline with a continuous two-needle seam of "E" nylon thread running full length. The mid-tape bend is made around the lower edge of the sail below the longest ringslot, sandwiching the cloth between the two halves. The long upper end is folded back 1/2 inch and bent over the upper sail edge to cover the short end even with the sail edge.

* Nominal tension is sufficient to straighten the material for maintenance of dimensional consistency without undue stretching, usually about 5 lbs carefully measured each time.

8.6 CIRCUMFERENTIAL BANDS

The vent, skirt, and intermediate bands (if any) are marked under nominal tension in accordance with the marking diagrams on the drawing, which include provisions for lap splices. Temporary marking jigs are used until the spacing take-up allowance has been verified on the prototype assembly.

8.7 SUSPENSION LINES AND VENT LINES

Suspension lines and vent lines are marked in accordance with the marking diagrams while subjected to a uniform tension, usually 20 lbs. As in any circular parachute the purpose is to produce a high degree of uniformity in the length of lines around the canopy. The material should be rolled off the spool and allowed to "relax" for 24 hours before marking. Recently some manufacturers have not stored their line material spools but store it loosely in boxes. In these cases it is not necessary to relax the material for 24 hours. If lines are unusually long, tension may be applied with the lines routed around a pulley.

8.8 RISERS

Riser materials are measured, cut and assembled in conformance with the best standard practices using n-point cross-stitch patterns. Box stitch patterns are not used.

8.9 THE CANOPY ASSEMBLY

The canopy assembly consists of N gore subassemblies, N/2 vent lines, vent and skirt bands, and any mid-canopy circumferential reinforcing bands that may be required. If a permanently attached pilot chute is required, the apex bridle harness will be a part of the canopy assembly.

The canopy is assembled gore-by-gore with three-needle fell seams of "F" nylon thread. In each seam the two radial tapes are folded together to one-half width with the cloth sandwiched between. The upper and lower tapes are held together and fed through the sewing machine from sail edge to sail edge in a way that will minimize differential gathering of the cloth and displacement between adjoining sail edges across the seam. A maximum misalignment of $\pm 1/4$ inch is acceptable and provides adequate continuity of structure around the canopy. A skilled operator requires only a few minutes learning time to produce work within this tolerance. Seam folding aids may be used but are not essential.

When a canopy is to be made up of several large segments, each assembled by a different operator, care must be exercised to ensure that each operator employs the same main seam stitching technique in joining the gores so that the radial take-up will be uniform all around. Common practice is to stitch the seam downward from vent to skirt so that the radial tape tabs can be easily fanned out as the seam runs off the bottom. Tab fanning is done to facilitate the wrap-around operation when the suspension line joints are finished.

Vent, skirt, and intermediate bands are stitched to their appropriate ring edges so that each mark falls on a radial centerline. Care is exercised to effect a uniform distribution of cloth fullness between marks. If any difficulties are encountered here, a satisfactory change in the shrink allowances can usually be negotiated with the engineering department. Band lap splices are made, each centered on a different radial seam, and stitched as specified on the drawing.

Vent lines are installed in the conventional manner on top of the canopy with end lap joints secured with one row of double-throw zigzag stitching running one-half inch off each end of the lap.

The bridle harness, if one is required, is attached to the apex of the canopy as illustrated in Figure 71.

8.10 THE PARACHUTE ASSEMBLY

The standard parachute assembly consists of one canopy assembly, N suspension lines, N-2 reefing rings, two cutter pockets with doublers, two cutter lanyards, one riser assembly, and a set of links.

Each suspension line is stitched to the skirt of the canopy with one row of double-throw zigzag stitches starting 1/2-inch above the cord end and extending to 1/2-inch below the radial tab end. The radial tape tabs are wrapped snugly around the cord for a distance of 1.5 to 2 inches below the skirt and secured as the row of zigzag stitches is run through to the end of the pattern.

Each reefing ring must be attached rigidly to the inside of the canopy at the intersection of the radial with the skirt band. The ring attachment should consist of 5 turns of waxed #6 nylon cord doubled and tied off on the outside with a surgeon's knot and an overhand knot. Machine stitched hold-down cleats of tape are acceptable if mid-gore reefing is used.

The cutter pockets with doublers are installed on opposite sides of the canopy at the skirt in the conventional manner. The short cutter actuating lanyards or suspension line cord are attached to the appropriate suspension lines in conformance with best practice for the tubular insertion-type joint known popularly as the "Chinese Finger Trap." The location specified for this attachment will be far enough below the skirt to ensure complete extraction of the firing pin from the cutter.

The suspension line attachment to the riser link is made as a snug loop around the bar (preferably two turns when space permits) with the bitter end inserted into the tubular cord and secured with a short zigzag stitch pattern (approximately 2 to 4 inches long) near the link bar.

8.11 DIMENSIONAL TOLERANCES

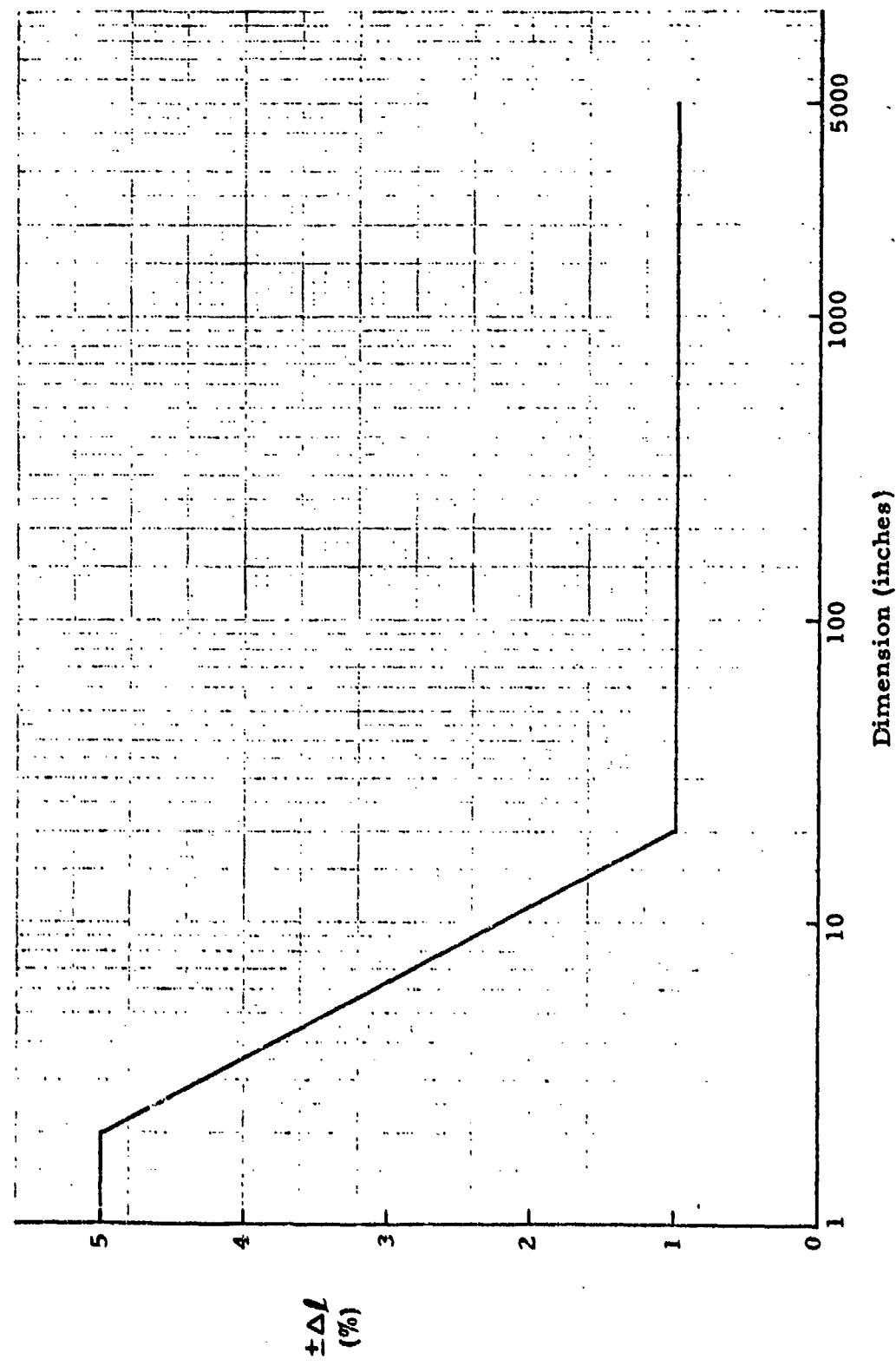
The characteristic stress-strain curve of parachute textiles affords inherent forgiveness for errors of fabrication that distort the polysymmetry of the structure. As shown in Figure 67, an initial elongation of one percent is attended by a load of only 3 percent of the ultimate strength of a typical material. For all dimensions longer than 20 inches ± 1 percent would constitute a generous tolerance. The shortest critical dimension is the width of the gore at the vent band (typically 2 to 3 inches in the Ringsail) for which a variation of $\pm .1$ inch or ± 5 percent is reasonable. On this basis it is possible to construct a diagram of acceptable dimensional tolerances as shown in Figure 72. Use of these tolerances for the finished dimensions of Ringsail parachutes is recommended when they do not conflict with tighter standards dictated by specific operational considerations.

8.12 QUALITY CONTROL

The methods of construction employed in the Ringsail parachute lend themselves to good in-process control by the sewing machine operator as well as easy post-assembly inspection. Close control of the folding of the inter-gore fell seams by the radial tapes is one example. Good practice is to inspect all patterns and marking boards and witness call cutting of material. In-process inspection points can be established to insure basting of the gore assemblies are proper before assembly and that all gores are properly assembled prior to installing the vent and skirt bands.

The important dimensions of the final parachute assembly that must be uniform around the canopy within reasonable tolerances to ensure good polysymmetry of the structure are as follows:

Figure 72. Acceptable Tolerances for Finished Dimensions of the Ringsail Parachute



- a. Vent line length
- b. Width of gore at vent band
- c. Length of radial from vent to skirt
- d. Width of gore at skirt band
- e. Suspension line length
- f. Riser length

In general, dimensional inspection of 10% of items (a) through (e) above, taken at uniformly distributed points around the canopy are sufficient to insure good quality. Although the width of the gore at intermediate points between vent and skirt is also important, the method of assembly prevents large discrepancies and it usually is not feasible to check such dimensions except at intermediate circumferential bands.

If the measuring and marking of components is controlled to within close tolerances, then the inspection of the coincidence of matching marks can provide one measure of the dimensional accuracy of the assembly.

The line lengths are easily checked to the design dimension by applying the same tension used in their fabrication (usually 20 lbs). Checking the lengths of the canopy assembly along stitched seams is more difficult. During the manufacturing process a canopy cut to the design dimensions "shrinks," i. e., becomes shorter along all stitched seams due to takeup caused by thread tension, etc. Owing to interlaminar friction, it usually requires more than a little tension to stretch such seams back to the original length, and verification of uniformity around the canopy is inconvenienced. However, the inconvenience is not great, requiring merely the determination of an average dimension on the first production model to be checked at nominal tension (say 20 lbs).

A parachute, during the inflation process, stretches and it happens that under the nominal loading of steady descent the elongation of all components is more than sufficient to restore the assembly to its design dimensions; indeed, considerable over-expansion of the area is the rule for Ringsail parachutes larger than 40 ft D_0 . Therefore, the requirements for the fabricator to apply a shrink-scale to the measurement of some of the canopy tapes tapes and bands, to make trial canopy assemblies, and to juggle measuring tensions until the parachute can indeed be checked against the design dimensions is superfluous. Quality control of the polysymmetry of the canopy can be effected very simply by measuring the first production model under a standardized constant tension and establishing the average dimension of each component to be satisfied on the inspection table.

REFERENCES

1. WADC TR 53-78, A Study to Establish a Parachute Research and Development Program, Vol. II, Sec. V (Design and Fabrication), Radioplane Co. Report No. 756, Aug. 1953.
2. Ewing, E.G., Engineering Proposal for Development of the Skysail Personnel Parachute and Container, Radioplane Co. Report No. 882, April 1954.
3. Ewing, E.G., Development of the Light Weight Ringslot Parachute for Stage III Recovery of the XQ-4 Drone, Radioplane Company Technical Memorandum AMM-12-1, Nov. 1955.
4. Anon; Design Development of a Universal Aerial Recovery System Phase III (Product Improvement), SAMSQ 68-244, Northrop Ventura Report No. 6174, June 1968.
5. Graham, C. R.; Heavy Vehicle Ringsail Parachute Century Series - 124.5 ft D₀ & 123 ft D₀, Northrop Ventura Report No. 3856, May 1965.
6. Ewing, E.G., Design Analysis 128.8 ft D₀ Century Ringsail (Project 1821), Northrop Ventura Report No. 4051, June 1966.
7. Nash-Boulden, S.S.; Apollo Aerial Drop Test Summary, Northrop Ventura PTM-763, Nov. 1963.
8. Ewing, E.G.; Development Program for a Ringsail Parachute (Century Series) Final Report, Northrop Ventura Report No. 5028, Dec. 1966.
9. Norman, L. C. and Suit, K. L.; An Investigation of the Initial Century Series Ringsail Parachute, NASA TND-5968, Manned Spacecraft Center, Aug. 1970.
10. Gimbalouski, E.A.; Development of a Final Stage Recovery System for a 10,000 Pound Weight, WADC TR 59-109, Pioneer Parachute Co., Dec. 1958.
11. Moeller, J. H.; Preliminary Evaluation of the Effect of 100% Vertical Tapes and Midpanel Reefing on Reducing Aerodynamic Interference in PDS 1543 Cluster Operation, Northrop Ventura internal memo. APT/64-222, 2 April 1964.
12. Moeller, J.H.; Basic Loads for Apollo Block I Spacecraft Earth Landing System, Northrop Ventura Report 3772A, Oct. 1966.

13. Mullins, W.M., Reynolds, D.T., Lindh, K.G. & Bottorff, M.R.; Investigation of Prediction Methods for the Loads and Stresses of Apollo Type Spacecraft Parachutes Vol. II Stresses, Northrop Corp., Ventura Div., Report NVR-6432, June 1970.
14. Mickey, F.E., McEwan, A.J., Ewing, E.G., Huyler, W.C. Jr., and Khajeh-Nouri, B.; Investigation of Prediction Methods for the Loads and Stresses of Apollo Type Spacecraft Parachutes Vol. I Loads, Northrop Corp., Ventura Div. Report NVR-6431, June 1970.
15. Groat, J.F. and Nash-Boulden, S.S.; Analysis of Apollo Main Parachute Wind Tunnel Test Using Full, Half, and Third Scale Models, Northrop Ventura Report 2928, Jan. 1964.
16. Nash-Boulden, S.S. and Coe, D.C.; Analysis of the Full Scale and Clustered One-third Scale Apollo 88 foot Ringsail Parachute Tests in the Ames 40 x 80 foot Wind Tunnel - Second Series. Northrop Ventura Report 3518, April 1964.
17. Riley, V.F.; Final Report Glidesail Development Program Contract NAS9-140, Northrop Ventura Report PTM-524A Dec. 1962.
18. Murrow, H.N., and McFall, J.C. Jr.; Summary of Experimental Results Obtained from the NASA Planetary Entry Parachute Program, AIAA Paper No. 68-934, Sept. 1968.
19. Stone, J.W.; Rate of Descent Analysis of the Apollo Earth Landing System with the Basic PDS-1543 88-foot Parachutes, Northrop Ventura Report 2972, July 1964.
20. French, K.E.; Model Law for Parachute Opening Shock, AIAA Journal, Vol. 2, No. 12, Dec. 1964, pp. 2226-2228.
21. Riffle, A.B.; Determination of the Aerodynamic Drag and Static Stability of Reefed Parachute Canopies, Wright Patterson AFB Ohio, Jan. 1965.
22. Ewing, E.G.; Deployable Aerodynamic Deceleration Systems, NASA SP-8066, June 1971.
23. Greene, G.C.; Opening Distance of a Parachute, Journal of Spacecraft and Rockets, Vol. 7, No. 1, Jan. 1970, pp 90-100.
24. Anon., Performance of and Design Criteria for Deployable Aerodynamic Decelerators, ASD-TR-61-579, AFSC, Dec. 1963.

25. McEwan, A. J., Huyler, W. C., Jr., Mullins, W. M and Reynolds, D. T.; Description of Computer Programs for the Analysis of Apollo Parachutes, Northrop Ventura Report 6428, June 1969.
26. Ewing, E. G.; Ringsail Parachute Characteristics, Radioplane Company PTM-323A, Jan. 1961.
27. Weller, E. J.; Design Approval Test Report - Asset Recovery System, Northrop Ventura PTM 571, Apr. 1963.
28. Graham, C. R. and Baker, J. T.; Recovery Parachute - Stanley Escape Capsule Component Verification Tests, Radioplane Report No. 2392A, March 1962.
29. Buhler, W. C.; Project Mercury Landing Parachute Development and Qualification, Radioplane Report No. 2312-B, Oct. 1961.
30. Nash-Boulden, S. S.; Summary Report Gemini Main Parachute Development Tests 7 through 20, 28 through 30 and 32, Northrop Ventura Report No. 2932, Jan. 1964.
31. Swanson, J. N. and Dedon, W. W.; Flight Qualification Test Program - Gemini Parachute Landing System Spacecraft 3 Configuration, Northrop Ventura Report No. 3796, July 1965.
32. Belknap, S. and Goar, K.; Summary Analysis Report of Drop Tests Performed During the Apollo Main Parachute Improvement Program; Drop Test Series 40, 41 and 44, Northrop Ventura Report No. 3722, Dec. 1964.
33. Murray, H. L.; Apollo Block II Increased Capability Earth Landing System - Final Report of Drop Test Series 80 and 81, Northrop Corp., Ventura Div. Report NVR-6106, May 1968.
34. Ewing, E. G.; Another Look at the Filling Problem of Clustered Parachutes, Northrop Ventura Report No. 3502, April 1964.
35. Anon.; 20K Parachute System Final Report, Irving Air Chute Co. Inc., Report No. GIR85-15, Aug. 1967.

APPENDIX A

PROMINENT RINGSAIL PARACHUTES

This Appendix presents design information on a number of the better known Ringsail parachutes. This information is presented for the benefit of the designer to provide some insight into the various methods and techniques used in the structural design. Figures 73 thru 76 presents still photographs of Mercury, Gemini, Apollo and Century Series Parachutes. The Century Parachutes in cluster are shown in the Frontispiece.

The Ringsail parachutes shown in Table XXVI and the figures referenced were selected as representative of the full spectrum of system operational requirements that can be met with negligible development risk. A guide to reading the fullness distribution curves presented in Figures 78 through 105 is shown in Figure 77.

TABLE XXVI
REPRESENTATIVE RINGSAIL PARACHUTES

D_o (ft)	Program or Operational System	Figure
29.6	Project ASSET	78
41.0	B-58 Escape Capsule and SUD Aviation Nose Cone recovery	79
63.1	Mercury Capsule Landing System	80
84.2	Gemini Spacecraft Landing System	81
85.6	Apollo Earth Landing System (including various development configurations)	82 thru 104
128.8	Century Series	105

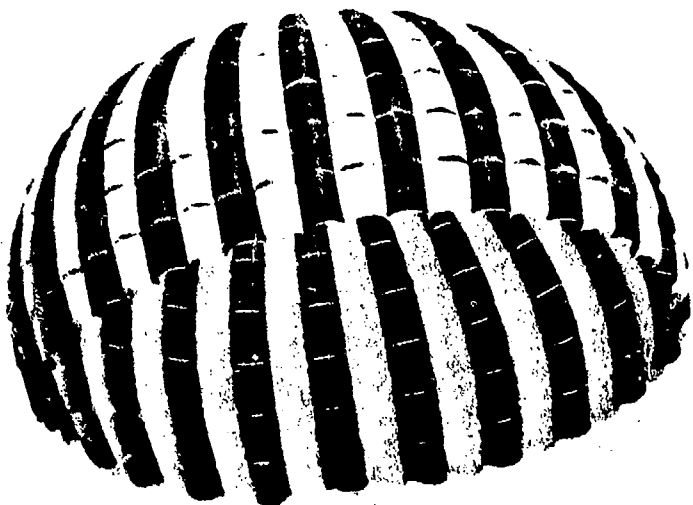
Included with the information relating to the final design version of the modified Ringsail of the Apollo ELS cluster is a group of construction data sheets for significant test specimens of the many prior versions fabricated and tested during the development program. The original Apollo main parachute had a nominal diameter of $D_o = 88.1$ ft. Subsequent versions differed in two basic ways, embodying:

- a. Basic design modifications aimed at improving cluster operation and reducing weight.
- b. Changes in materials of construction during the structural evolution required to strengthen critical members and meet increasing design limit loads as the spacecraft weight grew from 9,500 to 13,000 lbs.

Two classes of parachutes are represented in Figures 78 through 105 and the data sheets which follow:

- a. 72 gore Ringsails of standard and modified designs all having nominal diameters in the range of 87 to 88 feet.
- b. 68 gore, 85.6 ft D_o Ringsails modified by removing 4 gores from the standard 72 gore model and by removing 75 percent of the width of ring 5.

The 72 gore canopies with the exception of PDS 3120 have a constructed shape that is essentially a spherical segment to which fullness has been added as shown in the diagrams. The 68 gore canopies being assembled from spherical gores have a truncated ogival shape with an apex angle of 19 degrees, and the same fullness distribution as the standard 72 gore model. The constructed shape of PDS 3120 is a truncated ogive with an apex angle of 15 degrees. For convenience the 85.6 ft D_o ogival shaped canopies were designated "conical" in the drawing titles and the popular nominal diameter of 83.5 ft is retained to agree with the original documentation.



Reproduced from
best available copy.



Figure 73. Mercury Capsule Landing System, 63.1 ft D₀ Ringsail



Reproduced from
best available copy.



Figure 74. Gemini Spacecraft Landing System, 84.2 ft D₀ Ringsail

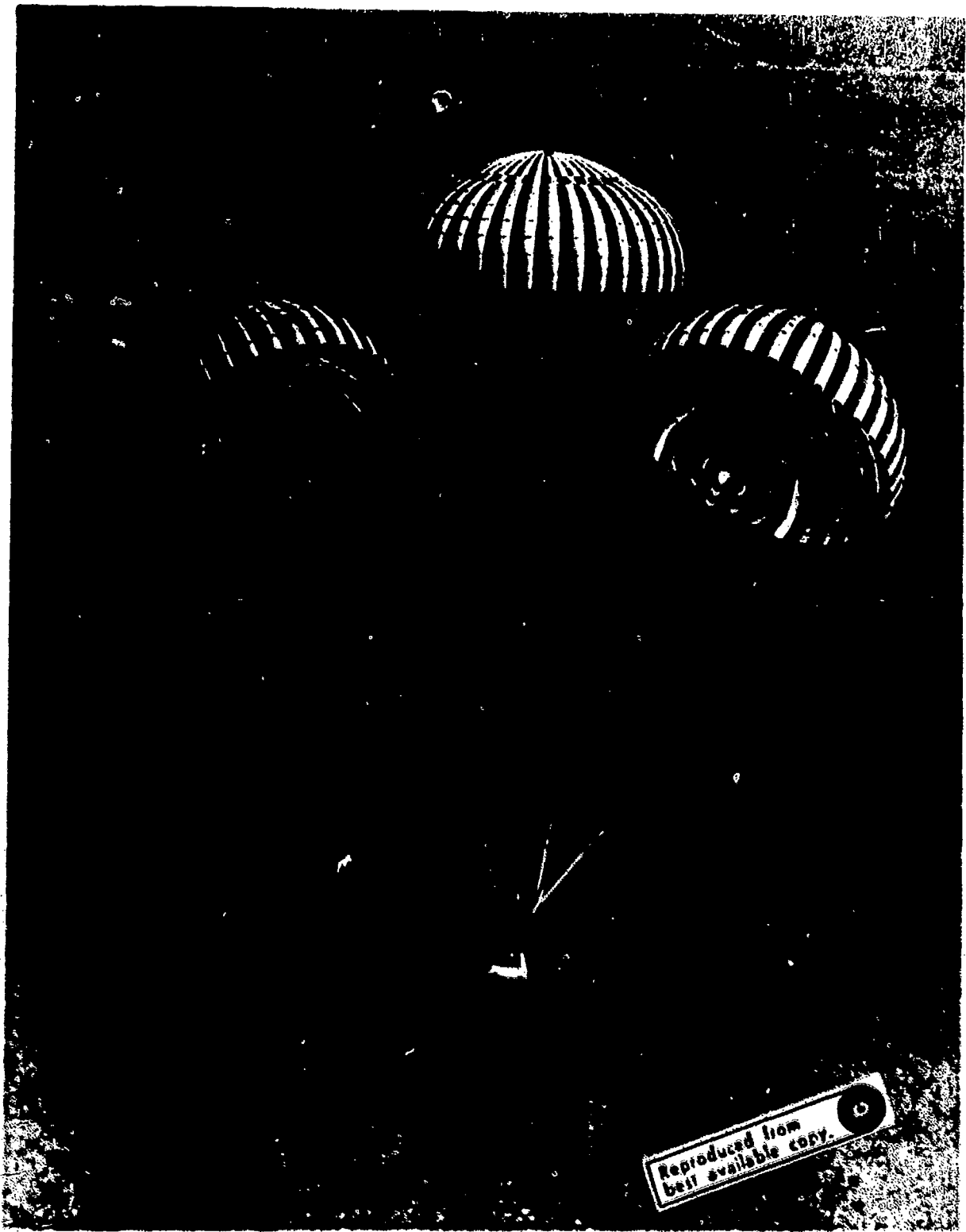
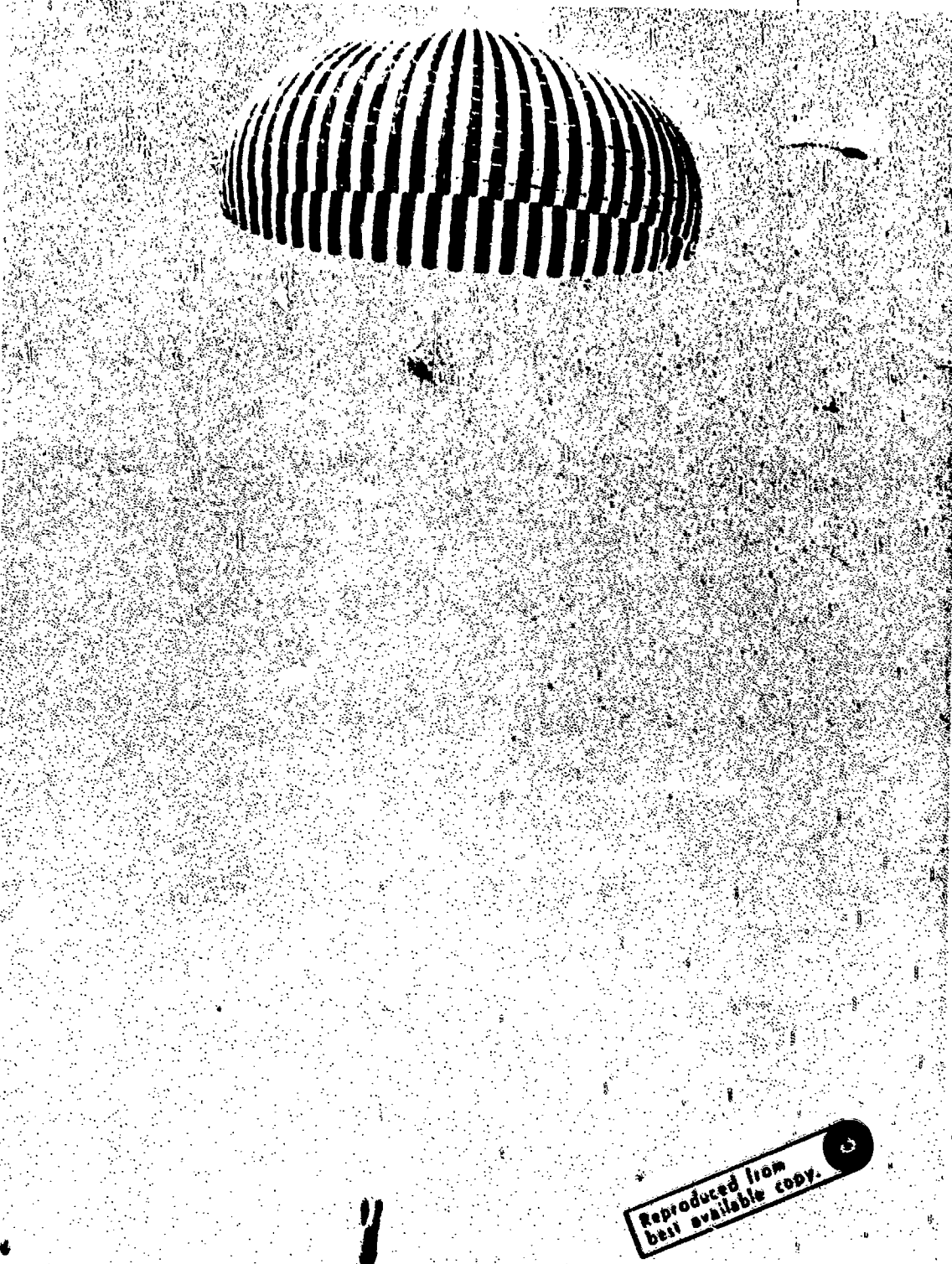


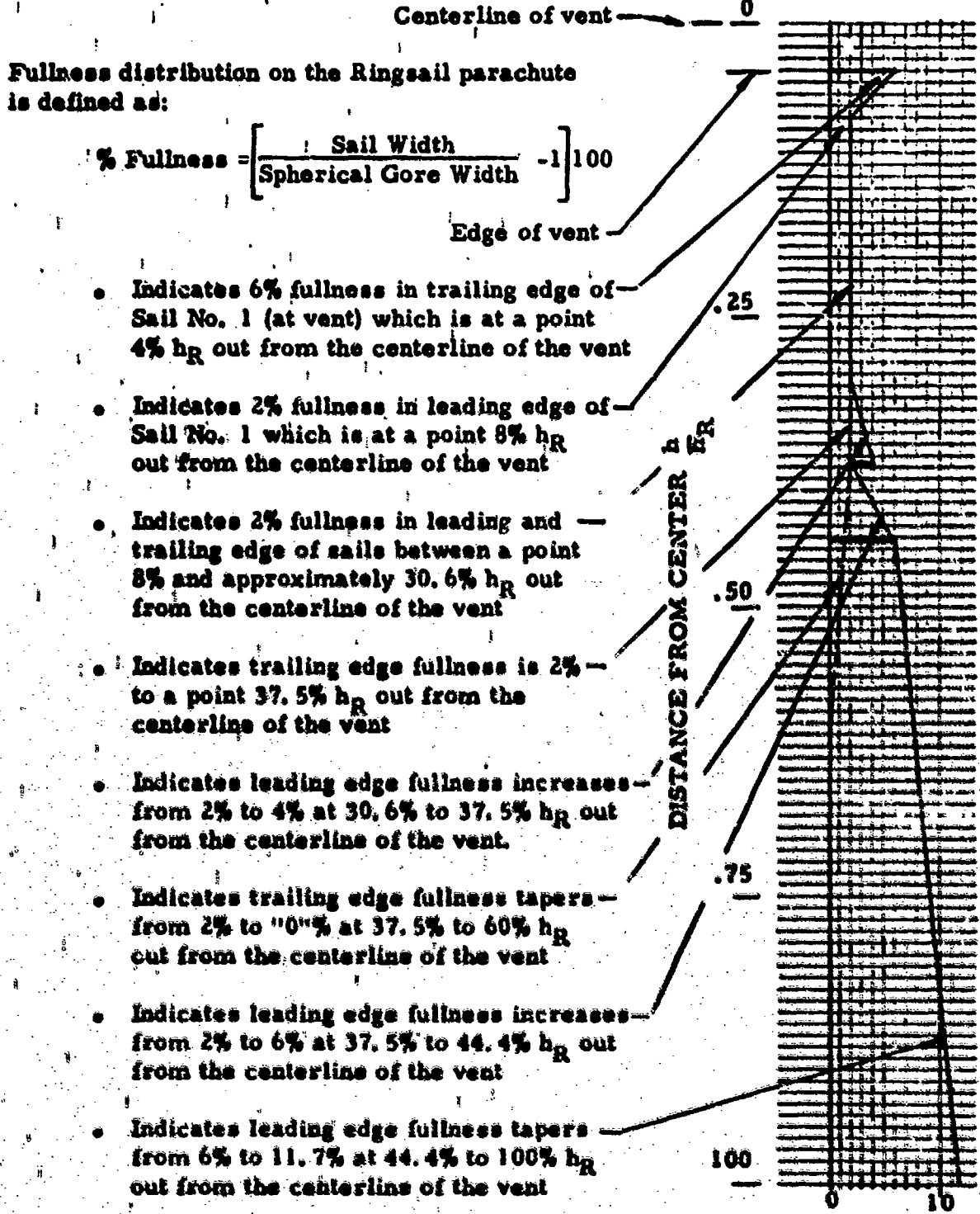
Figure 75. Apollo Spacecraft Earth Landing System, Cluster of Three 85.6 ft D₀ Ringsail Parachutes

Reproduced from
Bell available copy.



Reproduced from
best available copy.

Figure 76. 128.8 Ft D₀ Century Ringsail Parachute



FULLNESS DISTRIBUTION (%)

Figure 77. Guide to Fullness Distribution Curves
Presented in Figures 78 through 105

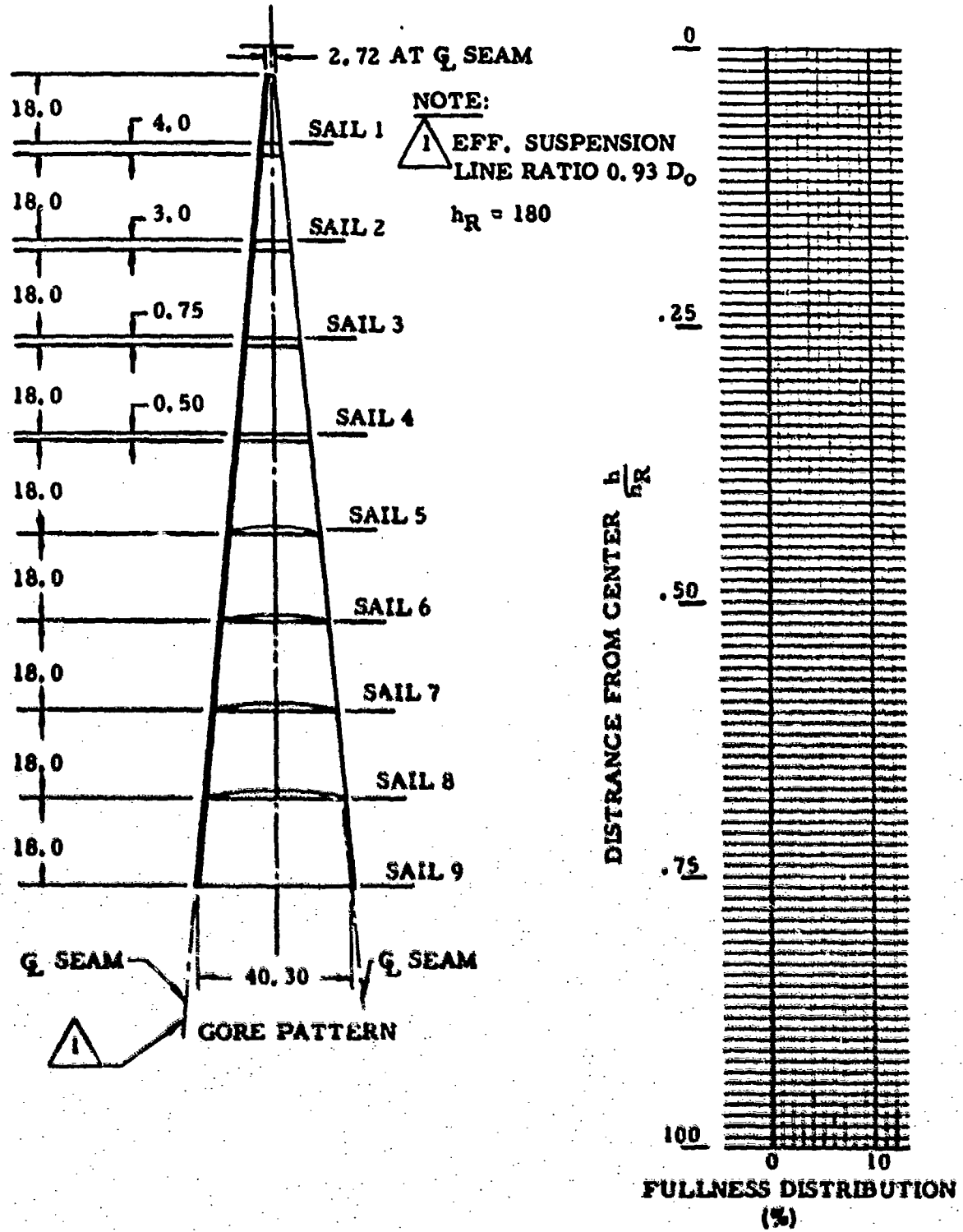


Figure 70. Gore Pattern and Fullness Distribution

R5616-1 29.6 ft D₀ Ringseil Parachute

PART NO.: R5616-1

TITLE: PARACHUTE, 29.6 ft D₀ RINGSAIL

NO. GORES: 24

TYPE OF REEFING: RADIAL

ITEM	MATERIAL		
VENT LINES	550 LB NYLON CORD		
VENT BAND	900 LB NYLON TAPE, 1.0 WIDE		
RING NUMBER	CLOTH WEIGHT OZ/YD ² (a)	TAPE	
1	2.25	P _r , LB	WIDTH, IN.
2	2.25	90 (b, f)	.62
3	2.25	90 (c, f)	.62
4	1.1	90 (c, f)	.62
5	1.1	None	None
6	1.1	None	None
7	1.1	None	None
8	1.1	None	None
9	1.1	None	None
VERTICAL TAPE	90 LB NYLON TAPE, .62 WIDE (e)		
SKIRT BAND	300 LB NYLON TAPE, 1.0 WIDE		
RADIALS (2 EACH)	300 LB NYLON TAPE, 1.0 WIDE		
SUSPENSION LINES	550 LB NYLON CORD		

(a) TRIPLE-SELVAGE CLOTH

(b) LEADING EDGE ONLY

(c) LEADING AND TRAILING EDGE
(d) TRAILING EDGE ONLY
(e) NO. 1 THRU NO. 5 SAIL DOUBLED, CENTER OF CORE TO TOP NO. 5 SAIL,
THEN DIAGONALS & TERMINATES AT RADIAL AT BOTTOM OF NO. 5 SAIL

(f) CIRCUMFERENTIAL REINFORCEMENT

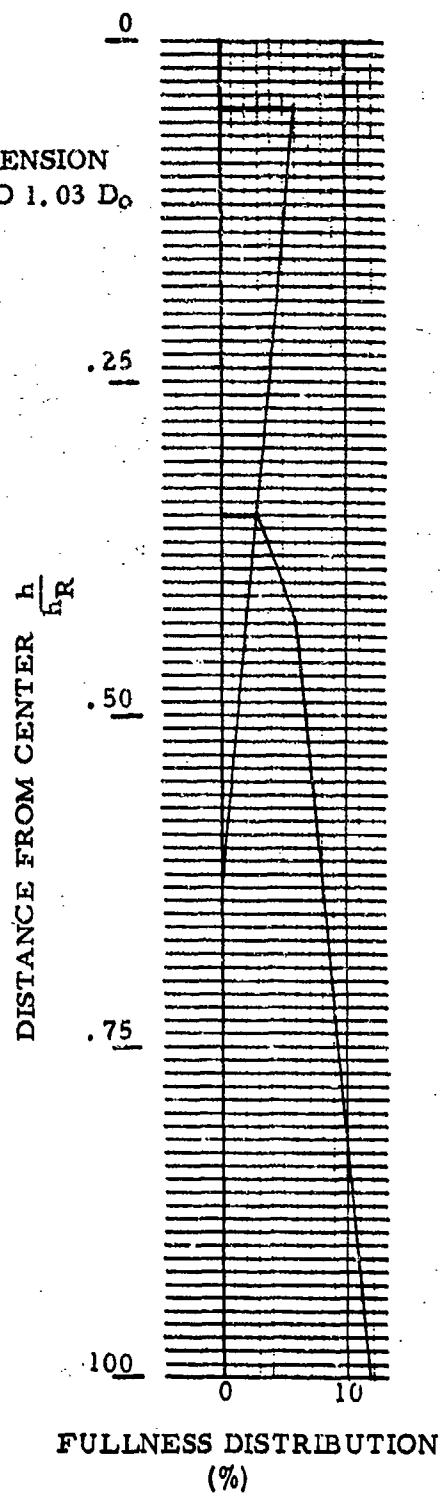
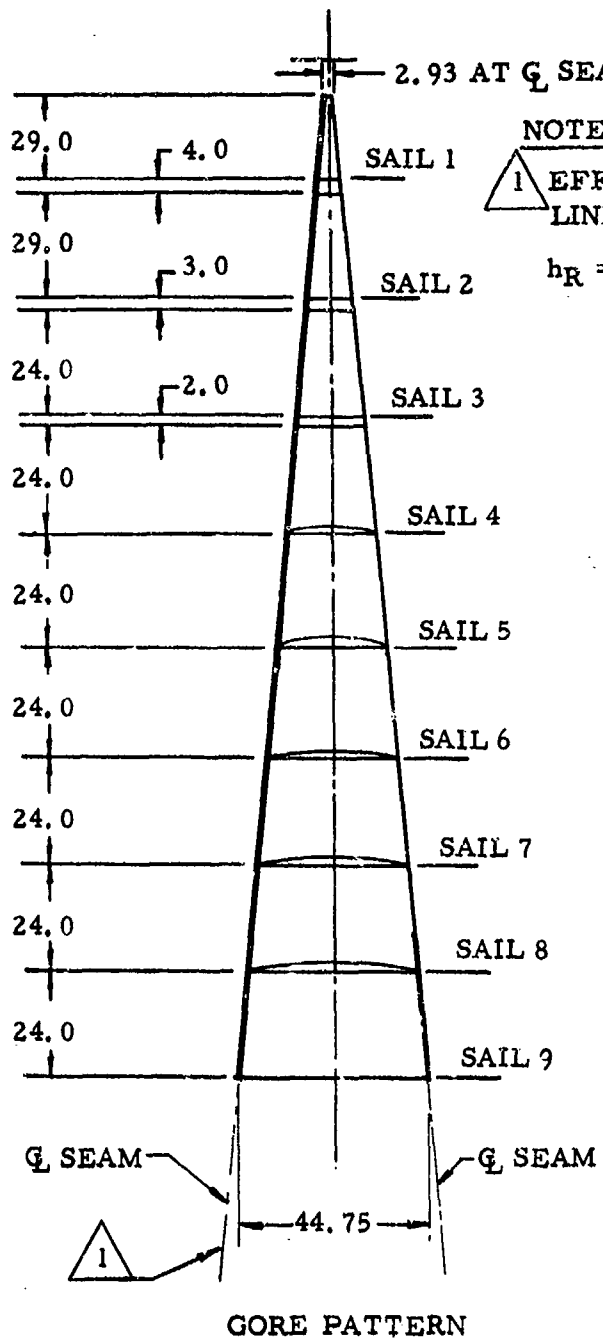


Figure 79. Gore Pattern and Fullness Distribution
R5044-501 41 ft D₀ Ringsail Parachute

PART NO.: R5044-501

TITLE: PARACHUTE, 41 ft D₀ RINGSAIL

NO. CORES: 32

TYPE OF REEFING: RADIAL

ITEM	MATERIAL		
VENT LINES	550 lb NYLON CORD		
VENT BAND	900 lb NYLON TAPE, 1.0 WIDE		
KING NUMBER	CLOTH WEIGHT OZ/YD ² (a)	TAPE P _r , LB	WIDTH, IN.
1	2.25	300 (b)	1.0
2	2.25	300 (c)	1.0
3	1.1	90 (d)	.62
4	1.1	90 (d)	.62
5	1.1	90 (d)	.62
6	1.1	None	None
7	1.1	None	None
8	1.1	None	None
9	1.1	None	None
VERTICAL TAPE	NONE		
SKIRT BAND	300 lb NYLON TAPE, 1.0 WIDE		
RADIALS (2 EACH)	300 lb NYLON TAPE, 1.0 WIDE		
SUSPENSION LINES	550 lb NYLON CORD		

(a) TRIPLE-SELVAGE CLOTH
(b) LEADING EDGE ONLY

(c) LEADING AND TRAILING EDGE
(d) TRAILING EDGE ONLY

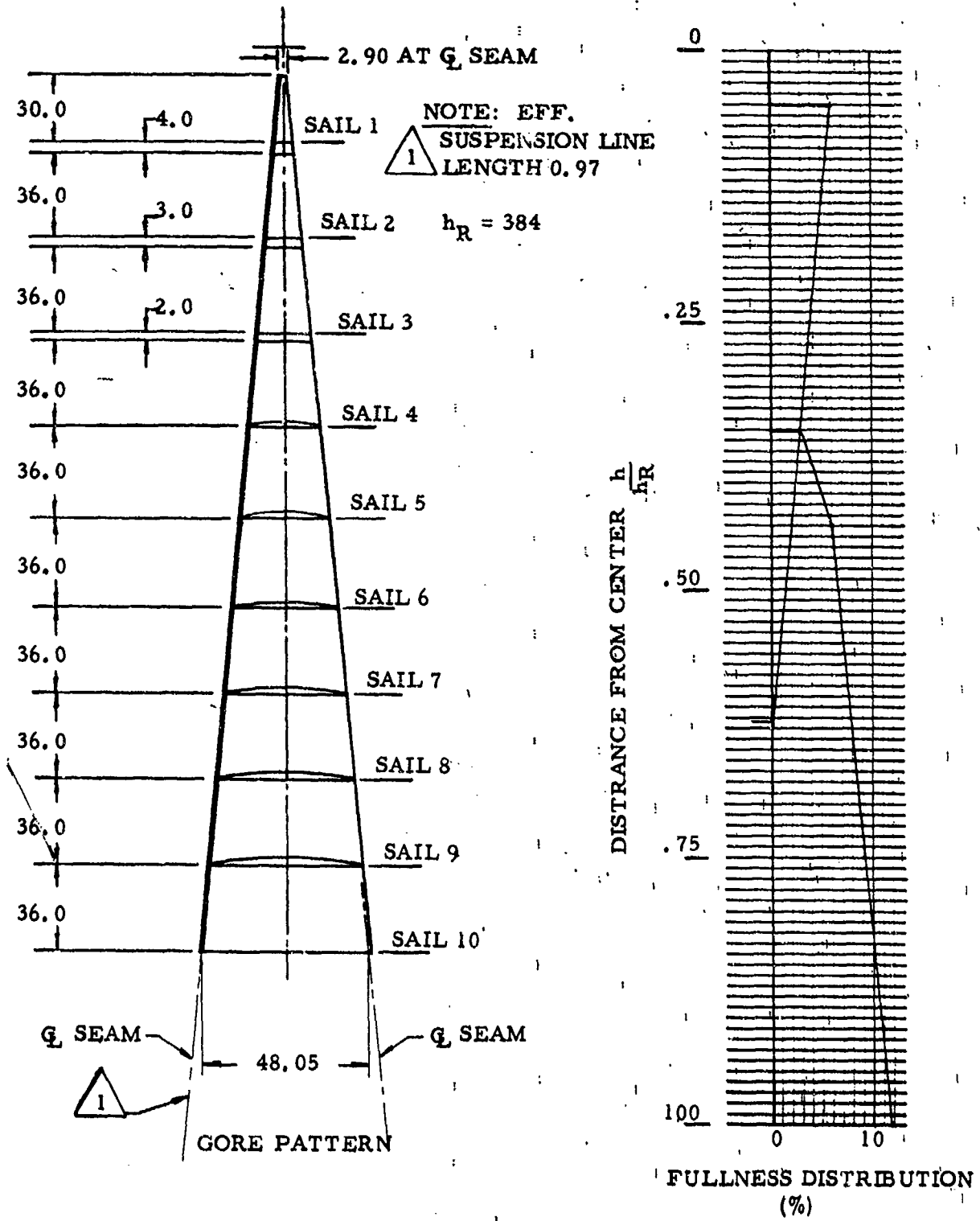


Figure 80. Gore Pattern and Fullness Distribution
R5157-321 63.1 ft D_o Ringsail Parachute

PART NO.: R5157-321

TITLE: PARACHUTE, 63.1 ft D₀ RINGSAIL

NO. GORES: 48

TYPE OF REEFING: RADIAL

ITEM	MATERIAL		
VENT LINES	550 lb NYLON CORD		
VENT BAND	900 lb NYLON TAPE, 1.0 WIDE		
RING NUMBER	CLOTH WEIGHT OZ/YD ² (a)	TAPE P _r , LB	WIDTH, IN.
1	2.25	90 (b)	.62
2	2.25	90 (c)	.62
3	2.25	90 (c)	.62
4	2.25	90 (d)	.62
5	1.1	70 (d)	.62
6	1.1	70 (d)	.62
7	1.1	70 (d)	.62
8	1.1	70 (d)	.62
9	1.1	None	None
10	1.1	None	None
VERTICAL TAPE			
SKIRT BAND	300 lb NYLON TAPE 1.0 WIDE 525 lb NYLON WEBBING, 1.0 WIDE		
RADIALS (2 EACH)	300 lb NYLON TAPE, 1.0 WIDE		
SUSPENSION LINES	550 lb NYLON CORD		

(a) TRIPLE-SELVAGE CLOTH
(b) LEADING EDGE ONLY

(c) LEADING AND TRAILING EDGE
(d) TRAILING EDGE ONLY

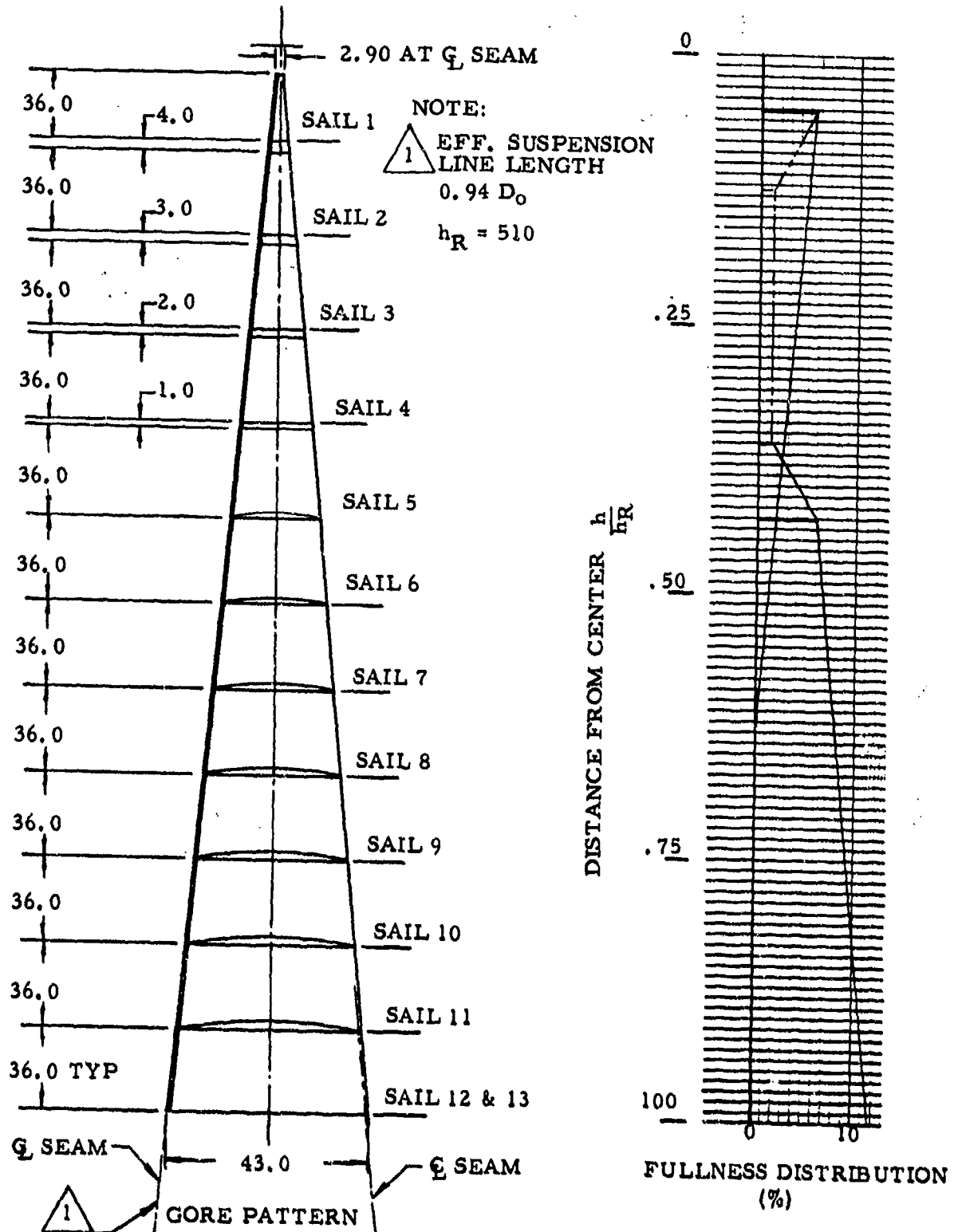


Figure 81. Gore Pattern and Fullness Distribution

R6220-525 84.2 ft D_o Ringsail Parachute

PART NO.: R6220-525

TITLE: PARACHUTE, 84.2 ft D₀ RINGSAIL

NO. GORES: 72

TYPE OF REEFING: RADIAL

ITEM	MATERIAL		
VENT LINES	550 lb NYLON CORD		
VENT BAND (2)	900 lb NYLON TAPE, 1.0 WIDE		
RING NUMBER	CLOTH WEIGHT OZ/YD ² (a)	TAPE	
1	2.25	P _r , LB	WIDTH, IN.
2	2.25	300 (b, e)	1.0
3	2.25	300 (c, e)	1.0
4	2.25	300 (c, e)	1.0
5	2.25	525 (d, e)	1.0
6	1.1	90 (d, e)	.62
7	1.1	70 (d, e)	.62
8	1.1	70 (d, e)	.62
9	1.1	70 (d, e)	.62
10	1.1	70 (d, e)	.62
11	1.1	70 (d, e)	.62
12 & 13	1.1	70 (d, e)	.62
VERTICAL TAPE	NONE		
SKIRT BAND	500 lb NYLON WEBB, 1.0 WIDE		
RADIALS (2 EACH)	300 lb NYLON TAPE, 1.0 WIDE		
SUSPENSION LINES	550 lb NYLON CORD		

- (a) TRIPLE-SELVAGE CLOTH
- (b) LEADING EDGE ONLY
- (c) LEADING AND TRAILING EDGE
- (d) TRAILING EDGE ONLY
- (e) CIRCUMFERENTIAL REINFORCEMENT

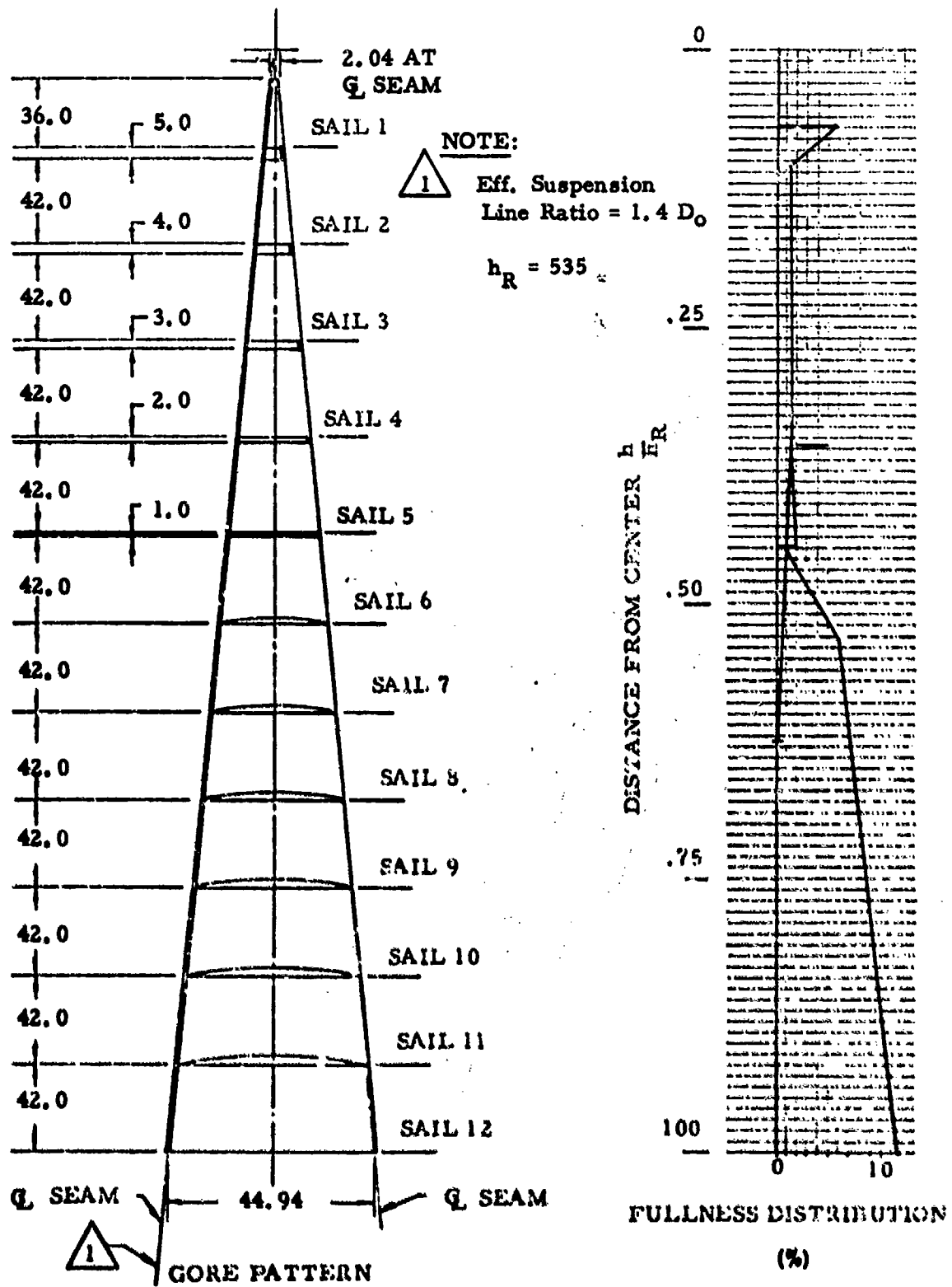


Figure 82. Gore Pattern and Fullness Distribution
PDS 808-1 88.1 ft D_0 Ringsail Parachute

PART NO.: PDS 808-1

TITLE: Parachute, 88.1 Ft D₀ Ringsail

NO. GORES: 72

TYPE OF REEFING: Radial

ITEM	MATERIAL		
VENT LINES	400 Lb Nylon Cord		
VENT BAND	900 Lb Nylon Tape, 1.0 Wide		
RING NUMBER	CLOTH WEIGHT OZ/YD ² (a)	TAPE P _r , LB	WIDTH, IN.
1	1.1	None	None
2	1.1	None	None
3	1.1	None	None
4	1.1	None	None
5	1.1	None	None
6	1.1	None	None
7	1.1	None	None
8	1.1	None	None
9	1.1	None	None
10	1.1	None	None
11	1.1	None	None
12	1.1	None	None
VERTICAL TAPE	None		
SKIRT BAND	500 Lb Nylon Webbing, .56 Wide		
RADIALS (2 EACH)	200 Lb Nylon Tape, 1.06 Wide		
SUSPENSION LINES	400 Lb Nylon Cord		

(a) TRIPLE-SELVAGE CLOTH
(b) LEADING EDGE ONLY

(c) LEADING AND TRAILING EDGE
(d) TRAILING EDGE ONLY

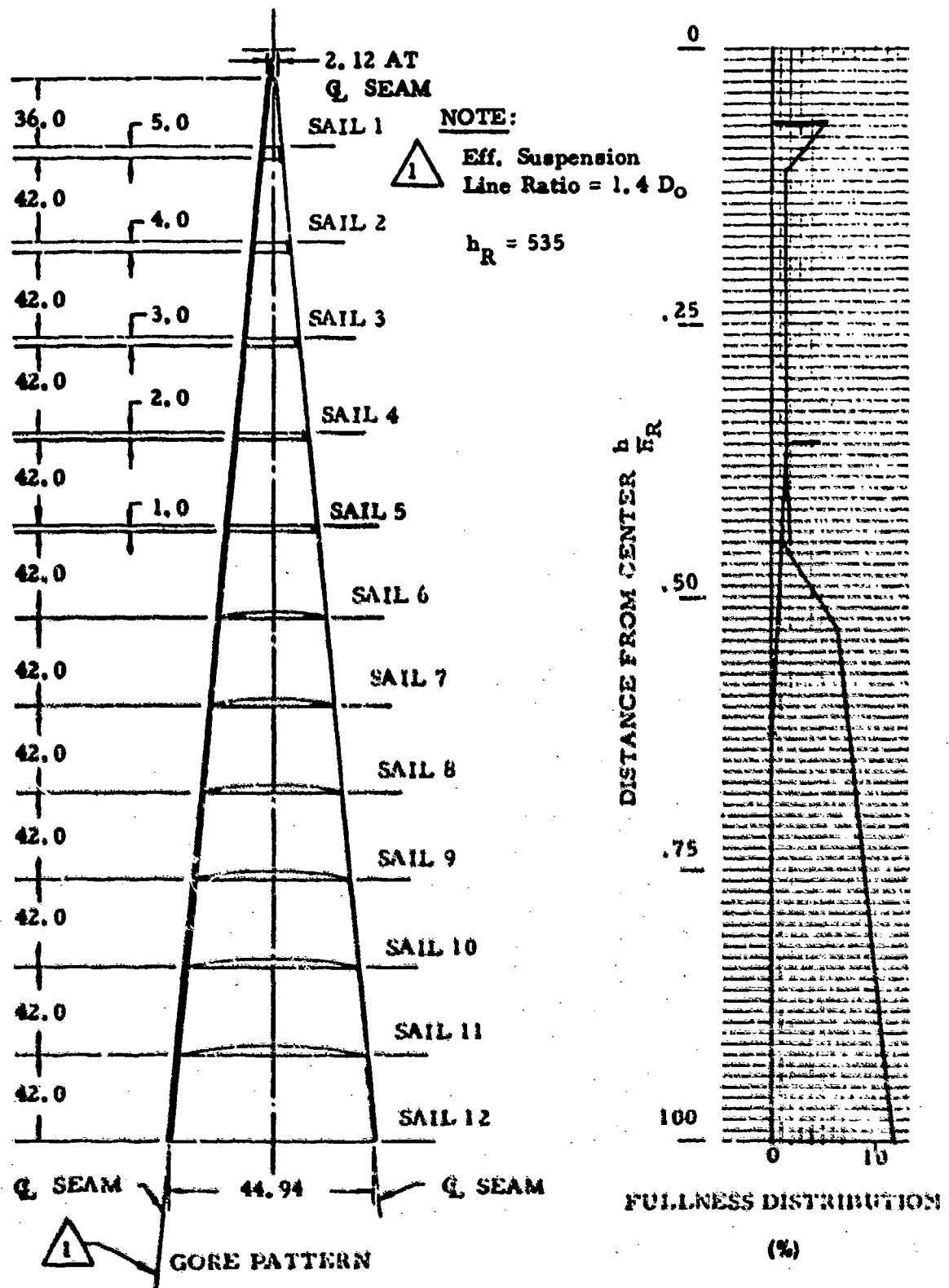


Figure 83. Gore Pattern and Fullness Distribution,
PDS 926-1 88.1 ft D_0 Ringsail Parachute

PART NO.: PDS 926-1

TITLE: Parachute, 88.1 Ft D₀ Ringsail

NO. GORES: 72

TYPE OF REEFING: Radial

ITEM	MATERIAL		
VENT LINES	400 Lb Nylon Cord		
VENT BAND (3 each)	900 Lb Nylon Tape, 1.0 Wide		
RING NUMBER	CLOTH WEIGHT OZ/YD ² (a)	TAPE	
1	2.25	P. _{r.} LB	WIDTH, IN.
2	2.25	200 (b)	1.06
3	2.25	200 (c)	1.06
4	1.1	200 (c)	1.06
5	1.1	90 (d)	.62
6	1.1	90 (d)	.62
7	1.1	None	None
8	1.1	None	None
9	1.1	None	None
10	1.1	None	None
11	1.1	None	None
12	1.1	None	None
VERTICAL TAPE	None		
SKIRT BAND	500 Lb Nylon Webbing, .56 Wide		
RADIALS (2 EACH)	200 Lb Nylon Tape, 1.06 Wide		
SUSPENSION LINES	400 Lb Nylon Cord		

(a) TRIPLE-SELVAGE CLOTH
(b) LEADING EDGE ONLY

(c) LEADING AND TRAILING EDGE
(d) TRAILING EDGE ONLY

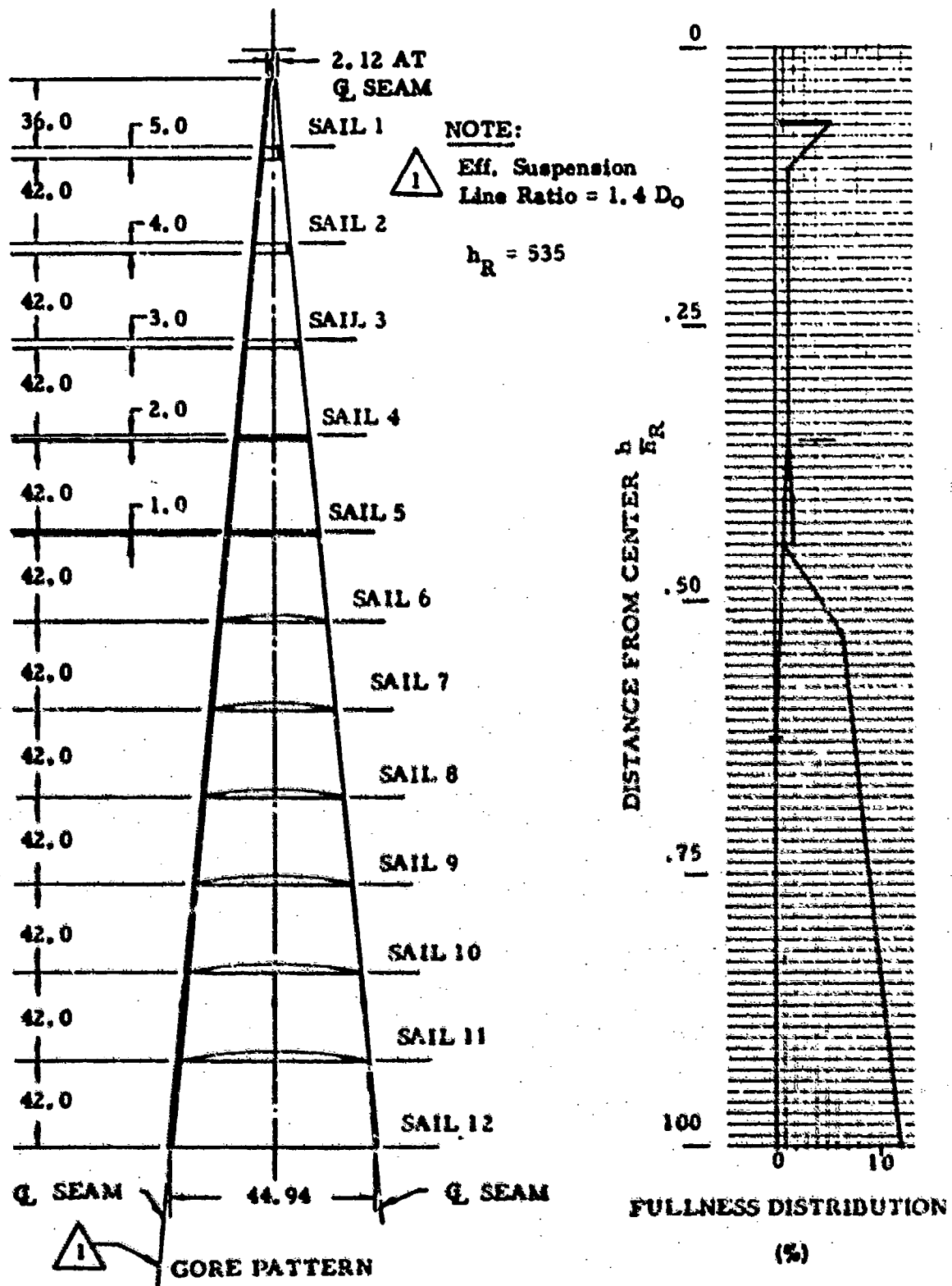


Figure 84. Gore Pattern and Fullness Distribution,
 PDS 927-1 88.1 ft D_0 Ringtail Parachute

PART NO.: PDS 927-1

TITLE: Parachute, 88.1 Ft D₀ Ringsail

NO. CORES: 72

TYPE OF REEFING: Radial

ITEM	MATERIAL		
VENT LINES	400 Lb Nylon Cord		
VENT BAND (3 each)	900 Lb Nylon Tape, 1.0 Wide		
RING NUMBER	CLOTH WEIGHT OZ/YD ² (a)	TAPE P. _F , LB	WIDTH, IN.
1	1.1	200 (b)	1.06
2	1.1	200 (c)	1.06
3	1.1	200 (c)	1.06
4	1.1	200 (c)	1.06
5	1.1	90 (d)	.62
6	1.1	90 (d)	.62
7	1.1	None	None
8	1.1	None	None
9	1.1	None	None
10	1.1	None	None
11	1.1	None	None
12	1.1	None	None
VERTICAL TAPE	None		
SKIRT BAND	500 Lb Nylon Webbing, .56 Wide		
RADIALS (2 EACH)	200 Lb Nylon Tape, 1.06 Wide		
SUSPENSION LINES	400 Lb Nylon Cord		

(a) TRIPLE SELVAGE CLOTH
(b) LEADING EDGE ONLY

(c) LEADING AND TRAILING EDGE
(d) TRAILING EDGE ONLY

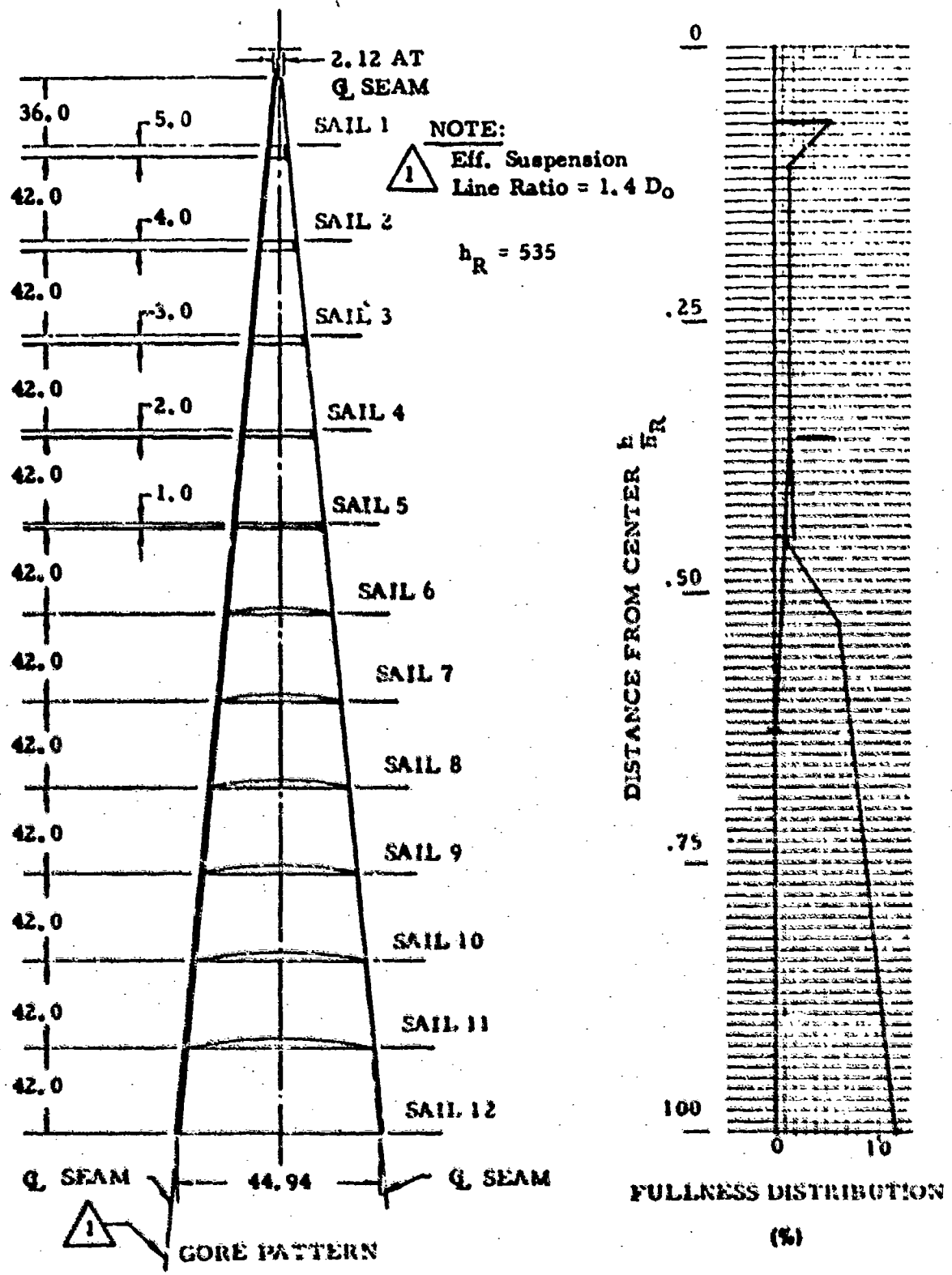


Figure 85. Gore Pattern and Fullness Distribution,
PDS 1226-1 thru -505 88.1 ft D_0 Ringsail Parachute

PART NO.: PD9 1226-1

TITLE: Parachute, 68.1 Ft D, Ringsail

NO. GORES: 72

TYPE OF REEFING: Radial

ITEM	MATERIAL		
VENT LINES	400 Lb Nylon Cord		
VENT BAND (3 each)	900 Lb Nylon Tape, 1.0 Wide		
RING NUMBER	CLOTH WEIGHT OZ/YD ² (a)	TAPE	WIDTH, IN.
1	2.25	90 (b, c)	.62
2	2.25	90 (c, e)	.62
3	2.25	90 (c, e)	.62
4	1.1	90 (c, e)	.62
5	1.1	90 (d, e)	.62
6	1.1	90 (d, e)	.62
7	1.1	None	None
8	1.1	None	None
9	1.1	None	None
10	1.1	None	None
11	1.1	None	None
12	1.1	None	None
VERTICAL TAPE	None		
SKIRT BAND	500 Lb Nylon Webbing, .56 Wide		
RADIALS (2 EACH)	200 Lb Nylon Tape, 1.06 Wide		
SUSPENSION LINES	400 Lb Nylon Cord		

(a) TRIPLE-SELVAGE CLOTH
(b) LEADING EDGE ONLY

(c) LEADING AND TRAILING EDGE
(d) TRAILING EDGE ONLY
(e) CIRCUMFERNENTIAL REINFORCEMENT

PART NO.: PDS 1226-501

TITLE: Parachute, 88.1 Ft D₀ Ringsail

NO. GORES: 72

TYPE OF REEFING: Radial

ITEM	MATERIAL		
VENT LINES	550 Lb Nylon Cord		
VENT BAND (3 each)	900 Lb Nylon Tape, 1.0 Wide		
RING NUMBER	CLOTH WEIGHT OZ/YD ² (a)	TAPE	
1	2.25	P _r , LB	WIDTH, IN.
2	2.25	90 (b, e)	.62
3	2.25	90 (c, e)	.62
4	1.1	90 (c, e)	.62
5	1.1	90 (d, e)	.62
6	1.1	90 (d, e)	.62
7	1.1	None	None
8	1.1	None	None
9	1.1	None	None
10	1.1	None	None
11	1.1	None	None
12	1.1	None	None
VERTICAL TAPE	None		
SKIRT BAND	500 Lb Nylon Webbing, .56 Wide		
RADIALS (2 EACH)	200 Lb Nylon Tape, 1.06 Wide		
SUSPENSION LINES	400 Lb Nylon Cord		

(a) TRIPLE-SELVAGE CLOTH
(b) LEADING EDGE ONLY

(c) LEADING AND TRAILING EDGE
(d) TRAILING EDGE ONLY
(e) CIRCUMFERENTIAL REINFORCEMENT

PART NO.: PDS 1226-503

TITLE: Parachute, 88.1 Ft D₀ Ringsail

NO. CORES: 72

TYPE OF REEFING: Radial

ITEM	MATERIAL		
VENT LINES	550 Lb Nylon Cord		
VENT BAND (3 each)	900 Lb Nylon Tape, 1.0 Wide		
RING NUMBER	CLOTH WEIGHT OZ/YD ² (a)	TAPE P _r , LB	WIDTH, IN.
1	2.25	90 (b, c)	.62
2	2.25	90 (c, e)	.62
3	2.25	90 (c, e)	.62
4	1.1	90 (c, e)	.62
5	1.1	90 (d, c)	.62
6	1.1	90 (d, e)	.62
7	1.1	None	None
8	1.1	None	None
9	1.1	None	None
10	1.1	None	None
11	1.1	None	None
12	1.1	None	None
VERTICAL TAPE	None		
SKIRT BAND	500 Lb Nylon Webbing, .56 Wide		
RADIALS (2 EACH)	200 Lb Nylon Tape, 1.06 Wide		
SUSPENSION LINES	400 Lb Nylon Cord		

(a) TRIPLE-SELVAGE CLOTH
(b) LEADING EDGE ONLY

(c) LEADING AND TRAILING EDGE
(d) TRAILING EDGE ONLY
(e) CIRCUMFERENTIAL REINFORCEMENT

PART NO.: PDS 1226-505

TITLE: Parachute, 88.1 Ft D₀ Ringsail

NO. GORES: 72

TYPE OF REEFING: Radial

ITEM	MATERIAL		
VENT LINES	550 Lb Nylon Cord		
VENT BAND (3 each)	900 Lb Nylon Tape, 1.0 Wide		
RING NUMBER	CLOTH WEIGHT OZ/YD ² (a)	TAPE P. _r , LB	WIDTH, IN.
1	2.25	90 (b, e)	.62
2	2.25	90 (c, e)	.62
3	2.25	90 (c, e)	.62
4	1.1	90 (c, e)	.62
5	1.1	90 (d, e)	.62
6	1.1	90 (d, e)	.62
7	1.1	None	None
8	1.1	None	None
9	1.1	None	None
10	1.1	None	None
11	1.1	None	None
12	1.1	None	None
VERTICAL TAPE	None		
SKIRT BAND	500 Lb Nylon Webbing, .56 Wide		
RADIALS (2 EACH)	200 Lb Nylon Tape, 1.06 Wide		
SUSPENSION LINES	400 Lb Nylon Cord		

(a) TRIPLE-SEWAGE CLOTH
(b) LEADING EDGE ONLY

(c) LEADING AND TRAILING EDGE

(d) TRAILING EDGE ONLY

(e) CIRCUMFERENTIAL REINFORCEMENT

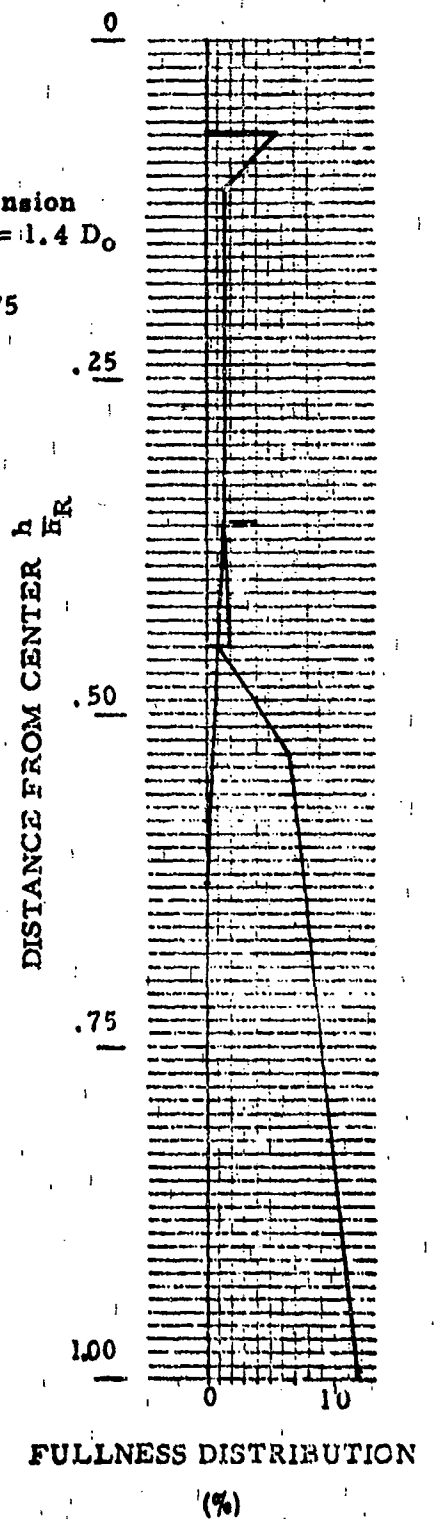
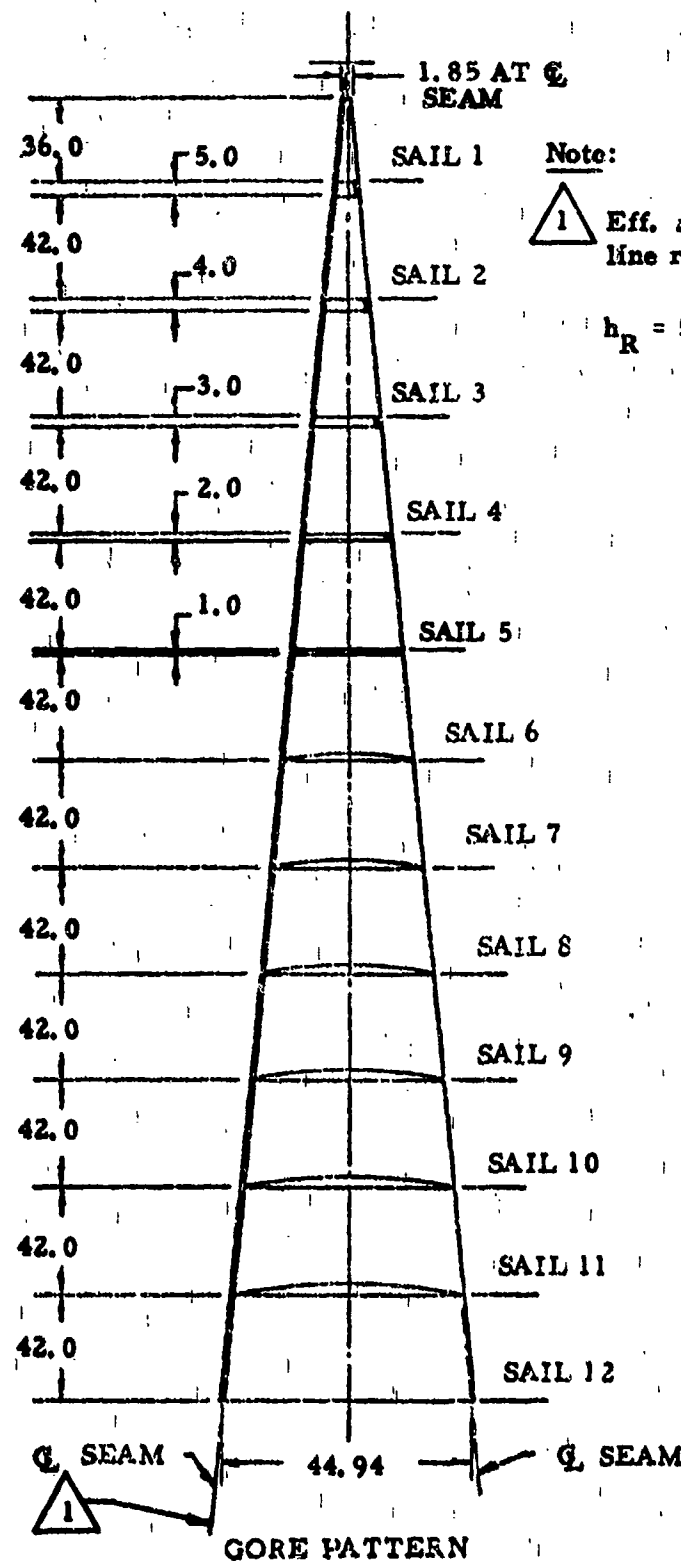


Figure 86. Gore Pattern and Fullness Distribution,
PDS 1543-1, 535 and -553 88.1 and 85.6 ft D_0 Ringsail Parachute

PART NO.: PDS 1543-1

TITLE: Parachute Assy., 88.1 Ft D_o Ringsail

NO. GORES: 72

TYPE OF REEFING: Radial

ITEM	MATERIAL		
VENT LINES	550 Lb. Nylon Cord		
VENT BAND	4000 Lb. Nylon Webbing, 1.0 Wide		
RING NUMBER	CLOTH WEIGHT OZ/YD ² (a)	TAPE	
1	2.25	200(b)	1.06
2	2.25	200(c)	1.06
3	2.25	200(c)	1.06
4	1.1	200(c)	1.06
5	1.1	200(d)	1.06
6	1.1	90(d)	.62
7	1.1	90(d)	.62
8	1.1	90(d)	.62
9	1.1	None	None
10	1.1	None	None
11	1.1	None	None
12	1.1	None	None
VERTICAL TAPE	90 Lb. Nylon Tape, .62 Wide (c)		
SKIRT BAND	300 Lb. Nylon Tape, 1.0 Wide 500 Lb. Nylon Webbing, .56 Wide		
RADIALS (2 EACH)	300 Lb. Nylon Tape, 1.0 Wide		
SUSPENSION LINES	550 Lb. Nylon Cord		

(a) TRIPLE-SELVAGE CLOTH
(b) LEADING EDGE ONLY

(c) LEADING AND TRAILING EDGE
(d) TRAILING EDGE ONLY
(e) NO. 1 THRU NO. 5 SAIL, DOUBLED,
CENTER OF GORE

PART NO.: PDS 1543- 535

TITLE: Parachute Assy., 88.1 Ft D₀ Ringsail

NO. GORES: 72

TYPE OF REEFING: Radial

ITEM	MATERIAL		
VENT LINES	550 Lb. Nylon Cord		
VENT BAND	4000 Lb. Nylon Webbing, 1.0 Wide		
RING NUMBER	CLOTH WEIGHT OZ/YD ² (a)	TAPE	
1	2.25	200(b)	.1.06
2	2.25	200(c)	1.06
3	2.25	200(c)	1.06
4	1.1	200(c)	1.06
5	1.1	200(d)	1.06
6	1.1	90(d)	.62
7	1.1	90(d)	.62
8	1.1	90(d)	.62
9	1.1	None	None
10	1.1	None	None
11	1.1	None	None
12	1.1	None	None
VERTICAL TAPE	90 Lb. Nylon Tape, .62 Wide (e)		
SKIRT BAND	300 Lb. Nylon Tape, 1.0 Wide 500 Lb. Nylon Webbing, .56 Wide		
RADIALS (2 EACH)	300 Lb. Nylon Tape, 1.0 Wide		
SUSPENSION LINES	550 Lb. Nylon Cord		

(a) TRIPLE-SELVAGE CLOTH
(b) LEADING EDGE ONLY

(c) LEADING AND TRAILING EDGE
(d) TRAILING EDGE ONLY
(e) NO. 1 THRU NO. 12 SAIL, DOUBLED,
CENTER OF GORE

PART NO.: PDS 1543 - 553

TITLE: Parachute Assy., 85.6 Ft D₀ Ringsail

NO. GORES: 68

TYPE OF REEFING: Radial

ITEM	MATERIAL		
VENT LINES	550 Lb. Nylon Cord		
VENT BAND	4000 Lb. Nylon Webbing, 1.0 Wide		
RING NUMBER	CLOTH WEIGHT OZ/YD ² (a)	TAPE	
1	2.25	P _r , LB	WIDTH, IN.
2	2.25	200(b)	1.06
3	2.25	200(c)	1.06
4	1.1	200(c)	1.06
5	1.1	200(d) 300/300(f)	1.06 1.00/1.00
6	1.1	90(d)	.62
7	1.1	90(d)	.62
8	1.1	90(d)	.62
9	1.1	None	None
10	1.1	None	None
11	1.1	None	None
12	1.1	None	None
VERTICAL TAPE	90 Lb. Nylon Tape, .62 Wide (e)		
SKIRT BAND	300 Lb. Nylon Tape, 1.0 Wide 500 Lb. Nylon Webbing, .56 Wide		
RADIALS (2 EACH)	300 Lb. Nylon Tape, 1.0 Wide		
SUSPENSION LINES	550 Lb. Nylon Cord		

(a) TRIPLE-SELVAGE CLOTH (c) LEADING AND TRAILING EDGE

(b) LEADING EDGE ONLY (d) TRAILING EDGE ONLY

(f) CIRCUMFERENTIAL REINFORCEMENT, (e) NO. 1 THRU NO. 12 SAIL, DOUBLED,
SAILS 9.5 & 20.0 FROM BOTTOM OF CENTER OF GORE

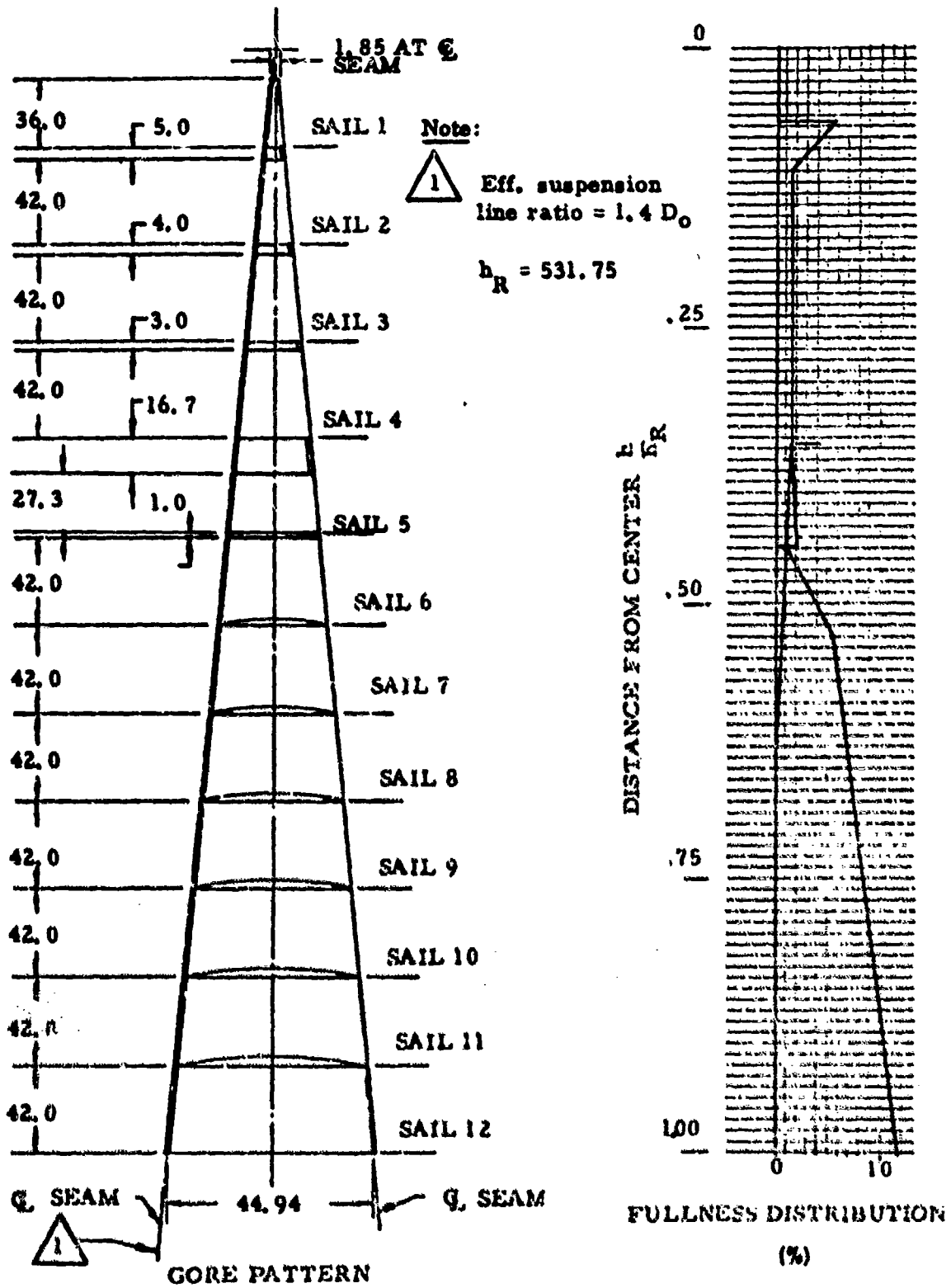


Figure 87. Gore Pattern and Fullness Distribution,
PDS 1543-521 and -523 88.1 ft D_0 Ringsail Parachute

PART NO.: PDS 1543-521

TITLE: Parachute Assy., 88.1 Ft D₀ Ringsail

NO. CORES: 72

TYPE OF REEFING: Radial

ITEM	MATERIAL		
VENT LINES	550 Lb. Nylon Cord		
VENT BAND	4000 Lb. Nylon Webbing, 1.0 Wide		
RING NUMBER	CLOTH WEIGHT OZ/YD ² (a)	TAPE	
1	2.25	P _r , LB	WIDTH, IN.
2	2.25	200(b)	1.06
3	2.25	200(c)	1.06
4	1.1	200(c)	1.06
5 (35% Removed Top)	1.1	300(d, f) 300(f, g)	1.00 1.00
6	1.1	90(d)	.62
7	1.1	90(d)	.62
8	1.1	90(d)	.62
9	1.1	None	None
10	1.1	None	None
11	1.1	None	None
12	1.1	None	None
VERTICAL TAPE	90 Lb. Nylon Tape, .62 Wide (e)		
SKIRT BAND	300 Lb. Nylon Tape, 1.0 Wide 500 Lb. Nylon Webbing, .56 Wide		
RADIALS (2 EACH)	300 Lb. Nylon Tape, 1.0 Wide		
SUSPENSION LINES	550 Lb. Nylon Cord		

- (a) TRIPLE-SELVAGE CLOTH (g) 6.3 INCHES DOWN FROM TOP OF RING 5
 (b) LEADING EDGES ONLY (c) LEADING AND TRAILING EDGE
 (f) CIRCUMFERENTIAL REINFORCE (d) TRAILING EDGE ONLY
 (e) NO. 1 THRU NO. 12 SAIL, DOUBLED,
 mean CENTER OF GORE

PART NO.: PDS 1543- 523

TITLE: Parachute Assy., 88.1 Ft D₀ Ringsail

NO. GORES: 72

TYPE OF REEFING: Radial

ITEM	MATERIAL		
VENT LINES	550 Lb. Nylon Cord		
VENT BAND	4000 Lb. Nylon Webbing, 1.0 Wide		
RING NUMBER	CLOTH WEIGHT OZ/YD ² (a)	TAPE	
		P. _r , LB	WIDTH, IN.
1	2.25	200(b)	1.06
2	2.25	200(c)	1.06
3	2.25	200(c)	1.06
4	1.1	200(c)	1.06
5 (35% Removed, Top)	1.1	300(d, f) 200(f, g)	1.00
6	1.1	90(d)	.62
7	1.1	90(d)	.62
8	1.1	90(d)	.62
9	1.1	None	None
10	1.1	None	None
11	1.1	None	None
12	1.1	None	None
VERTICAL TAPE	90 Lb. Nylon Tape, .62 Wide (e)		
SKIRT BAND	300 Lb. Nylon Tape, 1.0 Wide		
SUSPENSION LINES	550 Lb. Nylon Cord		

- (a) TRIPLE-SELVAGE CLOTH (g) 6.3 INCHES DOWN FROM TOP OF RING 5
 (b) LEADING EDGE ONLY (c) LEADING AND TRAILING EDGE
 (d) CIRCUMFERENTIAL REINFORCEMENT (d) TRAILING EDGE ON 1/7
 (e) NO. 1 THRU NO. 5 SAIL, DOUBLED,
 CENTER OF GORE

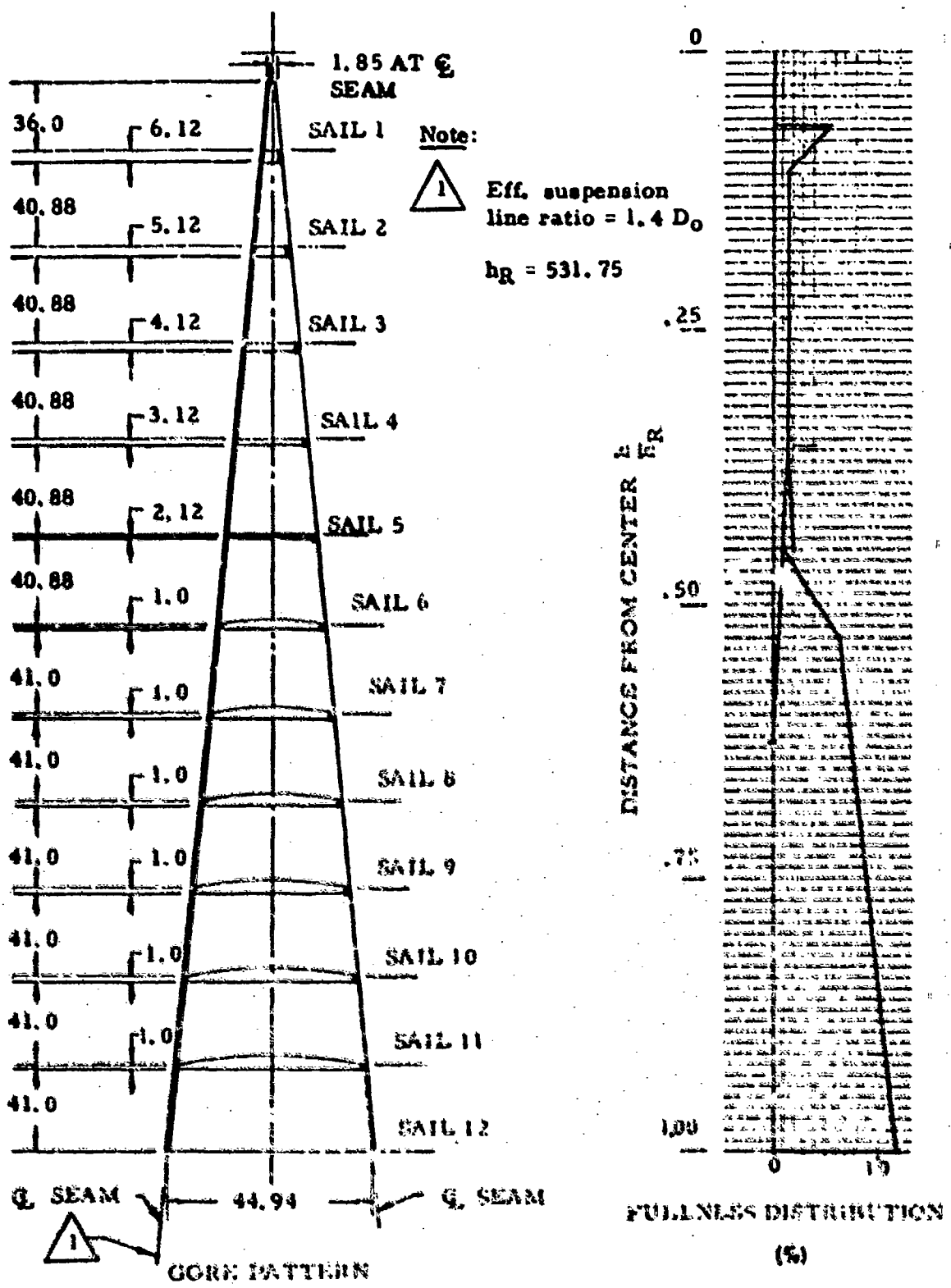


Figure 88. Gore Pattern and Fullness Distribution,
PDS 1543-529 88.1 ft D_0 Ringseal Parachute

PART NO.: PDS 1543- 529

TITLE: Parachute Assy., 88.1 Ft D_o Ringsail

NO. GORES: 72

TYPE OF REEFING: Radial

ITEM	MATERIAL		
VENT LINES	550 LB. Nylon Cord		
VENT BAND	4000 LB. Nylon Webbing, 1.0 Wide		
RING NUMBER	CLOTH WEIGHT OZ/YD ² (a)	TAPE	
1	2.25	P _r , LB	WIDTH, IN.
2	2.25	200(b)	1.06
3	2.25	200(b) 300(d, f)	1.06 1.00
4	2.25	200(b) 300(d, f)	1.06 1.00
5	1.1	200(b) 300(d, f)	1.06 1.00
6	1.1	100(d, f)	.62
7	1.1	90(d, f)	.62
8	1.1	90(d, f)	.62
9	1.1	90(d, f)	.62
10	1.1	90(d, f)	.62
11	1.1	90(d, f)	.62
12	1.1	90(d, f)	.62
VERTICAL TAPE	90 LB. Nylon Tape, .62 Wide (a)		
SKIRT BAND	300 LB. Nylon Tape, 1.0 Wide 500 LB. Nylon Webbing, .55 Wide		
RADIALS (2 EACH)	300 LB. Nylon Tape, 1.0 Wide		
SUSPENSION LINES	550 LB. Nylon Cord		

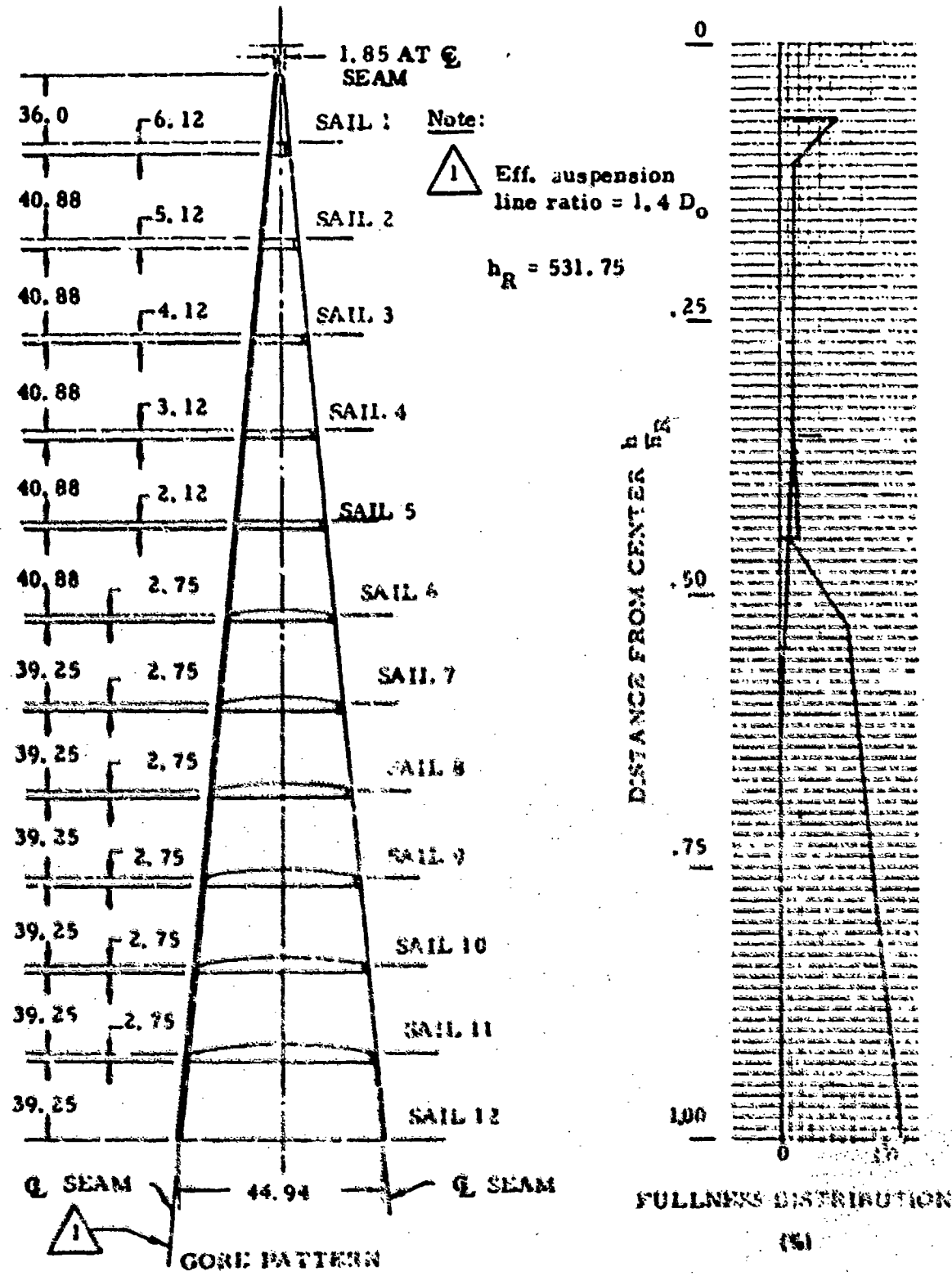


Figure 89. Gore Pattern and Fullness Distribution,
PDS 1543-531 and -543 88.1 ft D_0 Ringsail Parachute

PART NO.: PDS 1543-531

TITLE: Parachute Assy., 88.1 Ft D_o Ringsail

NO. GORES: 72

TYPE OF REEFING: Radial

ITEM	MATERIAL		
VENT LINES	550 Lb. Nylon Cord		
VENT BAND	4000 Lb. Nylon Webbing, 1.0 Wide		
RING NUMBER	CLOTH WEIGHT OZ/YD ² (a)	TAPE	
1	2.25	P _r , LB	WIDTH, IN.
2	2.25	200(b)	1.06
3	2.25	200(b) 300(d, f)	1.00
4	1.1	200(b) 300(d, f)	1.06
5	1.1	300(d, f)	1.00
6	1.1	300(d, f)	1.00
7	1.1	90(d, f)	.62
8	1.1	90(d, f)	.62
9	1.1	90(d, f)	.62
10	1.1	90(d, f)	.62
11	1.1	90(d, f)	.62
12	1.1	90(d, f)	.62
VERTICAL TAPE	90 Lb. Nylon Tape, .62 Wide (a)		
SKIRT BAND	300 Lb. Nylon Tape, 1.0 Wide 300 Lb. Nylon Webbing, .56 Wide		
RADIALS (2 EACH)	300 Lb. Nylon Tape, 1.0 Wide		
SUSPENSION LINES	550 Lb. Nylon Cord		

(ii) TRIPLE-SELVAGE CLOTH

(N) LEAPING EDGES ONLY

in CIRCUIT

MENT

(c) LEADING AND TRAILING EDGE

(b) TRAILING EDGE ONLY

(e) NO. 1 THRU N

(e) NO. 1 THRU NO. 5 SALE, EXCLUDED,
CENTER OF GENE

PART NO.: PDS 1543-543

TITLE: Parachute Assy., 88.1 Ft D_o Ringsail

NO. GORES: 72

TYPE OF REEFING: Radial

ITEM	MATERIAL		
VENT LINES	550 Lb. Nylon Cord		
VENT BAND	4000 Lb. Nylon Webbing, 1.0 Wide		
RING NUMBER	CLOTH WEIGHT OZ/YD ² (a)	TAPE	
		P _r , LB	WIDTH, IN.
1	2.25	200(b)	1.06
2	2.25	200(b) 300(d,f)	1.06 1.00
3	2.25	200(b) 300(d,f)	1.06 1.00
4	1.1	200(b) 300(d,f)	1.06 1.00
5	1.1	300(d,f)	1.00
6	1.1	90(d,f)	.62
7	1.1	90(d,f)	.62
8	1.1	90(d,f)	.62
9	1.1	90(d,f)	.62
10	1.1	90(d,f)	.62
11	1.1	90(d,f)	.62
12	1.1	90(d,f)	.62
VERTICAL TAPE	90 Lb. Nylon Tape, .62 Wide (e)		
SKIRT BAND	300 Lb. Nylon Tape, 1.0 Wide 500 Lb. Nylon Webbing, .56 Wide		
RADIALS (2 EACH)	300 Lb. Nylon Tape, 1.0 Wide		
SUSPENSION LINES	550 Lb. Nylon Cord		

- (a) TRIPLE-SELVAGE CLOTH
- (b) LEADING EDGE ONLY
- (f) CIRCUMFERENTIAL REINFORCEMENT
- (c) LEADING AND TRAILING EDGE
- (d) TRAILING EDGE ONLY
- (e) NO. 1 THRU NO. 12 SAIL, DOUBLED, CENTER OF GORE

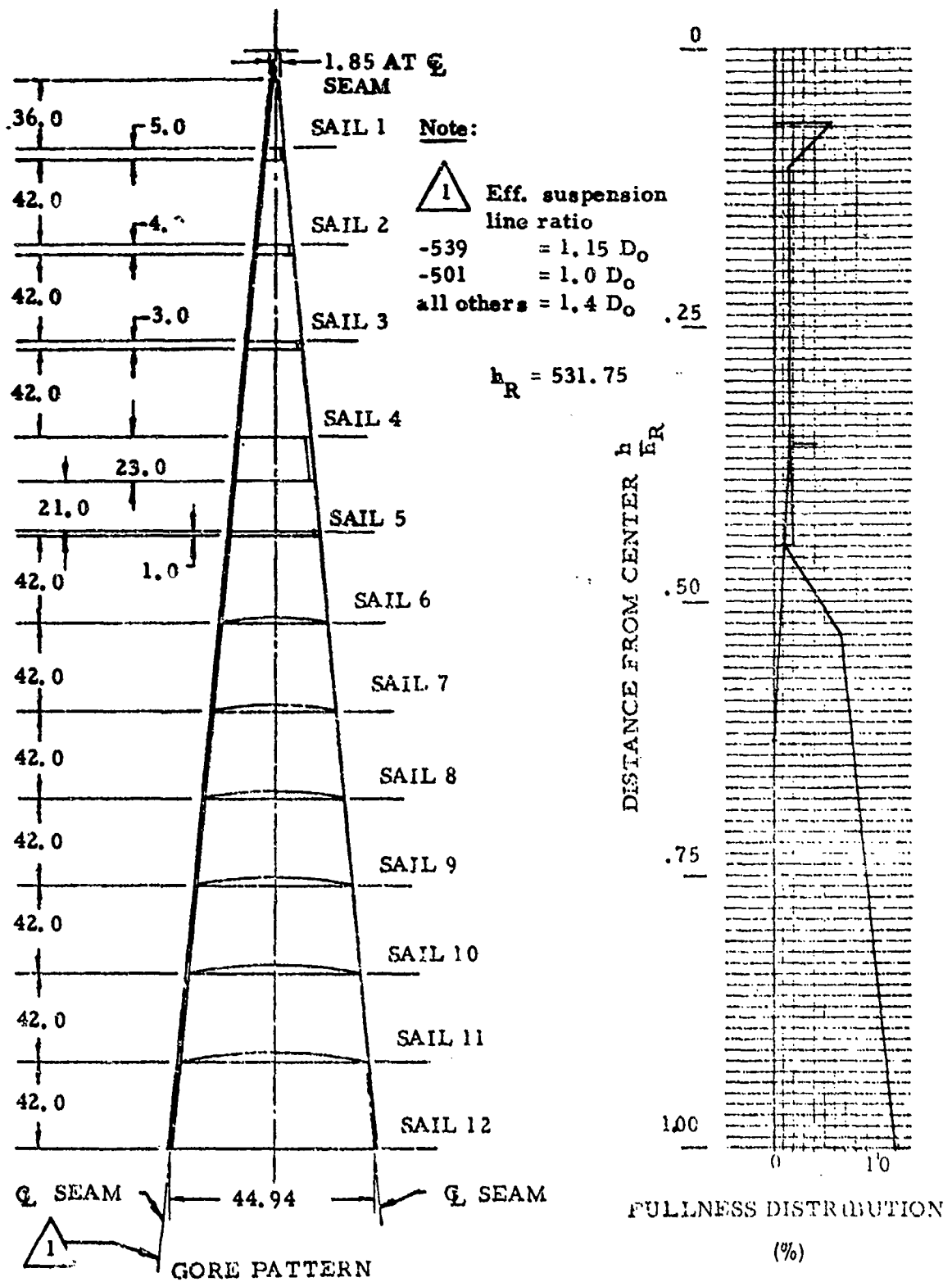


Figure 90. Gore Pattern and Fullness Distribution,
PDS 1543-525, -533, -539 and -551 88.1 and 85.6 ft D₀ Ringsail Parachute

PART NO.: PDS 1543- 525

TITLE: Parachute Assy., 88.1 Ft D_o Ringsail

NO. GORES: 72

TYPE OF REEFING: Radial

ITEM	MATERIAL		
VENT LINES	550 Lb. Nylon Cord		
VENT BAND	4000 Lb. Nylon Webbing, 1.0 Wide		
RING NUMBER	CLOTH WEIGHT OZ/YD ² (a)	TAPE	
1	2.25	200(b)	1.06
2	2.25	200(c)	1.06
3	2.25	200(c)	1.06
4	1.1	200(c)	1.06
5(50% Removed, Top)	1.1	300(d,f)	1.00
6	1.1	90(d)	.62
7	1.1	90(d)	.62
8	1.1	90(d)	.62
9	1.1	None	None
10	1.1	None	None
11	1.1	None	None
12	1.1	None	None
VERTICAL TAPE	90 Lb. Nylon Tape, .62 Wide (e)		
SKIRT BAND	300 Lb. Nylon Tape, 1.0 Wide 500 Lb. Nylon Webbing, .56 Wide		
RADIALS (2 EACH)	300 Lb. Nylon Tape, 1.0 Wide		
SUSPENSION LINES	550 Lb. Nylon Cord		

(a) TRIPLE-SELVAGE CLOTH

(c) LEADING AND TRAILING EDGE

(b) LEADING EDGE ONLY

(d) TRAILING EDGE ONLY

(f) CIRCUMFERENTIAL REINFORCE-
MENT

(e) NO. 1 THRU NO. 5 SAIL, DOUBLED,
CENTER OF GORE

PART NO.: PDS 1543-533

TITLE: Parachute Assy., 88.1 Ft D₀ Ringsail

NO. GORES: 72

TYPE OF REEFING: Radial

ITEM	MATERIAL		
VENT LINES	550 Lb. Nylon Cord		
VENT BAND	4000 Lb. Nylon Webbing, 1.0 Wide		
RING NUMBER	CLOTH WEIGHT OZ/YD ² (a)	TAPE	
		P _r , LB	WIDTH, IN.
1	2.25	200(b)	1.06
2	2.25	200(c)	1.06
3	2.25	200(c)	1.06
4	1.1	200(c)	1.06
5(50% Removed, Top)	1.1	300(d, f)	1.00
6	1.1	90(d)	.62
7	1.1	90(d)	.62
8	1.1	90(d)	.62
9	1.1	None	None
10	1.1	None	None
11	1.1	None	None
12	1.1	None	None
VERTICAL TAPE	90 Lb. Nylon Tape, .62 Wide (c)		
SKIRT BAND	300 Lb. Nylon Tape, 1.0 Wide 500 Lb. Nylon Webbing, .56 Wide		
RADIALS (2 EACH)	300 Lb. Nylon Tape, 1.0 Wide		
SUSPENSION LINES	550 Lb. Nylon Cord		

- (a) TRIPLE-SELVAGE CLOTH
- (b) LEADING EDGE ONLY
- (c) LEADING AND TRAILING EDGE
- (d) TRAILING EDGE ONLY
- (e) NO. 1 THRU NO. 5 SAIL, DOUBLED,
MENT
- (f) CIRCUMFERENTIAL REINFORCE-
MENT
- (g) NO. 1 THRU NO. 5 SAIL, DOUBLED,
CENTER OF GORE

PART NO.: PDS 1543 - 539

TITLE: Parachute Assy., 85.6 Ft D₀ Ringsail

NO. GORES: 68

TYPE OF REEFING: Radial

ITEM	MATERIAL		
VENT LINES	550 Lb. Nylon Cord		
VENT BAND	4000 Lb. Nylon Webbing, 1.0 Wide		
RING NUMBER	CLOTH WEIGHT OZ/YD ² (a)	TAPE	
		P _r , LB	WIDTH, IN.
1	2.25	200(b)	1.06
2	2.25	200(c)	1.06
3	2.25	200(c)	1.06
4	1.1	200(c)	1.06
5 (50% Removed Top)	1.1	300(d,f)	1.00
6	1.1	90(d)	.62
7	1.1	90(d)	.62
8	1.1	90(d)	.62
9	1.1	None	None
10	1.1	None	None
11	1.1	None	None
12	1.1	None	None
VERTICAL TAPE	90 Lb. Nylon Tape, .62 Wide (e) 300 Lb. Nylon Tape, 1.0 Wide		
SKIRT BAND	500 Lb. Nylon Webbing, .56 Wide		
RADIALS (2 EACH)	300 Lb. Nylon Tape, 1.0 Wide		
SUSPENSION LINES	550 Lb. Nylon Cord		

- (a) TRIPLE-SELVAGE CLOTH
- (b) LEADING EDGE ONLY
- (c) LEADING AND TRAILING EDGE
- (d) TRAILING EDGE ONLY
- (f) CIRCUMFERENTIAL REINFORCEMENT (e) NO. 1 THRU NO. 5 SAIL,
DOUBLED, CENTER OF GORE

PART NO.: PDS 1543- 551

TITLE: Parachute Assy., 88.1 Ft D₀ Ringsail

NO. GORES: 72

TYPE OF REEFING: Radial

ITEM	MATERIAL		
VENT LINES	550 Lb. Nylon Cord		
VENT BAND	4000 Lb. Nylon Webbing, 1.0 Wide		
RING NUMBER	CLOTH WEIGHT OZ/YD ² (a)	TAPE	WIDTH, IN.
1	2.25	200(b)	1.06
2	2.25	200(c)	1.06
3	2.25	200(c)	1.06
4	1.1	200(c)	1.06
5(50% Removed, Top)	1.1	300(d,f)	1.00
6	1.1	90(d)	.62
7	1.1	90(d)	.62
8	1.1	90(d)	.62
9	1.1	None	None
10	1.1	None	None
11	1.1	None	None
12	1.1	None	None
VERTICAL TAPE	90 Lb. Nylon Tape, .62 Wide (e)		
SKIRT BAND	300 Lb. Nylon Tape, 1.0 Wide 500 Lb. Nylon Webbing, .56 Wide		
RADIALS (2 EACH)	300 Lb. Nylon Tape, 1.0 Wide		
SUSPENSION LINES	550 Lb. Nylon Cord		

(a) TRIPLE-SELVAGE CLOTH

(c) LEADING AND TRAILING EDGE

(b) LEADING EDGE ONLY

(d) TRAILING EDGE ONLY

(f) CIRCUMFERENTIAL REINFORCE-
MENT

(e) NO. 1 THRU NO. 5 SAIL, DOUBLED,
CENTER OF GORE

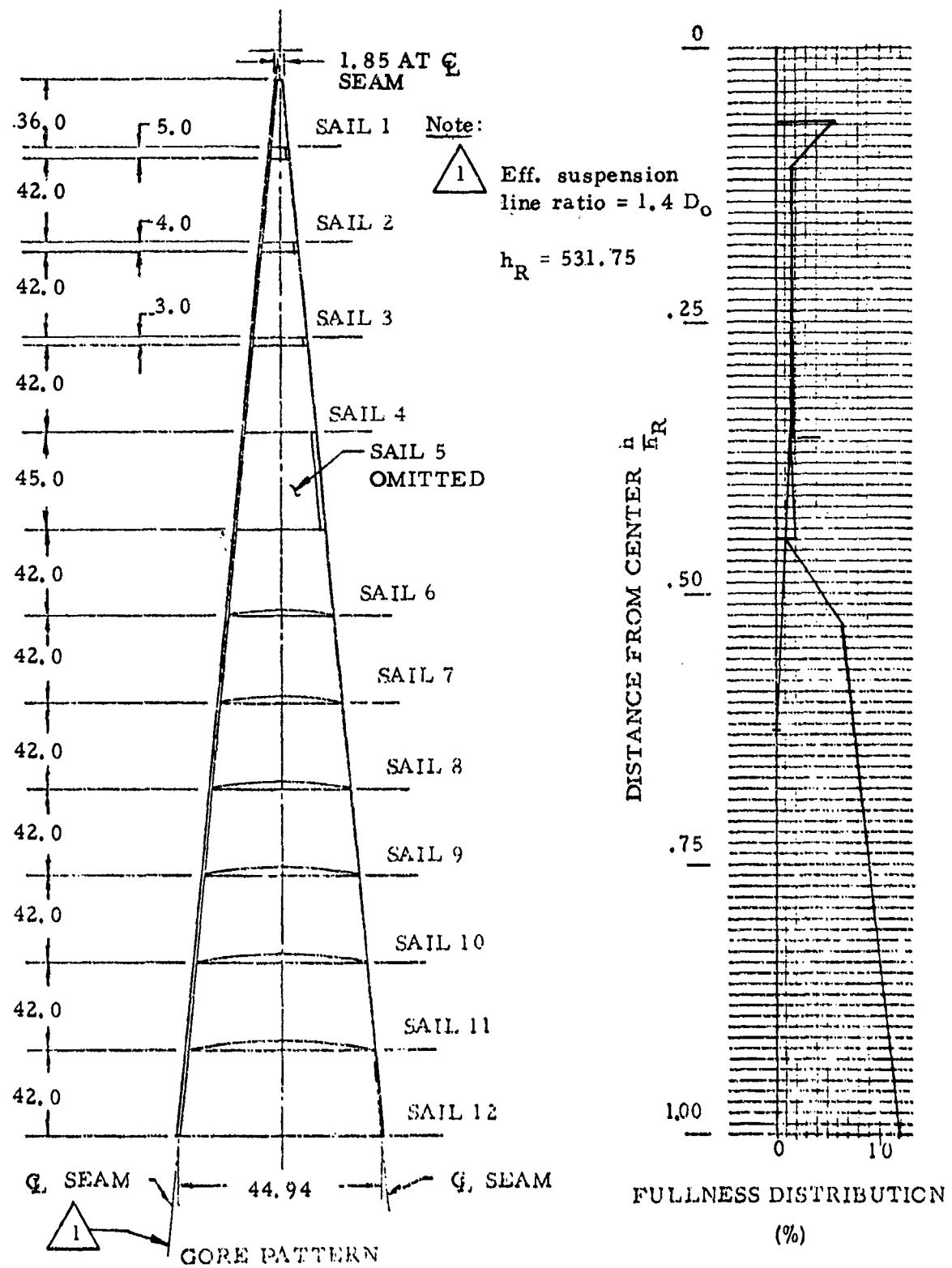


Figure 91. Gore Pattern and Fullness Distribution,
PDS 1543-547 88.1 ft D_0 Ringsail Parachute

PART NO.: PDS 1543- 547

TITLE: Parachute Assy., 38.1 Ft D₀ Ringsail

NO. GORES: 72

TYPE OF REEFING: Radial

ITEM	MATERIAL		
VENT LINES	550 Lb. Nylon Cord		
VENT BAND	4000 Lb. Nylon Webbing, 1.0 Wide		
RING NUMBER	CLOTH WEIGHT OZ/YD ² (a)	TAPE	
1	2.25	P _r , LB	WIDTH, IN.
2	2.25	200(b)	1.06
3	2.25	200(c)	1.06
4	1.1	200(c)	1.06
5(100% Removed)	None	None	None
6	1.1	90(d)	.62
7	1.1	90(d)	.62
8	1.1	90(d)	.62
9	1.1	None	None
10	1.1	None	None
11	1.1	None	None
12	1.1	None	None
VERTICAL TAPE	90 Lb. Nylon Tape, .62 Wide (e)		
SKIRT BAND	300 Lb. Nylon Tape, 1.0 Wide 500 Lb. Nylon Webbing, .56 Wide		
RADIALS (2 EACH)	300 Lb. Nylon Tape, 1.0 Wide		
SUSPENSION LINES	550 Lb. Nylon Cord		

(a) TRIPLE-SELVAGE CLOTH
(b) LEADING EDGE ONLY

(c) LEADING AND TRAILING EDGE
(d) TRAILING EDGE ONLY
(e) NO. 1 THRU NO. 4 SAIL, DOUBLED,
CENTER OF GORE

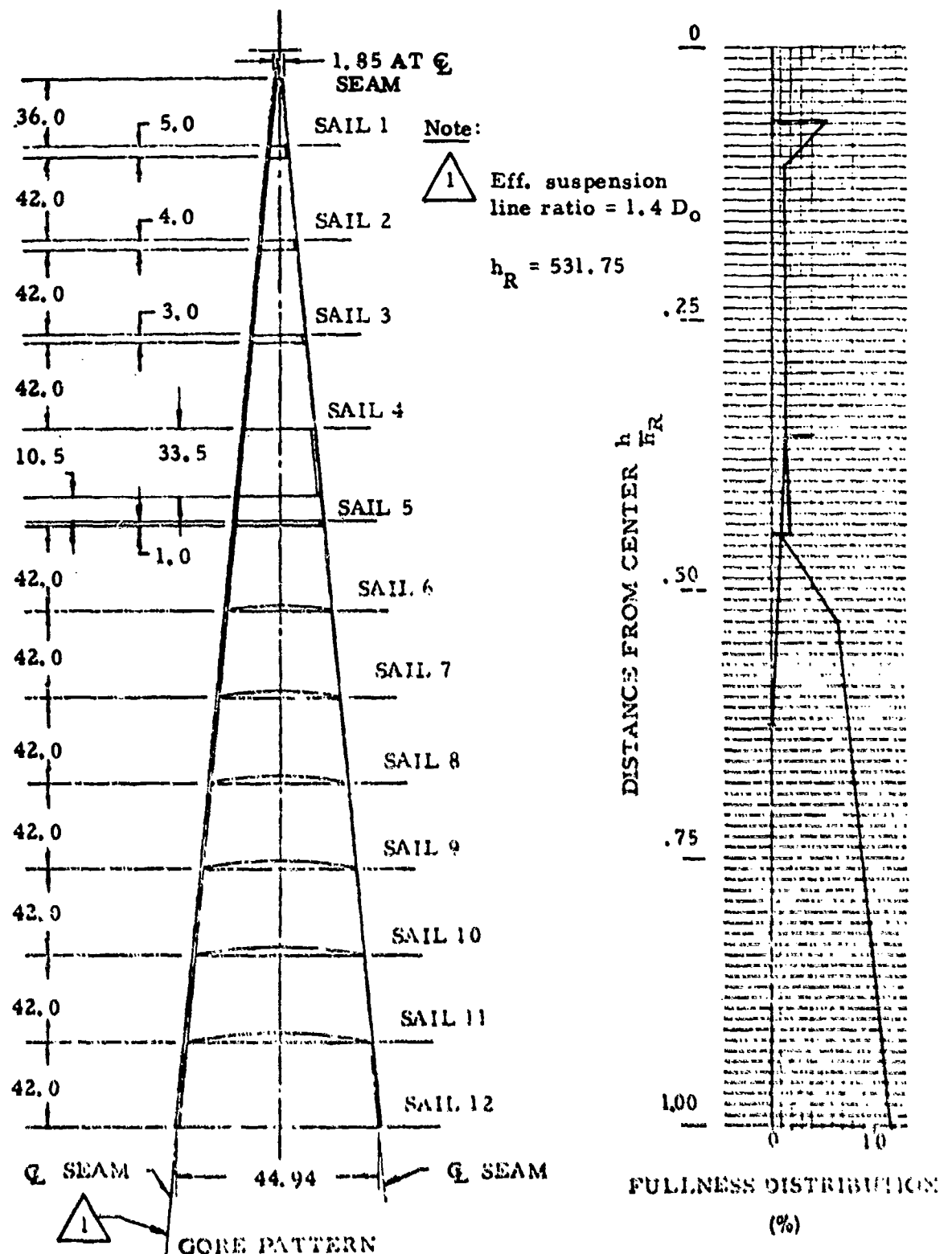


**Figure 92. Gore Pattern and Fullness Distribution,
PDS 1543-555 85.6 ft D_o Ringsall Parachute**

PART NO.: PDS 1543 - 555

TITLE: Parachute Assy., 85.6 Ft D₀ Ringsail

NO. GORES: 68

TYPE OF REEFING: Radial

ITEM	MATERIAL		
VENT LINES	550 Lb. Nylon Cord		
VENT BAND	4000 Lb. Nylon Webbing, 1.0 Wide		
RING NUMBER	CLOTH WEIGHT OZ/YD ² (a)	TAPE	WIDTH, IN.
1	2.25	200(b)	1.06
2	2.25	200(c)	1.06
3	2.25	200(c)	1.06
4	1.1	200(c)	1.06
5 (75% Removed Top)	1.1	300(d, f)	1.00
6	1.1	90(d)	.62
7	1.1	90(d)	.62
8	1.1	90(d)	.62
9	1.1	None	None
10	1.1	None	None
11	1.1	None	None
12	1.1	None	None
VERTICAL TAPE	90 Lb. Nylon Tape, .62 Wide (e)		
SKIRT BAND	300 Lb. Nylon Tape, 1.0 Wide		
SUSPENSION LINES	550 Lb. Nylon Cord		

(a) TRIPLE-SELVAGE CLOTH

(c) LEADING AND TRAILING EDGE

(b) LEADING EDGE ONLY

(d) TRAILING EDGE ONLY

(f) CIRCUMFERENTIAL REINFORCEMENT (e) NO. 1 THRU NO. 5 SAIL,
DOUBLED. CENTER OF CORE

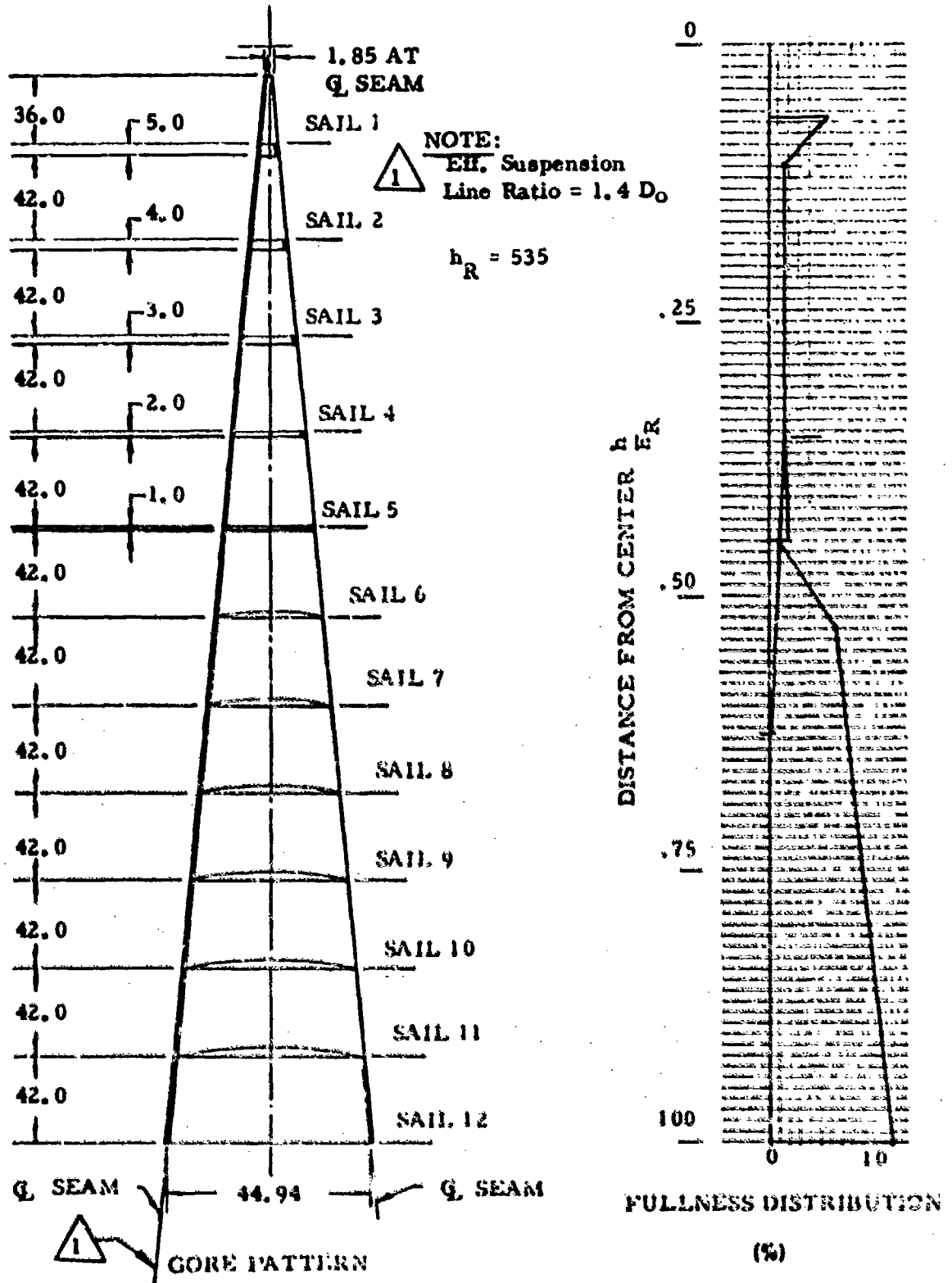


Figure 93. Gore Pattern and Fullness Distribution,
PDS 1544-1 and -501 88.1 ft D_0 Ringsail Parachute

PART NO.: PDS 1544-1

TITLE: Parachute, 88.1 Ft D₀ Ringsail

NO. GORES: 72

TYPE OF REEFING: Radial

ITEM	MATERIAL		
VENT LINES	550 Lb Nylon Cord		
VENT BAND	4000 Lb Nylon Webbing, 1.0 Wide		
RING NUMBER	CLOTH WEIGHT OZ/YD ² (a)	TAPE	
1	2.25	P. L.D.	WIDTH, IN.
2	2.25	90 (b, f, g)	.62
3	2.25	90 (c, f, g)	.62
4	1.1	90 (c, f, g)	.62
5	1.1	90 (d, f, g)	.62
6	1.1	90 (d, f)	.62
7	1.1	90 (d, f)	.62
8	1.1	90 (d, f)	.62
9	1.1	None	None
10	1.1	None	None
11	1.1	None	None
12	1.1	None	None
VERTICAL TAPE	None		
SKIRT BAND	525 Lb Nylon Tape, 1.0 Wide 500 Lb Nylon Webbing, .56 Wide		
RADIALS (2 EACH)	200 Lb Nylon Tape, 1.06 Wide (e) 200 Lb Nylon Tape, 1.06 Wide		
SUSPENSION LINES	550 Lb Nylon Cord		

- (a) TRIPLE-SELVAGE CLOTH
- (b) LEADING EDGE ONLY
- (c) CIRCUMFERENTIAL REINFORCEMENT

- (g) DOUBLED
- (c) LEADING AND TRAILING EDGE
- (d) TRAILING EDGE ONLY
- (e) ONE REQUIRED PER RADIAL SEAM.
DOUBLED & SEWN AS A RADIAL REINF.

PART NO.: PDS 1544-501

TITLE: Parachute, 88.1 Ft D₀ Ringsail

NO. GORES: 72

TYPE OF REEFING: Radial

ITEM	MATERIAL		
VENT LINES	550 Lb Nylon Cord		
VENT BAND	4000 Lb Nylon Webbing, 1.0 Wide		
RING NUMBER	CLOTH WEIGHT OZ/YD ² (a)	TAPE	
1	2.25	90 (b, f, g)	.62
2	2.25	90 (c, f, g)	.62
3	2.25	90 (c, f, g)	.62
4	1.1	90 (c, f, g)	.62
5	1.1	90 (d, f, g)	.62
6	1.1	90 (d, g)	.62
7	1.1	90 (d, g)	.62
8	1.1	90 (d, g)	.62
9	1.1	None	None
10	1.1	None	None
11	1.1	None	None
12	1.1	None	None
VERTICAL TAPE	90 Lb Nylon Tape (b)		
SKIRT BAND	525 Lb Nylon Tape, 1.0 Wide		
RADIALS (8 EACH)	500 Lb Nylon Webbing, .46 Wide 200 Lb Nylon Tape, 1.06 Wide (e) 500 Lb Nylon Tape, 1.06 Wide		
SUSPENSION LINES	550 Lb Nylon Cord		

(a) DOUBLED

(b) TRIPLE-SELVAGE CLOTH

(c) LEADING EDGE ONLY

(d) NO. 1 THRU NO. 5 SAIL,

DOUBLED, CENTER OF GORE

(f) CIRCUMFERENTIAL REINFORCEMENT

(g) LEADING AND TRAILING EDGE

(h) TRAILING EDGE ONLY

(i) ONE REQUIRED FOR RADIAL SEAM,

DOUBLED & SEWN AS A RADIAL REIN.

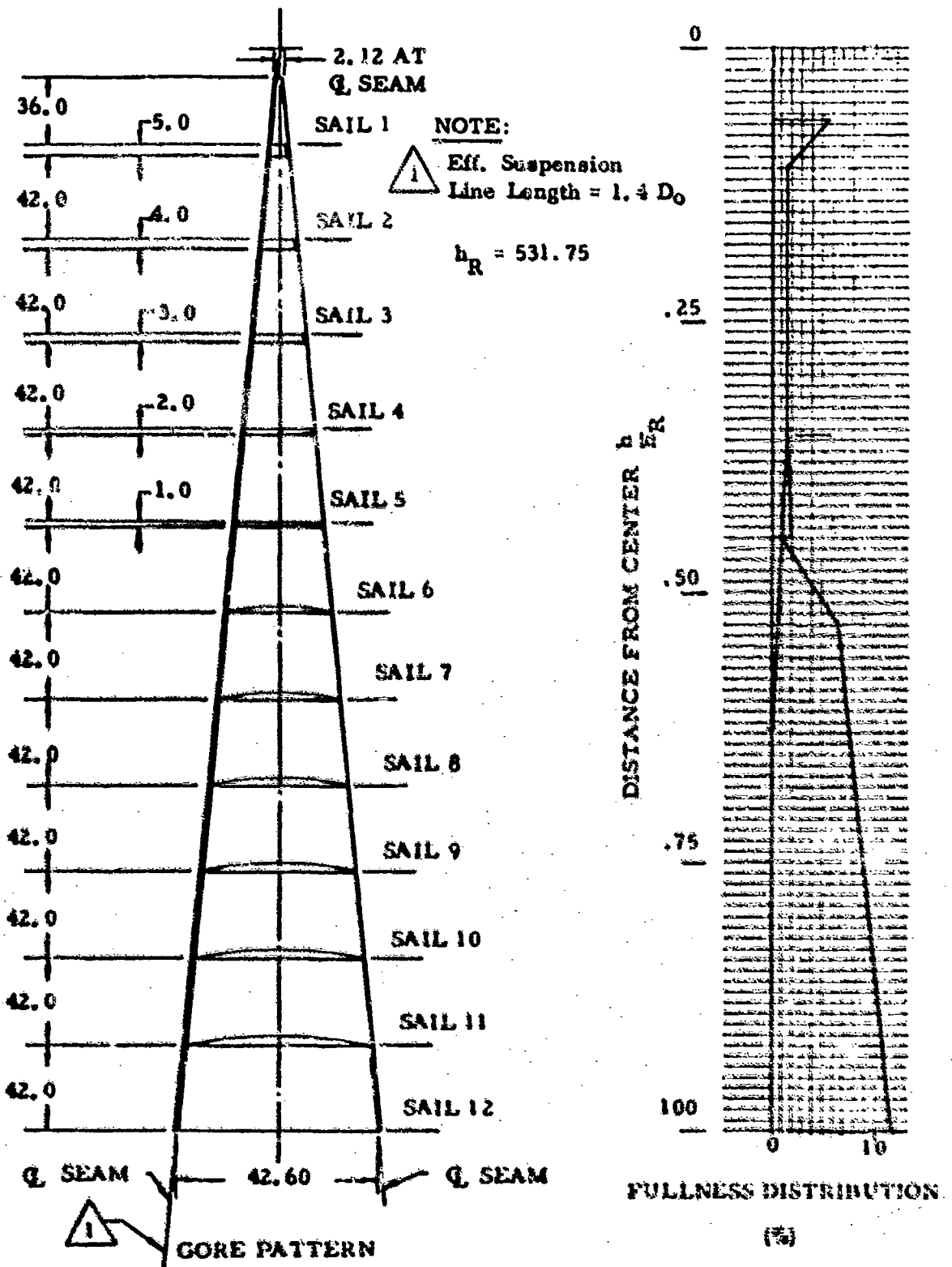


Figure 94. Core Pattern and Fullness Distribution,
PDS 1650-1 and -501 07.1 R D_0 Ringtail Parachute

PART NO.: PDS 1650-1

TITLE: Parachute, 87.1 Ft D_C Ringsail

NO. GORES: 72

TYPE OF REEFING: Radial

ITEM	MATERIAL		
VENT LINES	550 Lb Nylon Cord		
VENT BAND	4000 Lb Nylon Webbing, 1.0 Wide		
RING NUMBER	CLOTH WEIGHT OZ/YD ² (a)	TAPE	
1	2.25	P _r , LB	WIDTH, IN.
2	2.25	200 (b)	1.06
3	2.25	200 (c)	1.06
4	1.1	200 (c)	1.06
5	1.1	200 (d)	1.06
6	1.1	90 (d)	.62
7	1.1	90 (d)	.62
8	1.1	90 (d)	.62
9	1.1	None	None
10	1.1	None	None
11	1.1	None	None
12	1.1	None	None
VERTICAL TAPE	90 Lb Nylon Tape, .62 Wide (e)		
SKIRT BAND	500 Lb Nylon Webbing, .56 Wide		
RADIALS (2 EACH)	300 Lb Nylon Tape, 1.0 Wide		
SUSPENSION LINES	550 Lb Nylon Cord		

(a) TRIPLE-SELVAGE CLOTH
(b) LEADING EDGE ONLY

(c) LEADING AND TRAILING EDGE
(d) TRAILING EDGE ONLY
(e) NO. 1 THRU NO. 5 SAIL, DOUBLED,
CENTER OF GORE

PART NO.: PDS 1650-501

TITLE: Parachute, 87.1 Ft D_o Ringsail

NO. GORES: 72

TYPE OF REEFING: Radial

ITEM	MATERIAL		
VENT LINES	550 Lb Nylon Cord		
VENT BAND	4000 Lb Nylon Webbing, 1.0 Wide		
RING NUMBER	CLOTH WEIGHT OZ/YD ² (a)	TAPE	
1	2.25	P _r , LB	WIDTH, IN.
2	2.25	200 (b)	1.06
3	2.25	200 (c)	1.06
4	1.1	200 (c)	1.06
5	1.1	200 (d)	1.06
6	1.1	90 (d)	.62
7	1.1	90 (d)	.62
8	1.1	90 (d)	.62
9	1.1	None	None
10	1.1	None	None
11	1.1	None	None
12	1.1	None	None
VERTICAL TAPE	90 Lb Nylon Tape, .62 Wide (e)		
SKIRT BAND	500 Lb Nylon Webbing, .56 Wide		
RADIALS (2 EACH)	300 Lb Nylon Tape, 1.0 Wide		
SUSPENSION LINES	550 Lb Nylon Cord		

(a) TRIPLE-SELVAGE CLOTH

(c) LEADING AND TRAILING EDGE

(b) LEADING EDGE ONLY

(d) TRAILING EDGE ONLY

(e) NO. 1 THRU NO. 12 SAIL, DOUBLED,
CENTER OF GORE

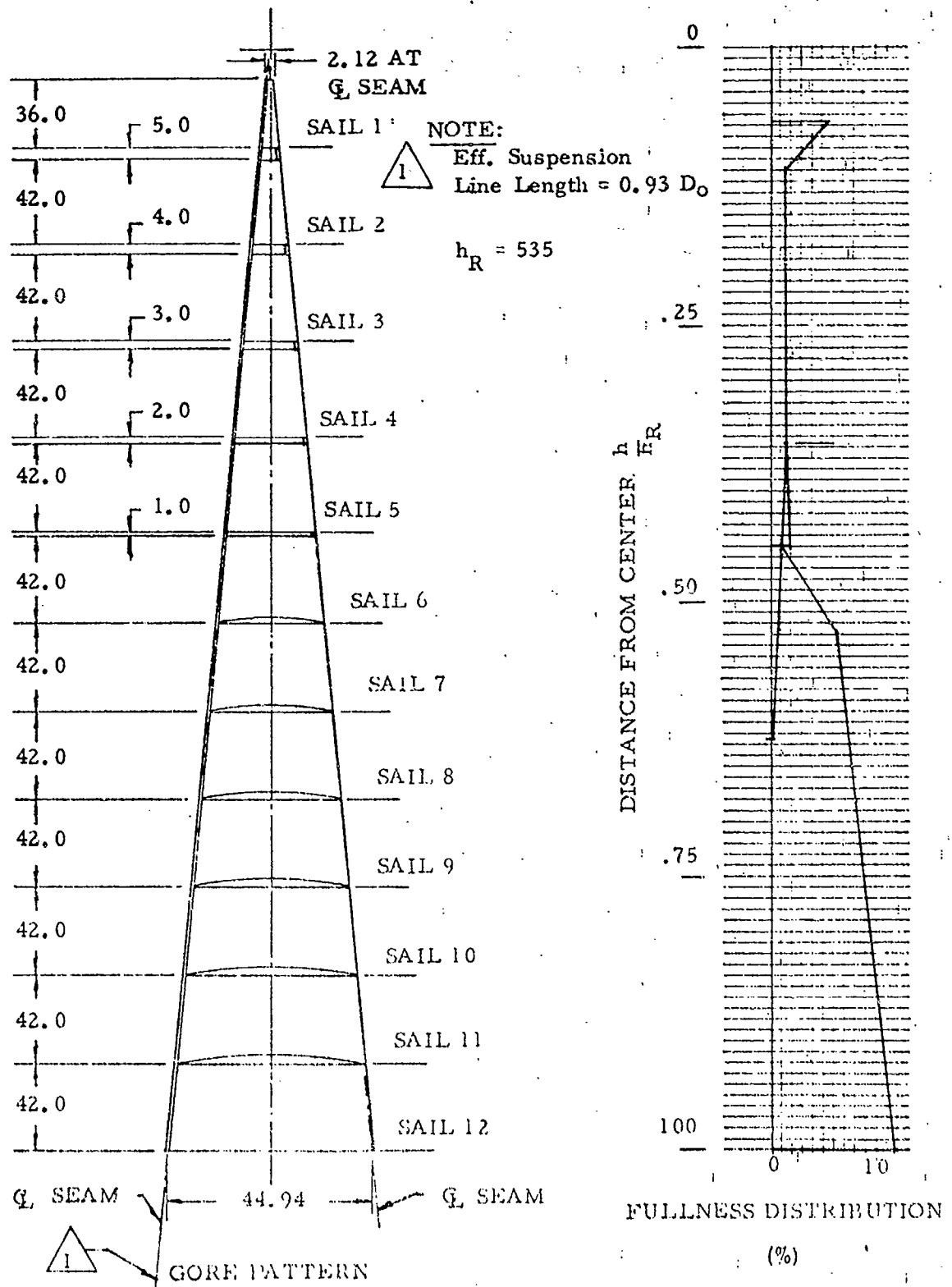


Figure 95. Gore Pattern and Fullness Distribution,
PDS 2021-1 88.1 ft D_0 Ringsail Parachute

PART NO.: PDS 2021-1

TITLE: Parachute, 88.1 Ft D₀ Ringsail

NO. CORES: 72

TYPE OF REEFING: Radial

ITEM	MATERIAL		
VENT LINES	550 Lb Nylon Cord		
VENT BAND (3 each)	900 Lb Nylon Tape, 1.0 Wide		
RING NUMBER	CLOTH WEIGHT OZ/YD ² (a)	TAPE	
1	2.25	90 (b, c)	.62
2	2.25	90 (c, e)	.62
3	2.25	90 (c, e)	.62
4	1.1	90 (c, e)	.62
5	1.1	90 (d, e)	.62
6	1.1	90 (d, e)	.62
7	1.1	None	None
8	1.1	None	None
9	1.1	None	None
10	1.1	None	None
11	1.1	None	None
12	1.1	None	None
VERTICAL TAPE	None		
SKIRT BAND	500 Lb Nylon Webbing, .56 Wide		
RADIALS (2 EACH)	200 Lb Nylon Tape, 1.06 Wide		
SUSPENSION LINES	400 Lb Nylon Cord		

(a) TRIPLE-SELVAGE CLOTH

(b) LEADING EDGE ONLY

(c) LEADING AND TRAILING EDGE

(d) TRAILING EDGE ONLY

(e) CIRCUMFERENTIAL REINFORCEMENT

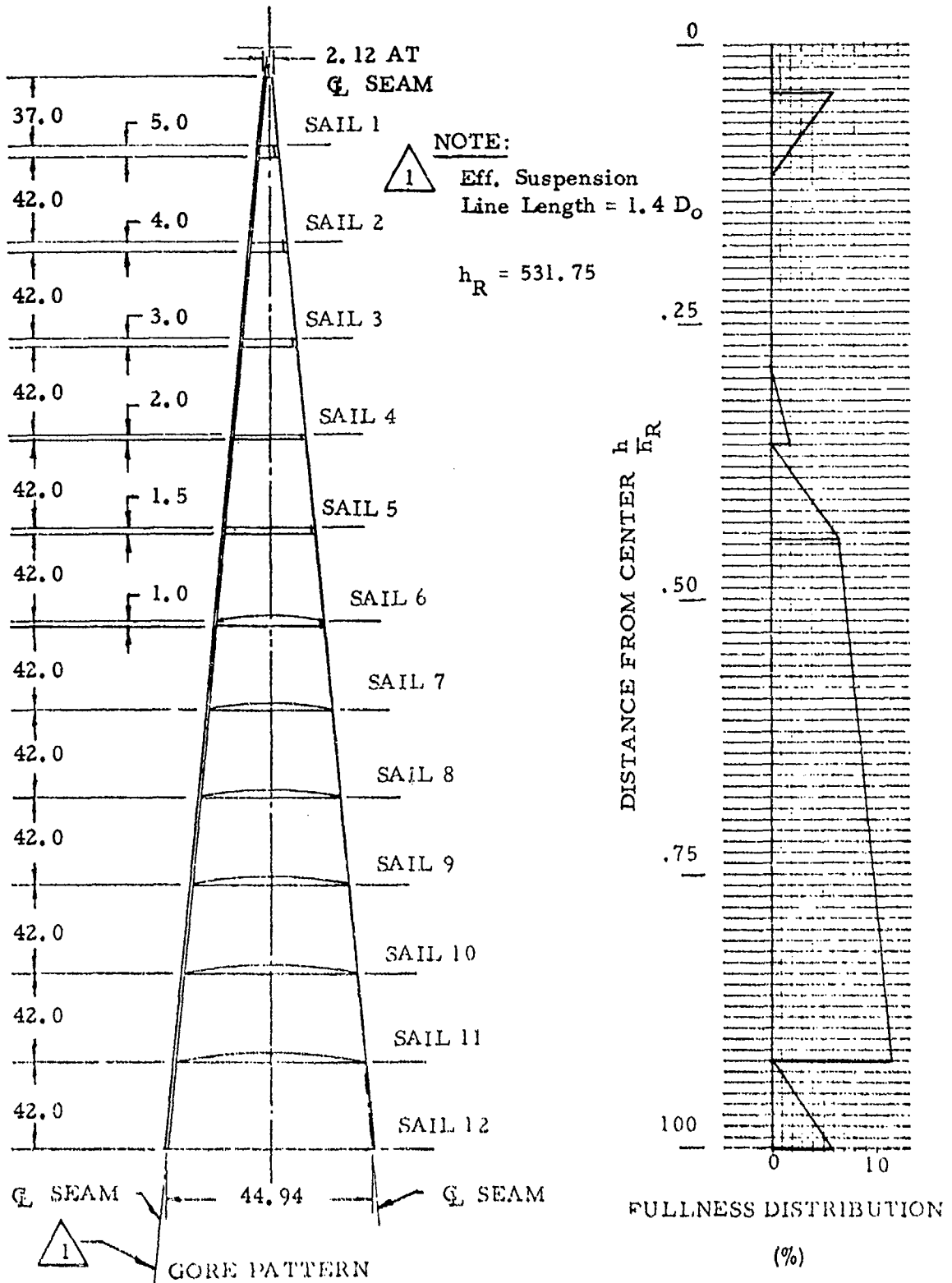


Figure 96. Gore Pattern and Fullness Distribution,
PDS 2071-1 88.1 ft D_o Ringsail Parachute

PART NO.: PDS 2071-1

TITLE: Parachute, 88.1 Ft D₀ Ringsail

NO. GORES: 72

TYPE OF REEFING: Radial

ITEM	MATERIAL		
VENT LINES	550 Lb Nylon Cord		
VENT BAND	4000 Lb Nylon Webbing, 1.0 Wide		
RING NUMBER	CLOTH WEIGHT OZ/YD ² (a)	TAPE P _r , LB	WIDTH, IN.
1	2.25	200 (b)	.1.06
2	2.25	200 (c)	1.06
3	2.25	200 (c)	1.06
4	1.1	200 (c)	1.06
5	1.1	200 (d)	1.06
6	1.1	90 (d)	.62
7	1.1	90 (d)	.62
8	1.1	90 (d)	.62
9	1.1	None	None
10	1.1	None	None
11	1.1	None	None
12	1.1	None	None
VERTICAL TAPE	90 Lb Nylon Tape, .62 Wide (e)		
SKIRT BAND	300 Lb Nylon Tape, 1.0 Wide		
RADIALS (2 EACH)	300 Lb Nylon Tape, 1.0 Wide		
SUSPENSION LINES	550 Lb Nylon Cord		

(a) TRIPLE-SELVAGE CLOTH
(b) LEADING EDGE ONLY

(c) LEADING AND TRAILING EDGE
(d) TRAILING EDGE ONLY
(e) NO. 1 THRU NO. 7 SAIL, DOUBLED,
CENTER OF GORE

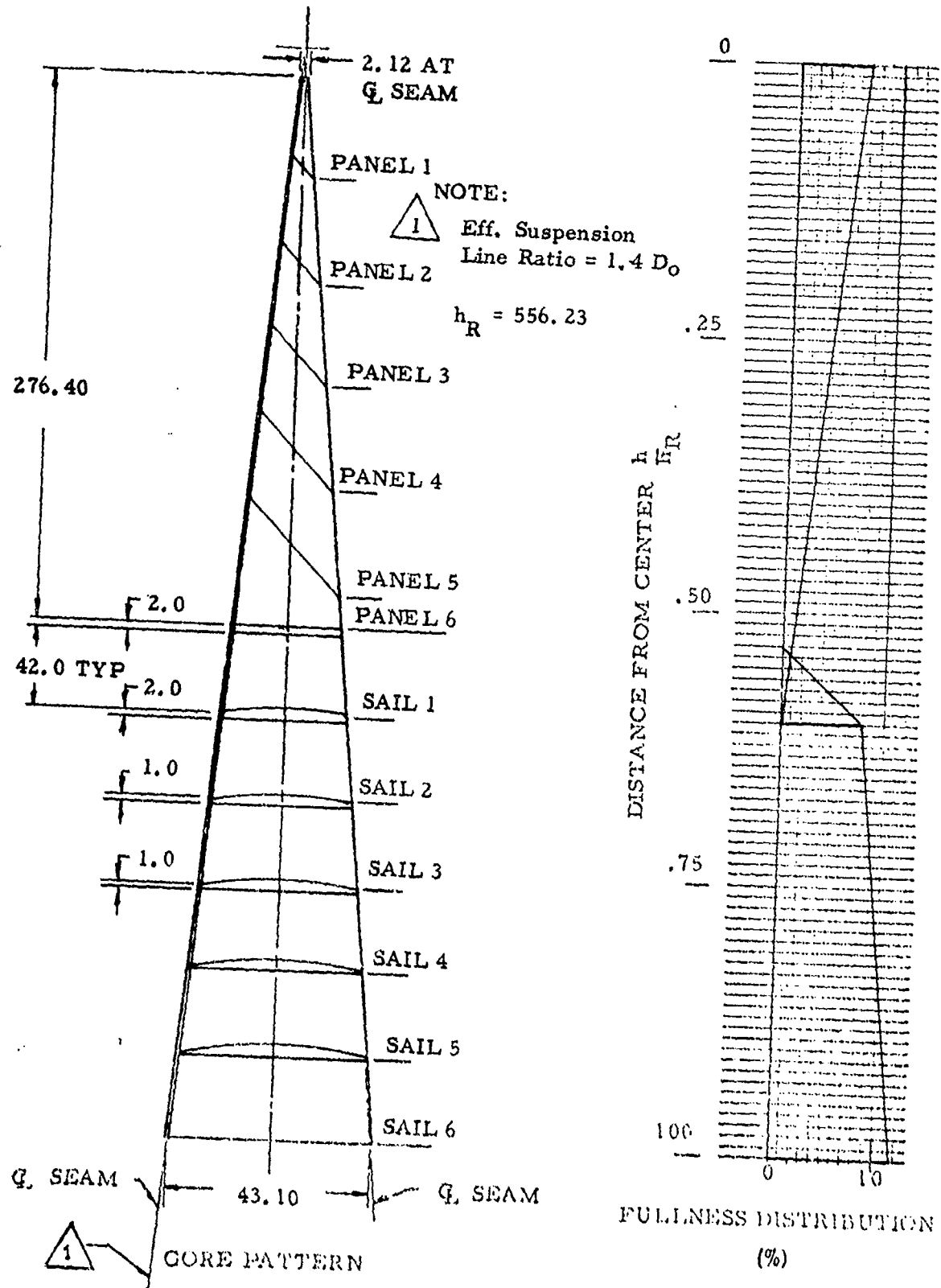


Figure 97. Gore Pattern and Fullness Distribution,
PDS 2072-1 87.9 ft D_0 Conical Ring/Solid Parachute

PART NO.: PDS 2072-1

TITLE: Parachute, 87.9 Ft D_o Conical Ring/Solid

NO. CORES: 72

TYPE OF REEFING: Radial

ITEM	MATERIAL		
VENT LINES	550 Lb Nylon Cord.		
VENT BAND	4000 Lb Nylon Webbing, 1.0 Wide		
RING NUMBER	CLOTH WEIGHT OZ/YD ² (a)	TAPE	
		P _r , LB	WIDTH, IN.
1 (Panel)	2.25	None	None
2 (Panel)	2.25	None	None
3 (Panel)	2.25	None	None
4 (Panel)	2.25	None	None
5 (Panel)	1.1	None	None
6 (Panel)	1.1	None	None
1	1.1	90 (d)	.62
2	1.1	90 (d)	.62
3	1.1	None	None
4	1.1	None	None
5	1.1	None	None
6	1.1	None	None
VERTICAL TAPE	None		
SKIRT BAND	900 Lb Nylon Tape, 1.0 Wide		
RADIALS (2 EACH)	300 Lb Nylon Tape, 1.0 Wide		
SUSPENSION LINES	550 Lb Nylon Cord		

(a) TRIPLE-SELVAGE CLOTH
(b) LEADING EDGE ONLY

(c) LEADING AND TRAILING EDGE
(d) TRAILING EDGE ONLY

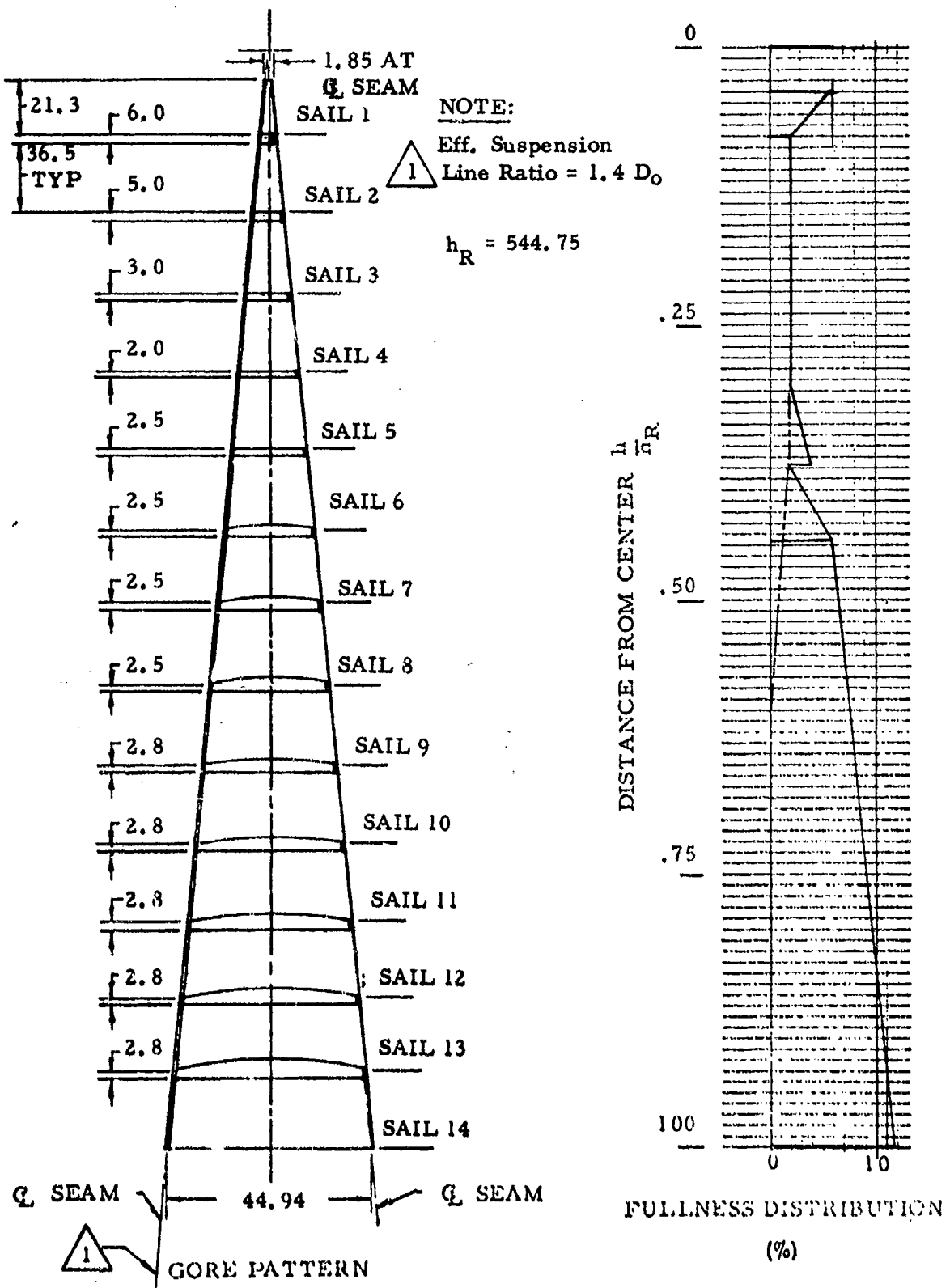


Figure 98. Gore Pattern and Fullness Distribution,
PDS 3120-1 88.3 ft D_0 Ringsail Parachute

PART NO.: PDS 3120-1

TITLE: Parachute, 88.3 Ft D₀ Ringsail

NO. GORES: 72

TYPE OF REEFING: Radial

(Pocket Bands)

ITEM	MATERIAL		
VENT LINES	550 Lb Nylon Cord		
VENT BAND	4000 Lb Nylon Webbing, 1.0 Wide		
RING NUMBER	CLOTH WEIGHT OZ/YD ² (a)	TAPE	
		P _r , LB	WIDTH, IN.
1	2.25	200 (b)	1.06
2, 3, 4	2.25	200 (c)	1.06
5	1.1	200 (c)	1.06
6	1.1	200 (d) 90 (b)	1.06 .62
7	1.1	90 (c)	.62
8	1.1	90 (c)	.62
9	1.1	90 (c)	.62
10	1.1	None	None
11	1.1	None	None
12	1.1	None	None
13	1.1	None	None
14	1.1	None	None
VERTICAL TAPE	90 Lb Nylon Tape, 1.0 Wide		
SKIRT BAND	500 Lb Nylon Webbing, .56 Wide		
RADIALS (2 EACH)	300 Lb Nylon Tape, 1.0 Wide		
SUSPENSION LINES	550 Lb Nylon Cord		

(a) TRIPLE-SELVAGE CLOTH
(b) LEADING EDGE ONLY

(c) LEADING AND TRAILING EDGE
(d) TRAILING EDGE ONLY
(e) NO. 1 THRU NO. 14 SAIL, DOUBLED,
CENTER OF GORE

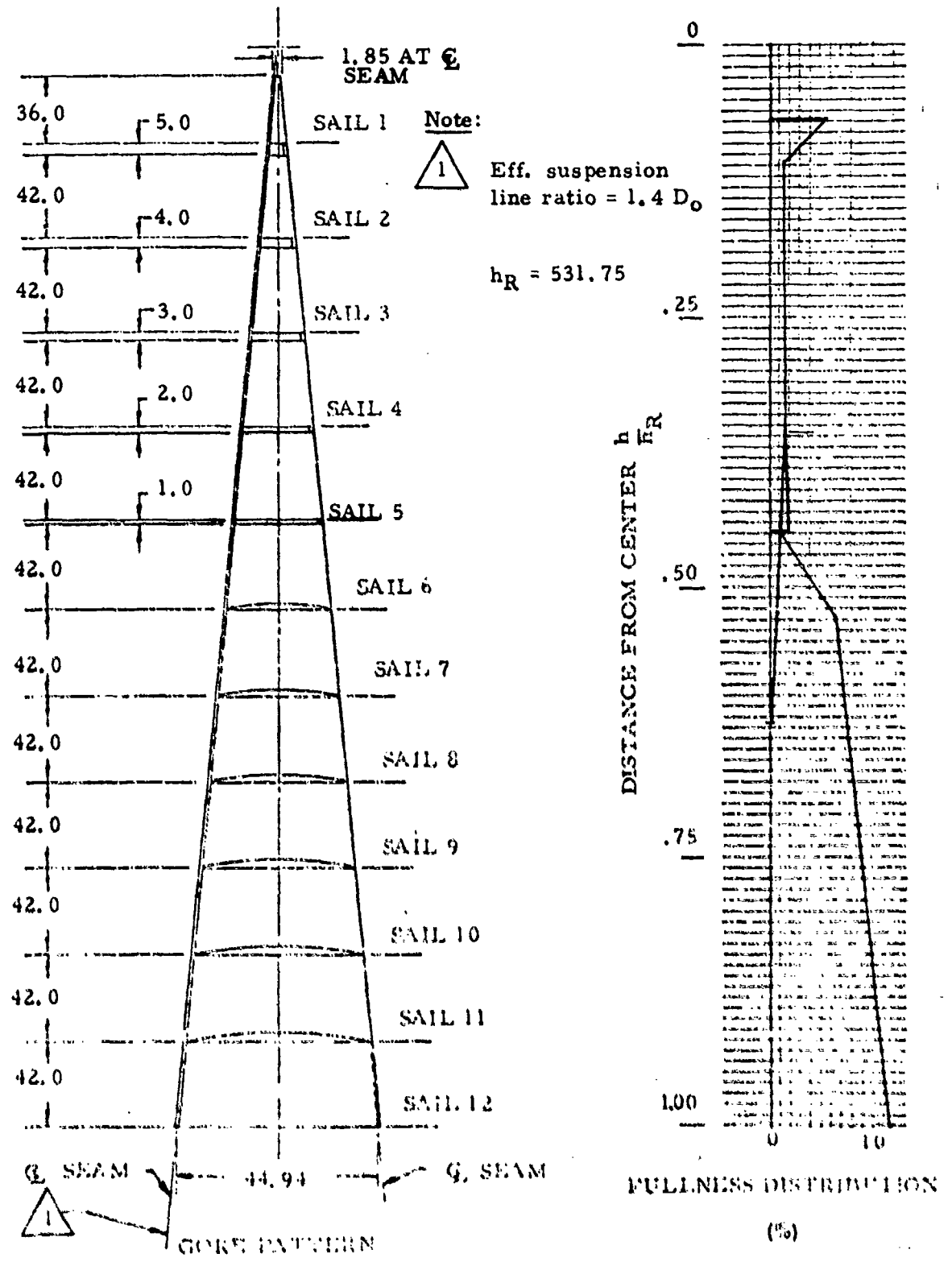


Figure 99. GORE Pattern and Fullness Distribution.
R7118-1, -501, -503 and -513 88.1 ft D_0 Ringsail Parachute

PART NO.: R7118-1

TITLE: Parachute, 88.1 Ft D₀ Ringsail

NO. GORES: 72

TYPE OF REEFING: Radial

ITEM	MATERIAL		
VENT LINES	550 Lb Nylon Cord		
VENT BAND	4000 Lb Nylon Webbing, 1.0 Wide		
RING NUMBER	CLOTH WEIGHT OZ/YD ² (a)	TAPE	
		P _r , LB	WIDTH, IN.
1	2.25	200 (b)	1.06
2	2.25	200 (c)	1.06
3	2.25	200 (c)	1.06
4	1.1	200 (c)	1.06
5	1.1	200 (d)	1.06
6	1.1	90 (d)	.62
7	1.1	90 (d)	.62
8	1.1	90 (d)	.62
9	1.1	None	None
10	1.1	None	None
11	1.1	None	None
12	1.1	None	None
VERTICAL TAPE	90 Lb Nylon Tape, .62 Wide (e)		
SKIRT BAND	300 Lb Nylon Tape, 1.0 Wide 500 Lb Nylon Webbing, .56 Wide		
RADIALS (2 EACH)	300 Lb Nylon Tape, 1.0 Wide		
SUSPENSION LINES	550 Lb Nylon Cord		

(a) TRIPLE-SELVAGE CLOTH
(b) LEADING EDGE ONLY

(c) LEADING AND TRAILING EDGE
(d) TRAILING EDGE ONLY
(e) NO. 1 THRU NO. 5 RING, DOUBLED,
CENTER OF GORE

PART NO.: R7118-501

TITLE: Parachute, 88.1 Ft D₀ Ringsail

NO. GORES: 72

TYPE OF REEFING: Radial

ITEM	MATERIAL		
VENT LINES	550 Lb Nylon Cord		
VENT BAND	4000 Lb Nylon Webbing, 1.0 Wide		
RING NUMBER	CLOTH WEIGHT OZ/YD ² (a)	TAPE	
1	2.25	P. _E , LB (b)	1.06
2	2.25	200 (c)	1.06
3	2.25	200 (c)	1.06
4	1.1	200 (c)	1.06
5	1.1	200 (d)	1.06
6	1.1	90 (d)	.62
7	1.1	90 (d)	.62
8	1.1	90 (d)	.62
9	1.1	None	None
10	1.1	None	None
11	1.1	None	None
12	1.1	None	None
VERTICAL TAPE	90 Lb Nylon Tape, .62 Wide (e)		
SKIRT BAND	300 Lb Nylon Tape, 1.0 Wide 500 Lb Nylon Webbing, .56 Wide		
RADIALS (2 EACH)	300 Lb Nylon Tape, 1.0 Wide		
SUSPENSION LINES	550 Lb Nylon Cord		

(a) TRIPLE-SELVAGE CLOTH

(c) LEADING AND TRAILING EDGE

(b) LEADING EDGE ONLY

(d) TRAILING EDGE ONLY

(e) FULL GORE HEIGHT, DOUBLED,
CENTER OF GORE

PART NO.: R7118-503

TITLE: Parachute, 88.1 Ft D₀ Ringsail

NO. GORES: 72

TYPE OF REEFING: Radial and Mid-Gore

ITEM	MATERIAL		
VENT LINER	550 Lb Nylon Cord		
VENT BAND	4000 Lb Nylon Webbing, 1.0 Wide		
RING NUMBER	CLOTH WEIGHT OZ/YD ² (a)	TAPE	WIDTH, IN.
1	2.25	P. _r , LB (b)	1.06
2	2.25	P. _r , LB (c)	1.06
3	2.25	P. _r , LB (c)	1.06
4	1.1	P. _r , LB (c)	1.06
5	1.1	P. _r , LB (d)	1.06
6	1.1	P. _r , LB (d)	.62
7	1.1	P. _r , LB (d)	.62
8	1.1	P. _r , LB (d)	.62
9	1.1	None	None
10	1.1	None	None
11	1.1	None	None
12	1.1	None	None
VERTICAL TAPE	50 Lb Nylon Tape, .62 Wide (e)		
SKIRT BAND	300 Lb Nylon Tape, 1.0 Wide 500 Lb Nylon Webbing, .50 Wide		
RADIALS (2 EACH)	100 Lb Nylon Tape, 1.0 Wide		
SUSPENSION LINES	550 Lb Nylon Cord		

(a) TRIPLE-SELVAGE CLOTH
(b) LEADING EDGE ONLY

(c) LEADING AND TRAILING EDGE
(d) TRAILING EDGE ONLY
(e) NO. 1 THRU NO. 5 RING, DOUBLED,
CENTER OF GORE

PART NO.: R7118-513

TITLE: Parachute, 88.1 Ft D_o Ringsail

NO. GORES: 72

TYPE OF REEFING: Radial

ITEM	MATERIAL		
VENT LINES	550 Lb Nylon Cord		
VENT BAND	4000 Lb Nylon Webbing, 1.0 Wide		
RING NUMBER	CLOTH WEIGHT OZ/YD ² (a)	TAPE P _r , LB	WIDTH, IN.
1	2.25	200 (b) 200 (b, f)	1.06
2	2.25	200 (c) 200 (c, f)	1.06
3	2.25	200 (c) 200 (c, f)	1.06
4	1.1	200 (c) 200 (c, f)	1.06
5	1.1	200 (d) 200 (d, f)	1.06
6	1.1	90 (d) 200 (d, f)	.62 1.06
7	1.1	90 (d) 200 (d, f)	.62 1.06
8	1.1	90 (d)	.62
9	1.1	None	None
10	1.1	None	None
11	1.1	None	None
12	1.1	None	None
VERTICAL TAPE	90 Lb Nylon Tape, .62 Wide (e)		
SKIRT BAND	300 Lb Nylon Tape, 1.0 Wide 500 Lb Nylon Webbing, .56 Wide		
RADIALS (2 EACH)	300 Lb Nylon Tape, 1.0 Wide		
SUSPENSION LINES	550 Lb Nylon Cord		

(a) TRIPLE-SELVAGE CLOTH

(d) TRAILING EDGE ONLY

(b) LEADING EDGE ONLY

(e) NO. 1 THRU NO. 5 RING, DOUBLED,
CENTER OF GORE

(c) LEADING AND TRAILING EDGE

(f) CONTINUOUS REINFORCEMENT

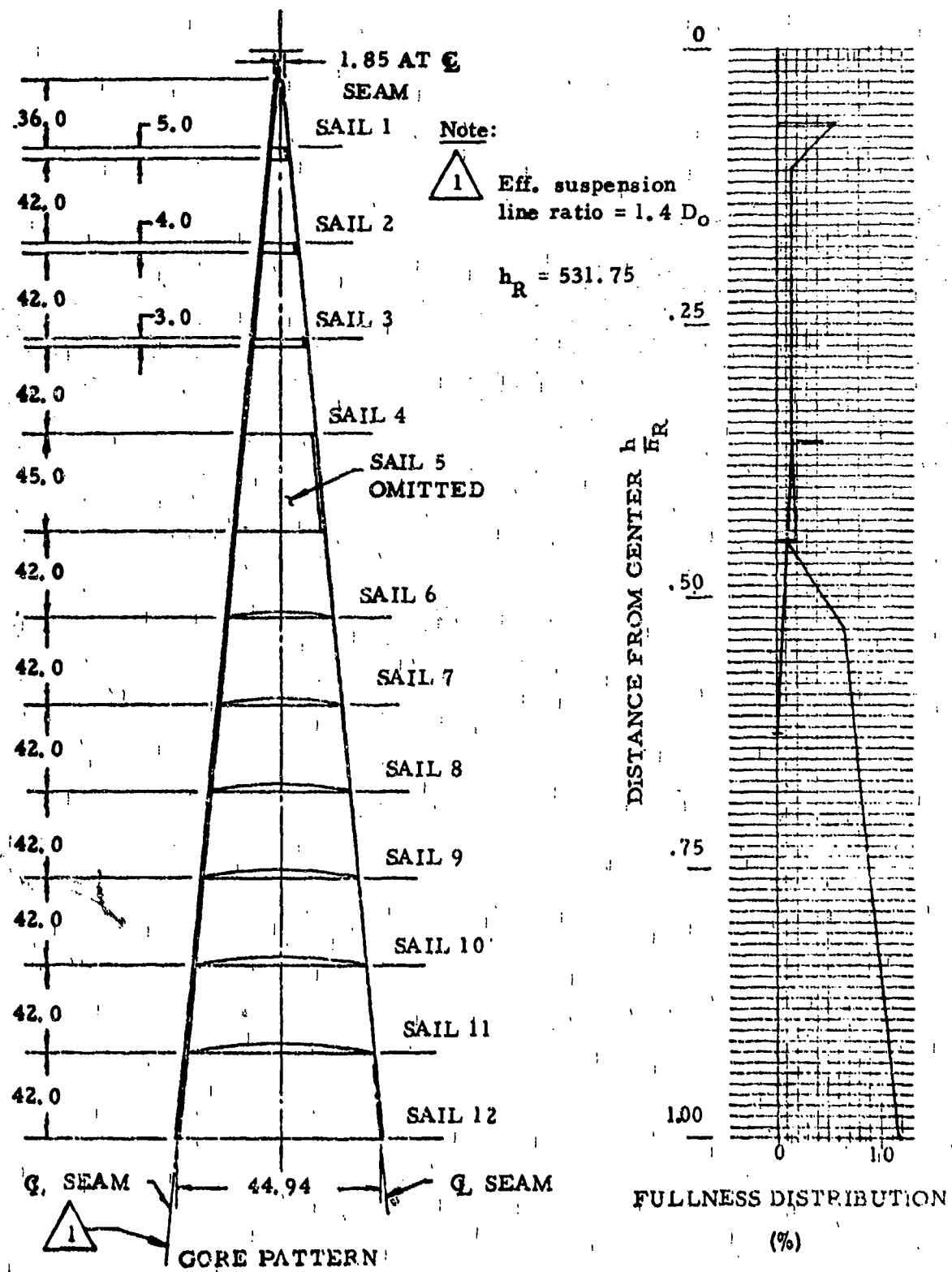


Figure 100. Gore Pattern and Fullness Distribution,
R7118-507 88.1 ft D_o Ringsail Parachute

PART NO.: R7118-507

TITLE: Parachute, 88.1 Ft D₀ Ringsail

NO. GORES: 72

TYPE OF REEFING: Radial

ITEM	MATERIAL		
VENT LINES	550 Lb Nylon Cord		
VENT BAND	4000 Lb Nylon Webbing, 1.0 Wide		
RING NUMBER	CLOTH WEIGHT OZ/YD ² (a)	TAPE	
1	2.25	P _r , LB 200 (b)	WIDTH, IN. 1.06
2	2.25	200 (c)	1.06
3	2.25	200 (c)	1.06
4	1.1	200 (c)	1.06
5	None	None	None
6	1.1	90 (d)	.62
7	1.1	90 (d)	.62
8	1.1	90 (d)	.62
9	1.1	None	None
10	1.1	None	None
11	1.1	None	None
12	1.1	None	None
VERTICAL TAPE	90 Lb Nylon Tape, .62 Wide (e)		
SKIRT BAND	300 Lb Nylon Tape, 1.0 Wide 500 Lb Nylon Webbing, .56 Wide		
RADIALS (2 EACH)	300 Lb Nylon Tape, 1.0 Wide		
SUSPENSION LINES	550 Lb Nylon Cord		

(a) TRIPLE-SELVAGE CLOTH
(b) LEADING EDGE ONLY

(c) LEADING AND TRAILING EDGE
(d) TRAILING EDGE ONLY
(e) NO. 1 THRU NO. 4 RING, DOUBLED,
CENTER OF GORE

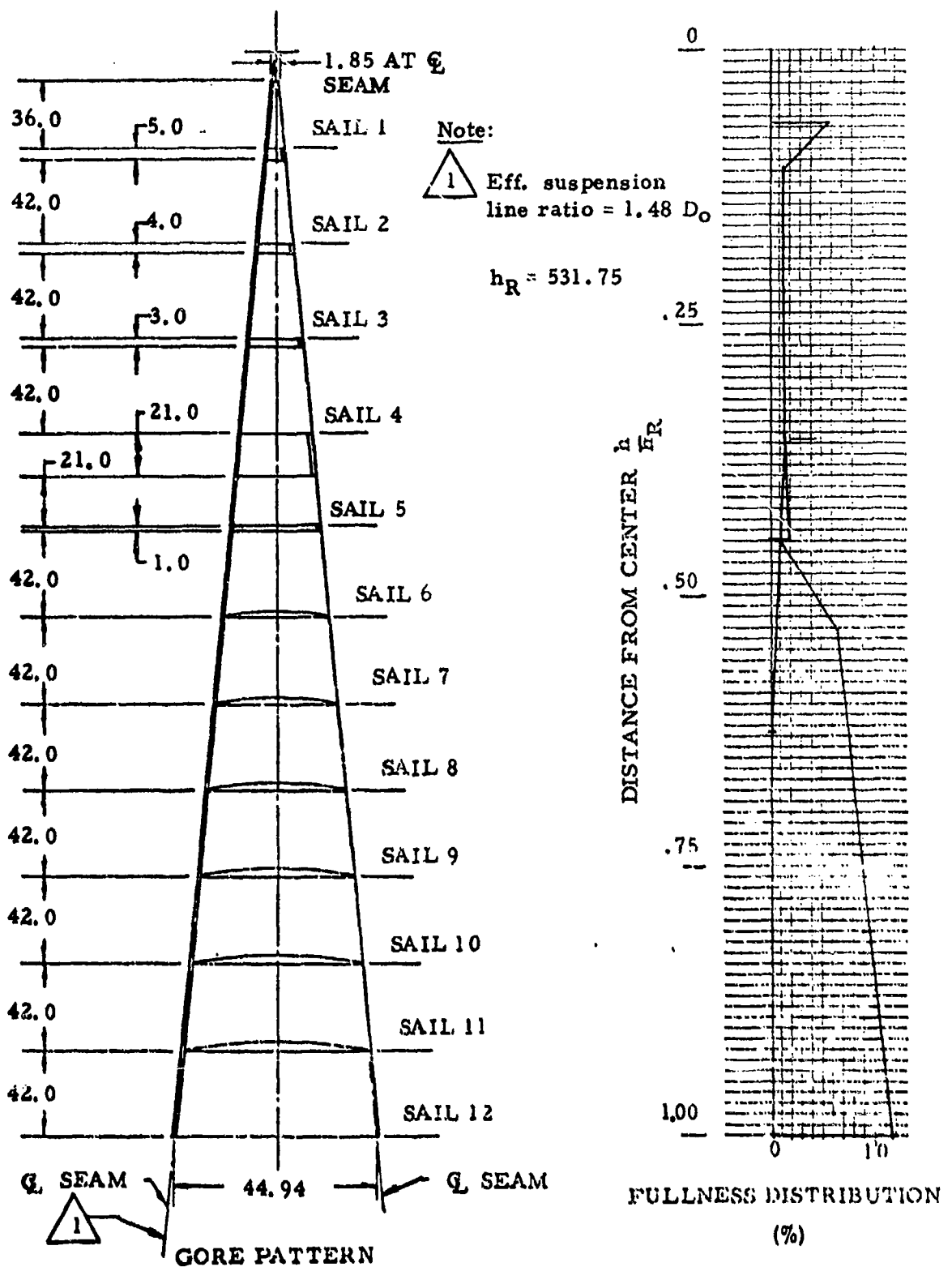


Figure 101. Gore Pattern and Fullness Distribution,
R7118-515 88.1 ft D_o Ringsail Parachute

PART NO.: R7118-515

TITLE: Parachute, 88.1 Ft D_o Ringsail

NO. GORES: 68

TYPE OF REEFING: Mid-Gore

ITEM	MATERIAL		
	CLOTH WEIGHT OZ/YD ² (a)	TAPE	
RING NUMBER		P _r , LB	WIDTH, IN.
1	2.25	200 (b)	1.06
2	2.25	200 (c)	1.06
3	2.25	200 (c)	1.06
4	1.1	200 (c)	1.06
5 (50% Removed Top)	1.1	200 (d)	1.06
6	1.1	90 (d)	.62
7	1.1	90 (d)	.62
8	1.1	90 (d)	.62
9	1.1	None	None
10	1.1	None	None
11	1.1	None	None
12	1.1	None	None
VERTICAL TAPE	90 Lb Nylon Tape, .62 Wide (e)		
SKIRT BAND	300 Lb Nylon Tape, 1.0 Wide 500 Lb Nylon Webbing, .56 Wide		
RADIALS (2 EACH)	300 Lb Nylon Tape, 1.0 Wide		
SUSPENSION LINES	550 Lb Nylon Cord		

(a) TRIPLE-SELVAGE CLOTH
(b) LEADING EDGE ONLY

(c) LEADING AND TRAILING EDGE
(d) TRAILING EDGE ONLY
(e) NO. 1 THRU NO. 5 SAIL, DOUBLED,
CENTER OF GORE

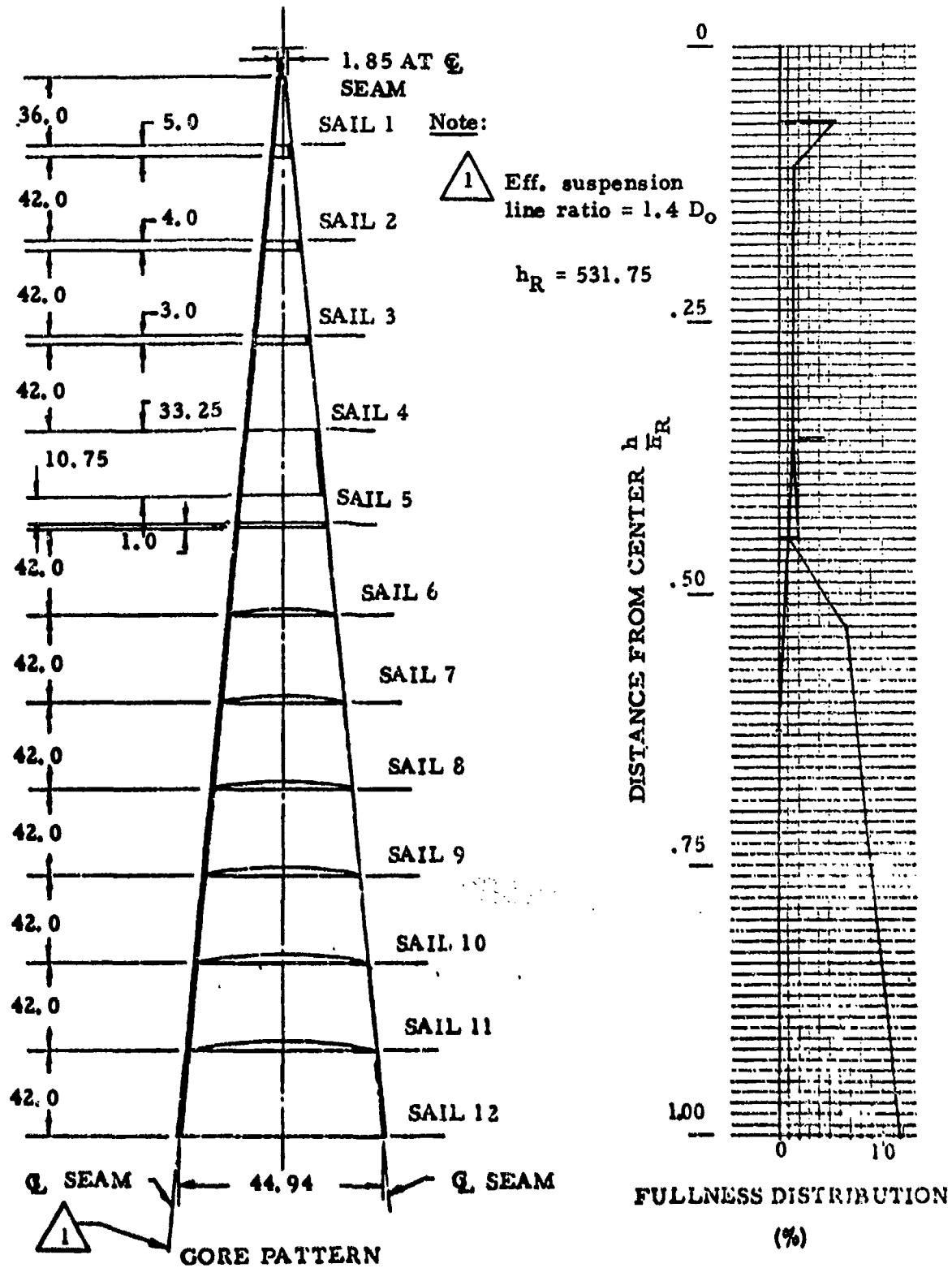


Figure 102. Core Pattern and Fullness Distribution,
R7527-1 and -503 85.6 ft D_o Conical Ringsail Parachute

PART NO.: R7527-1

TITLE: Parachute, 85.6 Ft D_o Conical Ringsail

NO. GORES: 68

TYPE OF REEFING: Mid-Gore

ITEM	MATERIAL				
VENT LINES	550 Lb Nylon Cord				
VENT BAND	4000 Lb Nylon Webbing, 1.0 Wide				
RING NUMBER	CLOTH WEIGHT OZ/YD ² (a)	TAPE		WIDTH, IN.	
1	2.25	P _r , LB	(b, f)	.62	
2	2.25	90	(c, f)	.62	
3	2.25	90	(c, f)	.62	
4	1.1	90	(c, f)	.62	
5 (75% Removed Top)	1.1	200	(d, f)	1.06	
6	1.1	90	(d, f)	.62	
7	1.1	None		None	
8	1.1	None		None	
9	1.1	None		None	
10	1.1	None		None	
11	1.1	None		None	
12	1.1	None		None	
VERTICAL TAPE	90 Lb Nylon Tape, .62 Wide, (e)				
SKIRT BAND	300 Lb Nylon Tape, 1.0 Wide 500 Lb Nylon Webbing, .56 Wide				
RADIALS (2 EACH)	300 Lb Nylon Tape, 1.0 Wide				
SUSPENSION LINES	650 Lb Nylon Cord				

PART NO.: R7527-503

TITLE: Parachute, 85.6 Ft D_o Conical Ringsail

NO. GORES: 68

TYPE OF REEFING: Mid-Gore

ITEM	MATERIAL			
VENT LINES	550 Lb Nylon Cord			
VENT BAND	4000 Lb Nylon Webbing, 1.0 Wide			
RING NUMBER	CLOTH WEIGHT OZ/YD ² (a)	TAPE		WIDTH, IN.
1	2.25	90	(b, f)	.62
2	2.25	90	(c, f)	.62
3	2.25	90	(c, f)	.62
4	1.1	90	(c, f)	.62
5	1.1	200	(d, f)	1.06
6	1.1	90	(d, f)	.62
7	1.1	None		None
8	1.1	None		None
9	1.1	None		None
10	1.1	None		None
11	1.1	None		None
12	1.1	None		None
VERTICAL TAPE	90 Lb Nylon Tape, .62 Wide (c)			
SKIRT BAND	300 Lb Nylon Tape, 1.0 Wide 500 Lb Nylon Webbing, .56 Wide			
RADIALS (2 EACH)	300 Lb Nylon Tape, 1.0 Wide			
SUSPENSION LINES	650 Lb Nylon Cord			

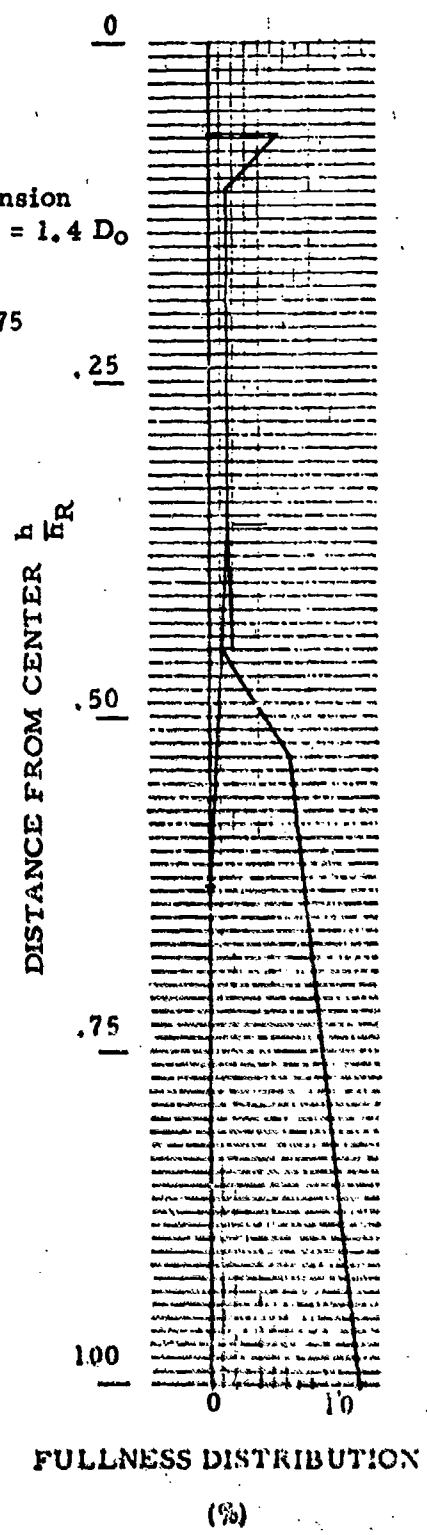
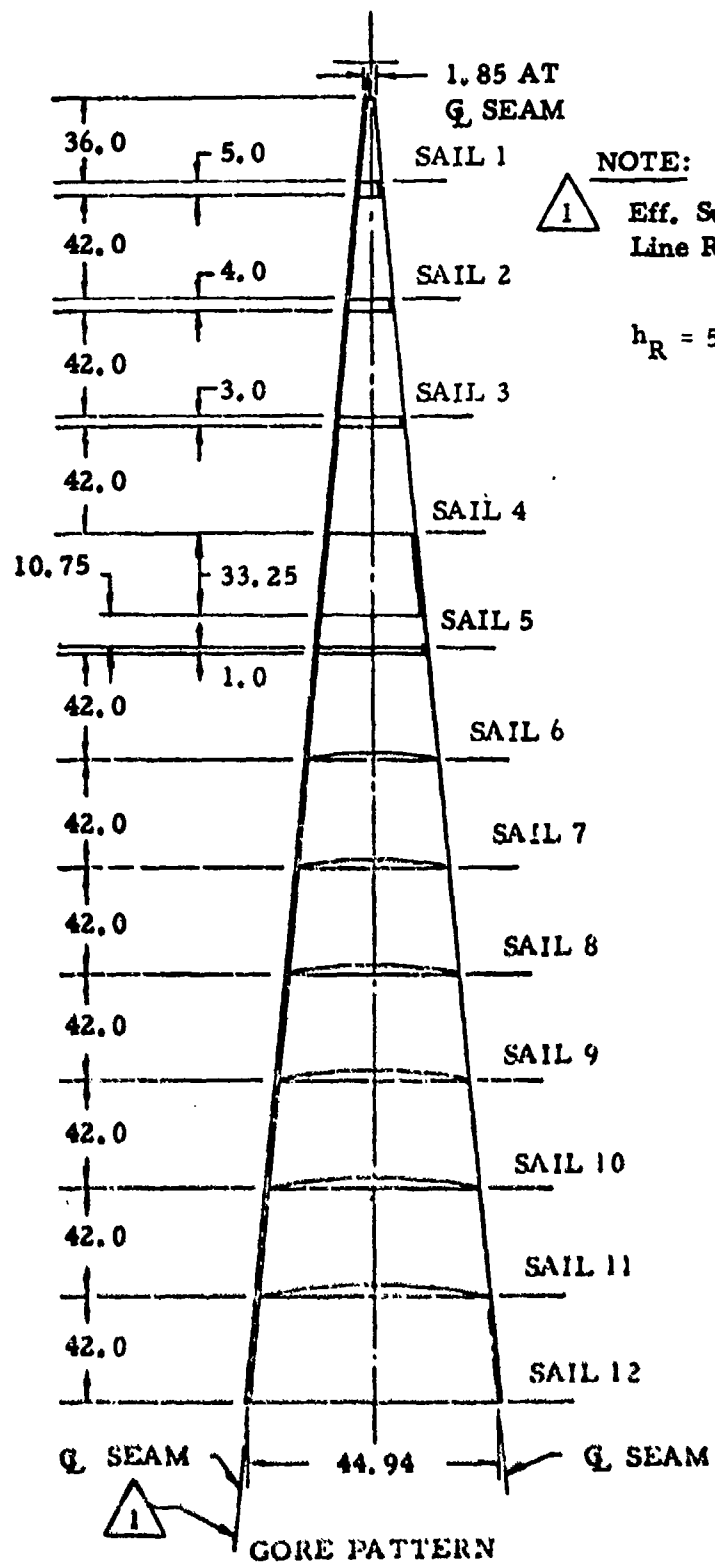


Figure 103. Gore Pattern and Fullness Distribution,
DR 7661-1 and -527 83.5 ft D_0 Conical Ringsail Parachute.

PART NO.: DR 7661-1

TITLE: Parachute, 83.5 Ft D₀ Conical Ringsail

NO. CORES: 68

TYPE OF REEFING: Mid-Gore

ITEM	MATERIAL		
VENT LINES	650 Lb Nylon Cord		
VENT BAND	4000 Lb Nylon Webbing, 1.0 Wide		
RING NUMBER	CLOTH WEIGHT OZ/YD ² (a)	TAPE (i)	
1	2.25	P. lb	WIDTH, IN.
2	2.25	200 (b)	1.06
3	2.25	200 (c)	1.06
4	2.25	200 (c)	1.06
5 (75% Removed Top)	1.1	200 (d)	1.06
6	1.1	90 (d)	.62
7	1.1	90 (d)	.62
8	1.1	90 (d)	.62
9	1.1	None	None
10	1.1	None	None
11	1.1	None	None
12	1.1	None	None
VERTICAL TAPE	90 Lb Nylon Tape, .62 Wide (e)		
SKIRT BAND	250 Lb Nylon Tape, 1.0 Wide 900 Lb Nylon Webbing, .56 Wide		
RADIALS (2 EACH)	350 Lb Nylon Tape, 1.0 Wide		
SUSPENSION LINES	650 Lb Nylon Cord		

- (a) TRIPLE-SELVAGE CLOTH
- (b) LEADING EDGE ONLY
- (c) CIRCUMFERENTIAL REIN-
FORCEMENT

- (d) LEADING AND TRAILING EDGE
- (e) TRAILING EDGE ONLY
- (f) NO. 1 THRU NO. 5 SAIL, DOUBLED,
CENTER OF GORE

PART NO.: DR 7661 - 527

TITLE: Parachute, 83.5 Ft D_o Conical Ringsail

NO. GORES: 68

TYPE OF REEFING: Mid-Gore

ITEM	MATERIAL		
VENT LINES	650 Lb Nylon Cord		
VENT BAND	1200 Lb Nylon Webbing, 1.0 Wide 4000 Lb Nylon Webbing, 1.0 Wide		
RING NUMBER	CLOTH WEIGHT OZ/YD ² (a)	TAPE (f)	WIDTH, IN.
1	2.25	200 (b)	1.06
2	2.25	200 (c)	1.06
3	2.25	200 (c)	1.06
4	2.25	200 (d) 350 (b)	1.06 1.00
5 (75% Removed, Top)	1.1	625 (d) 200 (b)	1.00 1.06
6	1.1	350 (d), 200 (h) 90 (b)	1.00/1.06 .62
7	1.1	350 (d), 200 (h) 90 (b)	1.00/1.06 .62
8	1.1	200 (d), 200 (h) 90 (b)	1.06/1.06 .62
9	1.1	90 (d)	.62
10	1.1	None	None
11	1.1	None	None
12	1.1	None	None
VERTICAL TAPE	90 Lb Nylon Tape, .62 Wide (e)		
SKIRT BAND	1200 Lb Nylon Webbing, 1.0 Wide (g)		
RADIALS (2 EACH)	350 Lb Nylon Tape, 1.0 Wide		
SUSPENSION LINES	650 Lb Nylon Cord		

(g) DOUBLED

(h) MID-RING

(a) TRIPLE-SELVAGE CLOTH

(c) LEADING AND TRAILING EDGE

(b) LEADING EDGE ONLY

(d) TRAILING EDGE ONLY

(f) CIRCUMFERENTIAL REIN-
FORCEMENT

(e) NO. 1 THRU NO. 5 SAIL, DOUBLED,
CENTER OF COPE

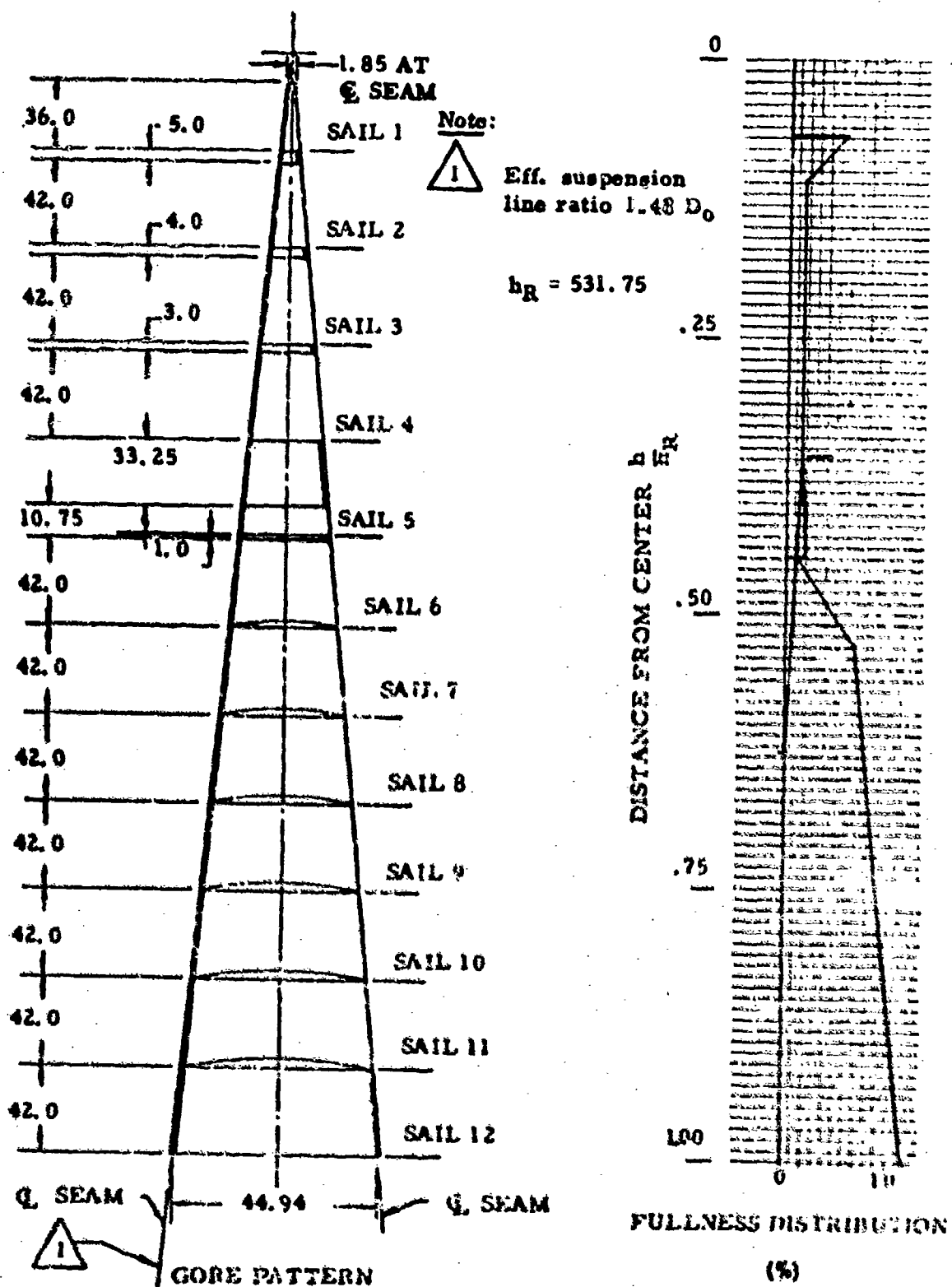


Figure 104. Gore Pattern and Fullness Distribution,
R7661-1 thru -519 83.5 ft D_0 Conical Ringsail Parachute

PART NO.: R7661-1

TITLE: Parachute, 83.5 ft D₀ Conical Ringsail

NO. GORES: 68

TYPE OF REEFING: Mid-Gore

ITEM	MATERIAL		
VENT LINES	650 Lb Nylon Cord		
VENT BAND	4000 Lb Nylon Webbing, 1.0 Wide		
RING NUMBER	CLOTH WEIGHT OZ/YD ² (a)	TAPE	
		P _r , LB	WIDTH, IN.
1	2.25	200 (b)	1.06
2	2.25	200 (c)	1.06
3	2.25	200 (c)	1.06
4	2.25	200 (c)	1.06
5 (75% Removed, Top)	1.1	200 (d)	1.06
6	1.1	90 (d)	.62
7	1.1	90 (d)	.62
8	1.1	None	None
9	1.1	None	None
10	1.1	None	None
11	1.1	None	None
12	1.1	None	None
VERTICAL TAPE	90 Lb Nylon Tape, .62 Wide (e)		
SKIRT BAND	350 Lb. Nylon Tape, 1.0 Wide 500 Lb. Nylon Webbing, .56 Wide		
RADIALS (2 EACH)	350 Lb Nylon Tape, 1.0 Wide		
SUSPENSION LINES	650 Lb Nylon Cord		

(a) TRIPLE-SELVAGE CLOTH
(b) LEADING EDGE ONLY

(c) LEADING AND TRAILING EDGE
(d) TRAILING EDGE ONLY
(e) NO. 1 THRU NO. 5 SAIL, DOUBLED,
CENTER OF GORE

PART NO.: R7661-501

TITLE: Parachute, 83.5 Ft D_o Conical Ringsail

NO. GORES: 68

TYPE OF REEFING: Mid-Gore

ITEM	MATERIAL		
VENT LINES	650 Lb Nylon Cord		
VENT BAND	4000 Lb Nylon Webbing, 1.0 Wide		
RING NUMBER	CLOTH WEIGHT OZ/YD ² (a)	TAPE	
1	2.25	P _r , LB 200 (b)	WIDTH, IN. 1.06
2	2.25	200 (c)	1.06
3	2.25	200 (c)	1.06
4	2.25	200 (c)	1.06
5 (75% Removed Top)	1.1	200 (d)	1.06
6	1.1	90 (d)	.62
7	1.1	90 (d)	.62
8	1.1	90 (d)	.62
9	1.1	None	None
10	1.1	None	None
11	1.1	None	None
12	1.1	None	None
VERTICAL TAPE	90 Lb Nylon Tape, .62 Wide (e)		
SKIRT BAND	350 Lb Nylon Tape, 1.0 Wide 500 Lb Nylon Webbing, .56 Wide		
RADIALS (2 EACH)	350 Lb Nylon Tape, 1.0 Wide		
SUSPENSION LINES	650 Lb Nylon Cord		

(a) TRIPLE-SELVAGE CLOTH
(b) LEADING EDGE ONLY

(c) LEADING AND TRAILING EDGE
(d) TRAILING EDGE ONLY
(e) NO. 1 THRU NO. 5 SAIL, DOUBLED,
CENTER OF GORE

PART NO.: R7661-503

TITLE: Parachute, 83.5 Ft D₀ Conical Ringsail

NO. GORES: 68

TYPE OF REEFING: Mid-Gore

ITEM	MATERIAL		
VENT LINES	650 Lb Nylon Cord		
VENT BAND	4000 Lb Nylon Webbing, 1.0 Wide		
RING NUMBER	CLOTH WEIGHT OZ/YD ² (a)	TAPE	
		P _r , LB	WIDTH, IN.
1	2.25	200 (b)	1.06
2	2.25	200 (c)	1.06
3	2.25	200 (c)	1.06
4	2.25	200 (c)	1.06
5 (75% Removed, Top)	1.1	200 (d)	1.06
6	1.1	90 (d)	.62
7	1.1	90 (d)	.62
8	1.1	90 (d)	.62
9	1.1	None	None
10	1.1	None	None
11	1.1	None	None
12	1.1	None	None
VERTICAL TAPE	90 Lb Nylon Tape, .62 Wide (e)		
SKIRT BAND	350 Lb Nylon Tape, 1.0 Wide 500 Lb Nylon Webbing, .56 Wide		
RADIALS (2 EACH)	350 Lb Nylon Tape, 1.0 Wide		
SUSPENSION LINES	650 Lb Nylon Cord		

(a) TRIPLE-SELVAGE CLOTH
(b) LEADING EDGE ONLY

(c) LEADING AND TRAILING EDGE
(d) TRAILING EDGE ONLY

PART NO.: R7661-505

TITLE: Parachute, 83.5 Ft D₀ Conical Ringsail

NO. GORES: 68

TYPE OF REEFING: Mid-Gore

ITEM	MATERIAL		
VENT LINES	650 Lb Nylon Cord		
VENT BAND	4000 Lb Nylon Webbing, 1.0 Wide		
RING NUMBER	CLOTH WEIGHT OZ/YD ² (a)	TAPE	WIDTH, IN.
1	2.25	200 (b)	1.06
2	2.25	200 (c)	1.06
3	2.25	200 (c)	1.06
4	2.25	200 (c) 90 (b)	1.06 .62
5 (75% Reinov'd Top)	1.1	200 (d, f,)	1.06
6	1.1	200 (d) 90 (d)	1.06 .62
7	1.1	200 (d) 90 (d)	1.06 .62
8	1.1	90 (d, f)	.62
9	1.1	None	None
10	1.1	None	None
11	1.1	None	None
12	1.1	None	None
VERTICAL TAPE	90 Lb Nylon Tape, .62 Wide (e)		
SKIRT BAND	1200 Lb Nylon Webbing, 1.0 Wide		
RADIALS (2 EACH)	350 Lb Nylon Tape, 1.0 Wide		
SUSPENSION LINES	650 Lb Nylon Cord		

(a) TRIPLE-SELVAGE CLOTH
(b) LEADING EDGE ONLY
(f) DOUBLED

(c) LEADING AND TRAILING EDGE
(d) TRAILING EDGE ONLY
(e) NO. 1 THRU NO. 5 SAIL, DOUBLED,
CENTER OF GORE

PART NO.: R7661-507

TITLE: Parachute, 83.5 Ft D_o Conical Ringsail

NO. GORES: 68

TYPE OF REEFING: Mid-Gore

ITEM	MATERIAL.		
VENT LINES	650 Lb Nylon Cord		
VENT BAND	4000 Lb Nylon Webbing, 1.0 Wide		
RING NUMBER	CLOTH WEIGHT OZ/YD ² (a)	TAPE	
1	2.25	P _r , LB	WIDTH, IN.
2	2.25	200 (b)	1.06
3	2.25	200 (c)	1.06
4	2.25	200 (c) 90 (b)	1.06 .62
5 (75% Removed, Top)	1.1	200 (d, f) 90 (b, f)	1.06 .62
6	1.1	200 (d) 90 (d)	1.06 .62
7	1.1	200 (d) 90 (d)	1.06 .62
8	1.1	90 (d, f)	.62
9	1.1	None	None
10	1.1	None	None
11	1.1	None	None
12	1.1	None	None
VERTICAL TAPE	90 Lb Nylon Tape, .62 Wide (e)		
SKIRT BAND	350 Lb Nylon Tape, 1.0 Wide 500 Lb Nylon Webbing, .56 Wide		
RADIALS (2 EACH)	350 Lb Nylon Tape, 1.0 Wide		
SUSPENSION LINES	650 Lb Nylon Cord		

(a) TRIPLE-SELVAGE CLOTH
(b) LEADING EDGE ONLY
(f) DOUBLED

(c) LEADING AND TRAILING EDGE
(d) TRAILING EDGE ONLY
(e) NO. 1 THRU NO. 5 SAIL, DOUBLED
CENTER OF GORE

PART NO.: R7661-509

TITLE: Parachute, 83.5 Ft D₀ Conical Ringsail

NO. GORES: 68

TYPE OF REEFING: Mid-Gore

ITEM	MATERIAL		
VENT LINES	650 Lb Nylon Cord		
VENT BAND	1200 Lb Nylon Tape, 1.0 Wide 4000 Lb Nylon Webbing, 1.0 Wide		
RING NUMBER	CLOTH WEIGHT OZ/YD ² (a)	TAPE	
		P _r , LB	WIDTH, IN.
1	2.25	200 (b)	1.06
2	2.25	200 (c)	1.06
3	2.25	200 (c)	1.06
4	2.25	200 (d) 350 (b)	1.06 1.00
5 (75% Removed, Top)	1.1	625 (d) 200 (b)	1.00 1.06
6	1.1	350 (d), 90 (b), 200 (f)	1.00, .62, 1.06
7	1.1	350 (d), 90 (b), 200 (f)	1.00, .62, 1.06
8	1.1	200 (d), 90(b), 200 (f)	1.06, .62, 1.06
9	1.1	90 (d)	.62
10	1.1	None	None
11	1.1	None	None
12	1.1	None	None
VERTICAL TAPE	90 Lb Nylon Tape, .62 Wide (c)		
SKIRT BAND	Doubled 1200 Lb Nylon Tape, 1.0 Wide		
RADIALS (2 EACH)	350 Lb Nylon Tape, 1.0 Wide		
SUSPENSION LINES	650 Lb Nylon Cord		

- (a) TRIPLE-SELVAGE CLOTH
- (b) LEADING EDGE ONLY
- (c) LEADING AND TRAILING EDGE
- (d) TRAILING EDGE ONLY
- (f) MID-RING CIRCUMFERENTIAL REINFORCEMENT
- (v) NO. 1 THRU NO. 5 SAIL, DOUBLED CENTER OF GORE

PART NO.: R7661-511

TITLE: Parachute, 83.5 Ft D_o Conical Ringsail

NO. GORES: 68

TYPE OF REEFING: Mid-Gore

ITEM	MATERIAL		
VENT LINES	650 Lb Nylon Cord		
VENT BAND	1200 Lb Nylon Tape, 1.0 Wide 4000 Lb Nylon Webbing, 1.0 Wide		
RING NUMBER	CLOTH WEIGHT OZ/YD ² (a)	TAPE	
		P _r , LB	WIDTH, IN.
1	2.25	200 (b)	1.06
2	2.25	200 (c)	1.06
3	2.25	200 (c)	1.06
4	2.25	200 (d) 350 (b)	1.06 1.00
5 (75% Removed, Top)	1.1	625 (d) 200 (b)	1.00 1.06
6	1.1	350 (d), 90 (b), 200 (f)	1.00, .62 1.06
7	1.1	350 (d), 90 (b), 200 (f)	1.00, .62, 1.06
8	1.1	200 (d), 90 (b), 200 (f)	1.06, .62, 1.06
9	1.1	90 (d)	.62
10	1.1	None	None
11	1.1	None	None
12	1.1	None	None
VERTICAL TAPE	90 Lb Nylon Tape, .62 Wide (e)		
SKIRT BAND	Doubled 1200 Lb Nylon Tape, 1.0 Wide		
RADIALS (2 EACH)	350 Lb Nylon Tape, 1.0 Wide		
SUSPENSION LINES	650 Lb Nylon Cord		

- (a) TRIPLE SELVAGE CLOTH
- (b) LEADING EDGE ONLY
- (c) LEADING AND TRAILING EDGE
- (d) TRAILING EDGE ONLY
- (e) NO. 1 THRU NO. 5 SAIL, DOUBLED
REINFORCEMENT
- (f) NO. 1 THRU NO. 5 SAIL, CENTER OF GORE

PART NO.: R7661-513

TITLE: Parachute, 83.5 Ft D_o Conical Ringsail

NO. GORES: 68

TYPE OF REEFING: Mid-Gore

ITEM	MATERIAL		
VENT LINES	650 Lb Nylon Cord		
VENT BAND	1200 Lb Nylon Tape, 1.0 Wide 4000 Lb Nylon Webbing, 1.0 Wide		
RING NUMBER	CLOTH WEIGHT OZ/YD ² (a)	TAPE	
1	2.25	P _r , LB	WIDTH, IN.
2	2.25	200 (b)	1.06
3	2.25	200 (c)	1.06
4	2.25	200 (d) 350 (b)	1.06 1.00
5 (75% Removed, Top)	1.1	625 (d) 200 (b)	1.00 1.06
6	1.1	350 (d), 90 (b), 200 (f)	1.00, .62, 1.06
7	1.1	350 (d), 90 (b), 200 (f)	1.00, .62, 1.06
8	1.1	200 (d), 90 (b), 200 (f)	1.06, .62, 1.06
9	1.1	90 (d)	.62
10	1.1	None	None
11	1.1	None	None
12	1.1	None	None
VERTICAL TAPE	90 Lb Nylon Tape, .62 Wide (e)		
SKIRT BAND	Doubled 1200 Lb Nylon Tape, 1.0 Wide		
RADIALS (2 EACH)	350 Lb Nylon Tape, 1.0 Wide		
SUSPENSION LINES	650 Lb Nylon Cord		

- (a) TRIPLE-SELVAGE CLOTH
- (b) LEADING EDGE ONLY
- (c) LEADING AND TRAILING EDGE
- (d) TRAILING EDGE ONLY
- (f) MID-RING CIRCUMFERENTIAL REINFORCEMENT
- (e) NO. 1 THRU NO. 5 SAIL, DOUBLED, CENTER OF GORE

PART NO.: R7661-515

TITLE: Parachute, 83.5 Ft D_o Conical Ringsail

NO. GORES: 68

TYPE OF REEFING: Mid-Gore

ITEM	MATERIAL		
VENT LINES	650 Lb Nylon Cord		
VENT BAND	1200 Lb Nylon Webbing, 1.0 Wide 4000 Lb Nylon Webbing, 1.0 Wide		
RING NUMBER	CLOTH WEIGHT OZ/YD ² (a)	TAPE	
		P _r , LB	WIDTH, IN.
1	2.25	200 (b)	1.06
2	2.25	200 (c)	1.06
3	2.25	200 (c)	1.06
4	2.25	200 (b) 350 (d)	1.06 1.00
5 (75% Removed, Top)	1.1	625 (d), 1200 (d) 200 (b)	1.00, 1.00, 1.06
6	1.1	350 (d), 90(b), 200 (f)	1.00, .62, 1.06
7	1.1	350(d), 90(b), 200 (f)	1.00, .62 1.06
8	1.1	200 (d), 90 (b) 200 (f)	1.06, .62, 1.06
9	1.1	1200 (d) (g) 90 (d)	1.00 .62
10	1.1	200 (d)	1.06
11	1.1	None	None
12	1.1	None	None
VERTICAL TAPE	90 Lb Nylon Tape, .62 Wide (e) Doubled		
SKIRT BAND	1200 Lb Nylon Tape, 1.0 Wide		
RADIALS (2 EACH)	150 Lb Nylon Tape, 1.0 Wide		
SUSPENSION LINES	650 Lb Nylon Cord		

(g) DOUBLED

(a) TRIPLE-SELVAGE CLOTH

(c) LEADING AND TRAILING EDGE

(b) LEADING EDGE ONLY

(d) TRAILING EDGE ONLY

(6) MID-RING CIRCUMFERENCE

(c) NO. 1 THRU NO. 5, SAIL, DOUBLED
CENTERED ON CODE

REINFORCEMENT

CENTER OF GORE

PART NO.: R 7661-517

TITLE: Parachute, 83.5 Ft D₀ Conical Ringsail

NO. GORES: 68

TYPE OF REEFING: Mid-Gore

ITEM	MATERIAL		
VENT LINES	650 Lb. Nylon Cord		
VENT BAND	1200 Lb. Nylon Webbing, 1.0 Wide 4000 Lb. Nylon Webbing, 1.0 Wide		
RING NUMBER	CLOTH WEIGHT OZ/YD ² (a)	TAPE	
1	2.25	P _r , LB 200(b)	WIDTH, IN. 1.06
2	2.25	200(c)	1.06
3	2.25	200(c)	1.06
4	2.25	200(b) 350(d)	1.06 1.00
5(75% Removed, Top)	1.1	625(d), 1200(d) 200(b)	1.00, 1.00, 1.06
6	1.1	350(d), 90(b), 200(f)	1.00, .62 1.06
7	1.1	350(d), 90(b), 200(f)	1.00, .62 1.06
8	1.1	200(d), 90(b) 200(f)	1.06, .62 1.06
9	1.1	1200(d) (g) 90(d)	1.00 .62
10	1.1	200(d)	1.06
11	1.1	None	None
12	1.1	None	None
VERTICAL TAPE	90 Lb. Nylon Tape, .62 Wide (e)		
SKIRT BAND	Doubled 1200 Lb. Nylon Tape, 1.0 Wide		
RADIALS (2 EACH)	350 Lb. Nylon Tape, 1.0 Wide		
SUSPENSION LINES	650 Lb. Nylon Cord		

- (a) TRIPLE-SELVAGE CLOTH
- (b) LEADING EDGE ONLY
- (c) DOUBLELED
- (d) TRAILING EDGE ONLY
- (e) MID-RING CIRCUMFERENTIAL REINFORCEMENT
- (f) NO. 1 THRU NO. 5. SAIL, DOUBLED CENTER OF GORE

PART NO.: R7661-519

TITLE: Parachute, 83.5 Ft. D₀ Conical Ringsail

NO. GORES: 68

TYPE OF REEFING: Mid-Gore

ITEM	MATERIAL		
VENT LINES	650 Lb. Nylon Cord		
VENT BAND	1200 Lb. Nylon Webbing, 1.0 Wide 4000 Lb. Nylon Webbing, 1.0 Wide		
RING NUMBER	CLOTH WEIGHT OZ/YD ² (a)	TAPE	
1	2.25	P _r , LB	WIDTH, IN.
2	2.25	200(b)	1.06
3	2.25	200(c)	1.06
4	2.25	200(b) 350(d)	1.06 1.00
5 (75% Removed Top)	1.1	625(d), 1200(d) 200(b)	1.00, 1.00, 1.06
6	1.1	350(d), 90(b), 200(f)	1.00, .62, 1.06
7	1.1	350(d), 90(b), 200(f)	1.00, .62 1.06
8	1.1	200(d), 90(b) 200(f)	1.06, .62 1.06
9	1.1	1200(d) (g) 90(d)	1.00 .62
10	1.1	200(d)	1.06
11	1.1	None	None
12	1.1	None	None
VERTICAL TAPE	90 Lb. Nylon Tape, .62 Wide (e)		
SKIRT BAND	Doubled 1200 Lb. Nylon Tape, 1.0 Wide		
RADIALS (2 EACH)	350 Lb. Nylon Tape, 1.0 Wide		
SUSPENSION LINES	650 Lb. Nylon Cord		

(g) DOUBLED

(a) TRIPLE-SELVAGE CLOTH

(c) LEADING AND TRAILING EDGE

(b) LEADING EDGE ONLY

(d) TRAILING EDGE ONLY

(f) MID-RING CIRCUMFERENTIAL
REINFORCEMENT

(e) NO. 1 THRU NO. 5, SAIL, DOUBLED,
CENTER OF GORE

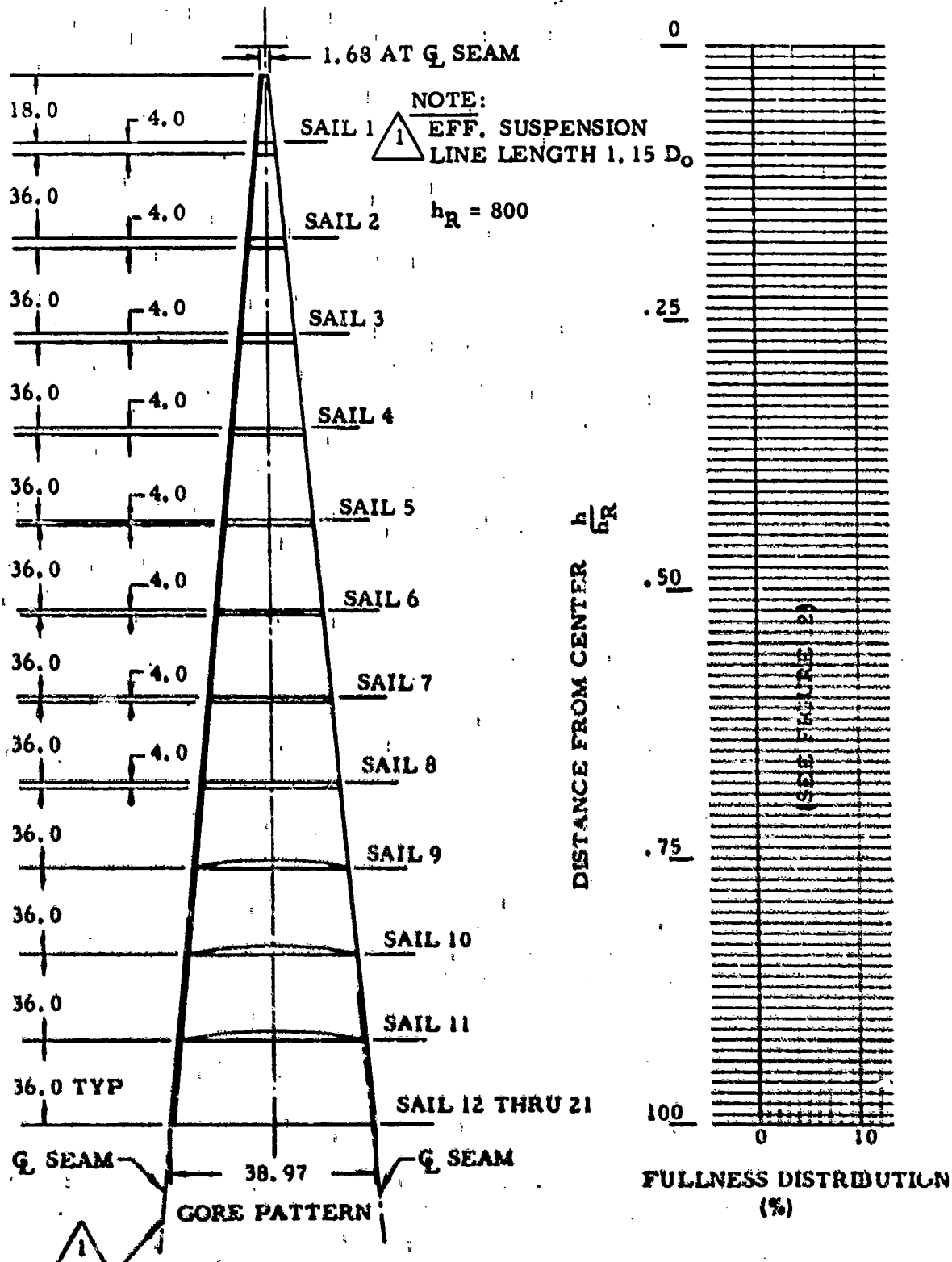


Figure 105. Gore Pattern and Fullness Distribution

R7811-1 128.8 ft D_0 Ringsail Parachute

PART NO.: R7811-1

TITLE: PARACHUTE, 128.8 ft D₀ RINGSAIL

NO. GORES: 112

TYPE OF REEFING: RADIAL

ITEM	MATERIAL		
VENT LINES	550 lb NYLON CORD		
VENT BAND	4000 lb NYLON WEBBING, 1.0 WIDE		
RING NUMBER	CLOTH WEIGHT OZ/YD ² (a)	TAPE	
		P _r , LB	WIDTH, IN.
1	2.25	200 (b)	.1.0
2	2.25	200 (c)	.1.0
3	2.25	200 (c)	.1.0
4	2.25	90 (c)	.62
5	2.25	90 (c)	.62
6	1.6	90 (c)	.62
7	1.6	90 (c)	.62
8	1.6	90 (c)	.62
9	1.1	1000 (d, e)	.50
10	1.1	70 (d)	.62
11 AND 12	1.1	70 (d)	.62
13 THRU 21	1.1	70 (d)	.62
VERTICAL TAPE	90 lb NYLON TAPE, .62 WIDE (e)		
SKIRT BAND	1000 lb NYLON WEBBING, .5 WIDE		
RADIALS (2 EACH)	300 lb NYLON TAPE, 1.0 WIDE		
SUSPENSION LINES	550 lb NYLON CORD		

(a) TRIPLE-SELVAGE CLOTH
 (b) LEADING EDGE ONLY
 (c) CIRCUMFERENTIAL REIN-
 FORCEMENT

(c) LEADING AND TRAILING EDGE
 (d) TRAILING EDGE ONLY
 (e) NO. 1 THRU NO. 9 SAIL DOUBLED,
 CENTER OF GORE

APPENDIX B

SPECIAL RINGSAIL PARACHUTE APPLICATIONS

Modified Ringsail parachute designs were developed for applications other than the Apollo ELS cluster. Development of the "Glidesail" steerable version was initiated in 1960 when interest in the potential utility of a controllable gliding parachute was beginning to gain momentum. In 1967 the Ringsail parachute design was adapted to the need for an aerial pickup target canopy of good efficiency and positive opening characteristics. About the same time the NASA Langley Research Center developed a new Ringsail design with a wide peripheral slot (similar to the Disc-Gap-Band parachute) for the Planetary Entry Parachute Program. The salient characteristics of these parachutes are summarized in the following sections.

1.0 The Glidesail Steerable Parachute

The Glidesail parachute was conceived as a minimal modification of the Ringsail design to produce a fully dirigible parachute having a maximum ratio of lift to drag in the range of 0.5 to 1.0. It was one of the first new gliding parachute designs to provide for L/D control from zero to maximum. In this respect it was an improvement over its steerable contemporaries, most of which had fixed built-in glide ratios between 0.3 and 0.5.

The Glidesail control system, for which a patent was applied in June 1961 and granted in January 1964 (Patent No. 3,117,753), consisted of a broad trailing edge flap having in the final configuration a radial depth above the skirt of $0.15 D_0$ and spanning .37N to .4N gores. The group of suspension lines on the flap were attached to a common control riser. Steering was effected by retracting suspension lines on either side of the canopy which caused the Glidesail to turn by shifting the system center of gravity. The parachute was deployed with the flap fully retracted so that all suspension lines would be of equal length through the opening transient. After the system reached a steady descent condition, the flap control riser was extended to initiate glide.

One of the 63 ft D_0 Glidesail models is shown in Figure 196 descending in full glide with flap extended. The NASA-sponsored development program reported in Reference 17 included tethered control tests of a variety of 18 ft D_0 models in the AMES 40 x 80 wind tunnel and aerial drop tests of 36 ft D_0 and 63 ft D_0 models with a radio-controlled test vehicle. One test was also performed with a cluster of three canopies secured together in a delta configuration of which only two were Glidesails. The leading canopy was a standard Ringsail inherited from the Mercury program. All of the test

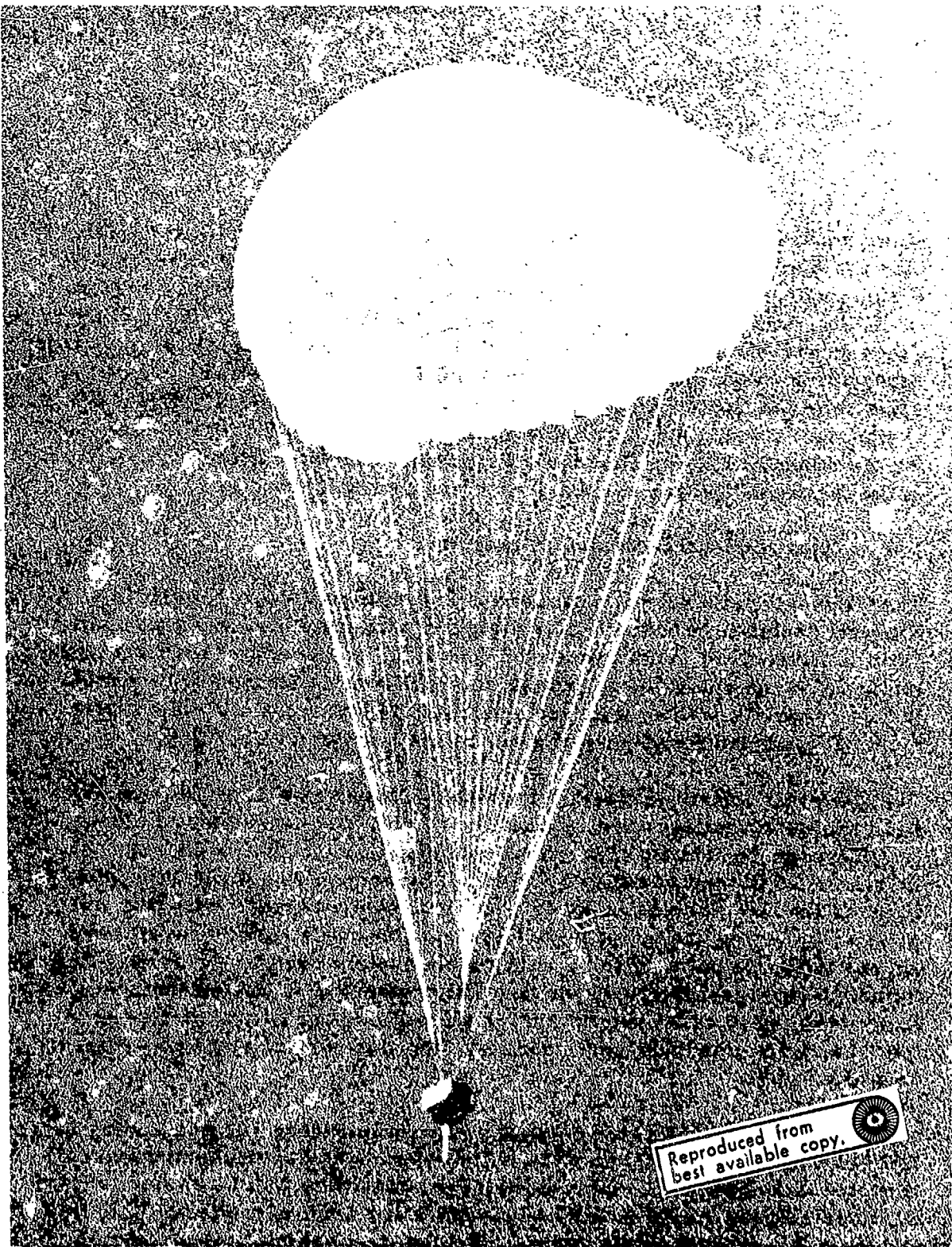


Figure 106. 63 ft D_0 Glidesail Parachute Gliding at
 L/D (max) ~ 0.7 with 2580 pounds

specimens were made from standard parachute cloth and most of them had an effective suspension line length of $0.8 D_o$. Because the test instrumentation was not adapted for cancelling the effect of wind except when a straight course was flown, only rough L/D measurements were obtained. The reported performance is presented in Table XXVII.

TABLE XXVII
MEASURED GLIDESAIL PERFORMANCE

System Configuration	Single	Single	Cluster of 3
Glidesail, D_o (ft)	36.	63	63
Descent weight, (lb)	184	2580	2750
Rate of descent, (fps)	15.0	29.5	18.0
Average Turning Rate, (deg. /sec.)	-	4	5
Control riser extension	.125 D_o	.125 D_o	.120 D_o
Average L/D	~ .4	~ .7	~ .6

Once the glide had been initiated, system stability during the descent was excellent, pendular oscillations being imperceptible.

One of the major program objectives was to produce a controllable gliding parachute as a minimum modification of the Ringsail in order to gain full benefit from the demonstrated high opening reliability of the Ringsail design. This objective was attained, but the design goal of $L/D = 1.0$ was not. Subsequent experience taught that the use of low porosity cloth in the major area of the canopy around the ringslot crown probably would have enabled attainment of the design goal.

2.0 The Ringsail Aerial Pickup Target

The canopy of the Ringsail aerial pickup target parachute is of standard design. As shown in Figure 107 the modification required to adapt it for the annular parachute aerial recovery system consists of an added set of multiple suspension lines attached to the apex of the annular canopy. The target parachute also carries an interwoven web of heavy reinforcements for transmission of the engagement and pickup loads through the annular

specimens were made from standard parachute cloth and most of them had an effective suspension line length of $0.9 D_o$. Because the test instrumentation was not adapted for cancelling the effect of wind except when a straight course was flown, only rough L/D measurements were obtained. The reported performance is presented in Table XXVII.

TABLE XXVII
MEASURED GLIDESAIL PERFORMANCE

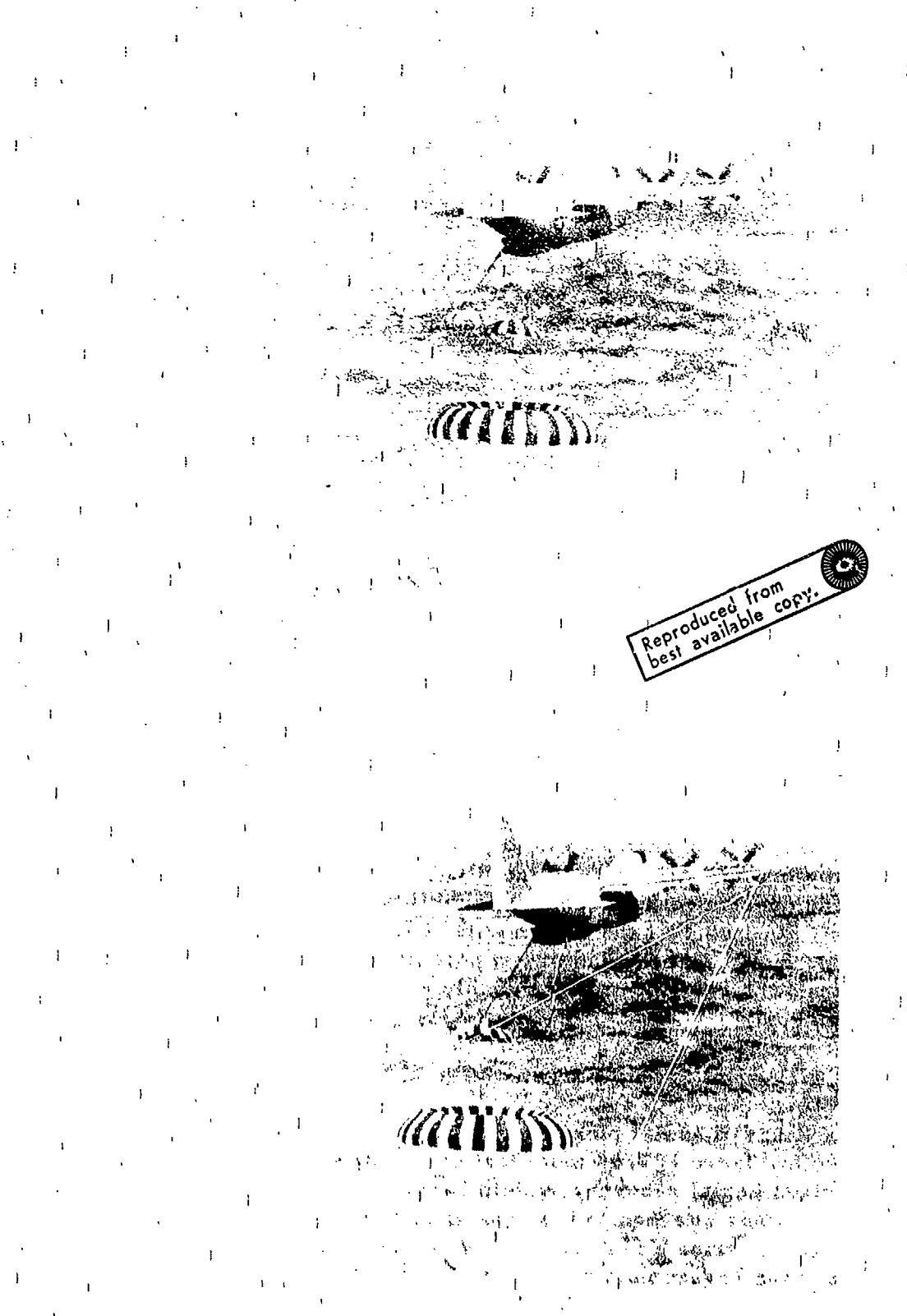
System Configuration	Single	Single	Cluster of 3
Glidesail, D_o (ft)	36	63	63
Descent weight, (lb)	184	2580	2750
Rate of descent, (fps)	15.0	29.5	18.0
Average Turning Rate, (deg. / sec.)	-	4	5
Control riser extension	$.125 D_o$	$.125 D_o$	$.120 D_o$
Average L/D	~ .4	~ .7	~ .6

Once the glide had been initiated, system stability during the descent was excellent, pendular oscillations being imperceptible.

One of the major program objectives was to produce a controllable gliding parachute as a minimum modification of the Ringsail in order to gain full benefit from the demonstrated high opening reliability of the Ringsail design. This objective was attained, but the design goal of $L/D = 1.0$ was not. Subsequent experience taught that the use of low porosity cloth in the major area of the canopy around the ringslot crown probably would have enabled attainment of the design goal.

2.0 The Ringsail Aerial Pickup Target

The canopy of the Ringsail aerial pickup target parachute is of standard design. As shown in Figure 107 the modification required to adapt it for the annular parachute aerial recovery system consists of an added set of multiple suspension lines attached to the apex of the annular canopy. The target parachute also carries an interwoven web of heavy reinforcements for transmission of the engagement and pickup loads through the annular



A black and white aerial photograph showing a large, dark, rectangular target canopy suspended from a aircraft. The canopy has a distinct wavy or undulating pattern across its surface. The aircraft's wing and engine are visible on the left side of the frame. The background is a bright, textured sky.

Reproduced from
best available copy.

Figure 107. Aerial Engagement of 17.5 ft D₀ Ringsail Target Canopy on 42 ft D₀ Annular Parachute with 800 Lb Dummy Payload

parachute to the payload. The number of suspension lines of the target parachute is equal to the number of lines on the annular parachute, while the ratio of the number of gores in the two canopies is made either 1/2 or 1/3, depending on the relative size. Thus, the Ringsail target parachute has either two or three suspension lines attached to the skirt of the canopy at each radial seam. This attachment is made to a loop formed by turning back the ends of the double radial tapes, each line-end being bent through the loop and inserted back into itself to form the familiar Chinese finger trap splice.

Because the length of the suspension lines is determined by the relative sizes of target and annular canopies, the effective lengths of the Ringsail target rigging varied from $l_e/D_o = .76$ to 1.49 during the development program reported in Reference 4. One of the unique advantages of this type of parachute system is that the target canopy is used first as a drogue (either reefed or nonreefed) to decelerate the system to a low velocity for opening of the nonreefed annular canopy. During the drogue working interval the suspension line confluence is retained by a temporary keeper formed by the upper end of the sleeve in which the annular canopy is deployed. A pair of standard reefing line cutters is used to release this keeper a predetermined time interval after the deployment bag has been stripped off.

The information obtained from the system development tests provides the only data available on the performance of small, heavily loaded Ringsail parachutes. In the majority of the tests the equilibrium descent velocity at the end of the "drogue" working interval fell between 53 and 93 fps (EAS); the corresponding unit canopy loadings were in the range of $W/C_{DS_o} = 3.5$ to 10.3 psf. Measured drag coefficients and opening load factors of these parachutes are included in Figures 22 and 28 respectively. The data presented in Table XXVIII are representative of the best performance of the four different models tested. To insure structural integrity for the test program these Ringsails were made of the conservative "mid-weight" construction incorporating pickup reinforcements of 9000 lb 1 inch webbing and 10,000 lb braided cord.

3.0 The Modified Ringsail Parachutes of the PEPP Program

During the Planetary Entry Parachute Program conducted by the NASA Langley Research Center (Reference 18) a modified Ringsail parachute design was subjected to several tests at speeds up to Mach 2.9 and altitudes in excess of 120,000 feet. Experimental models having nominal diameters of 31.2, 40, and 54.5 feet were tested. These parachutes were deployed nonreefed at dynamic pressures in the range of 9 to 12 psf. Total geometric

TABLE XXVIII
RINGSAIL TARGET PARACHUTE PERFORMANCE AS A
DROGUE IN THE UAR SYSTEM

(Symbol) D_o - (ft)	□ 17.5	◇ 23.0	△ 28.5	▷ 34.0	
Number of gores	20	20	30	30	
Number of lines	60	60	60	60	
Rigging (l_e/D_o)	1.49	1.13	.91	.76	
Reefing $(\%/D_o)$	31	24	24	17.6	
Test No.	6	7	5	9	
Descent weight, (lb)	1779	1835	2010	2090	
Altitude, (ft)	15800	16000	16100	12560	
q_s (psf)	44.3	48.3	47.9	41.1	
Opening Loads: Reefed, (lb)	3940	3010	5660	5000	
Disreef, (lb)	5270	5410	7110	7500	
C_K :					
Reefed	.97	.80	.70	.76	
Disreef	1.52	.79	1.35	.91	
W/C _D S:					
Reefed, (psf)	20.0	23.6	11.8	13.0	
F.O., (psf)	10.3	6.3	4.5	3.6	
v_e	fps (EAS)	92.6	72.8	60.3(1)	54.0
C_{D_o}		.72	.70	.66(2)	
Parachute weight* (lb)	27.0	30.4	34.8	41.0	

NOTE: (1) Averages for 4 tests (2) Averages for 2 tests

*Includes canopy and lines of "mid-weight" construction and pickup reinforcements.

porosities were typically about 13% S_o , most of which (9% S_o) was concentrated in a wide slot near the periphery of the inflated canopy as shown in Figure 108.

This modification was derived from the Disc-Gap-Band parachute configuration developed by LRC in an attempt to produce a parachute system that would be reasonably stable in very low density air corresponding to conditions expected on the planet Mars. Although the PEPP Ringsail's subsonic performance as a parachute was mediocre, both its subsonic and supersonic performance appeared to be better than that of the DGB. Degradation of parachute performance in supersonic flow is expected, but the poor showing of the PEPP parachutes subsonically can be attributed to faulty aerodynamic shaping of the skirt area below the peripheral slot.* In operation the canopies inflated to the peripheral slot, while the skirt annulus, functioning like an extension of the suspension lines, contributed little more than skin friction to total drag. This fault could have been corrected.

*With reference to Modified Ringsail and DGB only; the Cross designs tested were disqualified earlier for even poorer performance.

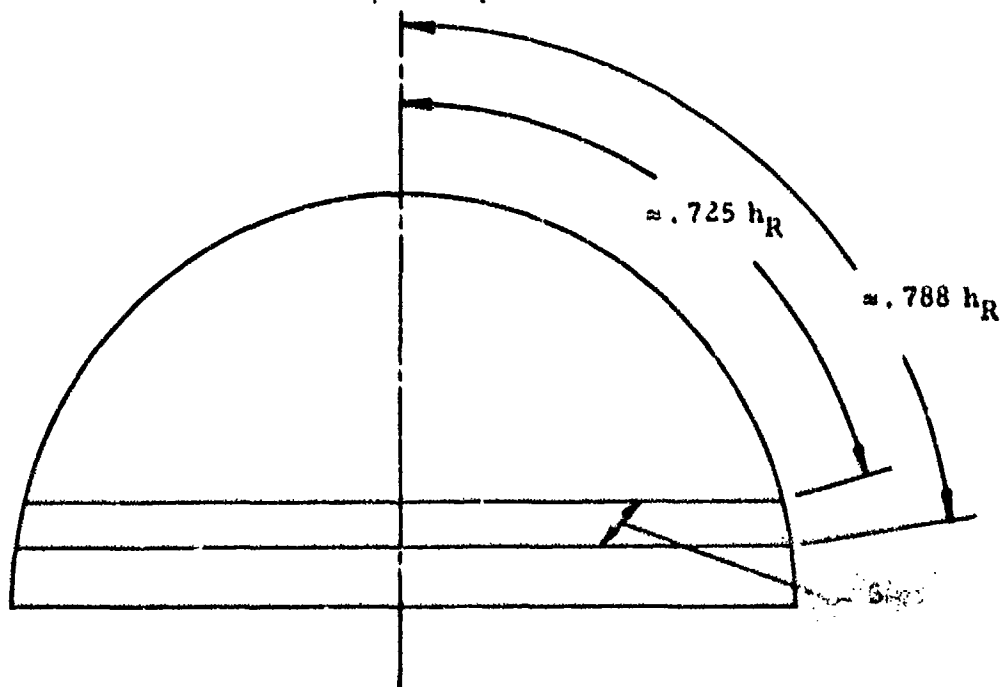


Figure 108. Schematic of the PEPP Ringsail
(40 ft D_o)

Deployed supersonically these parachutes exhibited high opening shock ($C_K = .92 - 1.05$ nonreefed) followed by severe longitudinal pulsations and load fluctuations as shown comparatively in Figure 109. The crown geometric porosity of the Ringsail models was too low, and the roof porosity of the DGB was even lower, the latter due in part to operation at a supercritical differential pressure across the cloth pores. Experience with supersonic drogues would suggest the need for more geometric porosity in the canopy roof than in the sidewalls. In the DGB configuration the effective sidewalls would be an annulus of the canopy roof above the peripheral slot, the cylindrical band functioning more as a brake on canopy opening.

The difference between the constructed shapes of the two canopies in the skirt area is reflected in their filling rates, comparison of dimensionless filling intervals showing the filling distance of the modified Ringsail with flared skirt to be 75 to 80 percent that of the DGB with cylindrical skirt (at the same Mach number). Significant contribution of the Planetary Entry Parachute Program was the finding reported in Reference 18 that the parachute filling distance increased with Mach number (see Figure 58, Section 6.2.5). This is accounted for by the effect of compressibility on the air inflow rate, the canopy volume to be filled remaining essentially constant.

Subsonic drag coefficient measurements were subject to considerable uncertainty; average values obtained for each different model are presented in Table XXIX.

TABLE XXIX
PEPP MEASURED DRAG COEFFICIENTS

Modified Ringsail		Disc-Gap-Band	
D_0 (ft)	C_{D_0}	D_0 (ft)	C_{D_0}
31.2	.55	30.0	.52
40.0	.62	40.0	.53
54.5	.60	40.0	.48
		64.7	.58

NOTE: C_{D_0} is based on S_0 computed with slot area included

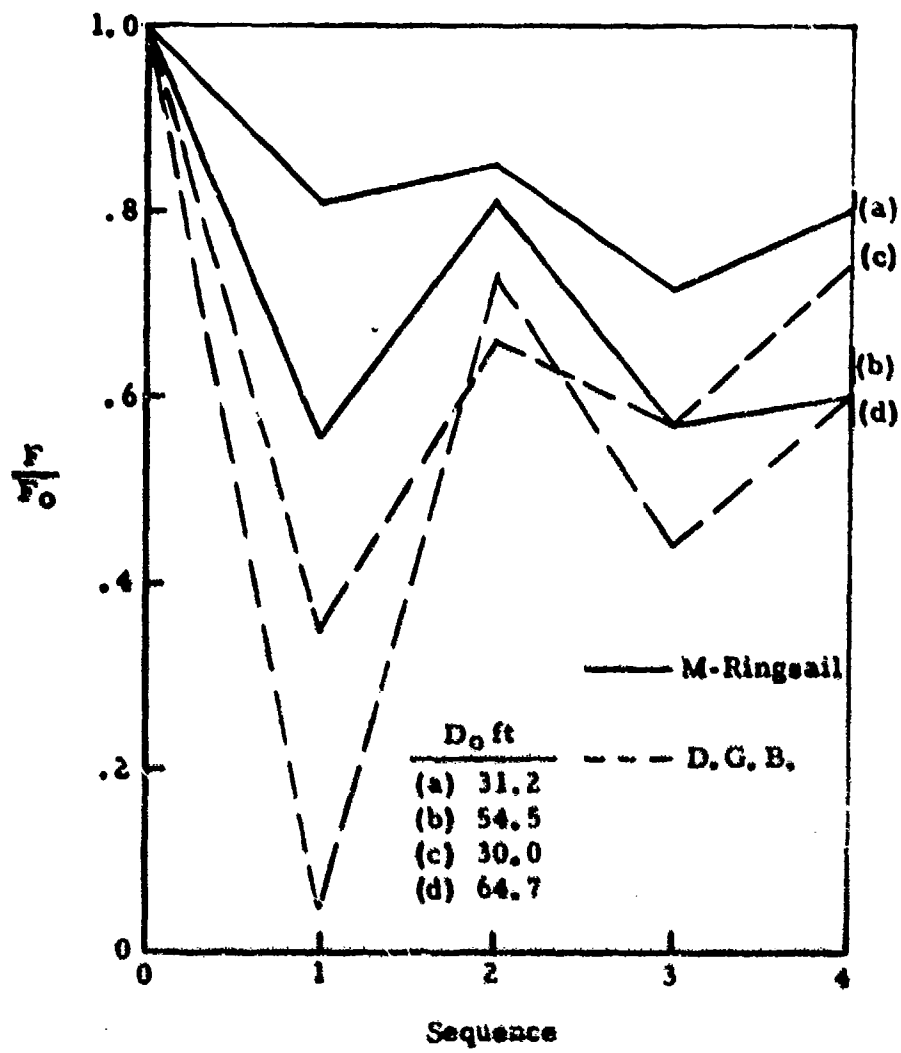


Figure 109. Opening Load Fluctuations of PEPP Parachutes Following Line Stretch at Mach 1.4 - 1.6

The difference between the small and large models may indicate a scale effect, but probable errors are large. The low drag coefficients of these Ringsail models, allowing for the wide peripheral slot, indicates a design problem. For parachutes larger than 48 ft D_0 , a drag coefficient of less than $C_{D_0} = 0.70$ would normally be considered unacceptable.

APPENDIX C

SAMPLE DESIGN PROBLEM

Ringsail parachute design procedures are clarified by a practical numerical example based on the requirements for recovery of a 2340 lb vehicle. The maximum allowable rate of descent at 5000 ft MSL is 33 fpm. Because a high rate of deceleration is desired to ensure safe recovery at very low altitudes, the maximum allowable opening load factor is 5.5 g in level flight. The parachute is to be deployed at 225 KEAS by a forcibly ejected pilot chute aided, if necessary, by an ejector bag under the pack. The installed weight and volume shall be a minimum compatible with the most advanced state of the art.

The canopy area required is derived by aerodynamic analysis as follows:

- To allow for the normal variation in the observed rate of descent of parachute systems let the design rate of descent be

$$v_e = 33 / 1.06 = 31.1 \text{ fpm} \quad (\text{rule of thumb})$$

- The equivalent rate of descent at sea level

$$v_e = 31.1 / 1.077 = 28.9 \text{ fpm} \quad (\sigma^{-1/2} = 1.077)$$

- The equilibrium dynamic pressure

$$q_e = 1.0 \text{ psf}$$

- The required effective drag area

$$C_D S_0 = W/q_e = 2340 \text{ ft}^2$$

- For $L_e/D_0 = 1.15$ and $v_e = 29 \text{ fpm}$

$$C_{D_0} = 0.81 \quad (\text{Figure 22})$$

- The canopy area

$$S_0 = C_D S_0 / C_{D_0} = 2882 \text{ ft}^2$$

The following steps are numbered to conform with Section 5.1

Ringsail Basic Dimensions

1. Nominal diameter: $D_0 = 60.6 \text{ ft}$
2. Number of gores: $N = 46 \text{ to } 53$

From the loads analysis:

$$F_{LIM} = 5.5 W \text{ max.}$$
$$= 13,000 \text{ lbs}$$

From the structural analysis:

$$(D.F.) F_{LIM} = 24,700 \text{ lbs}$$

$$N_R = 4 \text{ (risers)}$$

$$P_R = 550 \text{ lbs (suspension line cord)}$$

$$\text{For } N = 48 \quad N P_R = 26,400 \text{ lbs}$$

and the ratio $N P_R / (D.F.) F_{LIM} = 1.068$ is satisfactory.

3. Length of suspension lines:

effective length $l_e = 1.15 D_0 = 70 \text{ ft}$ (to the nearest foot)

let risers $l_R = 3 \text{ ft}$

line length $l_e = 67 \text{ ft}$

4. Gore height $h_g = .519 D_0 = 377 \text{ inches}$

5. Area of crown ventilation:

$$\lambda_{gc} = 2.75\% S_0 \quad (\text{from Figure 21})$$

$$S_{gc} = 79.3 \text{ ft}^2$$

Vertical tapes on gore centerlines crossing the crown slots will be used.

6. Woven width of cloth: $h_w = 36 \text{ inches}$

To conform with best practice for Ringsails of $D_0 = 56 \text{ feet and larger}$

7. Vertical spacing of sails in the gore:

- a) First approximation:

$$\text{Number of sails in gore: } h_R/h_w = 10.5$$

$$n = 10$$
$$n_f = 9$$

Number of ring slots: $(.4 h_R / h_w) - 1 = 3.2$

$$n_g \approx 3$$

Vent height: $h_v = 15$ to 22 inches

Start with $h_v = 18$ inches

Slot width dimension (Δh_g):

Estimate position of mean slot as shown in Sketch (a) Figure 110.

$$.4 h_R = 151 \text{ in.}$$

$$h_g = (.4 h_R - h_v)/2 + h_v = 84.5 \text{ in.}$$

Length of mean slot:

$$\bar{C}_g = 6.44 (h_g/N) \sin(h_g/h_R) 54^\circ \text{ (per Figure 12)}$$

$$h_R/N = 7.86$$

$$h_g/h_R = 84.5/377$$

$$\bar{C}_g = 6.44 (7.86) \sin 12.1^\circ$$

$$= 50.6 (.209) = 10.6 \text{ in.}$$

Open area per gore:

Neglect area covered by radials and vertical tapes.

$$\frac{\Sigma S_{gc}}{N} = 238 \text{ in.}^2 \quad (\Sigma S_{gc} \text{ from step 5})$$

Estimated area of vent sector = 18 in.²

Area of mean slot per gore:

$$\frac{S_g}{6} = (238-18)/3 = 73 \text{ in.}^2$$

Approximate slot width:

$$\Delta h_g = 73/10.6 = 6.9 \text{ in.}$$

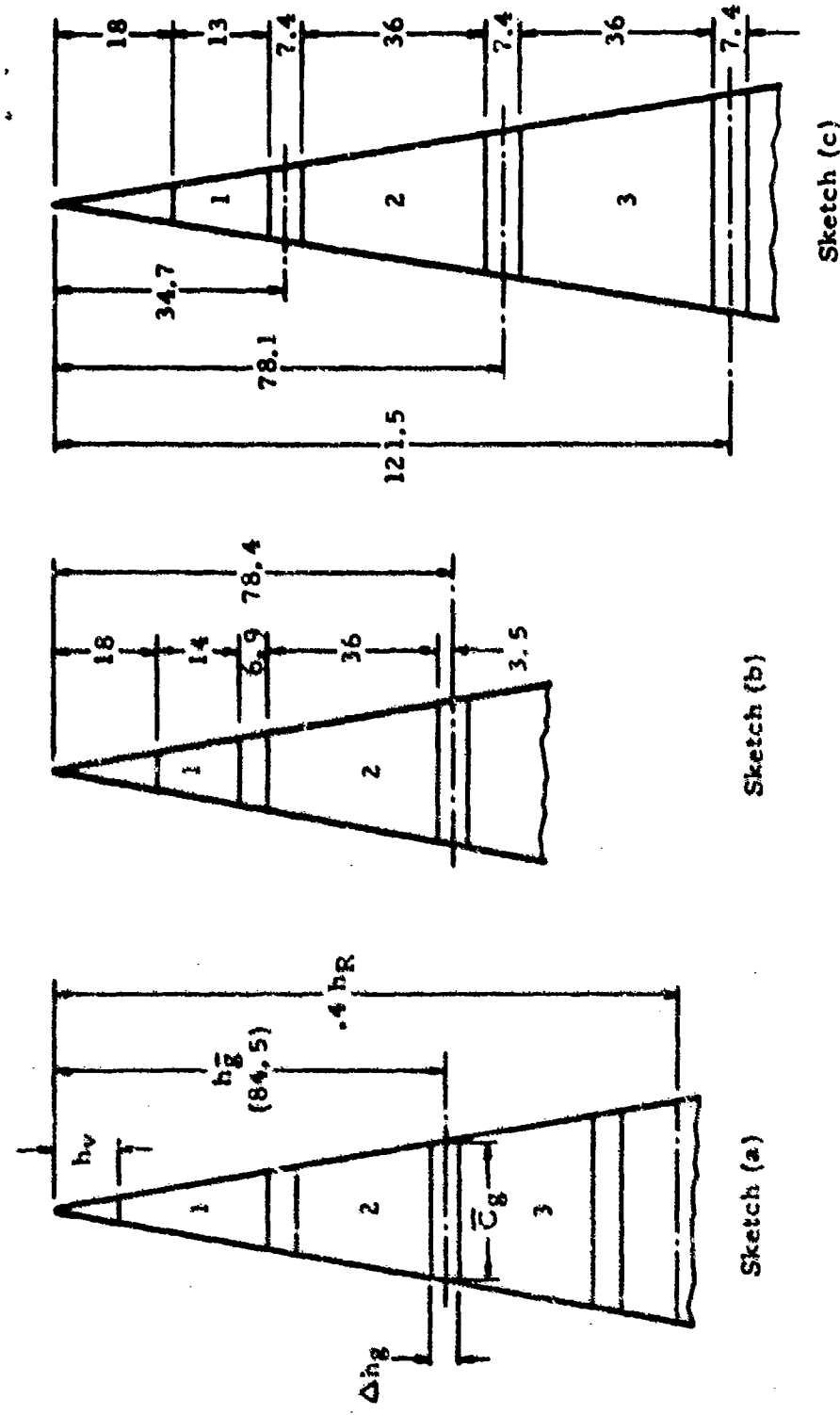


Figure 110. Trial Gore Layouts of Crown Ventilation per Gore

Check width of sail No. 1

$$n_F h_w = 324 \text{ in.}$$

$$n_g \Delta h_g = 20.7 \text{ in.}$$

$$h_v = \underline{18} \text{ in.}$$

Total 362.7 in

$$h_1 = 377 - 363 = 14 \text{ in.}$$

b) Second approximation:

The dimensional adjustment needed may be deduced from the size and position of the mean slot in Sketch (b) Figure 110.

Since the radial position is less than estimated the slot area also will be less. Try increasing the slot width to

$$\Delta h_g = 6.9 (84.5/78.4) = 7.4 \text{ in.}$$

Then

$$n_g \Delta h_g = 22.2 \text{ in.}$$

and

$$h_1 = 377 - 364 = 13 \text{ in.}$$

The crown geometric porosity of the adjusted layout shown in Sketch (c) is now checked by the calculations summarized in Table XXX.

Note that $C_g = 6.44 (h_R/N) \sin\phi = 50.6 \sin\phi$; rough slide rule accuracy is adequate. (Figure 12)

$$\Sigma S_{gc} = 239 (48)/144 = 79.6 \text{ ft}^2$$

- c) The result is very close to the design value from step 5 above. Therefore, a third approximation is not required. Since the vent dimension was not changed, no size check is needed here.

TABLE XXX
SUMMARY OF CROWN GEOMETRIC POROSITY

Slot No.	h^* (in.)	$\frac{h}{h_R}$	$\phi = \sin^{-1} \left(\frac{h}{h_R} \right) 54^\circ$	$\sin \phi$	C_g (in.)	Δh (in.)	Area (in. 2 /gore)
(Vent)	9	.024	1.3	.023	1.16	18	21
1-2	34.7	.092	5.0	.087	4.40	7.4	33
2-3	78.1	.207	11.2	.194	9.92	7.4	73
3-4	121.5	.322	17.4	.299	15.1	7.4	112

Per gore Total 239 in. 2

* Per Figure 110 (C).

8. Gore Coordinates: $C = 50.6 \sin \left(\frac{h}{h_R} \right) 54^\circ$

9. Fullness factors: Read K_A & K_B from Figure 54

10. Sail widths: $C_A = K_A C; C_B = K_B C$

11. Verification of canopy area and nominal diameter:

The calculations required for steps 8 through 11 are summarized in Table XXXI. The sample calculations were carried out with a 24-inch slide rule. However, use of a desk computer and four-place table of trigonometric functions is recommended.

The total area of the slots and sails in one gore is obtained from the last column in Table XXXI.

Area = 8669 in. 2 per gore

$$S_o = (8669/144) 43 = 2890 \text{ ft}^2$$

$$D_o = 60.65 \text{ feet}$$

TABLE XXXI
CANOPY DIMENSIONAL CALCULATIONS ($N = 48$ GORES)

Soil No.	Δh (in)	h (in)	$\frac{h}{h_r}$	ϕ (degrees)	$\sin \phi$	C (in)	K_A	$\frac{C_A}{C_B}$	C (in)	A_{proj} (in 2)
(Vent)							K_B			
1	13	18	.0478	2.58	.0450	2.280	1.055	2.41	1.2	21.6
	31	.0823	4.45	.0777	3.931	1.052	4.14	3.28	42.7	
(slot)	7.4								4.63	34.2
2	36	38.4	.1020	5.51	.0962	4.870	1.050	5.11	7.43	267.3
	74.4	.1975	10.67	.1853	9.380	1.040	9.75			
(slot)	7.4								10.21	75.5
3	36	81.8	.2170	11.71	.2030	10.28	1.036	10.67		
	17.8	.3125	16.89	.2907	14.71	1.029	15.15	12.91	465	
(slot)	7.4								15.13	112
4	36	125.2	.3321	17.95	.2907	14.71	1.027	15.11		
	161	.427	23.09	.392	19.83	1.017	20.16	17.64	635	
(slot)	7.4									
5	36	161	.427	22.09	.3920	19.83	1.017	20.16		
	197	.523	28.26	.4735	23.97	1.018	25.89	23.03	829	
(slot)	7.4									
6	36	197	.523	28.26	.4735	23.97	1.008	24.12		
	233	.618	33.39	.5502	27.85	1.008	30.10	27.11	976	
(slot)	7.4									
7	36	233	.618	33.39	.5502	27.85	1.00	27.85		
	269	.714	38.58	.6235	31.53	1.008	34.06	30.96	1114	
(slot)	7.4									
8	36	269	.714	48.58	.6235	31.53	1.00	31.53		
	305	.809	43.70	.6999	34.96	1.008	37.79	34.66	1247	
(slot)	7.4									
9	36	305	.809	43.70	.6909	34.96	1.00	34.96		
	341	.905	48.90	.7536	38.12	1.008	41.20	38.08	1370	
(slot)	7.4									
10	36	341	.905	48.90	.7536	38.12	1.00	38.12		
	377	1.000	54.00	.8090	40.93	1.008	44.20	41.16	1480	
(h_r)										

Note:   No need to carry fractions of inches beyond this point
From Figure 54

The final crown geometric porosity is

$$\Sigma S_{gc} = (244.3/144) 48 = 81.4 \text{ ft}^2$$

$$\lambda_{gc} = 2.816 \% S_o$$

This is slightly greater than the previous calculation due to a small increment added by the fullness factors.

The finished vent diameter with $C_v = 2.28$ in. is

$$D_v = 48 (2.28)/\pi = 34.80 \text{ inches}$$

and $S_v = 952 \text{ in.}^2 = 6.60 \text{ ft}^2$
 $= .00228 S_o$

Note also that the slot between sails 4 and 5 has no differential fullness because it falls in the region above $h/h_R = 0.45$ (Figure 54). This coincidence seldom happens but is harmless. The effective area of the slot is not zero but is less than it would be normally. Although the transition point on the diagram can be treated flexibly as a band between $h/h_R = 0.4$ and 0.5, no corrective adjustment is called for because, in this area of the canopy, strength is more important than porosity. The designer could elect the option of adding a fourth ringslot to the canopy at this point, reducing the width of all accordingly.

12. Sail pattern dimensions (Table XXXII)

Add 1.6 inches to C_A and C_B

Add 2.0 inches to h_1

TABLE XXXII
SAIL PATTERN DIMENSIONS

Sail No.	H	A	B
1	15.0	3.74	5.74
2	36.5	6.71	11.35
3		12.27	16.75
4			
5		(etc.)	(etc.)
6	△		
7			
8			
9			
10	36.5	39.72	45.8

Note: △ The cloth is woven 36.5 ± 0.5 inches

Calculation of the sail pattern dimensions is not essential to the preliminary design analysis and can be deferred until prototype fabrication drawings are needed.

Selection of Materials

Assign design factors that are compatible with the desired safety factors and a parachute structure of minimum weight:

Component	Canopy	Lines	Risers
Let S.F. =	1.5	1.5	2.0
Use D.F. =	1.9	1.9	2.5

The design limit load from the loads analysis is the same for both opening stages

$$F_{LIM} = F_R = F_0 = 13,000 \text{ lbs}$$

The reefed opening load is for a canopy reefed with a skirt line diameter $D_R = 9.5\% D_0$ (radial reefing) for which

$$\begin{aligned} C_{DSR} &= .054 C_{DS_0} && (\text{Figure 47b}) \\ &= 126 \text{ ft}^2 \end{aligned}$$

$$C_{D_p} = .65 \quad (\text{Figure 55b})$$

$$\begin{aligned} \text{and } S_p &= 194 \text{ ft}^2 \\ D_p &= 15.7 \text{ ft} \end{aligned}$$

Canopy cloth: $P'_R = 1.9 T_c$

$$T_c = 13,000/\pi D_p$$

In the crown when reefed:

$$\begin{aligned} T_c &= 13,000/\pi (15.7) \\ &= 264 \text{ lb/ft} = 22 \text{ lb/in.} \\ P'_R &= 41.8 \text{ lb/in.} \end{aligned}$$

Although the possibility of employing 1.1 oz. cloth with $P_R = 42$ lb/in. is indicated, this likely would be marginal in a canopy of this size due to the relatively high dynamic pressure (172 psf) at deployment.

Therefore, use 1.6 oz./yd² ripstop cloth with $P_R = 50$ lb/in.

The crown area to be covered with the heavy cloth is estimated for $D_p = 15.7$ ft.

$$h_c = (\pi/4) 15.7 (12) = 148"$$

Although this extends into ring 4 (Table XXXI) only rings 1, 2, and 3 need be made of the selected cloth, because the unit load in ring 4 is much less than T_c near the vent.

Checking a transition annulus of:

$$D_{p_2} = (4/\pi) .5 (377/12) = 20 \text{ ft} \quad (\text{Equation 24})$$

$$\begin{aligned} T_c &= 13,000/\pi(20) = 207 \text{ lb/ft} \\ &= 17.2 \text{ lb/in.} \end{aligned}$$

$$P'_R = 1.9 (17.2) = 32.8 \text{ lb/in.}$$

Therefore, over the balance of the canopy (rings 4 through 10) 1.1 oz. ripstop with $P_R = 42$ lb/in. will be used.

Suspension lines and vent lines:

$$P'_R = 1.9(13,000)/48 = 515 \text{ lbs}$$

Use 550 braided nylon cord

Radial tapes:

$$P'_R = 0.9 (515)/2 = 232 \text{ lbs}$$

Use 300 lb 1 inch nylon tape

(A 250 lb 1 inch tape would be a better choice if such were available.)

Mid-Canopy Circumferential Band:

Assume: $S_p = .7 S_{p_0}$

$$\text{and } D_p = 1.1 (4 S_p / \pi)^{1/2} \quad (\text{Equation 71 Section 6})$$

$$S_{p_0} = (2/3)^2 S_0 = 1284 \text{ ft}^2$$

$$S_p = 900 \text{ ft}^2 \quad D'_p = 33.9 \text{ ft} \quad (\text{unstretched})$$

$$D_p = 1.1 D'_p = 37.2 \text{ ft when } Y = 13,000 \text{ lbs}$$

$$T_c = 13,000 / \pi (37.2) = 111.3 \text{ lb/ft}$$

$$= 9.28 \text{ lb/in.}$$

Location of canopy equator on gore:

$$h' = \pi D'_p / 4 = 26.6 \text{ ft}$$

≈ 319 inches

Place the band near $h'/2 \sim 160$ or the top edge of ring 5 at $h'_b = 151$ inches

$$\text{Under load } h_b \sim 1.1 h'_b = 177 \text{ inches}$$
$$h_b - h_v \approx 159 \text{ inches}$$

$$\text{Then: } T_b = 159 (9.28) / 2 = 738 \text{ lbs}$$

$$P'_R = 1.9 T_b = 1400 \text{ lbs}$$

Use 1500 lb 9/16 in. tubular webbing.

$$\text{Risers: } P' = \frac{2.5(13,000)}{4} = 8120 \text{ lbs}$$

Although 8700 lb type X webbing at 3.7 oz/yd satisfies the strength requirement, 10,000 lb type XIX webbing at 4.1 oz/yd is preferred because of its superior flexibility.

The remaining materials are selected in accordance with the guidelines given in Section 7. Table XXXIII presents a complete list of the textile materials that should be used in prototype models of the new 60.6 ft D_o Ringsail parachute.

TABLE XXXIII

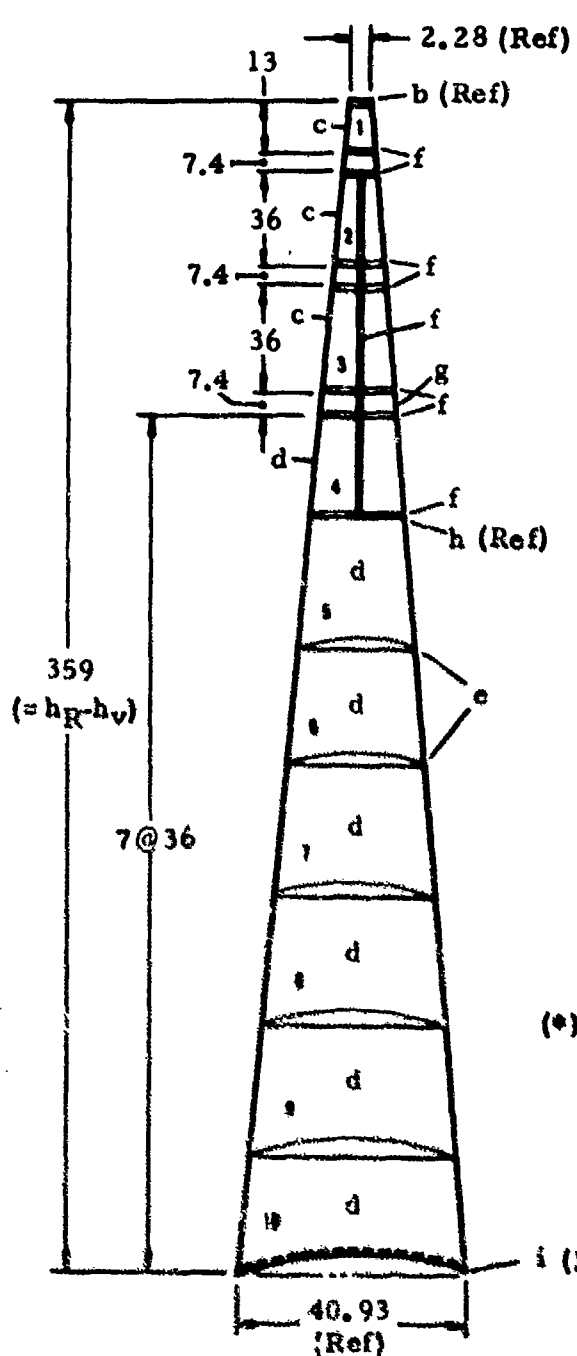
MATERIAL LIST FOR THE 60.6 ft D_o RINGSAIL PARACHUTE

Member	Material	Code	Specification
Vent lines	550 lb braided cord	a	MIL-C-7515B Type II
Vent band	4000 lb 1 in. tubular web	b	MIL-W-5625D
Rings 1, 2, & 3	1.6 oz/yd ² nylon cloth	c	MIL-C-7020D Type III
Rings 4 thru 10	1.1 oz/yd ² ripstop	d	MIL-C-7020D Type I
Saledge tapes: L	70 lb 5/8 in. tape	e	MIL-T-5608E Type III CL B
M	90 lb 5/8 in. tape	f	MIL-T-5608E Type III CL B
Vertical tapes	90 lb 5/8 in. tape	f	MIL-T-5608E Type III
Radial tapes	300 lb 1 in. tape	g	MIL-T-6134A Type II
Ripstop band	1500 lb 9/16 in. tubular web	h	MIL-W-5625D
Skirt band	1000 lb 1/2 in. tubular web	i	MIL-W-5625D
Suspension lines	550 lb braided cord	a	MIL-C-7515B Type II
Risers	10,000 lb 1 3/4 in. web	j	MIL-W-4088D Type XDX
Reefing line	1000 lb braided cord	k	MIL-C-7515B Type IV
Thread & Cord	nylon	B E F #6	V-T-295 Type I CL 1

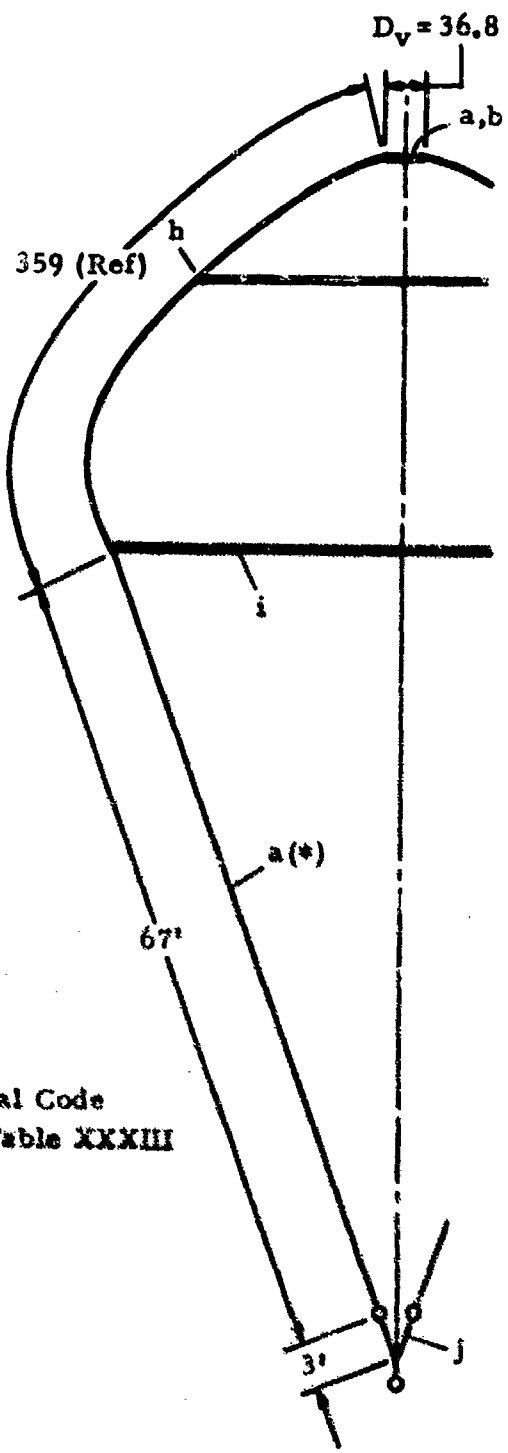
The prototype preliminary design is completed and presented for more detailed analysis in Figure 111.

Hardware

Reefing rings: Use part No. USAF48H7995



Gore Layout



Parachute Diagram

Figure 111. Prototype Design Dimensions and Materials for 60.6 Ft D_0 Ringsail Parachute

Line to riser links:

$$\text{Proof test load } P_T = 13,000/4 = 3250 \text{ lbs}$$

$$P'_R = 1.5 P_T = 4880 \text{ lbs}$$

Use MS22021-1 speed link (if qualifiable) for minimum weight (.184 lbs), otherwise use AF52B6660 "U" link.

Preliminary weight estimate

The parachute structure falls in the medium weight category for which

$$W_p = 51 \text{ lbs} \quad (\text{Figure 53})$$

The probable pack weight is:

$$1.12 W_p = 57 \text{ lbs}$$

The pack volume for different packing methods would be:

Method	lb/in. ³	Volume in. ³
Manual (hard)	.016	3560
Light press	.020	2850
Heavy press	.024	2380

APPENDIX D
SPECIFICATION, TRIP SELVAGE CLOTH

1. INTRODUCTION

- 1.1 **PURPOSE** - This Specification contains requirements for the fabrication, inspection and control of one type of reinforced selvage for use on parachute cloths.
- 1.2 **SCOPE** - This Specification shall be used only in conjunction with a specification for parachute cloth.
- 1.3 **APPLICABILITY** - This Specification shall be applicable when specified on the Engineering Drawing, on the Purchase Order or in a Material Procurement and Design Specification for parachute cloth.
 - 1.3.1 **ADDITIONAL CALLOUTS** - In addition to calling out this basic specification, the following items must also be specified:
 - (a) A Specification for parachute cloth
 - (b) The nominal width of the parachute cloth
 - (c) Government Source Inspection, when applicable (P. O. only)

2. REFERENCES - The latest revision of the following documents form a part of this Specification to the extent specified herein:

FEDERAL

Textile Test Methods CCC-T-191

MILITARY

Cloth, Nylon Parachute	MIL-G-7020
Cloth, Nylon Parachute	MIL-G-7350

3. REQUIREMENTS

3.1 WIDTH

3.1.1 **NOMINAL WIDTH OF CLOTH** - The nominal width of the base parachute cloth shall be specified on the Engineering Drawing and shall be selected from the list shown in Table L

3.1.2 WOVEN WIDTH OF CLOTH AND TOLERANCES - The woven width and allowable tolerances for the finished cloth with reinforced selvage on both edges shall be as shown in Table I.

TABLE I: WIDTH REQUIREMENTS

Nominal Width Of Cloth Specified (inch)	Required Woven Width And Tolerances (inch)
42	42 1/2 ± 1/2
36	36 1/2 ± 1/2
24	24 1/4 ± 1/4
18	18 1/4 ± 1/4

3.1.3 WIDTH OF SELVAGE - The width of the reinforced area of each selvage shall be $1/2 \pm 1/16$ inch.

3.2 MECHANICAL PROPERTIES OF THE REINFORCED SELVAGE

3.2.1 MINIMUM BREAKING STRENGTH - The minimum breaking strength of each reinforced selvage in the warp direction shall be as follows:

$$S_s (\text{min}) = 1.38 S_c$$

where:

S_s (min) - Minimum breaking strength of the reinforced selvage in the Warp direction in pounds per selvage.

S_c - Breaking strength of the base cloth in the Warp direction in pounds per inch.

3.3 TEAR RESISTANCE - The resistance of the reinforced selvage to both Tearing and Weave separation shall be increased to the greatest extent possible by suitable locking warp members in each edge. The exact construction shall be left to the discretion of the fabricator but every effort should be made to obtain maximum resistance for these properties while remaining compatible with the other requirements specified herein.

3.4 CONSTRUCTION

- 3.4.1 WEAVE** - The weave used shall be at the discretion of the fabricator but shall be compatible with the requirements shown herein.
- 3.4.2 DESIGN** - The reinforced selvage may be integrally woven with the cloth or it may be woven separately of plied threads provided the finished cloth satisfies the requirements shown herein.
- 3.4.3 MULTIPLE WIDTH WEAVES** - The 18 inch cloth only may be woven in two parallel widths provided all inside, reinforced selvages are effectively locked against fraying by suitable warp members.
 - 3.4.3.1 FILLING WIDTH** - The width of the filling space between inside selvages in multiple width cloth shall be $5/16 \pm 1/16$ inch.

4. QUALITY ASSURANCE CRITERIA

4.1 SAMPLING

- 4.1.1 SAMPLING FOR EXAMINATION** - Sampling for Examination shall be in accordance with MIL-C-7020.
- 4.1.2 SAMPLING FOR MECHANICAL PROPERTY TESTING** - Sampling for Mechanical Property Testing shall be in accordance with MIL-C-7020, Sampling Plan B.

4.2 METHOD OF TEST

- 4.2.1 EXAMINATION** - Both Yard-by-Yard and Overall Examinations shall be conducted on the selvages in accordance with MIL-C-7020.
- 4.2.2 MECHANICAL PROPERTY TEST** - The Breaking Strength of the selvage alone shall be determined in accordance with CCC-T-191, Method S104.1 with the following exceptions:
 - (a) The original specimen shall be approximately $3/4$ inch wide, 6 inch minimum length, and shall include the selvage plus approximately $1/4$ inch of the base cloth. It shall be taken in the warp direction.

- (b) The warp threads of the base cloth shall be removed by raveling until only the actual selvage remains.
- (c) The remaining selvage shall be used as the test specimen.
- (d) The selvage breaking strength value shall be reported in pounds (per each selvage).

4.3 ACCEPTANCE CRITERIA

4.3.1 EXAMINATION

4.3.1.1 DEFINITIONS OF DEFECTS - Defects shall be as defined in FED-STD-4.

4.3.1.2 CLASSIFICATION, FLAGGING AND ACCEPTABLE QUALITY LEVELS FOR DEFECTS - The classification, flagging and acceptable quality levels shall be in accordance with MIL-C-7020 and, in addition, the defects shown in Table II shall be classified as shown and full allowance given for each in determining acceptable quality levels.

TABLE II ADDITIONAL CLASSIFICATION OF DEFECTS

MAJOR DEFECTS	MINOR DEFECTS
Multiple Floats over 1/8" square.	Loopy or Stringy Selvage projecting up to 1/16 inch
Stringy Selvage showing separation or looseness.	Loose Selvage in which the scallops cannot be pulled smooth under a tension applied to the adjoining fabric, equal to or less than 5% of the nominal strength of the fabric.
Loops in Selvage extending in excess of the 1/16 inch.	Tight Selvage in which the fullness in the adjoining fabric cannot be pulled smooth under a tension applied to the selvage, equal to or less than 50% of the nominal strength of the selvage.
Fuzzy selvage indicating frayed or broken warp or fill threads.	

- 4.3.1.3 ALLOWANCE FOR DEFECTS - An allowance of 1/2 yard shall be added for each major defect.
- 4.3.2 MECHANICAL PROPERTY - The minimum Breaking Strength of the selvage shall be shown in Section 3.2.
- 4.4 CERTIFICATION AND TEST REPORTS - A statement of conformance to this Specification and a report on the Examination shall be included in the Certificate of Conformance and Test Report for the base cloth.
- 4.5 ACCEPTANCE - Acceptance or approval of material in the course of fabrication shall in no case be construed as a guarantee of the acceptance of the finished product.
- 4.6 QUALITY CONTROL OPTION - Quality Control shall have the option of requiring the reinspection of the product, regardless of prior inspections.
- 4.7 REJECTION - Material not conforming to the requirements of this Specification is subject to rejection.
- 4.7.1 RESUBMITTAL OF REJECTED MATERIAL - Rejected material shall not be resubmittal for approval without furnishing full particulars concerning the previous rejection(s) and the measures taken to overcome and/or eliminate the defects.

5. PROCUREMENT CRITERIA

- 5.1 GOVERNMENT SOURCE INSPECTION - The Purchase Order shall specify Government Source Inspection when required.
- 5.2 PACKAGING, PACKING AND MARKING - The Packaging, Packing and Marking shall conform to the requirements of the applicable specification for the base cloth.

APPENDIX E

RINGSAIL PARACHUTE DESIGN COMPUTER PROGRAM WG 176A-10

This Appendix presents a computer printout of the Ringsail design program, WG 176A-10 referenced in Section 5, page 136. Included on the bottom of page 358 and all of page 359 is sample input data to aid the user.

C
C
C

PROGRAM TO DESIGN RINGSAIL PARACHUTES

REAL LLW

```
COMMON/C DATA/CDOX(50),DOX(50),ICD
COMMON/RGTBL/PSVR(50),PRSL(50),IPD
COMMON/CNTRL/VCB(150),CTRL(100),TITLE(12)
COMMON/FULDAT/HHR(50),XKA(50),XKB(50),IFD
COMMON/SAILS/XA(50),XB(50),XAB(50),XARY(50),SALNGT(50)
COMMON/READAT/CDS,DSUB0,DZL,SLST,CDO,XNO,XH
1      ,XLS,XLR,DV,XHR,SALNO,SEAM,VLNO
2      ,CRANG,CCDEF,CKOEF,GRCOE,RLCOE,PESLO,XNMBR
3      ,SLW,LLW,SRH,VBK,RTW,RSH,VLN
4      ,CRNPOR,GEOPOR,TOTPOR,CLHPOR,VNTPOR,XIXMU
COMMON/SDATA/SPC(50),SLARA,XHT,XHV,NMBR,XXCOE,ANRAD,SLTAR(50)
COMMON/SDIM/XYY(2,50),XYCA(50),XYCB(50),XYC(2,50),XVH(50),XYA(50),
1 XVP(50),XIMU,XAREA,VAREA,IS(50),RWTOP(50),RWBOT(50),IK(50),
2 PRCRN,PRGOR,PRCLTH,PROTO,ASATL,ARI(50),SD
DIMENSION RDCHK(35),STDRD(35),XXX(10),ADA(35)
EQUIVALENCE(RDCHK(1),CDS)
DOUBLE PRECISION ENDATA,ENDTST,VCB,TITLE,ADA
DATA ENDATA/'ENDATA'/
```

C
C
C

READ PROGRAM VOCABULARY DATA

```
COLS          DESCRIPTION
2 - 4        STARTING NUMBER          JJ
5 - 8        ENDING NUMBER           KK
11 - AS REQUIRED ADDITIONAL VOCABULARY WORDS   VCB(11)
IN GROUPS OF SIX LETTERS OR SPACES
NINE WORDS OF SIX LETTERS MAXIMUM
USE AS MANY CARDS AS REQUIRED WITH LAST CARD AS FOLLOWS
COLS 2 - 4 AND 5 - 7 MUST CONTAIN 150
COLS 11 - 16 MUST CONTAIN THE LETTERS 'ENDATA'
```

C
C
C

VOCABULARY DATA AS USED IN PROGRAM WG176

```
C 1 10  CHUTE DIA.    * CANOPY AREA DRAG AREA NO. OF CORESL/CHUT
C 11 20  E DIA.DES.CDO  RIGGING LGTHLINE LENGTH RISER LENGTHGORE L
C 21 30  ENGYH 6.64 HP/N VENT RADIUS VENT DIA. OVLAMBDA SUB C SUB G
C 31 40  SUR T SUB MSAIL AREA H SUB R / D FEET SQ.FT.,INCHESPOUNDS
C 41 50  PERS. SO.IN.SYS. WEIGHT TOTAL AREA DIAMETER NO.OF
C 51 52  RISERS N/S
```

```

C150150 ENDDATA
C
C      5 READ(5,303)JJ,KK,(VCB(I),I=JJ,KK)
C      IF(VCB(JJ),NE,ENDATA)GO TO 5
C
C      READ PARAMETRIC CDO DATA
C
C      COLS          DESCRIPTION
C      1 - 10        VALUE OF CDO
C      11 - 20        VALUE OF CORRESPONDING D SUB 0
C      USE AS MANY CARDS AS REQUIRED (50 MAX)
C      LAST DATA CARD TO BE FOLLOWED BY CARD WITH ENDDATA IN COLS 75 - 80
C
C      I=0
10   I=I+1
      READ(5,302)CDOX(I),DOX(I),ENDTST
      DOX(I)=DOX(I)*12.0
      IF(ENDTST,NE,ENDATA)GO TO 10
      TCD=I-1

C      READ PARAMETRIC CDO MOD VS LINE LENGTH DATA
C
C      COLS          DESCRIPTION
C      1 - 10        PERCENTAGE VARIATION PRODUCED IN CDO
C      11 - 20        PERCENTAGE VARIANCE FROM OPTIMUM
C      RIGGING LENGTH
C      LAST DATA CARD TO BE FOLLOWED BY CARD WITH ENDDATA IN COLS 75 - 80
C      USE AS MANY CARDS AS REQUIRED (50 MAX)
C
C      I=0
12   I=I+1
      RFAD(5,302)PSVR(I),PRSL(I),ENDTST
      IF(ENDTST,NE,ENDATA)GO TO 12
      TPD=I-1

C      READ FULLNESS DISTRIBUTION
C
C      COLS          DESCRIPTION
C      1 - 10        VALUE OF THE RATIO H/HR
C      11 - 20        VALUE OF KA
C      21 - 30        VALUE OF KB
C      USE AS MANY CARDS AS REQUIRED (50 MAX)
C      LAST DATA CARD TO BE FOLLOWED BY CARD WITH ENDDATA IN COLS 75 - 80
C
C      I=0
14   I=I+1
      RFAD(5,306)HHR(I),XKA(I),XKB(I),ENDTST
      IF(ENDTST,NE,ENDATA)GO TO 14
      TFD=I-1

C      READ INPUT DATA

```

C
C DATA CARD NO 1

C C COLS DESCRIPTION
C 1 72 TITLE TO APPEAR ON DATA
C 80 CARD SEQUENCE NUMBER , MUST CONTAIN 1
C C TITLE(12)
C IXXX(I)

C 9999 READ(5,300)(TITLE(J),J=1,12),IXXX(1)

C C INITIALIZE SAIL MATERIAL WEIGHT

C DO 9 J=1,50
9 SALWGT(J)=0.0

C C DATA CARD NO 2

COLUMNS		DESCRIPTION		COLS
1 - 10	CDS OF PARACHUTE	(SQ FT)	DSUBO	
11- 20	DIAMETER OF PARACHUTE	(FEET)	DZL	
21- 30	DESIGN LOAD	(LBS)	SLST	
31- 40	ADJUSTED SUSPENSION LINE STRENGTH	(LBS)	CDO	
41- 50	DRAG COEFFICIENT		XNO	
51- 60	NUMBER OF GORES		XH	
61- 70	WIDTH OF SAIL MATERIAL	(INCHES)	IXXX(1)	
80	CARD SEQUENCE NUMBER , MUST CONTAIN	2		

C C READ(5,304)CDS,DSUBO,DZL,SLST,CDO,XNO,XH,IXXX(1)

C C DATA CARD NO 3

COLUMNS		DESCRIPTION		COLS
1 - 10	SUSPENSION LINE LENGTH	(FEET)	XLS	
11- 20	RISER LENGTH	(INCHES)	XLR	
21- 30	VENT DIAMETER	(INCHES)	DV	
31- 40	GORE LENGTH	(INCHES)	XHR	
41- 50	NUMBER OF SAILS		SALNO	
51- 60	WIDTH OF SAIL MATERIAL REQUIRED FOR SEAM (INCHES)		SEAM	
61- 70	NUMBER OF VENT LINES		VLNO	
80	CARD SEQUENCE NUMBER , MUST CONTAIN	3	IXXX(1)	

C C READ(5,304)XLS,XLR,DV,XHR,SALNO,SEAM,VLNO,IXXX(3)

C C DATA CARD NO 4

COLUMNS		DESCRIPTION		COLS
1 - 10	CROWN ANGLE	(DEGREES)	CRANG	
11- 20	COEFFICIENT ANGLE FOR GORE WIDTH	(DEGREES)	CCOEF	
21- 30	COEFFICIENT FOR GORE WIDTH C		CKOEF	
31- 40	GORE LENGTH COEFFICIENT		GRCOE	
41- 50	RIGGING COEFFICIENT		RLCOE	
51- 60	PERCENTAGE OF GORE LENGTH WITHOUT SLOTS (PERCENT)	PESLO		

C 61- 70 NUMBER OF SLOTS XNMBR
 C 80 CARD SEQUENCE NUMBER , MUST CONTAIN 4 XXX(1)
 C
 READ(5,304)CRANG,CCDEF,CKDEF,GRCOE,RLCOE,PESLO,XNMBR,XXX(4)
 C
 DATA CARD NO 5
 C
 COLS DESCRIPTION
 C 1 - 10 WEIGHT OF SAIL MATERIAL (LBS/SQ FT) SLW
 C 11- 20 SUSPENSION LINE WEIGHT (LBS/FT) LLW
 C 21- 30 SKIRT BAND WEIGHT (LBS/FT) SBW
 C 31- 40 VENT BAND WEIGHT (LBS/FT) VBW
 C 41- 50 RADIAL TAPE WEIGHT (LBS/FT) RTW
 C 51- 60 RISER WEIGHT (LBS/FT) RSW
 C 61- 70 VENT LINE WEIGHT (LBS/FT) VLW
 C 80 CARD SEQUENCE NUMBER , MUST CONTAIN 5 XXX(1)
 C
 READ(5,304)SLW,LLW,SBW,VBW,RTW,RSW,VLW,XXX(5)
 C
 DATA CARD NO 6
 C
 COLS DESCRIPTION
 C 1 - 50 INFORMATION RELATIVE TO SAIL REINFORCEMENT IS(1)
 C COLUMN NUMBER CORRESPONDS TO SAIL NO.
 C IF COLUMN BLANK - NO REINFORCING
 C IF 1 IN COLUMN - REINFORCED TOP ONLY
 C IF 2 IN COLUMN - REINFORCED TOP AND BOTTOM
 C 80 CARD SEQUENCE NUMBER , MUST CONTAIN 6 XXX(1)
 C
 READ(5,321)(IS(J),J=1,50),XXX(6)
 C
 DATA CARD NO 7
 C
 COLS DESCRIPTION
 C 1 - 50 INFORMATION RELATIVE TO REINFORCING TAPE WEIGHT
 C COLUMN NUMBER CORRESPONDS TO SAIL NO.
 C IF COLUMN BLANK - THIS WEIGHT TAPE NOT USED ON
 C SAIL
 C IF 1 IN COLUMN - THIS WEIGHT BOTH TOP AND BOTTOM
 C IF 2 IN COLUMN - THIS WEIGHT TOP
 C IF 3 IN COLUMN - THIS WEIGHT BOTTOM
 C 51- 60 WEIGHT OF REINFORCING TAPE (LBS/FOOT)
 C 70 IF THIS IS THE LAST REINFORCING TAPE CARD PUT A 2
 C IN THIS COLUMN
 C DATA CARDS 7A THRU 7(N) N = NUMBER OF CARDS REQUIRED
 C SAME AS CARD NO 7 NOTE A 2 IN COLUMN 70 OF THE
 C LAST CARD ONLY
 C 80 CARD SEQUENCE NUMBER , MUST CONTAIN 7 XXX(1)
 C
 15 READ(5,322)(IX(J),J=1,50),RFTW,KTEST,XXX(7)
 DO 1150 J=1,40

```

IF(IIX(J).EQ.0) GO TO 1150
IF(IIX(J).EQ.2) RWTOP(J)=RFTW/12.0
IF(IIX(J).EQ.2) GO TO 1150
IF(IIX(J).EQ.3) GO TO 1149
RWTOP(J)=RFTW/12.0
1149 RWBOT(J)=RFTW/12.0
1150 CONTINUE
IF(KTEST.EQ.0) GO TO 15

```

C
C DATA CARD NO 8

COLS	DESCRIPTION	(PERCENT)	
1 - 10	DESIRED CROWN POROSITY	(PERCENT)	CRNPOR
11- 20	DESIRED GEOMETRIC POROSITY	(PERCENT)	GEOPOR
21- 30	DESIRED TOTAL POROSITY	(PERCENT)	TOTPOR
31- 40	POROSITY OF SAIL CLOTH	(PERCENT)	CLHPOR
41- 50	POROSITY OF VENT	(PERCENT)	VNTPOR
51 - 60	NUMBER OF RISERS	(XIXMU)	
80	CARD SEQUENCE NUMBER . MUST CONTAIN	8	IXXX(1)

READ(5,304)CRNPOR,GEOPOR,TOTPOR,CLHPOR,VNTPOR,XIXMU,DUM,IXXX(8)

C
C DATA CARD NO 9

COLS	DESCRIPTION	
1 - 50	INFORMATION RELATING TO SAIL MATERIAL AND SAIL NUMBER	
	COLUMN NUMBER CORRESPONDS TO SAIL NUMBER	
	IF COLUMN IS BLANK - STANDARD SAIL MATERIAL WILL BE USED	
	IF '1' THIS WEIGHT MATERIAL WILL BE USED	
51 - 60	WEIGHT OF SAIL CLOTH TO BE USED	
70	IF THIS IS THE LAST SPECIAL WEIGHT PUT '1' IN THIS COL	
	DATA CARDS 9A THRU 9(N) N=NUMBER OF CARDS REQUIRED	
	SAME AS CARD 9 NOTE A 1 IN COLUMN 70 OF LAST CARD ONLY	

```

1115 READ(5,322)(IIX(J),J=1,50),SPSWT,KTEST,IXXX(9)
DO 1116 J=1,50
IF(IIX(J).EQ.0) GO TO 1116
SALHGT(J)=SPSWT/144.0
1116 CONTINUE
IF(KTEST.EQ.0) GO TO 1115

```

C
C READ DATA CARD NO 10

COLS	DATA	SYMBOL
1 - 10	DIMENSION DOWN TO FIRST SAIL	XHV
11 - 20	HEIGHT OF TOP SAIL	XHT
21 - 25	SLOT DIMENSIONS	SPC(1)
26 - 30		SPC(2)
31 - 35		SPC(3)
36 - 40		SPC(4)
41 - 45		SPC(5)

C	46 - 50	6	SPC(6)
C	51 - 55	7	SPC(7)
C	56 - 60	8	SPC(8)
C	61 - 65	9	SPC(9)
C	66 - 70	10	SPC(10)
C	71 - 75	11	SPC(11)
C	79 - 80 CARD SEQUENCE NO. MUST BE 10		IXXX(10)

C READ(5,336) XHV,XHT,(SPC(I),I=1,11),IXXX(10)
 336 FORMAT(2F10.0,1F5.0,3X,I2)
 C CHECK CARDS FOR COMPLETENESS AND ORDER
 C
 DO 1151 I=1,10
 IF(IXXX(I).NE.1) GO TO 1152
 1151 CONTINUE
 GO TO 1170
 C
 WRITE ERROR MESSAGE REGARDING INPUT DATA
 C
 1152 WRITE(6,323)
 CALL EXIT
 C
 C INITIALIZE CONTROL DATA
 C
 1170 DO 16 I=1,100
 16 CTRL(I)=0.0
 C
 C CONVERT DATA TO PROPER UNITS
 C
 XXSLT=0.0
 DO 2115 I=1,11
 XXSLT=XXSLT+SPC(I)
 2115 CONTINUE
 IF(XXSLT.NE.0.0) CTRL(95)=7.0
 CDS=CDS*144.0
 DSUBD=DSUBD*12.0
 XLS=XLS*12.0
 CRANG=CRANG*.017453
 CCDEF=CCOFF*.017453
 SLW=SLW/144.0
 LLW=LLW/12.0
 SRW=SRW/12.0
 VRW=VRW/12.0
 RTW=RTW/12.0
 RSK=RSW/12.0
 VLN=VLN/12.0
 CRNPOR=CRNPOR/100.0
 GEOPOR=GEOPOR/100.0
 TOTPOR=TOTPOR/100.0
 CLHPOR=CLHPOR/100.0
 VNTPOR=VNTPOR/100.0

```

PESLO=PESLO/100.0
TXMU=XIXMU

C   INITIALIZE STANDARD VALUES
C
C   DD 1100 J=1,33
33 STORD(1)=0.0
STORD(7)=36.0
STORD(9)=36.0
STORD(13)=1.6
STORD(15)=.26180
STORD(16)=.94248
STORD(17)=6.44
STORD(18)=.523
STORD(19)=1.15
STORD(20)=0.5
STORD(29)=.02
STORD(33)=.003

C   CHECK FOR SPECIFICATION INPUT SET CONTROLS
C
C   DD 1100 I=1,34
IF(RDCHK(I),EQ.0.0)CTRL(I)=1.0
IF(CTRL(I),EQ.0.0)GO TO 1100
IF(STORD(I),NE.0.0)CTRL(I)=0.0
RDCHK(I)=STORD(I)

1100 CONTINUE

C   CHECK REINFORCING TAPE DATA
C
C   DD 1053 J=1,50
IF((IS(J),EQ.1).AND.(RWTOP(J),EQ.0.0))GO TO 1054
IF((IS(J),EQ.2).AND.((RWTOP(J),EQ.0.0).OR.(RWBOT(J),EQ.0.0)))GO TO
1 1054
1053 CONTINUE
GO TO 1055
1054 CTRL(36)=1.0

C   WRITE INPUT INFORMATION
C
1055 CALL INIUPA
C   DETERMINING IF CHUTE CAN BE DESIGNED
C
IF((CTRL(1)+CTRL(2)),LT,2.0)GO TO 94
C   WRITE ERROR INPUT IF CHUTE CANNOT BE DESIGNED
C
1113 WRITE(6,301)(TITLE(J),J=1,12)
WRITE(6,305)
CALL EXIT

```

```

C
C      CHECK FOR CDS PROVISION
C
C      94 WRITE(6,330)
330 FORMAT(23H1 CHUTE CAN BE DESIGNED)
IF(CTRL(2).EQ.0.0)GO TO 18
C
C      CALCULATE SD  CDO  DSUB0 WHEN CDS IS GIVEN
C
C      CALL SOCAL(SD,0)
GO TO 20
C
C      CALCULATE SD  CDO  COS WHEN DSUB0 GIVEN
C
18 SD=3.1416*DSUB0**2/4.0
CALL SOCAL(SD,2)
WRITF(6,331)DSUB0,CDS,SD,CDO
331 FORMAT(14HO SOCAL CALLED,4E12.3)
20 IF(CTRL(8).EQ.0.0)GO TO 1021
C
C      SUSPENSION LINE LENGTH LENGTH NOT PROVIDED   CALCULATE RIGGING
C      LENGTH
C
C      XL=RLCOE*DSUB0
CTRL(8)=0.0
GO TO 21
1021 XL=XLS+XLR
C
C      IF GORE LENGTH UNSPECIFIED CALCULATE GORE LENGTH
C
21 XLS=XL-XLR
CTRL(9A)=XL
IF(CTRL(111).EQ.0.0)GO TO 22
XHA=GRCOE*DSUB0
C
C      SET BOTTOM LIMIT ON GORES
C
22 LONU=.76*DSUB0/12.0
C
C      SET TOP LIMIT ON GORES
C
IHNU=.89*DSUB0/12.0
C
C      DETERMINE NUMBER OF RISERS
C
I=0
IF(IXMU.NE.0)GO TO 2222
IXMU=4.0
IF(LONU.LT.30) IXMU=2
IF(LONU.GT.60) IXMU=5
IF(LONU.GT.80) IXMU=8

```

```

2222 XINU=IXNU
C
E   SET GORE NUMBER BY STANDARD SET
C
C   IF NO OF GORES UNSPECIFIED CALCULATE NO
C
E   IF(CTRL(6).EQ.0.01GO TO 2023
23 I=I+IXNU
IF(I.GT.LONU).AND.(I.LT.IHNUI)GO TO 24
GO TO 23
C
E   DETERMINE IF GORES CALCULATED FROM LOADS
C
24 XNO=1
IF((CTRL(31)+CTRL(41).NE.0.01)CTRL(34)=1.0
IF(CTRL(34).EQ.1.01GO TO 1125
C
C   IF LOADS PROVIDED CALCULATE MINIMUM LINES
C
XXNO=(EZL/SLST)*1.9
IXXNO= INT(XXNO)+1
I=0
C
E   IF LOAD PROVIDED DETERMINE NO OF GORES
C
124 I=I+IXNU
IF(I.LT.IXXNO)GO TO 124
XNO=1
GO TO 1125
C
C   CHECK IF NO OF GORES IS COMPATABLE
C
2023 XXNO=XNO/XINU
IF((INT(XXNO)-XXNO).EQ.0.01GO TO 1125
WRITE(6,2024)
2024 FORMAT(51H REQUESTED GORES INCOMPATABLE TAKING ALTERNATEROUTE)
GO TO 23
1125 WRITE(6,337)XNO,XINU,XHR
332 FORMAT(22HO GORES AND RISERS SET,3E12.3)
C
C   CHECK IF NO OF SAILS PROVIDED
C
IF(CTRL(112).EQ.1.01GO TO 25
C
C   IF GORE DATA GIVEN BYPASS SAIL NO CHECK
C
IF(CTRL(45).EQ.2.01GO TO 25
C
C   IF SAILS PROVIDED CHECK IF NUMBER COMPATABLE
C
IF( SALNO*XN.GT.XHR)GO TO 1126

```

```

XXXXX=XHR-SALNO*XH
YYYYY=CKDEF*(XHR/XNO)*SIN(XXXXY*CCDEF/XHR)
XXXX=XXXXY*YYYYY/(2.0*S0)
IF(XXXX .LT. GEOPORIG TO 25

C
C WRITE ERROR STATEMENT REGARDING SAILS
C
1126 WRITE(6,301)TITLE
WRITE(6,324)
CALL EXIT
C DETERMINE SAIL CONFIGURATION UP TO START OF SLOTS
C
C ESTABLISH CONSTANTS
C
25 I=0
XXCOE=CKDEF*(XHI/XNO)
ANRAD=CCDEF /XHR
Y=XHR
YSTOP=XHR-PFSLO*XHR
IF(CTRL(95).EQ.2.0)YSTOP=XHR-(SALNO-(XNHBR+.5))*XH
DELY=XH
26 I=I+1
C
C DETERMINE POSITION OF BOTTOM OF SAIL
C
C XXXII,I)=Y
C
C DETERMINE GORE WIDTH AT BOTTOM OF SAIL
C
CCC=XXCOE*SIN(Y*ANRAD)
YYCII,I)=CCC
C
C DETERMINE FULLNESS CONSTANT
C
CNSY=Y/XHR
CALL KSF1(CNST,XKRB,I)
C
C DETERMINE FREE SAIL BOTTOM DIMENSION
C
XXCII,I)=XXKB*CCC
C
C DETERMINE SAIL BOTTOM CONSTRUCTION DIMENSION
C
XB(I,I)=YYCII,I)+SEAM
C
C SET SAIL HEIGHT
C
YYH(I,I)=DELY
C
C DETERMINING POSITION OF TOP OF SAIL

```

```

V=Y-DELY
XYY(2,1)=Y
C DETERMINE GORE WIDTH AT TOP OF SAIL
C CCC=XXCOE*SIN(V*ANRADI)
XVC(2,1)=CCC
C DETERMINE FULLNESS CONSTANT
C CNST=Y/XHR
CALL KSET(CNST,XXKA,2)
C DETERMINE FREE SAIL TOP DIMENSION
C XYCA(1)=XXKA+CCC
C DETERMINE SAIL TOP CONSTRUCTION DIMENSION
C XA(1)=XYCA(1)+SEAM
C CHECK FOR END OF NO SLOT REGION
C IF(Y.GT.YSTOP)GO TO 26
C SET NUMBER OF SAILS WITHOUT SLOTS
C SALNO=1
WRITE(6,333)SALNO
333 FORMAT(12SH0,SAILS WITHOUT SLOTS SET,E12.3)
C DETERMINE POROSITY INFO
C CALL SLOCAL
WRITE(6,334)ASAIL
334 FORMAT(12SH0,VENTILATION RATIO SET,E12.3)
C CHECK IF WEIGHT CAN BE DETERMINED
C IF(CTRL(23).EQ.0.01)GO TO 1184
VLW=LLW
CTRL(23)=0.0
1184 IF(CTRL(14).EQ.0.01)GO TO 1185
VLWD=XNO/2.0
CTRL(14)=0.0
1185 DO 83 JJ=22,28
83 CTRL(35)=CTRL(35)+CTRL(JJ)
CTRL(35)=CTRL(35)+CTRL(36)
IF(CTRL(75).NE.0.01) GO TO 1084
C IF SUFFICIENT WEIGHT DATA CALCULATE CHUTE WEIGHT

```

```

C
      CALL WEIGHT(WGT)
      CTRL(99)=WGT
      GO TO 84
1084 WRITE(6,301)TITLE
      WRITE(6,325)

C
C      CALCULATE CHUTE POROSITY
C
      86 CALL PORSIT(2)
C
C      WRITE OUTPUT
C
      CALL OUTRIT
300 FORMAT(12A6.7X,1I1)
301 FORMAT(1H1,24X,12A6)
302 FORMAT(2F10.0,54X,A6)
303 FORMAT(1X,2I3,3X,10A6)
304 FORMAT(7F10.0,9X,1I1)
305 FORMAT(14H0 INSUFFICIENT DATA PROVIDED TO DESIGN CHUTE)
306 FORMAT(3F10.0,44X,A6)
307 FORMAT(1H0,24X,12A6)
308 FORMAT(1H1,42X,45HR I N G S A I L   C H U T E   D E S I G N)
309 FORMAT(1X,3A6,F10.3,1X,A6,12X,3A6,F10.3,1X,A6,12X,3A6,F10.3,1X,A6)
310 FORMAT(1H1)
311 FORMAT(14H CHECK ON AREA AND DIA. FROM SAIL SUMMATION)
312 FORMAT(1H0,43X,42ND O R F   A N D   S A I L   D E S I G N)
313 FORMAT(E BANDSAIL DISTANCE   SAIL WIDTH SAIL WIDTH GORE WIDTH
      1 HEIGHT      FREE SAIL AREA)
314 FORMAT(9H4),     FROM APEX LESS SEAM          AT SAIL
      1 OF SAIL 50, 14, PERCENT SOI
315 FORMAT(14H TIP,2X,6I12,3)
316 FORMAT(1X,12,50X,3E12,3)
317 FORMAT(1H BOTTOM,4E12,3)
318 FORMAT(50X,11HECINTINUED))
319 FORMAT(10H0SLOT NO. +13,42X,3E12,3)
320 FORMAT(12HVENTILATION CRESCENT SLOT,51X,2E12,3)
321 FORMAT(150I1,20X,1I1)
322 FORMAT(150I1,1E12,3X,13,9X,1I1)
323 FORMAT(14H DATA FREE MISSING OR OUT OF ORDER,5X,12I)
324 FORMAT(12H014PROPER NT OF SAILS GIVEN)
325 FORMAT(14H0INSUFFICIENT DATA TO PROVIDE CHUTE WEIGHT)

C
C      GLOSSARY OF SYMBOLS USED IN PROGRAM 4G176
C
C      ASAIL - VENTILATION AREA OF LOWER SAILS
C      CGO - GORE WIDTH AT POINT IN QUESTION
C      CCOFF - COEFFICIENT ANGLE FOR DETERMINING C NOMINALLY =54 DEG
C      CDD - ESTABLISHED DRAG COEFFICIENT OF DESIGN
C      CDXY(I,J) - CD DATA IN THE CD VS DD TABLE
C      COS - DESIRED DRAG AREA OF PARACHUTE INCHES

```

C	CKOFF	- COEFFICIENT FOR DETERMINING C Nominally=6.44
C	CNST	CONSTANT FOR FINDING FULLNESS COEFFICIENT
C	CRANG	- CROWN ANGLE NOMINALLY = 15 DEGREES
C	CRNPOR	- CROWN POROSITY DESIRED
C	CTRL(1)	- CONTROL NUMBERS AND LOGIC DATA (SEE ASSIGNMENTS)
C	DAT1	OUTPUT DATA
C	DAT2	OUTPUT DATA
C	DAT3	OUTPUT DATA
C	DELY	SAIL HEIGHT
C	DLDTST	DIMENSION LEFT FOR SLOTS
C	DOX(1)	- DO DATA IN THE CD VS DO TABLE
C	DSUND	- NOMINAL CHUTE DIAMETER
C	DV	- VENT DIAMETER NOMINALLY $2\pi HV \cos(\text{CROWN ANGLE})$
C	DZL	- DESIGN LOAD
C	ENDATA	SYMBOL TO INDICATE END OF DATA DECK
C	ENDTST	CHECK FOR LAST DATA CARD
C	FPTW	- REINFORCING TAPE WEIGHT AS READ FROM CARD
C	GEOPOR	- GEOMETRIC POROSITY DESIRED
C	GRCOE	- GORE LENGTH COEFFICIENT NOMINALLY = .515
C	GSLA	- SLOT AREA PER CORE
C	MHR(1)	- M/H/R DATA FOR THE FULLNESS DISTRIBUTION DATA
C	HT	HEIGHT OF TOP SAIL
C	I	INDEX USED IN LOOPS
C	TCO	- NUMBER OF DATA POINTS IN THE CD VS DO TABLE
C	TFD	- NUMBER OF DATA POINTS IN THE FULLNESS DATA
C	TNU	UPPER LIMIT ON NO OF GORES
C	TPD	- NUMBER OF DATA POINTS IN RIGGING TABLE
C	TSTP	FIXED POINT NO OF SLOTS
C	TSNO	FIXED POINT NO OF SAILS
C	TS(1)	- SAIL NUMBERS REQUIRING REINFORCING TAPE J=2 BOTH J=1 TOP
C	TXXND	FIXED POINT VALUE OF XXND
C	TYMU	FIXED POINT NUMBER OF LINES PER RISER
C	XXX(1)	- CHECK FOR DATA CARD COMPLETENESS AND ORDER
C	XXCT	- CODE TO ESTABLISH REINFORCING TAPE WEIGHT
C	J	INDEX USED IN LOOPS
C	JJ	INDEX FOR VOCABULARY READ
C	K	INDEX FOR SLOT ADJUSTMENT
C	KK	INDEX FOR VOCABULARY READ
C	KNXX	COUNTER FOR ADJUSTING SLOT DIMENSIONS
C	KTEST	CHECK TO SEE IF MORE DATA CARDS FOLLOW
C	LIN	- LINE WEIGHT LBS/FOOT
C	LONU	LOWER LIMIT ON NO OF GORES
C	NMFR	- NUMBER OF SLOTS IN I FORMAT XNMFR IN F FORMAT
C	N/S	- NOT SPECIFIED
C	PERSD	PERCENTAGE DEVIATION FROM DESIRED SLOT AREA
C	PERSD	- PERCENTAGE OF CORE FOR FULL SAILS NOMINALLY .5
C	PRSO	SAIL AREA PERCENTAGE OF SO
C	PRCLTH	- POROSITY OF CLOTH PERCENT OF S SUR O (DESIGN)
C	PRCN	- POROSITY OF CROWN PERCENT S SUR O (DESIGN)
C	PRCPR	- GEOMETRIC POROSITY PERCENT S SUR O (DESIGN)
C	PRCTO	- TOTAL POROSITY PERCENT OF S SUR O

C PRSL(I) - PERCENT OF OPTIMUM RIGGING LENGTH FROM DO VS RIG. TABLE
C PSVR(I) - PERCENTAGE CHANGE IN DO FROM DO VS RIGGING TABLE
C RFTW - REINFORCING TAPE WEIGHT TO BE ASSIGNED
C RLCOE - RIGGING COEFFICIENT NOMINALLY = 1.15
C RSW - RISER WEIGHT LBS/FOOT
C RTW - RADIAL TAPE WEIGHT LBS/FOOT
C RWBOT(I) - REINFORCING TAPE WEIGHT BOTTOM LBS/FT
C RWTOP(I) - REINFORCING TAPE WEIGHT TOP LBS/FT
C SALNO - NUMBER OF SAILS USED
C SRW - SKIRT BAND WEIGHT LBS/FOOT
C SEAM - WIDTH OF SAIL REQUIRED FOR SEAM NOMINALLY = 1.5 IN.
C SKAB(I) - CONSTANTS FOR THE FULLNESS DISTRIBUTION DATA
C SLTO - DISTANCE USED TO CHECK SLOT WIDTHS
C SLSPC - FIRST TRY AT SLOT SPACING
C SLARA - SLOT AREA TOTAL
C SLST - ADJUSTED SUSPENSION LINE STRENGTH
C SLW - SAIL WEIGHT LBS/SQ FOOT
C SNO - NUMBER OF GORES
C SD - CANOPY AREA SD IN
C SPSWT - SPECIAL SAIL MATERIAL WEIGHT
C SPCTOT - TOTAL SLOT DIMENSION
C TAREA - SUMMATION OF SAIL MATERIAL
C TITLE(I) - TITLE OF JOB FOR USE IN DATA HEADINGS
C TOTDST - CROWN DISTANCE TO BE FILLED WITH SLOTS AND SAILS
C TOARA - TOTAL POROSITY AREA
C TOTPOR - TOTAL POROSITY DESIRED
C TPOR - TOTAL CHUTE POROSITY -PERCENT OF S SUB 0 NOMINAL =.02
C VARFA - VENT AREA
C VBW - VENT BAND WEIGHT LBS/FOOT
C VCB(I) - VOCABULARY DATA STORED IN A FORMAT (SEE LIST)
C VENO - NUMBER OF VENTLINES NORMALLY SC/2
C VEW - VENTLINE WEIGHT LBS/FT NOMINALLY SAME AS LLW
C VNTPOR - VENT POROSITY DESIRED
C VPOK - VENT POROSITY - PERCENT OF S SUB 0 NOMINAL =.003
C WGT - TOTAL CHUTE WEIGHT
C XA(I) - WIDTH OF SAIL AT THE TOP
C XB(I) - WIDTH OF SAIL AT THE BOTTOM
C XDO - DIAMETER CALCULATED FROM TAREA
C XH - WIDTH OF CLOTH FOR SAILS
C XHR - GORE LENGTH
C XHV - DIMENSION DOWN TO TOP SAIL OF GORE
C XIMU - NUMBER OF LINES PER RISER
C XL - RIGGING LENGTH
C XLR - RISER LENGTH NOMINALLY = 36 IN.
C XLS - SUSPENSION LINE LENGTH
C XXND - LINES REQUIRED BY LOADING
C XXXXX - DIMENSION TO CHECK SAIL NO COMPATABILITY
C XXXX - AREA FOR CHICKEN SAIL NO COMPATABILITY
C XXKA - KA COEFFICIENT OF FULLNESS
C XXKR - KB COEFFICIENT OF FULLNESS
C XYA(I) - FREE SAIL AREA

XYCA11 - FREE LENGTH OF THE SAIL TOP
 XYCB11 - FREE LENGTH OF THE SAIL BOTTOM
 XYC13,13 - GORE WIDTH J=1-BOTOF SAIL J=2 - TOP OF SAIL
 XVM013 - SAIL HEIGHT
 XYB15 - PERCENTAGE OF FREE SAIL AREA TO S SUB 6
 XYV15,15 - BOTTOM AND TOP POSITIONS OF SAILS J=3-BOT J=2-TOP
 Y VERTICAL DIVISION
 XYX15 DIMENSION TO CHECK SAIL NO COMPATABILITY

CONTROL NUMBER ASSIGNMENT IN PROGRAM WG176

* INDICATES STANDARD ** INDICATES CALCULATED
CONTROL NUMBER ASSIGNMENT YES = 0 NO = 1

	NORMAL
CTRL(1) HAS A CDS VALUE BEEN PROVIDED	** 0
CTRL(2) HAS A NOMINAL DIAMETER BEEN GIVEN	** 1
CTRL(3) HAS A DESIGN LOAD BEEN PROVIDED	0
CTRL(4) HAS AN ADJUSTED SUSPENSION LINE LOAD GIVEN	0
CTRL(5) HAS A DRAG COEFFICIENT BEEN PROVIDED	** 1
CTRL(6) WERE THE NUMBER OF GORES SPECIFIED	** 1
CTRL(7) WAS THE WIDTH OF CLOTH SPECIFIED	* 0
CTRL(8) WAS THE SUSPENSION LINE LENGTH SPECIFIED	** 1
CTRL(9) WAS THE RISER LENGTH SPECIFIED	* 1
CTRL(10) WAS THE VENT DIAMETER SPECIFIED	** 0
CTRL(11) WAS THE GORE LENGTH SPECIFIED	** 1
CTRL(12) WAS THE NUMBER OF SAILS SPECIFIED	** 1
CTRL(13) HAS THE SEAM WIDTH SPECIFIED	* 1
CTRL(14) WERE THE NUMBER OF VENT LINES GIVEN	** 0
CTRL(15) HAS THE CROWN ANGLE SPECIFIED	* 1
CTRL(16) WAS THE COEFFICIENT ANGLE FOR C SPECIFIED	1 1
CTRL(17) WAS THE COEFFICIENT FOR C SPECIFIED	* 1
CTRL(18) WAS THE GORE LENGTH SPECIFIED	* 1
CTRL(19) WAS THE RIGGING COEFFICIENT SPECIFIED	* 1
CTRL(20) WAS THE PERCENT OF GORE WITHOUT SLOTS SPECIFIED	* 1
CTRL(21) WAS THE NUMBER OF SLOTS SPECIFIED	** 1
CTRL(22) IS SAIL MATERIAL WEIGHT PROVIDED	0 0
CTRL(23) WAS LINE WEIGHT PROVIDED	0 0
CTRL(24) WAS SKIRT BAND WEIGHT PROVIDED	0 0
CTRL(25) WAS VENT BAND WEIGHT PROVIDED	0 0
CTRL(26) WAS RADIAL TAPE WEIGHT PROVIDED	0 0
CTRL(27) WAS THE RISER WEIGHT PROVIDED	0 0
CTRL(28) WAS THE VENT LINE WEIGHT GIVEN	0 0
CTRL(29) HAS THE CROWN POROSITY SPECIFIED	** 1
CTRL(30) HAS THE GEOMETRIC POROSITY SPECIFIED	** 1
CTRL(31) HAS THE TOTAL POROSITY SPECIFIED	* 1
CTRL(32) HAS THE SAIL CLOTH POROSITY SPECIFIED	** 1
CTRL(33) HAS THE VENT POROSITY SPECIFIED	** 1
CTRL(34) LOADS ARE TO BE USED TO DEFINE NO. OF GORES	1 1
CTRL(35) IS THERE SUFFICIENT INFO TO PROVIDE WEIGHT	0 0
CTRL(36) HAS REINFORCING TAPE WEIGHT PROVIDED	0 0
CTRL(37) HAS THE SAIL NUMBER FOR REINFORCING GIVEN	0 0

```

GO TO 9999
END
SUBROUTINE SOCAL(SO,IXX)
C
C SUBROUTINE TO CALCULATE CANOPY AREA GIVEN REQD. DRAG AREA
C
COMMON/CNTRL/VCS(150),CTRL(100),TITLE(12)
COMMON/CDATA/CDOX(50),DOX(50),ICD
COMMON/READAT/CDS,DSUB0,DZL,SLST,CDO,XND,XH
1      ,XLS,XLR,DV,XHR,SALNO,SEAH,VLND
2      ,CRANG,CCOEF,CKDEF,GRCOE,RLC06,PESLO,XNM0R
3      ,SLW,LLW,SBW,VBW,RTH,RSW,VLW
4      ,CRNP0R,GEOP0R,TOTP0R,CLHP0R,VNTP0R,XIXMU
COMMON/RGTBL/PSVR(50),PRSL(50),IPD
DOUBLE PRECISION VCB,TITLE

C
C ITERATIVE PROCESS TO CALCULATE SO
C
C DETERMINE IF CDS OR D SUB 0 IS GIVEN
C
X00=DSUB0
IF(IXX.NE.2)GO TO 1
SM=X00**2*.7854
GO TO 3
C
C INITIALIZE FOR D SUB 0 CASE
C
1 S0PLUS=1000.0
DELS1=1.0
S0=CDS
C
C INITIALIZE D SUB 0
C
2 X00=SQRT(4.0*S0/3.1416)
3 IF(CTRL(8).EQ.1.0)GO TO 4
XL=XLS+XLR
GO TO 5
4 XL=RLCOE*X00
C
C OPTIMUM RIGGING LENGTH
C
5 OPTL=1.15*X00
C
C CALCULATE PERCENT OF OPTIMUM RIGGING LENGTH
C
PERSD=100.0*(XL-OPTL)/OPTL
IF(PERSD.EQ.0.0)GO TO 26
C
C FIND PROPER CDO MODIFIER IN RIGGING TABLE,
C
DO 20 I=2,IPD

```

```

      IF((PRSL(I-1).LE.PERSD).AND.(PRSL(I).GE.PERSD))GO TO 22
20 CONTINUE
      WRITE(6,301)
      CALL EXIT

C     INTERPOLATE IN RIGGING TABLE
C
22 CALL EXTRP(PRSL(I-1),PSVR(I-1),PRSL(I),PSVR(I),PERSD,PSVRX)
      GO TO 26
24 PSVRX= 0.0
C     FIND PROPER D SUB 0 IN DO TABLE
C
26 DO 28 I=2,ICD
      IF((DOX(I-1).LE.XDO).AND.(DOX(I).GE.XDO))GO TO 30
28 CONTINUE
      WRITE(6,302)
301 FORMAT(24HO RIGGING TABLE EXCEEDED)
302 FORMAT(33HO DRAG COEFFICIENT TABLE EXCEEDED)
      CALL EXIT

C     INTERPOLATE IN DO TABLE
C
30 CALL EXTRP(DOX(I-1),CDOX(I-1),DOX(I),CDOX(I),XDO,CDO)
C     CALCULATE CDO
C
      CDO=CDO+CDO*PSVRX/100.0
      IF(IXX.EQ.2)GO TO 44
C     CALCULATE TRIAL SO
C
      SOX=CDO/CDO
C     CHECK FOR CHANGES REQUIRED IN DO
C
      DELSZ=SOX-SO
      IF((DELSZ*DELSZ).LE.0.01)SOPLUS=SOPLUS*(-.5)
      DIVA=100.0*DELSZ/SO

C     SEE IF DO IS WITHIN 5 PERCENT
C
      IF(ARS(DIVA).LT.0.5)GO TO 40
      ITEST=TEST+1
      SO=SO+SOPLUS
C     CHECK FOR RUN-AWAY LOOP
C
      IF(TEST.LT.51)GO TO 2
      WRITE(6,303)
303 FORMAT(28HO UNABLE TO FIND VALUE OF SO)

```

```

    CALL EXIT
40  SO=SOX

C C
    CALCULATE D SUB 0 FOR COS CASE
C C
    DSUB0=SORT(4.0*SO/3,1416)
    RETURN
C C
    CALCULATE COS FOR D SUB 0 CASE
C C
44  CDS=SO*CDO
    RETURN
    END
    SUBROUTINE KSET(CNST,XXX,ITYP)
C C
    SUBROUTINE TO PERFORM TABLE LOOK-UP AND SET FULLNESS RATIO
C C
    COMMON/FULDAT/HHR(50),XKA(50),XKR(50),IFD
C C
    FIND POINT IN TABLE FOR INTERPOLATION
C C
    DO 20 I=2,IFD
    IF((HHR(I-1).LE.CNST).AND.(HHR(I).GE.CNST))GO TO 24
20  CONTINUE
    WRITE(6,310)
310 FORMAT(95HOUNABLE TO ESTABLISH FULLNESS RATIO)
    CALL EXIT
24  IF(ITYP.EQ.2)GO TO 28
C C
    INTERPOLATE FOR SAIL BOTTOM
C C
    CALL EXTRP(HHR(I-1),XKB(I-1),HHR(I),XKB(I),CNST,XXX)
    RETURN
C C
    INTERPOLATE FOR SAIL TOP
C C
28  CALL EXTRP(HHR(I-1),XKA(I-1),HHR(I),XKA(I),CNST,XXX)
    RETURN
    END
    SUBROUTINE PORSIT(ITYP)
C C
    SUBROUTINE TO CALCULATE POROSITY OF CHUTE
C C
    COMMON/SDATA/SPC(50),SLARA,XHT,XHV,NMBR,XXCOE,ANRAD,SLTAR(50)
    COMMON/READAT/CDS,DSUB0,DZL,SLST,CDO,XNO,XH
    1      ,XLG,XLR,DV,XHR,SALNO,SEAM,VL40
    2      ,CRANG,CCDEF,CKOEF,GRCOE,RLCOE,PESLO,XNMBR
    3      ,SLW,LLW,SAW,VBW,RTW,RSH,VLW
    4      ,CRNPOR,GEOPOR,TOTPOR,CLHPOR,VNTPOR,XIXMU
    COMMON/SDIM/XYY(2,50),XYCA(50),XYCB(50),XYC(2,50),XVH(50),XVA(50),
1  XYP(50),XIMU,XAREA,VAREA,IS(50),RWTOP(50),RBOT(50),IX(50),

```

```

2 PRCRN,PRGOR,PRCLTH,PROTO,ASAIL,AR(501,SD
IF(IITYP .EQ.1)GO TO 9
C
C   FLOAT NUMBER OF SLOTS IN CROWN
C
C   SLNO=NMBR
C
C   CROWN POROSITY CALCULATION
C
C   PRCRN=((VAREA+XAREA*XNO)/SD1*100.0
C   GO TO 24
C
C   NUMBER OF SAILS WITHOUT SLOTS BETWEEN
C
C   5 CRNO=SLNO
C
C   NUMBER OF SPACES FOR INFLATION POROSITY
C
C   JJ=CRNO
C
C   CALCULATE POROSITY OF INFLATION
C
C
C   SET RATIO OF SPACE RADII
C
C   R1=XYCB(2)/3.1416
C   R2=XYCA(JJ)
C   DIS1=XYY(1,2)
C   DIS2=XYY(1,JJ)
C   ASAIL=0.0
C
C   CALCULATE AREAS
C
DO 20 I=2,JJ
A=XYCA(I-1)
B=XYCB(I)
DIST=XYY(1,I)
CALL EXTRP(DIS1,R1,DIS2,R2,DIST,RB)
II THETAB=B/(RB*2.0)
CORD=RB*SIN(THETAB)
IF(CORD.LE.0.1)GO TO 12
WRITE(6,304)B,A,CORD
304 FORMAT(29HOSAIL FULLNESS DOES NOT MATCH/30X,4I1H      8      A
1     RA          CORD/30X,4F10.4)
RA=RB-.25
GO TO 11
12 LOPN=1
ADR=10.0
DELT=1.0
RA=RB
15 THETAA=A/(RA*2.0)

```

```

XX=RA*SIN(THETAA)
DEL=CORD-XX
IF((ABS(DEL)/CORD).LT..01)GO TO 19
IF((DEL*DEL0).LT.0.01)ADR=ADR*(-.5)
RA=RA+ADR
DEL0=DEL
IF(LOPN.GT.20)GO TO 18
LOPN=LOPN+1
GO TO 15
18 WRITE(6,305)I
305 FORMAT(34H LOOP BLOWUP IN PORSIT AT SAIL NO.,I3)
RA=0.0
19 YB=RB*COS(THETAB)
YA=RA*COS(THETAA)
AREAB=(RB**2*THETAB)-YB*CORD
AREAAB=(RA**2*THETAA)-YA*CORD
AR(I)=AREAB-AREAAB
ASAIL=ASAIL+AR(I)
20 CONTINUE
ASAIL=ASAIL*XNO/S0
RETURN

C
C      GEOMETRIC POROSITY
C
24 PRGOR=PRCRN+ASAIL*100.0
C
C      CLOTH POROSITY
C
CLPOR=0.0383*(.75-(PRGOR/100.0))
PRCLTH=CLPOR*100.0
C
C      TOTAL POROSITY
C
PROTO=PRCLTH+PRGOR
RETURN
END
SUBROUTINE SLTARE(PERSO)
C
C      SUBROUTINE TO CALCULATE TOTAL SLOT AREA
C
COMMON/SDATA/SPC(50),SLARA,XHT,XHV,NMBR,XXCOE,ANRAD,SLTAR(50)
COMMON/READAT/CDS,DSUB0,DZL,SLST,CDO,XND,XH
1      ,XLS,XLR,DV,XHR,SALND,SEAM,VLND
2      ,CRANG,CCDEF,CKDEF,GRCOE,RLCOE,PESLO,XNMBR
3      ,SLW,LLW,SBW,VBW,RTW,RSW,VLW
4      ,CRNPOR,GEOPOR,TOTPOR,CLHPOR,VNTPOR,XIXMU
COMMON/SDIM/XYY(2,50),XYCA(50),XYCB(50),XYC(2,50),XYH(50),XYA(50),
1 XYP(50),XIMU,XAREA,VAREA,IS(50),PWTOP(50),RWBOT(50),IX(50),
2 PRCRN,PRGOR,PRCLTH,PROTO,ASAIL,AR(50),S0
C
C      INITIALIZE

```

```

C
C      GSLA=SLARA/XNO
C      XAREA=0.0
C
C      POSITION OF TOP OF FIRST SLOT
C
C      YT=XHV+XHT
C      DO 20 I=1,NMBR
C
C      GORE WIDTH AT TOP OF SLOT
C
C      C=XXCOE*SIN(YT*ANRADI)
C
C      CALCULATE FULLNESS CONSTANT
C
C      CNST=YT/XHR
C      CALL KSET(CNST,XXKA,2)
C
C      SLOT WIDTH AT TOP
C
C      TOP=XXKA*C
C
C      POSITION OF BOTTOM OF SLOT
C
C      YB=YT+SPC(1)
C
C      CALCULATE FULLNESS CONSTANT
C
C      CNST=YB/XHR
C      CALL KSET(CNST,XXKB,1)
C
C      SLOT WIDTH AT BOTTOM
C
C      C=XXCOE*SIN(YB*ANRADI)
C      RTM=XXKB*C
C
C      AREA OF SLOT
C
C      SLTAR(I)=SPC(I)*(TOP+RTM)/2.0
C
C      TOTAL AREA OF SLOTS
C
C      XAREA=XAREA+SLTAR(I)
C      YT=YB+XH
C      20 CONTINUE
C
C      SLOT POROSITY
C
C      PERSD= ABS(XAREA-GSLA )/GSLA
C      RETURN
C      END

```

SUBROUTINE WEIGHT(WGT)

SUBROUTINE TO CALCULATE THE WEIGHT OF THE CHUTE

REAL LLW

COMMON/SAILS/XA(50),XB(50),XAB(50),XABY(50),SALWGT(50)

COMMON/CNTRL/VCB(150),CTRL(100),TITLE(12)

COMMON/READAT/CDS,DSURO,DZL,SLST,CDO,XNO,XH

1 .XLS,XLR,DV,XHR,SALNO,SEAM,VLNO

2 .CRANG,CCOEF,CKOEF,GRCOE,RLCOE,PESLO,XNMBR

3 .SLW,LLW,SBW,VBW,RTW,RSM,VLW

4 .CRNPOR,GEOPOR,TOTPOR,CLHPOR,VNTPOR,XIXMU

COMMON/SDIM/XYY(2,50),XYCA(50),XYCB(50),XYC(2,50),XYH(50),XYA(50),

1 XYP(50),XIMU,XAREA,VAREA,IS(50),RWTOP(50),RWBOT(50),IX(50),

2 PRCRN,PRGOR,PRCLTH,PROTO,ASAIL,AR(50),SO

DOUBLE PRECISION VCB,TITLE

C NUMBER OF SAILS

JJ=SALNO

SLA=0.0

CLA=0.0

C CLOTH WEIGHT

DO 9 J=1,50

IF(SALWGT(J).EQ.0.0)SALWGT(J)=SLW

9 CONTINUE

C CALCULATE SAIL AREA

DO 10 I=1,JJ

KK=JJ-I+1

CLAR=(XA(I)+XB(I))/2.0*XH(I)*SALWGT(KK)

CLA=CLA+CLAR

10 CONTINUE

C SAIL WEIGHT

CLA=CLA*XNO

C SUSPENSION LINE WEIGHT

SLA=XNO*(XLS+12.0)*LLW

C RISER WEIGHT

RIA=(XLR+12.0)*(XNO/XIMU)*RSW

C WEIGHT OF RADIALS

```

      RAA=XNO*2.0*(XHP+2.0)*RTW
  307 FORMAT(1HO,12A6)
  308 FORMAT(1H1,42X,45HR I N G S A I L   C H U T E   D E S I G N)
C
C   WEIGHT OF SKIRT BAND -
C
SKA=(XNO*XVCB(1)+6.0)*SBW
C
C   WEIGHT OF VENT BAND
C
VBA=(XNO*XVCA(JJ)+6.0)*VBW
C
C   WEIGHT OF VENT LINES
C
VLA=(DV+6.0)*VLNO*VLW
C
C   WEIGHT OF REINFORCING TAPES
C
RTA=0.0
RWTOP(1)=0.0
DO 20 I=1,JJ
ISL=JJ-I+1
IF(ISL .LT. 1) GO TO 20
WGG=(XNO*XVCB(ISL)+6.0)*RWTOP(I)
IF(ISL .LT. 2) GO TO 19
WGG=WGG+(XNO*XVCB(ISL)+6.0)*RWBOT(I)
19 RTA=RTA+WGG
20 CONTINUE
MGT=CLA+SLA+RIA+RAA+SKA+VBA+VLA+RTA
C
C   WRITE WEIGHT DATA
C
WRITE(6,308)
WRITE(6,307)(ITLF(J),J=1,12)
WRITE(6,319)
319 FORMAT(23HWEIGHT DATA)
WRITE(6,320)
320 FORMAT(30H(ALL WEIGHTS GIVEN IN POUNDS))
WRITE(6,321)CLA
321 FORMAT(23HOSAIL FABRIC WEIGHT = ,F10.3)
WRITE(6,322)SLA
322 FORMAT(26HOSUSPENSION LINE WEIGHT = ,F10.3)
WRITE(6,323)RIA
323 FORMAT(17HORISER WEIGHT = ,F10.3)
WRITE(6,324)RAA
324 FORMAT(22HWEIGHT OF RADIALS = ,F10.3)
WRITE(6,325)SKA
325 FORMAT(27HOSKIRT BAND WEIGHT = ,F10.3)
WRITE(6,326)VBA
326 FORMAT(21HOVENT BAND WEIGHT = ,F10.3)
WRITE(6,327)VLA

```

```

327 FORMAT(21H0VENT LINE WEIGHT = ,F10.3)
      WRITE(6,328)RTA
328 FORMAT(32H0WEIGHT OF REINFORCING TAPES = ,F10.3)
      WRITE(6,329)WGT
329 FORMAT(36H-TOTAL PARACHUTE ASSEMBLY WEIGHT = ,F10.3)
      RETURN
      FND
      SUBROUTINE EXTRP(X1,Y1,X2,Y2,AX,AY)
C
C      SUBROUTINE TO PERFORM EXTRAPOLATION
C
      DELX=X2-X1
      DELY=Y2-Y1
      AY=((DELY*(AX-X1))/DELX)+Y1
      RETURN
      END
      SUBROUTINE INDATA
C
C      SUBROUTINE TO PRINT INPUT DATA
C
      COMMON/CODATA/DOOX(50),DOX(50),ICD
      COMMON/RGTBL/PSVR(50),PRSL(50),IPD
      COMMON/CNTRL/VCB(150),CTRL(100),TITLE(12)
      COMMON/FULDAT/HHR(50),XKA(50),XKB(50),IFD
      COMMON/SATLS/XA(50),XB(50),XAB(50),XABY(50),SALWGT(50)
      COMMON/READAT/CDS,DSUB0,DZL,SLST,CDO,XNO,XH
      1      ,XLS,XLR,DV,XHR,SALNO,SEAM,VLVD
      2      ,CRANG,CCDEF,CKDEF,GRCOE,RLCOE,PESLO,XNMBR
      3      ,SLW,LLW,SBW,VBW,RTW,RSW,VLW
      4      ,CRNPOR,GEOPOR,TOTPOR,CLMPOR,VNTPOR,XIXMU
      COMMON/SDATA/SPC(50),SLARA,XHT,KHV,NMBR,XXCOF,ANRAD,SLTAR(50)
      COMMON/SDIM/YYY(2,50),XYCA(50),XYCB(50),XYC(2,50),XYH(50),XYA(50),
      1 XYP(50),XIMU,XARFA,VAREA,TS(50),RWTDP(50),RWBDT(50),IX(50),
      2 PRCRN,PRGDR,PRCLTH,PROTO,ASAIL,AR(50),SD
      DIMENSION RDCHK(35),STD(35),TXXX(9),ADA(35)
      DOUBLE PRECISION VCA,TITLE,ADA
      EQUIVALENCE(RDCHK(1),CDS)
C      WRITE TABLE DATA
C
      1055 WRITE(6,308)
      WRITE(6,307)TITLE
      WRITE(6,326)
      WRITE(6,327)
      326 FORMAT(1H0,25X,22H N P U T D A T A)
      327 FORMAT(1H0,5X,9HC00 DATA,8X,14HRIGGING VS C00,13X,14HFULLNESS TABL
      1E1
      WRITE(6,328)
      328 FORMAT(9H0 D SUB 0,6X,3HC00,4X,26HPERS,OPT. PERS,C00 H/HR,7X,2H
      1KA,RX,7HKB/1H0)
      JJ=MAX0(1CD,1PD,1FD)
      DO 1040 J=1,JJ

```

```

DOAX=00X(J)/12.0
IF(J.EQ.40)WRITE(6,328)
WRITE(6,329)DOAX ,CDOX(J),PRSL(J),PSVR(J),MHR(J),XKA(J),XKB(J)
1040 CONTINUE
329 FORMAT(1X,F9.3,6F10.3)
WRITE(6,308)
WRITE(6,307)TITLE
WRITE(6,326)
WRITE(6,318)
REWIND 12
DO 1056 I=1,34
IF(CTRL(1).EQ.0.0)GO TO 1956
IF(CTRL(1).EQ.1.0)WRITE(12,331)VC8(52)
GO TO 1056
1956 DAO=RCHK(1)
IF(1.EQ.1)DAO=DAO/144.0
IF(1.EQ.2.OR.1.EQ.8)DAO=DAO/12.0
IF(1.EQ.34)GO TO 1961
IF(1.EQ.11)GO TO 1961
IF(1.LT.15)GO TO 1963
IF(1.EQ.20)DAO=DAO*100.0
IF(1.EQ.15)DAO=DAO/.017453
IF(1.LT.22)GO TO 1965
IF(1.EQ.22)DAO=DAO*144.0
IF(1.GT.22).AND.(1.LT.29)DAO=DAO*1.2.0
IF(1.LT.29)GO TO 1967
DAO=DAO*100.0
GO TO 1965
1961 WRITE(12,1962)DAO
1962 FORMAT(F6.0)
GO TO 1056
1963 WRITE(12,1964)DAO
1964 FORMAT(F6.2)
GO TO 1056
1965 WRITE(12,1964)DAO
1966 FORMAT(F6.1)
GO TO 1056
1967 WRITE(12,1968)DAO
1968 FORMAT(F6.5)
1056 CONTINUE
REWIND 12
DO 1057 I=1,34
READ(12,331)ADA(1)
1057 CONTINUE
330 FORMAT(F6.3)
331 FORMAT(A6)
WRITE(6,332)ADA(11),ADA(2)
WRITE(6,333)ADA(3),ADA(4)
WRITE(6,334)ADA(5),ADA(6)
WRITE(6,335)ADA(7),ADA(8)
WRITE(6,336)ADA(9),ADA(10)

```

```

      WRITE(6,337)ADA(11),ADA(12)
      WRITE(6,338)ADA(13),ADA(14)
      WRITE(6,339)ADA(15),ADA(16)
      WRITE(6,340)ADA(17),ADA(18)
      WRITE(6,341)ADA(19),ADA(34)
      WRITE(6,342)ADA(20),ADA(21)
      WRITE(6,343)ADA(22),ADA(23)
      WRITE(6,344)ADA(24),ADA(25)
      WRITE(6,345)ADA(26),ADA(27)
      WRITE(6,346)ADA(28),ADA(29)
      WRITE(6,347)ADA(30),ADA(31)
      WRITE(6,348)ADA(32),ADA(33)
      WRITE(6,308)
      WRITE(6,307)TITLE
      WRITE(6,326)
      WRITE(6,318)
      WRITE(6,369)
340 FORMAT(1H0,10X,52HSAIL INPUT DATA (REINFORCING OR NON-STANDARD WEI
IGHT))
      WRITE(6,350)
350 FORMAT(1H0,9H SAIL NO.10X,9HTOP TAPE,10X,11HBOTTOM TAPE,10X,12HCLD
ITH WEIGHY)
      DO 1990 I=1,50
      IF((SALWGT(I),EQ,0.01,AND,(IS(I),EQ,0))GO TO 1990
      DAD=SALWGT(I)*144.0
      IF(DAD,EQ,0.01)DAD=SLW*144.0
      DATOP=RWTOP(I)*12.0
      DAROT=RWDOT(I)*12.0
      XXX=IS(I)+1
      GO TO(1970,1971,1972),XXX
1970 WRITE(6,1973),DAD
      GO TO 1990
1971 WRITE(6,1974),DATOP,DAD
      GO TO 1990
1972 WRITE(6,1975),DATOP,DAROT,DAD
1973 FORMAT(1H0,.9X,12.16X,23HNFS,16X,23HNFS,14X,F10.6)
1974 FORMAT(1H0,.9X,12.11X,F10.6,12X,23HNFS,14X,F10.6)
1975 FORMAT(1H0,.9X,12.11X,F10.6,9X,F10.6,11X,F10.6)
1990 CONTINUE
372 FORMAT(1SH DRAG AREA = ,A6,30X,1THCHUTE DIAMETER = ,A6)
373 FORMAT(1SH DESIGN LOAD = ,A6,20X,23HSUSPENSION LINE LOAD = ,A6)
374 FORMAT(1SH DRAG COEF. = ,A6,20X,18HNUMBER OF GORES = ,A6)
375 FORMAT(1SH CENTER WIDTH = ,A6,27X,24HSUSPENSION LINE LENGTH = ,A6)
376 FORMAT(1SH RISER LENGTH = ,A6,27X,16HVENT DIAMETER = ,A6)
377 FORMAT(1SH GORE LENGTH = ,A6,27X,18HNUMBER OF SAILS = ,A6)
378 FORMAT(1SH SEAM ALLOWANCE = ,A6,25X,23HNNUMBER OF VENT LINES = ,A6)
379 FORMAT(1SH CROWN ANGLE = ,A6,20X,19HGORE ANGLE COEF. = ,A6)
380 FORMAT(1SH GORE WIDTH COEF. = ,A6,23X,20HGORE LENGTH COEF. = ,A6)
381 FORMAT(24H RIGGING LENGTH COEF. = ,A6,19X,19HNNUMBER OF RISERS = ,A
1A1
382 FORMAT(12H PER S. GORE TO SLOTS = ,A6,20X,18HNNUMBER OF SLOTS = ,A6)

```

343 FORMAT(21H SAIL CLOTH WEIGHT = ,A6,22X,25HSUSPENSION LINE WEIGHT =
1 ,A6)

344 FORMAT(21H SKIRT BAND WEIGHT = ,A6,22X,19HVVENT BAND WEIGHT = ,A6)

345 FORMAT(22H RADIAL TAPE WEIGHT = ,A6,21X,15HRISER WEIGHT = ,A6)

346 FORMAT(20H VENT LINE WEIGHT = ,A6,23X,17HCROWN POROSITY = ,A6)

347 FORMAT(22H GEOMETRIC POROSITY = ,A6,21X,17HTOTAL POROSITY = ,A6)

301 FORMAT(1H1,24X,12A6)

307 FORMAT(1H0,12X,12A6)

348 FORMAT(18H CLOTH POROSITY = ,A6,25X,16HVVENT POROSITY = ,A6)

308 FORMAT(1M1,12X,45HR I N G S & S L CHUTE DESIGN)

318 FORMAT(1H0,33X,11H(CONTINUED)/1H0)

RETURN

END

SUBROUTINE SLOCAL,

C

C SUBROUTINE TO CALCULATE SLOT POSITION AND DIMENSIONS

C

COMMON/COATA/CDOX(50),DOX(50),ICD

COMMON/RGTRBL/PSVR(50),PRSL(50),IPD

COMMON/CNTRL/VCB(150),CTRL(100),TITLE(12)

COMMON/FULDAT/HMR(30),XKA(50),XKB(50),IFD

COMMON/SAILS/XA(50),XB(50),XAB(50),XABY(50),SALWGT(50)

COMMON/READAT/CDS,DSUB0,DZL,SLST,CDO,XNO,XH

1 ,XLS,XLR,DV,XMR,SALMO,SEAN,VLN0

2 ,CRANG,CCDEF,CKDEF,GRCOE,RLCOE,PESLD,XNMNR

3 ,SLW,LLW,SBW,VBW,RTW,RSW,VLN

4 ,CRMPOR,GEOPOR,TOTPOR,CLMPOR,VMPOR,XIXMU

COMMON/SADATA/SPC(50),SLARA,XHT,XHV,NMBR,XXCOE,ANRAD,SLTAR(50)

COMMON/SOI%/XXX(2,50),XYCA(50),XYCB(50),XYC(2,50),XYH(50),XYA(50),

1 .XYP(50),XIMU,XAREA,VAREA,TS(50),RWTOP(50),RMBOT(50),IX(50),

2 PRCRN,PRGOR,PRCLTH,PROTO,ASATL,AR(50),SO

DIMENSION RDCHK(35),STDRD(35),XXX(9),ADA(35)

EQUIVALENCEIRDCHK(1),CDSI

DOUBLE PRECISION YCB,TITLE,ADA

C

C CALCULATE VENTELATION POROSITY

C

CALL PORSIT()

C

VENT AREA CALCULATION

C

VAREA=50*VNTPOR

C

VENT DIAMETER CALCULATION

C

DV=SQRT(VAREA*1.23724)

C

CALCULATE DIMENSION DOWN TO TOP SAIL

C

IF(CTRL(95).NE.2.0)GO TO 90

IF(XHV.EQ.0.0)XHV=DV/(2.0*COS(CRANG))

Best Available Copy

```

SLD=0.0
NMBR=XNMBR
XMARO=SALNO*XNMBR-1.0
DO 95 I=1,NMBR
95 SLD=SLD+SPC(I)
XHT=XHR-(XMARO*XH+SLD+XHV)
DV=XHV*(2.0*COS(CRANG))
SLARA=100.0
CALL SITARE(PERSD)
GO TO 80
90 XHV=DV/(2.0*COS(CRANG))

C      CALCULATE TOTAL POROSITY AREA REQUIRED
C
TOARA=SO*TOTPOR

C      CALCULATE SLOT AREA REQUIRED
C
IF(CTRL(30).EQ.1.0)GO TO 1127
SLARA=SO*(GEOPOR-ASAIL)-VAREA
GO TO 1129
1127 IF(CTRL(31).EQ.1.0)GO TO 1128
SLARA=TOARA-(VAREA+ASAIL*SO)
GO TO 1129
1128 SLARA=SU*CRNPOR-VAREA

C      CALCULATE AREA PER GORE IN SLOTS
C
1129 GSLA=SLARA/XNO

C      LARGEST WHOLE NUMBER OF SAILS OF HEIGHT H THAT CAN BE ADDED
C
IXNBR=SALNO
TOTDST=XXX(2,IXNBR)-XHV
NMBR=INT(TOTDST/XH)
XNMBR=NMBR
IF(NMBR.GT.(50-IXNBR))GO TO 1130

C      DIMENSION LEFT FOR SLOWS
C
DLDIST=TOTDST-XNMBR*XH
C      ROUGH EQUAL SLOT SPACING
C
SLSPC=0.0
GO TO 28
1130 WRITE(6,380)XNMBR,SALNO
380 FORMAT(16HO TOO MANY SAILS,2E12.3)
CALL EXIT
C

```

```

C      CALCULATE CLOSEST EQUAL SPACING WITHIN .25 INCH
C
28 SLSPC=SLSPC+.25
      SLTO=1.0*MBR*SLSPC
      IF(SLT0.LT.OLDIST)GO TO 28
      SLSPC=SLSPC-.25
C
C      SET IDENTIFIED SLOT SPACES
C
      DO 30 I=1,NMBR
      SPC(I)=SLSPC
30 CONTINUE
C
C      ADJUST SPACES (UNEQUAL) TO MATCH DIST. TO WITHIN .25 INCH
C
      KNXX=1
      DO 40 I=1,NMBR
      SPCTOT=0.0
C
C      ADD .25 INCH TO TOP SLOTS
C
      DO 34 J=1,KNXX
      SPC(J)=SPC(J)+.25
34 CONTINUE
C
C      CALCULATE TOTAL SLOT DISTANCE
C
      DO 36 J=1,NMBR
      SPCTOT=SPCTOT+SPC(J)
36 CONTINUE
C
C      CHECK FOR SPACING MATCH
C
      IF(SPCTOT.GT.OLDIST)GO TO 42
      KNXX=KNXX+1
40 CONTINUE
C
C      SET TOP SAIL HEIGHT
C
      42 XHT=XH
C
C      CALCULATE SLOT AREA
C
      CALL SELTARF(PERSD)
C
C      CHECK FOR POROSITY MATCH
C
      IF(PERSD.LT..05)GO TO 80
C
C      LOGIC CHECK FOR SLOT DIMENSION CHANGE

```

```

C IFIXAREA.LT.GSLA GO TO 56
C
C FIX POINT NO OF SLOTS
C
C ISTP=NMBR/2
C
C REDUCE SLOT AREA BY INCREASING TOP SLOT AND REDUCING BOTTOM SLOT
C
C KNXX=1
C DO1242 I=1,ISTP
C DO1240 J=1,KNXX
C SPC(J)=SPC(J)+.25
C K=NMBR-J
C SPC(K+1)=SPC(K+1)-.25
1240 CONTINUE
C
C CALCULATE SLOT AREA
C
C CALL SLTARE(PERSD)
C
C CHECK FOR POROSITY MATCH
C
C IF(PERSD.LT..05)GO TO 80
C KNXX=KNXX+1
C
C CHECK TO SEE IF BOTTOM SLOT REMOVED
C
C IF(SPC(NMBR).LE.0.0)GO TO 50
1242 CONTINUE
C
C REMOVE ALL SLOTS IF PRECEDING DOES NOT PROVIDE SOLUTION
C BY ADDING ANOTHER SAIL
C
C 50 NMBR=NMBR+1
C
C SET HEIGHT OF NEW TOP SAIL
C
C XHT=OLDDIST
C
C RESET IDENTIFIED SLOTS TO ZERO
C
C DO 52 I=1,NMBR
C SPC(I)=0.0
52 CONTINUE
C
C INCREASE SLOTS BY .25 INCH AT A TIME REMOVING MATERIAL FROM TOP
C SAIL
C
C 56 DO 58 I=1,NMBR
C SPC(I)=SPC(I)+.25
C XHT=XHT-.25

```

```

58 CONTINUE
C
C   CALCULATE SLOT AREA
C
C   CALL SLTARE(PERSD)
C
C   CHECK FOR POROSITY MATCH
C
C   IF(PERSD.LT..05)GO TO 80
C
C   CHECK FOR AREA GREATER THAN REQUIRED
C
C   IF(XAREA.LT.GSLA) GO TO 56
C   KNXX=1
C
C   MATCH AREA BY REMOVING FROM BOTTOM SLOTS AND ADDING TO TOP SAIL
C
C   DO 68 I=1,NMBR
C   DO 66 J=1,KNXX
C   K=NMBR-J
C   SPC(K+1)=SPC(K+1)-.25
C   HT=HT+.25
66 CONTINUE
C   CALL SLTARE(PERSD)
C
C   CHECK FOR CLOSEST CONDITION LESS THAN REQUIRED AND ACCEPT SOLUTION
C
C   IF(XAREA.LT.GSLA) GO TO 80
C   KNXX=KNXX+1
C
C   IF BOTTOM SLOT IS REMOVED ACCEPT SOLUTION
C
C   IF(SPC(NMBR).LE.0.0)GO TO 80
68 CONTINUE
C
C   CALCULATE SLOTS WHERE AREA IS LESS THAN REQUIRED
C
C   R0 DELY=XH
C
C   NUMBER OF SAILS AND SLOTS IN FIXED POINT FORM
C
C   I=SALNO
C   J=NMBR
C   IF(I+J).GT.50)GO TO 1130
C
C   DETERMINE LOCATION OF SAILS IN SLOT RETCON
C
C   R2 I=I+1
C
C   DETERMINE SAYL BOTTOM LOCATION

```

```

Y=XXX(2,I-1)-SPC(JJ)
XXX(1,I)=Y

C DETERMINE GORE WIDTH AT BOTTOM OF SAIL
C
CCC=XXCOE*SIN(Y*ANRADI)
XYC(I,I)=CCC

C DETERMINE SAIL HEIGHT
C
XYH(I)=DELY

C DETERMINE FULLNESS CONSTANT
C
CNST=Y/XHR
CALL KSET(CNST,XXKB,1)

C DETERMINE FREE SAIL WIDTH AT SAIL BOTTOM
C
XYCB(I)=XXKB*CCC

C DETERMINE CONSTRUCTION WIDTH AT SAIL BOTTOM
C
XR(I)=XYCB(I)+SEAM

C CALCULATE POSITION OF TOP OF SAIL
C
Y=Y-DELY
XXX(2,I)=Y

C CALCULATE GORE WIDTH AT TOP OF SAIL
C
CCC=XXCOF*SIN(Y*ANRADI)
XYC(2,I)=CCC

C CALCULATE FULLNESS CONSTANT
C
CNST= Y/XHR
CALL KSET(CNST,XXKA,2)

C DETERMINE FREE SAIL WIDTH AT SAIL TOP
C
XYCA(I)=XXKA*CCC

C CALCULATE CONSTRUCTION WIDTH AT SAIL TOP
C
XA(I)=XYCA(I)+SEAM

C CHECK IF TOP SAIL
C
IF(I,J,EQ,2)DELY=XHT

```

J=J-1
IF(J.GT.0) GO TO 82

C
C
C
SET NEW NUMBER FOR TOTAL SAILS FLOATING AND FIXED

SALNO=1
ISNO=1
XHV=XVV(2,ISNO)
DV=XHV*(2,0*COS(CRANG))
RETURN
END
SUBROUTINE OUTIT

C
C
SUBROUTINE TO WRITE OUTPUT INFORMATION
C

COMMON/CODATA/DOX(50),DOX(50),ICD
COMMON/RGTBL/PSVR(50),PRSL(50),TPD
COMMON/CNTRL/VCB(150),CTRL(100),TITLE(12)
COMMON/FULDAT/HHR(50),XKA(50),XKB(50),IFD
COMMON/SAILS/XA(50),XB(50),XAN(50),XABY(50),SALHGT(50)
COMMON/READAT/CDS,DSUB0,DZL,SLST,CDD,XND,XH
1 ,XLS,XLR,DV,XHR,SALNO,SEAM,VLNO
2 ,CRANG,CCDEF,CKDEF,GRCOE,RLCOE,PESLO,XNMBR
3 ,SLW,LLW,SBW,VBW,RTH,RSW,VLW
4 ,CRNPOR,GEOPOR,TOTPOR,CLHPOR,VNTPOR,XIXMU
COMMON/SDATA/SPC(50),SLARA,XHT,XHV,NMBR,XXCOE,ANRAD,SLTAR(50)
COMMON/SGIN/XVV(2,50),XVCA(50),XVCB(50),XVC(2,50),XYH(50),XYA(50),
1 XYP(50),XTBU,XAREA,VAREA,TS(50),RWTOP(50),RWBOT(50),IX(50),
2 PRCRN,PRGOR,PRCLTH,PROTO,ASAIL,AR(50),SO
DIMENSION RDCHK(35),STDRI(35),IXX(9),ADA(35)
EQUIVALENCE(RDCHK(1),CDS)
DOUBLE PRECISION VCB,TITLE,ADA
SI TOT=0.0
PRSLT=0.0
CRYTOT=0.0
PRSTOT=0.0
WRITE(6,308)
WRITE(6,307)(TITLE(J),J=1,12)
DAT1=DSUB0/12.0
DAT2=SD/164.0
DAT3=CDS/164.0
WRITE(6,310)
1 WRITE(6,309)VCB(1),VCH(2),VCB(3),DAT1,VCB(37),VCB(4),VCB(5),VCB(3)
1 ,DAT2,VCB(38),VCH(6),VCB(7),VCB(3),DAT3,VCB(39)
DAY1=XND
NGT=CTRL(59)
DAT2=HGT
DAT3=CDD
WRITE(6,310)
1 WRITE(6,109)VCB(9),VCH(2),VCB(3),DAT1,VCB(45),VCB(43),VCB(44),VCB(13),
1 ,DAT2,VCB(40),VCH(12),VCB(13),VCB(11),DAT3

```

XL=CTRL(98)
DAT1=XL/12.0
DAT2=XLS/12.0
DAT3=XLR/12.0
WRITE(6,310)
WRITE(6,309) VCB(14), VCB(15), VCB(3), DAT1, VCB(37), VCB(16), VCB(17), VC
1B(3), DAT2, VCB(37), VCB(18), VCB(19), VCB(3), DAT3, VCB(37)
DAT1=XL/DSUB0
DAT2=100.0*DVENT*2*.7854/S0
VENDO=DAT2
VENT=DVENT*2*.7854/144.0
DAT3=DVENT
WRITE(6,310)
WRITE(6,309) VCB(10), VCB(11), VCB(3), DAT1, VCB(45), VCB(53), VCB(54), VC
1B(3), DAT2, VCB(41), VCB(26), VCB(27), VCB(3), DAT3, VCB(39)
DAT1=XHR
DAT2=XHR/DSUB0
DAT3=6.44*XHR/XNO
WRITE(6,310)
WRITE(6,309) VCB(20), VCB(21), VCB(3), DAT1, VCB(39), VCB(35), VCB(36), VC
1B(3), DAT2, VCB(45), VCB(22), VCB(23), VCB(3), DAT3, VCB(39)
DAT1=PRCLTH
DAT2=PRCRN
DAT3=PROTO
WRITE(6,310)
WRITE(6,309) VCB(28), VCB(32), VCB(3), DAT1, VCB(41), VCB(28), VCB(29), VC
1B(3), DAT2, VCB(41), VCB(28), VCB(31), VCB(3), DAT3, VCB(41)
DAT1=PRGOR
DAT2=XIMU
WRITE(6,310)
WRITE(6,309) VCB(28), VCB(30), VCB(3), DAT1, VCB(41), VCB(50), VCB(51), VC
1B(3), DAT2
WRITE(6,310)
WRITE(6,311)
WRITE(6,310)
ISNO=SALNO
TAR=0.0
TAREA=0.0
DO 50 I=1, ISNO
ARA=XYH(I)*(XYCA(I)+XYCB(I))/2.0
TAR=TAR+ARA
XYA(I)=ARA
XYP(I)=100.0*ARA/S0
SLOX=0.0
IF(I.LF.NMRR1.SL0)X=SL*TAR(I)
TAREA=TAREA+ARA+SLOX
50 CONTINUE
TARFA=TAREA*XNO+VENT
XDD=SQRT(4.0*TAREA/3.1416)/12.0
TAREA=TAREA/144.0
DAT1*TAREA

```

```

DAT2=XOO
DAT3=TAREA+CDO
TAREA=TAR*XNO/144.0
TPDR=TAREA*100.0/(SO/144.0)
WRITE(6,309)VCB(46),VCB(47),VCB(3),DAT1,VCB(38),VCB(48),VCB(49),VC
1B(3),DAT2,VCB(37),VCB(6),VCB(7),VCB(3),DAT3,VCB(38)
WRITE(6,308)
WRITE(6,307)(TITLE(K),K=1,12)
WRITE(6,312)
WRITE(6,313)
WRITE(6,314)
DO 90 I=1,ISNO
J=ISNO-I+1
XYP(J)=XYP(J)*XNO
HHHRT=XYY(2,J)/XHR
HHHRB=XYY(1,J)/XHR
XSOF=XYA(J)*XNO/144.0
WRITE(6,315)XYY(2,J),HHHRT,XYC(J),XA(J),XYC(2,J)
WRITE(6,316)I,XYH(J),XYA(J),XSOF,XYP(J)
WRITE(6,317)XYY(1,J),HHHRB,XYC(J),XB(J),XYC(1,J)
IF(I.GT.NMBRIGO TO 1284
PRSD=(SLTAR(I)/SO)*100.0*XNO
XSOF=XNO*SLTAR(I)/144.0
SLTOT=SLTOT+XSOF
PRSLT=PRSLT+PRSD
WRITE(6,319)I,SPC(I),SLTAR(I),XSOF,PRSD
GO TO 88
1284 IF(I.EQ.ISNO)GO TO 88
PRSD=(AR(J)/SO)*100.0*XNO
XSOF=XNO*AR(J)/144.0
CRTOT=CRSTOT+XSOF
PRSTOT=PRSTOT+PRSD
WRITE(6,320)AR(J),XSOF,PRSD
88 IF((I.EQ.5).OR.(I.EQ.10)).OR.(I.EQ.15))GO TO 89
IF((I.EQ.20).OR.(I.EQ.25)).OR.(I.EQ.30))GO TO 89
IF((I.EQ.35).OR.(I.EQ.40)).OR.(I.EQ.45))GO TO 89
GO TO 90
89 IF(I.EQ.ISNO)GO TO 90
WRITE(6,308)
WRITE(6,307)(TITLE(K),K=1,12)
WRITE(6,312)
WRITE(6,313)
WRITE(6,314)
90 CONTINUE
WRITE(6,308)
WRITE(6,307)(TITLE(K),K=1,12)
WRITE(6,323)SLTOT
WRITE(6,324)PRSLT
WRITE(6,325)CRSTOT
WRITE(6,324)PRSLT

```

```

      WRITE(6,327)VENT
      WRITE(6,324)VENPO
      WRITE(6,329)TAREA
      WRITE(6,324)TPDR
323 FORMAT(19HOTAL SLOT AREA = ,F12.3,TH SQ.FT.)
324 FORMAT(17H PERCENT OF SO = ,F12.3)
325 FORMAT(28HOTAL CRESCENT SLOT AREA = ,F12.3,TH SQ.FT.)
327 FORMAT(19HOTAL VENT AREA = ,F12.3,TH SQ.FT.)
329 FORMAT(20HOTAL CLOTH AREA = ,F12.3,TH SQ.FT.)
300 FORMAT(12A6,7X,[1]
301 FORMAT(1H1,24X,12A6)
302 FORMAT(2F10.0,54X,A6)
303 FORMAT(1X,213,3X,9A6)
304 FORMAT(7F10.0,9X,11)
305 FORMAT(44H INSUFFICIENT DATA PROVIDED TO DESIGN CHUTE)
306 FORMAT(3F10.0,44X,A6)
307 FORMAT(1H0,24X,12A6)
308 FORMAT(1H1,42X,45HR IN G S A I L   C H U T E   D E S I G N)
309 FORMAT(1X,3A6,F10.3,1X,A6,12X,3A6,F10.3,1X,A6,12X,3A6,F10.3,1X,A6)
310 FORMAT(1H )
311 FORMAT(43H CHECK ON AREA AND DIA. FROM SAIL SUMMATION)
312 FORMAT(1H0,43X,42MG D R E   A N D   S A I L   D E S I G N)
313 FORMAT(105HOSAIL DISTANCE          M/HR SAIL WIDTH SAIL WIDTH
      1 GORE WIDTH     HEIGHT          FREE SAIL AREA)
314 FORMAT(117H NO.   FROM APEX          LESS SEAM
      1 AT SAIL      OF SAIL      SQ. TH.  SQ FT/RING PERS SO/RING)
315 FORMAT(5H0 TOP,2X,5F12.3)
316 FORMAT(3X,12,62X,4F12.5)
317 FORMAT(7H BOTTOM,5F12.3)
318 FORMAT(50X,11H(CONTINUED))
319 FORMAT(10HOSLOT NO. ,13,54X,4F12.5)
320 FORMAT(14HOCRESCENT SLOT,65X,3F12.3)
321 FORMAT(50I1,29X,11)
322 FORMAT(50I1,F10.0,9X,11,9X,11)
      RETURN
      END
      BLOCK DATA
COMMON/CODATA/CDOX(50),DOX(50),ICD
COMMON/RGTBL/PSVR(50),PRSL(50),IPD
COMMON/FULDAT/HHR(50),XKA(50),XKB(50),IFD
      DATA CDOX,DOX,PSVR,PRSL,HHR,XKA,XKB/50*0.,50*0.,50*0.,50*0.,
      50*0.,50*0.,50*0./
      END

```

1 10	CHUTE DIA.	=	CANOPY AREA DRAG AREA	NO. OF GORES/CHUT
11 20	E DIA. DFS.CDO		RIGGING LGTHLINE LENGTH	RISER LENGTH/GORE L
21 30	ENGTH 6.44 HR/N		VENT RADIUS VENT DIA.	DVLAMBDA SUB C SUB G

Best Available Copy

	SUB T	SUB MSAIL AREA	M SUB R / D FEET	SQ.FT. INCHES POUNDS
PERS.	SQ. IN. SYS.	WEIGHT	TOTAL AREA	DIAMETER NO. OF
RISERS	M/S VENT PDR.			

150150 ENDTA

.715	10.0
.715	20.0
.716	30.0
.717	34.0
.730	40.0
.736	45.0
.795	48.0
.809	50.0
.820	55.0
.825	60.0
.830	70.0
.832	80.0
.834	90.0
.835	100.0
.835	110.0
.835	120.0
.835	130.0

ENDTA

-24.8	-47.8
-18.5	-39.1
-14.3	-30.4
-9.79	-21.7
-5.50	-13.05
-1.59	-6.35
0.0	0.0
1.59	4.35
4.65	13.05
7.09	21.7
9.03	30.4
10.6	39.1

ENDTA

0.00	1.06	1.06
0.45	1.015	1.015
0.45	1.015	1.08
0.60	1.0	1.08
1.0	1.0	1.08

ENDTA

/*

Best Available Copy